THE TWENTY-THIRD ANNUAL CONFERENCE ON MASS SPECTROMETRY AND ALLIED TOPICS

MAY 25-30, 1975
HOUSTON, TEXAS

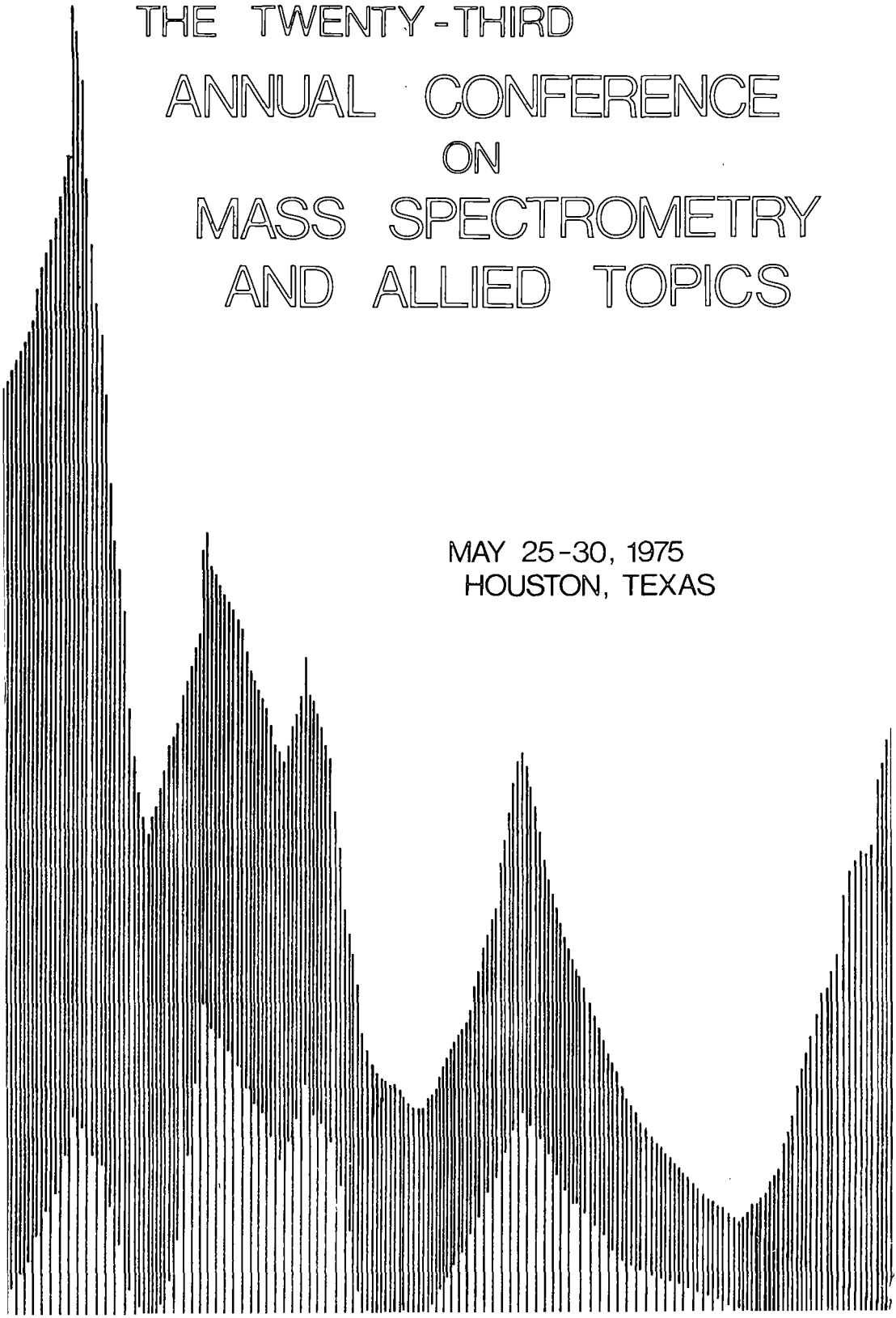

THE TWENTY-THIRD ANNUAL CONFERENCE ON MASS SPECTROMETRY AND ALLIED TOPICS

MAY 25-30, 1975

HOUSTON, TEXAS

TABLE OF CONTENTS

1.	Introduction	1
2.	Acknowledgements	3
3.	Proceedings of the Twenty-Third Annual Conference	4
4.	Author Index	668
5.	ASMS Committees and ASTM E-14 Subcommittees	675
6.	Committee and Subcommittee Reports	676
7.	ASMS Constitution and Bylaws	696
8.	ASTM Publications	705
9.	Mass Spectrometry Organizations	707

Introduction

This volume is a collection of papers presented at the Twenty-Third Annual Conference on Mass Spectrometry and Allied Topics, held in Houston, Texas, May 25-30, 1975. It is intended that this volume be distributed only to members of ASMS, and registrants of the Conference, and therefore it should not be considered as a publication.

It is suggested that any future reference to individual reports be cited in the form: author(s), presented at the Twenty-Third Annual Conference on Mass Spectrometry and Allied Topics, Houston, Texas, May 25-30, 1975.

The final collection, editing, and assembly of the papers for this volume were carried out at Rice University, and it is a pleasure to recognize the meticulous and dedicated efforts of Wayne and Sandra Timmer in the actual preparation of the publication copy and the cover design.

John L. Margrave
Houston, Texas

ASMS

President: H.J. Svec, Department of Chemistry, Iowa State University, Ames, Iowa 50010

Vice President (Program): J. H. Futrell, Department of Chemistry, University of Utah, Salt Lake City, Utah 84112

Vice President (Arrangements): Wilson M. Brubaker, Hewlett-Packard, 1954 Highland Oaks, Arcadia, California 91006

Secretary: J. A. McCloskey, Department of Biopharmaceutical Sciences, University of Utah, Salt Lake City, Utah 84112

Treasurer: M. T. Laug, Argonne National Laboratory, Box 2528, Idaho Falls, Idaho 83401

Past President: F. H. Field, Department of Chemistry, Rockefeller University, New York, New York 10021

Directors-at-Large:

P. Kebarle, Department of Chemistry, University of Alberta, Edmonton 7, Alberta, Canada

J. L. Margrave, Office of Advanced Studies and Research, Rice University, Houston, Texas 77001

The American Society for Mass Spectrometry is grateful for support of the 1975 Conference through sponsorship by the following organizations.

Company	Representative
AEI SCIENTIFIC APPARATUS, INC. 500 Executive Boulevard Elmsford, New York 10523	Dr. W. A. Wolstenholme
AVCO CORPORATION 10700 East Independence Street Tulsa, Oklahoma 74115	Mr. Bill Hopper
CAMECA INSTRUMENTS, INC. 101 Executive Boulevard Elmsford, New York 10523	Mr. Robert J. Hessler
COLUMBIA SCIENTIFIC INDUSTRIES 3625 Bluestein Boulevard P. O. Box 6190 Austin, Texas 78762	J. M. Cotton
CYPHERNETICS CORPORATION P. O. Box 175 Ann Arbor, Michigan 48106	Mr. John Spiegelmyer
CVC PRODUCTS, INC. 1775 Mt. Read Boulevard Rochester, New York 14603	Mr. Robert M. Kolb
E. I. DUPONT DE NEMOURS & CO., INC. 1500 S. Shamrock Avenue Monrovia, California 91016	Dr. E. M. Chait
EXTRANUCLEAR LABORATORIES, INC. P. O. Box 11512 Pittsburgh, Pennsylvania 15238	Mr. Michael C. McKeown
FINNIGAN CORPORATION 845 W. Maude Avenue Sunnyvale, California 94086	Dr. Robert E. Finnigan
HEWLETT-PACKARD Scientific Instruments Division 1601 California Avenue Palo Alto, California 94304	Mr. D. B. Harrington
HEYDEN & SON LTD Spectrum House Alderton Crescent London NW4 3XX England	Mr. Peter M. Williams
INCOS 1332 Sixth Street Berkeley, California 94710	Dr. D. E. Hagge

JEOL (U.S.A.), INC. 235 Birchwood Avenue Cranford, New Jersey 07016	Dr. R. H. Obenauf
THE KEARNS GROUP AND VG INSTRUMENTS 58 Buckingham Drive Stamford, Connecticut 06902	Mr. G. L. Kearns
KOCH ISOTOPES, INC. 72 Rogers Street Cambridge, Massachusetts 02142	Dr. Paul Vickery
MERCK AND COMPANY, INC. 111 Central Avenue Teterboro, New Jersey 07608	Mr. Donn M. Gordon
3M COMPANY 3M Center St. Paul, Minnesota 55101	Mr. David P. Smith
NUCLIDE CORPORATION 642 East College Avenue State College, Pennsylvania 16801	Dr. L. F. Herzog
SCIENTIFIC RESEARCH INSTRUMENTS 6707 Whitestone Road Baltimore, Maryland 21207	Dr. Gordon Fergusson
STOHLER ISOTOPE CHEMICALS, INC. 49 Jones Road Waltham, Massachusetts 02154	Mr. J. Turgel
SYSTEM INDUSTRIES 535 Del Rey Avenue Sunnyvale, California 94086	Mr. Neville L. Crook
UTHE TECHNOLOGY INTERNATIONAL 325 No. Mathilda Avenue Sunnyvale, California 94086	Dr. Bruce Raby
UNIVERSAL MONITOR CORPORATION 430 No. Halstead Street Pasadena, California 91107	Mr. D. P. Littlejohn
VARIAN MAT/U.S. OPERATIONS 25 Route 22 Springfield, New Jersey 07081	Mr. Helmut Raddatz

PROCEEDINGS OF THE TWENTY-THIRD ANNUAL CONFERENCE

Paper No. Page No.

PL-1 * Primordial Cosmochemistry and the Origin of Life.
C. Ponnamperuma----------

PL-2 * Studies in Reaction Dynamics.
Y. T. Lee----------

Trace Analysis of Environmental Samples

A-1 Oxygen as a Reagent Gas for the Analysis of 2,3,7,8-Tetra-Chloro-p-Dioxin (TCDD) by Negative Ion Chemical Ionization Mass Spectrometry.
T. M. Harvey, D. F. Hunt, and J. W. Russell---------- 34

A-2 The Monitoring of Poly(Vinyl chloride) Decomposition Products Via GC/MASS Fragmentography.
J. W. Lewis---------- 35

A-3 Survey Analysis for Trace Elements.
C. E. Taylor---------- 38

A-4 GC-MS (EI-CI) Examination of Fish & Bird Extracts for Toxaphene and other Organic Contaminants in Fish.
D. L. Stalling and J. W. Hogan---------- 38

A-5 The Application of Selected Ion Monitoring to Organic Pollutant Analysis.
W. L. Budde and J. W. Eichelberger------- 39

A-6 Computerized GC/EIMS Used to Monitor Herbicide Clean-up of Contaminated Pond.
B. F. Dudenbostel, Jr. and D. N. Speis---------- 40

A-7 GC/MS Analysis of New Orleans Drinking Water.
M. H. Carter, A. W. Garrison, L. H. Keith, J. M. McGuire, and J. D. Pope----- 40

A-8 New Procedures for the Analysis of Volatile Organics by Gas Chromatography-Mass Spectrometry.
J. W. Eichelberger and W. L. Budde------- 41

A-9 Applications of Pyrolysis/GC/MS in the Analysis of Organic Nitro Compounds.
C. Merritt, Jr.---------- 42

*Plenary Lecture

Paper No. Page No.

A-10 The Identification of Organic Contaminants in Water.
F. E. Saalfeld and R. A. Saunders---------45

A-11 Applications of Field Desorption and Field Ionization Mass Spectrometry to Environmental Analysis.
J. F. Ryan, R. L. Harless and R. G. Lewis----------46

A-12 Positive and Negative Chemical Ionization Mass Spectra of Some Pyrethrins, Carbamates and Organophosphorous Compounds.
D. F. Hunt and S. J. Stout----------49

Field Desorption Symposium

B-1 Recent Advances in Field Desorption Mass Spectrometry.
H.R. Schulten and H. D. Beckey----------50

B-2 Field Desorption Mass Spectrometry Studies of Biorganic Compounds.
K. L. Rinehart, Jr. and J. C. Cook, Jr.----------53

B-3 Structure Elucidation Using Field Desorption Mass Spectrometry (FDMS).
C. N. McEwen----------54

B-4 Field Desorption Mass Spectrometry (FDMS) Of Biogenic Amines and Isoquinoline Alkaloids.
G. W. Wood and N. Mak----------56

B-5 The Complex Effects of Sodium and Potassium Ions in the Field Desorption Mass Spectrometry of Barbiturates.
J. N. Gerber, B. Soltman, J. F. Holland, and C. G. Sweeley----------58

B-6 Thermally-Promoted Field Desorption Mass Spectrometry.
D. F. Barofsky, L. Jacob and E. Barofsky----------60

B-7 Some Applications of Field Desorption (FD) and Field Ionization (FI) Mass Spectrometry.
D. E. Games, A. H. Jackson and M. Rossiter----------62

Paper No. Page No.

B-8 High Temperature Activated Carbon Emitters For Field Desorption Studied by ESR.
R. H. Obenhauf ---------- 64

B-9 Mass Spectrometric Studies of Alamethicin.
R. C. Pandey, J. C. Cook, Jr., and K. L. Rinehart, Jr. ---------- 67

B-10 EI and FD Mass Spectra of Rifamycins.
L. F. Zerilli, M. Landi, and G. G. Gallo ---------- 68

Instrumentation I

C-1 Stigmatic, Second Order, Double Focusing Mass Spectrometer.
S. Taya, H. Tsuyama, I. Kanomata, and H. Matsuda ---------- 70

C-2 Applications of Double Beam Mass Spectrometry to Accurate Mass Measurement.
M. L. Aspinal, K. R. Compson, A. A. Dowman, R. M. Elliott, D. Hazelby ---------- 73

C-3 Micro-Analyser Using Electron Beam Guiding Ion Source.
T. Takagi, T. Kishi, and I. Yamada ---------- 76

C-4 A Two-Filament Rotary Source for Surface Ionization Mass Spectrometry.
R. J. Dupzyk ---------- 76

C-5 Multiple Ion Detection by Accelerating Voltage Alternation in Conjunction with Voltage Sweeping.
L. D. Gruenke, J. C. Craig, and D. M. Bier ---------- 77

C-6 CI-EI Combination Source for MAT 112.
P. Dobberstein, G. Kappus, H. Michelsen, and R. Alberti ---------- 80

C-7 A Dual Field Desorption Electron Ionization Source for Applications in Biomedical Research.
E. M. Chait, C. R. McKinney, and M. Czuha ---------- 83

C-8 Application of the Ion-Drift Spectrometer to Macromass Spectroscopy.II
M. Dole and J. Gieniec ---------- 84

Paper No. Page No.

C-9 Improvement of Interfacing of Quadrupole Mass Filters with Multipoint Field Ionization Sources.
H. L. Brown and R. H. Cross---------- 87

C-10 Potentialities of Quadrupole Mass Spectrometers in Field Ionization/ Field Desorption Investigators.
H. J. Heinen, H. H. Gierlich and H. D. Beckey---------- 90

C-11 Attachment of a Simple Ion Probe to an MS-9 Mass Spectrometer.
R. J. Blattner, D. S. Simons, and C. A. Evans, Jr.---------- 92

C-12 A High Sensitivity GC/MS Utilizing Digitally Programmed Ion Energy.
E. J. Argelander, B. N. Colby, C. W. Hull, T. W. Whitehead---------- 93

C-13 Applications of a New High Sensitivity GC/MS System.
R. G. Beimer, E. M. Chait and C. W. Hull---------- 95

C-14 Gas Chromatography/Chemical Ionization Mass Spectrometry.
F. Hatch and B. Munson---------- 96

C-15 Minaturized Magnetic Sector Mass Spectrometer for Use with Gas Chromatograph.
A. D. Tomassian---------- 98

C-16 Semipermeable Membrane GC/MS Interface.
D. P. Littlejohn----------101

C-17 GC-MS Interface for a CEC 21-104 Mass Spectrometer.
J. Zaletel and J. R. Knighton----------104

C-18 The Use of Leaky Dielectrics for the Separation of Fringe Fields of Quadrupole Mass Filters.
W. L. Fite----------107

C-19 General Time Focusing Relations, a Classical Uncertainty Relation, and the Evaluation of the Limits of Time-of-Flight Mass Spectrometers.
R. P. Stein----------108

Paper No. Page No.

C-20 A New Approach to Time-of-Flight Mass Spectroscopy.
D. F. Torgerson and R. D. MacFarlane-----111

C-21 Miniature Time-of-Flight Mass Spectrometer for Ion Composition Measurements in the Lower Ionosphere.
B. R. Kendall and R. F. Reiter----------113

Primary Processes

D-1 Photoionization Mass Spectrometric Study of CO_2 and H_2O in the Extreme Ultraviolet.
P. L. Kronebusch and J. Berkowitz--------114

D-2 Ion-Pair Formation in H_2, HD, and D_2.
J. Berkowitz and P. L. Kronebusch--------117

D-3 Formation of Fragment Ions by Autoionization and Predissociation of Molecular Rydberg States.
K. E. McCulloh and V. H. Dibeler---------119

D-4 Double Ionization in the Rare Gases Induced by Electron Impact.
L. P. Johnson and J. D. Morrison---------120

D-5 Determination by Charge-transfer Collisional Spectroscopies of the Electronic States Present in a Mass-analyzed Ion Beam.
J. Appell, M. Durup, P. Dong, and J. Durup----------122

D-6 Kinetic Energy Distributions from Unimolecular Dissociations.
C. E. Klots----------125

D-7 Kinetic Energy Release from Ions in Selected Internal Energies.
B. P. Tsai, T. Baer, and A. S. Werner----------126

D-8 Translational Energies of Ions from Ionic Fragmentation.
D. E. Carter and J. L. Franklin----------128

D-9 Breakdown Curves of the Ethylene and Ethylene-d_4 Ions Obtained by Threshold Photoelectron-Photoion Coincidence Mass Spectrometry.
R. Stockbauer and M. G. Inghram----------131

D-10 Photodissociation of Negative Ions.
G. Mauclaire, M. L. Vestal, and J. H. Futrell----------132

Paper No. Page No.

D-11 Photoionization Processes at Threshold I. Threshold Photoelectron Spectra and Photoionization of CO_2.
C. F. Batten, J. A. Taylor, and G. G. Meisels---------- 135

D-12 Evaluation of Kinetic Shifts by Pulsed Source Mass Spectrometry.
S. M. Gordon and N. W. Reid---------- 138

D-13 Associative Ionization and Secondary Reactions in U + O_2 and U + N_2O Systems.
W. L. Fite, H. H. Lo, and M. W. Siegel---------- 139

D-14 Predissociation Processes in Biatomic Ions from Kinetic Energy Distributions and from Metastable Studies.
J. Momigny, R. Locht, and H. Wankenne----- 140

D-15 Energetics of the Ionization and Fragmentation of Arsenic Trifluoride by Electron Impact.
R. E. Pabst, R. G. Meador, J. L. Margrave, and J. L. Franklin---------- 143

D-16 Optically Modified Mass Spectra (OMMS) of COS^+.
A. B. Denison, J. M. Phillips, and J. H. Weber---------- 146

D-17 Electronic States of Fragmentation in the Mass Spectrometer.
L. J. Hendricks and R. H. Shapiro--------- 148

D-18 Iterative Deconvolution of Negative Ion Mass Spectra.
J. L. Franklin and F. J. Hadley---------- 150

D-19 Negative Ion Electron Impact Studies of Group IVA Tetrahalides.
R. E. Pabst, D. L. Perry, J. L. Margrave, and J. L. Franklin---------- 153

D-20 Negative Ion Formation in Conjugated Monocyclic Perchlorocarbons.
A. F.-T. Chen and C. L. Brown---------- 156

D-21 New Studies of Complex Gaseous Halides.
G. D. Blue and J. L. Margrave---------- 158

Paper No. Page No.

Ion Molecule Reactions II

E-1 * The Application of Transition State Theory to Ion-Molecule Reactions.
H. Gershinowitz---------- 159

E-2 Applications of Phase Space Theory to Polyatomic Ion-Molecule Reactions.
W. J. Chesnavich and M. T. Bowers--------- 165

E-3 The Dependence of the Lifetime of Intermediate Ion-Molecule Reaction Complexes on Internal Energy.
G. G. Meisels and F. Botz---------- 165

E-4 Reaction Intermediates and Temperature Dependence of Ion Molecule Reactions. The System: $C_2H_5^+ \cdot CH_4$.
K. Hiraoka and P. Kebarle---------- 166

E-5 Recent Ion Cluster Stability Measurements: $H_3^+(H_2)_n$, $CH_5^+(CH_4)_n$, H_3^+CO, $H(CO)_n^+$, $H(N_2)_n^+$, $Cl^-(HA)$.
K. Hiraoka, M. French and P. Kebarle------ 167

E-6 Reversible Reactions of Gaseous Ions. X The Determination of the Stability of Several Cyclic Alkyl Carbonium Ions.
J. J. Solomon and F. H. Field---------- 168

E-7 Decomposition Rates of Excited Reaction Complexes Temperature and Pressure Effects in Association Reactions Involving NH_4^+, $CH_3NH_3^+$ and $(CH_3)_2NH_2^+$.
M. Meot-Ner and F. H. Field---------- 169

E-8 Equilibrium Study of the $NO^+ \cdot N_2$ Ion Cluster.
D. L. Turner and D. C. Conway---------- 170

E-9 Biomolecular Formation of Long-Lived Complexes in Ion-Molecule Reactions.
W. N. Allen and F. W. Lampe---------- 171

E-10 The Generation of Radical Anions by Reaction of O^- Ions with Organic Substrates.
J. H. J. Dawson, A. J. Ferrer-Correia, and K. R. Jennings---------- 174

E-11 The Gas-Phase Reactivity of Disubstituted Aromatic Compounds with Ionic Acetylating Reagents.
D. A. Chatfield, T. A. Elwood, and J. H. Futrell---------- 176

*Invited Paper

Paper No. Page No.

E-12 Collision Induced Dissociation Reaction of Molecular Negative Ions CO_3^-, N_2O^-, and NO_2^-.
R. L. C. Wu and T. O. Tiernan---------- 179

Symposium on Profiling of Physiologic Fluids

F-1 Use of Mass Spectrometry for Orthomolecular Diagnosis.
A. B. Robinson, M. Weiss, W. E. Reynolds, and L. R. Robinson---------- 182

F-2 Application of High Resolution Liquid Chromatography to the Analysis of Physiologic Fluids.
J. E. Mrochek and C. D. Scott---------- 185

F-3 Gas Chromatography - Mass Spectrometry in Clinical Chemistry.
O. Stokke, E. Jellum, and L. Eldjarn---------- 186

J. L. Franklin Symposium *

G-1 Structures and Stabilities of C_4 and C_5 Hydrocarbon Ions.
F. P. Lossing and J. C. Traeger---------- 189

G-2 Proton-Transfer Reactions by Trapped-Ion Mass Spectrometry.
A. G. Harrison, P.-H. Lin, and C. W. Tsang---------- 190

G-3 Some Aspects of Negative Ion Chemistry.
E. E. Ferguson---------- 191

G-4 What is Important to Everyone in High Pressure Ion Molecule Reactions.
P. Kebarle---------- 192

G-5 Molecular Orbital Studies of the Energies and Structures of Polyatomic Cations.
J. A. Pople---------- 193

G-6 Ion Kinetic Energy Spectrometry.
J. H. Beynon and R. G. Cooks---------- 194

G-7 Carbonium Ions and Protonated Cyclopropanes.
G. M. Kramer---------- 195

* Abstracts only. Manuscripts submitted to the International Journal of Mass Spectrometry and Ion Physics.

Paper No. Page No.

Special Analytical Techniques

H-1 Comparative Experience with Computerized GC/MS Systems.
R. B. Spencer---------- 196

H-2 A Comparison of Integrative Recording Techniques for Selected Ion Recording.
S. P. Markey, R. L. Hawks, and G. W. A. Milne---------- 197

H-3 Kinetics of Polyvinyl Chloride Pyrolysis by On-line Thermogravimetric Analysis and Mass Spectrometry.
K. Voorhees, R. W. Mickelson, P. W. Ryan, D. Chatfield, I. N. Einhorn, and J. H. Futrell---------- 200

H-4 A Gas Chromatograph - Mass Spectrometer - Computer System Using High Resolution Pressure Ionization (API) Techniques.
D. I. Carroll, C. Oertli, I. Dzidic, R. N. Stillwell, and E. C. Horning-------- 203

H-5 Mass Spectrometric Gas Analysis in Steam Water.
G. L. Carlson and A. Pebler---------- 203

H-6 Determination of Concentration of Explosives in Air by Isotope Dilution.
G. A. St. John, J. H. McReynolds, and M. Anbar---------- 204

H-7 Thermal Stability of Thin Films by Modulated Beam Mass Spectrometry.
M. A. Frisch and W. Reuter---------- 207

H-8 Quantitative Analysis of Complex Samples by Computer Controlled Mass Spectrometry.
D. Schuetzle, T. J. Prater, D. E. Hagge, and R. L. Knights---------- 208

H-9 Simultaneous Ion Scattering and Secondary Ion Mass Spectrometry.
M. J. Vasile and D. L. Malm---------- 211

H-10 Identification of Bacteria by Pyrolysis Mass Spectrometry Combined with Multivariate Analysis.
H. L. C. Meuzelaar, P. G. Kistemaker and W. Eshuis---------- 212

H-10S Mass Spectrometric Determination of Water Desorbed from Solids.
G. M. Wood, B. T. Upchurch, and D. B. Hughes---------- 213

Paper No. Page No.

H-11 Use of Automatic Data Acquisition/Reduction with EI/FD Mass Spectrometry in Analysis of Crude Extracts of Biological Samples.
W. D. Jamieson and F. G. Mason---------- 222

H-12 Mass Spectral Study of a High-Boiling Saturate Fraction from Petroleum.
F. D. Guffey and J. H. Weber---------- 225

H-13 Mass Spectrometric Analysis of the Hydrocarbons-Ethers from Coal Liquids and from the Products Obtained Upon Their Hydrogenation-Hydrogenolysis.
S. E. Scheppele, G. J. Greenwood, and B. L. Crynes---------- 226

H-14 MS Analysis of Coal Liquefaction Products.
T. Aczel and H. E. Lumpkin---------- 228

H-15 Coal Gasification Studies by Field Ionization Mass Spectrometry.
E. J. Kempster, R. Schnitzer, and M. Anbar---------- 231

H-16 Analysis of Volatiles from Fresh Coal Surfaces Using High Resolution Mass Spectrometry and Computer Processing of Data.
M. C. Hamming, F. J. Radd, and A. B. Carel---------- 234

H-17 The Application of Ultra High Resolution Dynamic Scanning to the Analysis of Sulfur-Containing Petrochemicals.
H. E. Lumpkin, R. M. Elliott, S. Evans, D. Hazelby, and W. A. Wolstenholme---------- 235

H-18 Some Observations on the Application of Groups of Mass Chromatograms to the Characterization of Very Complex Unresolved Mixtures: Petroleum Oils.
W. V. Ligon, Jr. and R. L. Johnson, Jr.---------- 238

H-19 Mass Spectrometry Investigation of Catalyst Deactivation.
A. G. Sharkey, Jr., R. G. Lett, and J. L. Shultz---------- 241

H-20 Rapid Survey Analysis of Complex Environmental Samples Using High Accuracy Mass Chromatography.
T. J. Prater, D. Schuetzle, and D. E. Hagge---------- 242

Paper No. Page No.

Instrumentation II

I-1 A Modular Electronic Output System for Improved Fast-Response Time-of-Flight Mass Spectrometric Measurements.
K. A. Lincoln---------- 245

I-2 An Intracavity Dye-Laser Technique for the Study of Laser-Induced Ionic Processes.
J. R. Eyler---------- 248

I-3 Design Modifications on a Varian Atlas CH-4B Mass Spectrometer for Chemical Ionization.
R. S. Ampulski---------- 250

I-4 A Cold Cathode Sampling Orbitron Ionization Gauge.
K. M. Jackson, P. C. McLeod, and M. K. Testerman---------- 253

I-5 A Digital Mass Readout for Magnetic Sector Mass Spectrometers.
A. M. Hogg---------- 256

I-6 Dynagraph Raster Graphics Display System.
G. L. Brezler---------- 259

I-7 Voltage Coefficients of High Value Resistors.
L. F. Herzog and T. J. Eskew---------- 262

I-8 Fast Switching of Ion Accelerating Potential: Some Limitations and a New Circuit.
T. J. Eskew---------- 266

Biological and Biomedical Applications I

J-1 Pharmacokinetic Studies Using CI Mass Spectrometry.
J. Nowlin, G. Kellermann, R. M. Hill and M. G. Horning---------- 267

J-2 Pharmacokinetic Studies of Methaqualone Using Isotope Dilution Analysis and Field Ionization Mass Spectrometry.
H. d'A. Heck, J. H. McReynolds, and M. Anbar---------- 268

J-3 Mass Spectrometric Studies on Drug Metabolism Using Stable Isotopes--A New Quantifying Method.
Y. Nakagawa, K. Iwatani, S. Hashimoto, and S. Takahashi---------- 271

Paper No. Page No.

J-4 Studies of Drug Metabolism by GC-MS-Computer Methods.
W. G. Stillwell, P. Gregory, N. Booher and R. N. Stillwell---------- 274

J-5 Use of Mass Spectrometry in the Chemical Ionization Mode for the Study of in vitro Drug Metabolism.
K. R. Sommer, M. G. Horning, and J. P. Thenot---------- 274

J-6 Determination of 6-Acetyl Morphine in Biological Fluids by GC-MS-COM Techniques.
J. P. Thenot and E. C. Horning---------- 275

J-7 Application of GC-MS Techniques to Metabolism Studies on Novel Uricosuric-Saluretic Agents.
A. G. Zacchei and T. Wishousky---------- 276

J-8 Quantification of Phencyclidine (PCP) in Body Fluids and Identification of Major Metabolites.
D. C. K. Lin, R. L. Foltz, R. D. Forney, Jr., and I. Sunshine---------- 279

J-9 Determination of Ribavirin and Pyrazofurin in Serum by Gas Chromatography-Chemical Ionization-Selected Ion Monitoring Technique.
J. Roboz, R. Suzuki, M. Perloff, and T. Ohnuma---------- 280

J-10 Identification of L-DOPA Metabolites in CSF of Parkinsonian Patients by GC-MS.
S. E. Hattox and R. C. Murphy---------- 281

J-11 Identification of Metabolites of Monensin from Rats.
A. L. Donoho and J. L. Occolowitz---------- 284

Reaction Dynamics

K-1 * Kinematics of Ion-Molecule Collisions.
Z. Herman---------- 285

K-2 Crossed-beam Studies of the Reactions of Ar^+/Kr^+ with CH_4.
S. Y. Tang, R. L. C. Wu, E. G. Jones, and T. O. Tiernan---------- 292

K-3 Dynamics of the $Kr^+ + H_2$ Reaction.
S. Chivalak and P. M. Hierl---------- 293

*Invited Paper

Paper No. Page No.

K-4 Energy Disposal in Partial Charge Transfer Reactions.
C. Cole and P. M. Hierl---------- 296

K-5 Kinematics of the Reaction: $H_2O^+ + H_2 = H_3O^+ + H$.
A. J. Yencha, V. Pacak, and Z. Herman---------- 298

K-6 Crossed-Beam Studies of Charge Exchange and Elastic Scattering in Rare Gas Ion-Atom Collisions.
M. L. Vestal, C. R. Blakley, and J. H. Futrell---------- 301

K-7 A Crossed Beam Study of Proton Transfer From Hydronium Ions to Water Molecules.
P. W. Ryan, M. L. Vestal, C. R. Blakley, and J. H. Futrell---------- 303

K-8 Low Energy He^+/H_2 Interactions.
E. G. Jones, B. M. Hughes, D. G. Hopper, and T. O. Tiernan---------- 305

K-9 Kinematics of Charge Transfer $Kr^+ + CH_4$ at Low Collision Energies.
Z. Herman, V. Pacak and K. Birkinshaw---------- 306

K-10 Wavelength Dependence of the Branching Ratio for Competitive Photodissociation of Butene Cation.
M. Riggin, R. Orth, and R. C. Dunbar---------- 309

K-11 Dye-Laser Induced Photodetachment of Electrons From Gaseous SH^- Ions.
J. R. Eyler and G. H. Atkinson---------- 310

K-12 Dye Laser-Induced Photodissociation of $C_7H_8^+$ Ions in Gaseous Toluene.
J. R. Eyler---------- 313

Environmental

L-1 Application of Atmospheric Pressure Ionization to Monitoring of Organic Contaminants in Air.
D. I. Carroll, I. Dzidic, W. H. McFadden and J. R. Reeher---------- 316

L-2 Determination of Carcinogenic Pollutants in Ambient Air Using a GC- MS- Computer System.
R. C. Lao, R. S. Thomas, and J. L. Monkman---------- 320

Paper No. Page No.

L-3 Development of a Cryogenic Separator for CI Analysis of Environmental Air Samples.
H. S. Swofford, Jr., I. C. Wang, D. P. Martinsen, and S. E. Buttrill, Jr.---------- 322

L-4 The Analysis of Halocarbons in the Atmosphere by GC-MS.
E. P. Grimsrud and R. A. Rasmusson-------- 325

L-5 GC/MS Techniques, Including Interscan Display, in the Analysis of Trace Contaminants in Great Lakes Fish.
D. W. Kuehl, G. D. Veith, and G. E. Glass---------- 327

L-6 Identification of Plant Metabolites of "Vydate" Oxamyl Insecticide/Nematicide by Mass Spectrometry.
R. W. Reiser and J. Harvey, Jr.---------- 329

L-7 Negative Chemical Ionization Mass Spectrometry Screening for Environmental Contamination: Application to Human Urines.
R. C. Dougherty and K. Piotrowska--------- 332

L-8 A New Device for the Vapor Phase Transfer of Adsorbed Organics Directly from an Adsorbent to a Gas Chromatograph-Mass Spectrometer.
W. V. Ligon, Jr. and R. L. Johnson, Jr.--- 333

L-9 Characterization of Polycyclic Aromatic Hydrocarbons in Diffusion Flames by GC/MS.
P-H Lin and R. A. Hites---------- 335

L-10 Determination of Tetrachlorodibenzo-p-Dioxin in Chemical and Environmental Matrices.
M. L. Taylor, B. M. Hughes, T. O. Tiernan, R. L. C. Wu, and D. T. Terwilliger---------- 337

L-11 Development of Solid Sorbent-Mass Spectrometric Techniques for Low Level Monitoring of NO and NO_2 in Air.
C. Chang, T. O. Tiernan, B. M. Hughes, and M. L. Taylor---------- 341

Paper No. Page No.

Biological and Biomedical Applications II

M-1 Quantitative Analysis of the Major Urinary Metabolite of Prostaglandin E in Man by Selected Ion Monitoring.
B. J. Sweetman, H. W. Seyberth, J. C. Frolich and J. A. Oates---------- 343

M-2 Polyhydroxybutyric Acids Detected in Urine Extracts by GC-MS.
J. A. Thompson, P. V. Fennessey, and S. P. Markey---------- 345

M-3 Molecular Weight Profiles of Carboxylic Acids in Urine Obtained by Field Ionization Mass Spectrometry and Their Clinical Applications.
R. L. Dyer, M. E. Scolnick, R. R. Sperry, and M. Anbar---------- 347

M-4 Mass Spectrometric Characterization of Human Urinary Metabolites of Cyproheptadine.
W. J. A. VandenHeuvel, V. F. Gruber, B. H. Arison, D. C. Titus, and C. C. Porter---------- 350

M-5 Application of GC-MS in the Analysis of Volatile Compounds in Urine and Ascitic Fluid of Normal and Tumor Bearing Mice.
A. M. Lovett, E. Sherwood, J. Oro, and D. A. Flory---------- 351

Solids

N-1 The Analysis of Epitaxial Films by Spark Source Mass Spectrometry.
G. G. Sweeney and H. B. Kim---------- 354

N-2 Multi-Element Isotope Dilution Spark-Source Mass Spectrometry.
J. C. Franklin, J. A. Carter, D. L. Donohue, and R. W. Stelzner---------- 355

N-2 Evaluation of the Joyce-Loebl Automated Microdensitometer for Spark Source Mass Spectra.
M. A. Haney---------- 357

N-4 Molecular Beam Mass Spectrometric Studies of Laser Plumes Formed at Atmospheric Pressure.
F. T. Greene and G. Radolovich---------- 358

N-5 Time Resolving Mass Spectra Produced by Laser Vaporization of Solids.
E. J. Rolinski, C. J. Oblinger, and C. R. Thomas---------- 360

Paper No. Page No.

N-6 Laser Source Mass Spectroscopy of Inclusions in Solids.
K. R. Thompson---------- 362

N-7 Evaporation of Solids by Laser Pulses.
D. R. Olander---------- 363

N-8 Initial Energy Distributions of Secondary (+) Ions from the Sputtering of Non-Metallic Solids with Ar^+ (3KeV to 10KeV).
F. G. Satkiewicz---------- 365

N-9 Improvements in Quantitative Analysis of Solids by SIMS.
K. Kusao, Y. Yoshioka, N. Nakamura, and F. Konishi---------- 368

N-10 A Coaxial Cathode Gas Discharge Source for Solids Analysis.
W. A. Mattson and W. W. Harrison---------- 371

N-11 A Pulsed Mode Hollow Cathode Ion Source for Solids Analysis.
W. W. Harrison and W. A. Mattson---------- 371

Biological and Biomedical Applications II

O-1 Measurement of *In Vivo* Incorporation of Multilabeled Thymidine into DNA using Field Ionization Mass Spectrometry.
J. H. McReynolds, H. d'A. Heck, and M. Anbar---------- 372

O-2 The Quantitative Determination of Dopamine in Brain Tissue by Methane CI-MS.
M. S. Silberberg, M. E. Rennekamp, and D. V. Bowen---------- 374

O-3 Electron Impact Induced Fragmentation Pathways of Morphine and Its Derivatives.
D. K. Haegele---------- 376

O-4 Basic Mass Spectrometric Investigations of Amino Acid-Fluorescamine Derivatives.
J. J. Shieh, K. L. Leung, and D. M. Desiderio---------- 377

O-5 Ionization of Steroidal Epoxides Under Electron Impact and Chemical Ionization Conditions.
S. S. Lau and E. C. Horning---------- 378

O-6 Electron Impact, Chemical Ionization and Atmospheric Pressure Ionization Mass Spectra of the Tocopherols.
S-N. Lin and E. C. Horning---------- 378

Paper No. Page No.

O-7 Identification and Quantitation of Biogenic Phenolalkylamines in the Subpicomol Range Using a GC Coupled to a Small Double Focusing Mass Spectrometer.
M. Donike, K. H. Maurer, U. Rapp, and A. Zune---------- 379

O-8 Fragmentation of the MO-TMS Derivatives of Cortisol and Ecdysterones.
A. Hung, S. S. Lau, W. G. Stillwell, and M. G. Horning---------- 387

O-9 Mass Spectra of Dihydrodiols.
C. Butler, W. G. Stillwell, and M. G. Horning---------- 387

O-10 A Convincing Case for the Utilization of Electron Impact Mass Spectrometry for the Assignment of Configuration to Stereoisomers.
M. M. Green and J. L. Martin---------- 388

O-11 The Comparable Low Hydrogen Deuterium Isotope Effects in Intramolecular Hydrogen Transfer Rearrangement Reactions in Mass Spectrometers and in Solution: The Reason for the Low Isotope Effect of the McLafferty Rearrangement.
M. M. Green, J. M. Moldowan, J. Artus, and M. Armstrong---------- 392

Ion Molecule Reaction I

P-1 High Pressure Ion-Molecule Reactions in Fluoromethanes.
M. J. Pabst, H. S. Tan and J. L. Franklin---------- 396

P-2 Mass Spectrometric Study of Ion-Molecule Reactions in C_2H_3F and $C_2H_2F_2$.
H. S. Tan, M. J. Pabst and J. L. Franklin---------- 399

P-3 Ion Molecule Reactions in Ar Gas.
W-C.F. Liu and D. C. Conway---------- 402

P-4 Proton Abstraction Reactions in the Systems H_2O-NH_3, H_2CO-NH_3, CH_3OH-NH_3, and CH_3OH-H_2O.
Z. Karpas and F. S. Klein---------- 403

P-5 Negative Ion Molecule Reactions at Low Ion Energies.
I. Dotan (Duchovny) and F. S. Klein---------- 405

Paper No. Page No.

P-6 Endoergic Ion-Molecule-Collision of I^- and H_2O.
K. M. A. Refaey and J. L. Franklin-------- 408

P-7 Negative Ion Spectra of Some Sulphides and Some Oxides of Nitrogen.
K. M. A. Refaey---------- 411

P-8 Measurement of Thermal Electron Dissociative Attachment Rates for Halogen Gases.
G. D. Sides and T. O. Tiernan---------- 414

P-9 Dissociative Attachment and Ion Molecule Reactions in Phosphorus and Arsenic Chlorides.
J. G. Dillard, R. Pauls, and C. E. Compton---------- 415

P-10 Mass Spectrometric Sampling of the Ionic and Neutral Species Present in Different Regions of an RF Discharge in Methane.
M. J. Vasile and G. Smolinsky---------- 416

P-11 Relative Proton Affinities of Ethylene and Water.
Y-H Li and L. I. Bone---------- 417

Biological and Biomedical Applications IV

Q-1 Long Range Trimethylsilyl Group Migrations in Steroid Mass Spectra.
C. J. W. Brooks, S. J. Gaskell, and A. G. Smith---------- 418

Q-2 Selective Introduction of TMS Groups in Tryptamine: Preparation of N-TMS Derivatives of Tryptamines.
N. Narasimhachari and K. Leiner---------- 421

Q-3 IO, II-dihydroxy-protriptyline: Formation Via a Stable Epoxide Intermediate.
C. Pantarotto, G. Belvedere, R. Fanelli, V. Rovei, and A. Frigerio-------- 423

Q-4 GC/MS of Thermally Stable Sulfonylurea Derivatives.
H. C. Ashline and W. E. Braselton, Jr.---------- 424

Q-5 Precision and Accuracy in Measuring Picomole Quantities of Norepinephrine by Quadrupole-Selected Ion Monitoring.
R. C. Murphy, J. A. Zirrolli, K. Clay, S. E. Hattox, and R. Helbig--------- 427

Paper No. Page No.

Q-6 Differentiation of Endogenous N-methyl Derivatives in Serum Extracts from Artifacts Caused by N-methylation in the Injector of the Gas Chromatograph.
L. K. Wong, C. E. Costello, and K. Biemann---------- 430

Q-7 Negative Ion Mass Spectral Studies of Some Underivatized Nucleosides.
C. L. Brown and V. Hanson---------- 433

Q-8 Structural Studies on the Modified Nucleoside Q, Isolated from E.coli Transfer RNA.
H. Kasai, Z. Ohashi, F. Harada, S. Nishimura, N. J. Oppenheimer, P. F. Crain, J. G. Liehr, D. L. von Minden, and J. A. McCloskey---------- 434

Q-9 Hydrogen Rearrangement Reactions in the Mass Spectra of Nucleosides.
S. E. Hattox, K. H. Schram, and J. A. McCloskey---------- 435

Q-10 Sterically Crowded Silyl Groups as Directors of Fragmentation in the Mass Spectra of 2'-Deoxynucleosides.
J. B. Westmore, M. A. Quilliam and K. K. Ogilvie---------- 437

Q-11 The Characterization of N-Phosphonomethylglycine and its metabolite Aminomethylphosphonic Acid by GC/MS/COM and Isotopic Dilution Techniques.
M. L. Rueppel and J. T. Marvel---------- 439

Q-12 Identification of Novel Diterpenoid Alkaloids in Delphinium Ajacis by Mass Spectrometry.
G. R. Waller and R. H. Lawrence, Jr.---------- 440

Q-13 EI and FI Mass Spectra of the Fluorescamine Derivatives of Some Biologically Important Primary Amines Including Amphetamines and Amino Acids.
N. Narasimhachari, E. Kempster, and M. Anbar---------- 444

Ion Molecule Reactions III

R-1 Proton Transfer Reactions from H_3^+ Ions to N_2, O_2, and CO Molecules.
W. T. Huntress, Jr. J. K. Kim, and L. P. Theard---------- 446

Paper No. Page No.

R-2 Internal Energy Effects and Isotope Effects in Hydron Transfer Reactions to Ethane.
R. D. Smith and J. H. Futrell---------- 447

R-3 ICR Study of the Gas Phase Chemistry of Li^+, Na^+, K^+.
J. Allison and D. P. Ridge---------- 450

R-4 Temperature Dependence of Ion-Molecule Reactions Studied by ICR.
S. E. Buttrill, Jr. and G. Ringer--------- 452

R-5 Fourier Transform Ion Cyclotron Resonance Spectroscopy.
M. Comisarow and A. G. Marshall---------- 453

R-6 Charge Transfer to Hydrogen Halide and Halogen Molecules from Atomic and Diatomic Ions.
S. G. Lias---------- 456

R-7 Comparison of Energy Dependencies of Ion-Molecule Reactions.
W. Lindinger, F. C. Fehsenfeld, D. A. Albritton, A. L. Schmeltekopf, and E. E. Ferguson---------- 459

R-8 A Quantitative Investigation of the Role of Franck-Condon Factors in Charge-Transfer Reactions.
J. Gale, M. Henchman, and J. F. Paulson---------- 460

R-9 Excitation Functions from Rate Constants Measured under Non-Maxwellian Conditions.
J. Ige and M. Henchman---------- 463

R-10 Heats of Formation of Gaseous Hydrocarbon Ions.
A. Goren and B. Munson---------- 466

R-11 Proton Affinities of Inorganic Compounds.
D. Smith and B. Munson---------- 468

Isotopic Measurements

S-1 Precision and Accuracy in Isotope Ratio Determinations.
R. S. Newbury---------- 469

S-2 The Triple Filament Thermal Ionization Source (TFTIS) and High Precision Isotope Abundance Ratios.
L. J. Moore---------- 470

Paper No. Page No.

S-3 Iron Concentration in Porcine Blood and Standard Reference Material Copper Benchmarks by Isotope Dilution Mass Spectrometry.
E. L. Garner and L. P. Dunstan---------- 472

S-4 Determination of the Absolute Isotopic Abundance and Atomic Weight of Terrestrial Potassium.
E. L. Garner, T. J. Murphy, J. W. Gramlich, P. J. Paulsen, L. A. Machlan, I. L. Barnes, and S. S. Goldich-- 474

S-5 Simultaneous Detection of Uranium Isotopes.
R. E. Powell, N. R. Daly, and N. J. Freeman---------- 476

S-6 Uranium Isotope Analysis On-Site by Quadrupole Mass Spectrometry.
M. W. Siegel and F. E. Jones---------- 477

S-7 Carbon Dating Mass Spectrometry--Background Reduction Techniques.
R. Schnitzer, W. H. Aberth, and M. Anbar---------- 479

S-8 Isotope Ratios from GCMS.
D. E. Matthews and J. M. Hayes---------- 482

Computer Applications

T-1 An International Mass Spectral Search System (MSSS).
S. R. Heller, G. W. A. Milne, H. M. Fales, A. Bridy, and R. S. Heller---------- 485

T-2 A General Method for Molecular Ion Prediction.
R. G. Dromey, B. G. Buchanan, D. H. Smith, J. Lederberg, and C. Djerassi---------- 486

T-3 Automatic Identification of Mass Spectra. A Goodness of Fit Measure Derived from Hypothesis Testing.
S. L. Grotch---------- 489

T-4 A Probability Based Matching System Applicable to a Large Diverse File of Reference Mass Spectra.
F. W. McLafferty, G. M. Pesyna H. E. Dayringer, and R. Venkataraghavan--- 490

Paper No. Page No.

T-5 What is a "Factor" in the Factor Analysis of Mass Spectra.
R. W. Rozett and E. M. Petersen---------- 491

T-6 A Simple Search System for Mass Spectra.
J. F. Smith, R. J. Mathews, and
J. D. Morrison---------- 493

T-7 Applications of a GC-MS Data System Using a New Library Search System.
J. R. Chapman, K. R. Compson,
R. M. Elliott, D. Hazelby, and
G. Schackleton---------- 496

T-8 An Extension to the Role of the Dedicated Data System in GC-MS.
P. Powers, M. J. Wallington,
J. A. V. Hopkinson, and G. L.
Kearns---------- 499

T-9 Real-Time Gas Chromatography-High Resolution Mass Spectrometry and the Analysis of Complex Organic Mixtures.
B. J. Kimble, F. C. Walls, R. W.
Olsen, and A. L. Burlingame---------- 503

T-10 Instrumentation and Data Reduction for Collisional Activation Spectra.
T. Wachs, P. F. Bente,III, F. W.
McLafferty, and C. C. Van De Sande-------- 506

T-11 A Computer-controller AVA Unit for Routine Biological Assay Processing.
R. B. Spencer and R. W. Walker---------- 506

T-12 Low-Cost Computer System for Quadrupole Mass Spectrometers.
P. S. Berger, P. D. Norbert, and
W. F. Holmes---------- 507

T-13 Extension of the Mass Range for Selected Ion Monitoring by Computer Control of the Magnetic Field.
N. D. Young, J. F. Holland, J. N.
Gerber and C. C. Sweeley---------- 508

T-14 The Use of a Programmable Calculator for Mass Spectrometer Control and Data Processing.
J. L. Hayden, T. C. D. Knight,
and S. W. Smith---------- 513

T-15 Voltage Scanning of a Double Focussing Mass Spectrometer Under Computer Control.
K. B. Denson, S. P. Taylor, and
J. M. Hayes---------- 513

Paper No. Page No.

T-16 On-Line Control of High Resolution Mass Spectrometers. I. Peak Matching.
D. W. Bissett, C. Cone, and F. C. Maseles---------- 514

T-17 Sequence Determination of Oligodeoxy-Ribonucleotides by Mass Spectrometry and Computerized Pattern Recognition.
J. L. Wiebers, J. A. Shapiro, S. P. Perone, and D. R. Burgard---------- 515

T-18 UPACS - Computerized Mass Spectrometry System.
L. Baczynskyj, J. F. Zierserl, M. D. Kenny, J. B. Aldrich, and D. J. Duchamp---------- 516

Biological and Biomedical III

U-1 Plasma Amino Acid Analysis by Isotope Ratio GC/MS/Computer Techniques.
M. F. Schulman and F. P. Abramson--------- 519

U-2 Determination of ^{3}H, ^{14}C, and ^{18}O by GC-MS. Application to Sterol Metabolism.
B. S. Middleditch, M. Gut, and S. Burstein---------- 519

U-3 High Precision Isotope Ratio Measurements by CI/MS.
D. L. Hachey, P. A. Szczepanik, W. F. Bryant, and P. D. Klein---------- 520

U-4 A Procedure to Measure Total Body Water in Infants Using $H_2{}^{18}O$.
J. A. Zirrolli and R. C. Murphy---------- 523

U-5 A Comparison Between $^{14}CO_2$ and $^{13}CO_2$ Measurements in the Breath of Rats Fed Sodium Acetate.
R. S. Ampulski and R. W. Boggs---------- 526

U-6 In Vivo Measurement of Glucose Metabolism in Children with Stable Isotopically Labelled Metabolites.
D. M. Bier, K. J. Arnold, M. Haymond, L. D. Gruenke, and D. M. Kipnis---------- 529

U-7 GC/MS Analysis of Polypeptides and Proteins Containing Arginine, Lysine and Proline Using Dipeptidylaminopeptidase Mixtures.
W. F. Seifert and R. M. Caprioli---------- 531

U-8 Detection of Asparagine and Glutamine in Peptides Sequenced by Dipeptyidylaminopeptidase I Via Gas Chromatorgaphy-Mass Spectrometry.
Y. A. Young and D. M. Desiderio---------- 532

Paper No. Page No.

U-9 Identification of Oligopeptides in Mixtures by Microdistillation in a Mass Spectrometer.
R. D. Grigsby, E. J. Norman, and P. E. Pulley---------- 534

U-10 Mass Spectrometry of Some Borane-Reduced Dipeptides and the Permethylation Products.
R. M. Thompson, F. L. Weitl, and R. W. Roeske---------- 535

U-11 Chemical Ionization Mass Spectra of Derivitized Peptides.
M. Mudgett, D. V. Bowen, and F. H. Field---------- 537

Solids

V-1 Experimental Results and an Attempt at an Interpretation for Secondary Ion Emission from Targets Bombarded by a C_s^+ Ion Beam.
P. Vallerand and M. Baril---------- 539

V-2 Low Energy Ion Scattering Spectrometry (ISS) of the SiO_2/Si Interface.
W. L. Harrington, R. E. Honig, R. Williams, and A. M. Goodman---------- 542

V-3 Boron Implanted Silicon - A Comparison of SIMS Total Concentration Profiles with Electrical Measurements.
C. W. Magee, W. L. Harrington, R. E. Honig, and C. P. Wu---------- 545

V-4 Test of a Quantitative Correction Procedure for SIMS Analysis.
D. S. Simons, J. E. Baker, and C. A. Evans, Jr.---------- 548

V-5 Ion Microprobe Analysis for Niobium Hydride in Hydrogen-Embrittled Niobium.
P. Williams, C. A. Evans, Jr., M. L. Grossbeck and H. K. Birnbaum-------- 551

V-6 Positive and Negative Ion Mass Spectra of Metal Complexes of Nickel (II) with Hydrazine-S-Methyl-Dithiocarboxylate Ligands.
J. G. Dillard and C. F. Battrell---------- 552

V-7 Negative Ion Chemistry of the Molybdenum Fluorides.
D. L. Hildenbrand---------- 553

Paper No. Page No.

V-8 Application of Field Desorption Mass Spectrometry to Inorganic Chemistry.
M. Anbar and G. A. St. John---------- 554

V-9 Mass Spectra of Silver Salts.
G. D. Roberts and E. White, V---------- 557

V-10 Thermal Stability of Thin Films by Modulated Beam Mass Spectrometry.
M. A. Frisch and W. Reuter---------- 560

Chemical Ionization

W-1 Mechanisms in Methane Chemical Ionization Spectra.
B. L. Jelus and B. Munson---------- 563

W-2 Atmospheric Pressure Ionization (API) Mass Spectrometry. Relation of Sensitivity of Detection to the Ion Source Pressure.
I. Dzidic, D. I. Carroll, and E. C. Horning---------- 565

W-3 A New Hypersensitive System for Trace Gas Analysis.
N. M. Reid, J.B. French, and J.A. Buckley--- 566

W-4 Argon-Ozone-Water CIMS: A New Method for Determining the Location of Double Bonds.
D. F. Hunt, F. W. Crow and T. M. Harvey---------- 568

W-5 High Resolution CIMS: A General Method.
D. F. Hunt and W. F. Reid---------- 571

W-6 Negative Chemical Ionization Mass Spectrometry: A Potential New Method for Analyzing Mixtures of High Molecular Weight Aromatic Hydrocarbons.
D. F. Hunt, G. C. Stafford, and J. W. Russell---------- 572

W-7 Water Chemical Ionization of Lipid Materials.
S. E. Buttrill, Jr.---------- 575

W-8 Reagent Gas Cluster Ion Additions to Neutral Molecules.
H. S. Swofford, Jr., P. Price, D. P. Martinsen, and S. E. Buttrill Jr.---------- 577

W-9 Proton Localization in Chemical Ionization Fragmentation.
I. Jardine and C. Fenselau---------- 580

Paper No. Page No.

W-10 Reactions of Ammonia and Water in the Chemical Ionization Mass Spectrometry of Bifunctional Acids and Esters.
R. J. Weinkam and J. Gal---------- 582

W-11 Hydrogen Rearrangements in Esters Following Chemical Ionization.
F. M. Benoit and A. G. Harrison---------- 585

W-12 Chemical Ionization Mass Spectrometry of Compounds of Biological Interest.
M. E. Rennekamp, J. Shabanowitz, and D. V. Bowen---------- 587

W-13 Mechanistic Studies of the Decomposition of Urethane Foams Using Chemical Ionization Mass Spectrometry.
F. D. Hileman, K. J. Voorhees, L. H. Wojcik, J. H. Futrell, and I. N. Einhorn---------- 589

W-14 On-Line Hydrogen/Deuterium Exchange in Capillary Gas Chromatography/Chemical Ionization Mass Spectrometry (GC-CIMS) as a Means of Structure Analysis of Complex Mixtures.
W. J. Richter, W. Blum, and J. G. Liehr---------- 591

W-15 The Analysis of Polymer Degradation Products by Chemical Ionization Mass Spectrometry.
D. A. Chatfield, F. Hileman, K. J. Voorhees, J. H. Futrell, and I. N. Einhorn---------- 593

W-16 Surface Chemical Ionization of Arginine and Two Isobaric Tripeptides.
R. D. MacFarlane, R. Showronski, A. Hassell, and D. F. Torgerson---------- 594

W-17 Quantitiative Analysis of Fatty Acids in Biological Systems by Chemical Ionization Reconstructed Mass Chromatography.
J. D. Wander, S. M. Sabesin, L. B. Kuiken, N. W. Flynn, J. B. Ragland, and F. Petty---------- 595

W-18 Proton Transfer Mass Spectrometry of Rapidly Heated α-Amino Acids.
R. C. Pierce and L. Friedman---------- 597

W-19 Positive and Negative CIMS of N-Trifluoroacetyl-n-butyl Esters of Amino Acids.
D. F. Hunt, G. C. Stafford, and C. Devine---------- 600

Paper No. Page No.

W-20 Bacterial Fingerprinting with Isobutane Chemical Ionization Mass Spectrometry.
F. Petty, R. C. Rendtorff, R. W. Chandler, N. Flynn, and J. D. Wander------ 602

W-21 Chemical Ionization Mass Spectrometry of Penicillin.
T. L. Chang and C. F. Kuhlman---------- 603

W-22 Quantitative Determination of Glycine (and Other Amino Acids) in Subnanomole Quantities Using Chemical Ionization Mass Fragmentography.
N. W. Flynn, H. N. Tucker, S. V. Molinary, J. D. Wander, and F. Petty------ 605

W-23 Determination of Active Hydrogen in Organic Compounds Using GC/EIMS or CIMS.
C. N. McEwen and F. G. Kitson---------- 607

Metastable Ions

X-1 Absolute Unimolecular Decay Rates of Energy Selected Metastable Ions.
T. Baer, A. S. Werner and B. P. Tsai---------- 609

X-2 Field Ionization Kinetics (FIK). Decomposition and Isomerization of $C_4H_8^+$ Radical Ions.
R. P. Morgan and P. J. Derrick---------- 611

X-2S A New Method for Structure Determination of Ion-Molecule Reaction Products.
P. P. Dymerski and F. W. McLafferty------- 612

X-3 Field Ionization Kinetics Studies of Cleavage and Rearrangement Reactions in Ketones and Alcohols.
D. G. Patterson, R. B. Scott, and P. Brown---------- 613

X-4 Unimolecular Decomposition of Metastable Ions Over an Extended Time of 10^{-6}-10^{-3} sec.
R. D. Smith and J. H. Futrell---------- 614

X-5 Simultaneous Observation of First and Second Field Free Region Metastable Processes in an Instrument of Reversed Nier-Johnson Geometry.
W. V. Ligon, Jr. and J. L. Webb---------- 616

X-6 The Observation of Metastable Transitions in a Double Focussing Mass Spectrometer Using a Linked Scan of Accelerating Voltage and Electric Sector Voltage.
A. F. Weston, K. R. Jennings, R. M. Elliott, and S. Evans---------- 617

Paper No. Page No.

X-7 Energy Partitioning and Ring Size in Cyclic Transition States.
R. G. Cooks, R. W. Kondrat, and J. H. Beynon---------- 619

X-8 Metastable Transition Analysis.
E. J. Gallegos---------- 620

Organic Applications

Y-1 The Structures of Fragmenting $C_2H_4O^{+\cdot}$ Ions.
J. K. Terlouw and J. L. Holmes---------- 628

Y-2 The Energetics and Metastable Characteristics of Fragmenting $C_3H_6^{+\cdot}$ Ions.
J. L. Holmes, G. M. Weese, and J. K. Terlouw---------- 630

Y-3 The Effect of Ortho-and 2,6-Substitution Patterns on the Loss of NO· from Substituted Nitrobenzenes.
M. K. Hoffman and M. D. Friesen---------- 632

Y-4 Semiempirical Molecular Orbital Calculations Used to Study Substituent Effects.
G. H. Loew, R. F. Kirchner, and J. G. Lawless---------- 632

Y-5 Some Aspects of the Ionic Chemistry of C_6H_6.
M. L. Gross, S. B. Bronczyk, R. Aerni, D. H. Russell, G. A. Gallup, and D. Steinheider---------- 633

Y-6 Chlorine and Bromine Kinetic Isotope Effects from Isotope-Ratio Mass Spectrometry.
J. W. Taylor, D. G. Graczyk, J. F. Willey, and R. L. Julian---------- 635

Y-7 Mass Fragmentographic Studies of Sulfur Compounds: Some 1-(5-Ethyl-2-thienyl)-1-thiaalkanes.
P. Chandrasurin, N. G. Foster, and R. W. Higgins---------- 636

Y-8 TGA-MS-Computer Analysis of Polyphosphazene Composites.
M. L. Bazinet, W. G. Yeomans, and C. Merritt, Jr.---------- 638

Y-9 The Mass Spectra of an Amide and Some Thioamide.
R. I. Reed and R. Borhani---------- 641

Paper No. Page No.

Y-10 Topological Studies by Bifunctional Interactions in Mass Spectrometry.
S. Najm, G. Wolff, G. Teller, and R. E. Wolff---------- 644

Y-10S Field Desorption Studies on Peptides and Peptide Antibiotics on an MS902 Spectrometer.
H. R. Morris, K. E. Batley, and E. C. Barton---------- 645

Y-11 Organic Ion Structures from Collisional Activation Spectra.
B. Van De Graaf, P. P. Dymerski, C. C. Van De Sande, T. Nishishita, N. M. M. Nibbering, and F. W. McLafferty---------- 647

Y-12 Interpretation of the Mass Spectrum of an Ornithine-Containing Lipid.
M. L. Gross, D. R. Hilker, H. W. Knoche, and J. M. Shively---------- 648

Y-13 Mass Spectrometry of Cyclopropyl alkyl Benzenes.
T. H. Kinstle and S. Andrewson---------- 650

Y-14 New Reference Compounds for M/E Above 1000.
R. King and K. B. Baucom---------- 651

Y-15 Ionization and Fragmentation of Some Sulfoxides and Sulfones Induced by Electron Impact.
R. W. Kiser---------- 652

Y-16 Studies on the Proteins Ribitol Dehydrogenase, Chloramphenicol Transacetylase, Dihydrofolate Reductase, Azurin and Prothrombin by Mixture Analysis Mass Spectrometry.
H. R. Morris, A. Dell, and K. E. Batley---------- 655

Special Techniques

Z-1 Analytical Applications of Photodissociation Spectroscopy.
R. C. Dunbar---------- 658

Z-2 Particulate Impact Mass Spectrometry.
F. T. Greene---------- 659

Z-3 Preparative Mass Spectrometry.
R. G. Cooks and B. H. Solka---------- 660

Paper No. Page No.

Z-4 The Kinetics of Radiolytic Gas Phase Reactions by Modulated Molecular Beam Mass Spectrometry.
V. R. Kruger and D. R. Olander---------- 661

Z-5 Analysis of μg/kg (ppb) Level Hydrocarbons in Intertidal Zone Sediments and Water by Gas Chromatography-Mass Spectrometry.
H. S. Hertz, W. E. May, S. N. Chesler, and B. H. Gump---------- 663

Z-6 Measurement of Reactive Species in Low Temperature Combustion
J. R. Wyatt, J. J. DeCorpo and F. E. Saalfeld---------- 666

OXYGEN AS A REAGENT GAS FOR THE ANALYSIS OF 2,3,7,8-TETRA-CHLORO-p-DIOXIN (TCDD) BY NEGATIVE ION CHEMICAL IONIZATION MASS SPECTROMETRY

T. Michael Harvey
Research Triangle Institute
P. O. Box 12194
Research Triangle Park, N. C. 27709

and

Donald F. Hunt and John W. Russell
Department of Chemistry
University of Virginia
Charlottesville, Virginia 22901

In this report we describe a convenient low resolution negative CIMS technique for TCDD analysis which is at least 25 times more sensitive than the presently used procedure involving EI high resolution MS coupled to a CAT. Single ion monitoring on a 2 pg solid-probe sample of TCDD by the NCIMS method affords a signal to noise ratio >50:1 on the MS-902. When oxygen at 1 torr is used as a reagent gas in our Townsend electric discharge source, TCDD affords a NCI spectrum containing an abundant ion at m/e 176 ($M^- + O_2$-$C_6H_2ClO_2$). This ion, which presumably results from attachment of O_2 to M^- followed by cleavage of the ether linkages in TCDD, is characteristic of structure, carries 80% of the sample ion current, and is well out of the mass range containing ions due to contaminating chlorocarbons such as the PCBs DDT and DDE. When TCDD was analyzed by this technique in the presence of a ten-fold quantity of DDE, DDT and Arachlor 1254, no interfering ions were encountered and the observed signal to noise ratio was >20:1.

THE MONITORING OF POLY(VINYL CHLORIDE) DECOMPOSITION PRODUCTS VIA GC/MASS FRAGMENTOGRAPHY

Joseph W. Lewis
Research & Development Department
Union Carbide Corporation
Bound Brook, New Jersey 08805

INTRODUCTION

PVC was first prepared in the laboratory by free radical polymerization by E. Baumann, (Ann., 163, 312) in 1872. It is the second largest tonnage of plastics in the world, second only to Polyethylene. PVC may be produced by the processes shown in Table I. Many PVC resins are made by the suspension process. Each process leaves its own characteristic residuals in the polymer. The decomposition of Poly(vinyl chloride) (PVC) has been under investigation for over a quarter of a century. Intensive research is currently being carried out in many laboratories around the world due to health hazard concern. Madorsky and co-workers at NBS were the early workers to employ mass spectrometry as an instrumental tool to study products of decomposition.

More recently, excellent research has been achieved by Boettner, Ball and Weiss[1] in characterizing the volatile degradation products from PVC homopolymer, VC/VA copolymer, wire insulating resins and PVC floor tile resin. These studies were unique. The environment for decomposition was air and IR and GC/MS were used to qualitatively and quantitatively determine the volatile products of decomposition over the 280°C-580°C temperature range. They indicated the presence of vinyl chloride from 280°-510°C and a maxima of VCM between 280°-350°C from homopolymer. No mention of the amount of residual monomer is made. Very little VCM is observed up to 280°C therefore it is inferred that VCM is produced. In addition, they conclude that the amount of vinyl chloride is five times greater in the formulated resins than in homopolymer when degraded from 200°-600°C at 3°C/min. However, acetaldehyde may be a contributing factor, since it elutes with VCM.

Druesedow and Gibbs[2] observed a marked catalytic effect of HCl on PVC degradation in air but not in nitrogen. Chait and Beimer[3] coupled a TGA to a GC/MS and report vinyl chloride produced in greater abundance with helium environment than in air. This seems inconsistent with the findings of Druesedow and Gibbs who have shown that evolution of HCl is more rapid in O_2 and air than in nitrogen. If during a heat test, carried out in air a nitrogen stream is introduced, the rapid liberation of HCl diminishes. HCl is twice as autocatalytic in the presence of stationary air as in dynamic air environment.

ION MONITORING

The degradation instrumentation consists of a Pyrolysis unit, Figure 1, connected to a controlled atmosphere chamber which is interfaced with a GC/MS System (Quadrupole Filter). A data system permits real time ion output and multiple ion monitoring. The chromatographic column initially was a 6 ft. Porapak QS with 6-inch fore-column of NaOH on Chromosorb, at 175°C. We later substituted a 6 ft. Carbowax 1500 on Carbopak A operated at 90°C. The resin was a Poly(vinyl chloride) homopolymer made by the suspension process at 60°C. The M_w=60,000, M_n=36,000 and had a V_I=1.0. It is an atactic polymer with a residual monomer content <0.5 PPM.

Thermogravimetric Analysis was employed and the weight loss curves determined at rates of 10°C/min and 40°C. At 10°C/min a weight loss of 10% was observed at 290°C while at 40°C/min the temperature was slightly greater than 300°C. The weight loss curves indicated very slight decomposition in the fabricating range for vinyls of 175°C-225°C, in Figure 2. GC/MS was employed at temperatures of 175°C and 225°C. In air we observed HCl and benzene and a number of aromatics and aliphatics. The sample residue after thermal treatment was severely discolored. We gathered complete mass spectra rather than ion monitoring and observed no vinyl chloride.

As mounting interest in low levels of vinyl chloride was evidenced, we turned to multiple ion monitoring (MID) or mass fragmentography. Low level standards of vinyl chloride in THF may be prepared whereby nanograms/microliter may be injected and ion monitored. Although 105 picograms can be detected we utilized a 1.0 µl of 1.05 PPM VCM in THF or 1.0 ng of VCM as a lower limit of detection. Milligram samples of PVC homopolymer were held at 175°C, 225°C, 350°C and 500°C in air and helium for 120 seconds and the degradation products transferred to the GC/MS. Ions were monitored for vinyl chloride and the ppm of VC plotted against temperature as shown in Figure 3. PVC degraded in air at a heating rate of 1000°C/sec. reaches a maxima at 35 PPM vinyl chloride at 350°C. The sample is quite dark after treatment at 350°C in air. Degradation of homopolymer in helium produces a maxima at 6 PPM of vinyl chloride at 500°C. At the temperatures of fabrication 175°C-225°C the level of vinyl chloride is approximately 1 PPM.

REFERENCES

1. E. A. Boettner, G. Ball and B. Weiss, J. App. Poly. Sci., Vol. 13, 377 (1969).

2. R. G. Beimer and E. M. Chait, 22nd Annual Conference on Mass Spectrometry and Allied Topics, 344 (1974).

3. D. Druesedow and C. F. Gibbs, Natn. Bur. Stand. Circular 525, p. 69 (1953).

Process	Particle Size	Rel.Visc. Mol. Wt.	VCM (PPM)
Suspension	50-150 μm	1.6-3.1	200-1000
Emulsion (Dispersion)	0.5-2.0 μm	2.0-3.1	< 1.0
Bulk (non-solvent)	70-125 μm	1.7-3.0	<20
Solvent (Solution)	60-800 μm	1.3-2.0	<10

TABLE 1. Methods for preparing PVC and properties.

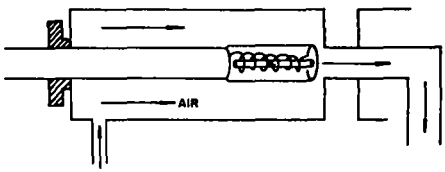

FIGURE 1. Pyrolysis Chamber - Coil Probe and Sample in Capillary.

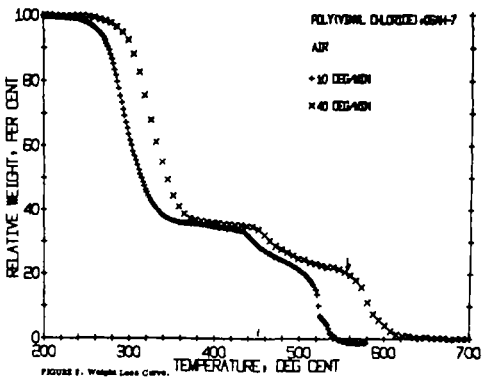

FIGURE 2. Weight Loss Curve.

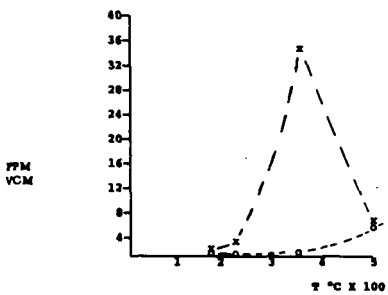

FIGURE 3. Evolution of Vinyl Chloride vs. Temp.

A-3

Survey Analysis for Trace Elements. Charles E. Taylor, Southeast Environmental Research Laboratory, Environmental Protection Agency, Athens, Georgia. 30601.

The spark source mass spectrometer will take an increased respected role as a complete survey method for trace elements in materials that affect or are of our existing environment. Spark source mass spectrometry methods have been successfully applied to a variety of samples.

The survey capabilities of SSMS are compared with other instrumental techniques. Spark source mass spectrometry analyses will routinely supply data on more elements in a single run than most other techniques available.

A-4

GC-MS (EI-CI) Examination of Fish & Bird Extracts for Toxaphene, and Other Organic Contaminants in Fish.
D. L. Stalling and J. W. Hogan, U.S.D.I., FWS, Columbia, Mo. 65201 and C. Shew, EPA, Ada, Oklahoma 74820.

Environmental toxaphene analysis can be enhanced by chemical ionization (CI) GC-MS. Several hundred components which compose toxaphene are poorly resolved by GC. Electron impact (EI)-MS produces spectra with few molecular ions, and a large complex of other ion fragments. $M-Cl^+$ ions are predominant in CI-MS spectra. Extracts of brook trout, channel catfish, and redwing blackbrids exposed chronically to toxaphene, and a carp collected from the Yazoo River, were examined by CI-GC-MS. Silicic acid proved superior for separation of PCBs from toxaphene. Fatty acid methyl esters, not removed by Florisil, precluded concentration of the extracts for CI-GC-MS. GPC effectively removed these esters from the extracts. Comparison of reconstructed gas chromatograms (RGCs) derived from $M-Cl^+$ ion intensities, revealed little difference between toxaphene and its residues in fish. Significant differences were apparent between the bird residues and toxaphene. We suggest that birds dehydrohalogenate toxaphene at these RGCs were similar to RGCs of chemically reduced toxaphene.[1]

[1]Holmstead, P.L., et al., J. Agri. Food Chem. 22:939 (1974).

The Application of Selected Ion Monitoring to Organic Pollutant Analysis*

William L. Budde and James W. Eichelberger
U. S. Environmental Protection Agency
Environmental Monitoring and Support Laboratory
Cincinnati, Ohio 45268

Abstract

Selected Ion Monitoring is defined as the dedication of a mass spectrometer to the acquisition of ion abundance data at only selected ionic masses in real time. This application is in contrast to conventional operations in which a regular sequence of ion abundances is measured to generate a mass spectrum. The development of the digital computer controlled quadrupole mass spectrometer opened the possibility of much more extensive application of selected ion monitoring. With the computerized quadrupole most of the inherent limitations that exist with other types of spectrometers were eliminated. In environmental studies there are a large number of potential applications for selected ion monitoring. Some of those to be discussed include the analysis of chlorinated solvents in drinking water, the identification of PCB's in the presence of chlorinated hydrocarbon pesticides, and the measurement of polycyclic aromatic hydrocarbons in waste samples.

---

*The full text of this paper will appear in the forthcoming EPA GC/MS procedural manual for environmental measurements.

A-6

Computerized GC/EIMS Used to Monitor Herbicide Clean-up of Contaminated Pond. B. F. Dudenbostel, Jr. and David N. Speis, U.S. EPA, Region II, Edison, NJ 08817.

Computerized GC/EIMS was used to monitor well water (drinking supplies) and the clean-up of a small lake following careless and excessive use of a herbicide to kill weeds. Twenty-five gallons of DNBP (2,4 dinitro - 6 - sec butyl phenol) were used full strength. Rain washed the herbicide into the lake and caused a large scale fish-kill. Fear of contamination of nearby drinking water supplies led to the use of a special mobile (50 ton) filtering unit to remove the DNBP from the lake. The well water supplies were found to contain less than 0.1 μg/l of DNBP (min. detect. level) by computerized GC/EIMS. This technique was used to monitor the filtration until safe levels were achieved in the lake. Bioassays were also carried out.

A-7

GC/MS Analysis of New Orleans Drinking Water. Mike H. Carter, A. W. Garrison, L. H. Keith, J. M. McGuire, and J. D. Pope. Anal. Chem. Bran., SERL, EPA, Athens, Georgia 30601

Samples from the drinking water supply of the City of New Orleans were analyzed for trace organic pollutants. Sixty-three compounds in a concentration range of four parts per trillion to five parts per billion were identified. The identifications were made using GC/low resolution EI-MS, GC/low resolution CI-MS, and GC/high resolution Ei-MS.

The use of computer mass spectral matching programs resulted in the identification of approximately 40% of the GC peaks.

New Procedures for the Analysis of Volatile Organics by Gas Chromatography-Mass Spectrometry*

James W. Eichelberger and William L. Budde

U. S. Environmental Protection Agency
Environmental Monitoring and Support Laboratory
Cincinnati, Ohio 45268

Abstract

The first sample work-up methods used with GC/MS in organic water pollutant analysis were minor modifications of standard solvent extraction procedures that were developed for pesticide analyses. These procedures are very effective for compounds that are readily separated from the solvent by gas chromatography. However, there are a large number of pollutants that are too volatile for liquid-liquid extraction because they are either lost during concentration of the solvent extract or they cannot be separated from the solvent during chromatography. New procedures that will be discussed were developed to concentrate, identify, and measure this class of pollutants. The procedures include direct aqueous injection, entrainment with an inert gas and trapping, pre-distillation, and extraction with a heavy solvent.

---

*The full text of this paper will appear in the forthcoming EPA GC/MS procedural manual for environmental measurements.

APPLICATIONS OF PYROLYSIS/GC/MS IN THE ANALYSIS OF ORGANIC NITRO COMPOUNDS

C. Merritt, Jr.

US Army Natick Laboratories, Natick, Massachusetts 01760

Pyrolysis has become a very useful adjunct technique to gas chromatography and mass spectrometry in the study of environmental problems. At the ASMS Meeting in Atlanta we described its use as an analytical tool and at the last symposium on environmental studies, held at the ASMS Meeting in San Francisco, we showed how it may be used to simulate incineration or other thermal degradation processes on a micro scale.

Munitions wastes, constitute one of the major pollution problems in certain areas of the United States and the efforts to abate this pollution have resulted in the need for special methods to separate, detect and determine aromatic nitro compounds. Pyrolysis/gc/ms has been used extensively in these studies.

The combined pyrolysis/gc/ms analysis system has been described previously[1]. The system is designed to provide the means for carrying out a wide variety of pyrolysis studies using various types of pyrolyzers and under varying conditions of time, temperature, atmospheric environment, and physical state of the sample. The pyrolysis products are separated by the gas chromatograph and the individual components identified by mass spectrometry.

Preliminary results in pollution abatement studies suggest that some very useful insights may be obtained about processes that may be adapted for pollution control. One of the main problems of concern is disposal of munition wastes, and this in turn leads to a consideration of incineration processes. It is simple enough to solve the water pollution problem by separating the contaminants from the water by absorption or extraction, or any other suitable process. The problem remains, however, of how to dispose of the separated concentrate, and the usual approach is to convert the water pollution problem to an air pollution problem by burning the wastes. Since munitions are generally nitro compounds of some type, simple combustion, or even thermolytic degradation in inert atmospheres, yields oxides of nitrogen which are undesirable gases to evolve into the atmosphere. Consideration of the problem led to the idea that pyrolysis in a reducing atmosphere might yield more innocuous products and it seemed desirable to study these reactions on a microgram scale in a pyrolysis/gs/ms apparatus where the explosion hazards are minimized, and the reaction products readily determined.

In one method of treatment of water wastes the components are absorbed on charcoal - The question then arises as to the feasibility of thermal regeneration of the charcoal. Micro simulation has proven particularly useful in this study.

In the studies of TNT pyrolysis behavior, TNT was found to be thermally very stable. Although TNT is readily detonated by mechanical shock, it can be heated on the solids pyrolyzer to about 700-800°C without apparent decomposition.

In the vapor phase pyrolyzer after distilling it from the wire at 250°, no decomposition of TNT was observed up to ca. 450°C. At 600°C,

in the vapor phase pyrolyzer, the gc eluate shows the presence of several decomposition products, such as NO, CO_2, HCN, ØH, $ØCH_3$ and $ØNO_2$.

These experiments lead to the conclusion that TNT could indeed be distilled from the charcoal. A solid sample of TNT confirmed the vapor phase pyrolysis data in that no breakdown products are observed until the temperature is well above 600-700°C. No volatile compounds are produced when heating charcoal alone up to 1000°C. When absorbed on charcoal however, the TNT is totally decomposed to CO_2 and N_2. It appears that with rapid heating in bulk, TNT decomposes into several products, but that when heated slowly on the surface of charcoal only CO_2 and N_2 are obtained.

The results with TNT encouraged us to study other munitions such as RDX and HMX. These results are summarized below:

TNT	$\longrightarrow$ NO, NO_2, CO, CO_2, C_2H_2, HCN,	
	+C$\longrightarrow$ N_2,CO_2	
RDX	$\longrightarrow$ N_2O, NO, CO_2, HCN, C_2, HCN, C_2N_2,	imidazoles
	+C$\longrightarrow$ N_2O, NO, CO_2 (triazine)	
HMX	$\longrightarrow$ N_2O, NO, CO_2, HCN, C_2N_2, CH_3CN,	imidazole
	+ $\longrightarrow$ N_2O, NO, CO_2	

The compounds obtained from bulk pyrolysis are compared with those obtained when the munition is heated slowly on charcoal. In general, only N_2O, NO and CO_2 are the products when decomposition of RDX and HMX takes place on charcoal.

Among the various approaches to abatement of munitions wastes is microbial degradation - An important series of compounds obtained in this work is the nitrotoluidines for which a method is needed to determine the individual components. Some of the compounds encountered are seen in Figure 1.

The problem with this type of analysis is the ability to distinguish among the various isomers. Using pyrolysis techniques different pyrograms may be obtained which definitely characterize each of these isomers. Although the mass spectra of these compounds are not identical, in many cases they are quite similar and in nearly all cases identification depends on peak intensity differences which vary considerably with ion source conditions and other instrument parameters. In the case of pyrolysis, frequently, unique compounds are obtained which can be related specifically to the parent compound. Typical pyrograms are seen in Figure 2.

In these studies, pyrolysis/gc/ms continues to provide a very important diagnostic tool in the study of aromatic nitro compounds and we expect it to continue in the future to be a useful adjunct in all our studies involving mass spectrometry.

Reference:1.Proceedings 21st Annual Conference ASMS, San Francisco, 1973, p320.

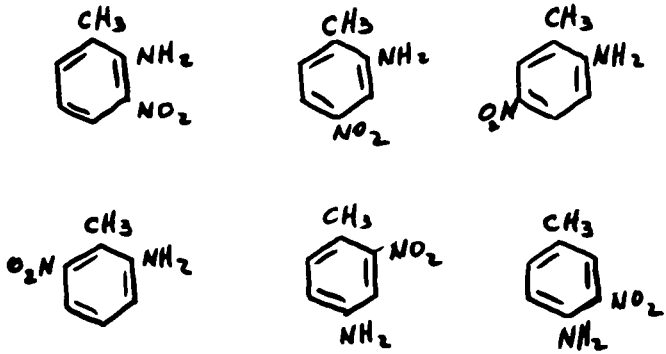

Figure 1

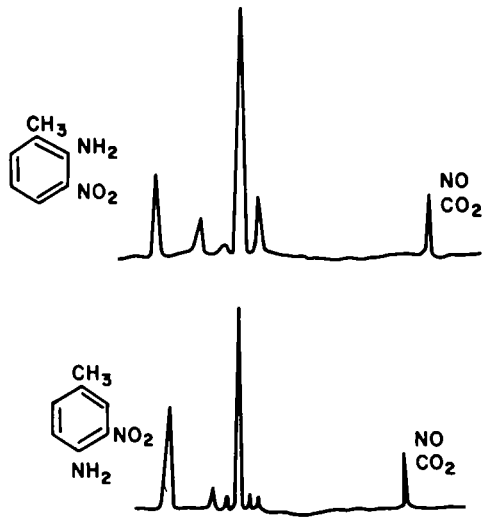

Figure 2

The Identification of Organic Contaminants in Water.

F. E. SAALFELD and R. A. SAUNDERS, Physical Chemistry Branch, Naval Research Laboratory, Washington, D. C. 20375

Analysis of the organic contaminants in water samples obtained from various sources (such as the District of Columbia; Potomac, James, and Merrimack Rivers; and rain water) have been carried out. The methods used to abstract the contaminants from the water samples (counter current helium purging and solvent extraction) were described. The concentrated organic contaminant mixture were analyzed with a gas chromatograph-mass spectrometer system. Some of the notable features of each of the above water samples were reported. The data, which will be reported in J. Biomedical Mass Spectrometry, showed more than 30 organic contaminants in each water sample.

APPLICATIONS OF FIELD DESORPTION AND FIELD IONIZATION MASS SPECTROMETRY TO ENVIRONMENTAL ANALYSIS. James F. Ryan, Robert L. Harless and Robert G. Lewis, Environmental Protection Agency, Pesticides and Toxic Substances Effects Laboratory, Research Triangle Park North Carolina, 27711.

The past several years have witnessed the advent of a new and exciting technique called field desorption mass spectrometry (FDMS), as well as a renewal of widespread interest in field ionization mass spectrometry (FIMS). Each of the above offers unique possibilities for the analysis of environmental toxicants, many of which cannot be examined using traditional electron ionization methods. Damico, Barron and Sphon(1) have previously examined the field ionization mass spectra of several chlorinated pesticides, while Becky and Schulten(2) have obtained the field desorption spectra of similar materials.

Figure 1 presents the field desorption mass spectra of cacodyllic acid, one of the arsenical pesticides. While metal identity is relatively easy to determine using such techniques as atomic absorption or even spark source mass spectrometry, these pesticides can be very difficult to analyze for chemical structure. In contrast to this, the field desorption spectrum exhibits abundant structural infromation in the form of a $(M+1)^+$ ion at m/e 139, a molecular ion at m/e 138 and an $(M-17)^+$, indicating the probable presence of a hydroxyl group, at m/e 121.

While field desorption, which produces intense molecular ions, can be very useful in the analysis of individual chemical compounds, mixtures are often difficult to analyze. However, by first chromatgographically separating the mixture into components, and then introducing each component to a field ionization mass spectrometer source, one can obtain spectra which will permit successful analysis of complex mixtures. Of course one of the drawbacks to a GC-FIMS system is that each component must have sufficient volatility to be chromatographed. Figure 2 presents the total ion current trace of a mixture of ten chlorinated pesticides which were introduced to a GC-FIMS system. As shown, even geometric isomers are resolved and can be identified, an important point since toxicity often depends on functional group position.

Figure 3 presents the mass spectrum associated with the fifth peak in the total ion current chromatogram. Even though the GC effluent peak is symmetrical, there appear two chlorine isotope clusters in the associated field ionization mass spectrum, one of which can be assigned to the molecular ion of dieldrin (m/e 378), and one to the molecular ion of p,p' DDE (m/e 316). By using a field ionization technique which produces predominantly molecular ions, one is able to resolve the identities of two pesticides which elute simultaneously.

Thus, field desorption is a unique and valuable complement to electron ionization and chemical ionization mass spectrometry in the analysis of relatively simple mixtures and pure compounds. For complex mixtures, the combination of a gas chromatograph and a field ionization mass spectrometer produces simple mass spectra, providing molecular weight information, and total ion current chromatograms, providing GC retention time indicies.

REFERENCES

1. J.N. Damico, R.P. Barron and J.A. Sphon, Int'l J. Mass Spectrom. and Ion Physics, 2, 161 (1969).

2. H.R. Schulten and H.D. Becky, J. Agr. and Food Chem., 21, 489 (1973).

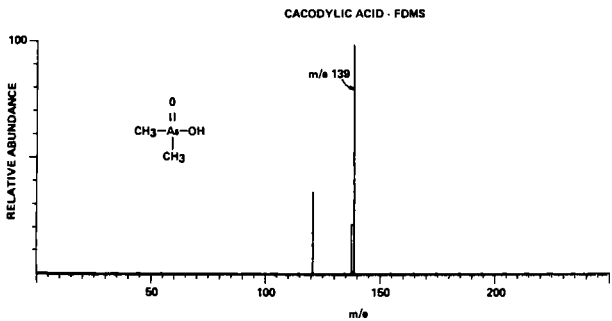

Figure 1. Field desorption mass spectrum of cacodyllic acid.

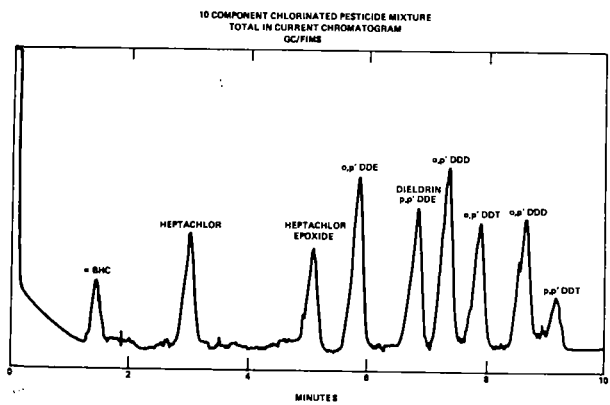

Figure 2. GC-FIMS total ion current chromatogram of ten component chlorinated pesticide mixture.

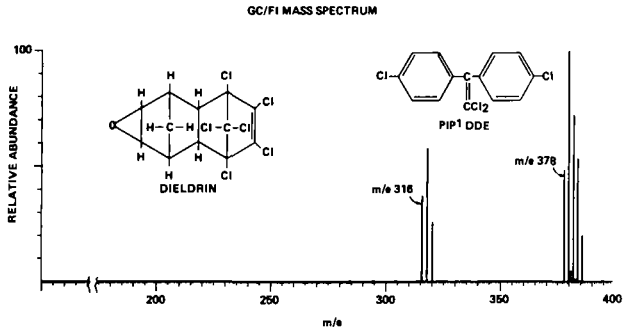

Figure 3. GC-FI mass spectrum of fifth eluting peak in Figure 2 total ion current chromatogram.

Positive and Negative Chemical Ionization Mass Spectra of Some Pyrethrins, Carbamates, and Organophosphorous Compounds.

Donald F. Hunt and Steven J. Stout, Department of Chemistry, University of Virginia, Charlottesville, VA 22901.

As part of a continuing effort to develop the analytical potential of CIMS we have studied the gas phase positive and negative ion-molecule chemistry of several pyrethrins, carbamates, and organophorous compounds. In this paper positive CI spectra recorded with methane, isobutane, and ammonia as reagent gases will be presented. Use of a Townsend discharge ion source to generate high sensitivity negative CI spectra with hydrogen and oxygen as reagents will also be discussed. Under CI conditions it is possible for the spectroscopist to devise ion-molecule reactions to suite the needs of the analytical problem at hand. Both the nature and extent of sample fragmentation, and therefore the structural information obtained, can be controlled by varying either the energy or type of ion molecule reaction employed.

Recent Advances in Field Desorption Mass Spectrometry

H.-R. Schulten and H.D. Beckey
University of Bonn, Institute of Physical Chemistry, 53 Bonn, Wegelerstr. 12, West-Germany

In Field Desorption (FD) Mass Spectrometry (MS) rapid progress has been achieved in two main areas of research:

1. Improvements of the method

1.1 Sensitivity

The sensitivity of various compounds has been measured with a single focusing mass spectrometer Varian MAT CH4 (modified as described in ref. (1)). At a m.s. entrance slit width of 0.1 mm and exit slit width of 0.2 mm the resolution was $M/\Delta M \simeq 350$. For cholesterol, which is often used as a standard for sensitivity tests in EI and FD mass spectrometry the following data were obtained. The $M^{+\cdot}$ and $(M+H)^+$ peaks were scanned repetitively until the sample was almost completely field desorbed from the emitter. Using the syringe technique (1) the sensitivity (in Coulomb/microgram of the sample loaded on the emitter) was 3.6×10^{-12} C/µg. Further a modified syringe technique (1,2) was applied. Using these somewhat sophisticated techniques the obtained increase in sensitivity was equivalent to about a factor of 100 (5×10^{-10} C/µg). The formula for the sensitivity S used here was:

$$S = \frac{\int_0^t U dt}{R \cdot A \cdot \text{Molarity} \cdot \mu l \cdot M} \; (C/\mu g),$$

where U is the voltage of the multiplier exit, t = time until the sample is almost completely desorbed (sec), R = output resistence of the multiplier (Ω), A = amplification factor of the multiplier, µl = the volume of solution deposited on the emitter, M = molecular weight. The sample was dissolved in a 1:100 mixture of CH_3OH/H_2O. The lowest concentration that gave useful FD spectra is about 10^{-8} M, the lowest sample amount for measurement of the $M^{+\cdot}$ and $(M+1)^+$ peaks lies at present in the range of 10^{-11} g at a signal/noise ratio of 3:1.

1.2 Reproducibility

The strongest influence on the quality of the FD spectra has the emitter quality. Therefore their emission properties should be checked prior to the FD experiments in the FI mode. A multiple activation apparatus should be used to produce emitters uniform in morphology (as shown in ref. 3) and with standard needle length (~30 µm). It appears that a salient parameter for the temperature in the emission centers is the average length of the carbon needles. An investigation on the correlation between emitter heating current and the emitter temperature in field desorption mass spectrometry has been performed (4). Calibration curves have been established that give an estimate of the temperature in the emission region of high temperature activated field desorption emitters. Two characteristic types of field anodes have been investigated: 1. Emitter wires carrying microneedles of 25-30 µm length, preferentially used for field desorption of organic compounds. 2. Emitters with microneedles of 50-60 µm length that are

used for the investigation of polymers by pyrolysis field desorption mass spectrometry. Further a total emission controlled time/temperature program for desorption is advantageous. As shown in Fig. 1 a thermogram of the sample can be recorded that gives information about the best anode temperature, enables a thermally gentle ionization for molecular weight determination (low emission threshold) or a pyrolysis field desorption to be performed. Prior to the evaluation of the obtained FD spectrum this thermogram gives a hint about the polarity of the sample molecules and an estimate about the amount of sample consumed in one FD measurement (plateau). In addition a plurality of steps in the thermogram serves for the diagnosis of mixtures that contain components in a wide polarity range, e.g. aerosols (5). A schematic drawing of the device for the controlled desorption program is shown in Fig. 2 (6).

2. Analytical Aspects

2.1 Organic and Inorganic Salts

The process of cluster formation has been discussed (7), e.g. for organic sulphonates, phosphates and glucuronides and for inorganic salts, e.g. alkali-halides, -nitrates, -azides and onium complexes. The results seem to suggest a whole range of new mass spectrometric applications in inorganic chemistry (8).

The parameters for cationization in FI and FD and the importance of this process for the production of kinetically and energetically favoured even electron ions was delineated. The fragmentation of the polar molecules resulting from a cationization by for instance alkali ions, has a higher activation energy than splitting off functional groups after a protonation. Cationization is therefore an interesting tool for the determination of molecular weights (9).

2.2 Mixtures

Complex mixtures of amino acids, peptides, pesticides, dye stuffs and other commercially available, technical products give with FD-MS remarkably simple and relatively easy identifiable spectra. Fractioned desorption is particularly useful with integrating recording systems such as the photoplate.

2.3 Macromolecules

Bio- and technical polymers (e.g. DNA, RNA; polyethylene) and high molecular weight environmental chemicals (e.g. chloroparaffins) give significant fingerprint spectra with Pyrolysis-FD-MS. The prospects for a correlation between the obtained spectra and the structure of these polymers were outlined.

References:

(1) H.D. Beckey and H.-R. Schulten, Angew. Chem. 87, 425 (1975) Angew. Chem., internat. Edit., 14, 403 (1975).

(2) B. Linden, H.U. Winkler and H.D. Beckey, to be published.

(3) H.-R. Schulten and H.D. Beckey, Org. Mass Spectrom. 6, 885 (1972).

(4) D. Kümmler and H.-R. Schulten, Org. Mass Spectrom., in press.

(5) H.-R. Schulten and U. Schurath, Atmos. Env., in press.

(6) H.-R. Schulten and N.M.M. Nibbering, Biomed. Mass Spec-

trom., submitted.

(7) H.-R. Schulten and F.W. Röllgen, Org. Mass Spectrom. 10, 649 (1975).

(8) H.-R. Schulten and F.W. Röllgen, Angew. Chem., August '75.

(9) F.W. Röllgen and H.-R. Schulten, Org. Mass Spectrom. 10, 660 (1975).

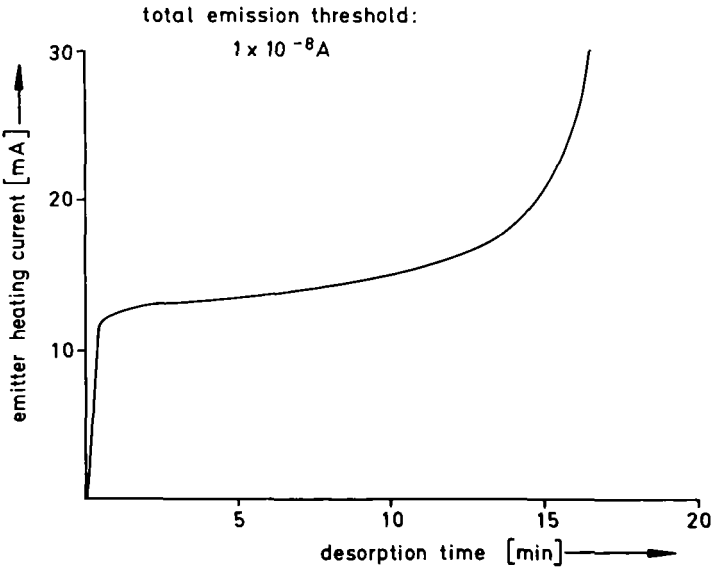

Fig. 1 Thermogram of a typical polar organic substance, BAT ~ 11 mA, real desorption time 14 minutes.

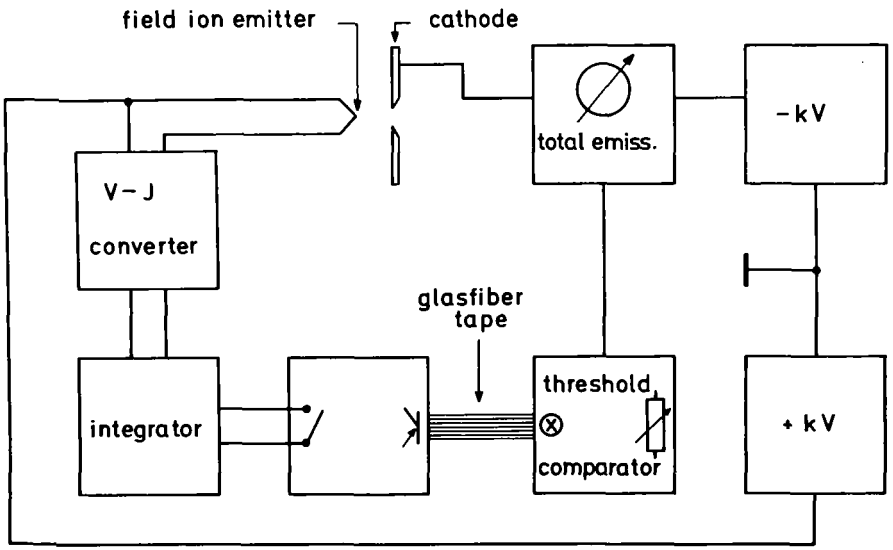

Fig. 2 Block diagram of the device for emission-controlled time/temperature profiles in FD-MS.

Field Desorption Mass Spectrometry Studies of Biorganic Compounds. K. L. Rinehart, Jr. and J. C. Cook, Jr., Sch. Chem. Sci. Univ. of Ill., Urbana, Ill. 61801

Studies of the field desorption technique in our laboratory have been primarily directed toward assaying the utility of the technique as a structural tool for compounds already under investigation. These include oligopeptide antibiotics such as the emerimicins and antiamoebin, polyene antibiotics such as hamycin and aureofungin, and both antibacterial agents and halogenated compounds of marine origin. Secondarily, we are testing the limits of the technique in other areas of interest, for example, with mycolic acids, marine toxins, and oligonucleotides. These studies require the development or modification of field desorption techniques--sample loading; new mass marker, high resolution--to suit these often difficult samples, and require the complementation of field desorption with field ionization and electron impact techniques.

STRUCTURE ELUCIDATION USING FIELD DESORPTION MASS SPECTROMETRY (FDMS)

C. N. McEwen
Central Research and Development Department
E. I. du Pont de Nemours and Company
Wilmington, Delaware 19898

The absence of structurally significant fragment ions in FDMS to identify thermally labile unknown compounds can often be compensated by high resolution FDMS, hydrogen/deuterium exchange of acidic hydrogens, and fragment ion information obtained from the complimentary EI or CI spectra. We use peak-matching to obtain accurate masses of ions unique to FDMS[1] and high resolution EIMS for accurate mass measurement of structurally important fragment ions found in the EI spectra. Some FD spectra, however, are complex (especially certain salts and pyrolysis FD spectra) and contain many ions not found in the corresponding EI or CI spectra. Mass measurement by photoplate recording is expedient for these compounds.[2]

We have developed a high resolution FD photoplate technique that is independent of the FI reference compounds used and can be processed by computer programs designed for high resolution EIMS. The procedure requires exposing the photoplate to field desorbed ions, followed by exposure of the field ionized reference ions under identical conditions and on the same photoplate position. The FI reference compounds can be emitter deactivating (temperature cycling reactivates the emitter) and up to 50 amu apart as with perfluoroalkyl iodides. After pumping out the FI reference compounds, an EI spectrum of PFK is exposed on the same photoplate position. A resolution in excess of 15,000 is desirable and a combination EI/FI/FD source is required by this method.

The computer program uses an EI generated PFK reference file and assigns the mass of the FI and FD ions relative to the EI generated PFK peaks. A plot of the nominal masses of the FI reference ions vs. the mass difference of the calculated and computer generated masses of these ions produces a curve (Figure 1) from which the accurate masses of the field desorbed ions are calculated assuming equal mass differences for FI and FD ions of the same nominal mass.

The use of H/D exchange to determine the acidic hydrogen content of thermally labile compounds is another valuable aid in structure determination, especially when the hetroatom content of the molecule has already been delineated by high resolution mass spectrometry. Because of large differences in the rate of exchange of different kinds of hydrogens (amide, amine, carbon bonded, etc.) it may be possible to distinguish hydrogens according to their rate of exchange in D_2O or CH_3OD. This method is complicated by a variable M^+/MH^+ ratio.[3]

A Du Pont 21-110 mass spectrometer equipped with an EI/FI/FD source has been used for these experiments. The photoplate data was automatically digitized using a Grant comparator connected with a Datex digitizer. The data collected on magnetic tape was processed on a PDP-10 computer using programs written by R. M. Hilmer and modified by H. J. Stoklosa of the Du Pont Central Research and Development Department.

---

1. C. N. McEwen and A. G. Bolinski, Biomed. Mass Spectrom., 2, (1975).

2. H. R. Schulten and H. D. Beckey, Org. Mass Spectrom., 7, 861 (1973).

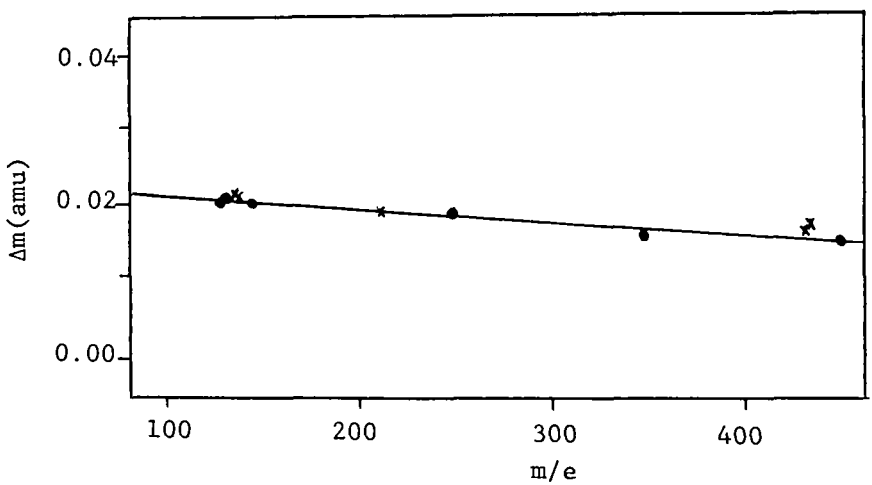

Figure 1. Graph for determining mass of field desorbed ions. Δm is subtracted from computer generated masses of FD ions to obtain accurate mass.

● FI references $(CH_3C(O)(CH_2)_nCH_3$ and $CF_3(CF_2)_nI$.

x FD ions from trimethylphenylammonium benzenesulfonate.

FIELD DESORPTION MASS SPECTROMETRY (FDMS) OF BIOGENIC AMINES AND ISOQUINOLINE ALKALOIDS

Gordon W. Wood and Ning Mak
Department of Chemistry, University of Windsor,
Windsor, Ontario, Canada N9B 3P4

A variety of amines which share the 2-arylethylamine (aryl=phenyl or 3-indolyl) structure are important in brain function. Current interest in these compounds is heightened by a biochemical theory of alcoholism which implicates their acetaldehyde condensation products (isoquinolines) in the development of addiction. Although mass spectral techniques of derivatization and analysis exist for several of these compounds, a recent publication has demonstrated the potential of chemical ionization for analysis of the underivatized amines(1).

We report here some of our results for the biogenic amines and the pertinent isoquinoline relatives using FDMS. Some comparisons will be made with chemical ionization (NH_3) results obtained by Dr. Alan Hogg, Dept. of Chemistry, The University of Alberta, Edmonton, as well as published chemical ionization(isobutane) and electron impact results.

The following amine hydrochlorides desorb smoothly from the field anode to give simple spectra in which the molecular ion(of the free amine) is the base peak: p-tyramine, 3-methoxytyramine, dopamine, L-epinephrine, DL-normetanephrine, tryptamine, 5-methoxytryptamine. Peaks corresponding to β-cleavage (M-30, 30 or M-44, 44 in epinephrine), which commonly give rise to the base peak in electron impact experiments, were generally 10-20% of base at best anode temperature. In contrast to published CI results(1), there was little evidence of NH_3 loss, nor was H_2O loss from normetanephrine observed. Generally, free bases gave results similar to hydrochlorides but salts of less volatile (stronger?) acids desorbed mainly as ammonium ions. For example, p-tyramine hydrogen sulfate gave protonated amine as the base peak (free amine = 5%) and the p-toluenesulfonate salt gave only the protonated amine peak. For the latter, the region above the protonated molecular ion showed peaks corresponding to association of that ion with anion and with one and two complete salts (i.e. BH.A, BH.BHA, BH.2BHA). The behavior of sulfate salts under field desorption conditions is further illustrated by serotonin creatinine sulfate which gave two base peaks: m/e 176 (serotonin) and m/e 113 (creatinine). This salt also showed protonation peaks (m/e 177, 114) and considerable β-cleavage (m/e 146 = 60%), the latter probably a reflection of the high anode current (20ma).

Four isoquinolines obtained by condensation of acetaldehyde with the appropriate 2-phenylethylamine (Pictet-Spengler reaction conducted by Dr. Maurice Hirst, Dept. of Pharmacology, University of Western Ontario) are shown below.

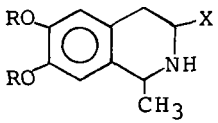

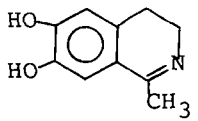

1: R = H, X = H

2: R = CH_3, X = H

3: R = H, X = COOH

4

The hydrochloride of each of these compounds was field desorbed and chemical ionization (NH_3) was carried out by Dr. A. Hogg for comparison. Catecholamine derivatives (1,3,4) gave M+1 as base peak and a fairly complex molecular ion region (M-1 to M+3), whereas for the dimethoxy compound 2 the most intense peak corresponded to M and the only other peak in the spectrum was M+1 at approximately the expected isotope value. Compound 3 gave several additional ions related to carboxyl loss, of which M-45(31%), M-44(31), and $M-44^{++}$(33) are most intense.

Aside from some complications of ammonia peaks and ammonia addition to base peak, the chemical ionization spectra of the isoquinolines were generally clear-cut with the anticipated quasimolecular ion as base peak. The one exception arose with compound 4 where m/e 192, not m/e 178, was the base peak. Whether this error arose from the preferential distillation of a methyl homologue which has since been shown to be an impurity, or from an unusual reaction with ammonia is presently under investigation.

For any mass spectral technique to assume practical importance in analysis of body fluids or extracts therefrom, several hurdles must be overcome(1). While field desorption has a major advantage in its ability to handle non-volatile materials, contamination from alkali metals is a potentially crippling disadvantage. In this connection it should be mentioned that in no case did such interference arise in this work. Further, addition of massive amounts of either NaCl or CsI to the isoquinoline papaverine failed to produce any change in the spectrum.

[1] G.W.A. Milne, H.M. Fales, and R.W. Colburn, Analyt. Chem. 45, 1952 (1973).

(A more detailed account of this work will be submitted for publication in Analytical Chemistry.)

The Complex Effects of Sodium and Potassium Ions in the Field Desorption Mass Spectrometry of Barbiturates. JAMES N. GERBER, BERND SOLTMAN, JOHN F. HOLLAND and CHARLES C. SWEELEY, Biochemistry Department, Michigan State University, East Lansing, Mich. 48824.

Preliminary results of studies of the effects of sodium ions on the field desorption mass spectrometry of barbiturates indicated that the formation of complex ions is extremely dependent upon the emitter current, while pH seems to have very little effect. By varying the emitter current throughout the range from 20 mA to 50 mA, the following complex ions have been observed.

m/e	Ions
185	$(M+H)^+$
207	$(M+Na)^+$
229	$(M+2Na-H)^+$
251	$(M+3Na-2H)^+$
137	$(M+4Na-2H)^{2+}$
99	$(M+5Na-2H)^{3+}$

M = 184, the molecular weight of barbituric acid

Only with great difficulty were these experiments repeatable and the selection and maintenance of sample temperature was determined to be the limiting parameter. Based on these and other experimental data, it became apparent that emitter current control, both static and programmed, was a necessary condition for obtaining meaningful and reproducible mass spectra. An emitter current programmer (ECP) has been fabricated and employed to meet this need.

The design of the ECP is shown in Fig. 1. It is an all solid state device using integrated circuits and modular components. A low voltage digital circuit accepts switch register commands that set the initial and final values for a programmed linear current "sweep." The programmer controls the current in the emitter by means of a digital to analog converter and subsequent analog closed loop regulating circuits, all at a potential of 3 KV. Optical couplers ensure insulation between the low and high voltage circuits, while providing the path for the control signals.

The ECP, which combines directly with the Varian MAT CH-5 DF mass spectrometer, can generate emitter currents between 0 and 63 ± 0.1 mA and can provide linear programs at any of four selected rates. Experimental results indicate this control produces effective temperature regulation commensurate to a current precision of ± 0.4 mA. This enables the operator to easily obtain optimum anode temperatures and provides the capability to analyze complex mixtures by using a thermal gradient during repetitive scanning in the field desorption mode. The device is easily adaptable to operation under computer control.

Details of the fabrication of the ECP and experimental studies using this device will be submitted for publication in *Analytical Chemistry*.

Acknowledgments

Design and fabrication of the emitter current programmer were accomplished by James W. Maine in the Instrument Shop of the Biochemistry Department of Michigan State University. Our thanks to Norman D. Young of this department for helpful discussions during these studies.

This work was supported by NIH Grant RR-00480.

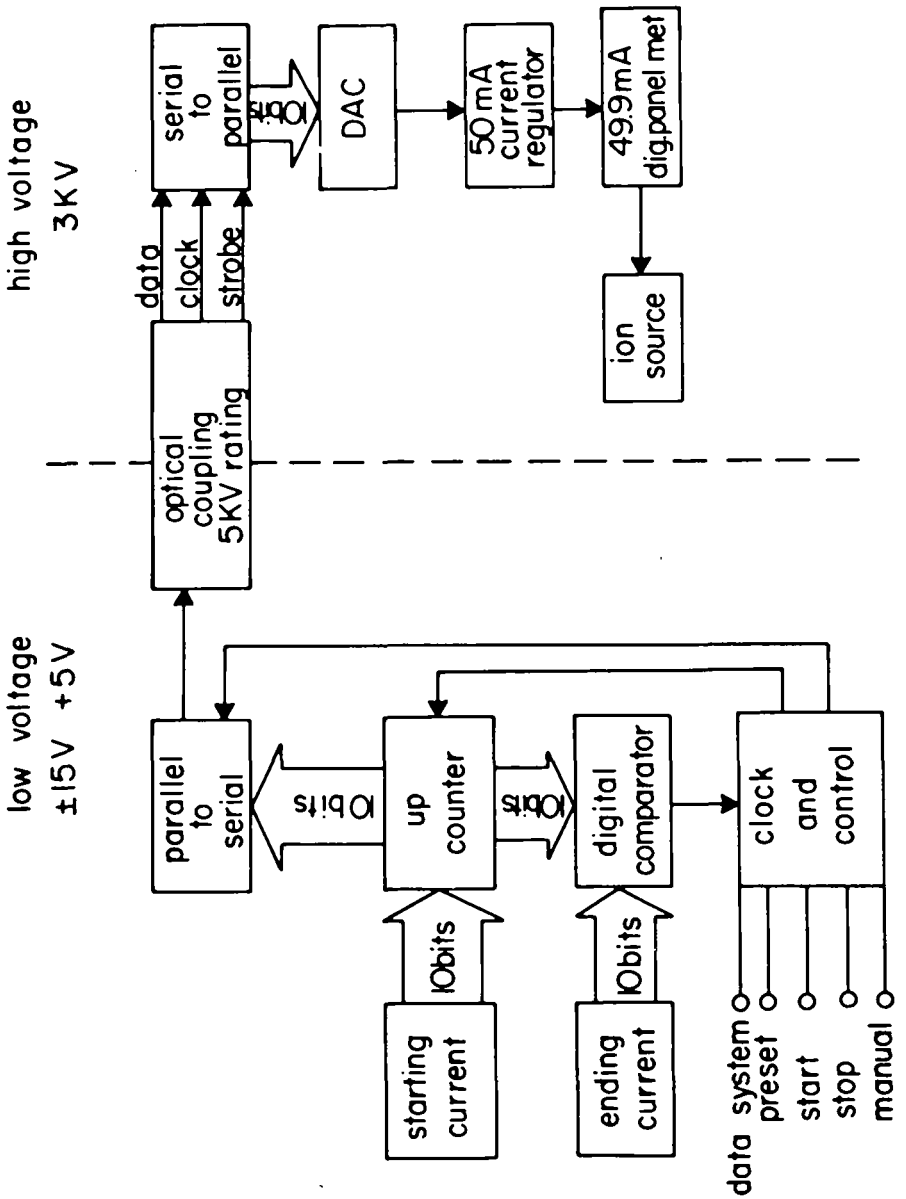

THERMALLY-PROMOTED FIELD DESORPTION MASS SPECTROMETRY*

Douglas F. Barofsky, Larry Jacob and Elisabeth Barofsky
Oregon Graduate Center, Beaverton, Oregon 97005

Field desorption (FD) mass spectrometry (MS) has enjoyed rapid growth during that last three years in its applications to organic chemistry. However, there are several uncertainties associated with the technique which hinder its standardization. Amongst these are the relationship between emitter temperature and the recording and interpretation of FD mass spectra.

Emitter temperature is used to control the onset of emission current and, when desired for structural information, to control thermal decomposition of the sample under investigation. In scanning sector field instruments, in particular, the ease with which a spectrum can be recorded is very sensitive to the onset and duration of ion emission as controlled by emitter temperature. Attempts to define an operational emitter temperature, usually referred to as the "best anode temperature"[1] (BAT), at which spectra can be usefully recorded do not seem universally applicable to all types of compounds. The definition of sensitivity and the significance of relative peak intensities must be strongly tied to the thermal history of the emitter relative to the recording history, i.e., the time sequence of recording and the scanning rate; however, the nature of this dependence has not yet been investigated.

The present work was undertaken to establish a more quantitative basis for the emitter temperature's role in FDMS. To this end a new, programmable heating current power supply was constructed. This unit has a programmable heating current range of 0-20 mA (adequate for the activated 8μ wire used in our laboratory); a booster range of 35-60 mA is incorporated into the unit for emitter cleaning by flash heating. The heating current is regulated to within 0.01 mA. The power supply controls are at a low voltage level and are optically coupled to the power supply which is maintained at the emitter voltage (2000-3600 v). The thirteen channel optical couplers used are of our own design and construction. Output connectors are provided for recording the heating current. An ammeter for monitoring total emission current is also built into the heating unit. The emission current ammeter has a resolution of 0.1 nA, and its output is optically coupled to low level for recording purposes.

This instrumentation was used to record FD thermograms generated from a Hitachi RMU-7 single focusing mass spectrometer. A FD thermogram is a X-Y-Y[1] plot of total ion emission (Y) and transmitted

*Submitted for publication in Int. J. Mass Spec. and Ion Phys.

ion current at one specific mass number (Y^1) versus heating current (X). During the preliminary experiments, the heating current was normally scanned at 0.04 mA/sec.

Our observations indicate that FD thermograms can be usefully employed in studying the effects of emitter geometry and sample distribution on the emitter. The thermogram provides an excellent qualitative picture of the desorption history of the sample and can, thus, be usefully employed in determining how best to record mass spectra. In addition, our preliminary observations show that thermograms can probably be used to make absolute quantitative measurements and to define an absolute index of sensitivity.

Beyond using thermograms to improve the operational basis of FDMS, we have also preliminarily investigated their analytical applications. Experiments performed on the xyloside, tetramethyloregonin[2], have demonstrated that FD thermograms can be used to distinguish between different fragmentation pathways. Thermograms generated from a simple mixture, consisting of the polycyclic aromatic hydrocarbons anthracene, perylene, and coronene, proved to be thermochromatograms showing specific peaks corresponding to the mixture components at different specific temperatures. This additional analytical facility may be of considerable utility in future analyses of mixtures.

1. H. U. Winkler and H. D. Beckey, Org. Mass Spectrom. 6, 655 (1972).

2. J. J. Karchesy, M. L. Laver, D. F. Barofsky and E. Barofsky, J. C. S. Chem. Comm. 1974, 649.

SOME APPLICATIONS OF FIELD DESORPTION (FD) AND FIELD IONIZATION (FI) MASS SPECTROMETRY

D.E. Games, A.H. Jackson and M.Rossiter,
Department of Chemistry, University College, P.O.Box 78, Cardiff CF1 1XL, U.K.

We have been concerned with the application of FD and FI GC-MS techniques for structural studies and the detection of thermally labile and/or involatile materials in three main areas:

1. Natural compounds which are available in a pure form or present in crude mixtures,
2. Drugs and their metabolites,
3. Synthetic organic and organo-metallic compounds.

FD has proved particularly effective for molecular weight determination of a variety of natural products of unknown structure e.g. antibiotics, bile pigments, coumarins and glycosides. High resolution data was obtained in some cases by peak matching the FD ion of interest with a suitable standard in the FI mode. For the glycosides the thermally induced fragment ions obtained at higher emitter currents were structurally informative and high resolution EI spectra provided information regarding the nature of the aglycone.

Direct examination of crude natural extracts is an area where FD is particularly useful. Crude natural extracts of e.g. alkaloids, coumarins, carotenoids, porphyrins and phaeophytins have been examined in this way, and a rapid finger print of the molecular species present is provided in each case. Apart from indicating the possible presence of new species the technique serves as a useful check for the absorption or decomposition of compounds when the extracts are subjected to GC-MS or high pressure liquid chromatography (HPLC).

Although FI GC-MS does not have the sensitivity of EI GC-MS, it provides molecular weight information in many cases, where the latter technique does not, e.g. unsaturated alcohols and acetates, and we have found it a particularly useful aid in our studies of the composition of insect secretions.

The major aim of our FD studies of drugs and their metabolites has been to utilise FD as a means of detection and identification of these compounds and their conjugates in crude biological extracts. Ions corresponding to diphenylhydantoin and phenobarbitone and some of their metabolites have been detected in urine extracts of rats fed with these drugs. However attempts to detect conjugates in crude extracts have so far been unsuccessful, although FD spectra of taurine, glycine and glucuronic acid conjugates of a number of different types of drugs have been obtained.

Our third area of study has involved synthetic compounds which do not provide useful EI spectra. Molecular weight and often some additional structural information is readily obtained from the FD

spectra of e.g. Wittig salts, sodium and potassium salts of sulphonates and sulphates, organo-metallic compounds, quaternary ammonium salts and dimeric compounds. One feature of the FD spectra of the salts is the formation of cluster ions which enable identification of both anion and cation in many cases. The intensity of the cluster ions varied with the wire current and solvent used, and in the case of the phosphonium and quaternary ammonium salts was also dependent on the nature of the anion i.e. the anions of stronger acids yielded more intense cluster ions.

Full details of these studies will be published in appropriate journals.

HIGH TEMPERATURE ACTIVATED CARBON EMITTERS FOR FIELD DESORPTION STUDIED BY ESR.

R.H.OBENAUF, JEOL ANALYTICAL INSTRUMENTS, INC., CRANFORD, NEW JERSEY 07016.

M.TAKEUCHI,S.ENOMOTO,Y.ITAGAKI AND K.AOYAGI, JEOL, ANALYTICAL INSTRUMENTS DIVISION,TOKYO,JAPAN.

One of the most critical techniques in field desorption mass spectroscopy is the production of reliable emitters. Without great confidence in the reproducibility of the activation process, one cannot know if the failure in obtaining an FD spectrum is due to the nature of the sample, a poisoning impurity, or simply - a poor emitter. In an effort to develop a reliable test for emitter efficiency, we have used electron spin resonance to test the FD emitters under various conditions.

All experiments were run on emitters produced by the high temperature activation technique of Beckey et al.[1] In each case, the 10 micron tungsten wire was treated using Barofsky's[2] pre-roughening method followed by activation with benzonitrile. Activation conditions were carefully controlled to produce emitters which yielded the highest sensitivity FD spectra. All spectra were taken on a JEOL JMS-01SG-2 operated with electrical detection.

Scanning electron micrographs of each emitter were obtained using a JEOL JMS-3-A. Physical differences in needle growth as a result of different activation temperatures were quite apparant. Emitters yielding the best sensitivity were produced at 1200 - 1250°C. The dense needles were finely divided and 30 ~ 40 microns long. Sustained thermally induced fragmentation could also be produced using higher emitter temperatures during desorption.

In order to obtain an ESR spectrum, the emitter wire had to be removed from the emitter mount and placed in the ESR sample tube as shown in Figure 1. Here the emitter is shown in the ESR cavity with a capillary inlet to the tube for introduction of PFK or other gas. All spectra were obtained on a JEOL JES-PE-3X ESR spectrometer. This technique precludes the possibility of obtaining mass spectra from an emitter after taking the ESR spectrum. We were, however,able to obtain reproducible results based on many runs taking electron micrographs and FDMS sensitivity checks prior to breaking the emitter.

The result of a blank run is shown in Figure 2. The top spectrum is that of the bare pre-roughened tungsten wire and the lower spectrum that of the wire after introduction of PFK. The noise level change is due only to a difference in amplifier response.

Figure 3 (upper trace) is a typical ESR spectrum of a high temperature activated emitter which exhibited high sensitivity. The spectrum consists of a single sharp peak. The important features are a very narrow line width of about 0.7 gauss (peak to peak) and a G value of 2.0026. This indicates that the center of the unpaired electron is localized with high density and that motional exchange line narrowing exists. The spin density calculates about $10^{14} \sim 10^{15}$ spins per emitter. I would like also to point out that the emitter G value lies quite close to that of the free electron 2.0023.

We can qualitatively say that the sharpness of the ESR signal is related to the quality of the FD emitter. The line widths of our "good" emitters did vary somewhat, however, they were all less than about 1.5 gauss.

It is, of course, well known that the desorption efficiency can be affected by the presence of certain sample solvents, impurities, or reference gases. We have noted an irreversible change in the ESR signal upon introduction of PFK. In Figure 3, the same emitter was used for both spectra, however, the lower spectrum was taken about 30 minutes after introduction of PFK. As can be seen this results in a marked broadening of the line and loss in intensity. These results indicate that the center of the unpaired electron is localized at or near the surface of the carbon needles, thus permitting deactivation by PFK.

The results of a separate experiment, as shown in Figure 4 bear mention. Here the ESR spectra of catalaytic carbon (carbon black) were taken for both activated and non-activated carbon. The upper spectrum has a line width of about 1.5 gauss while the lower is much broader; a striking similarity to the two spectra in Figure 3.

1. H.D.Beckey et al., a)Messtechnik,79,196(1971) and b) Org. Mass Spectrom.6,885(1972).

2. D.F.Barofsky and E.Barofsky, Int.J.Mass Spectrom.Ion Phys., 14,3(1974).

ESR MEASUREMENT

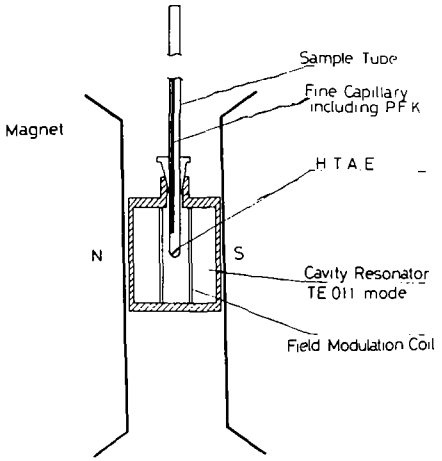

FIGURE 1

ESR of Non-activated Emitter

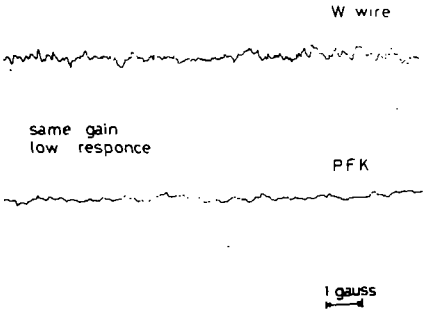

FIGURE 2

ESR of H.T.A.E.

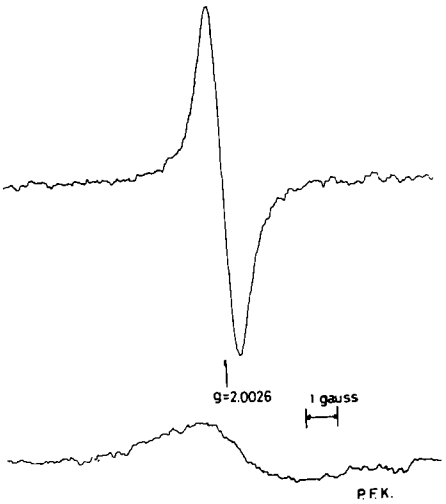

FIGURE 3

ESR of Catalytic Carbon

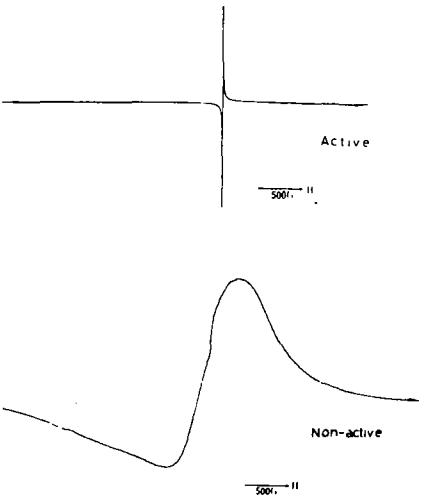

FIGURE 4

Mass Spectrometric Studies of Alamethicin. Ramesh C. Pandey, J. Carter Cook, Jr., and Kenneth L. Rinehart, Jr., Dept. of Chem., Univ. of Ill., Urbana, Ill. 61801.

Recently, two groups[1,2] have assigned the structure of alamethicin, an oligopeptide antibiotic from *Trichoderma viride*[3] that can transport cations and induce action potentials in synthetic membranes. We have reinvestigated the structure of alamethicin, employing field desorption mass spectrometry as a major tool, and find that the previously assigned structure must be revised since alamethicin contains components other than those reported.[1,2,3] A revised structure based on our mass spectrometric data for alamethicin will be discussed.

[1] J. W. Payne, R. Jakes, and B. S. Hartley, *Biochem.J.*, 117, 757 (1970)

[2] Yu. A. Ovchinnikov, A. A. Kiryushkin, I. V. Kozhevnikova, *J. Gen. Chem. USSR*, 41, 2105 (1971).

[3] C. E. Meyer and F. Reusser, *Experientia*, 23, 85 (1967).

EI AND FD MASS SPECTRA OF RIFAMYCINS

L. F. Zerilli, M. Landi, G. G. Gallo

Lepetit Research Laboratories, 20158 Milano (Italy)

K. H. Maurer and U. Rapp

Varian MAT GmbH, 28 Bremen 10 (West Germany)

Rifamycins are a family of antibiotics, obtained by fermentation and chemical modification, (1) acting against Gram-positive and Gram-negative bacteria and on mycobacteria (2). The structure of rifamycins S is reported as representative:

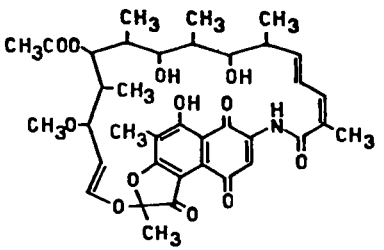

Electron impact (EI) mass spectrometry has been shown a powerful tool in structural work also in the field of rifamycins (3,4). In fact, even if the presence of many polar groups in the molecule brings about low volatility, in some cases significant spectra have been shown by the products as such. Anyhow, for the majority of rifamycins the thermal lability of the compounds prevents good spectra to be obtained. Derivatization improves the volatility, but mixtures of various derivatives usually form and the interpretation of the spectra is difficult. Thus, field desorption (FD) mass spectrometry appears the best way for overtake these limitations. Furthermore FD allows molecular weight information to be obtained on rifamycins sodium salts as well. In table 1 EI and FD molecular (M^+) or quasi-molecular ion intensities of rifamycins are compared.

Table 1

Rifamycin	MW	EI M^+ rel.int.	FD base peak
S	695	14%	M^+
SV Na salt	719	absent	$[M+Na]^+$
B	755	absent	$[M+H]^+$
O	753	2%	M^+
Desacetyl S	653	absent	M^+
AF	725	5%	M^+
AMP	822	absent	M^+
W	655	2%	M^+

Field desorption mass spectra of rifamycins of analytical pure grade were carried out on a Varian MAT 731 instrument, equipped with a combination field desorption-field ionization-electron impact ion source. A benzonitrile conditioned tungsten wire emitter carrying a potential of 9 KV (extraction voltage: -4 KV) was used. Source Temperature, 60°. The emitter wire current was optimized to give best anode temperatures (BAT) for molecular ions at a resolution of 1,000. The m/e values were determined by comparison with those of an electron impact mass spectrum of perfluorokerosene. Electron impact mass spectra of rifamycins were run on a Perkin Elmer 270 instrument with an electron beam energy of 70 eV, using the direct inlet system. Source temperature 150°.

References

1. P. Sensi, N. Maggi, S. Furesz and G. Maffii, Antimicr. Agents and Chemoth., 1966, 699 (1967).

2. S. Riva and L. G. Silvestri, Ann.Rev.Microbiol., 26, 199 (1972).

3. L. F. Zerilli and G. G. Gallo, Eur.Report, 4765 f.i.e., 217 (1971).

4. L. F. Zerilli, M. Landi, N. Rimorini and G. G. Gallo, Ann.Chim. (Rome), 64 199, (1974).

Stigmatic, Second Order, Double Focusing Mass Spectrometer

S. Taya, H. Tsuyama, I. Kanomata and H. Matsuda *
Central Research Laboratory, Hitachi Ltd.,
Kokubunji, Tokyo, Japan.
*Institute of Physics, College of General Education,
Osaka University, Toyonaka, Japan.

In order to improve the transmission and the resolution of a double focusing mass spectrometer, two ion optical considerations are carried out. One is to use electric and magnetic sector fields which have, not only a radial focusing but also an axial focusing property, namely stigmatic focusing fields. The other is to strictly correct the second order image aberration of the ion optical system. Therefore, such an instrument can be called a stigmatic, second order, double focusing mass spectrometer.

Generally, a radial focusing image width x_2 is given in the second order approximation as follows;

$$x_2 = A_x x + A_\alpha \alpha + A_\delta \delta + A_{xx} xx + A_{x\alpha} x\alpha + A_{x\delta} x\delta + A_{\alpha\alpha}\alpha\alpha + A_{\alpha\delta}\alpha\delta + A_{\delta\delta}\delta\delta + A_{yy} yy + A_{y\beta} y\beta + A_{\beta\beta}\beta\beta, \quad (1)$$

where x and y denote the radial and axial distances from the optical axis, α and β the radial and axial inclinations and δ the relative velocity deviation of the incident ion beam. Since the ion source slit width is normally very narrow, the terms of eq.(1) including x are not important. Therefore, the parameters of the ion optical system are determined to diminish the six coefficients $A_{\alpha\alpha}, A_{\alpha\delta}, A_{\delta\delta}, A_{yy}, A_{y\beta}, A_{\beta\beta}$ as much as possible. In the calculation of the second order aberration coefficients, the influence of the extended fringing field is very important.* Therefore, the calculation in this paper is carried out by means of the second order transfer matrix method in which the fringing field effects are taken into account.

The ion optical system of the stigmatic, second order, double focusing mass spectrometer is obtained as shown in Fig.1. It consists of a toroidal electric sector field having a concave edge at the entrance side (c=0.5, r_e=212mm, Φ_e=85.2°, ρ_1=-106mm), and of a uniform magnetic sector field of non-zero entrance and exit angles (r_m=200mm, Φ_m=90°, ε_1=30°, ε_2=-9.6°).

The axial focusing property of this ion optical system is calculated as shown in Fig.2. The incident parallel beam is focused at the entrance and the diverging beam from the ion source slit at the exit of the magnetic sector. Therefore, a high transmission can be expected, because the ion beam can pass through the narrow magnet gap.

The second order aberration coefficients are calculated and compared with those of the high resolution mass spectrometers in which the second order aberrations are partially corrected, as shown in Table 1. In this calculation, the same fringing field distribution is taken into account, and each magnetic radius is normalized at 1m.

Table 1. The Second Order Aberration Coefficients.

Instrument	$A_{\alpha\alpha}$	$A_{\alpha\delta}$	$A_{\delta\delta}$	A_{yy}	$A_{y\beta}$	$A_{\beta\beta}$
This Work	0.00	0.04	-0.10	-0.09	-0.43	-1.50
MINNESOTA	0.13	-0.06	0.32	-0.87	-9.94	-28.7
MANITOBA	0.12	0.19	0.31	-0.52	-5.00	-13.3
MAINZ	0.01	-6.12	-2.53	-6.42	-126.	-613.
ARGONNE	0.19	3.12	-2.45	-2.68	-2.40	-0.31
GARCHING	12.7	-1.36	0.00	-1.31	1.41	-2.02

* H. Matsuda, T. Matsuo; Int. J. Mass Spectrom. Ion Phys., 6, 385 (1971).

The schematic diagram of the instrument is shown in Fig.3.
The resolving power of this instrument is measured under the following condition;

Accelerating Voltage : 3.7kV,
Sample Gas : CO, N_2, C_2H_4 Mixture Gas,
Ion Beam Spread : x=1μm, α=0.003rad, δ=0.001, y=1mm, β=0.001rad.

The mass spectrum at the maximum resolution is shown in Fig.4. (2)
From this spectrum a resolving power of 67,000 at 10 % valley separation is obtained. The theoretical resolving power including the second order aberration ΣAb is given as;

$$R.P. = \frac{r_e(1+X_e)X_m}{k_e^2(X_eX_mS_i+S_c+\Sigma Ab)} = \frac{212}{0.57\,S_i+S_c+\Sigma Ab}$$

$$(r_e=212\text{mm},\ X_e=0.61,\ X_m=0.93,\ k_e^2=1+c=1.5\ ), \qquad (3)$$

where r_e denotes the electric sector radius, X_e and X_m the magnifications of the electric and magnetic sector fields and S_i and S_c the ion source slit and the collector slit widths, respectively.

Under the experimental condition of the ion beam spread given in eq.(2), the theoretical resolving power is calculated at 73,000. The experimental value 67,000 reaches 90 % of this theoretical one.

The transmission is defined as the ratio of the ion current passing through the each sector field to the incident one. The experimental results are obtained as 81 % for the electric sector, 53 % for the magnetic sector, therefore the total transmission is obtained at 43 %.

The shape of the focusing image is observed by photographic plates, and is shown in Fig.5. The ion source slit width is 0.1 x 2 mm^2. From this image the crescent shape of the second order aberration which is concerned with the axial spread of the incident beam (y,β) is not observed.

The theoretical axial focusing width y_2 is given as follows;

$$y_2 = (1.9y + 280\beta)\ \text{mm}. \qquad (4)$$

From the experimental condition of the axial spread (y=1mm, β=0.001rad), the theoretical axial width is evaluated at 4.4mm, while the experimental image length is observed at 3.8mm from the axial focusing width of the photographic plate.

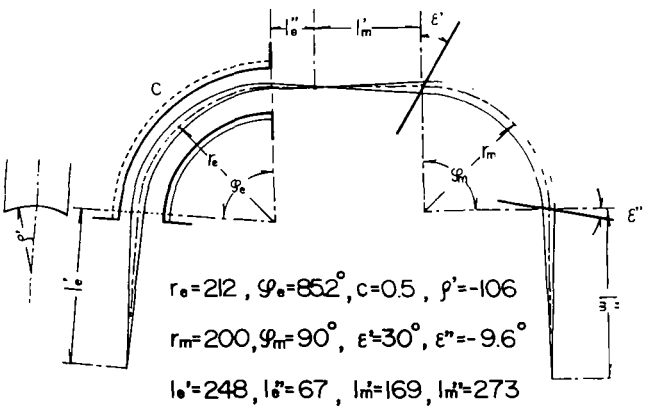

Fig. 1. The Ion Optical System

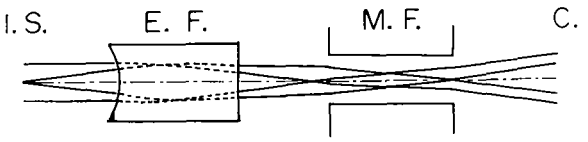

Fig. 2. The Axial Focusing Property

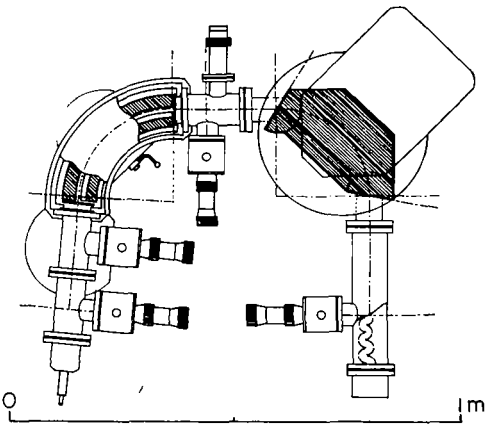

Fig. 3. The Experimental Instrument

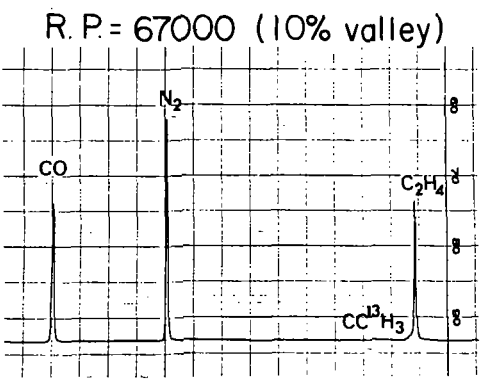

Fig. 4. The Mass Spectrum of the Maximum Resolving Power

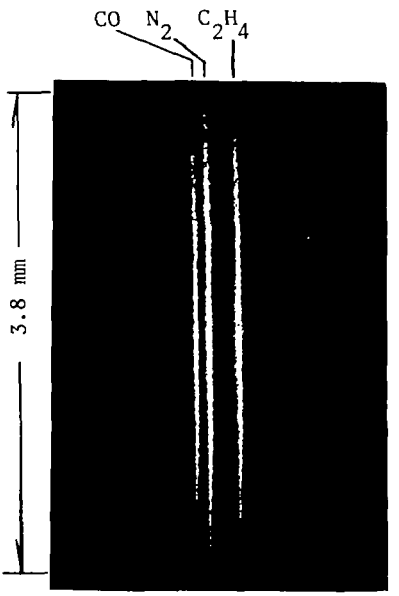

Fig. 5. The Axial Focusing Image

Applications of Double Beam Mass Spectrometry to Accurate Mass Measurement

M.L. Aspinal, K.R. Compson, A.A. Dowman, R.M. Elliott, D. Hazelby
AEI Scientific Apparatus Ltd, Barton Dock Road, Manchester M31 2LD, England

Double beam mass spectrometry is a valuable technique for reliable mass marking and mass measurement at low resolving power and fast scan speeds. Double beam mass marking is illustrated in figure 1 which is a field desorption spectrum obtained on the MS3074.

For accurate mass measurement, single beam instruments are forced to operate at high resolving power and consequently suffer from low sensitivity and reference compound suppression. These problems do not occur with double beam instruments in which the sample and reference are in separate sources and at low resolving power.

Figure 2 is a chromatogram of the volatile components of a cigarette smoke obtained from the DS50 data system by repetitively scanning the MS3074 at one second per decade. Table 1 illustrates the quality of the mass measurements. A small peak has been deliberately chosen for this example.

Table 1 Peak No. 264 Dimethyl Disulphide

Mass	Composition	Intensity (%)	Error (m Mu)
96	$C_2H_6\ ^{32}S^{34}S$	9	0.8
94	$C_2H_6\ ^{32}S_2$	100	-0.8
79	$C\ H_3\ ^{32}S_2$	52	1.8
61	$C_2H_5\ ^{32}S$	17	0.7

Figure 3 is a chromatogram of a mixture of two steroids eluted from a high resolution glass capillary column directly coupled to the MS1073 which is a low resolution double beam instrument. Figure 4 is a plot of the spectrum of the second of these compounds and table II illustrates the mass measurements that were obtained.

Table III MS1073 Double Beam Mass Measurements of Derivatized Steroid

Mass	Composition	Intensity (%)	Error (m Mu)
460	$C_{25}H_{41}NO_3\ ^{28}Si^{29}Si$	30	-2.7
459	$C_{25}H_{41}NO_3\ Si_2$	100	-3.4
428	$C_{24}H_{38}NO_3\ Si_2$	32	5.5
345	$C_{19}H_{29}\ O_2\ Si_2$	36	0.2

The accuracy of double beam mass measurement with chemical ionization was assessed using the drug pentazocine. Table IV gives the mass measurement errors of a typical scan.

Table VI Mass Measurement of Pentazocine CI (CH_4)

Mass	Composition	Intensity (%)	Error (m Mu)
287	$C_{18}{}^{13}C\ H_{28}\ NO$	20	-2.1
286	$C_{19}H_{28}NO$	100	1.3
285	$C_{19}H_{27}NO$	15	0.0
284	$C_{19}H_{26}NO$	13	1.0
230	$C_{15}H_{20}NO$	10	0.4

Six separate scans were made of this material, the mean mass measurement error of the quasi-molecular ion at mass 286 was 0.1 millimass units and the standard deviation was 1.45 millimass units.

In conclusion, these results show how double beam mass spectrometry improves the ease of operation and quality of the information in applications involving chemical ionization, field desorption and GC/MS at low resolution where its advantages for mass identification and mass measurement are particularly valuable.

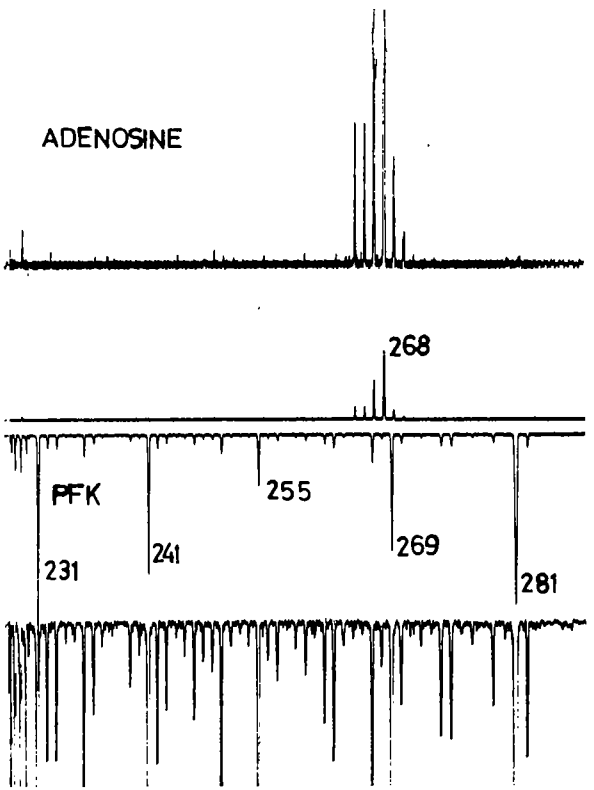

Fig.1

Fig.2

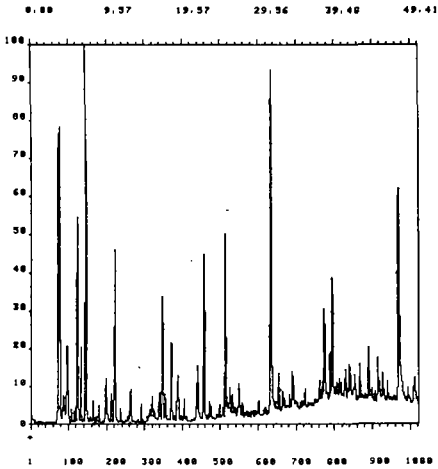

Fig.3

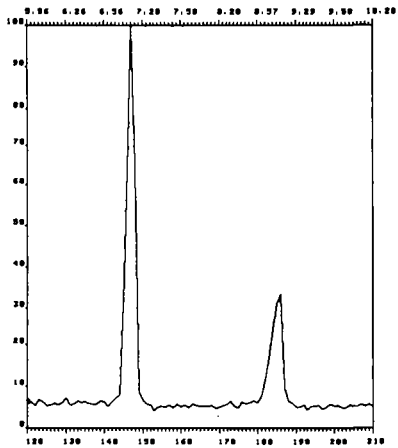

Fig.4

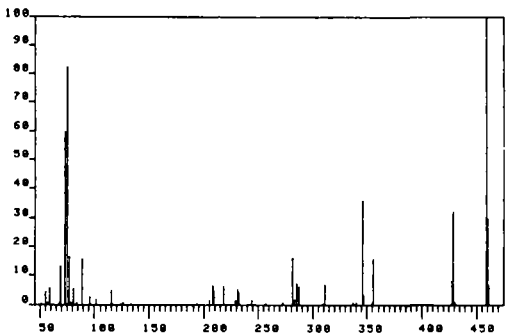

MS1073 SPECTRUM OF UNKNOWN STEROID

C-3

Micro-Analyser Using Electron Beam Guiding Ion Source.

T. Takagi, T. Kishi*and I. Yamada, Non Member, Kyoto Univ., Dept. of Elec., Kyoto and *Univ. of Osaka Pref., Dept. of E.E., Sakai, Japan

Recently authors have developed an electron beam guiding ion source which can be applied for an micro-mass analyser. When a fine high power density electron beam injected on to a solid sample S, the bombarded area is vaporized and the evaporated atoms are ionized by collisions with the incident or secondary electrons. These ions which are trapped in the negative potential well formed by injecting electron beam are extracted through a center of cathode K and analysed by usual mass analyser. Before and after the state of a sample surface can be displayed as the same principle as SEM by using the secondary electrons emitted from the sample surface. The injecting electron beam can be scanned by the coil D. At the present stage, the constant sensitivity and resolution are obtained in the range of about 5 or 6 mm scanning width.

C-4

A Two-Filament Rotary Source for Surface Ionization Mass Spectrometry.* RONALD JENE DUPZYK, Lawrence Livermore Laboratory, Livermore, California 94550

A two-filament thermal ionization source containing a six sample rotor has been built. Operating a high sensitivity 60 tandem magnet spectrometer, it has shown sample-to-sample cross contamination of less than 20 ppm. With overnight pump down, source operating pressures are nominally $<5 \times 10^{-8}$ torr. It is currently being used to analyze environmental U and Pu samples that are in the sub-nanogram range. Design parameters and system operating characteristics will be described.

* Work performed under the auspices of the U. S. Atomic Energy Commission.

MULTIPLE ION DETECTION BY ACCELERATING VOLTAGE ALTERNATION IN CONJUNCTION WITH VOLTAGE SWEEPING

L. D. Gruenke, J. C. Craig and D. M. Bier*

University of California, Schools of Pharmacy and Medicine*
Departments of Pharmaceutical Chemistry and Pediatrics
San Francisco, California 94143

An analog multiple ion detection system for magnetic sector instruments has been developed which is exceptionally easy to construct and operate and yet yields data superior to that obtained from conventional systems. The cost of this system (excluding the multipen recorder) is less than $100 and it requires only minor modifications of the accelerating voltage supply.

The key feature of the system is the use of a 60 Hz a.c. sine wave sweep voltage superimposed on the d.c. accelerating voltage. The purpose of the a.c. voltage sweep is four fold: 1.) it makes ion current measurement relatively immune to small drifts in the magnet current or accelerating voltage. 2.) the voltage sweep allows m/e peaks to be continuously displayed on an oscilloscope. Thus, focus conditions can be monitored and adjusted during data collection without affecting the results. 3.) the m/e peak shape can also be monitored for interference from ion current at the same nominal but different exact mass. 4.) real time visualization of a small adjustable mass range greatly facilitates the setting-up process.

The use of multiple ion detection in conjunction with voltage sweeping we abbreviate MID/VS. Figure 1 shows a block diagram of the MID/VS system designed for the AEI MS-12. High voltage switching is accomplished by switching the reference voltage of the MS-12 accelerating voltage supply between a fixed and a settable value, thus giving two channel AVA operation. This method of high voltage switching avoids the need for making modifications at the high voltage side of the power supply.

The voltage sweep causes the mass spectrometer to sweep back and forth over a small adjustable mass range which is centered at the mass determined by the d.c. component of the voltage. This means that an m/e peak centered in the sweep range will remain centered when the sweep range is widened or narrowed. By displaying the output of the mass spectrometer on an oscilloscope a nonflickering display of a mass spectrum over a very small mass range can be viewed in real time. A typical oscilloscope display is seen in Fig. 2. The oscilloscope has been adjusted so that the same m/e peak is shown here swept out three times. This is to aid exact focusing; when all three images are equally spaced the m/e peak is centered exactly in the middle of the sweep range.

The block diagram (Fig. 1) shows the recorder connections. A three pen recorder is connected so that two pens show the composite ion current data. The third recorder channel is connected through relay-2 to the mass spectrometer only during the measurement of one of the two ion currents. An RC network delays the switching of relay-2 for 300 milliseconds after the switching of the reference voltage by relay-1. This allows the accelerating voltage to settle at the proper voltage before the ion current measurement is made. A capacitor at the input of this channel of the recorder maintains the voltage at the input when relay-2 is open. This

sample-and-hold feature allows the gain of the data from the second AVA channel to be controlled independently.

Figure 3 shows a typical ion current profile obtained from the MID/VS system. The recorder pen can not respond quickly enough to trace out the m/e peak each time it is swept out every 1/120 of a second. As a result the pen deflection is proportional to the average ion current during the sweep rather than to its instantaneous value. This means that recorder tracings from the MID/VS system are identical in appearance to those obtained from conventional analog MID systems.

The middle curve seen in Fig. 3 alternates between the average ion currents for each m/e value. The sharp spikes seen at the bottom part of this curve near the center are due to the fall in ion current during the time the accelerating voltage is being switched from one value to the other. The bottom curve in Fig. 4 is identical to the middle curve but at lower recorder gain. The top curve is the sample and hold channel. The hold periods are clearly seen as flat portions in the curve. The top curve corresponds to the bottom of the middle curve but at higher recorder gain.

We have applied the MID/VS system to the measurement of stable isotope ratios in a wide variety of biomedical problems. Calibration curves obtained for alanine enriched with known amounts of its d_4 analog and for glucose enriched with dideuterioglucose are currently being used for the determination of blood glucose and alanine in children infused with tetradeuterioalanine and dideuterioglucose as part of a study on gluconeogenesis and glucose utilization *in vivo*.[1]

Similar calibration curves have been obtained for methyl palmitate enriched with methyl palmitate-d_4, in a study of lipid turnover, and for dideuterio-L-nicotine enriched with its natural analog in a study of nicotine levels in body fluids. In each case the precision of successive measurements (carried out in the picogram to nanogram range) was about 1%. There are reports in the literature[2-4] of other MID systems which utilize voltage sweeping. However these use *linear sweeps* and involve computer generation or computer analysis of the sweep waveform. The MID/VS system described above has the virtues of being inexpensive, simpler to construct, and easy to operate.

REFERENCES

1. Gruenke, L. D., Craig, J. C., and Bier, D. M., *Biomed. Mass Spectrom.*, 1:418-423 (1974).
2. Holland, J. F., Sweeley, C. C., Thrush, R. H., Teets, R. E., and Bieber, M. A., *Anal. Chem.*, 45:308-314 (1973).
3. Holmes, W. F., Holland, W. H., Shore, B. L., Bier, D. M., and Sherman, W. R., *Anal. Chem.*, 45:2063-2071 (1973).
4. Klein, P. D., Haumann, J. R., and Eisler, W. J., *Anal. Chem.*, 44:490-493 (1972).

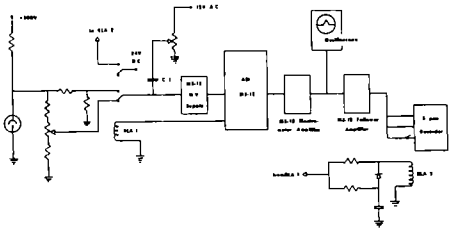

Fig. 1. Block diagram of the MID/VS system.

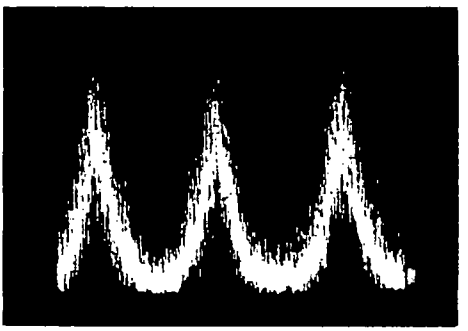

Fig. 2. Typical oscilloscope display of MID/VS system.

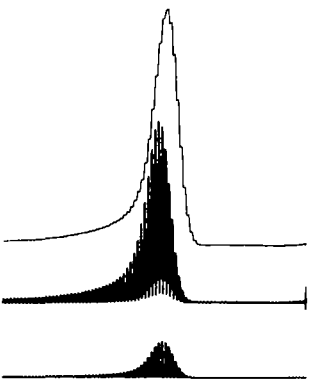

Fig. 3. Typical ion current profile from MID/VS system.

CI-EI Combination Source for MAT 112

P. DOBBERSTEIN, G. KAPPUS, H. MICHELSEN Varian MAT GmbH, Bremen, W. Germany, and R. ALBERTI, Varian MAT U.S. Operations, Springfield, N.J. USA

Since the CI-process is somehow specific to the pair reagent ion sample molecule it does not give the desired result for any unknown compound, in these cases it is usefull to have an electron impact spectrum in addition to the CI-spectrum. The new CI-EI source for mass spectrometer MAT 112 allows switching from one mode to the other within parts of a minute. The schematic (fig. 1) shows the source in the EI-mode where the CI-box acts as the pusher-electrode. When switching to CI the CI-box is shifted into the electron beam region (electron beam perpendicular to plane of drawing) by means of a moving rod. A microswitch connected to the moving rod initiates in the source supply the following functions:

1. shut off high voltage
2. operation of electropneumatic valves
3. switch source voltages from one mode to the other
4. switch on high voltage

The source supply has 2 complete sets of potentiometers for the source voltages allowing independent source optimation for each mode. Since the reagent gas is fed directly into the CI-box, change between different reagent gases is easy and does not influence the GC operation where we use He as carrier gas. The source is completely mounted on the ion source flange (fig. 2) and therefore it can be exchanged for the standard EI source without difficulties.

The total ion current (TIC) signal for the GC-trace (fig. 3) is obtained by means of a spectrum integrator at a scan speed of 200 u/sec. Mass range and scan speed can be chosen separately for recording of a single spectrum on the UV recorder (fig. 4), interrupting the integration for one scan.

Isobutane CI spectra of allobarbital (fig. 5) and secobarbital (fig. 6) recorded with Varian MAT data system 101 MS interfaced to m.s. MAT 112 demonstrate that spectra obtained with this source show very small fragmentation. About 1 µg of sample was injected into the GC (LM: original spectrum, LS: with background subtraction).

The spectra are shown with the permission of Carter Cook, University of Illinois, Urbana, who has our prototype source.

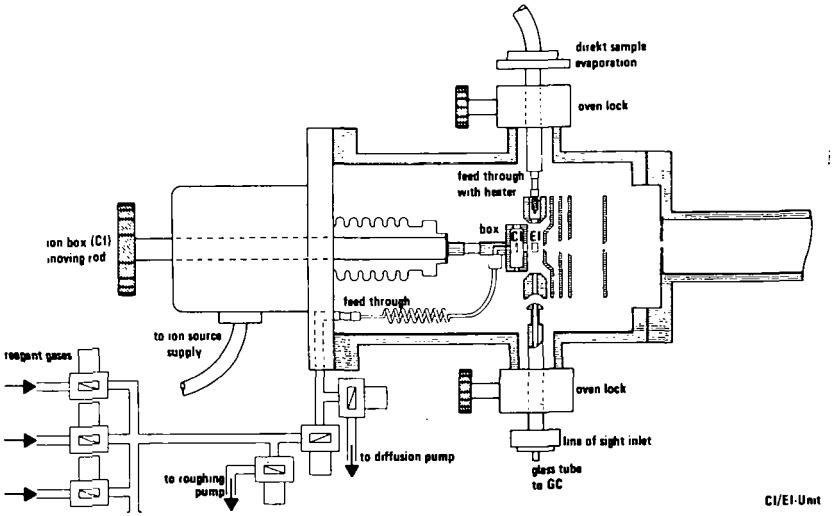
direkt sample
evaporation
oven lock
feed through
with heater
box
ion box (CI)
moving rod
feed through
to ion source
supply
reagent gases
oven lock
line of sight inlet
to diffusion pump
to roughing
pump
glass tube
to GC
CI/EI-Unit

fig. 1

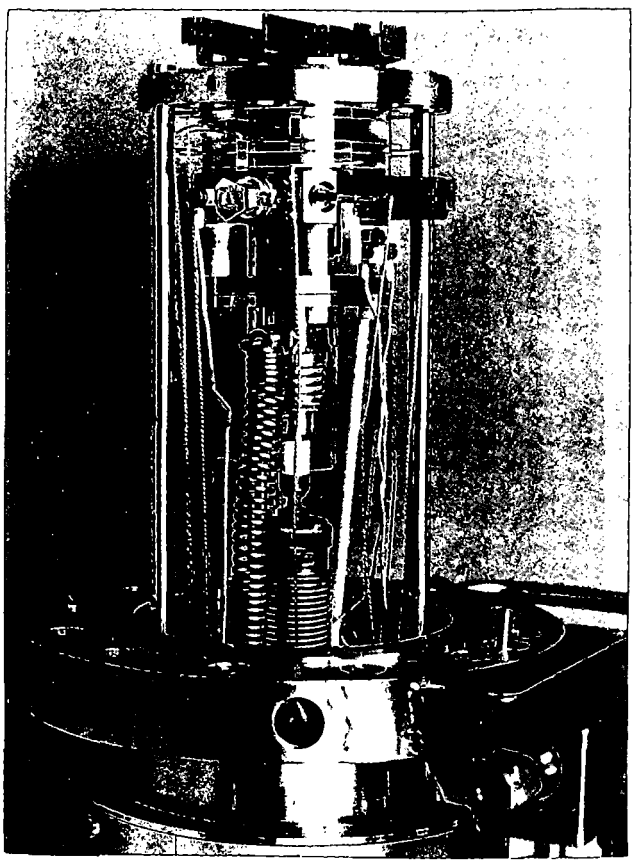

fig. 2

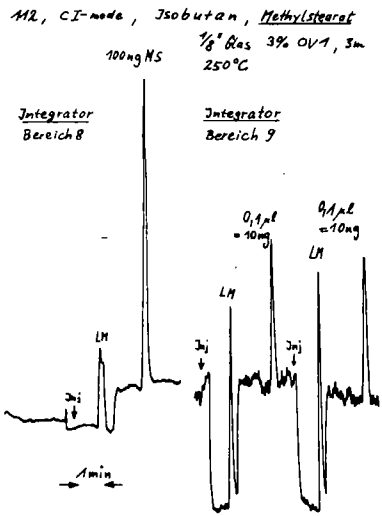

fig. 3

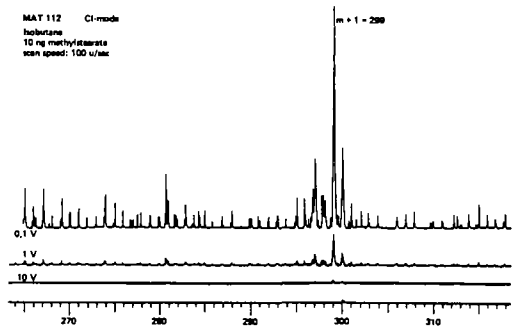

fig. 4

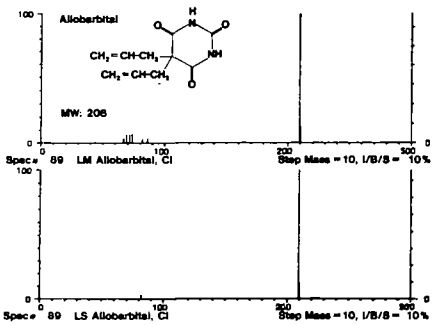

fig. 5

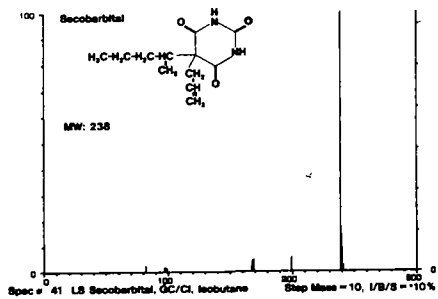

fig. 6

A Dual Field Desorption Electron Ionization Source for Applications in Biomedical Research. E. M. Chait, C. R. McKinney, M. Czuha, Du Pont Instruments, 1500 South Shamrock Avenue, Monrovia, CA 91016.

A dual field desorption/electron ionization source has been developed for a high resolution mass spectrometer. This source has been designed to exploit the recent development of metal dendrite emitter systems for field desorption. In addition, the source combined several features for optimal ease of operation making field desorption more accessible to researchers in biomedical fields. The operating parameters of this source have been studied with a stress on ease of operation and the ability to obtain reliable data. Examples of involatile and intractable materials will be shown to illustrate how field desorption may compliment other techniques such as electron ionization and chemical ionization. Various experimental considerations involved with the design optimization and operation of the source with a mass spectrometer utilizing electrical detection of the spectrum will be discussed.

APPLICATION OF THE ION-DRIFT SPECTROMETER TO MACROMASS SPECTROSCOPY. II

Malcolm Dole and J. Gieniec, Department of Chemistry, Baylor University, Waco, Texas 76703

At the Dallas meeting of the A.S.M.S. we reported[1] our first attempts to use the Plasma Chromatograph (PC) (T.M. Franklin GNO Corp.) to measure mobilities of macroions produced by an electrospray technique[2] in nitrogen at atmospheric pressure. A figure was given showing the variation of measured velocities of positive lysozyme macroions as a function of nitrogen flow rate through the drift cell of the PC. At that time the flow meter used to measure the gas flow rate had not been calibrated; this meter has been calibrated and we show the revised data in Fig. 2. The lysozyme macroion velocities were calculated from the drift times of the first three peaks of the plasmagram, Fig. 1(a). Peaks 4 and 5 are the solvent ions shown in Fig. 1(b). The ion velocities should increase by 7 cm/sec for each increase of 100 cc/sec in the flow rate of the gas if the macroions are entrained in the carrier gas. The lines have been drawn to reflect this linear increase in velocity. The available data points fit this line reasonably well above flow rates of about 150 cc/sec. At the lower flow rates it is expected that the ion velocities will be lower since loss of carrier gas through the interstices between the guard rings of the drift cell becomes significant.

The reduced mobilities were calculated from the drift velocities as extrapolated to zero flow rate. These values are collected in Table I along with radii (R) of the macroions as calculated for various values of z from the equation

$$R = 8.2\left(\frac{z}{K_o}\right)^{\frac{1}{2}} \qquad (1)$$

where K_o is the reduced mobility (i.e. the measured mobility calculated at S.T.P.) and z is the number of unit charges per macroion. Eq. (1) was derived from the equation[3]

$$K = \frac{3ze}{16N}\left[\frac{1}{m} + \frac{1}{m'}\right]^{\frac{1}{2}}\left(\frac{2\pi}{kT}\right)^{\frac{1}{2}}\frac{1}{\Omega_D} \qquad (2)$$

with e the electronic charge, m and m' the masses of the carrier gas molecules and macroions resp., k Boltzmann's constant, T the absolute temperature, N the carrier gas number density and Ω_D the average collision cross section. To obtain (1) from (2) we assumed a hard sphere model ($\Omega_D \simeq \pi R^2$).

TABLE I
Mobilities of Lysozyme Macroions

Peak No.	K_o, $cm^2V^{-1}sec^{-1}$	Estimated Ionic Radii (Å) z=1	z=2	z=3
1	0.24	17	24	29
2	.36	14	19	24
3	.52	11	16	20

The radius of a spherical lysozyme monomer (molecular wt. about 14,600) can be estimated to be about 17Å. This agrees with the experimental values for peaks 1 and 3 assuming z=1 and z=2 resp. Peak 2 might be due to doubly charged dimers. It can be seen in figure 1a that it is not well resolved.

In view of the uncertainty in the data, an alternate interpretation of the data is that peaks 1, 2 and 3 are all due to lysozyme monomers with z=1, z=2 and z=3 resp. Refinement of the technique and higher resolution should permit us to interpret the drift time data more precisely.

Further, we wish to describe some focusing experiments with macroions of 51,000 amu polystyrene electrosprayed from a 0.1 wt.% solution with 3 parts of cyclohexane and 2 parts of acetone as solvent. Using the experimental arrangement shown in Fig. 3 with the electrospray occurring at the tip of the needle marked V_N and with the macroions accelerated toward the grounded plate, we have photographed the polymer deposit on the plate and shown that the circular deposit decreases markedly in radius as the voltage between the conducting layer marked V_p and the grounded plate is increased. Keeping V_N 5 kV more negative than V_p we have been able to reduce the polystyrene area from a diameter of 4.5 cm to 0.7 cm as V_p was lowered to -6kV. Focusing occurred mostly in the first kV range, the diameter decreasing to 1.3 cm at 1kV. This demonstrates that the polymer molecules or aggregates are ionized and can be electrically focused as they pass into the drift cell. We have also demonstrated the same effect at the exit end of the drift cell; i.e. after the ions have passed through the drift tube. Although this focusing effect has not found direct application in the work with the PC to date, its potential advantages in providing increased intensities for macroion beams are immediately apparent.

ACKNOWLEDGMENTS

This research was supported by grant No. GP-27672 (now No. MPS 71-02618 A0T) of the National Science Foundation and by income from the chair in chemistry established at Baylor University by a gift from The Robert A. Welch Foundation.

REFERENCES

1. Gieniec, J., Cox H.L., Jr., Teer, D. and Dole, M., Proceedings of the 20th Conference on Mass Spectrometry and Allied Topics, Dallas, June 1972, p. 276.

2. Dole, M., Mack, L.L., Hines, R.L., Mobley, R.C., Ferguson, L.D., and Alice, M.B., J. Chem. Phys. 49, 2240 (1968).

3. McDaniel, E.W. and Mason, E.A. "The Mobility and Diffusion of Ions in Gases", John Wiley & Sons, N.Y., p 121 (1973).

Fig 1

a) Mobility spectra of positive lysozyme ions obtained by electrospraying a 0.0053 wt.% solution in 90% ethanol The carrier gas flow rate is 135 cm^3/sec.

b) Mobility spectra of positive solvent ions obtained by electrospraying 90% ethanol. The carrier gas flow rate is 200 cm^3/sec.

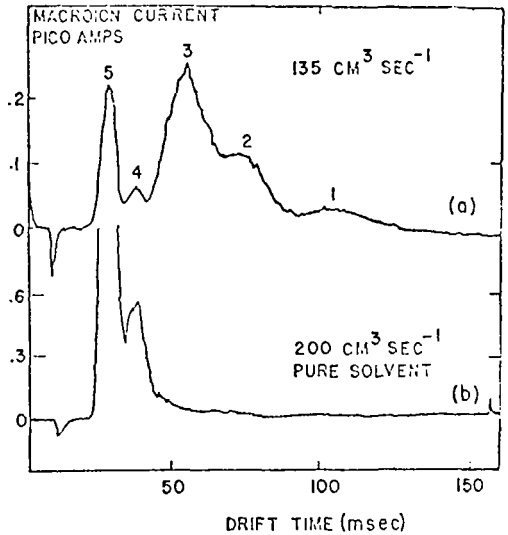

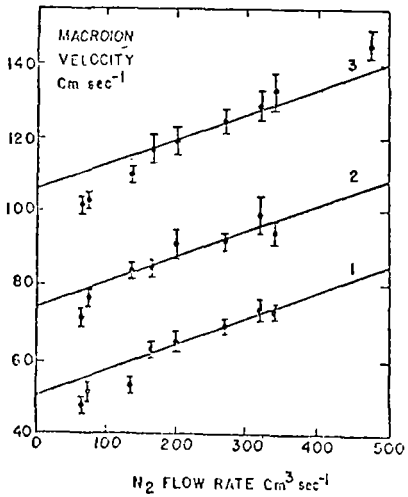

Fig 2

Positive lysozyme macroion velocities as a function of nitrogen gas flow rate. The numbers on the three lines refer to the numbers on the 5 peaks of the plasmagram as shown in Fig. 1(a).

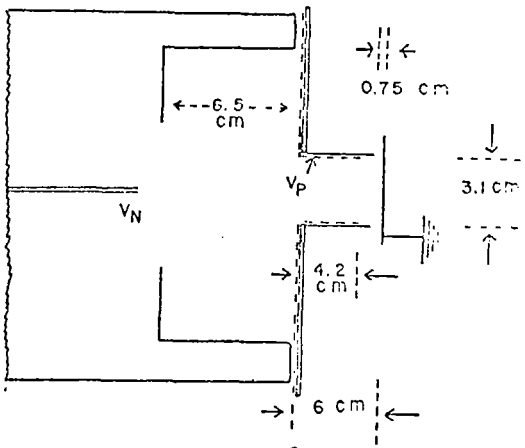

Fig 3

Arrangement of equipment for macroion focusing experiments.

Improvement of the Interfacing of Quadrupole Mass Filters with Multipoint Field Ionization Sources. H. L. Brown and R. H. Cross, Mass Spectrometry Research Center, Stanford Research Institute, Menlo Park, CA 94025

Efforts to interface the SRI multipoint FI source[1,2] with a quadrupole mass spectrometer show that the sensitivity of this instrumental arrangement is limited by a great deal of spectral noise and the loss of intensity due to the deceleration to a few eV of a highly divergent beam produced at a few keV. It is hypothesized that noise results from the following mechanism. Excited molecules result from neutralization of a certain fraction of the FI produced ions as they pass or collide with the grid which we can consider as an electron donor past which the ions move. For 3 kV potential grid-to-points the ions pass with a velocity comparable to the orbital velocity of a hydrogenic electron at $\sim$ 100 Å. An electron captured at that velocity and radius forms a Rydberg state with an effective principle quantum number $n^* \approx 11$, and a binding energy, $E_n \approx 0.12$ eV obtained from

$$E_n = R_y/(n^*)^2 \qquad (1)$$

where R_y is the Rydberg constant.

The free radiative lifetime τ_R of such a state is given by

$$\tau_R \approx \tau_{R_o}(n^*)^3 \qquad (2)$$

which for $n^* = 11$ yields a lifetime of $\sim$ 1.4 μsec, sufficiently long for the excited molecule to enter the quadrupole. The lifetime against FI, τ_I is given by:

$$\tau_I \approx \tau_{I_o} \exp\left(\frac{0.60\ I^{3/2}}{F}\right) \qquad (3)$$

where I can be replaced by E_n and F is the effective field at the molecule. Inserting the magnitudes of fields along the beam path and estimating the lifetime for FI from the experiment, one concludes that we observe Rydberg molecules formed with $n^* \geq 30$, corresponding to an ionization potential of < 0.010 eV and a free radiative lifetime of > 30 μsec. Ions produced from such fast excited neutrals along the beam path can only be partially decelerated at best and therefore pass through the quadrupole with little or no resolution to produce the spectral noise. At first those neutrals were eliminated by offsetting the FI source from the axis of the quadrupole.[2] However, formation of these states is velocity dependent whereas FI is field dependent so that reduction of both points to counter electrode voltage and spacing reduces this noise while maintaining the signal eliminating the need for deflection of the beam.

The problem of loss of intensity due to beam divergence was assessed from the results of the experiment shown in Fig. 1. This apparatus measures the angular divergence of the beam envelope for FI ions leaving the ionizer screen. Ions leave the ionizer with a velocity v_o at some angle θ_o with respect to the axis with $|v_o|$ determined by the potential V_o and mass of the ion.

To this velocity we add a second velocity vector, v_1, due to acceleration or deceleration in the gap between the ionizer and the face of the microchannel plate image intensifier. From the size of the image shown on the phosphor screen and the observables, to a first approximation one measures the divergence of the beam envelope by the equation shown at the bottom of the figure where D is the spot diameter and r is the separation of the ionizer screen and microchannel plate. Some results of such measurements are shown in Table 1.

Table 1: Angular Distribution of Ions Emitted from Multipoint FI Sources

	V_o (kV)		
	1.5	2.0	2.5
Thymine		$40.9^\circ \pm 2.2^\circ$	$42.0^\circ \pm 1.6^\circ$
Toluene	$41.7^\circ \pm 4.7^\circ$	$43.4^\circ \pm 1.9^\circ$	$46.2^\circ \pm 3.7^\circ$
Hydrogen		$39.4^\circ \pm 2.3^\circ$	$39.3^\circ \pm 2.4^\circ$

The salient information is that the beam divergence is large, and that it increases with the point to counter electrode potential. Consequently maximum sensitivity for a given FI instrument will be produced by the maximum allowable ion energy and the minimum allowable ionization field. Quadrupoles require ions at a few eV, so the instrumental options are limited in this case. Fig. 2 shows two approaches toward utilizing as much of the beam as possible. In the lower arrangement the ionizer is placed as close as possible to the quadrupole entrance to minimize losses due to loss of brightness of the divergent beam which falls off approximately as $1/r^2$. The upper schematic illustrates the use of a single stop acceleration-exponential deceleration arrangement. Here an initial acceleration reduces the beam divergence and then, since the quadrupole has a relatively large virtual acceptance aperture, one images a somewhat magnified beam with decreased divergence into the quadrupole. A comparison of the results of two techniques is shown in Fig. 3. The points marked QP#1 and QP#2 indicate count rates obtained from two different quadrupoles with closely spaced sources and the plotted data show the results from the same quadrupoles with an accel-decel lens. The two quadrupoles behaved dissimilarly; our expectations based on non-mass analyzed experiments lie between these two results.

The sensitivty obtained for thymine with either alternative is $\sim$ 55 pg with an overall instrumental efficiency of $\sim 6 \times 10^{14}$ ions/mole. Some applications of these instruments to routine analytical problems are presented in papers H-15 and M-3 of these proceedings.

References

1. C. A. Spindt, J. App. Phys. 39, 3504 (1968).
2. H. L. Brown and M. Anbar, Int. J. Rad. Phys. Chem. 7, 281 (1975).

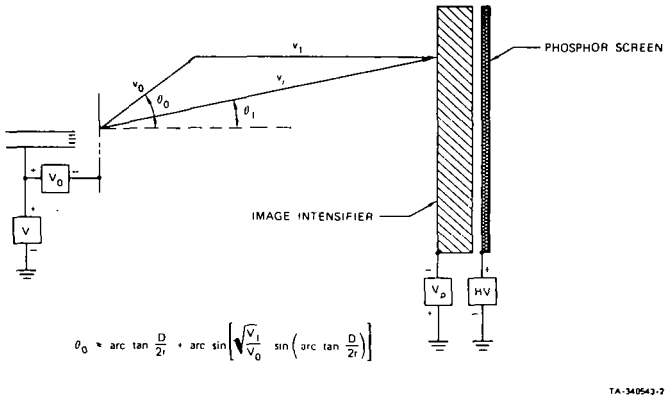

FIGURE 1 SCHEMATIC OF APPARATUS USED FOR ANGULAR DISTRIBUTION MEASUREMENTS

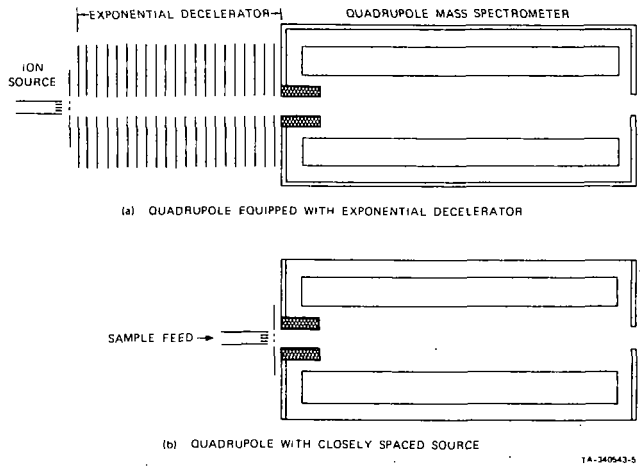

FIGURE 2

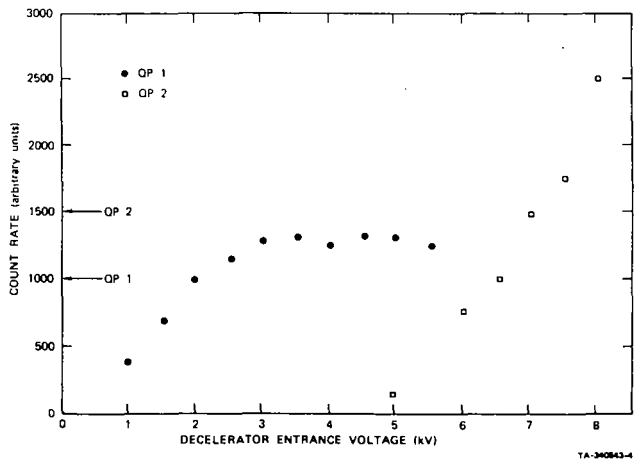

FIGURE 3 MASS ANALYZED COUNT RATE VERSUS DECELERATOR ENTRANCE VOLTAGE

POTENTIALITIES OF QUADRUPOLE MASS SPECTROMETERS IN FIELD IONIZATION/FIELD DESORPTION INVESTIGATIONS

H.J. Heinen, H.H. Gierlich and H.D. Beckey
Institut für physikalische Chemie der Universität Bonn,
53 Bonn, Wegelerstr. 12, W. Germany

Quadrupole mass filters offer considerable advantages in field desorption mass spectrometry (FD-MS) as they provide rapid repetitive mass scans over deliberately chosen mass ranges. The mass spectrum can be oscilloscopically displayed during the FD process. This allows a dynamical observation of the recording procedure of the FD mass spectrum, which implies that any influence of the instrumental parameters - and most importantly of the emitter temperature and of the field strength - on the mass spectrum can be directly controlled. This is of extreme advantage in the following cases:

1) The emitter heating current for the best anode temperature for molecular weight determination of an organic compound can be easily adjusted.
2) The fragmentation level in the FD mass spectra can be increased to a controlled degree.
3) Cluster ions can be identified by the observation of their temperature and field strength dependence.
4) In the case of qualitative analysis of mixtures the conditions of FD can be easily chosen so that the peaks of interest show up optimally.

On the technical problems involved in the combination of the quadrupole mass filter with the field desorption/field ionization source has been reported in detail earlier [1]. At the present the FD-quadrupole mass spectrometer operates satisfactorily up to mass 500 with unit mass resolution. The signal to noise ratio is 10^5 for the parent ion signal for the field ionization of acetone. The parent ion group of adenosine can be recorded peak resolved out of a 10^{-4} molar solution of adenosine by the emitter dipping technique. This corresponds to a minimal sample consumption of some nanograms.

The sensitivity of the instrument can be noticeably increased if the mass resolution is lowered from unit resolution. Thus rapid preinvestigations on the desorption onset with increasing emitter temperature as well as on the mass ranges of interest can be performed in a low resolution run with negligible sample consumption. The versatility of the FD-quadrupole mass spectrometer is demonstrated by the investigations of several drugs. A case is reported where three barbiturates were determined out of the crude chloroformic urine extract of a case of overdose of hypnotics [2]. It is shown that the dynamical observation of the FD recording procedure can give valuable information on the origin of the mass peaks which is of great help in the interpretation of the spectra. Thus the lack of high resolution mass determination with the quadrupole mass spectrometer is compensated in many applications.

References:

1) H.J. Heinen, Ch. Hötzel and H.D. Beckey, Int. J. Mass Spectrom. Ion Phys., 13, 55 (1974).

2) H.H. Gierlich, H.J. Heinen and H.D. Beckey, Biomed. Mass Spectrom., 2, 31 (1975).

Attachment of a Simple Ion Probe to an MS-9 Mass Spectrometer*

Richard J. Blattner, David S. Simons and Charles A. Evans, Jr.

Materials Research Laboratory

University of Illinois, Urbana, Illinois 61801

We have adapted an ion probe attachment to an AEI MS-902 mass spectrometer to utilize the mass resolution, peak matching and energy analysis capabilities of the instrument for the analysis of inorganic insulators and organic materials. The primary ion source and ion optics have been described previously.[1] Charge neutralization was accomplished by a masking technique which provided electron flooding of the sample during positive ion bombardment. Results obtained from the NBS 600 series of glass standards indicated that analyses could be obtained at the 1 ppm level at a working resolving power of 5000 for selected elements. Peak matching was useful for exact mass identification in this mode. Positive secondary ion mass spectra obtained from benzoic acid, salicylic acid and m-chlorobenzoic acid indicated that the spectra changed in time. Initially, the spectra were similar to electron impact spectra, but after extended ion bombardment they changed to essentially the graphite spectrum. This temporal change in the mass spectra was correlated with changes observed in the physical appearance of the sample surface. Doubly charged molecular species and metastable peaks were observed in the halide spectrum. Negative secondary ion mass spectra were characterized by the presence of the parent-minus-one molecular ion rather than by the presence of the parent ion as one of the most abundant species. In each negative secondary ion mass spectrum it was necessary to qualitatively subtract the obvious graphite subspectrum from the composite spectrum to make a reasonable interpretation.

A more complete account of this work will be submitted for publication in Analytical Chemistry.

* This work was supported in part by the National Science Foundation Grants DMR 72-03026 and MPS 74-05745.

1. R. J. Blattner, J. E. Baker, and C. A. Evans, Jr., Anal. Chem., 46, 2171 (1974).

A HIGH SENSITIVITY GC/MS UTILIZING DIGITALLY PROGRAMMED ION ENERGY

By

E.J. Argelander, B.N. Colby, C.W. Hull, T.W. Whitehead

E. I. du Pont de Nemours and Co. (Inc.)
1500 S. Shamrock Avenue
Monrovia, CA 91016

Recent trends in GC/MS applications have increased the demand for ultimate sensitivity and ease of operation. To meet these needs, a new design concept has been utilized in an integrated GC/MS. The basis for this system is digitally programmed ion energy which allows incorporation of many of the best features of both quadrupole and magnetic sector analyzers into a single instrument. These features include high sensitivity over the full mass range, fast scanning for an oscilloscope display, linear mass scan, and complete digital control.

High sensitivity is achieved in an all-glass system by close coupling the gas chromatograph through a jet separator to a highly efficient ion source-magnetic sector analyzer combination. The 58°, four-inch radius magnetic sector is operated at a constant field of 10,000 gauss and has a resolving power of 600. The spectrometer is scanned by digitally programming the ion accelerating voltage at up to 2048 amu/sec (6×10^5 v/s at m/e 43) from low to high mass values selected on the instrument keyboard.

In the past, voltage scanning has suffered from mass discrimination. To eliminate this problem, a two-stage ion source was developed. This source uses slits and extractor electrodes to separate the ion forming region from the scanned accelerating region. The ions are first extracted with a small constant potential and then accelerated to the scan potential into the magnetic field. The source voltage range is 12,500 to 540 volts which corresponds to a mass range of 43 to 1000 amu.

For display and recording purposes, it is desirable to produce peaks with similar widths at all mass positions. To achieve this, a beam modulation system is employed which artificially decreases resolution at low mass. This is done by applying a programmed 100 KHz signal to a set of deflection plates located between the magnet and the slit in front of the electron multiplier. The amplitude of this signal is functionally related to the mass in register so that the resultant spectra have nominal unit mass resolution to m/e = 600.

Due to the high accelerating voltages used for digitally programmed ion energy and the fact that the pressure within the glass jet separator is conducive to electrical discharge, electrical isolation techniques were employed in the GC/MS interface. All large voltage drops were arranged to occur either in high vacuum or at atmospheric pressure.

A typical GC/MS spectrum taken with this instrument is shown in Figure 1.

DIELDRIN

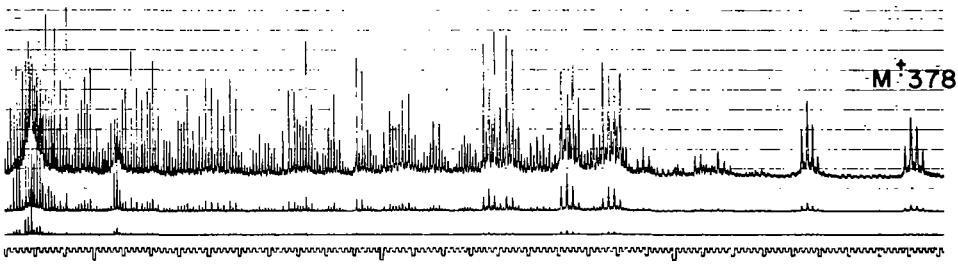

Figure 1

Applications of a New High Sensitivity GC/MS System.

R. G. Beimer, E. M. Chait and C. W. Hull, Du Pont Instruments, Monrovia, CA 91016

The last few years have seen steady progress in the technology of gas chromatography used in combination with mass spectrometry. GC/MS equipment has developed in such a fashion that it has become increasingly useful to researchers in industrial, clinical, biomedical, forensics and environmental fields of research. Modern GC/MS hardware is now accessorized with what have become necessary adjuncts to the analyses. These include mass spectrometer data systems for the handling of large amounts of data, multiple ion detection for very specific and sensitive analyses and alternative methods of ionization such as chemical ionization to permit an additional dimension in simplifying mass spectral data. The purpose of this paper is to describe a totally new GC/MS system with state of the art sensitivity. Applications of this new mass spectrometer will be discussed as they relate to current fields of research.

GAS CHROMATOGRAPHY/CHEMICAL IONIZATION MASS SPECTROMETRY

FRANK HATCH and BURNABY MUNSON

Department of Chemistry
University of Delaware
Newark, Delaware 19711

A simple interface has been made between a gas chromatograph (HP 7420A) and a mass spectrometer (duPont (CEC)21-110B) which eliminates the need for a separator. The interface consists of two microcapillary valves (Precision Sampling Corp.) in series, which are connected with a glass/ metal seal and a flexible bellows to the heated glass inlet lines leading to the source of the mass spectrometer. The inlet lines and the valves are insulated from the grounded gas chromatograph by a section of quartz tubing (5 cm x 0.1 cm i d). Microcapillary tubing (70 cm x 0.16 cm o d) connects the interface to the splitter connection in the gas chromatograph. The dead volume on the high pressure side is approximately 50 μl. The low pressure glass line is relatively long (100 cm x 0.6 cm o d) and contains three bends. To reduce the problems of electrical discharges, the glass lines are coated with Ceramacast 505 (Aremco Products, Inc.) and wrapped with asbestos tape and mica before the heating tapes are added. Operating temperatures are 250-300°C at a source potential of 4 kv and 200-250°C at a source potential of 6 kv. The source housing chamber is evacuated with a 4" diffusion pump (TM) of rated capacity, 680 lμ/sec. The pumping capacity at the source is estimated to be 280 lμ/sec.

Any carrier gas may be used with the gas chromatograph (He, H_2, N_2, and CH_4 were used) and if desired, a second gas can be mixed with the GC effluent before reaching the source of the mass spectrometer. Up to 20 ml/min (STP) of He of 10 ml/min of N_2 or CH_4 can be taken into the source. The total effluent or any fraction may be taken into the source by a simple adjustment of the valves. The performance of the system is not a sensitive function of the pressure or flow rate. For GC columns of 5-7000 theoretical plates, the resolution obtained from MS traces (peak width at half height) was essentially the same as the resolution obtained from the GC traces of the flame ionization detector for flow rates to the MS greater than about 2 ml/min (STP). Two source configurations were successfully used: an open one to give low source pressures (<0.05 torr) and near EI conditions (electron entrance = 0.045 cm^2; ion exit = 0.031 cm^2) and the other to give high source pressures (>0.5 torr) and CI conditions (electron entrance = 0.002 cm^2; ion exit = 0.002 cm^2). The spectra of compounds obtained with He as the carrier gas at low pressures are very

similar to the conventional 70 ev EI spectra and identification of compounds can be made from comparisons of these "near EI" spectra. Spectra obtained with He as the carrier gas at high source pressures (>0.5 torr) are significantly different from 70 ev EI spectra and show a much greater extent of fragmentation to lower molecular weight ions than is noted in the EI or "near EI" spectra. The high pressure charge exchange spectra obtained with N_2 (or He) as the carrier gas frequently contain abnormally high abundances of $(M+H)^+$ ions because of hydrogen-containing impurities in the gas. Typical CH_4 CI spectra can be obtained by mixing CH_4 with the He carrier gas. The spectra obtained from these mixtures are not sensitive functions of the composition of the mixtures: very similar spectra are obtained with 1/1 and with 1/8 CH_4/He mixtures.

GC traces can be obtained by monitoring the ion currents for selected ions in the spectra in either the low pressure mode of operation of high pressure charge exchange mode of operation. These traces will identify compounds with a common structural feature. The low molecular weight reactant ions can be defocussed at the beam monitor immediately preceeding the magnet and the output of this monitor can be used to determine the GC trace as the higher molecular weight species are formed. One can also monitor the ion current for one of the reactant ions and obtain a GC trace from the decrease in the ion current of the reactant ions as the compounds come through the mass spectrometer. GC traces could be obtained from the computer analyses of the data, but our system does not yet have computer capabilities. The magnetic scan system is presently being modified for computer acquisition of data.

MINIATURIZED MAGNETIC SECTOR MASS SPECTROMETER FOR USE WITH GAS CHROMATOGRAPH

By

Albert D. Tomassian

Perkin-Elmer Aerospace Division
Pomona, California 91767

The mass spectrometer of the Viking GCMS system is a miniaturized high resolution instrument, ruggedized for flight applications. Its overall dimensions are 8" x 6" x 3.5", weighs 5.5 lbs and requires 11 watts operating power including 9 watts to maintain ion source at 225°C.

Figure 1 outlines the mass spectrometer. It has the Nier-Johnson geometry with 90° electric and 90° magnetic sectors. The electric sector is cylindrical with a mean radius of 1.86". It has an aspect ratio of 3 and utilizes Rose shims for field uniformity. Herzog shunts are also used to reduce fringe field effects. The radius of the magnetic sector is 1.50", it has inlaid pole pieces with a 0.100" gap. In addition, part of the flux in the gap is used for the ion pump which is an integral part of the mass spectrometer. The pump has a speed of 500 cc/s and utilizes slotted cathodes for the improved pumping of inert gases. The ion source is conductance limited to 50 cc/s, and therefore differentially pumped by 10:1 which increases ion source sensitivity and reduces sample memory.

As shown in Figure 2, the ion source assembly has dual filaments, and the electron beam is magnetically confined to reduce dispersion in the ionizing region. The source utilizes a saddle lens to inhibit the leakage fields from the accelerating region transgressing into the ionizing region.

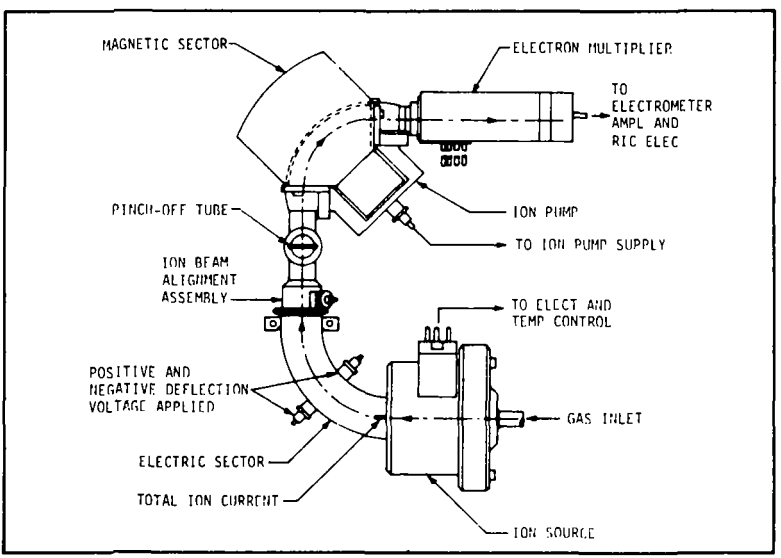

FIGURE 1. Mass Spectrometer Schematic Outline

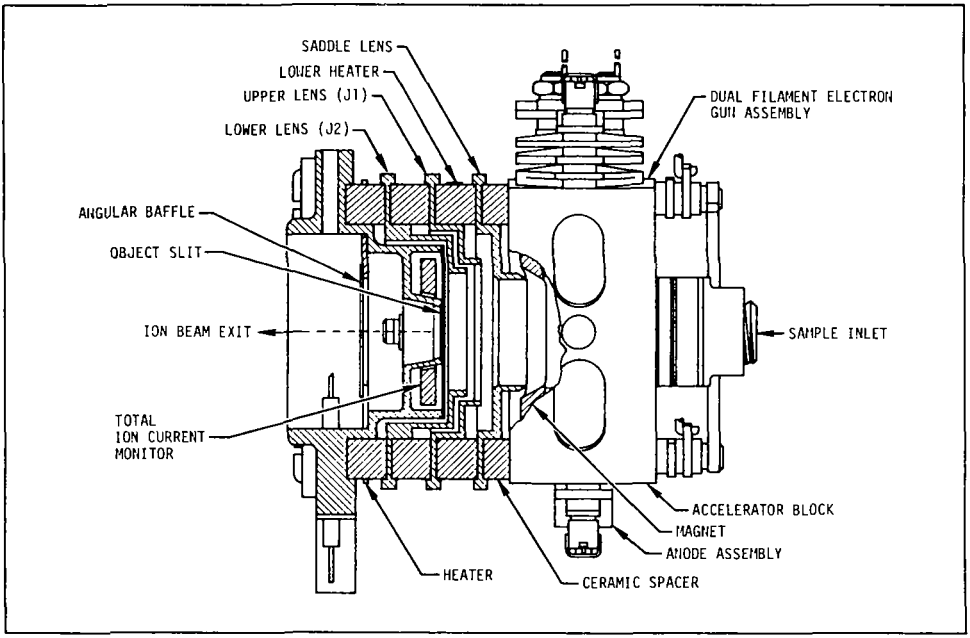

FIGURE 2. Ion Source Assembly

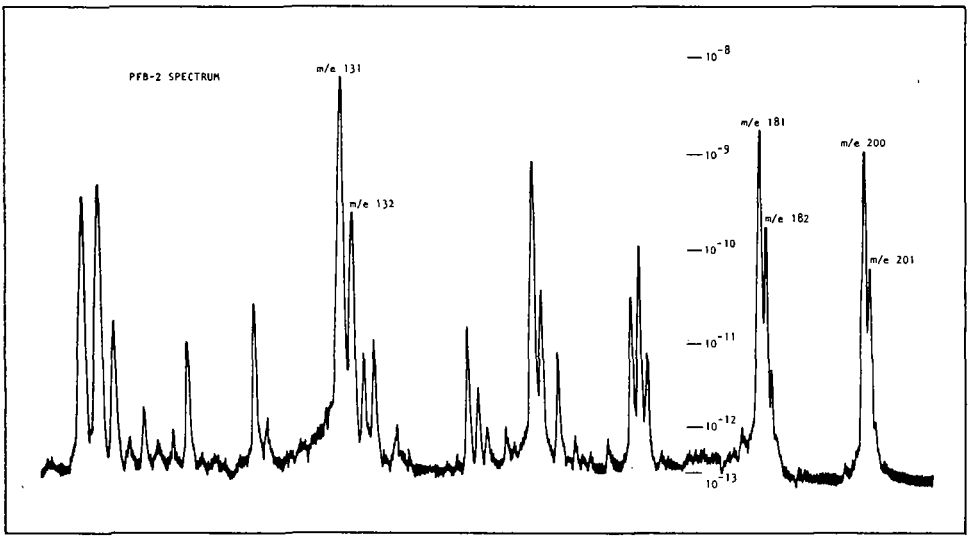

FIGURE 3. PFB-2 Spectrum from m/e 112 to m/e 201

The accelerating lenses are split to allow lateral motion of the ion beam. The total ion monitor, used for monitoring GC peaks, consists of a ring which intercepts the upper and lower portions of the ion beam.

The resolved ions are detected by a 12 stage electron multiplier located behind the image slit and is capable of a gain of 10^6. The image slit is 0.002" wide and is curved to compensate for Berry curvature.

The mass spectrometer is voltage scanning with an MV product of 28,000. It is designed to exponentially scan from m/e 12 to 200 in 10.2 seconds. However it is capable of scanning to higher masses and with faster scan rates.

The mass spectrometer efficiency for nitrogen (ions collected versus number of molecules flowing into ion source) is 10^{-5}. Its sensitivity is 7×10^{-6} amps/torr of pressure in the ion source, and which is equivalent to 1×10^{-6} amperes per nanogram per second of flow rate. The minimum detectable limit is 10^{-6} nanograms per second for nitrogen with a multiplier gain of 10^4. For the same multiplier gain, the sensitivity for the base peak of MEK, m/e 43, is 1.3×10^{-7} amperes per nanogram per second, and a minimum detectable limit of 8×10^{-6} nanograms per second of flow rate.

The instrument has a resolution of 400 at 5% peak height at m/e 12 and a resolution of 240 at m/e 200. Figure 3 shows a scan of PFB-2 sample covering the range of masses from m/e 112 to m/e 201.

This miniaturized high resolution, and high sensitivity mass spectrometer has potential as a portable trace contaminant monitor and may find application for environmental and industrial uses, as well as future manned space missions.

SEMIPERMEABLE MEMBRANE GC/MS INTERFACE

DUANE P. LITTLEJOHN
Universal Monitor Corporation
430 N. Halstead St.
Pasadena, CA. 91107

The use of semipermeable membranes as enrichment devices for Gas Chromatograph/Mass Spectrometer systems was first reported[1] in 1966 by P. M. Llewellyn. Since then several workers have built devices for their personal needs and several are in use today. Dr. William McFadden, in his book[2] on GC/MS techniques, has done an excellent review of progress to date on membrane enrichment systems by several workers.

This paper is devoted not to permeation theory but to performance of a dual stage system using 2 cm diameter membranes manufactured by Environmental Devices, 503 E. Bandell, Campbell, CA., and used with the Universal Monitor Corporation OLFAX ® II GC/MS/Computer System.

An enrichment device has value only if it can provide: an enrichment (E) of sample to carrier gas compatible with the vacuum system pumping capacity, a high yield (Y) of sample recovered and made available for analysis and time fidelity so as not to cause degradation of GC peak resolution.

Three compounds were chosen as characteristic of a range of compounds to illustrate the utility of the membrane system. Dodecane, Amobarbital and Cholesterol were used in the experiment.

EXPERIMENTAL

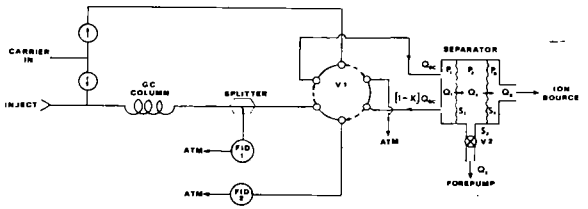

FIGURE 1

Figure 1 shows the flow diagram of the system used to measure, as a function of membrane temperature (T), the enrichment (E), the yield (Y) and the fractional recovery (K). Using the OLFAX II Mass Spectrometer, the time fidelity of the sample peak in the mass spectrometer is illustrated by comparing the time course of Cholesterol to the GC peak shape as measured by the flame ionization detector labeled FID_1.

In Figure 1, sample is injected on the GC column operated isothermally at 180°. The effluent is split 1:1 with one half going to FID_1 and the second half going to FID_2 through one port-pair of a Carle Instruments Inc. 1141 E. Ash Ave., Fullerton, CA. high temperature switching valve (V1) mounted in the detector oven and operated at 240°C. A second carrier flow is supplied to the input of the membrane separator through a second port-pair of the valve (V1) and exhausted to atmosphere through the third port-pair. By comparing the response of FID_1 and FID_2 to a single eluting peak with valve (V1) in the position shown, the relative sensitivity of the two detectors is established. The second carrier flow is used only to maintain one atmosphere of N_2 at the surface of the first membrane and consequently a fixed partial pressure of N_2 in the mass spectrometer ion source at a fixed membrane temperature.

With the valve (V1) in the alternate or dotted line position, eluting peaks (Q_{GC}) are directed across the surface of the first membrane, through the valve (V1) and then to the detector FID_2 and measured as a quantity $(1-K)Q_{GC}$. (K) is the fraction of (Q_{GC}) which permeated the first membrane

as the quantity (Q_1). As (K) approaches 1, Q_1 approaches Q_{GC} which means *total recovery of sample from the flowing stream by the first membrane.* The value of (K) will depend on the membrane temperature which affects solubility of the sample in the membrane material. The membranes used in this study are dual (2) cm diameter, and .025mm thick units made of hole-free, dimethylsilicone rubber supported mechanically by perforated metal grids.

In Figure 1, (Q_s) is the sample quantity reaching the mass spectrometer ion source as a result of a sample quantity to the first membrane of (Q_{GC}). Therefore, yield (Y) is given as:

$$Y = \frac{Q_s}{Q_{GC}} \quad \text{and:} \quad Q_s = Q_2 = (Q_1 - Q_3)$$

Q_3 is the fraction of Q_1 lost due to the vacuum pump required to pump away a major fraction of the carrier gas permeating the first membrane. The value Q_3 was established for nitrogen by measuring the pressure at the ion pump with the valve (V2) closed and open. Knowing pumping speeds of the ion pump, the pumping speed for nitrogen through the valve (V2) was established with the valve open (the normal operating condition). The pumping speed for the sample molecules of interest can then be calculated from the relation:

$$S_3 = S_{3(0)} \sqrt{\frac{M_1}{M_2}}, \quad \text{where:} \quad M_1 = 28 \text{ for } N_2$$

From these assumptions and known pressures and pumping speeds, the expressions for the operating parameters are derived as:

Yield: $$Y = \frac{Q_s}{Q_{GC}} = K\left(\sqrt{\frac{A^2}{4} + 1} - \frac{A}{2}\right) \quad \text{and:} \quad A = \frac{S_3 P_1}{K\, Q_{GC}}$$

Enrichment: $$E = \frac{Q_s}{Q_{GC}} \cdot \frac{F}{S_s} \cdot \frac{P_{atm.}}{P_s}$$

Recovery: $$K = 1 - \frac{FID_2}{FID_1}$$

and: S_s = source speed (N_2)
P_s = source pressure (N_2)
F = carrier flow

Multiple injections of Dodecane, Amobarbital and Cholesterol were made while the membrane temperature (T) was varied and the performance parameters calculated at the optimum temperature for each compound. These are given in Table 1 and plotted in Figure 2 normalized to the 100% value for each compound.

TABLE 1.....

COMPOUND	MW	T	K	YIELD	ENRICHMENT
DODECANE	170	110	.985	54%	2.8×10^4
CHOLESTEROL	386	230	.99	68%	5.3×10^4
AMOBARBITAL	226	130	.99	64%	3.8×10^4

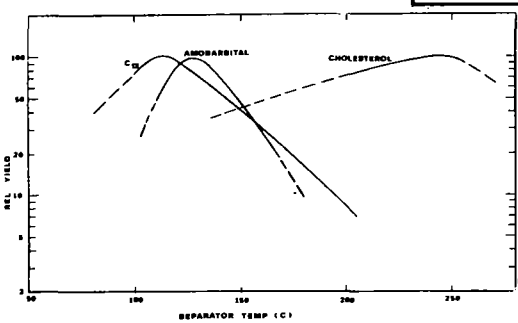

.....FIGURE 2

For Cholesterol the time course of the GC peak measured by FID_1 was compared to the time course of mass 275 of Cholesterol in the mass spectrometer by taking repeated scans of mass 275 at a known rate. The two resulting peaks were normalized and plotted on the same time scale and are shown in Figure 3.

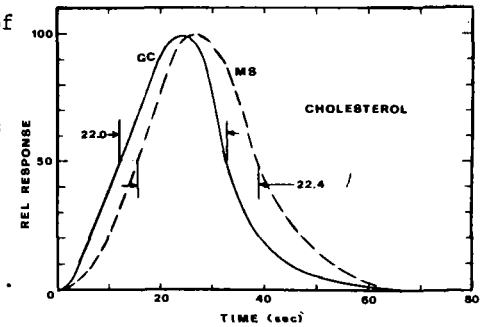

FIGURE 3.....

EVALUATION

The results given in Table 1 show that at the optimum membrane temperature (T), recovery (K) is very nearly 100% while yield (Y), even at enrichments greater than 10^4 is better than 50%. While the yield (Y) as a function of temperature, as shown in Figure 2, is acceptable even for the range of materials used, it is clear that a more ideal solution would be temperature programming of the membrane. This approach has been suggested and attempts have been made to place the membrane inside the column oven to take advantage of the programming control of the column. Indications are that although the programming rates are related, the absolute temperature values should be different suggesting that a separate temperature control is required for optimum conditions.

Finally the time course comparison of the GC and MS Cholesterol peaks show less than 2% peak spreading at half height and this includes the membrane effects plus pumpdown characteristics of the vacuum system which was operating at about 200°C.

CONCLUSIONS

The membrane enrichment device is of practical value given reasonable control of operating parameters. The range of compounds for which the device is useful in general, are those compounds which are separable by GC using silicone-like liquid phases such as SE-30 or OV-17. The operating temperature (to 300°C) places no serious restrictions on its use. A distinct advantage is the very high enrichment values which allow relatively small, clean and reliable ion pumping.

Since the carrier flow is independent of the vacuum system, full flexibility in carrier flow selection is allowed. Finally, lifetimes of years can be expected barring mechanical mistreatment.

REFERENCES

1. P.M. Llewellyn and D.P. Littlejohn, Combined GC/MS Techniques Symposium, Pittsburgh Conference on Analytical Chemistry and Applied Spectroscopy; February 1966.

2. W.H. McFadden, Techniques of Combined Gas Chromatography/Mass Spectrometry, Wiley-Interscience, New York 1973.

ACKNOWLEDGMENT

I would like to acknowledge the able help of Dr. R. H. Hertel and Mr. Christopher Kelly in the preparation of this work.

GC-MS INTERFACE FOR A CEC 21-104 MASS SPECTROMETER

John Zaletel and J. R. Knighton
Lorillard Research Center
Greensboro, N. C. 27420

This paper presents our effort to modify the CEC-104 mass spectrometer into an integrated GC-MS computer system. The initial stage of development had involved the construction and modification of a McCloskey probe assembly and a Teranishi separator. However, this unit could not be used because it developed leaks easily and had large dead volume. The valves and Swagelok Tee were replaced with a capillary tubing to reduce the possibility of cold spots and dead volume. Likewise, the Teflon probe tip was replaced because it would sag when heated and snag in the source.

The key functional part of the present assembly is a machinable ceramic tip. The tip has eliminated the breakage of the glass insulators inside the ion source and has prevented high voltage arcing in the source. At those points where couplings had to be used, the Swagelok fittings were replaced with Cajon fittings. With these fittings, assembly and disassembly can be accomplished repeatedly without creating leaks at pressures below 2×10^{-6} torr. It was difficult to achieve a seal between the metal heater blocks by simply compressing the Teflon gaskets because of the large surface area. In order to obtain a tight seal, the metal and Teflon surfaces were polished smooth and flat. The separator blocks were also polished to bond well with the membrane.

The separator utilizes a methyl silicone membrane in which about 0.75 cm^2 comes in direct contact with the gc effluent. Teranishi _et al_. recommend a surface area of 1 cm^2 or less to maintain an ion source pressure of less than 10^{-5} torr.

The capillary inside the hollow probe is resistance-heated through the capillary across the sleeve and through the probe shell. The original assembly proved unsatisfactory because the capillary would expand and contract when heated and cooled and would cause a short or break in the circuit. The sleeve on the probe tip was replaced by a Swagelok fitting and the capillary tube was insulated from the shell by Teflon tubing.

The CEC-104 mass spectrometer has severe deficiencies in the reproducibility and linearity of its magnet scan. Vassos and Ewing have traced the source of the non-reproducibility to an electrolytic capacitor. However, available software for computer data acquisition requires both a uniformly spaced and reproducible magnet scan.

Figure 1 shows how the magnet scan circuit was modified to meet these requirements. The magnet control amplifier board was replaced with a solid state amplifier board. A linear scan was obtained by using an operational amplifier which produces a linear ramp function with time. A linear ramp generator is added to the low limit set which sets the starting point for the scan. When the scan reaches the Hi limit set point, the circuit clamp maintains the output at that level. The

amplifier amplifies this signal and drives the optical isolator which generates the existing magnet control circuit.

The circuit was tested by measuring its static ability to focus on a specific ion. Initially, the instrument would drift completely off an ion peak within a short period of time. However, when a precision operational amplifier was inserted into the circuit, the stability of the magnet current was found to change only 400 ppm. The circuit was further evaluated by checking the pattern reproducibility of n-butane for three days. See Figure 2. For testing the high mass range, four sets of adjacent strong peaks from perfluoromethyltriazine (TFMT) were ratioed. The results show that these changes did not alter the original specifications for pattern reproducibility.

Figure 3 shows the circuit diagram used to interface the DuPont 093 mass marker with our CEC-104 mass spectrometer. The hardware supplied with the mass marker was mounted in the ion accelerator chassis. The voltage needed to operate the mass marker was obtained from terminal block 501 on the ion accelerator control chassis. Three resistors were changed to give the proper output voltage from an accelerating voltage of 1600 volts.

The mass marker was tested by running the spectra of perfluoromethyltriazine for 65 hrs. The mass marker is reproducible and stable for long periods of time without recalibration and is reliable even at the fastest scan rate of 3 sec/decade.

The venting system used in our GC-MS system is shown in Figure 4. This system permits a gas chromatograph to be operated independently or simultaneously with a mass spectrometer. A four way valve is operated manually to divert solvent peaks from the MS. Splitter A is attached to a heated collection vent which provides an exit connection to the separator. With this venting system, injections of 10-15 µl samples can be used without increasing the MS background of the sample.

Analysis of a smoke fraction revealed that certain compounds would not pass through the separator. Investigation was carried out with a wide class of compounds having a boiling point of 200°C to determine the cause. The study revealed that the cause was not due to the type of compound but rather a cold spot in the probe heater. After the cold spot was eliminated, peak distortion values for these compounds were quite normal for a membrane separator. This GC-MS combination was used to identify alkyl pyrazines from processed tobacco under various drying conditions. The FID and TIM chromatograms of the basic tobacco fraction shows that memory effects are very small in the interface unit.

ACKNOWLEDGMENTS: We wish to thank W. E. Routh, C. I. Lewis, and D. R. Smart for their participation, and D. B. Hughes (DuPont Instrument Div.) for valuable discussions on the electronic modifications.

A detailed account of this work will be submitted to Analytical Chemistry.

FIGURE 1

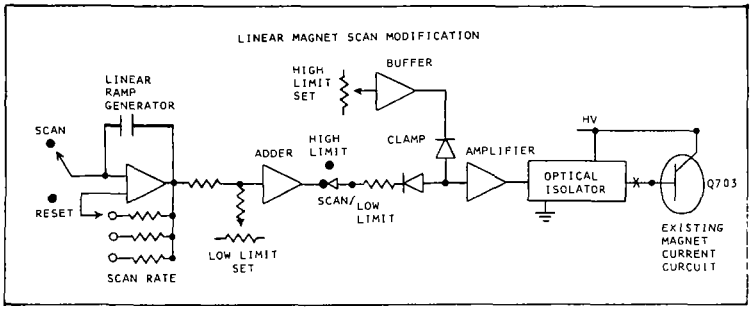

FIGURE 2

TEST OF PATTERN REPRODUCIBILITY

DAY	n-BUTANE	TFMT			
	$m/e\frac{58}{43}$	$m/e\frac{266}{285}$	$m/e\frac{102}{121}$	$m/e\frac{69}{76}$	$m/e\frac{31}{50}$
1ST	0.101	1.08	0.129	4.30	0.689
2ND	0.103	1.11	0.125	4.23	0.679
3RD	0.103	1.11	0.124	4.29	0.687
AVERAGE	0.102	1.10	0.126	4.27	0.688
% REL SD	1.12	1.57	2.01	0.89	1.39

FIGURE 3

DIAGRAM FOR INTERFACING DUPONT 21-093 MASS MARKER

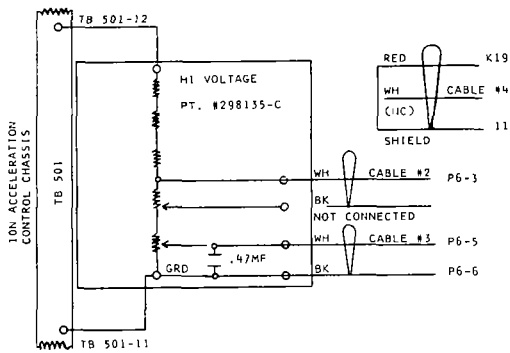

FIGURE 4

HP MODEL 5750 GC INTRODUCTION SYSTEM TO MS

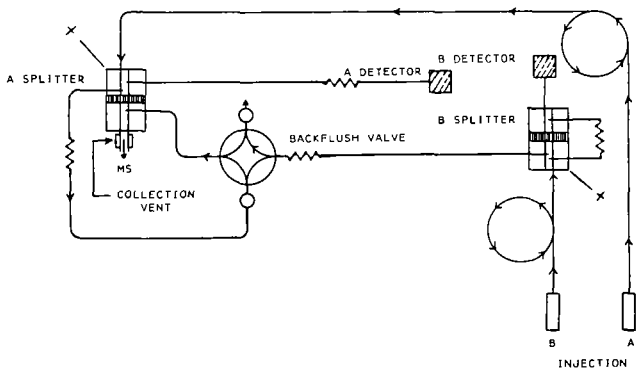

THE USE OF LEAKY DIELECTRICS FOR THE SEPARATION OF FRINGE FIELDS OF QUADRUPOLE MASS FILTERS

Wade L. Fite
Extranuclear Laboratories, Inc.
Pittsburgh, Pennsylvania 15238

Maxwell's equations reveal that materials with properly chosen dielectric constants and conductivities have the capability of shielding against DC and low frequency electric fields while not shielding or only partially shielding against RF fields at mass filter frequencies. The use of such materials near the ends of quadrupole mass filters can permit the ions to "see" the RF fields at a further distance than the DC fields and accomplish, in effect, a delayed DC ramp for entering and emerging ions. Two-dimensional solutions for the scalar potential inside a cylindrical tube of such a material yield the criteria for selection of the material and its geometry. Practical considerations of materials are also discussed. These effects, particularly as they apply to ELFS (U.S. Patent No. 3,867,632), are briefly treated. Experimental results verifying the theoretical conclusions are presented.

A full paper on this subject will be published elsewhere.

General Time Focusing Relations, a Classical Uncertainty Relation, and the Evaluation of the limits of Time-of-Flight Mass Spectrometers

Ronald P. Stein

Department of Physics, Tuskegee Institute, Ala. 36088*

The best possible time resolution (minimum) Δt of linear time of flight mass spectrometers has been analyzed.[1] This Δt was derived from a linear time focusing equation. Here, new time focusing equations for the centeral force system and a particle on a line are presented. Also, a very general time focusing relation appears to exist. The Δt in the linear case is found to have a form very closely related to two basic forms of the Heisenberg uncertainty principle, or; $\Delta x_o \Delta p_o \leq \Delta E_o \Delta t$ where ΔE_o is related to the uncertainty in the initial ion energy. With this new relationship, it is easier to assess the actual versus best possible performance of commercial and other existing time of flight mass spectrometers, and to quickly assess whether a new design idea is significantly better than those presently available.

A Classical Uncertainty Relation

Consider an ion or swarm of ions (or particles).

If:
1. the forces on the particle are conservative and constant in time
2. the motion of the particle is one-dimensional
3. the uncertainty in initial position Δx_o and the uncertainty in initial velocity Δv_o of the particle are uncorrelated

then[1]

$$v_o \frac{\partial t}{\partial x_o} + \frac{F_o}{m} \frac{\partial t}{\partial v_o} + 1 = 0$$ one-dimensional focusing equation

and since

$$\Delta t = \frac{\partial t}{\partial x_o} \Delta x_o + \frac{\partial t}{\partial v_o} \Delta v_o$$

We minimize Δt^2 by varying $\partial t/\partial x_o$ and $\partial t/\partial v_o$ and get

$$\Delta E_o \Delta t \geq \Delta x_o \Delta p_o$$ classical uncertainty relation

(This is Stein's[1] equation 16 with the time lag set to zero).

where: Δx_o = uncertainty in initial ion position
$\Delta p_o = m\Delta v_o$ = uncertainty in initial ion momentum
Δt = uncertainty in time of arrival of the ion at a detector
ΔE_o = uncertainty in the initial ion energy

* Now at Box 442A, Route #6, Carrollton, Georgia 30117

where $$\Delta E_0^2 = (F_0 \Delta x_0)^2 + (m v_0 \Delta v_0)^2$$

or

$$\Delta E_0^2 = \Delta U_0^2 + \Delta K_0^2$$

where,

ΔU_0 = uncertainty in initial ion potential energy
$\Delta K_0 = m v_0 \Delta v_0$ = uncertainty in initial ion kinetic energy

With the above identification of variables, the classical uncertainty relation makes a much clearer statement about the minimun Δt obtainable than Stein's equation 16. Knowing the uncertainty in the ion's source conditions $\Delta x_0, \Delta p_0, \Delta E_0$, it is now possible to predict the minimun uncertainty in t at the collector for one-dimensional constant energy time-of-flight mass spectrometers. This is very powerful since the best preformance (best time focusing) can now be evaluated without knowing the details of how that time focusing is achieved. Also, the uncertainty relation tells a mass spectrometrist when he has achieved the best time focusing. A more detailed discussion of this uncertainty relation is given in my thesis.[2]

Time Focusing Equations

The above classical uncertainty relation applies to a very limited class of time-of-flight mass spectrometers. However, the author has found this uncertainty relation to hold in all time-of-flight mass spectrometers in the published literature with only minor qualifications. Perhaps these qualifications can be clarified by finding more general uncertainty relations. This work has been started with the derivation of more time focusing equations. To sumarize the results:

If
1. the forces are conservative
2. the motion of the ion one-dimensional

then, by differentiating an integral expression for t, it can be shown,[1,2]

$$v_0 \frac{\partial t}{\partial x_0} + \frac{F_0}{m} + \frac{\partial t}{\partial v_0} + 1 = 0$$ one-dimensional focusing equation

If
1. the forces are conservative and central
2. the angular momentum ℓ is held constant

then by differentiating an integral expression for t, it can be shown,[2]

$$\dot{r}_0 \frac{\partial t}{\partial r_0} + \left[F_0 + \frac{\ell^2}{m r_0^3}\right] \frac{1}{m} \frac{\partial t}{\partial \dot{r}_0} + 1 = 0$$ central force focusing equation

If 1. the forces are conservative
2. the particle is constrained to a line

then by differentiating an integral expression for t, it can be shown,[2]

$$\dot{s}_o \frac{dt}{ds_o} + \frac{F_{s_o}}{m} \frac{dt}{d\dot{s}_o} + 1 = 0$$ particle on a line focusing equation

F_{s_o} = component of the force along the line on the particle at s_o.

A General Time Focusing Equation

The above three focusing equations are basically one-dimensional. A new approach is needed to get a more general equation. To get the one-dimensional focusing equation, an integral expression for t was found. It is possible to obtain this one-dimensional result without finding an integral expression for t.[2] This approach can be generalized to three-dimensional motion.

It was found that if:

1. the flight time is a continuous function of the initial position $\vec{r}_o$ and initial velocity $\dot{\vec{r}}_o$
2. the fields do not vary with time
3. Newton's laws hold

Then, $$\dot{\vec{r}}_o \cdot \frac{dt}{d\vec{r}_o} + \frac{\vec{F}_o}{m} \cdot \frac{dt}{d\dot{\vec{r}}_o} + 1 = 0$$

A simple equation for time varying fields probably exists. The above three-dimensional time focusing equation can now be used to develop a general classical uncertainty relation. This work is not yet complete.

Work completed at Pensylvania State University, with the partial support of NASA Grant NGL-39-009-032.

References

1. Ronald Stein, Int. J. Mass. Spectrom. Ion Physics 14, 205 (1974)
2. Ronald Stein, "The Limits of Time-of-Flight Mass Spectrometry: General Time Focusing Relations, and an Analysis of Cylindrical and Spherical Geometries," Doctorial Disseration, Pennsylvania State University, University Park, Pennsylvania 16802, (1974). Copies are available from the author at a nomial charge to cover printing and shipping. ($5.00)

A New Approach to Time-of-Flight Mass Spectroscopy

David F. Torgerson and Ronald D. Macfarlane
Cyclotron Institute and Department of Chemistry
Texas A&M University, College Station, Texas 77843

Time-of-flight mass spectroscopy is not normally associated with precision work due to well-known limitations. In this paper we describe the ^{252}Cf Plasma Desorption TOF mass spectrometer (PD) which overcomes some of these limitations, and its application to non-volatile biomolecules.

A schematic diagram of the mass spectrometer is shown in Fig. 1. Samples are dissolved in an appropriate solvent and are evaporated to dryness onto a 1 μm Ni foil to a thickness of ~100 μg/cm^2. The Ni sample foil is then aligned in the mass spectrometer with a ^{252}Cf source and an 8 m long TOF tube. The sample foil is maintained at ±10 kv depending on the polarity of the ions to be studied. Volatilization and ionization of the sample are accomplished using fission fragments from the ^{252}Cf source which comprise 3% of its total decay. Geometries are chosen such that for a fission fragment passing through the sample foil, the nearly colinear complementary fragment is detected using a scintillation counter from which a time zero marker is derived. Ions produced on the sample foil are immediately accelerated to 10 kv through a gridded lens system into the 8 m TOF tube. Ion containment is effected by using a thin wire centered on the axis of the tube on which ±10 v is maintained depending on the ion polarity. The resulting radial field maintains the ions in a spiral orbit about the wire with no change in their transverse velocities. Single ions are detected at the end of the tube using a windowless CEMA array. Time differences between initial ionization and detection in the CEMA array are measured using a time digitizer having a resolution better than 1 x 10^{-12} seconds. A mass spectrum is formed by storing and adding the results for each fission event in a 4096 memory array. Typically, 10^6 fission events are used to develop a mass spectrum. Since ions are formed on the same potential surface and at the same planar position, space-time focusing is automatically achieved. To volatilize a non-volatile biomolecule, two criteria must be fulfilled. Sufficient energy must be available to overcome the various forces holding the molecule in the solid and the energy must be deposited quickly enough to favor volatilization over decomposition.[1] As a fission fragment deposits 10 MeV of energy on a time scale of ~10^{-13} seconds in a 100 μg/cm^2 sample, both these criteria are apparently met and thermally labile molecules can be characterized without derivitization.

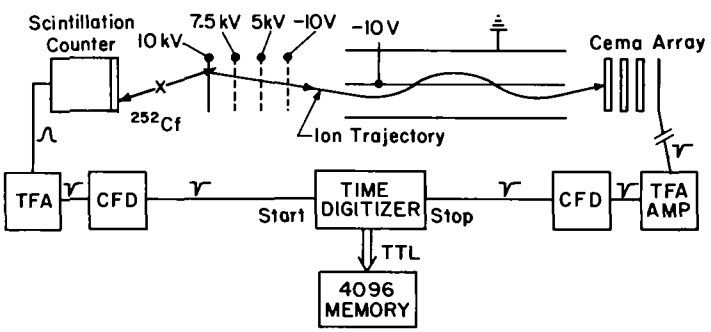

Fig. 1

Several classes of non-volatile biological molecules have been studied including amino acids,[2] peptides, nucleosides, nucleotides, organic salts, and other natural product molecules. As an example, Fig. 2 shows the ^{252}Cf PD mass spectrum of the nucleoside guanosine which, due to its high polarity, does not yield a parent ion using slow heating techniques.[3] In the present case, however, we observe an intense $(M + 1)^+$ quasi-molecular ion and an even stronger $(M - 1)^-$ quasi-molecular ion in the negative ion spectra. Fragmentation peaks are observed at lower masses which are associated with the base moiety.

We believe that ionization occurs primarily from proton transfer between parent ions once vaporization has occurred. This accounts for the presence of positive and negative ions in comparable abundances.

As ions are formed and detected in a consistent manner (same potential and flight path), masses of individual peaks can be measured to better than ~0.002 amu using statistical methods.[4] For example, a fragment in the negative ion guanosine spectrum at m/g 133 has been shown to be due to the loss of NH_3 from the base moiety and is not the sugar moiety, less H, which has the same nominal mass.

We should like to acknowledge the Robert A. Welch Foundation and the U. S. ERDA for financial support of this work.

References

1. R. J. Beuhler, E. Flanigan, L. J. Green, and L. Friedman, J. Amer. Chem. Soc. 96:12, 3990 (1974).
2. D. F. Torgerson, R. P. Skowronski, and R. D. Macfarlane, Biochem. Biophys. Res. Comm. 60, 616 (1974).
3. S. M. Hecht, A. S. Gupta, and N. J. Leonard, Anal. Biochem. 38, 230 (1970); P. Brown, G. R. Pettit, and R. K. Robins, Org. Mass Spectrom. 2, 521 (1969).
4. D. F. Torgerson, R. D. Macfarlane, and L. S. Spiegel, Proceedings of the Fifth International Conference on Atomic Masses and Fundamental Constants, Paris (1975), in press.

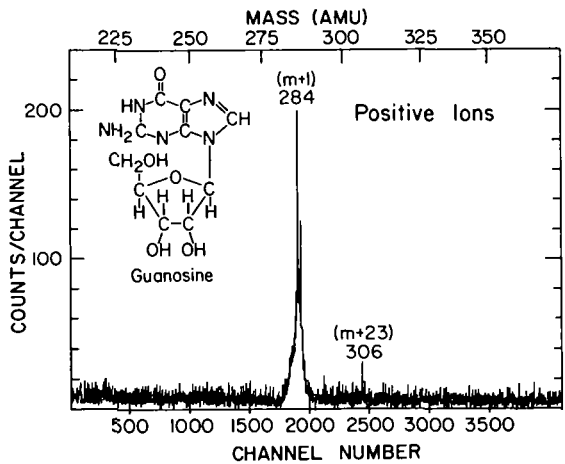

Fig. 2

MINIATURE TIME-OF-FLIGHT MASS SPECTROMETER FOR ION COMPOSITION MEASUREMENTS IN THE LOWER IONOSPHERE*

Bruce R. Kendall and Robert F. Reiter

The Pennsylvania State University
Department of Physics
and
Ionosphere Research Laboratory
University Park, Pennsylvania 16802

Extended Abstract

Most existing ion mass spectrometers for use in the altitude range 70-90 km utilize differential pumping to reduce internal pressures. An alternative approach is to use special types of mass spectrometers which can operate effectively while immersed in a high-density molecular environment. Once such type, a direction-focusing time-of-flight mass spectrometer of wedge configuration, appears particularly suitable for applications where extreme compactness and high sensitivity are required. It has been analyzed theoretically and subsequently developed into a form suitable for use on small sounding rockets. The total weight forward of the rocket motor is 7.5 Kg, including batteries, transmitter and telemetry equipment. The resolving power is approximately 8, which is sufficient to distinguish between many of the main ionic species thought to be present. Results of the first two flights with this apparatus suggest that a high proportion of the ions in the D-region have masses above 250 a.m.u.

*Research supported by NASA Grant No. NGL39-009-032.

Photoionization Mass Spectrometric Study of CO_2 and H_2O in the Extreme Ultraviolet by P. L. Kronebusch and J. Berkowitz.

This study was designed to investigate the fragmentation behavior of the molecular ion states formed by 584 Å to 304 Å incident radiation. The apparatus used in the experiments consisted of a hollow cathode lamp (which generated eight approximately equally spaced lines between 584 Å and 304 Å), a normal incidence vacuum ultraviolet monochromator, and a 12" radius magnetic mass spectrometer. It is to be noted that an ionic kinetic energy discrimination existed for values greater than 1 eV. Thus, in those cases for ions with such energy, the results presented here should be regarded as lower limits. However, few of the fragments investigated had more than thermal energy.

CO_2

The 584 Å (21.2 eV) photoelectron spectrum (Fig. 1) of CO_2 indicates the accessible states of CO_2^+ and their relative abundance. Because the states X, A, and B cannot dissociate and are thus observed as CO_2^+, only C will dissociate into the competitive channels, CO^+ and O^+. Our results agree well with the branching ratios given by Eland, O^+ = 0.045 total ionization and CO^+ = 0.025 total ionization. The higher energy states of importance are given in the x-ray (1254 eV) photoelectron spectrum of CO_2 (Fig. 2). The broad band between 30-40 eV indicate Σ_g and Σ_u states, 25-like molecular orbitals on C and O. This band decomposes predominantly into C^+ + 20 as indicated by a significant inset of C^+ at 30 eV(as opposed to the C^+ + O_2 channel possible at 22.7 eV) and by the continued growth of C^+, relative to the other ions, in the 30-40 eV range.

H_2O

The 584 Å (21.2 eV) photoelectron spectrum of H_2O is given in Fig. 3. The first two states cannot dissociate and are observed as H_2O^+. The thermochemical thresholds for the channels OH^+ + H (18. 11eV), H^+ + OH (18.72eV) O^+ + H_2 (18.65 eV) fall in the middle of the third accessible state. Our data indicate the OH^+(0.29 total ionization) and H^+(0.05 total ionization) as the competitive channels. The O^+ is very weak (0.0009 total ionization). These results agree well with Dibeler, et al. and Cairns, et al. except for the O^+ intensity, in which case our data average theirs.

Lorquet and Lorquet have recently introduced a theory for the fragmentation of this third state of H_2O^+, which is based on a predissociation model. This theory predicts a strong isotope effect in the formation of H^+ from H_2O as opposed to D^+ from D_2O, favoring the lighter isotope. No such isotope effect was observed with D_2O (experimental conditions were kept constant). Both the H^+ and the D^+ intensity were approximately 5% of the total ionization, a value larger than that predicted by the Lorquet theory even for the lighter isotope. It should be noted that the recent data of Eland also disagrees with the predicted isotopic yields.

As with CO_2 the x-ray photoelectron spectrum (through not given here) shows a large broad peak, designated as $1a_1$ in the 30-40 eV region. In addition to the processes described earlier, our data indicated the opening of the O^+ + 2H channel at 23.13 eV. The O^+ intensity slightly increased between 23.13 eV and 27.8 eV, with a rapid increase between 27.8 eV and 40.8 eV. In the latter region, the OH^+ and H^+ intensities dramatically decreased to such a degree that, at 40.8 eV, the O^+ channel matched the H^+ channel in

in relative intensity. Thus, from our experimental evidence, it is concluded that the $1a_1$ state of H_2O^+ decomposes predominantly via the O^+ + 2 H channel.

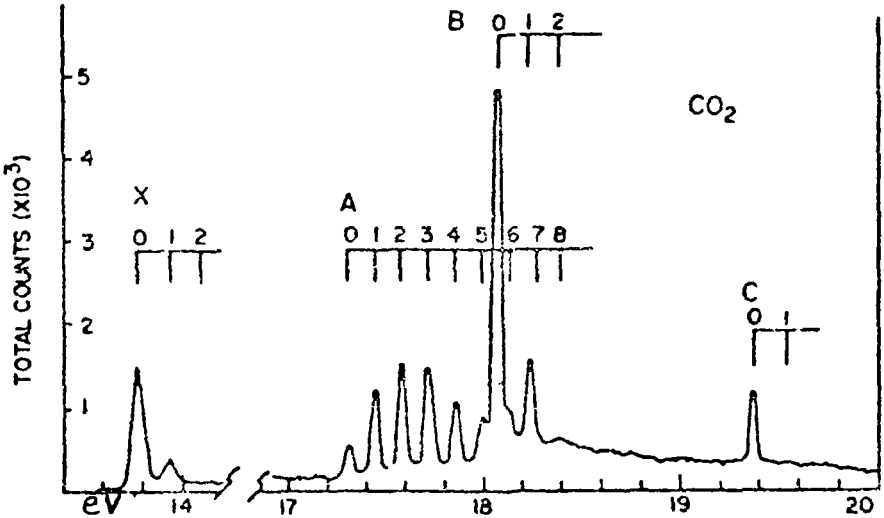

Fig 1.

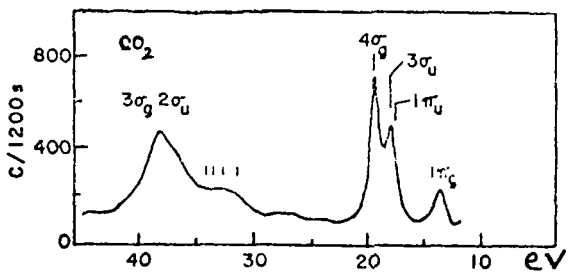

Fig 2

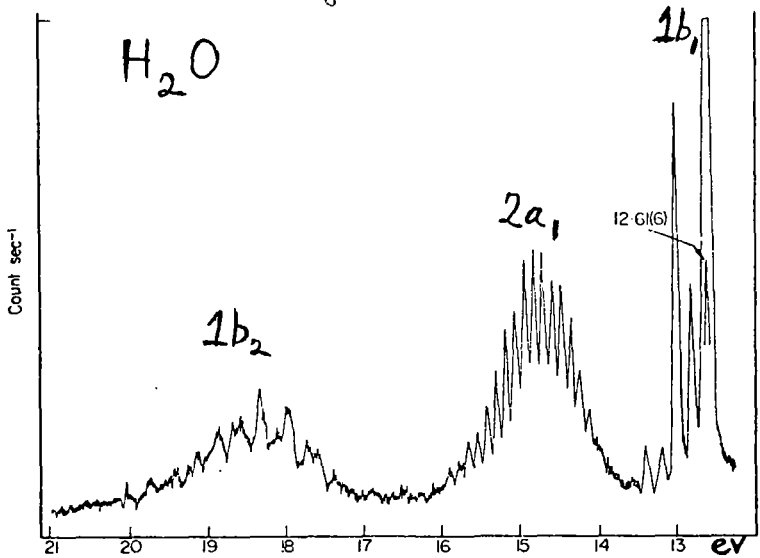

Fig 3

Ion-Pair Formation in H_2, HD, and D_2 by J. Berkowitz and P. L. Kronebusch

In 1967 we first reported the ion-pair formations, H^+-H^-, in the photoionization of H_2 in the threshold region (700-715 Å). It was a weak process, 10^{-3} of the H_2^+ intensity and displayed structure characteristic of a predissociation. The threshold appeared to be the thermodynamic threshold. This was later verified by the higher resolution work of McCalloh and Walker. They also speculated that the Rydberg levels converging to H_2^+ (ν = 9, N = 0) contributed to the predissociation near threshold. Since the limit (17.3365 eV) was just above the threshold for $H^+ + H^-$ from H_2^+ (17.3223 eV), most likely there is an accumulation of Rydberg levels near this threshold, forming a quasi-continum. For D_2, the thermodynamic threshold is slighty higher (17.4038 eV). Due to the smaller vibrational quanta in D_2^+, the predissociating Rydberg levels converge to D_2^+, V = 12 or V = 13. Peek's calculated Franck-Condon factor for $D_2(\nu'' = 0)$ to $D_2^+(\nu' = 13)$ is one-half that of $H_2(\nu'' = 0)$to H_2^+ (ν' = 9), which accounts for the correspondingly weaker intensity of the ion-pair process in D_2.

Intramolecular isotope effects, in HD, are reflected in the competing ion-pair channels, $H^+ + D^-$ and $H^- + D^+$. The thresholds are slightly displaced, $H^+ + D^-$ at 17.3575 eV and $H^- + D^+$ at 17.3616 eV. The predissociating Rydberg levels most likely converge to HD^+, v' = 10. The Franck-Condon factors for these levels are somewhat smaller than for H_2^+, v' = 9 but due to the two existing channels, the ion-pair intensities will be approximately halved. Fig. 1 shows D^- from HD, the lower energy process. The resolution is only 0.8 Å with fine structure approaching resolution. Fig. 2 shows H^- from HD, the higher energy process. This was more difficult to analyze because of a background due to the process $e^- + HD \rightarrow H^- + D$, a much more favorable process than $e^- + HD \rightarrow H + D^-$. Since the electrons come from the photoionization process, the background was minimized by reducing the pressure as much as possible. (Of course, the signal to noise ratio is correspondingly affected).

Within the uncertainty of the experiment, the H^-channel does not appear at higher energy as expected. The shape of the spectrum in both channels appears very similiar. To assess the isotope effect on the relative intensity of the two channels, the system was calibrated for the two species investigated. This was accomplished by examining H^+; H^- from H_2 intensity, which should differ only because of instrumental effects. Of course, all studies were normalized for pressure and light intensity in addition to maintaining the apparatus at identical, experimental conditions.

Our results indicate the H^-channel favored over the D^-channel by a factor of approximately 1.41 or $\sqrt{2}$, though the higher energy channel is the H^- channel. There is, as of yet, no satisfactory explanation for this fact. Also, a comparison of the ion-pair process in $H_2$the direct photoionization process in H_2 was made. Knowing the absorption coefficients, the integrated oscillator strength for the ion-pair formation in H_2 was found to be $0.8 * 10^{-4}$.

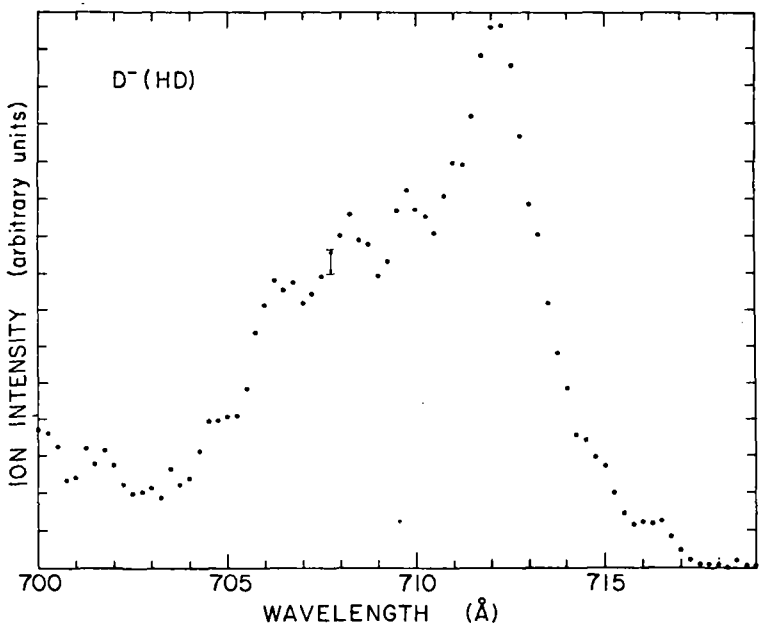
D⁻ (HD)
ION INTENSITY (arbitrary units)
700
705
710
715
WAVELENGTH (Å)

FIG 1

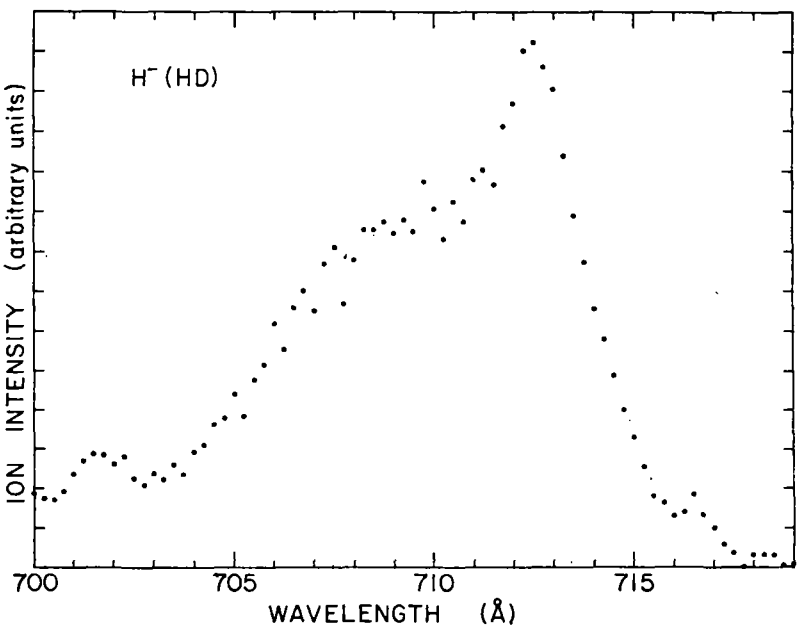
H⁻ (HD)
ION INTENSITY (arbitrary units)
700
705
710
715
WAVELENGTH (Å)

FIG 2

Formation of Fragment Ions by Autoionization and Predissociation of Molecular Rydberg States

K. E. McCulloh and Vernon H. Dibeler
National Bureau of Standards
Washington, DC 20234

ABSTRACT

It has been observed on the basis of photoionization studies that fragment-ion thresholds for a number of molecules occur at energies where the photoelectron spectra reveal no vertically accessible states. Rydberg structure observed just above threshold on the photoion yield curve of O^+ from CO_2 suggests the occurrence of predissociation coupled with autoionization. Similar behavior is inferred for H_2S and ketene. The observed photoionization yield of OH^+ from H_2O rises more rapidly from threshold and approaches the plateau at lower photon energy than does the yield curve calculated from the photoelectron spectrum on the assumption that OH^+ is produced exclusively by predissociation of $H_2O^+(^2B_2)$, suggesting that Rydberg states converging to $H_2O^+(^2B_2)$ make significant contributions to OH^+ production. In the photoionization of N_2O between 18 and 20 eV the curves for the three fragment ions NO^+, N_2^+, and O^+ exhibit strinkingly similar Rydberg structure. Autoionization to a common precursor of the three fragments is suggested.

DOUBLE IONIZATION IN THE RARE GASES INDUCED BY ELECTRON IMPACT

L.P. Johnson and J.D. Morrison

Department of Physical Chemistry, La Trobe University,
Bundoora, Victoria, 3083, Australia

Ionization efficiencies for the singly charged rare gases excited by electron impact have been extensively studied. Changes in gradient in the curves can be correlated with excited electronic states of the ions, arising by direct ionization processes, while other structure is accountable in terms of autoionization processes.

Multiply-charged rare gases have also been studied but since the cross section for such ionization are very much lower than those for single ionization, the experimental data are much less satisfactory.

In the present work, a quadrupole mass spectrometer was used in combination with a computer data-collection system, to obtain ionization efficiency curves for doubly charged neon, argon, krypton and xenon. The electron source used for ionization was a rhenium filament, giving electrons with an energy spread of about 0.6 eV half width. The curves presented are each the result of time averaging 2000 individual sweeps of the IE curves, sampled at 1024 points. By this means the signal to noise ratio is significantly improved. The energy scale in each case is calibrated by comparison with a singly-charged rare gas ion.

The first derivative IE curves obtained for Ne^{++} and Kr^{++} are shown in Figures 1 and 2. The values for the various states of the doubly charged ions recorded spectroscopically are shown above each curve.

In all cases, the lowest double ionization potentials are within 0.1 eV of the spectroscopic value. The curves consist of linear segments, which are consistent with a square-law threshold behaviour. In the case of the excited levels, the agreement is poor or non-existent particularly for the $^1D_2$ state. Other structure is present in the curves, whose shape suggests the presence of delayed ionization processes. There are two such processes possible:

$$Ne + e \rightarrow Ne^{+*} + 2e \rightarrow Ne^{++} + e$$

$$Ne + e \rightarrow Ne^{**} + e \rightarrow Ne^{++} + 2e$$

These would be expected to have differing threshold behaviour, the signal to noise ratio is still not good enough to decide which is present.

Spectroscopic data have always been used as the yardstick by which all electron impact measurements are assessed, and the present discrepancy is of some concern. Either our ideas of threshold laws need modification or the spectroscopic values are in error. In this connection it is perhaps significant that the assignment of the $^1D_2$ level depends on a single intercombination line in the visible, observed in a nebular spectrum. It is possible that these assignments may be incorrect.

It is also possible that there may be so much autoionization present that it completely submerges the upper direct ionization processes. A more careful examination is presently being made using monoenergetic electrons, in an attempt to clarify this.

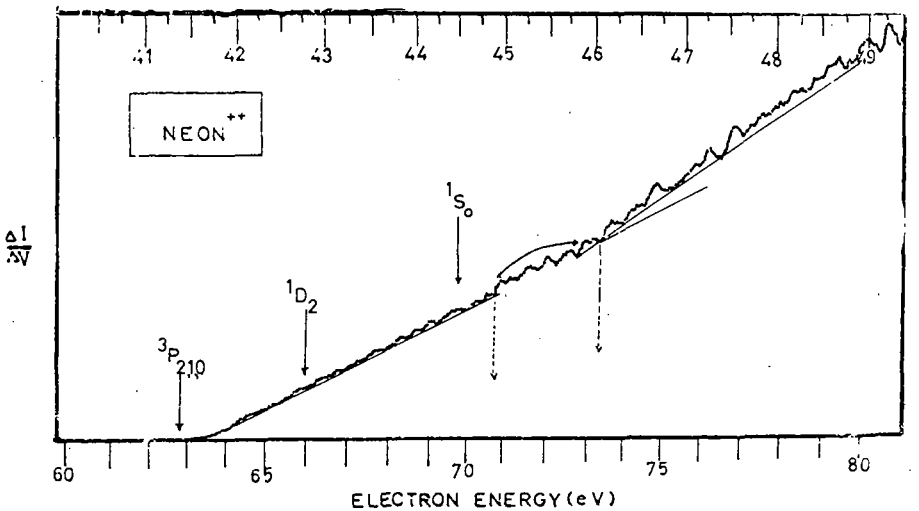

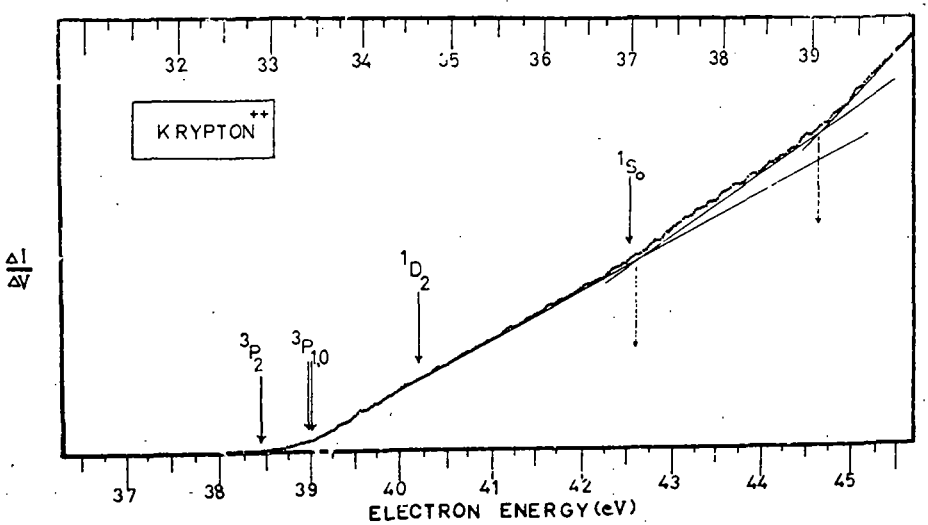

Determination by charge-transfer collisional spectroscopies of the electronic states present in a mass-analyzed ion beam

Jacqueline APPELL*, Marie DURUP**, PHAM Dong* and Jean DURUP*

*Laboratoire des Collisions Ioniques† and **Laboratoire de Physico-Chimie des Rayonnements†, Université de Paris-Sud, 91405-Orsay, France

Charge transfer spectroscopies may be developed in various ways, including spectroscopy of the energy levels of negative ions.

In experiment A the primary positive ions undergo neutralization in a first chamber where they become fast neutrals, the remaining ions being ejected by a deflecting field; in a second chamber the neutrals undergo a second collision where they are reionized, then the ions are energy-analyzed by a magnetic sector. The K. E. loss spectrum of Ar^+ ions neutralized on Ar and reionized on O_2 at 3 keV is shown in fig. 1. Two peaks are observed which we ascribe to primary Ar^+ ions in ground or metastable states. This illustrates the possibility in principle to measure the metastable content of the primary Ar^+ beam. But this requires some calibration; although both peaks are of the same magnitude the population of the metastable state may be much smaller than that of the ground state, since the former ions undergo two processes without much energy change, whereas the latter ones undergo first an efficient resonant charge transfer and thereafter a very inefficient one because very endoenergetic.

The left-hand spectrum of fig. 2 is a K. E. spectrum of H^- from collisions of H^+ on Xe in one chamber; it is identical to those obtained by Fournier et al (2). Now in the two-chamber experiment the two events of the double-collision process can be investigated separately. This is illustrated on the right-hand spectra of fig. 2; the two possible states of Ar^+ are too close to each other to be distinct and the two peaks in each spectrum correspond to the formation of Xe^+ either in the $^2P_{3/2}$ or in the $^2P_{1/2}$ state.

Reionization of H (from neutralization of H^+ on Ar) on various targets (O_2, CO, Ar, H_2) at 3 keV was investigated with the hope of seeing ion-pair formation on O_2. Actually a single H^+ kinetic-energy peak appears, at the position corresponding to about zero-energy electron ejection, apparently through autoionization of the H^++target quasi-molecule. Only at lower collision energy (1 keV) was some splitting of the $H + O_2 \rightarrow H^+ + O_2^-$ or $O_2 + e^-$ peak observed.

In experiment B which is a single-chamber experiment double charge transfer spectra of O^+ + Ar were registered. The one-collision spectra are too intricate to be of much interest but the two-collision spectra show the various states of O^+ present in the incident beam. An absolute calibration of the energy scale using the primary O^- peak permits an unambiguous identification of the peaks. As can be seen in fig. 2 the relative amounts of the various states (the ground state $^4S°$ and the metastable states $^2D°$ and $^2P°$) are different according to the molecule used for production of the O^+ ions.

†Associated to the C.N.R.S.

Interesting conclusions on the mechanisms of dissociative ionization can be drawn but here again any quantitative analysis requires a knowledge of the cross sections for each state. Interpretation of such spectra has to be taken with caution: the evolution of the spectrum with increasing target gas (Ar) pressure shows that the relative magnitude of the ground state peak increases with respect to the metastable one. The position of a given peak reflects the energy balance of the whole process and, since there is only one stable state of the product O^-, each peak corresponds to a given initial state of O^+ as indicated in fig. 2 whatever be its intermediate history. The explanation for the faster increase of the ground state peak with target gas pressure is then that the ion first undergoes a state-changing collision which converts it into a metastable state which will simply have a higher cross section for the double charge transfer process or conversely that the metastable state undergoes a state-changing collision which converts it into the ground state.

This result shows that collisions with a change in the total spin, $O^+(^4S°) + Ar \rightleftarrows O^+(^2D° \text{ or } ^2P°) + Ar$, do take place significantly although the spin-orbit coupling is small for light atoms. The few known examples of spin-changing collisions have in common that the transition takes place between molecular states of the same electron configuration, with unpaired electrons on two orbitals of different symmetry. A simple expression for the cross section in such systems can be derived in the semi-classical formalism.

References

(1) J. Appell, J. Durup, F. C. Fehsenfeld, P. Fournier, J. Phys. B 7 (1974) 406 and references therein.

(2) P. Fournier, C. Benoit, J. Durup, R. E. March, C. R. Acad. Sci. 278B (1974) 1039.

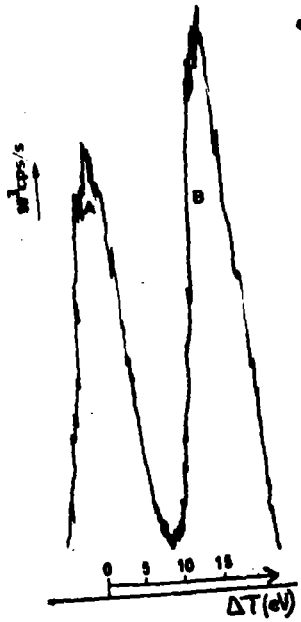

$O^+(O_2) \xrightarrow{Ar} O^-$

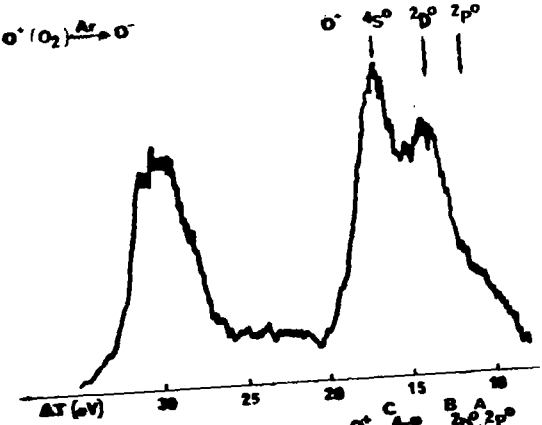

$O^+(CO_2) \xrightarrow{Ar} O^-$

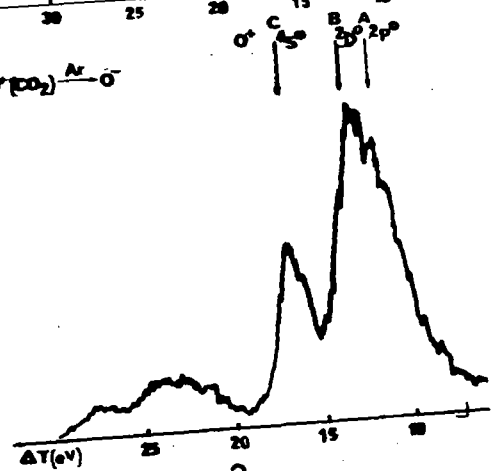

A $\begin{cases} Ar^{+*} + Ar \rightarrow Ar^* + Ar^+ \\ Ar^* + O_2 \rightarrow Ar^+ + O_2^- \end{cases}$

B $\begin{cases} Ar^+ + Ar \rightarrow Ar + Ar^+ \\ Ar + O_2 \rightarrow Ar^+ + O_2^- \end{cases}$

Figure 1

Figure 3

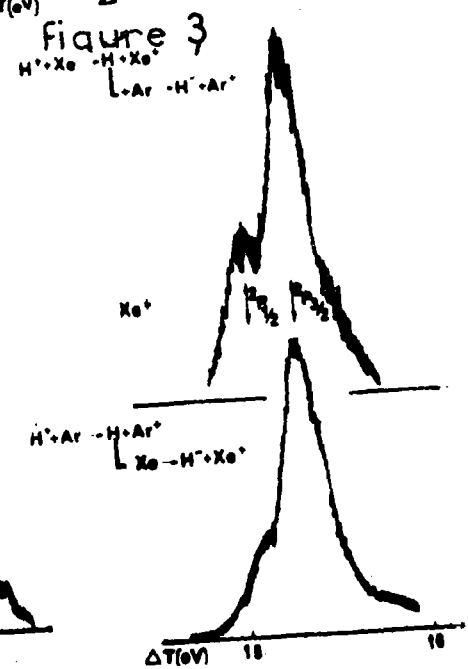

Figure 2

Kinetic Energy Distributions from Unimolecular Dissociations.* CORNELIUS E. KLOTS, Oak Ridge Natl. Lab., Oak Ridge, Tenn. 37830

Recently reported measurements of the distribution of kinetic energies shared by the products of unimolecular dissociations and of ion-molecule collision complexes have been analyzed within the framework of quasi-equilibrium theory. The available examples illustrate rather nicely the several limiting cases[1] which arise from the simplest of all possible models - the Langevin collision model. Data[2] for the dissociation $C_6H_5CN^+ \rightarrow C_6H_4^+ + HCN$, for example, illustrate the breakup of a species of low angular momentum on a "barrier-free" surface; the distribution is nearly that of a two-dimensional Boltzmann gas. A depletion of the leading edge of the distribution, accurately predicted by the model, arises from the intrusion of the small centrifugal barrier.

The dissociation $C_6H_6^+ \rightarrow C_6H_5^+ + H$, on the other hand is predicted to be a "barrier-dominant" dissociation. The depletion of the leading edge should be fully developed and an approximately three-dimensional Boltzmann distribution is expected. The data[3] reflect this broadening rather nicely.

The breakup of collision-complexes of high angular momenta should always show large depletion effects because of the inevitable presence of a large centrifugal barrier. Data[4] for the reaction $C_2H_4^+ + C_2H_4 \rightarrow C_4H_8^+ \rightarrow C_3H_5^+ + CH_3H_5^+ + CH_3$ accurately conform to predictions when this barrier is accurately evaluated.

The examples cited illustrate the need for the accurate numerical evaluation of quasi-equilibrium expressions, but also point to an important distinction. Quasi-equilibrium theory should not be confused with a model - in these instances the Langevin collision model. In particular, the possible failure of the latter does not imply a deficiency in the former.

*Research sponsored by the Energy Research and Development Administration under contract with the Union Carbide Corporation.

[1]C. E. Klots, Z. Naturforsch. 27a, 553 (1972).
[2]D. T. Terwilliger, J. H. Beynon, and R. G. Cooks, Proc. R. Soc. Lond. A341, 135 (1974).
[3]R. G. Cooks, private communication.
[4]A. Lee, R. L. Leroy, Z. Herman, and R. Wolfgang, Chem. Phys. Letts. 12, 569 (1972).

KINETIC ENERGY RELEASE FROM IONS IN SELECTED INTERNAL ENERGIES

B. P. Tsai, T. Baer, and A. S. Werner
Department of Chemistry
University of North Carolina
Chapel Hill, North Carolina 27514

Using the photoion-photoelectron coincidence technique (PIPECO)[1] in conjunction with dispersed radiation from the many-line hydrogen light source, we have investigated the ionization and fragmentation behavior of propargyl chloride and bromide.[2,3] This technique only collects those photoions detected in coincidence with an energy analyzed electron. Since the electron and photon energies are well known in the coincidence method, the internal energy of the ion is well defined. Ions are mass analyzed either by time of flight (TOF) or with the quadrupole mass spectrometer (QMS). Electrons are energy analyzed with a steradiancy analyzer.

We obtained PIPECO and zero kinetic energy (ZKE) electron spectra for both propargyl halide parent ions and the PIPECO spectra of $C_3H_3^+$, the only fragment ion observed below 13 eV, from both parent ions. The I.P.'s and A.P.'s extracted from these data are listed below.

	$C_3H_3Cl^+$	$C_3H_3^+/C_3H_3Cl^+$	$C_3H_3Br^+$	$C_3H_3^+/C_3H_3Br^+$
I.P. or A.P. (eV)	10.68±0.03	11.02±0.05	10.42±0.02	10.94±0.02

We then applied the PIPECO method to obtain TOF distributions at various fixed ionizing energies. These curves enabled us to determine the kinetic energy released upon fragmentation of the propargyl halide ions. The results for $C_3H_3^+/C_3H_3Cl^+$ and $C_3H_3^+/C_3H_3Br^+$ are shown in Figures 1 and 2.

The TOF spectra are double peaked because apertures prior to the detector discriminate against those ions initially ejected perpendicularly to the detector with substantial kinetic energy (K.E.). First consider the TOF distributions of $C_3H_3^+$ produced from $C_3H_3Cl^+$ at photon energy E in Figure 1. The best calculated fit to this data, obtained by using the TOF equations, corresponds to a K.E. release of 0.53 eV. This calculation neglects broadening due to an initial thermal energy distribution and isotopic differences since this effect is much smaller than the broadening due to K.E. release. Furthermore, this program only considers a single value of K.E. release. A noticeable improvement in the fit was observed when a distribution of K.E.'s was included in the calculation. However, this judgement was primarily based on the improved fit of the dip between the maxima. The calculated best fit corresponded to a gaussian distribution with a full width at half maximum of 0.10 ± 0.025 eV centered around 0.58 ± 0.05 eV.

At approximately 11.5 eV, a third peak starts to appear and increases with energy relative to the large K.E. release component. Initially, we attributed this third peak to either an impurity or an experimental artifact. However, upon eliminating these alternatives, we proposed that this new peak is due to a new fragmentation channel also producing $C_3H_3^+$. Lossing[4] has proposed that two structures of $C_3H_3^+$ exist but no previously published direct evidence has confirmed their existence. We present such evidence and attribute this new channel to production of a linear form of $C_3H_3^+$ and the lower energy channel to production of a cyclic form.

While the heats of formation for the linear[4] and cyclic[1] $C_3H_3^+$ structures have been published and are fairly well established, the heat of formation for the neutral molecule is not accurately known. By using our experimentally measured values for the I.P., A.P. and K.E. release as well as the known heats of formation for $C_3H_3^+$, we constructed schematic potential energy curves. From the heats of formation for the fragment ion and chlorine, the dissociation asymptotes are fixed. The energy

activation barriers for fragmentation are determined from the I.P. and A.P., and the K.E. release value sets a lower limit to the reverse activation barrier. Using only the fragmentation channel for the production of the cyclic structure, we determined a lower limit to the heat of formation of the neutral of 45 kcal mol^{-1}, 3 kcal mol^{-1} higher than the value determined from the group equivalent method in the NBS Table of I.P.'s, A.P.'s and Heats for Formation.[5] We believe our value to be correct because the calculated onset for the linear product derived from our neutral heat of formation is in good agreement with the experimental A.P.; the discrepancy is only 1 kcal mol^{-1}.

Figure 2 shows the TOF curves for propargyl bromide. Two K.E. components are observed at the fragmentation onset. The best calculated fit to the data corresponds to a K.E. release of 0.60 eV for production of the cyclic form of $C_3H_3^+$. As the internal energy of the parent ion increases, the linear ion contribution increases relative to that of the cyclic structure.

A schematic potential energy curve for fragmentation of $C_3H_3Br^+$ was constructed and a lower limit of 57 kcal mol^{-1} was determined for the heat of formation of neutral propargyl bromide in a manner similar to C_3H_3Cl. This value is 6 kcal mol^{-1} higher than the group equivalent method value and yields a calculated onset for the linear product in good agreement with the experimental determination. Note that in the propargyl bromide fragmentation, about 55% of the reverse activation energy is released as translational energy while in the propargyl chloride case, almost all of this barrier is channeled into kinetic energy.

1. A. S. Werner and T. Baer, J. Chem. Phys. 62, 2900 (1975).
2. T. Baer, A. S. Werner and B. P. Tsai, J. Chem. Phys. 62, 2497 (1975).
3. B. P. Tsai, A. S. Werner and T. Baer, to be published.
4. F. P. Lossing, Canad. J. Chem. 50, 3973 (1972).
5. J. L. Franklin, J. G. Dillard, H. M. Rosenstock, J. T. Herron, K. Draxl and F. H. Field, NSRDS-NBS 26, U.S. Government Printing Office (1969).

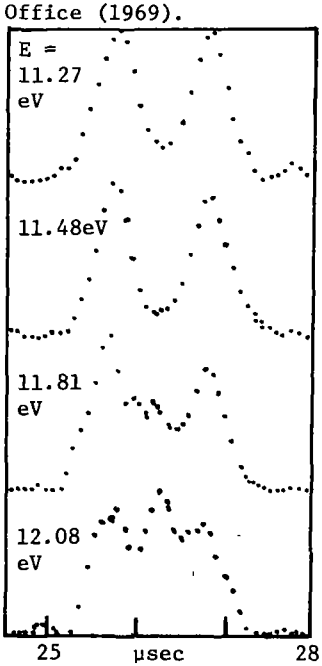

←Figure 1. TOF Distribution of $C_3H_3^+/C_3H_3Cl$

Figure 2.→ TOF Distribution of $C_3H_3^+/C_3H_3Br^+$

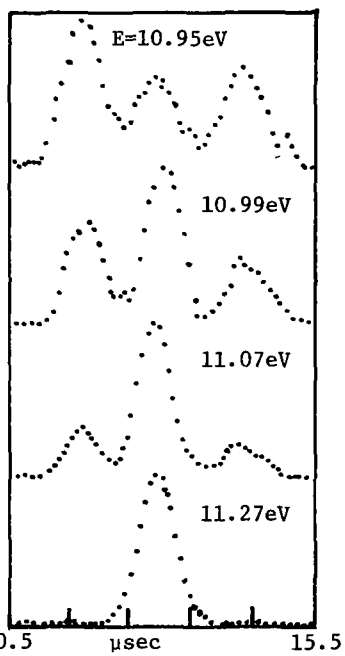

TRANSLATIONAL ENERGIES OF IONS FROM IONIC FRAGMENTATION

Duane E. Carter and J. L. Franklin
Chemistry Department, Rice University
Houston, Texas 77001

ACKNOWLEDGMENT

The authors are pleased to acknowledge support of this work by the Robert A. Welch Foundation.

Dissociative attachment reactions provide a relatively simple experimental means of studying the translational energies of fragments of ionic decomposition as a function of the energy of the system over a range of internal energies. Over the last several years a number of such reactions have been studied experimentally[1-4] with results in apparent conflict with statistical reaction theories. In general, the translational energies have been found to be greater than predicted.

The transition state version of the quasiequilibrium theory (QET) gives the following expression for the average translational energy of the products:[5]

$$\bar{\varepsilon}_t = \frac{\int_0^{E^*} \varepsilon_t \, \rho^{\neq}(E^* - \varepsilon_t) d\varepsilon_t}{\int_0^{E^*} \rho^{\neq}(E^* - \varepsilon_t) d\varepsilon_t} \tag{1}$$

where E* is the excess energy available to be partitioned into rotational, vibrational and translational energies. The density of vibrational states in the transition state is denoted by $\rho^{\neq}$. Phase space theory as applied by Klots[6] results in the following expression for the average translational energy:

$$\bar{\varepsilon}_t = F_t \times \frac{\int_0^{E^*} \rho(E_{vib}) \, (E^* - E_{vib})^{S+1} \, dE_{vib}}{\int_0^{E^*} \rho(E_{vib}) \, (E^* - E_{vib})^{S} \, dE_{vib}} \tag{2}$$

where ρ represents the density of vibrational states in the products, and F_t and S are constants that depend upon the geometry of the reaction. If the density of states is evaluated using the classical expression, both equations reduce to $\bar{\varepsilon}_t = E^*/N$ where N is the number of oscillators in the complex for the QET theory, but N may differ from the number of oscillators by at most two in the phase space theory. Equations (1) and (2) were evaluated for a number of systems, using for the density of states term a direct count of vibrational states, combined with the Whitter-Rabinovitch approximation.[7] The results for a representative small reaction, that of $P_4^- \rightarrow P_2^- + P_2$ are shown in Figure 1. Agreement with experimental results[4] is poor. For larger molecules, the two theories give similar prediction, usually in serious conflict with experimental results.

In an attempt to understand this failure of the statistical theories, we constructed a classical model of a triatomic molecule resembling CO_2^-. The statistical theories were tested by applying them to the model and comparing the predictions with the results of a large number of trajectories that were computed by numerically integrating Hamilton's

equations of motion for the system.[8] The conceptual framework for this study is shown in Figure 2. The first problem in either applying the statistical theory or constructing the model is determining energy parameters of the activated complex. For the CO_2^- $^2A_1$ state, these were taken from an ab initio study by Kraus and Neumann[9] and included a well depth of 3.6 eV. A reasonable potential function was written as a function of the two bond lengths and the bond angle. It included a Lennard-Jones 8-4 potential for each bond to simulate the ion-induced dipole attractive forces and an angular potential function with a minimum at 135°. The function included coupling terms so the angular dependence dropped out and the C-O bond strength increased as the molecule dissociated. It is important to note that the statistical theories should describe the model even if it does not accurately represent a real molecule. All quantum effects have been neglected but by letting Planck's constant approach zero the model should still be described.

The initial conditions for the trajectories were selected in a way that resembles a Franck-Condon transition. They were selected from Gaussian weighted random distribution centered around the equilibrium position for neutral CO_2. During the trajectories for molecules with less than 2 eV excess energy the bonds would undergo a complicated Lissajous motion for several tens of vibrations before finally dissociating. The translational, rotational and vibrational energies of the products were computed after a bond had exceeded 10Å.

The translational energies of a large number of trajectories were 20-point smoothed to obtain the plot of average translational energy vs the excess energy shown in Figure 3. Clearly, at low excess energies where the statistical theories should work best and experimental data may be obtained, the translational energies exceed that predicted by either theory. Figure 4 shows the distributions of translational, vibrational and rotational energies for a number of trajectories with 1.0 eV excess energy. These are compared to the predictions of Klots application of phase space theory.[6] The translational energy of the products is increased at the expense of the rotational energy. It is not yet clear whether these discrepancies represent a breakdown of the quasi-equilibrium hypothesis itself. Phase space theory requires a knowledge of the cross-section of the ion molecule reaction which is the inverse of the decomposition. The Langevin theory which Klots uses may be inadequate for reactions involving large rotational energies. It is clear that statistical reaction theories as presently formulated are inadequate to explain observed translational energies.

REFERENCES

1. P. W. Harland and J. L. Franklin, J. Chem. Phys., 61, 1621 (1974)
2. S. L. Bennett, R. E. Pabst, J. L. Margrave and J. L. Franklin, Int. J. Mass Spectrom. Ion Phys., 15, 451 (1974)
3. P. W. Harland, J. L. Franklin and D. E. Carter, J. Chem. Phys., 58, 1430 (1973)
4. S. L. Bennett, J. L. Margrave and J. L. Franklin, J. Chem. Phys., 61, 1647 (1974)
5. E. L. Spotz, W. A. Seitz and J. L. Franklin, J. Chem. Phys., 51, 5142 (1969)
6. C. E. Klots, Z. Naturforsch, 27a, 553 (1972); C. E. Klots, J. Phys. Chem., 75, 1526 (1971)
7. G. Z. Whitten and B. S. Rabinovitch, J. Chem. Phys., 38, 2466 (1963); D. C. Tardy, B. S. Rabinovitch and G. Z. Whitten, J. Chem. Phys., 48 1427 (1968)

8. D. L. Bunker, J. Chem. Phys., 37, 3931 (1962)
9. M. Kraus and D. Neuman, Chem. Phys. Lett., 14, 26 (1972)

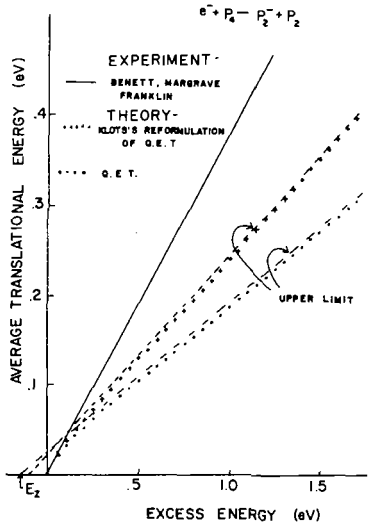

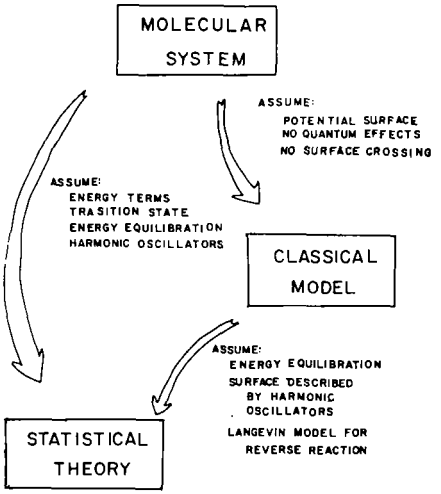

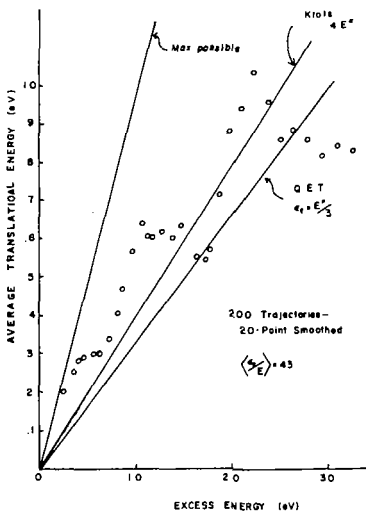

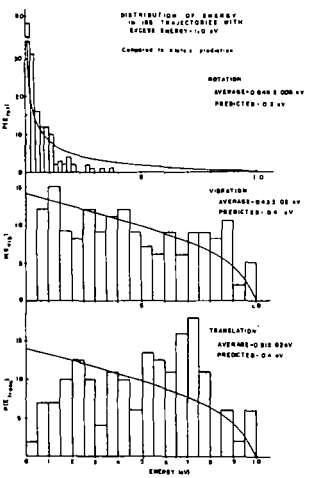

FIGURE CAPTIONS

Figure 1. Statistical theory predictions of average translational energy vs. excess energy for $P_4^- \rightarrow P_2^- + P_2$. The upper line shows the experimental results.

Figure 2. Conceptual framework of the trajectory study.

Figure 3. Translational energies of the trajectory products vs. the excess energy.

Figure 4. Distributions of translational, rotational and vibrational energies for trajectories with 1.0 eV excess energy.

Breakdown Curves of the Ethylene and Ethylene-d_4 Ions Obtained by Threshold Photoelectron-Photoion Coincidence Mass Spectrometry.

ROGER STOCKBAUER*
National Bureau of Standards
Washington, DC 20234

and

MARK G. INGHRAM
Department of Physics
University of Chicago
Chicago, IL 60637

The fragmentation processes in ethylene and ethylene-d_4 have been studied using the threshold photoelectron-photoion coincidence technique. Breakdown curves have been obtained from the fragmentation onset to 10 eV above the onset. The breakdown curves are in qualitative agreement with curves obtained from quasi-equilibrium calculations and with photo-ionization mass spectrometry results over the energy range where such data is available. There are substantial differences between the present data and data from charge exchange. It is believed that the differences are due to ion-molecule reactions dominating the charge exchange results at certain energies. The loss of two H atoms from ethylene is particularly interesting. It should be possible to deduce qualitatively, the form of the $C_2H_3^+$ fragment internal energy distribution from the shape of the breakdown curve for the two H atom loss process.

A detailed account of this work has been published in the Journal of Chemical Physics, 62, 4862 (1975).

*NRC-NBS Postdoctoral Associate

PHOTODISSOCIATION OF NEGATIVE IONS

G. Mauclaire, M.L. Vestal and J.H. Futrell
Department of Chemistry
University of Utah, Salt Lake City, Utah 84112

The recent results reported here have been obtained with the tandem quadrupole photodissociation described earlier.[1] The high pressure mercury lamp used in our previous work has been used, as well as a pulsed tunable dye laser, which in the visible region, increases dramatically both sensitivity and resolution. Figure 1 summarizes the results obtained with both light sources for the photodissociation of CO_3^-.

The spectral region near 6000 Å, which has been studied in detail using the tunable dye laser, shows some interesting fine structure which probably corresponds to a low frequency bending mode of CO_3^-. This region is shown in more detail in Figure 2 for points obtained at 25 Å increments. This region was also investigated by obtaining cross sections at 5 Å increments, but no additional structure was evident. However, the structure shown in Figure 2 was accurately reproduced.

The cross section for the photodissociation of CO_3^- increases rapidly with decreasing wavelength in the vicinity of 6500 Å (1.9 eV), but dissociation is observed out to at least 6700 Å (1.85 eV) with a small, but finite, cross section $6 \pm 2 \times 10^{-21}$ cm^2). Definite assignment of a thermochemical threshold for this reaction will require additional high resolution measurements in the wavelength range between 6200 and 7000 Å. The photodissociation of CO_3^- has also been studied by Moseley et al.,[2] and our value of $.95 \times 10^{-18}$ cm^2 for photodissociation at 4430 Å is quite compatible with their total photodestruction rate of $.91 \times 10^{-18}$ cm^2 at 4579 Å. Recently, these authors have extended their measurements in the range 5650 to 6400 Å, using a tunable dye laser.[3] They observe a very detailed structure, whose general shape is similar to the one we observe, but the cross section they measure is about 20 times greater than ours (3.5×10^{-18}cm^2 instead of 1.6×10^{-19}cm^2, for the peak at 6000 Å.) At this time, we have no explanation for this discrepancy.

Table 1 gives the photodissociation cross sections relative to different positive and negative ions formed in pure oxygen. The reaction $O_3^+ + h\nu \rightarrow O^+ + O_2$ exhibits the largest photodissociation cross section observed thus far in this work. This is particularly remarkable in that, based on available thermochemical data, this reaction is not energetically possible in this wavelength region if the O_3^+ is initially formed in its ground electronic and vibrational state. However, recent measurements of the photoelectron spectra of O_3 have shown the existence of three low-lying electronically excited states of O_3^+.[5] A recent theoretical calculation predicts the energies of these three states in good agreement with the experiments.[4] However, the theoretical calculations also predict five additional low-lying states of O_3^+ which are not observed in the photoelectron spectra. Since these states correspond to the ionization of one electron of O_3 and excitation of a second electron, it is not surprising that these states are not observed in the photoelectron spectra. Nevertheless, these states should be observable in the photodissociation spectra and we anticipate that further photodissociation experiments on O_3^+ planned for the immediate future may lead to the first experimental observation and characterization of these excited states. Clearly, a substantial fraction of the O_3^+ ions produced by ion-molecule reactions in the ion source from O_2 at 0.1 torr are in long-lived excited states. An example of the extremely high sensitivity which is available with this apparatus is provided by the results on the reaction

$$CH_3Br^+ + h\nu \rightarrow CH_3^+ + Br$$

which was studied in the wavelength range between 580 nm and 620 nm using Rhodamine 6G in the dye laser. In this range, near the thermochemical threshold for the reaction, we were able to measure photodissociation cross sections of ca. 2 x $10^{-20}cm^2$ with a precision of ± 1 percent in a total measurement time of one minute even though the laser was operated at only 5 percent of its nominal output power. The bandwidth of the radiation used in these experiments was 3 cm^{-1} (0.37 meV). While this reaction is admittedly a favorable case for the technique, these results illustrate the extremely high combination of sensitivity and resolution which can be attained.

TABLE I

Photodissociation Cross Sections at 6000 Å (1)

Reactions	σ (2)
$CH_3Br^+ \rightarrow CH_3^+ + Br$	0.022 ± 0.001
$CO_3^- \rightarrow O^- + CO_2$	0.16 ± 0.01
$O_3^- \rightarrow O^- + O_2$	1.7 ± 0.4
$O_3^- \rightarrow O_2^- + O$	1.3 ± 0.6
$O_2^+ \rightarrow O^+ + O$	0.19 ± .01
$O_3^+ \rightarrow O^+ + O_2$	11.8 ± 0.3
$O_3^+ \rightarrow O_2^+ + O$	0.9 ± 0.2
$O_4^+ \rightarrow O_2^+ + O_2$	3.9 ± 0.4

(1) 2.07 eV
(2) Units of $10^{-18}cm^2$

References

1. M.L. Vestal and J.H. Futrell, Chem. Phys. Lett., 28, 559 (1974)
2. J.T. Moseley, R.A. Bennett and J.R. Peterson, Chem. Phys. Lett., 26, 288 (1974)
3. J.R. Peterson, private communication.
4. P.J. Hay, T.H. Dunning Jr., W.A. Goddard III, J. Chem. Phys. 62, 3912 (1974)
5. D.C. Frost, S.T. Lee, and C.A. McDowell, Chem. Phys. Lett. 24, 149 (1974)

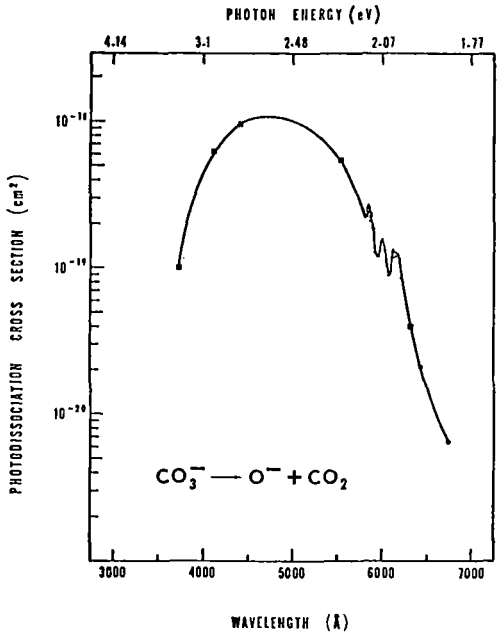

Fig. 1. Photodissociation cross section for the reaction $CO_3^- \rightarrow O^- + CO_2$ measured with the high pressure mercury lamp (▪) and the tunable dye laser (x); the points (•) represent an average of several measurements taken with the dye laser within an 100 Å band centered at the indicated wavelength.

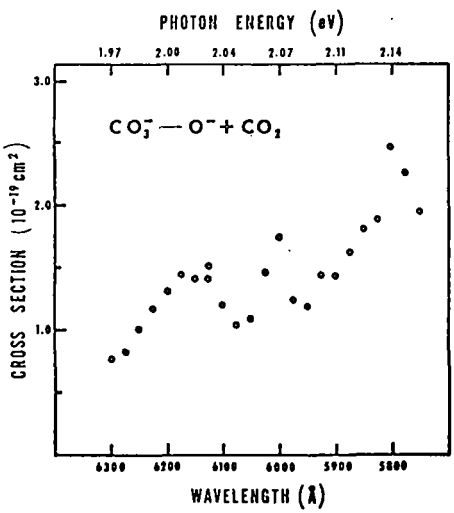

Fig. 2. Photodissociation cross section for the reaction $CO_3^- \rightarrow O^- + CO_2$ using Rhodamine 6G in the tunable dye laser.

PHOTOIONIZATION PROCESSES AT THRESHOLD I. THRESHOLD PHOTOELECTRON SPECTRA AND PHOTOIONIZATION OF CO_2.

C. F. Batten, J. A. Taylor, and G. G. Meisels
Department of Chemistry, University of Nebraska-Lincoln
Lincoln, Nebraska 68508

INTRODUCTION. Threshold Photoelectron Spectra (TPES) result from the selective detection of photoelectrons produced with nominally zero kinetic energy by a monochromatic photon beam of variable energy. TPES should have measurable intensity only when the photon energy exactly equals the threshold energy for the production of a particular ionic state. They provide accurate energies of such states but differ from conventional photoelectron spectra (PES) in several ways. TPES intensities reflect transition probabilities at threshold without possibility of energy discrimination in an electron velocity analyzer. PES measure relative abundances of states produced at some higher energy; they are related to threshold transition probabilities by energy dependent cross section functions whose behavior depends on the transition, and is frequently unknown. Also, atoms and molecules usually have autoinizing states (bound or dissociative) close in energy to their lower direct ionization thresholds; these will be excited and lead to ionization at resonance only. Since resolution of TPES detectors is not definite and excitation of autoionizing states may have a large cross section, states which autoionize to a lower-lying level of the ion may lead to some structure not resulting from threshold photo-electrons. These may be identified from photoion spectra or by changing energy resolution of the electron detector. In this presentation, we compare TPES, PES, and Photoion spectra for carbon dioxide over the wavelength range 901 to 875 Å, spanning the lowest electronic state ($2\pi g$) of the CO_2^+ ion.

EXPERIMENTAL. A one meter vacuum UV monochromator with a resolution of 0.42 Å (FWHM) is coupled to a threshold electron detector based on a collimated hole structure (1); the combination affords an energy resolution of 0.014 eV. (FWHM) and enables the location of a maximum with an optimum accuracy of 0.002 eV (0.10 Å). Details will be published elsewhere.

RESULTS AND DISCUSSION. Two segments of photoion and photoelectron spectra obtained concurrently are illustrated in figures 1 and 2 and the energy states of CO_2^+ identified from photoelectron spectra are collected in Table I. The total photoion current in the region 901 to 885 Å is virtually identical to that reported earlier (2). From the midpoint of the steep rise at onset we calculate a lowest ionization potential of 13.771 eV (900.30 Å) which agrees well with the Rydberg absorption series limit of 900.4 Å (13.770 eV) (3). Several peaks appear to be superimposed on the shorter wavelength side of this ionization onset, almost certainly as a result of autoionization. Some of these may be assigned to Rydberg series but interpretation remains incomplete.

The TPES rises steeply in the same range, from onset to a well defined peak at 13.776 eV (900.00 Å), which may be attributed to formation of the $\nu(0,0,0)$ level of the $2\pi_{3/2}$ component of ground state CO_2^+. Toward shorter wavelength the TPES shows additional structure which may be interpreted in terms of ionization to other known states of CO_2^+. The only electronic state of CO_2^+ which falls in this region is the $2\pi g$ state which is split into a lower $2\pi_{3/2}$ and an upper $2\pi_{1/2}$ component. Additional data of Mrozowski, Koryoshkin and Herzberg from optical spectroscopy (see Table I) were used to locate the positions of the vibrational levels for this state in our spectra.

The photoelectron peak at 13.797 eV (898.65 Å) occurs at almost exactly the energy at which the $2\pi_{1/2}$ component of $\nu(0,0,0)$ should be observed ($\Delta h\nu$ = 160 cm^{-1}, c of Table I). However, the photoion spectrum indicates the occurrence of an autoionizing state at this energy and it is not possible to separate autoionization from direct ionization simply.

The threshold photoelectron peak at 13.837 eV (896.05 Å) shows no interference from autoionization. The only state of CO_2^+ falling near this energy would be the $\nu(0,1,0)$ level. Population of this level by direct ionization is forbidden (4). The selection rule would not apply if this state were reached by autoionization from a neutral bent valence state which is believed to occur in this energy range (5). Autoionization from this state, if it has a broad energy cross section, may add to any peak resulting from direct ionization at lower energies or may be the exclusive contributor as seems most likely here. If this explanation is correct then the bending mode of CO_2^+ would have a fundamental frequency of 492 cm^{-1} rather than the value of 531 cm^{-1} reported by Koryoshkin.

The TPES between 895.45 Å and 890.50 contains several weak peaks as does the ion spectrum. All features except a peak at 13.894 eV (892.35 Å) appear to be the result of unsuppressed autoionization from Rydberg states. This peak is relatively too intense and can be attributed to formation of the $\nu(0,2,0)$ level. It is significant that neither of the first two CO_2^+ bending levels have been observed in nonthreshold spectra. No evidence for production of higher levels in this mode is found in our spectra. The energies of two incompletely resolved peaks at 13.937 eV (889.60 Å) and 13.994 eV (888.55 Å) agree with optical values for the two components of the $\nu(1,0,0)$ level. In the 885 and 875 Å region the TPES contains a weak broad feature which appears to consist of two poorly resolved contributions for which we calculate maxima of 14.092 eV (879.85 Å) and 14.109 eV (878.75 Å). These are consistent with the energies and spin orbit splitting of the $\nu(2,0,0)$ level and the envelope is similar to that assigned to the lower member of this mode.

Finally, we see no indication for production of the $\nu(0,0,2)$ level or any other level of the asymmetric stretching mode. This disagrees with a conclusion which Turner et al. (6) draw from their nonthreshold spectrum and with a Franck-Condon Factor calculation by Inghram (7) and coworkers, but agrees with the experimental results of the latter group.

1. R. Spohr, P.M. Guyon, W. A. Chupka, and J. Berkowitz, Rev. Sci. Instr. 42 1872.
2. K. E. McCulloh, J. Chem. Phys., 59, 4250(1973).
3. Y. Tanaka, A.S. Jursa, F.J. LeBlanc, J. Chem. Phys. 32, 1199(1960).
4. T. E. Sharp, H. M. Rosenstock, J. Chem. Phys. 41, 3343(1964).
5. M. Krauss, et al. J. Geophys. Res. 76, 3773(1971).
6. Villarejo, Stockbauer, and Inghram, J. Chem. Phys. 48, 3392(1968).
7. D. W. Turner, et al.; Molecular Photoelectron Spectroscopy, Wiley Interscience, New York 1970, p. 73.

Footnotes to Table 1

a) Reference 7, pp 62 and 63, splitting not resolved
b) Tanaka, Jursa and LeBlanc, J. Chem. Phys. 32, 119 (1960)
c) Mrozowski, Phys. Rev. 60, 730(1941), 62, 270(1942), 72, 682 & 691(1947)
d) Calculated by adding spacing of ref. c to our IP for $\nu(0,0,0)$
e) V. A. Koryoshkin, Dokl. Akad. Nauk. SSSR, 167, 1035(1966)
f) Calculated by adding spacing of ref e to our IP for $\nu_1(000)$
h) G. Herzberg, Molec. Spectra & Structure, IIID, Van Nostrand,NY.,1967
k) Calculated by adding spacing of ref h to our IP for $\nu_1(000)$
j) Spacing between this and next lowest level in same vibrational mode

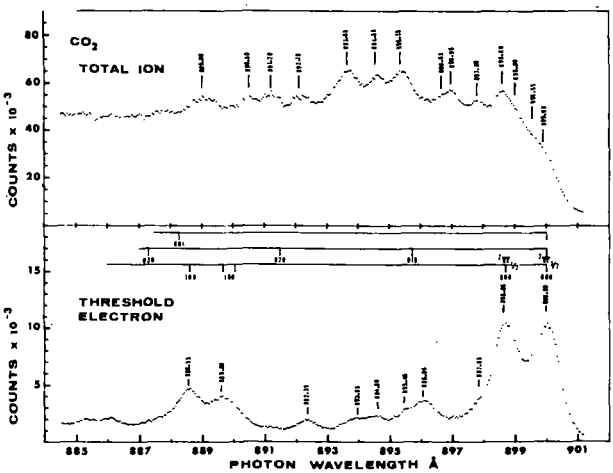

Figure 1. Photoionization and threshold photoelectron spectra of CO_2. Sample pressure 0.2 mtorr slits 50 μ, extraction potential 4 Volts.

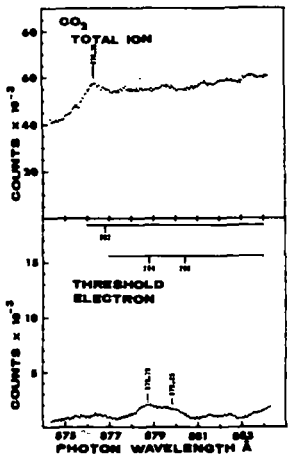

Figure 2. Photoionization and threshold photoelectron spectra of CO_2. Sample pressure 0.2 mtorr, slits 50 μ, extraction potential 10 Volts.

TABLE I
OBSERVED ENERGY STATES OF CO_2^+

State	IP by TPE	IP by PE	IP Optical	Δv TPE	Δv Other
$^2\Pi_{1/2}$					
v_{000}	13.776±.005eV	13.788[a]eV	13.770[b]eV		
v_{100}	13.937		13.933[d]	1299 cm^{-1}	1287.32[c] cm^{-1}
v_{200}	14.092		14.083[d]	1250	1209.55[c]
v_{300}			14.233[d]		
v_{010}	13.837		13.842[f]	492	531[e]
v_{020}	13.894		13.908[f]	460	
v_{001}	–		13.958[h]		1469[h], 1420[e]
v_{002}	–		14.140[h]		
$^2\Pi_{3/2}$					
v_{000}	13.797	13.788[a]	13.792[b]		
v_{100}	13.954		13.950[b]	1280	1265.75[c], 1210[e]
v_{200}	14.110		14.109[d]	1258	1256.89[c]

EVALUATION OF KINETIC SHIFTS BY PULSED SOURCE MASS SPECTROMETRY**

S. M. Gordon and N. W. Reid*

Atomic Energy Board
Private Bag X256
Pretoria
South Africa

ABSTRACT

An ion-trapping technique has been used in the determination of the full kinetic shift for normal fragment ions. As expected, significant kinetic shifts are found for the production of daughter ions from benzonitrile, benzene and toluene, while that involved in the decomposition of ethylene is essentially zero. Appearance potentials determined at long trapping times are in general agreement with thermochemical values. The dependence of kinetic shift on ion source residence-time is discussed in terms of experimentally derived rate-coefficient versus energy data.

*Permanent address: Department of Chemistry, University of Natal, Pietermaritzburg, South Africa.

**Accepted for publication in Int. J. Mass Spectrom. & Ion Phys.

ASSOCIATIVE IONIZATION AND SECONDARY REACTIONS IN $U + O_2$ AND $U + N_2O$ SYSTEMS

W.L. Fite and H. H. Lo
Department of Physics, University of Pittsburgh
Pittsburgh, Pennsylvania 15238

and

M.W. Siegel
Extranuclear Laboratories, Inc.
Pittsburgh, Pennsylvania 15238

Crossed beam experiments have yielded the cross section for $U + N_2O \rightarrow UO^+ + N_2 + e$, from the previously measured cross section for $U + O_2 \rightarrow UO_2^+ + e$. In a second experiment a beam of U atoms crossed a magnetic bottle field where gas was added. Ions formed and trapped in the bottle field were examined. With N_2O, UO_2^+ was also present, arising from the ion-molecule reaction $UO^+ + N_2O \rightarrow UO_2^+ + N_2$. With O_2, UO_3^+ was also present but arising, we believe from energy considerations, from the associative ionization process $UO^* + O_2 \rightarrow UO_3^+ + e$, with the UO coming from $U + O_2 \rightarrow UO^* + O$. The appearance of UO_3^+ suggests possible errors in the known energetics of the uranium-oxygen system. The experiments are described and the results discussed. Possible uses of magnetically confined plasmas of such ions are considered.

Supported in part by the NSF and in part by the Defense Nuclear Agency through AFCRL.

Predissociation processes in biatomic ions from kinetic energy distributions and from metastable studies.

J. MOMIGNY, R. LOCHT, H. WANKENNE - Depat of Chem.
University of Liège, 4000 - LIEGE (Belgium)

Predissociation processes are detectable, irrespective to their lifetimes, by the modulation of the K.E. distribution of the fragment ions through the vibrationnal distribution of the predissociated state. Such modulations have been observed recently, by a retarding potential technique, in K.E. distributions of O^+ from O_2^+ and of N^+ from N_2^+. The FWHM of a thermal peak in the K.E. distribution is of about 60 mV in these experiments. Plots of K.E. values against electron energies allows the determination of the pertaining dissociation limits [1-3]. Using this method, predissociation processes have been detected for the appearance of the following processes : $CO \longrightarrow C^+ + O^-$(A.P. for zero K.E. : 20.9 eV); $CO \longrightarrow C^+ + O$(A.P. for zero K.E. : 22.37 eV). The structures observed above these respective dissociation limits are given in Fig.Nr 1 and compared in Table Nr 1 to results from absorption spectroscopy [4] or from photoelectron spectroscopy [5]. Agreement between such mass spectroscopic and optical spectroscopic results allows us to attribute the following mechanism to these predissociations : the first process is due to the predissociation through an ionic state converging to the $C^+ + O^-$ asymptote of the 3 pσ Rydberg state of a Rydberg series converging to the doubly excited $^2\Sigma^+$ and $^2\Pi$ states of CO^+ ; the second process is due to the predissociation of the $D^2\Pi$ state of CO^+, as shows the agreement between the observed structure and the vibrationnal progression of this state, as observed from photoelectron spectroscopy.

TABLE 1 : Position of the submaxima (meV) observed in the first diffrentiated ion retarding curve of C^+ from CO^*.

(a)Electron energy 21-23 eV		(b) Electron energy 24-30eV		
This work*	Abs.Spectr.(3)	This work*	Photoelectr. Spectr.	
			(4)	(5)
0 ± 5	(-34 ± 7)			
152 ± 24	166 ± 7	21 ± 7	16±10	33±10
325 ± 35	336 ± 7	178 ± 26	183±10	196±10
469 ± 23	512 ± 7	352 ± 17	350±10	365±10
625 ± 40	649 ± 7	523 ± 31	516±10	535±10
		693 ± 21	686±10	695±10
		875 ± 24	851±10	861±10
		1052 ± 17	1003±10	1014±10

* Quoted values in column 1 and 3 correspond to 28/16 the energy measured by the position of the submaxima.

Within a lifetime window of about 10^{-5} to 10^{-7} second, the observation of predissociated states as "metastable transitions", is possible, with high K.E. resolution, in the first field free region of a double focussing M.S., by using a narrow exit slit on the electrostatic sector.

In such a way, we have recently been able to resolve the fine structure of the non-collision induced predissociation of N_2^+, as shown in Fig. Nr 2. Rough determinations of energy thresholds of the two main structures (A and C) as the spacing in energy between these levels indicates that almost two electronic states of N_2^+ are involved in this predissociation. Precise A.P. determinations are in progress.

References

(1) J.Schopman, R.Locht.-Chem.Phys.Lett.26 (596)1974

(2) R.Locht, J.Schopman,- Int.J.Mass.Sp.Ion.Phys. 15 (361) 1974

(3) R. Locht, J. Schopman, H. Wankenne, J.Momigny - Chem.Phys. 7 (393) 1975

(4) (5) K.Codling, A.W. Potts - J.Phys.B.7 (163)1974

(5) L. Asbrink, C. Fridh, E. Lindholm, K. Codling - Phys. Scripta 10 (183) 1974

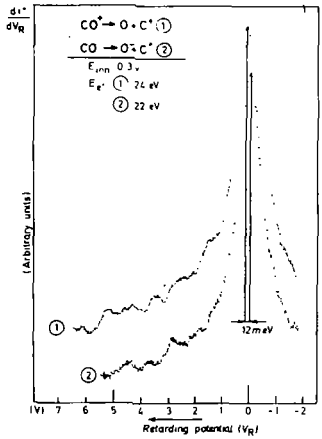

Fig. 1

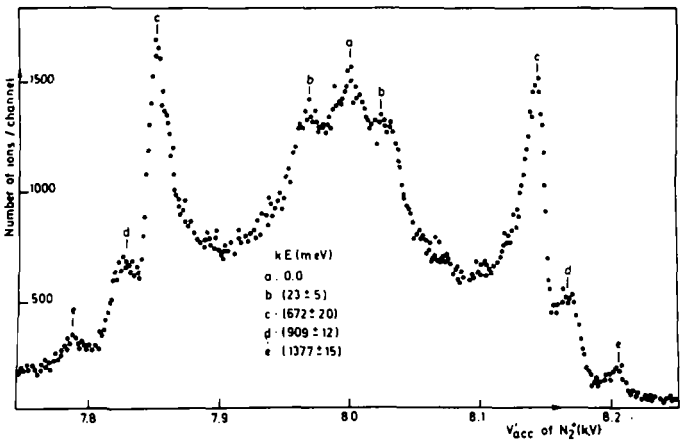

Fig. 2

ENERGETICS OF THE IONIZATION AND FRAGMENTATION OF ARSENIC TRIFLUORIDE BY ELECTRON IMPACT

R. E. Pabst, R. G. Meador, J. L. Margrave and J. L. Franklin
Chemistry Department, Rice University
Houston, Texas 77001

ACKNOWLEDGMENT

The authors are pleased to acknowledge support of this work by the Office of Naval Research, U.S. Navy, under contract No. 67-A-0145-0002.

There has been considerable interest in the ionization of monomeric halides of the main Group V elements both from an experimental and a theoretical viewpoint. The current state of research has been summarized by Torgerson and Westmore[1] in their study of PF_3. Our research stemmed from negative ion studies of the arsenic trihalides, the results of which will be presented elsewhere, but the values derived from AsF_3 will be summarized here.

The mass spectrum of AsF_3 showed peaks for F^+, F_2^+, As^+, AsF^+, AsF_2^+ and AsF_3^+. Although some $AsOF_3$ was present, it was only 2-3% that of AsF_3 initially and must be attributed to hydrolysis in the inlet line; it decreased to a negligible level before the studies were conducted. The study was done on a Bendix Time-of-Flight mass spectrometer equipped with a 3015 scanner to enable translational energies to be measured.

The appearance potential (A.P.) of AsF_3^+ was determined from the experimental data by two procedures, "extrapolated potential difference" (e.p.d.) and the "semilogarithmic plot" (s.l.p.), using xenon to calibrate the energy scale. Appearance potentials for fragment ions were determined by the e.p.d. method if the curves for fragment ion and Xe^+ were not parallel; and the s.l.p. method was used in the other cases. The results in Table 1 represent the mean of several determinations.

AsF_3^+: Values for the A.P. of this ion by both methods are given in Table 1. A value of 12.3 ± 0.1 is taken as the average. The vertical I.P. has been reported as 13.0[3] from photoelectron spectroscopy. Our measurement, taken at onset rather than at the maximum of the probability presumably gives an appearance potential that is closer to adiabatic than that determined by photoelectron spectroscopy.

AsF_2^+: There are two plausible reactions which could lead to production of this ion:

$$AsF_3 + e \rightarrow AsF_2^+ + F^- + e \qquad (1)$$

$$AsF_3 + e \rightarrow AsF_2^+ + F + 2e \qquad (2)$$

AsF_2^+ is formed with thermal energy at onset and increases linearly in translational energy with increasing electron energy. The negative ion spectrum of AsF_3 shows F^- to be formed by a dissociative resonance capture process with a maximum at 9.6 eV and another process having an onset near 11.8eV. Thus there are at least two resonant processes near the appearance potential of AsF_2^+. These would obscure the onset for F^- by a pair production process. However, the linear increase in translational energy of AsF_2^+ indicates it to be formed by a single process in this region and we conclude that it is a pair production process. We compute the ionization potential of AsF_2 to be 12.1 eV.

AsF^+: The appearance potential of this ion was 19.6 eV and the translational energy at onset was thermal. Four reaction processes are

possible:

$$AsF_3 + e \rightarrow AsF^+ + F_2^- + e \quad (3)$$

$$AsF_3 + e \rightarrow AsF^+ + F^- + F + e \quad (4)$$

$$AsF_3 + e \rightarrow AsF^+ + F_2 + 2e \quad (5)$$

$$AsF_3 + e \rightarrow AsF^+ + 2F + 2e \quad (6)$$

From a knowledge of the A.P. and the excess energy[1,4] it is possible to calculate an upper limit for the I.P. of AsF, depending on the reaction path used. The values derived thereby are 14.6, 13.3, 11.4, and 9.8 for reactions 3, 4, 5, and 6 respectively. When compared to the I.P. of AsF_3, the first two values seem excessive. Both reactions 5 and 6 seem reasonable, but the 11.4 eV value is preferred from the analogy to PF and PF_3 where the ionization potentials are nearly equal.[1]

$\underline{F_2^+}$: This ion is formed by two processes, the first being thermal at onset at 23.8 eV, and having a linear increase in translational energy to an electron energy of 27.7 eV, whereupon the translational energy of F_2^+ begins to decrease. This second process is assumed to be near thermal at onset, as all of the other processes for AsF_3 are thermal at onset. Four processes are assumed reasonable

$$AsF_3 + e \rightarrow F_2^+ + AsF^- + e \quad (7)$$

$$AsF_3 + e \rightarrow F_2^+ + AsF + 2e \quad (8)$$

$$AsF_3 + e \rightarrow F_2^+ + As + F^- + e \quad (9)$$

$$AsF_3 + e \rightarrow F_2^+ + As + F + 2e \quad (10)$$

From the negative ion studies of AsF_3, the heat of formation of AsF^- was found to be less than -29 kcal. Process (7) would give $\Delta H_f(AsF^-)$ as -1 kcal, which does not agree within limits. Process (8) is reasonable, and gives $\Delta H_f(AsF)$ to be -1 kcal in fair agreement with the results of O'Hare et al.[4] Reactions (9) and (10) would be endoergic at 23.8 eV. However process (10) will occur as a thermal process at 27.7 eV. We conclude, then, that process (8) and (10) account for the onsets of F_2^+ at 23.8 and 27.7 eV.

$\underline{F^+}$: This ion showed a low intensity process of thermal nature that was difficult to determine an appearance potential for. It also showed two other processes of considerable intensity, the first of which showed a considerable increase of excess energy after a thermal onset, and the second showed a steady decrease in the total excess energy after its onset, probably due to an overlapping of the two processes. The lower energy process could occur by pair production or by dissociative ionization with AsF_2 formed as the neutral species. The ionization efficiency curve for AsF_2^- shows no new process near this energy and so pair production can be eliminated. Dissociative ionization gives $\Delta H_f(AsF_2)$ to be -111 kcal/mole in good agreement with the proposed value of O'Hare[5] using $\Delta H_f(AsF_{3,g})$ as -187.8 kcal/mole.[6]

Several reactions might conceivably account for the processes occurring at 29.3 and 31 eV. However, the only ones giving reasonable agreement with known thermochemical data give the neutral products as As + F_2 and As + 2F respectively.

REFERENCES

1. D. F. Torgerson and J. B. Westmore, Can. J. Chem., 53, 933 (1975)
2. R. E. Pabst, S. L. Bennett, J. L. Margrave and J. L. Franklin (to be published)
3. A. W. Potts, H. J. Lempka, D. G. Streets and W. C. Price, Phil. Trans. Roy. Soc. Lond., A268, 59 (1970)
4. P. A. G. O'Hare, A. Batana and A. C. Wahl, J. Chem. Phys., 59, 6495 (1973)
5. P. A. G. O'Hare. ANL-7456 (Nov. 1968)
6. V. B. Parker, Natl. Bur. Stand., Washington, D.C. Private communication. Value based on $\Delta H_r(AsF_3, \ell) + 8.5$ kcal mole^{-1} [H. Russell, R. E. Rundel and D. M. Yost, J. Amer. Chem. Soc., 63, 2825 (1941)] and $\Delta H_f(AsF_3, \ell) = -196.3$ kcal mole^{-1}. The latter value is from heats of solution measurements [D. M. Yost and J. E. Sherborne, J. Amer. Chem. Soc., 57, 700 (1935)] and has been adjusted for changes in the auxiliary heats of reaction. The values reported in NBS Circular 500 and NBS 270-3 based on the same measurements are incorrect.

TABLE 1. TRANSPOTENTIALS AND HEATS OF FORMATION

Ion Neutral	Ap eV	ΔH_f pos ion kcal/mole	Ip eV	Method
AsF_3^+	12.35 ±0.1 12.25 ±0.1	96	12.3	s.l.p. e.p.d.
AsF_2^+ F^-	12.8 ±0.1	168	12.1	e.p.d.
$AsF^+ + F_2$	19.6 ± 0.1	265	11.4	s.l.p.
$F_2^+ + AsF$	23.8 ± 0.1	- 1*		s.l.p.
$F_2^+ + As + F$	27.7 ± 0.2	D(As-F) = 89		e.p.d.
$F^+ + AsF_2$	21.6 ± 0.4	-111*		e.p.d.
$F^+ + As + F_2$	29.3 ± 0.1	66**		e.p.d.
$F^+ + As + 2F$	31.0 ± 0.2	68**		e.p.d.

* ΔH_f of the neutral

** ΔH_f(As); to be compared to the accepted value of 72 kcal/mole.

OPTICALLY MODIFIED MASS SPECTRA (OMMS) OF COS^+ *

Arthur B. Denison, John M. Phillips
Department of Physics and Astronomy
Laramie, Wyoming 82071

James H. Weber
Laramie Energy Research Center, ERDA
Laramie, Wyoming 82070

Recent work[1,2] has shown the value of simultaneous electron impact-optical radiation spectroscopy in understanding the excited state processes involved in molecular ionization and fragmentation. The COS system appeared particularly interesting in that the ion and fragment intensities changed markedly with the addition of light to the normal impact electrons in the ionization chamber of a time-of-flight mass spectrometer. Both the absolute magnitude and relative intensities of the fragment mass peaks change with the addition of light. Although the mechanism responsible for the optical modification is not known, definite experimental results can be reported.

The main fragments of COS, in addition to the parent ion, are S^+, CO^+ and CS^+. The ion increase with the addition of light is most pronounced as the electron impact energies approach the normal appearance potentials. The CS ion seems to play a key role since the intensity of this ion changes the most rapidly following the introduction of the light beam into the ionization chamber. The maximum increase of this ion, by a factor of five, occurs within a few seconds. This increase, however, takes much longer than the corresponding effect in CO_2[1], which reaches a maximum within milliseconds. The mechanism by which the CS^+ is produced is not clear at the present time. It is known that with the optical radiation present the total energy of electron impact plus photon energy can never be less than 10.5 eV. The electron impact energy can be lowered to 7.3 eV with 5500Å light present to produce CS^+. Below this electron impact energy the light is not effective in increasing the ion intensity. For electron impact energies above 7.3 eV, longer wavelengths do give rise to increased ion intensity.

In the course of this study a practical benefit of optically modified mass spectroscopy (OMMS) became apparent. It is difficult without a high resolution mass spectrometer to distinguish between CS^+ and an impurity

*This research was sponsored in part by the National Science Foundation through Grant GP36683X1

CO_2^+, both of which have the same nominal mass. Using optical irradiation we were able to clearly separate these ions. The CO_2 ion[1] is enhanced by the presence of irradiation only when the wavelength is less than 3000Å. The CS^+, on the other hand, can be increased with radiation at much longer wavelengths as mentioned above.

We are continuing the study of the COS system in an effort to understand the fragmentation routes and the particular appearance of the CS^+.

---

[1] R. E. Ellefson, B. A. Osterlitz, J. M. Phillips, A. B. Denison, J. H. Weber, "Optically Modified Mass Spectra of CO_2," Chem. Phys. Lett. 31, 364 (1975).

[2] R. E. Ellefson, A. B. Denison, J. H. Weber, "Optically Modified Mass Spectra of n-Pentane," Chem. Phys. Lett., in print June 1975.

ELECTRONIC STATES OF FRAGMENTATION IN THE MASS SPECTROMETER

L. J. Hendricks, Dept. of Chem., Colorado School of Mines, Golden, Colorado 80401, and R. H. Shapiro, Dept. of Chem., Univ. of Colorado, Boulder, Colorado 80301.

This work is a theoretical explanation of the observations reported by Hendricks and Shapiro (Mass Spec. and Ion Phys. 15 399, 1974) of correlation between mass spectrum fragmentation rate constant data and photoelectron spectra. The fragmentation rate constants were obtained from numerical solution of the absolute rate equations at fixed energies. These energies were those for which charge exchange ionization could be used to approximate monoenergetic excitation. By plotting the rate constants as a function of the monoenergetic excitations, the resultant curve shows correlation with the electronic states involved in the photoelectron spectrum of that compound.

To solve the involved equations numerically requires the choice of a particular fragmentation pathway. The only model used has been a two-step consecutive fragmentation, in which the parent ion fragments with rate constant, k_1, to a daughter ion, which in turns decomposes to a secondary fragment. The compounds examined were limited to those for which this particular pathway applies exactly or as a close approximation.

For monoenergetic excitation, the distribution function, F(E), will be a delta function in energy. Where the initial concentration of the parent ion appears in the elementary equations, the product of the distribution function and the "constant" concentration of unionized molecules will appear in correct differential equations for the chosen model. However, this distribution function always appears as a multiplicative factor in the solution for each ion concentration, and hence, when the ion abundance ratios are formed mathematically for comparison with the experimental data, the distribution function cancels out completely from all the equations. Thus, the correlation between the rate constant curves obtained by this method and the photoelectron spectrum cannot be explained on the basis of the distribution function.

The $k_1(E)$ has been measured at various energies. For some of these energies, the fragmentation arises from one excited electronic state. However, for other energies, the fragmentation, although still the same, may well be arising from a different state. (See Figure.) If both the daughter and the parent ion are being observed, the fragmentation is not a simple direct ionization. Fragmentation by direct ionization occurs on a time scale of about 10^{-12} sec.---too fast to be observed in the mass spectrum, and hence only the daughter ion is observed. If both parent and daughter ions are observed, the process is likely a two-step process, where the parent ion is produced in a "stable" state that decays to the daughter by a curve-crossing to the dissociative level of another state. If this process occurs on a time scale of 10^{-5} to 10^{-6} sec., both parent and daughter ions appear in the mass spectrum.

These molecular ions are produced as the ground state ion at the lowest energies, as the first excited state ion at slightly higher energies, and so forth. Frequently, however, several of these states of the molecular ion will fragment by curve crossing to the SAME dissociative state. Thus, each state of the molecular ion will have its own k_1 associated with it, but the mass spectrum will not distinguish these by mass,

since all the molecular ions are fragmenting to the same mass fragment ion for each of these different energy states. This is illustrated in the Figure.

As the monoenergetic excitation is increased from energy to energy, structure will appear in the plot of $k_1(E)$ as a function of energy due to the contributions of each separate k_1. Since this structure is related to the states giving rise to it, as is the structure appearing in the photoelectron spectrum, a correlation between these rate constant curves and the photoelectron spectrum should be expected.

The actual appearance of the $k_1(E)$ versus E curves would be as in the Figure, <u>if</u> the resolution of the rate constant measurements were adequate to resolve this much detail. However, the actual resolution is limited by the condition that measurements can only be made at energies at which charge exchange ionization can be produced. These plots cover a large range of energies compared with the range for any one state (or k_1), and so the full plot is not the plot of a single k_1 as a function of energy. Rather, the full plot shows the individual k_1's arising from the separate energy states over the range of energies appropriate to each state.

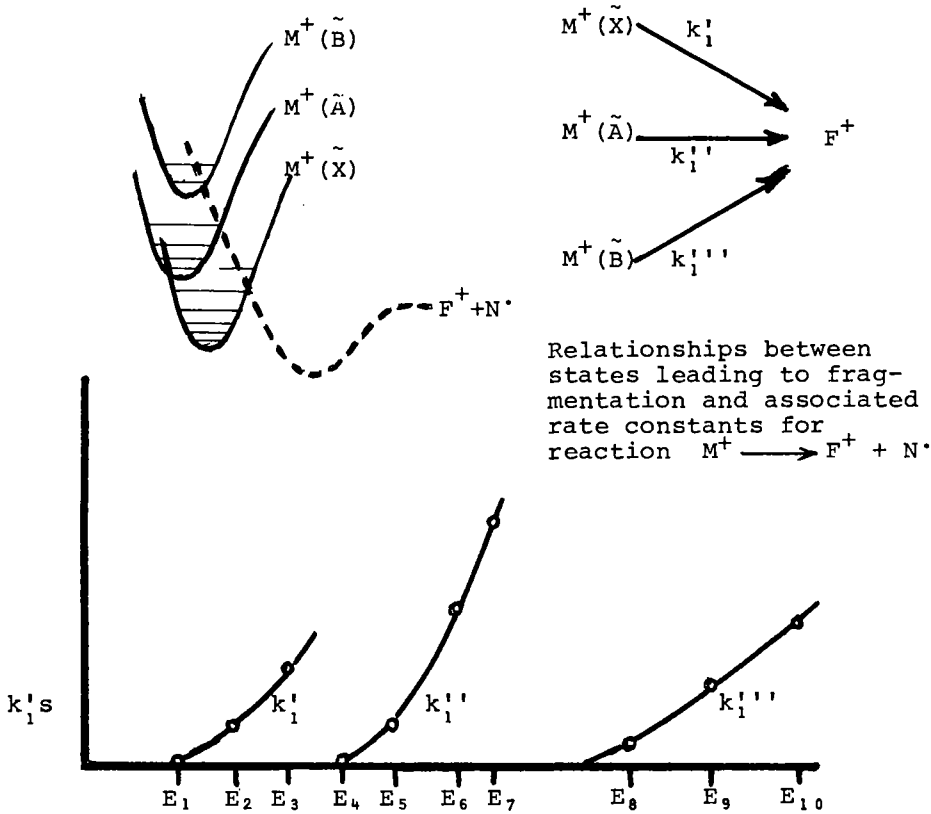

Thanks must be given to Dr. J. T. Hynes for many valuable discussions of this work.

ITERATIVE DECONVOLUTION OF NEGATIVE ION MASS SPECTRA

J. L. Franklin and F. J. Hadley
Chemistry Department, Rice University
Houston, Texas 77001

ACKNOWLEDGMENT

The authors are pleased to acknowledge support of this work by the Office of Naval Research, U.S. Navy, under contract No. 67-A-0145-0002.

In the present work, average translational energies and translational energy distributions were calculated for negative ions arising from dissociative resonance capture processes. This was done using the method of iterative deconvolution as developed by Morrison[1] and modified by MacNeil and Thynne.[2] The data were recorded on a TOF mass spectrometer and were taken from work done by Bennett, Pabst, Margrave and Franklin,[3] and Harland and Franklin.[4] Use of their data allowed us to compare our method with previous results. The systems considered were $TiCl_3^-/TiCl_4$, Br^- and $TiBr_3^-/TiBr_4$, and F^-/C_2F_6.

Franklin et al.[5] have shown that the kinetic energy with which an ion is formed in the ion source of a TOF mass spectrometer can be determined from the full-width at half-maximum (FWHM) of ion mass peaks and relating these to thermal ions of the same width.[3,4] In this way, the apparent mass of the ion could be calculated, leading directly to its average kinetic energy. Their study showed the widening effect of the gate pulse on the mass spectral peaks. This results, of course, from the gate pulse having a finite width.

We have attempted to remove this widening effect by the process of deconvolution, using the procedure of MacNeil and Thynne.[2] It involves 20 smoothing operations followed by an arbitrary number of unfoldings. The proper number of the latter was determined using known thermal ions at onset. Our gate pulse was represented by a 20 μsec FWHM gaussian peak. We allowed it to be rounded since gate pulses are not, in reality, square. Unfolding, then, leaves one with a more accurate profile of the mass peak (one-dimensional velocity distribution). From this we calculate both the corresponding three-dimensional velocity distribution and energy distribution.

Statistical theory predicts that any excess energy in a negative ion complex should be equally distributed among the various vibrational modes. That is,

$$\bar{\varepsilon}_t = \frac{E^*}{N}$$

where $\bar{\varepsilon}_t$ is the average ion kinetic energy and E* is excess energy. E* can be varied by varying the electron energy and the effect of this variation upon $\bar{\varepsilon}_t$ can be measured. It is found that a factor, α, must be introduced in the denominator, representing the fraction of effective oscillators in the complex.

Our results, and those of Bennett et al.,[3] find α to be about 0.12 for $TiCl_3^-/TiCl_4$ and $TiBr_3^-/TiBr_4$. This would have all excess energy appearing in the one vibrational mode that becomes translational energy. For Br^- from $TiBr_4$, on the other hand, α is found to be 0.70, representing a greater distribution of excess energy among vibrational modes. The difference in the cases of Br^- and $TiBr_3^-/TiBr_4$ is thought to arise from the nature of the remaining neutral species (i.e. $TiBr_3$ and Br).

Some discrepancy was found in the case of F^-/C_2F_6 when comparing the two methods being discussed. The results are shown in Figs. 1a and b. Although the resonance curve for F^- is smooth, it is apparent that two processes are involved. This is seen in Fig. 1b. There is a sharp decline in average kinetic energy between 4.4 and 5.2 eV. The rather broad energy distributions in Fig. 1a also lend support to this conclusion. The discrepancy in the results of the two methods is probably due to the fact that the peak width measurements method relates all mass peaks to thermal, near Gaussian peaks; whereas the present method considers the shape of the original mass peak.

The method of iterative deconvolution, then, can provide one with reasonable estimates to energy distributions and average ion energies. This, in turn affords one a clearer understanding of electronic states involved in the resonance processes as well as useful information concerning the unimolecular decomposition of negative ion complexes.

BIBLIOGRAPHY

1. J. D. Morrison, J. Chem. Phys., 39, 200 (1962)
2. K. A. G. MacNeil, J. C. J. Thynne, Int. J. Mass Spectrom. Ion Phys., 3, 35 (1969)
3. S. L. Bennett, R. E. Pabst, J. L. Margrave and J. L. Franklin, Int. J. Mass Spectrom. Ion Phys., 15, 451 (1974)
4. P. W. Harland and J. L. Franklin, J. Chem. Phys., 61, 1621 (1974)
5. J. L. Franklin, P. M. Hierl and D. A. Whan, J. Chem. Phys., 47, 3148 (1967)

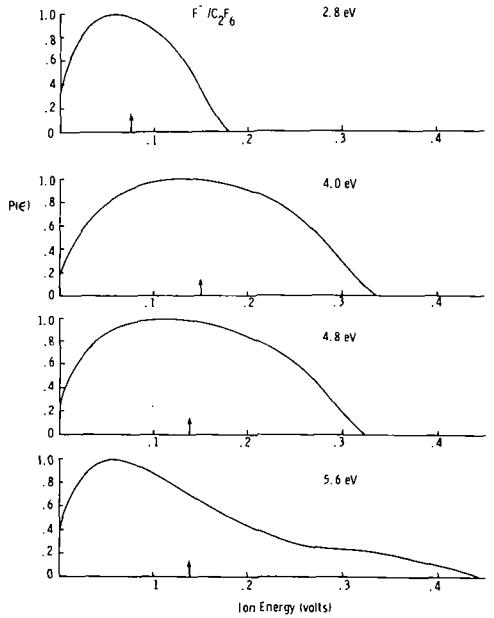

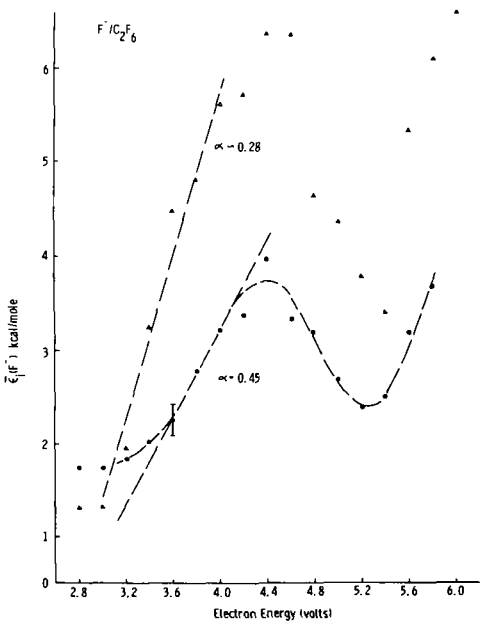

CAPTIONS

Fig. 1(a) Ion kinetic energy distributions for F^-/C_2F_6 at four electron energies over the resonance.

Fig. 1(b) Average translational energies for F^-/C_2F_6. The results of Harland and Franklin[4] (Δ); the present work (•).

NEGATIVE ION ELECTRON IMPACT STUDIES OF GROUP IVA TETRAHALIDES

R. E. Pabst, D. L. Perry, J. L. Margrave and J. L. Franklin
Department of Chemistry, Rice University
Houston, Texas 77001

ACKNOWLEDGMENT

The authors are pleased to acknowledge support of this work by the Office of Naval Research, U.S. Navy, under contract number 67-A-0145-0002.

The introduction of the vapors of $SiCl_4$, $SiBr_4$, $GeCl_4$, $SnCl_4$ into the ion source of a time-of-flight mass spectrometer, followed by low-energy electron impact, gave the ions X^-, X_2^-, MX_2^-, MX_3^-, and MX_4^-. Appearance potentials have been determined by deconvolution of the dissociative resonance capture curves, and translational energies of the ions have been measured through the resonance processes by the method of Franklin et al[1] and for higher energetic ions, by the modification of Pabst et al[2]. From the change in translational energy with electron energy the empirical constant α in the following equation can be determined:

$$E^*_{v,t} = \alpha N \epsilon_i \frac{m_i + m_m}{m_m}$$

where N is the number of vibrational modes, $E^*_{v,t}$ is the excess vibrational and translational energy, t_i is the translational energy of the ion and m_i and m_m are the masses of ion and neutral fragments. $E^*_{v,t}$ can be deducted from the appearance potential to give the heat of reaction to form thermal fragments. In some instances, one or more product may be electronically excited, however. It is thus possible to obtain good thermochemical values and/or electronic transitions.

The electron energy scale was calibrated with O^-/CO_2[3] and Cl^-/HCl[4]. Appearance potentials were obtained after deconvolution of the resonance curve by MacNeill and Thynne's[5] modification of Morrison's method[6].

The thermochemical data available on the Group IVA halides are limited. Heats of formation are known for the MX_4 and MX_2 species, but not for MX_3. The latter were estimated from average bond energies which give satisfactory results for several tetrahedral tetrahalides, including TiX_4[7], ZrX_4[8] and SiX_4 (this work).

The four compounds studied were $SiCl_4$, $SiBr_4$, $GiCl_4$ and $SnCl_4$. All gave the ions MX_3^-, MX_2^-, X_2^- and X^-. The MX_3^- were generally of rather small intensity and in the case of $SiCl_3^-$ and $SiBr_3^-$ translational energies could not be measured so the electron affinites (2.6 and 1.3 ev respectively) were lower limits. $GeCl_3^-$ had two resonances having the same α and with the difference in $E^*_{v,t}$ at onset being equal to the difference in appearance potential suggesting that there are two electronic states of $GeCl_4$ that have the same decomposition asymptote. Electron affinities of $GeCl_3$ and $SnCl_3$ were found to be 1.8 and 2.9 ev respectively.

All MX_2^- ions were of sufficient intensity to permit measuring translational energies and all gave values of $EA(MX_2)$ between 0.6 and 1.6 ev.

The X^- ion is sometimes formed from MX_4 at two different resonances, as was found by Wang et al[9] for $Cl^-/SiCl_4$. The lower resonance corresponds to the formation of $SiCl_3$ in the ground electronic state and the higher resonance corresponds to an electronically excited state of $SiCl_3$ for which we found $E^*_{e\ell}$ = 5.6 ev. The remaining compounds gave single X^-

resonances corresponding to the formation of electronically excited MX_3 with $E^*_{e\ell}$ of 4.7, .35 and 2.9 ev respectively for $SiBr_3$, $GeCl_3$ and $SnCl_3$.

The X_2^- ion was formed with small intensity ov r a very broad resonance indicating that two or more overlapping resonances were involved so that translational energies could be determined only for $Cl_2^-/GeCl_4$. All appear to formed along with MX_2 in an electronically excited state.[4] In the case of $GeCl_2$, $E^*_{e\ell}$ was found to be 1.9 ev. Ther remainder could only be estimated.

Our results are given in Table 1 and the thermochemical values employed are given in Table 2.

A wide range of values of α is to be seen in Table 1. Since α may be taken as the fraction of vibrational modes active in the decomposition process, it gives a clue in some instances to the dynamics of the process and the probable structure of the products. In the extreme, $TiCl_3^-/TiCl_4$, $TiBr_3^-/TiBr_4$ and $SnCl_3^-/SnCl_4$ have values of $\alpha N \approx 1$ which indicates all excess energy went into translation. This can be understood if the MX_3^- ions retained their tetrahedral structure. The reverse decompositions to for X^- + MX_3 all had larger α suggesting some distribution of vibrational energy, complete in the case of $Cl^-/GeCl_4$ and implying a change in structure of the MX_3, probably to a trigonal planor configuration.

In the formation of MX_2^-, the minimum number of effective oscillators expected is three, assuming no change in the X-M-X bond angle or M-X bond lengths. This would mean $\alpha \geq 0.33$, for $SiCl_2^-/SiCl_4$ and $SnCl_2^-/SnCl_4$ $\alpha = 0.30$, within experimental limits of the postulated value. The larger values of α for $SiBr_2^-$ and $GeCl_2^-$ suggest nearly complete equilibration of vibrational energy and a longer life time before decompostion.

REFERENCES

1. J. L. Franklin, P. M. Hierl and D. A. Whan, J. Chem. Phys. 47 3148, (1967).
2. R. E. Pabst, S. L. Bennet, J. L. Margrave and J. L. Franklin, to be published.
3. G. J. Schulz, Phys. Rev. 128, 178 (1962).
4. D. C. Frost and C. A. McDowell, J. Chem. Phys. 29, 503 (1958).
5. K. A. G. MacNeil and J. C. J. Thynne, Int. J. Mass Spectrom. Ion Phys. 3, 35 (1969).
6. J. D. Morrison, J. Chem. Phys. 39, 200 (1963).
7. JANAF Thermochemical Tables, Nat. Stand. Ref. Data Ser., Nat Bur. Stand. (U.S.) 37 (1971).
8. R. C. Feber, Heats of Dissociation of Gaseous Halides LA-3164, UC-4 Chemistry TID-4500 (40th Ed.) (1964).
9. J. Ling-FaiWang, J. L. Margrave and J. L. Franklin, J. Chem. Phys. 61, 1357-1360, (1974).
10. K. Jäger and A. Henglein, Z. Naturfarsch, 23a, 1122-27 (1968).
11. S. L. Bennett, R. E. Pabst, J. L. Margrave and J. L. Franklin, Int. J. Mass Spectrom, Ion Phys. 15, 451-461, (1974).
12. B. M. Huges, C. Lifshitz and T. O. Tierman, J. Chem. Phys. 59 3162 (1973).

TABLE 1

Specie	A.P. ev	Max ev	ei kcal/mole	α	$E^*_{v,f}$ kcal/mole	ΔH_f	Deduced, kcal/mole
$Cl-/SiCl_4$	0.9	1.7	2.2	0.43	9.8	$SiCl_3$	-100 ± 3
	6.8	7.6	6.6	0.36	26.2	$SiCl_3$*	29 ± 4
$Cl_2-/SiCl_4$	7.3	8.8	-	-	-	$SiCl_2$*	< 66
$SiCl_2-/SiCl_4$	7.5	8.5	3.2	0.30	17.4	$SiCl_2$	- 53 ± 3
$SiCl_3-/SiCl_4$	6.4	7.1	-	-	-	$SiCl_3-$	<-40
$Br-/SiBr_4$	5.2	5.7	4.5	0.40	20.1	$SiBr_3$*	51 ± 3
$Br_2-/SiBr_4$	5.3	5.9	-	-	-	$SiBr_2$*	< 75
$SiBr_2-/SiBr_4$	5.4	5.9	2.8	0.59	26.8	$SiBr_2-$	-50 ± 3
$SiBr_3-/SiBr_4$	4.7	5.6	-	-	-	$SiBr_3-$	<-28, ≈39
$Cl-/GeCl_4$	4.4	5.3	4.2	1.00	36.3	$GeCl_3$*	- 9 ± 3
$Cl_2-/GeCl_4$	4.5	5.6	2.4	1.00	28.2	$GeCl_2$*	0 ± 4
$GeCl_2-/GeCl_4$	5.2	6.3	2.5	0.93	48.8	$GeCl_2-$	-59, -100 ± 3
$GeCl_3-/GeCl_4$	1.6	2.1	1.4	0.26	9.5	$GeCl_3-$	-133 ± 4
	3.9	5.0	4.9	0.26	59.8	$GeCl_3-$	-130 ± 5
$Cl-/SnCl_4$	3.5	4.5	4.4	0.91	40.5	$SnCl_3$*	- 25 ± 3
$Cl_2-/SnCl_4$	4.6	5.5	-	-	-	$SnCl_2$*	< 39
$SnCl_2-/SnCl_4$	4.8	5.5	2.7	0.30	20.5	$SnCl_2-$	- 72 ± 4
$SnCl_3-/SnCl_4$	3.2	3.9	11.8	0.11	81.1	$SnCl_3-$	-158
$TiCl_3-/TiCl_4$	3.1	3.8	1.3	0.12	3.0	$TiCl_3-$	-142 ± 3
$TiBr_3-/TiBr_4$	2.4	3.1	1.6	0.14	5.2	$TiBr_3-$	-108, -188 ± 4

TABLE 2

GASEOUS HEATS OF FORMATION

Specie	ΔH_f,298 (kcal mole^{-1})				
$SiCl_4$	-157.1	[7]			
$SiCl_3$	-100	[A]			
$SiCl_2$	- 39.3	[7]			
$SiBr_4$	- 99.3	[8]			
$SiBr_3$	- 57	[B]			
$SiBr_2$	- 12.2	[8]			
$GeCl_4$	-130	[8]			
$GeCl_3$	- 89	[B]			
$GeCl_2$	- 44	[B]			
			Cl	28.92	[7]
$SnCl_4$	-120.9	[8]	Cl*	31.2	[7]
$SnCl_3$	- 91	[B]	Cl_2	0	[7]
$SnCl_2$	- 94.7	[8]	Cl_2*	51.0	[7]
Cl^-	- 55.9	[7]	Br	26.74	[7]
Cl_2^-	- 54.9	[12]	Br*	37.2	[7]
Br^-	- 50.8	[7]	Br_2	7.39	[7]
Br_2^-	- 52.1	[12]	Br_2*	46.9, 52.8	[7]

B - Estimated in this work * Excited

A - Experimental, from this work.

Negative Ion Formation in Conjugated Monocyclic Perchlorocarbons

Albert F.-T. Chen and Costello L. Brown

Chemistry Department
California State University
Los Angeles, California
90032

The formation of negative ions from conjugated monocyclic perchlorocarbons in a mass spectrometer has been investigated in our laboratory. Our initial efforts were concentrated on the formation of the pentachlorocyclopentadienide anion which possesses 6π-electrons and is considered to be aromatic. It was found that the pentachlorocyclopentadienide anion ($C_5Cl_5^-$) could easily be generated from both hexachlorocyclopentadiene and 1,2,3,4,5-pentachlorocyclopentadiene. In fact, except for the Cl^- ion, the $C_5Cl_5^-$ is the most intense ion in the negative ion spectrum of hexachlorocyclopentadiene.

The ionization efficiency curve for the formation of $C_5Cl_5^-$ from hexachlorocyclopentadiene showed two well resolved maxima at 2.08 eV and 3.80 eV. These maxima indicate that this ion is formed <u>via</u> a dissociative resonance capture process. Current investigations are in progress to see if we can determine the actual reaction or process each of these maxima represent.

The ionization efficiency curve for 1,2,3,4,5-pentachlorocyclopentadiene (C_5HCl_5) showed a rather diffuse dissociative resonance capture maximum for the $C_5HCl_4^-$ ion at 2.40 eV and a broad maximum at 3.80 eV for the $C_5Cl_5^-$ ion. The relative intensity of $C_5HCl_4^-$ in this spectrum is much more intense than that of the $C_5Cl_5^-$. In other words, cleavage of

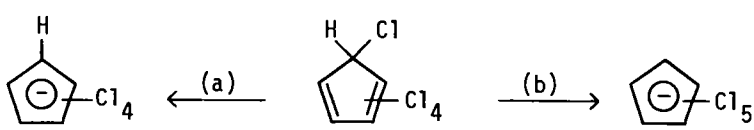

the C-Cl bond (process "a" above) is favored over cleavage of the C-H bond (process b). First order approximation of the dissociation energy difference between the allylic C-H and the allylic C-Cl bond is 20 Kcal/mole, which would favor the formation of the $C_5HCl_4^-$ anion.

Hexachlorobenzene was the only chlorocarbon investigated which exhibited a negative molecular ion. The occurrence of the molecular ion ($C_6Cl_6^-$) in this molecule is interesting from both mechanistic and theoretical point of view. Since hexachlorobenzene already has 6π-electrons, the added electron probably has to go into the antibonding level of the π-system. The ionization efficiency curve for $C_6Cl_6^-$ showed a maximum at 11 eV.

The molecular ion from octachlorocyclooctetraene was not observed. However, $C_8Cl_6^-$ was observed and found to have 4 I.E. maxima at 8.3, 4.7, 1.4 and 0.15 eV. The mechanism on the formation of $C_8Cl_6^-$ at different energies and their structural implications remains to be investigated.

New Studies of Complex Gaseous Halides. GARY D. BLUE and JOHN L. MARGRAVE, Rice University, Department of Chemistry, Houston, Texas 77001.

The high temperature mass spectrometric technique has been employed to identify reaction species and obtain thermodynamic data for equilibria in order to characterize the stability and importance of complex molecular species in the gas phase obtained on vaproization of inorganic halide condensed systems of a multicomponent or ternary compound compostition. The existence of new complex gaseous halide molecules may be inferred from a survey of the results of past activity in this research area. Among those systems chosen for investigation were: $AlCl_3 + MCl_x$ (e.g. M = Fe, Cr); mixed $M'Cl_x + M''Cl_y$, and $LiF + FeF_3$. A double-oven type sample system with Knudsen cell reactor served as the source of the molecular beam. The effects of considerable amounts of complex molecules in high temperature systems and also the possible practical importance to metallurgical applications will be considered. The need for supplemental work, i.e., transpiration studies, will be discussed.

The Application of Transition State Theory to Ion-Molecule Reactions

Harold Gershinowitz
The Rockefeller University
New York, New York 10021

I can think of no better way to begin this discussion of transition state than to quote from a very recent textbook, "There are a number of very useful approximation methods in molecular reaction theory which, while they bear a variety of names, are all based on one principle. They go under the name of Eyring (transition state) theory, the quasi-equilibrium theory, the RRKM theory, the statistical theory of mass spectra, the phase space theory and the variational theory of reaction rates. (R.D. Levine and R. B. Bernstein, Molecular Reaction Dynamics, (Oxford Univ. Press, 1974.))

My objective in this paper is to show that transition state theory (TST) can provide valuable information about the rates and mechanisms of ion-molecule reactions. In order to avoid any misunderstandings, I shall define precisely the nature of the phenomena I propose to treat by TST. First, the experimental conditions under which the reactions are studied are: (1) The reacting particles have thermal velocities. (2) The conditions in the reaction system are such that one may expect thermal equilibrium among the various degrees of freedom of the reactants. (3) The rate can be measured over a temperature range wide enough to distinguish among various forms of f(T). (4) Often the reaction can be measured over a range of pressures wide enough to determine whether or not the order of the reaction changes with pressure. Second, the principal experimental results to be explained are: (1) The reactions sometimes go much slower than the Langevin-Gioumousis-Stevenson (LGS) collision rate. (2) There is sometimes a marked dependence of the rate of reaction on temperature. Often the rate of reaction increases as the temperature is lowered. (3) Some of the reactions show a change in the order of the reaction as the pressure is changed.

Although the major part of the body of ion-molecule reactions does not fit these experimental criteria or display this behavior, more and more data are being reported which do. My own interest in this field was stimulated by the work being done on the high pressure pulsed mass spectrometer at The Rockefeller University by Field and his co-workers. Kebarle was one of the pioneers in the development of this type of apparatus and is reporting much data. The flowing and stationary afterglow, drift tube, and ICR mass spectrometers have also been used under the conditions which I have described.

Transition State Theory

One can state the sufficient conditions for validity of TST with deceptive simplicity. They are: (1) The reactants are in thermal equilibrium. (2) There is a critical configuration of the reactants called the activated complex. (3) Reaction occurs when this activated complex crosses a boundary which separates reactants from products. (4) The unit rate of reaction is given by the concentration of this complex times the frequency with which it crosses this boundary. (5) The state of the complex can be described by a set of normal coordinates, motion along one of which corresponds to the reaction path.

From these conditions one can derive an equation for the unit rate of

reaction, or the reaction rate constant k_r.

$$k_r(T) = c \cdot \frac{kT}{h} \cdot \frac{Q_a^{\ddagger}}{Q_n} \cdot \exp(-E_o/kT)$$

$Q_a^{\ddagger}$ is the partition function for the activated complex, excluding the reaction coordinate. Q_n is the partition function for the reactants. E_o is the difference in energy between the complex and reactants at absolute zero. c, called the transmission coefficient, is the probability that a system which crosses the boundary will not return. It is usually assumed to be unity.

When expanded, this equation becomes:

$$k_r(T) = c\frac{kT}{h} \frac{Q^{\ddagger}_{trans}\, Q^{\ddagger}_{rot}\, Q^{\ddagger}_{vib}\, Q^{\ddagger}_{elec}\, Q^{\ddagger}_{nuc}}{\prod_i (Q_i)_{trans}\, (Q_i)_{rot}\, (Q_i)_{vib}\, (Q_i)_{elec}\, (Q_i)_{nuc}} \exp(-E_o/kT)$$

As you know, all of these partition functions, except the nuclear, are functions of temperature. Hence, instead of the Arrhenius equation $k_r(T) = A \exp(-E_a/kT)$ in which A is independent of temperature, we get $k_r(T) = f(T) \exp(E_o/kT)$. When E_o is zero or very small all of the temperature dependence is in the pre-exponential term. At low temperatures, when the vibrational partition functions are unity, the relationship has the form $k_r(T) = BT^n$. At high temperatures when vibrational partition functions approach the value $kT/h\nu$ we have the same form with a different value for n. In the intermediate region f(T) does not have a simple analytical form.

Table 1 shows the form of the partition functions and their magnitudes. In the formation of an intermediate complex there may be a substantial change in the nature of the degrees of freedom. Many of the degrees of freedom which were translations or rotations in the reactants become vibrations in the complex. If we apply the TST equation to the collision of two atoms or two hard spheres, we find that the six degrees of freedom of translation in the reactants become three of translation, two of rotation and one of vibration in the complex. The resulting equation for the number of collisions is identical with that obtained from classical kinetic theory. For collisions of particles with internal degrees of freedom the rate is no longer the same. Table 2 shows the ratios, called the steric factor, between reactive collisions and hard sphere collisions, and also the temperature dependence of the pre-exponential term, for several kinds of reacting particles and intermediate complexes. I have shown these two tables only to point out that from the very general equation of TST one can immediately get order of magnitude rates and temperature dependences, with very few assumptions about the structure of the activated complex. For non-linear molecules with internal rotations, the steric factor and the temperature dependence can be substantially larger than those shown in Table 2.

I know that, at least for some readers, the question is not whether TST can explain the observed phenomena, but whether it is at all applicable to ion-molecule reactions. Let me, therefore, attempt to reply to some of the objections which have been made. In the first place, the conditions imposed do not include the often made assumptions that the transition state is at the maximum or saddle point of a potential energy surface or that the reaction must be adiabatic. The only restriction with regard to electronic states is that they must be accessible, i.e., not forbidden by quantum mechanical selection rules. The theory applies to reactions

with zero activation energy, provided that adequate attention is paid to conservation of angular momentum and to the zero point energy of newly formed vibrations. Another objection is that in an exothermic reaction it is not correct to use for the transition state the same temperature as for the reactants. This objection is not valid for the reaction conditions which I have postulated, namely that the reactants are in thermal equilibrium with each other and with their surroundings. In such a system the transition state is one of the configurations available to the reactants. Whether there is an activation energy or not, the volume of phase space corresponding to this configuration can be calculated by Maxwell-Boltzmann statistics. The exothermic heat of reaction is released after the system has passed through the transition state. Since the reaction system is assumed to be isothermal, this excess energy is dissipated by collisions with other molecules and with the walls, in the same way as the molecules for the reverse endothermic reaction gain their energy. In this respect ion-molecule reactions are no different from those of neutrals. For both kinds of reactions, it is only when this collisional mechanism of energy transfer fails that one must resort to non-Maxwell-Boltzmann statistics.

Transfer Reactions

TST postulates that a transfer reaction goes by the following mechanism $A^+ + B \rightleftharpoons (A^+ \text{---} B) \longrightarrow C^+ + D$. Since there are two particles on either side of the equation one would not anticipate any problems of dissipation of any excess energy which might be present in the transition state, since that could be absorbed in the relative kinetic energy of the separating products. If the transition state were loosely bound its partition function would be very similar to that of the reactants and one would calculate a rate about equal to the Langevin rate. However, if the transition state were tightly bound one would expect a substantial "steric factor" and a negative temperature dependence in the pre-exponential term. At low temperatures, when most of the vibrations are in their lowest state, it would take the form T^{-n}.

My own interest in the field of ion-molecules was aroused by the data on the hydride transfer reaction

$$t\text{-}C_4H_9^+ + i\text{-}C_5H_{12} \longrightarrow i\text{-}C_4H_{10} + t\text{-}C_5H_{11}$$

then being studied by Field and his co-workers. (J.J. Solomon, M. Meot-Ner & F. H. Field, J. Am. Chem. Soc. 96, 3727 (1974)). These authors have shown that by assigning a reasonable structure to the transition state the observed temperature dependence (T^{-3}) could be explained. The activation energy was found to be zero.

These authors also applied to this reaction a theory previously proposed by others which maintains that the rate is determined by the unimolecular decay of a long lived intermediate complex. It is my opinion that the introduction of such an intermediate is a complication not warranted by the experimental data. In the form used it involves unverifiable assumptions about the mechanism of the reaction, the structure of the intermediate complex, and the degree of excitation of the vibrations in the complex. These criticisms do not apply to the use of this theory for association reactions, which I shall discuss in a few minutes.

The successful application of TST to this reaction led us to examine a number of third order reactions, which I shall discuss later, and also the transfer reaction $O^+ + N_2 \longrightarrow NO^+ + N$. This reaction has been studied

over a much wider temperature range than most other ion-molecule reactions. The temperature coefficient is positive at high temperatures and becomes negative at low temperatures. We have shown (M. Meot-Ner, J.J. Solomon, F.H. Field and H. Gershinowitz, J. Phys. Chem. 78, 1773 (1974)) that by assuming that the activation energy is zero and that the transition state has a structure like that of the stable N_2O^+ ion one gets the results shown in Fig. 1. The change in slope is due to the fact that the vibrational partition functions, which are effectively unity at low temperature, approach the form $kT/h\nu$ at high temperatures and thus overpower the $T^{1/2}$ dependence of the rotational partition functions in the denominator of the rate expression.

Bimolecular Associations

For reactions of the type $A^+ + B \longrightarrow AB^+$ we have a more complicated kinetic and energy transfer problem. From the standpoint of TST one would write the mechanism as

$$A^+ + B \underset{k_2}{\overset{k_1}{\rightleftharpoons}} AB^+ \xrightarrow{k_2} AB^+$$

$AB^{+\ddagger}$ is at a higher energy level than AB^+, and unlike the case for transfer reactions this energy cannot be converted into the relative kinetic energy of two separating products. At high pressures, however, one would expect the number of collisions of $AB^{+\ddagger}$ with reactants or diluents to be sufficient to deactivate it before it re-dissociates into the reactants. Ordinary TST could therefore be used to calculate the high pressure rate and the temperature dependence of the reaction. It is clear, however, that this high pressure rate could, especially for polytomic ions and molecules, be appreciably less than the Langevin rate. For a true second order association there is no need to invoke an RRK energy transfer mechanism. However, many bimolecular associations do have a second order reaction rate constant which is a function of pressure. Consideration of these brings us into the field of third order reactions.

Third Order Association Reactions

At the low pressures of mass spectrometers, most ion-molecule association reactions are third order. In some cases, in which a relatively wide range of pressures is available, a transition from third order to second order kinetics is observed as the pressure is increased. Most of the reactions which have been studied show a negative temperature coefficient.

The theories of third order reaction have been mainly concerned with the combination of atoms to form diatomic molecules. In such cases there is no question that a third body will always be needed to absorb or carry away the energy of association. Such reactions can never be second order, except for those rare instances in which a radiative transition to a lower, more stable energy level can take place. Two mechanisms have been proposed and widely debated, the energy transfer (ET) and the bound complex (BC) mechanisms. Table 3 shows these two mechanisms. It has recently been shown (B. T. Park, R.L. Snow and W. D. Smith, J. Chem. Phys. 56, 926 (1972)) that both mechanisms contribute to atomic recombinations and that at low temperature and for heavy atoms the BC mechanism predominates. Despite this evidence, most of those who have been studying ion-molecule reactions have ignored the BC and concentrated on the ET mechanism. Although both of these mechanisms give the same formal expression for the third order rate constant, there is an important difference between them.

Looking at the Table we see that for the ET mechanism reaction (3) is an elastic collision, for the BC mechanism it is a transfer reaction. I recommend attention to this by those working on the effectiveness of third bodies.

TST can be applied to either of these mechanisms and does not distinguish between them, since in the TST equations any intermediate equilibria drops out. Last year we calculated the temperature dependence for eight third order reactions by TST, assuming that the vibrational partition functions are all close to unity. The results are shown in Table 4 and show an agreement between observed and calculated temperature dependence which is surprisingly good, considering the simplicity of the assumption.

It is only in the explanation of the rates in the intermediate region between second and third order that it becomes necessary to use theories of unimolecular decay. What one should use is a modification of the RRKM method which can take into account the possibility that the degrees of freedom in the activated complex are substantially different from those in the reactant molecules. The equation should be of the form

$$k_r(T) = \frac{kT}{h} \left(\frac{Q_a}{\prod_n Q_n}\right) \exp(-E_o/kT) \quad f(\epsilon)$$

where the Q's are the partition functions for the activated complex and the reactants and $f(\epsilon)$ is the RRKM expression for the distribution of energy among the vibrational degrees of freedom of the activated complex. This statement is equivalent to saying that in applying RRKM methods to association reactions one should use not the Langevin or a similar collision rate but the TST reaction rate for the formation of the complex. Recent work at The Rockefeller University by Michael Meot-Ner (M. Meot-Ner, Ph.D. Thesis, The Rockefeller University, 1975 and M. Meot-Ner and F. H. Field, J. Am. Chem. Soc. in press) indicates that for the association reactions of some large alkyl amine ions the high pressure second order reaction constant is substantially lower than the LGS rate.

Table 1

Q_{tr}	=	$\left(\frac{2\pi mkT}{h^2}\right)^{1/2} L$	$\sim$	10^8
Q_{rot}	=	$\left(\frac{8\pi^2 IkT}{h^2}\right)^{1/2}$	$\sim$	$10 - 10^2$
Q_{vib}	=	$(1-\exp(-h\nu/kT))^{-1}$	$\sim$	1 - 10
Q_{elec}	=	$\sum_{j=0}^{j} g_i e^{-E_j/kT}$	$\sim$	1 - 3
Q_{nuc}	=	$(2I + 1)$		usually 1

Table 2

Reactants	Complex	Steric Factor	Magnitude	n in T^n
A + L	L	$(Q_v/Q_r)^2$	10^{-2}	-1/2
L + L	N	$(Q_v/Q_r)^3$	10^{-3}	-1
L + N	N	$(Q_v/Q_r)^4$	10^{-4}	-3/2
N + N	N	$(Q_v/Q_r)^5$	10^{-5}	-2
L + L + L	N	$(Q_v/Q_r)^7$	10^{-7}	-7/2

Table 3

ET Mechanism	BC Mechanism		
$A + B \underset{(2)}{\overset{(1)}{\rightleftharpoons}} AB^*$	$A + M \underset{(2)}{\overset{(1)}{\rightleftharpoons}} AM^*$	or	$B + M \underset{(2)}{\overset{(1)}{\rightleftharpoons}} BM^*$
$AB^* + M \xrightarrow{(3)} AB + M$	$AM^* + B \xrightarrow{(3)} AB + M$		$BM^* + A \xrightarrow{(3)} AB + M$

Table 4[a]

Reaction	L	N	Expt'l
$He^+ + He + He \longrightarrow He_2^+ + He$	T^{-1}	$T^{-0.5}$	T^{-1}
$N^+ + N_2 + He \longrightarrow N_3^+ + He$	T^{-2}	$T^{-1.5}$	$T^{-1.7}$
$N_2^+ + N_2 + He \longrightarrow N_4^+ + He$	T^{-3}	$T^{-2.5}$	$T^{-1.6}$
$N^+ + N_2 + N_2 \longrightarrow N_3^+ + N_2$	T^{-3}	$T^{-2.5}$	$T^{-2.5}$
$O_2^+ + O_2 + O_2 \longrightarrow O_4^+ + O_2$	T^{-4}	$T^{-3.5}$	T^{-3}
$N_2^+ + N_2 + N_2 \longrightarrow N_4^+ + N_2$	T^{-4}	$T^{-3.5}$	$T^{-4.4}$
$H_3^+ + H_2 + H_2 \longrightarrow H_5^+ + H_2$	$T^{-4.5}$	T^{-4}	$T^{-4.6}$
$H_3O^+ + H_2O + CH_4 \longrightarrow H_5O_2^+ + CH_4$	$T^{-5.5}$	T^{-5}	$T^{-4.2}$

a. M. Meot-Ner, J.J. Solomon, F.H. Field & H. Gershinowitz, J. Phys. Chem. 78, 1773 (1974).

Figure 1

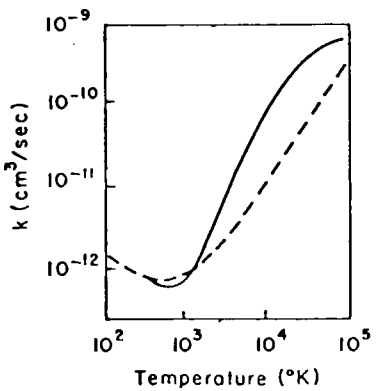

E-2

Applications of Phase Space Theory to Polyatomic Ion-Molecule Reactions. Walter J. Chesnavich and Michael T. Bowers, Univ. of California, Dept. of Chem., Santa Barbara, CA 93106

Phase space theory, originally formulated by Light and applied to unimolecular ion-molecule reactions by Klots, is extended to bimolecular reactions of polyatomic ions with polyatomic neutrals to give polyatomic products. In particular, expressions are derived for phase space volumes of oblate and prolate top molecules. In addition, ion-polar molecule potential functions are used to generate L-J angular momentum coupling relationships where appropriate. Applications of the theory to several ion-molecule systems will be made. These include the reactions of $NH_3^+ \cdot$ with NH_3 and H_2O studied by Chupka and Russell[1] and reactions of $t\text{-}C_4H_9^+$ ions with NH_3 and some methylamines studied in our laboratories.

[1]W. A. Chupka and M. E. Russell, J. Chem. Phys., 48, 1527 (1968).

E-3

The Dependence of the Lifetime of Intermediate Ion-Molecule Reaction Complexes on Internal Energy.* G. G. Meisels and F. Botz, Dept. of Chem., Univ. of Nebraska-Lincoln, Lincoln, NB 68508

A simple collision model which considers the contribution of rotational and vibrational energy was used in a mathematical analysis of the internal energy of the ion-molecule reaction complex. The effect of changing temperature, of varying applied fields, of inert gas additives, and of total pressure are included in the analysis. The resulting internal energy distribution functions are folded into RRKM calculations to obtain overall first order rate constants which are compared with rate constants obtained from differential arrival time distributions in high pressure mass spectrometry.

*A portion of this work was performed at the University of Houston. This investigation was supported in part by the USAEC.

Reaction intermediates and temperature dependence of ion molecule reactions. The system: $C_2H_5^+ \cdot CH_4$.

K. Hiraoka and P. Kebarle, Univ. of Alberta, Chem. Dept. Edmonton, Canada T6G 2E1.

The systems $C_2H_5^+$ and CH_4 studied at methane pressures in the torr range has very interesting temp. dependence. At lowest temperatures ($T < 125^oK$) the multiple clustering reaction: $C_2H_5^+ + 2CH_4 \overset{M}{=} C_3H_9^+ \cdot CH_4$ occurs. At somewhat higher temperatures t-$C_4H_9^+$ is synthesized by the sequence $C_2H_5^+ = (C_3H_9^+ \cdot CH_4)^* \rightarrow$ t-$C_4H_9^+ + 2H_2$. At still higher temperatures (160-210°K) protonated propane results from reaction (1): $C_2H_5 + CH_4 \overset{M}{=} C_3H_9^+$(1). Measurement of the equilibria leads to $\Delta H_1 = -6.6$ kcal/mole. ΔH_1 combined with literature data leads to $PA(C_3H_8) = 147$ kcal/mole. At higher temp. ($T > 250^oK$) the slow bimolecular reaction (2) occurs: $C_2H_5^+ + CH_4 = (C_3H_9^+)^* \rightarrow$ sec$C_3H_7^+ + H_2$. Reaction (2) has an activation energy $E_2 = 2.5$ kcal/mole. The activation energy is a consequence of an internal energy barrier of 9.1 kcal/mole. The nature of this barrier and the structures of $C_3H_9^+$ involved will be discussed. Similarly interesting reactions occur in the system $C_2H_5^+ \cdot C_2H_6$ at different temperatures.

Recent ion cluster stability measurements: $H_3^+(H_2)_n$, $CH_5^+(CH_4)_n$, H_3^+CO, $H(CO)_n^+$, $H(N_2)_n^+$, $Cl^-(HA)$.

K. Hiraoka, M. French and P. Kebarle, Univ. of Alberta, Chem. Department, Edmonton, Canada T6G 2E1.

Measurement of the clustering equilibrium in hydrogen show that the clusters $H_3^+(H_2)_n$ show a drop off in stability after $H_3^+(H_2)_3$. This is consistent with a triangular H_3^+ with one H_2 molecule at each corner. A drop off in stability of $CH_5^+(CH_4)_n$ clusters after $CH_5^+(CH_4)_2$ is consistent with three centre bond structure $CH_3{-}\begin{smallmatrix}H^+\\H^+\end{smallmatrix}$ of CH_5^+. H_3CO^+ formed by $H_2 + HCO^+ = H_3CO^+$ is not protonated formaldehyde but $COH^+ \cdot H_2$. The protium carbonyls $H^+(CO)_n$ show decreases of stability after $H^+(CO)_2$ and $H^+(CO)_6$. The $H^+(N_2)_n$ clusters show the same decreases, but there are significant and puzzling differences when comparison is made with the carbonyl clusters. The stabilities of $Cl^-(HA)$ complexes where HA are carbon and nitrogen acids do not increase with the gas phase acidity of HA.

REVERSIBLE REACTIONS OF GASEOUS IONS. X
THE DETERMINATION OF THE STABILITY
OF SEVERAL CYCLIC ALKYL CARBONIUM IONS

J. J. Solomon and F.H. Field

The Rockefeller University

New York, New York 10021

ABSTRACT

The hydride-transfer equilibria $t\text{-}C_4H_9^+ + RH \rightleftharpoons R^+ + i\text{-}C_4H_{10}$, where RH = several cyclic alkanes including methylcyclopentane, norbornane, and methyl norbornane have been investigated by pulsed electron beam high pressure mass spectrometry. These measurements have been undertaken to provide information useful in evaluating the extent of Σ bond delocalization (non-classical resonance energy) in norbornyl cation. The temperature dependence of the equilibrium constants over the range 320-520°K have been used to determine the relative values of several thermodynamic quantities of the cyclic carbonium ions. It is of interest that hydride ion transfer from norbornane to t-butyl ion (production of a secondary ion from a tertiary ion) is 1.2 kcal/mole exothermic.

DECOMPOSITION RATES OF EXCITED REACTION COMPLEXES

TEMPERATURE AND PRESSURE EFFECTS IN ASSOCIATION REACTIONS INVOLVING NH_4^+, $CH_3NH_3^+$ AND $(CH_3)_2NH_2^+$

Michael Meot-Ner and F.H. Field

ABSTRACT

Kinetic studies were made on clustering reactions involving NH_4^+, $CH_3NH_3^+$ and $(CH_3)_2NH_2^+$ between 250 and 400°K. The association reactions $BH^+ + B \xrightarrow{M} B_2H^+$ ($B = CH_3NH_2, (CH_3)_2NH$) exhibit transitions between second and third order kinetics in the pressure range 0.5 - 2.0 torr and the temperature range 250 - 400°K. The dependence of the overall forward rate constants on third-body pressure confirms the energy transfer mechanism $BH^+ + B \rightleftharpoons B_2H^{+*}$ followed by $B_2H^{+*} + M \xrightarrow{M} B_2H^+ + M$. The dissociation rate constants, k_b, of the excited complexes and their temperature dependences are:

Excited Complex	k_b^{350} (10^7 sec^{-1})	T Dependence of k_b
$(NH_4^+ \cdot NH_3)^*$	220	$T^{3.2}$
$(CH_3NH_3^+ \cdot CH_3NH_2)^*$	12	$T^{3.6}$
$((CH_3)_2NH_2^+ \cdot (CH_3)_2NH)^*$	6.0	$T^{7.2}$

The decrease of the rate constants with increasing molecular complexity and the increase with increasing temperature are quantitatively accounted for by calculations based on an RRKM quantum oscillator model.

Equilibrium Study of the $NO^+ \cdot N_2$ Ion Cluster*

D. L. Turner and D. C. Conway
Department of Chemistry
Texas A&M University
College Station, Texas 77843

ABSTRACT

The ion $NO^+ \cdot N_2$ plays a significant role in the aeronomy of the D-region of the ionosphere. To date, measurements of the bond energy and other thermodynamic parameters are marginal and probably questionable. A time-of-flight mass spectrometer has been used to study the equlilbrium $NO^+ + N_2 \rightleftharpoons NO^+ \cdot N_2$. Trace amounts of O_2 were added to increase the concentration of $NO^+ \cdot N_2$. The equilibrium constant has been determined for N_2 pressures from 3 to 12 torr and over the temperature range 178 to 273° K. Using a procedure described in the literature[1], the bond energy was computed as 5.0 ± 0.08 Kcal/mole at 298° K. Various other thermodynamic quantities were calculated by this method.

*This research was supported by the Robert A. Welch Foundation and the results are being prepared for publication.

[1]D. C. Conway and H. H. Teng, J. Chem. Phys. 59, 2316 (1973).

BIMOLECULAR FORMATION OF LONG-LIVED COMPLEXES IN ION-MOLECULE REACTIONS

W. N. Allen and F. W. Lampe

The Pennsylvania State University
University Park, Pennsylvania 16802

Results of recent experiments in our laboratory (Mayer and Lampe), in which SiH_3^+ ions were reacted with ethylene at 10^{-3} torr and low energy, suggested that the observed product ion, $SiC_2H_7^+$, was energy rich with a lifetime of about 10^{-5} seconds.

$$SiH_3^+ + C_2H_4 \rightarrow SiC_2H_7^{+*} \qquad (1)$$

This paper presents results of a further investigation of this system, the purpose of which was to clarify whether we were really seeing the energized ions or only the collisionally stabilized ones.

The experiments were carried out in a tandem mass spectrometer, the details of which have been described previously (Yu, Cheng, Kempter, and Lampe). Ions are produced by electron impact and the desired species selected by a quadrupole mass filter. The reactant ions then enter a collision cell containing a target gas where reaction occurs. The product ions which leave through an exit aperture, are mass analyzed with a second quadrupole mass filter, and detected with an electron multiplier.

When the reaction is carried out, $SiC_2H_7^{+*}$ is initially formed in the collision cell and can then undergo either of two processes, viz.,

$$C_2H_4 + SiC_2H_7^{+*} \xrightarrow{k_s} SiC_2H_7^+ + C_2H_4 \quad \text{Collision cell only} \qquad (2)$$

$$SiC_2H_7^{+*} \xrightarrow{k_a} SiC_2H_5^+ + H_2 \quad \text{Collision cell and detection system} \qquad (3)$$

A third possibility is that the ion remains energized and lives long enough to reach the detector. The complex ion is detected at m/e 59 and the dissociation product at m/e 57.

The ratio of the observed intensities of the 59 and 57 peaks is given by,

$$R = \frac{I_{59}}{I_{57}}_{obs} = \frac{I(SiC_2H_7^{+*}) + I(SiC_2H_7^+)}{I(SiC_2H_5^+)} \qquad (4)$$

A standard kinetic treatment of the quantities in the ratio gives a pressure-dependent expression, which, in the limit as the pressure approaches zero, reduces to the following:

$$\lim_{p \to 0} (R) = \frac{e^{-k_a(t_c+t_d)}}{1-e^{-k_a(t_c+t_d)}} \qquad (5)$$

where k_a is the rate constant for equation (3), t_c is the time the energized ion spends in the collision cell and t_d is the time the ion takes to reach the detector once it leaves the collision cell. Equation (5) shows that if the energized ion is being detected, then a plot of R as a function of collision cell pressure should have a positive intercept. Conversely, if k_a were too large, the energized ion would fall apart before reaching the detector and the intercept would be vanishingly small.

Figure (1) shows plots of R versus pressure for reaction energies of 1,2, and 5 eV in the lab system. Clearly, the plots for 1 and 2 eV have positive intercepts indicating that the energized ion is being detected at these energies. At 5 eV, k_a has apparently become so large that the ion dissociates before reaching the detector. The values of R accordingly do not appear to lead to positive intercepts. From the intercept of the 2 eV plot, a value of $k_a = 1.4 \times 10^5$ sec^{-1} was obtained.

Figure (2) shows a simple energy level diagram for the system. Energies shown in the diagram were obtained from thermochemical data (Franklin, Dillard, Rosenstock, Herron, Drexl, and Field; Wagman, Evans, Parker, Halow, Bailey and Schumm). For the reaction at E_{Lab} = 2 eV, using a value of 1.3 eV for E_o, a frequency factor of 10^{13} sec^{-1}, and s=24, simple RRK Theory gives a value of $k_a = 5 \times 10^5$ sec^{-1}. Although this is in good agreement with our experimentally determined value, the agreement is very probably fortuitous, since the RRK Theory is known to be inadequate for describing the unimolecular reaction process. A treatment of the system with the full Quasi-Equilibrium Theory is necessary and this is now in progress.

REFERENCES

Franklin, J. L., Dillard, J. G. Rosenstock, H. M., Herron, J. T., Drexl, K. and Field, F. W. (1969) Nat. Stand. Ref. Data Ser., Nat. Bur. Stand. (U.S.)

Mayer, T. M., and Lampe, F. W., (1974). J. Phys. Chem. 78, 2433

Wagman, D. D., Evans, W. H., Parker, V. B., Halow, I., Bailey, S. M. and Schumm, R. A. (1968) Nat. Bur. Stand. Tech. Note 270-3

Yu, T-Y., Cheng, T. M. H., Kempter, V. and Lampe, F. W., (1972) J. Phys. Chem. 76, 3321

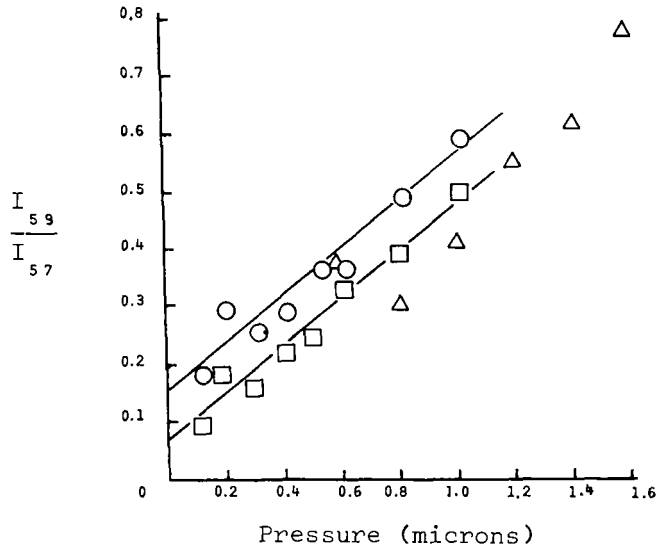

Figure 1. Ratio vs. Collision cell pressure: O, 1 eV; □, 2eV; Δ, 5eV.

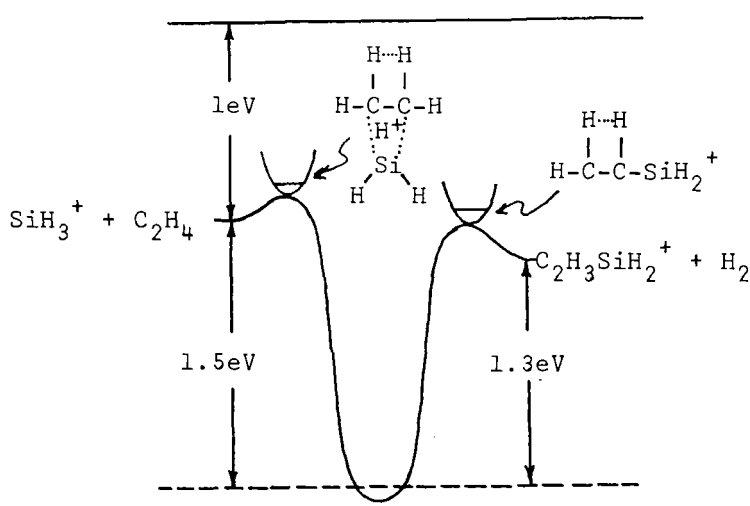

Figure 2. Suggested Energy Level Diagram

The Generation of Radical Anions by Reaction of O^- Ions with Organic Substrates

J. H. J. Dawson, A. J. Ferrer-Correia and K. R. Jennings
University of Warwick, Coventry, England, CV4 7AL

Ion cyclotron resonance techniques have been used to study the reactions of $O^{\cdot -}$ ions with a variety of unsaturated aliphatic compounds and with compounds containing electronegative substituents such as a halogen atom. The $O^{\cdot -}$ ions were generated from N_2O using electrons of nominal energy 0.5 eV and a trap current in the range 10-200 nA. Scattered electrons were ejected in the reaction region of the four-section drift cell by applying a signal of about 7 MHz across the trapping plates. A second electron ejection oscillator was connected across the trapping plates of the analyser region for experiments in which electrons formed in a detachment reaction were detected. The total current reaching the collector region was measured on a Keithley 602 electrometer.

Previous work[1] showed that in their reactions with CH_2CH_2 and CF_2CH_2, $O^{\cdot -}$ ions formed the radical anions $CH_2C^{\cdot -}$ and $CF_2C^{\cdot -}$ as major ionic products and this has been found to be a quite general reaction for many compounds. The four major processes leading to the formation of secondary ions are:

$$O^{\cdot -} + RH_2 \rightarrow R^{\cdot -} + H_2O \quad (1)$$

$$\rightarrow RH^- + OH\cdot \quad (2a)$$

$$\rightarrow RH\cdot + OH^- \quad (2b)$$

$$\rightarrow RHO^- + H\cdot \quad (3)$$

Reaction (1) is a major reaction channel for compounds containing a terminal $=CH_2$ group or an activated $>CH_2$ group and $R^{\cdot -}$ ions were found in the following systems:

$CH_2{=}CH_2$, $CH_2{=}C{=}CH_2$, $CH_2{=}CH{-}CH{=}CH_2$, $CHF{=}CH_2$, $CF_2{=}CH_2$, $CH_3CF{=}CH_2$, $CF_3CH{=}CH_2$, $CF_3(CH_3)C{=}CH_2$, $CNCH{=}CH_2$, $CH_3OCH{=}CH_2$, CH_3F, CH_2F_2, CH_3CN, CH_3CH_2CN, $CH_3CH_2CH_2CN$, $CH_3C{\equiv}CH$.

As more alkyl groups are attached to a molecule or the $>CH_2$ group becomes less activated, the importance of reaction (1) relative to reactions (2a) and (2b) falls, and no $R^{\cdot -}$ ions were observed in the propene and isobutene systems. This was further supported by the observation that $R^{\cdot -}$ ions are formed in the C_2H_5CN and n-C_3H_7CN systems, presumably by H_2 abstraction from the α-carbon atom, but not in the i-C_3H_7CN system in which H_2 abstraction from this carbon atom is impossible.

The relative importance of reactions (2a) and (2b) in each system was difficult to assess owing to the large difference in masses of the OH^- and RH^- ions, but there were significant qualitative differences, probably reflecting differences in the relative electron affinities of OH• and RH• and the stabilities of RH• and RH^-.

Reaction (3) was appreciably less common but occurred in several systems, such as the $CNCH{=}CH_2$ system, in which the reaction may possibly be formulated as

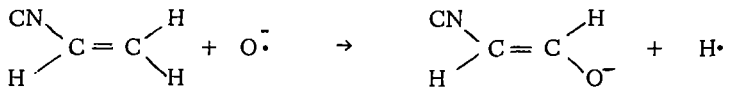

Although the radical anions were expected to be very reactive, no reaction of the type

$$R^{-}\cdot \quad + \quad RH_2 \quad \rightarrow \quad X^- \quad + \quad Y\cdot$$

was observed, but the ions $CH_2C^{-}\cdot$ and $CF_2^{-}\cdot$ were both observed to react with N_2O in reactions of the type

$$R^{-}\cdot \quad + \quad N_2O \quad \rightarrow \quad RN^- \quad + \quad NO\cdot$$

giving respectively CH_2CN^- and CF_2N^-.

In several other systems, an increase in pressure led to the loss of $R^{-}\cdot$ ions but no new ions were observed. In the acetonitrile system, the $CHCN^-$ ion was shown to react further to give neutral species plus a free electron by the use of two fixed ejection oscillators on the reaction and analyser trapping plates. A fixed frequency oscillator and a magnetic field scan were used to obtain total ion current (TIC) spectra[2] of the m/e = 39 ($CHCN^{-}\cdot$) and m/e = 40 (CH_2CN^-) ions in the presence and absence of the analyser region electron ejection. On switching on this ejection oscillator, the m/e = 40 signal was unaffected but the total "ion" current fell by an amount equal to the fall in m/e = 39 signal. This indicates that the $CHCN^{-}\cdot$ ion reacts to give free electrons in the analyser region which contribute to the current recorded in the collector region. Experiments with various added gases show that in most cases, the $CHCN^{-}\cdot$ ion is stabilised at higher pressures and that the reaction leading to the production of free electrons occurs specifically by reaction with CH_3CN molecules.

1. G. C. Goode and K. R. Jennings, Adv. in Mass Spectrometry, 6, 797 (1974).
2. G. C. Goode, R. M. O'Malley, A. J. Ferrer-Correia, R. I. Massey, K. R. Jennings, J. H. Futrell and P. M. Llewellyn, Int. J. Mass Spectrom. Ion Phys., 5, 393 (1970).

THE GAS-PHASE REACTIVITY OF DISUBSTITUTED AROMATIC COMPOUNDS WITH IONIC ACETYLATING REAGENTS

D.A. Chatfield, T.A. Elwood, and J.H. Futrell
Department of Chemistry
University of Utah, Salt Lake City, Utah 84]]2
M.M. Bursey, W.R. Kenan, Jr., Laboratories
University of North Carolina, Chapel Hill, North Carolina 275]4

Numerous reports have appeared in the literature that have utilized ion cyclotron resonance (ICR) mass spectrometry to differentiate between molecules containing various functional groups on a basis of their ion-molecule reactivity (1-4). A logical extension of this work has been the investigation of certain ion species as plausible chemical ionization (CI) reagent gases. Two compounds of interest in this laboratory which have shown characteristics of highly-selective reagent gases in the ICR are acetone and 2,3-butanedione (biacetyl). These two compounds behave as ionic acetylating reagents (Ac^+) by readily transferring CH_3CO^+ to many neutral molecules M. The acetylating reagent ions are formed from the fragmentation of and the ion-molecule reactions of acetone (Eq. 1 and 2) and biacetyl (Eq. 3 and 4):

$$\underset{m/e\ 58}{CH_3COCH_3^{+\cdot}} + CH_3COCH_3 \xrightarrow{k_1} \underset{m/e\ 101}{CH_3CO(COCH_3)CH_3^+} + CH_3\circ \qquad (1)$$

$$\longrightarrow \underset{m/e\ 43}{CH_3CO^+} + CH_3\circ \qquad (2)$$

$$\underset{m/e\ 86}{(CH_3CO)_2^{+\cdot}} + (CH_3CO)_2 \xrightarrow{k_1'} \underset{m/e\ 129}{(CH_3CO)_3^+} + CH_3CO\circ \qquad (3)$$

$$\longrightarrow \underset{m/e\ 43}{CH_3CO^+} + CH_3CO\circ \qquad (4)$$

The above reactions have been extensively studied by ICR techniques (5,6). The relative contributions of m/e 34, 58, and 101 from acetone reagent gas to the formation of a stable acetylated product ion of m/e (M+43), formed with a rate constant k_2, according to the reaction

$$Ac^+ + M \xrightarrow{k_2} (M + 43)^+ + N \qquad (5)$$

was dependent upon the specific composition and geometry of the species M. Similarly, the relative contributions of m/e 43, 86, and 129 from biacetyl, as determined using ICR double resonance techniques, reagent gas to stable (M + 43) ion formation proved to have a similar dependence upon M.

The gas-phase acetylation of ethylbenzene and the three isomers of xylene proved to be a most interesting study. In each instance, the rate constant k_2 for the formation of the $(M + 43)^+$ species was measured relative to the values of k_1 or k_1' (Eq. 1 and 3). Double resonance experiments indicated that the only precursor to the formation of a stable $(M + 43)^+$ product ion was CH_3CO^+. The results for ethylbenzene and xylene are shown in Table I. A 'priori, one would not predict that such a sticking reaction could form a stable product ion because any excess kinetic energy produced by the reaction cannot escape from the collision complex by the loss of a neutral product.

With these encouraging ICR results in mind, acetone and biacetyl were studied under CI conditions. The ion-molecule chemistry of acetone up to 1 Torr has been reported by MacNeil and Futrell (6), so it will not be discussed further at this time. Freshly distilled biacetyl was intro-

duced into an extensively-modified Varian MAT CH-7 mass spectrometer that has been equipped with a high pressure ion source (7). The mass spectrum of pure biacetyl was studied from 0.03 to 10 Torr pressure and between 100 and 300°C. Product ions other than m/3 129 appeared in the spectrum of biacetyl under CI conditions, including m/e 87, 101, 111, 155, and 173. When trace amounts of alkylbenzenes, anisole, phenetole, or aniline was introduced into the ion source at a pressure of 0.1 Torr of biacetyl, the anticipated $(M + 43)^+$ product ions appeared in the spectrum.

The ion-molecule reactions of xylene, acetone, and biacetyl were also studied on a more versatile instrument that removes the need to rely upon ICR double resonance techniques to determine reaction mechanisms. A unique tandem ICR mass spectrometer has been in operation for several years at the University of Utah in which a mass selected beam of ions are formed in a high pressure ion source and injected into a conventional ICR cell (8). Using this instrument, the reactions of biacetyl were studied from 5×10^{-5} to 1×10^{-3} Torr. Many of the ions that appeared in the CI spectrum of biacetyl were observed in the tandem ICR, and the following mechanisms were established:

$$\underset{\text{m/e 129}}{(CH_3CO)_3^+} + (CH_3CO)_2 \longrightarrow \underset{\text{m/e 87}}{(CH_3CO)_2H^+} + CH_2CO + (CH_3CO)_2 \qquad (6)$$

$$(CH_3CO)_3^+ + (CH_3CO)_2 \longrightarrow \underset{\text{m/e 101}}{C_5H_9O_2^+} + CO \qquad (7)$$

$$(CH_3CO)_3^+ \xrightarrow{\tau \geq 10^{-4}\text{sec}} \underset{\text{m/e 111}}{C_6H_7O_2^+} + H_2O \qquad (8)$$

$$\underset{\text{m/e 173}}{C_8H_{13}O_4^+} \xrightarrow{\tau \geq 10^{-4}\text{sec}} \underset{\text{m/e 155}}{C_8H_{11}O_3^+} + H_2O \qquad (9)$$

The m/e 111 species was believed to be a proton-bound dimer formed from m/e 87. Both m/e 129 and 173 were observed to readily undergo a slow metastable loss of water to form m/e 111 and 155, respectively, with lifetimes of $\tau \geq 10^{-4}$ sec.

And finally, a series of experiments were performed on the tandem ICR to observe the reaction of acetone and biacetyl with ethylbenzene and xylene. Acetone or biacetyl was admitted into the high pressure source and the m/e ratio of interest was injected into the ICR cell. Ethylbenzene or xylene was introduced into the differentially-pumped ICR cell and the intensity of the $(M + 43)^{\pm}$ ion was monitored. The relative contributions from the reagent ions of acetome and biacetyl to the $(M + 43)^+$ species are shown in Table II. It is evident from this data that the m/e 43 ion was not the only precursor ion that formed an acetylated adduct with the aromatic molecule. One must conclude from a comparison of the data presented in Tables I and II that either different reactions are being studied by the two experiments or that the ICR double resonance technique produced anomalous results. Since the ions were formed under similar conditions in both experiments, it is not obvious why the precursors to the reaction would differ. Additional work is currently underway to help and clarify this discrepancy.

TABLE I

Rate Constants for the Formation of $(M+43)^+$ Adduct in Units of 10^{-10}cc/molec-sec

Neutral	Acetone			Biacetyl		
	43^+	58^+	101^+	43^+	86^+	129^+
Ethylbenzene	0.01	0	0	0.03	0	0
o-Xylene	0.41	0	0	2.7	0	0
m-Xylene	0.20	0	0	0.85	0	0
p-Xylene	0.01	0	0	0.40	0	0

TABLE II

Ratios of Precursor Ions Contributing to the Formation of the $(M+43)^+$ Ion

Neutral	Acetone				Biacetyl		
	43^+	58^+	59^+	101^+	43^+	86^+	129^+
Ethylbenzene	2.8	1	1.2	1.3	2.2	9.4	1
o-Xylene	3.8	1.3	1	0	1.6	6.7	1
m-Xylene	3.6	0	1	1.2	1	8.6	1.7
p-Xylene	1.6	1.5	1.1	1	1.7	16	1

References

1. R.C. Dunbar, J. Shen, and G. Olah, J. Amer. Chem. Soc., 88, 3381(1966)
2. M.M. Bursey, T.A. Elwood, M.K. Hoffman, T.A. Lehman, and J.M. Tesarek, Anal. Chem., 42, 1370 (1970)
3. S.A. Benezra and M.M. Bursey, J. Amer. Chem. Soc., 94, 1024 (1972)
4. M.M. Bursey and M.K. Hoffman, Canad. J. Chem., 49, 3395 (1971)
5. A.K. Hoffman, T.A. Elwood, T.A. Lahman, and M.M. Bursey, Tet. Lett., 46, 4021 (1970)
6. K.A.G. MacNeil and J.H. Futrell, J. Phys. Chem., 76, 409 (1972)
7. M.L. Vestal, T.A. Elwood, L.H. Wojcik and J.H. Futrell, 20th Annual Conference on Mass Spectrometry and Allied Topics, Dallas, Texas, 1972, paper P10.
8. D.L. Smith and J.H. Futrell, 20th Annual Conference on Mass Spectrometry and Allied Topics, Dallas, Texas, 1972, paper S12.

Collision Induced Dissociation Reaction of Molecular Negative Ions CO_3^-, N_2O^- and NO_2^-

Richard L. C. Wu[†] and T. O. Tiernan[†]

Aerospace Research Laboratories (LJ)

Wright-Patterson Air Force Base, Ohio 45433

Collision-induced dissociation (CID) reactions of the type

$$XO_m^- + Y \rightarrow O^- + XO_{m-1} + Y \qquad (1)$$

[where $XOm^- \equiv CO_3^-$, N_2O^-, NO_2^- and $Y \equiv$ Xe, Kr, Ar, Ne, He, O_2, N_2, and NO] have been investigated in the recently modified ARL tandem mass spectrometer[1,2]. Cross sections for these reactions were studied as a function of translational energy. All of these processes exhibit endothermic thresholds. The post-threshold behavior was compared with the prediction of the statistical theory of Rebick and Levine[3]. The energy dependence of the cross section is assumed to have the form, $A(E_t-E_o)^n/E_{rel}$, where E_t and E_{rel} are, respectively, the total energy and the relative translational energy of the reactants and E_o is the threshold energy. The exponent n depends upon the mechanism of the process, with $1.9<n<2.2$ for a direct mechanism and $1.5<n<1.8$ for an indirect mechanism. For a given CID reaction, the calculated threshold function was convoluted, with the calculated energy distribution arising from the thermal motion of the target molecules (Doppler broadening[4]) and the energy spread of the incident ion beam. The calculated curves were then fitted to the experimental cross section in order to obtain the true energy threshold and the appropriate values of n.

Table I contains the values of E_o and n which gives the best fit to the experimental data for the CID reactions of the molecular negative ions CO_3^-, N_2O^- and NO_2^- impacted on various target gases. The exponent n given in Table I varies from 2.0 to 2.5; according to the statistical

theory, these CID processes are direct mechanisms - - not involving intermediate collision complexes. The bond dissociation energies were evaluated to be 1.95 ± 0.1, 0.43 ± 0.1, and 4.0 ± 0.1 eV, respectively, for the molecular negative ions CO_3^-, N_2O^-, and NO_2^-. The electron affinities of the corresponding neutral molecules were then calculated to be 3.1 ± 0.2, 0.22 ± 0.1, and 2.35 ± 0.1 eV, respectively, for the molecules CO_3, N_2O and NO_2.

This paper will be submitted for publication in the Journal of Chemical Physics.

TABLE I

Best Fit Value of E_0 and n for the Collision Induced Dissociation Reactions of CO_3^-, N_2O^-, and NO_2^- Impacted Upon Various Target Molecules and Electron Affinities of Corresponding Neutral Molecules.

Reactant Ion	Neutral Target	E_0(eV) (± 0.1)	n (± 0.1)	Electron Affinity (eV)
CO_3^-	Xe	1.9	2.2	
	Kr	1.9	2.0	
	Ar	1.9	2.2	3.1 ± 0.2[a] [CO_3]
	Ne	2.0	2.0	
	O_2	2.0	2.4	
	N_2	2.0	2.5	
		Ave. 1.95		
N_2O^-	Xe	0.5	2.5	
	Kr	0.4	2.3	
	Ar	0.4	2.4	0.22 ± 0.1[b] [N_2O]
	Ne	0.4	2.3	
	He	0.4	2.4	
	N_2	0.5	2.5	
		Ave. 0.43		

(TABLE I - Continued)

NO_2^-	Xe	4.0	2.0	
	Kr	4.0	2.2	
	Ar	4.0	2.2	
	Ne	4.0	2.1	2.35 ± 0.1^c [NO_2]
	He	4.0	2.4	
	N_2	4.0	2.4	
	NO	4.0	2.0	
		Ave. 4.0		

a. $EA(CO_3) = \Delta H_f^5(CO_3) - \Delta H_f^6(O^-) - \Delta H_f^6(CO_2) + D(O^- - CO_2)$

b. $EA(N_2O) = \Delta H_f^6(N_2O) - \Delta H_f(O^-) - \Delta H_f(N_2) + D(O^- - N_2)$

c. $EA(NO_2) = \Delta H_f^6(NO_2) - \Delta H_f(O^-) - \Delta H_f^6(NO) + D(O^- - NO)$

References

1. T. O. Tiernan and R. E. Marcotte, J. Chem. Phys. 53, 2107 (1970).

2. J. H. Futrell and T. O. Tiernan, in "Ion-Molecule Reactions," J. L. Franklin Ed., Plenum Press, New York 1972, Chapter 11.

3. C. Rebick and R. D. Levine, J. Chem. Phys. 58, 3942 (1973).

4. P. J. Chantry, Bull. Am. Phys. Soc. 16, 212 (1971); J. Chem. Phys. 55, 2746 (1971).

5. E. E. Ferguson, F. C. Fehenfeld and A. V. Phelps, J. Chem. Phys. 59, 1565 (1973).

6. J. L. Franklin, J. G. Dillard, H. M. Rosenstock, T. J. Herron, K. Draxl and F. H. Field, Ionization Potentials, Appearance Potentials and Heats of Formation of Gaseous Positive Ions, NSRDS-NBS26, 1969.

†Present Address: Department of Chemistry, Wright State University, Dayton, Ohio 45431

USE OF MASS SPECTROMETRY FOR ORTHOMOLECULAR DIAGNOSIS

by

Arthur B. Robinson, Mark Weiss, Walter E. Reynolds, and Laurelee R. Robinson
Linus Pauling Institute of Science and Medicine
2700 Sand Hill Road, Menlo Park, CA 94025

During the past six years, we have been striving to test the hypothesis that quantitative chromatography of body fluids followed by pattern recognition calculations could be used to develop indicators of human health that would be of use in preventive medicine, diagnosis, and evaluation of therapy. (1, 2, 3) We have also been interested in the possibility that body fluids might be introduced directly into mass spectrometers for diagnostic purposes. We first proposed this possibility to Dr. William Aberth of the Stanford Research Institute in 1971 as a potential use for the multipoint field ionization mass spectrometer that he was designing at that time. Since then, in collaboration with the Stanford Research Institute mass spectrometry group headed by Dr. Michael Anbar, we have carried out some promising experiments along those lines. That work will be published elsewhere. In addition, we have carried out some preliminary experiments using the chemical ionization source of a Finnigan Model 3200E mass spectrometer. These experiments are described below.

In conjunction with our work on orthomolecular diagnosis by various chromatographic means, we have carried out some work on experiments designed to compare the strength of patterns found by various kinds of chromatography and by direct mass spectrometry. Diagnostically useful patterns have been discovered for multiple sclerosis and Duchenne muscular dystrophy in humans and for aging in mice. In addition, potentially useful patterns have been discovered for breast cancer and mental retardation in humans.

Our paper at this ASMS meeting consisted of a 45 minute presentation that reviewed much of the chromatographic work that has been carried out in our laboratory during the past six years. In addition, preliminary results from experiments on human fasting, breast cancer, and multiple sclerosis that have been carried out with the Stanford Research Institute group were presented. Finally, a comparison of urine vapor chromatography, multipoint field ionization mass spectrometry, and chemical ionization mass spectrometry was made by evaluating the diagnostic power of these three procedures in distinguishing fasting normal subjects from non-fasting normal subjects.

Ten men provided a urine sample before and after a 24-hour fast. A month later the same ten men provided an additional pair of urine samples before and after a 24-hour fast. These 40 samples were introduced directly into the urine vapor analysis procedure.(4) In addition, 2.5 ml portions of the same samples were added to an equal volume of 50mM pH6.4 phosphate buffer along with 4 units of Sigma crystalline urease and maintained overnight at 22°C. The pH was adjusted to between 9 and 10 with 1M KOH and 10ml of a 1:1 mixture of n-butanol and ethyl acetate which had been presaturated with phosphate buffer was added to this mixture. The samples were mixed and centrifuged. 5.0 ml of the organic phase was evaporated to dryness at 50°C, dissolved in 0.2 ml methanol, and transferred to the solid probe of the mass spectrometer which was fitted with a chemical ionization source. After the methanol was evaporated at room temperature, the probe was inserted into the mass spectrometer and heated to a temperature of 100°C. After the total ion current had decreased, the temperature of the probe was raised to 200°C, and similarly finally raised to 250°C. The summed mass spectra from these three temperatures were collected as illustrated in Figure 1.

Figure 1.

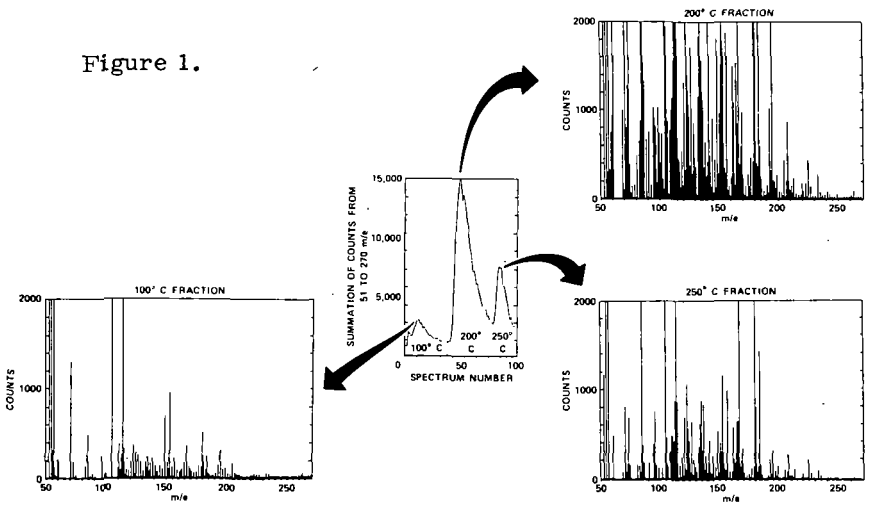

A non-parametric test of the hypothesis that the number of ions in each of the mass peaks in the 200°C fraction was systematically different between the fasting and nonfasting subjects was carried out as described in ref. 3. The calculation was carried out independently for each of the two groups of 20 samples and three mass peaks were selected as the most strongly correlating with fasting in both of the sets of 20 samples. The diagnostic power of these three peaks was then evaluated by means of a non-correlation index procedure as described in ref. 2. The resulting diagnostic value is shown in Figure 2. The diagnostic power of this chemical ionization procedure was 0.75 as compared with

0.71 for the multipoint field ionization mass spectrometry procedure and 0.90 for the urine chromatography procedure. We consider this a very promising result for both methods of mass spectrometry. Although the diagnostic power of these procedures as compared with the urine vapor chromatography is lower, these are our initial experiments with the mass spectrometry procedure, whereas the urine vapor procedure has undergone several years of developmental work.

Figure 2.

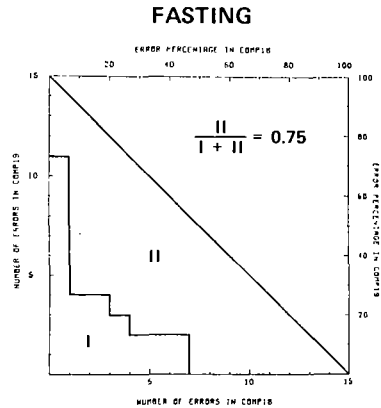

METHANE CHEMICAL IONIZATION MASS SPECTROMETRY
84, 113, AND 154 m/e

We think, on the basis of our initial experiments with the Stanford Research Institute group and on the basis of our initial experiments with the Finnigan chemical ionization source, that there is an excellent possibility that direct mass spectrometry of human body fluid samples without prior chromatographic separation will be a useful tool for orthomolecular diagnosis. We are especially interested in preventive medicine, and are therefore cautious about the economic practicability of the techniques that we are using. Chromatographic techniques are inherently slow, but have the advantage that the apparatus required is relatively inexpensive. Mass spectrometric procedures are inherently faster than the chromatography procedures but are carried out in more costly apparatus. Either of these technologies are economically practical if they are used independently. We suggest that direct introduction of human body fluid samples into various types of mass spectrometers and followed by computerized pattern recognition procedures should be vigorously explored as a potential method of choice for the quantitative determinations of human health that are needed in diagnostic, preventive, and therapeutic medicine.

References

1. Robinson, A.B. and Pauling, Linus, Orthomolecular Psychiatry, Chp. 3, W.H. Freeman & Co., San Francisco. 1973
2. Robinson, A.B. and Westall, F.C., J. Ortho. Psych. 3, 70 (1974)
3. Robinson, A.B. and Pauling, L., Clin. Chem. 20, 961 (1974)
4. Robinson, A.B., Partridge, D., Turner, M., Teranishi, R., and Pauling, L., J. Chromatography 85, 19 (1973)

Application of High Resolution Liquid Chromatography to the Analysis of Physiologic Fluids. John E. Mrochek and Charles D. Scott, ORNL*, P. O. Box X, Oak Ridge, TN 37830.

Automated, high-resolution, analytical systems based on liquid chromatographic separations are being used increasingly in clinical, biomedical research, and environmental laboratories. This is particularly true for separation and quantification of low molecular weight metabolites found in many physiologic fluids. A family of such analytical systems is now available. For example, high-pressure, ion exchange chromatography can be used to separate uv-absorbing compounds, carbohydrates, organic acids, amino acids, and others. Physiologic fluids can be separated without destroying labile molecular constituents since minimal pretreatment and mild separation conditions are used. Detailed studies of drug metabolism are possible by measuring many metabolites, including conjugates, in a single analysis. Biochemical indicators which may show the progression or regression of disease states such as cancer can be followed by monitoring constituents such as nucleosides, polyamines, and proteinbound carbohydrates.

*Operated for the Energy Research Development Administration by Union Carbide Corporation.

GAS CHROMATOGRAPHY - MASS SPECTROMETRY IN CLINICAL CHEMISTRY

Oddvar Stokke, Egil Jellum and Lorentz Eldjarn, Institute of Clinical Biochemistry, Rikshospitalet, Oslo, Norway.

Our GC-MS-computer system for analysis of biological material has gradually been developed during the last 8 years (1,2). With this system we are aiming at profiling as many as possible of the compounds present. In an ordinary urine sample we see between 500 and 1000 different GC peaks. Off line to the GC-MS-computer we have a computerized library which now contains about 60,000 abbreviated mass spectra.

We have used the system mainly in the following fields; (a) the diagnosis of inborn errors of metabolism, (b) studies of clinically well-defined, but biochemically obscure metabolic derangements like diabetes mellitus, acidotic conditions in children, different groups of neurological disorders, skin diseases, liver and kidney failure, (c) identification of noxious or toxic compounds, (d) determination of blood levels of drugs for therapeutic control, and (e) determination of compounds present in minute amounts (hormones etc.) (3).

The GC-MS system is not suited for screening of large numbers of patients, but for extensive screening of selected cases. The basis on which the patients to be studied are selected is therefore critical. For example, many of the inborn errors of metabolism present with one or more of the following symptoms: Metabolic acidosis, strange smell, recurrent vomiting, recurrent episodes of other symptoms, failure to thrive, neurological symptoms of unknown etiology, and simialr cases in the family. A thorough GC-MS screening should be performed in such cases.

Having decided to search for abnormal metabolites in a patient, it is important to eliminate as far as possible the influence of exogenous factors such as drugs and unusual food items. As a rule, we feel relatively safe if we can have a drug-free period of one week before the samples are collected. If this is impossible, we always ask for a list of the drugs which have been given. As to the diet, all excesses should be avoided before the sampling. Many strange compounds have been found which actually originated from diets and drugs (4,5). In order to avoid dietary artifacts, one could put the patients on a standardized diet the last few days before the sample collection. However,from a practical point this is both laborious and difficult. Instead, we prefer that the samples are collected early in the morning, before breakfast. At this time of the day the samples are less influenced by exogenous factors than later on.

No preservatives should be added to the samples, which should be deep-frozen if they cannot be brought to the laboratory immediately. It is common to store the samples in tubes, bottles or beakers made of plastic. One should then be aware of the possibility that plasticizers or other compounds may be eluted out of the plastic walls and contaminate the sample (5).

It should also be remembered that GC-MS is just one of many different techniques which can be used to disclose a metabolic abnormality. Many of the ordinary clinical chemical tests may be useful in addition to the GC-MS analysis. The choice of such tests differs with the symptoms. In general we determine the excretion in the urine of the major metabolic end-products, like urea, ammonia, creatinine and uric acid. We also determine the

urinary electrolytes and acid equivalents. The acid-base parameters of the blood and serum electrolytes enable us to calculate the anion gap, which may serve as a guide to the presence of any abnormal acid.

Our GC-MS system makes it possible to diagnose about 50 of the known inborn errors of metabolism. By this system we have also studied more closely some metabolic diseases (6,7), and detected and described some new ones. The metabolic defect in patients with Refsum's disease, involving storage of large amounts of phytanic acid, was, to a large extent, clarified by GC-MS (8).

In 1967 we described a new inherited disease which we called methylmalonic acidemia. A newborn infant with a severe acidosis excreted about 1 g per day of methylmalonic acid in the urine, due to an enzyme defect in the pathway converting propionic acid to succinic acid (9,10). Since then we have found several additional patients with the same disease, and also detected some other compounds accumulated as a secondary consequence of the primary defect (11).

The metabolites β-hydroxyisovaleric acid and β-methylcrotonylglycine were found in a child with neurological symptoms resembling Werdnig-Hoffmann's disease (12). The accumulation of the metabolites was probably due to a defective β-methylcrotonyl-CoA carboxylase in the degradation pathway of the amino acid leucine.

Five years ago we discovered a 19 year old male with a chronic metabolic acidosis who excreted 30-40 g of pyroglutamic acid (5-pyrrolidone-2-carboxylic acid) per day in the urine (13,14). Since then several similar patients have been found around the world, but in spite of intensive work, we still don't know what the biological significance of pyroglutamic acid is.

In conclusion, the GC-MS technique is a very powerful one, which enables us to diagnose conditions which would have been hard to detect by other means. In addition, its impact on clinical chemical research is substantial. However, the translation of the GC-MS result into meaningful biochemical language may in many cases take considerable time, and require the usage of many other methods and techniques.

References:

1. E. Jellum, O. Stokke and L. Eldjarn: Scand. J. clin. Lab. Invest., 27, 273 (1971).
2. E. Jellum, O. Stokke and L. Eldjarn: Analyt. Chem., 45, 1099 (1973).
3. L. Eldjarn, E. Jellum and O. Stokke: J. Chromatogr., 91, 353 (1974).
4. E. Jellum, H.C. Borresen and L. Eldjarn: Chim. Acta, 47, 191 (1973).
5. E. Jellum, O. Stokke and L. Eldjarn: Scand. J. clin. Lab. Invest., in press.
6. J.E. Pettersen, E. Jellum and L. Eldjarn: Clin. Acta, 38, 17 (1972).
7. J.E. Pettersen, S. Landaas and L. Eldjarn: Clin. Chim. Acta, 48, 213 (1973).
8. O. Stokke, K. Try and L. Eldjarn: Biochim. Biophys. Acta, 144, 271 (1967).

9. O. Stokke, L. Eldjarn, K.R. Norum, J. Steen-Johnsen and S. Halvorsen, Scand. J. clin. Lab. Invest., 20, 313 (1967).

10. S. Halvorsen, O. Stokke and L. Eldjarn: Lancet I, 765 (1968).

11. O. Stokke, E. Jellum, L. Eldjarn and R. Schnitler: Clin. Chim. Acta, 45, 391 (1973).

12. O. Stokke, L. Eldjarn, E. Jellum, H. Pande and P.E. Waaler: Pediatrics, 49, 726 (1972).

13. E. Jellum, T. Kluge, H.C. Borresen, O. Stokke and L. Eldjarn: Scand. J. clin. Lab. Invest., 26, 327 (1970).

14. L. Eldjarn, E. Jellum and O. Stokke: Clin. Acta, 49, 311 (1973).

Structures and Stabilities of C_4 and C_5 Hydrocarbon Ions.

F. P. Lossing and J. C. Traeger, Div. of Chem. Nat. Res. Council, Ottawa, Canada. K1A OR6.

At the Philadelphia meeting, preliminary results concerning the relative stabilities of a number of isomeric structures for $C_5H_7^+$ and $C_5H_9^+$ cations were presented. These experimental results, which were made by impact of a monoenergetic electron beam from an electrostatic velocity selector, have now been extended to a considerably larger number of isomeric olefinic and acetylenic species of nominal formula $C_4H_5^+$, $C_5H_5^+$, $C_5H_7^+$, and $C_5H_9^+$. The heats of formation of these isomeric cations, which correspond to generally abundant fragment ions in the mass spectra of hydrocarbons, are obtained by ionization potential measurements on free radicals of known structural identity generated by thermal decomposition reactions. Similar results on a few related ions containing the heteroatoms O and S have also been obtained. Comparisons with the energetics of fragment ion formation are instructive.

Proton-Transfer Reactions by Trapped-Ion Mass Spectrometry.

A.G. Harrison, P.-H. Lin, and C. W. Tsang, Dept. of Chem., University of Toronto, Toronto, Canada.

The variable reaction time (up to 4 ms.) available with the trapped ion technique[1] is ideally suited to the quantitative study of gas-phase proton transfer reactions. Results obtained in the following three areas will be discussed.

1. Rates of proton transfer from CH_5^+ and $C_2H_5^+$ to a variety of neutral molecules and comparison with theory.
2. Rates of symmetrical proton trnasfer reactions using isotopic labelling. $RXHD^+ + RXH \rightarrow RXH_2^+ + RXD$ ($RX=H_2N, CH_3NH, CH_3S, CH_3O, (CH_3)_2N$).
3. Relative proton affinities of oxygen-containing molecules from studies of proton-transfer equilibria $M_1H^+ + M_2 \rightarrow M_1 + M_2H^+$

[1] A.A. Herod and A.G. Harrison, Int. J. Mass Spectrom. Ion Phys., 4, 415, (1970).

Some Aspects of Negative Ion Chemistry.

Eldon E. Ferguson, Aeronomy Lab., NOAA, Boulder, Co. 80302.

In a classic early review on ion-molecule reactions,[1] a table of negative ion neutral reactions for which quantitative data were available had 9 entries. In a recent review on negative ion-neutral reactions alone,[2] tables of negative ion-neutral reaction rate constants included 174 reactions, reflecting the increase in knowledge in this field in a little over one decade. In this paper some of the negative ion-neutral reaction studies carried out at Boulder in a flowing afterglow system will be discussed. Some of the current research on both positive and negative ions in the recently developed Flow-Drift Tube will also be discussed, including both mobility and reaction rate constant measurements. The role of some of this negative ion chemistry in astrophysical and geophysical problems will also be discussed.

[1] F. W. Lampe, J. L. Franklin and F. H. Field, Prog. React. Kinetics 1, 1961.

[2] J. L. Franklin and P. W. Harland, Ann. Rev. of Phys. Chem. 25, 1974.

What is important to everyone in high pressure ion molecule reactions? P. Kebarle, Univ. of Alberta, Chem. Department, Edmonton, Canada T6G 2E1.

The presence of rapid deactivation and activation by third body collisions makes ion molecule reactions at high pressures (p > 1 torr) often distinctly different from those at low pressures. Most significantly, the reaction systems rapidly move towards thermodynamic equilibrium. Measurement of equilibrium constants has unlocked an unbelievably rich source of ion energetics: proton affinities, electron affinities, bond energies, ion solvation, etc. Recent work bridging the gap of proton affinities for water and ammonia based on: $B_1H^+ + B_2 = B_1 + B_2H^+$ will be used as illustration. Information on gas phase acidities of AH, electron affinities of A and bond energies D(A-H) for some carboxylic, carbon and nitrogen acids obtained from: $A_1^- + A_2H = A_1H + A_2^-$ will be given. At high pressure incipient solvation of the ions by clustering with solvent molecules Sℓ:ion + nSℓ = ion $(S\ell)_n$, shows what changes of energetics are introduced by solvation. Clustering in hydrocarbons often lead to synthesis of higher molecular weight hydrocarbon ions and study of such equilibria gives the heats of formation of these ions.

Molecular Orbital Studies of the Energies and Structures of Polyatomic Cations.

John A. Pople, Carnegie-Mellon Univ., Department of Chemistry, Pittsburgh, PA 15213

Molecular orbital techniques currently available for structural investigation are reviewed. These include the specification of basis sets for *ab initio* computations as well as methods for taking into account the effects of electron correlation. A critical examination is presented of such investigations of polyatomic cation structures made in recent years, with particular emphasis on ions containing hydrogen, carbon and oxygen. Systems discussed include H_3^+, CH_3^+, CH_5^+, $C_2H_3^+$, $C_2H_5^+$, $C_2H_6^+$, $C_2H_7^+$, $C_3H_3^+$, $C_3H_5^+$, and $C_3H_7^+$. The relative energies of various isomeric forms of these will also be treated.

Carbonium Ions and Protonated Cyclopropanes.

G. M. Kramer, Exxon Research and Engineering Co., Linden, New Jersey 07036.

Protonated cyclopropanes may be viewed as intermediates or transition states in various cationic systems. Their role in rearrangements involving alkyl, norbornyl and propyl cations in solution will be discussed. The positive identification of a protonated cyclopropane as an intermediate in any of these processes will be questioned as a result of various exchange and spectral studies. The relative stability of cations in solution and in the gas phase will also be discussed in light of recent data on ionic equilibria being obtained in these and other laboratories by hydride or halide transfer between ions and thermochemical solution studies. In some systems like, $iC_3H_7^+ + c\text{-}C_5H_{10} \rightleftharpoons C_3H_8 + c\text{-}C_5H_9^+$, close correspondence between solution and vapor phase behavior exists but in others preferential solution becomes a mitigating factor.

Ion Kinetic Energy Spectrometry.

J. H. Beynon and R. G. Cooks, Dept. of Chem., Purdue Univ., W. Lafayette, Indiana 47907.

This subject deals with changes in kinetic energies of ions accompanying either unimolecular or bimolecular reactions which occur in a field-free region of a mass spectrometer. The principle underlying the development of instrumentation for measuring these energy changes accurately is described. The determination of the kinetic energy release accompanying fragmentation and the kinetic energy loss or gain upon collision is especially stressed. Applications of the kinetic energy release measurement to the study of energy partitioning by mass spectrometry, to the determination of reaction mechanism and to the correction of ion enthalpies will be exemplified. The information obtainable from ion/molecule reactions at high kinetic energy will be discussed and applications to ion structure determination, measurement of isotopic incorporation and to state assignments in ionic reactants will be presented. Extensions of this methodology to ion/surface reactions, to ion/molecule reactions at non-zero scattering angles and to the study of the kinetics of highly excited species will be presented.

Comparative Experience with Computerized GC/MS Systems.

Robert B. Spencer, Merck & Co., Inc., West Point, Pa. 19486.

Combined gas chromatography/mass spectrometry is an important research tool in our laboratories. Two similar instruments, an LKB 9000 and an LKB 9000S, are used to perform the major portion of these analyses. Each system has been augmented by the addition of a data system. A Varian-MAT Spectro System 100 is interfaced to the LKB 9000, and a System Industries System 150 to the LKB 9000S. While these systems parallel each other in several respects, examples of runs on the two illustrate some of the important similarities and differences.

A COMPARISON OF INTEGRATIVE RECORDING TECHNIQUES FOR SELECTED ION RECORDING. Markey, S.P., Hawks, R.L., and Milne, G.W.A. NIMH, NIDA, and NHLI, National Institute of Health, Bethesda, Md. 20014.

Quantitative recording techniques for high sensitivity mass spectral analyses have been routinely utilized in numerous laboratories over the past several years. Because of the availability of significantly different computers, programs, interfaces, etc., a critical comparison of these available integration techniques has been made.

Biros[1] described the enhancement of mass spectral intensities using a time-averaging computer, or CAT of the type commonly employed in nmr spectroscopy. The same principles were employed by Murphy[2], et al demonstrating high precision and wide dynamic range with a minicomputer software version performing ensemble addition. Scans obtained with the maximum repetition rate permitted by the spectrometer (magnetic, accelerating voltage, or quadrupole) are continuously added in a point-by-point fashion. Signal will be enhanced in direct proportion to the number of scans, and noise with respect to the square root of that number. The resulting display contains m/e vs. intensity as in a single mass spectrum and intensities can be measured by area or peak height methods. A dynamic range of 2^{17} is attainable with the Varian C 1024 CAT.

Hard-wired multiple ion monitors are available for magnetic, accelerating voltage, and quadrupole scanning instruments. A variable number of channels (usually 2-8) can be selected, and each channel optimized for cycling to the top of the desired m/e value, integrating for a pre-selected period of time, and transmitting the signal to a multi-channel recorder. Because each channel can be optimized with respect to amplifier sensitivity, bucking, filtering, integration time, and recorder sensitivity, it is possible to record ions throughout the mass scale with wide dynamic range.

The most versatile of the major integrative techniques is based upon on-line computer systems to control mass spectrometers, sampling at preselected points in the mass scale, and storing the data for later graphic display, peak area determinations, or other manipulations. System versatility is obviously limited by software availability, but data systems have been described which can find the center of the ion and correct for mass defect,[3] and switch to different sets of ions throughout a chromatographic run[4] so that several compounds can be quantitated with maximum sensitivity in a single gc analysis.

With the availability of all three systems in our laboratories, a comparison was undertaken so that the most appropriate technique could be applied as required. Using the same samples, gc

column, and mass spectrometer, the three methods could be directly compared with regard to minimum detectable levels (signal/noise=3/1). A Finnigan 3200-GC-CI and GC-EI spectrometer was used with the Varian C 1024 CAT, Finnigan Programmable Multiple Ion Monitor (PROMIM), and Finnigan 6000 Data System (Revision G, corrected 3/10/75). Two sets of runs were made - the first, serially comparing all three techniques measuring the molecular ion region of cocaine (GC-CI), and the second with an updated ion monitoring program comparing the PROMIM and data system measuring three ions in the GC-EI spectrum of cholestane.

Table 1 permits a direct comparison of the CAT and PROMIM. Precise synchronization of spectrometer scan and CAT trigger rates was not possible so that scans of 50 msec duration were acquired every 100 msec. A range of eight m/e values was repetitively scanned, and that was determined only by visual appearance rather than optimal sensitivity. The results of identical analyses with the PROMIM, monitoring four ions with 100 msec integration led to a fourfold improvement in minimum detectable level. Of particular importance is the fact that retention time data is lost in ensemble addition, but mass resolution and ion profiles are retained.

Table 1 compares data obtained from equivalent analyses of cholestane using the multiple ion monitor and data system. Both were optimized with respect to mass defect and other operating parameters. Approximately a twofold improvement of PROMIM vs. data system was observed.

Data obtained from an earlier set of experiments with the data system was transferred to the NIH computer center for further massaging. A smoothing routine (MLAB) was applied to data with low signal/noise ratios permitting a cleaner graphic display to be derived. Incorporating smoothing and deconvoluting routines into ms data systems will allow greater confidence levels to be obtained.

A summary of the three major modes of integrative recording for gc-ms is given in Table III.

References:

[1]Biros, F.J.: Anal. Chem. 42: 537, 1970.

[2]Albrecht, B.H., Plattner, J.R., Hagerman, D., Markey, S.P., and Murphy, R.C.: 20th Ann. Conf. on Mass Spectrometry and Allied Topics, 1972.

[3]Holmes, W.F., Holland, W.H., Shore, B.L., Bier, D.M., and Sherman, W.R.: Anal. Chem. 45: 2063, 1973.

[4]Young, N.D., Holland, J.F., Gerber, J.N., and Sweeley, C.C.: Proc. 23 Conf. on Mass Spectrometry and Allied Topics, 1975.

TABLE I - SUMMARY

		MINIMUM DETECTABLE LEVEL THIS TEST ONLY
TIME AVERAGE (CAT)	•Limited to single isotope cluster •Sensitive to chemical background •Wide dynamic storage range for intensities •Superior for techniques with low chemical noise (FI, FDMS) and for high resolution analysis (peak shapes)	4 ng
MULTIPLE ION MONITOR-ANALOG RECORDER	•Sensitivity inversely proportional to number of mass channels monitored •Individual mass channel optimization, gives low noise, highest sensitivity •Wide dynamic recording range - m/e or intensity •Highest throughput of samples - instrumentation not used for data reduction	.5-1 ng
DATA SYSTEM	•Sensitivity inversely proportional to number of mass channels monitored •Single threshold for all ions plus software requirements make it less sensitive than multiple ion monitor •Digital data amenable to automated area calculations, peak smoothing, data storage •Software control permits change of mass channels during chromatographic analysis	1-2 ng

Kinetics of Polyvinyl Chloride Pyrolysis by On-line Thermogravimetric Analysis and Mass Spectrometry

KENT VOORHEES, R. W. MICKELSON, P. W. RYAN, D. CHATFIELD, I. N. EINHORN, J. H. FUTRELL, The Flammability Research Center and the Depts. of Chemistry and Material Science, The Univ. of Utah, Salt Lake City, Utah 84112

The kinetics of the thermal decomposition of polyvinyl chloride in the region of the initial 62% weight loss has been extensively studied. The results are somewhat conflicting, but in general, a reaction order of 3/2 is reported primarily from HCl formation data. Unfortunately, in most cases the weight loss of the polyvinyl chloride has not been followed. The thermal analysis (TGA) graph of an Aldrich PVC sample shows a small deflection in the 210-350°C region (Figure 1). A plot of percent conversion vs rate of conversion for this region (Figure 2) shows at least 3 separate processes occur in temperature range that had previously been treated as a single process region. It is these TGA advantages, both isothermal and dynamic, for polymer decompositions which have led to the interface of the thermal analyzer to mass spectrometer for effluent gas analysis for kinetic determinations.

A Mettler Model 1 thermal analyzer has been coupled to a computerized HP 5930A mass spectrometer through a Varian molecular leak valve. Heated Teflon lined stainless steel was used for transfer lines.

Figure 3 shows the HCl and benzene formation using the standard mass spectral reconstruct computer software. For this particular material, in the temperature range to 350°C, HCl and benzene are the major products produced. A 3/2 order plot for the benzene formation (Figure 4) of actual and calculated values is shown in Figure 5. Acceptable agreement using this approach between actual and calculated values can only be obtained after the 1st half life. Using an extended method (1) of Wall's Theory (2) for polymer degradations, an excellent fit can be obtained as shown in Figure 6. Although the results are preliminary, they do show that TGA-MS can be an extremely powerful tool for studying polymer decomposition mechanisms.

1. R. W. Mickelson, unpublished results.
2. J. H. Flynn and L. A. Wall, J. of Research of the Natl. Bureau of Stds., 70A, 487(1966).

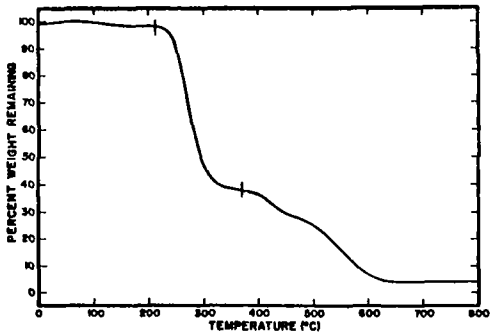

Figure 1. Thermogravimetric analysis of PVC in nitrogen at a heating rate of 10°C/min.

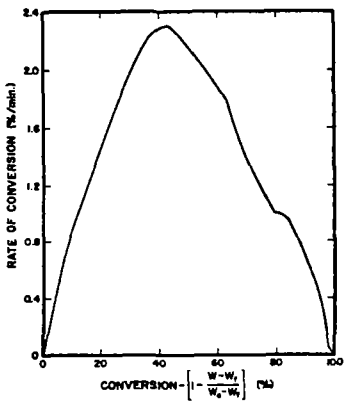

Figure 2. Major decomposition area of PVC showing an additional possible change in mechanism.

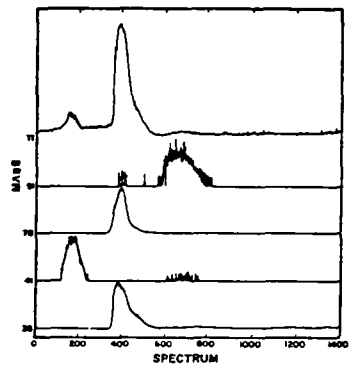

Figure 3. Specific ion abundance for PVC decomposed at a heating rate of 10°C/min.

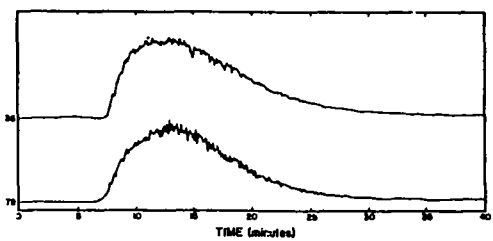

Figure 4. Specific ion abundance as a function of pyrolysis time at 240°C.

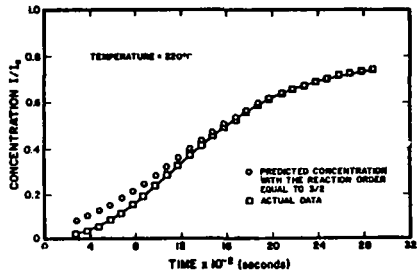

Figure 5 . Predicted concentration of benzene as a function of time using a power-model kinetic equation.

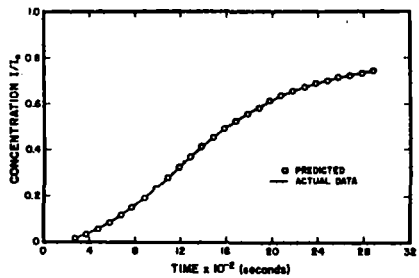

Figure 6 . Concentration of benzene as a function of time at 220°C.

H-4

A Gas Chromatograph-Mass Spectrometer-Computer System Using High Resolution Pressure Ionization (API) Techniques.

D. I. Carrol, C. Oertli, I. Dzidic, R. N. Stillwell, and E. C. Horning, Baylor College of Medicine, Houston, TX 77025.

A low dead volume API source, for use with high resolution glas open tubular columns, will be described. Column effluents and reactant gases enter the source separately. This prevents possible damage to the phase. The source can use either ^{63}NI or an electrical corona for ionization of the reactant gases. Corona and ^{63}NI positive ion spectra for the reactant gases isobutane, nitric oxide and amonia will be compared. Examples of high sensitivity detection and analytical applications will be discussed.

H-5

Mass Spectrometric Gas Analysis in Steam and Water.

G. L. CARLSON and A. PEBLER, Westinghouse Research Laboratories, Pittsburgh, Pennsylvania 15235.

A mass spectrometric method for the determination of trace quantities of gases in water has been developed. The technique has been applied to the detection and quantitative analysis of H_2, O_2, N_2, CO_2, and other trace gaseous impurities in high pressure and temperature steam from boilers and turbines. The procedure involves the collection of aliquots of steam at the actual turbine pressure and temperature conditions in two-port sampling cylinders which are then transferred to a gas mass spectrometer. Water is selectively removed with a dry ice trap, and the non-condensable impurities are quantitatively determined and referred to the collected amount of water. Some examples of actual impurity concentrations in turbine steam from operating power plants will be presented. The possibility of using the method for the determination of the solubilities of gases in water will also be discussed.

Determination of Concentration of Explosives in Air by Isotope Dilution. G. A. St. John, J. H. McReynolds, and M. Anbar, Stanford Research Institute, Mass Spectrometry Research Center, Menlo Park, CA 94025

In order to specify the required sensitivity for air monitoring systems designed to detect explosives, an absolute determination of the vapor pressures of six basic high explosives was performed. This was achieved using stable isotope labeled explosives as carriers and internal standards and field ionization mass spectrometry for detection and quantitation. Three of the explosives, ethylene glycol dinitrate (EGDN), nitroglycerin (NG), and pentaerythritol tetranitrate (PETN) were multiply labeled with ^{18}O in the nitro groups by synthesis from 89% $HN^{18}O_3$.[1] Deuterated toluene (d_8) and hexamine (d_{12}) were used to synthesize d_6-DNT, d_5-TNT, and d_6-cyclomethylene trinitramine (RDX).

Field ionization mass spectra of both the labeled and unlabeled explosives were determined on a single focusing magnetic sector instrument equipped with a SRI multipoint field ionization source.[2] Samples were introduced using a solid probe or a glass gas inlet system. Due to their high electron affinity these materials have a low field ionization efficiency even at the highest field strengths available with our sources. Operation at high fields produces a degree of field induced fragmentation, although this is difficult to distinguish from thermal fragmentation in these sensitive materials.

All of the materials studied exhibited strong molecular ions with varying levels of fragment ions from O, NO, NO_2 and M-NO_2. The spectrum of unlabeled RDX is given in Fig. 1. Many of the smaller peaks at m/e values below and above the molecular ion are due to background components in the sample and source which are ionized at very high efficiencies due to the high fields needed to ionize the explosives.

Equilibrium vapor pressures of the six explosives listed were measured by allowing a few milligrams of each unlabeled material to reach equilibrium in a 3-liter glass vessel at atmospheric pressure at 25°C. After equilibration 50cc of the equilibrated air were sucked into an evacuated bulb which had been previously loaded with a known quantity of the labeled explosive. The contents of the sample bulb were analyzed using the gas inlet system or eluted with solvent and transferred to the solid probe for the less volatile TNT, RDX, and PETN. During vaporization of the sample into the ion source the molecular ion region was repetitively scanned electrostatically and the ion counts integrated on a multichannel analyzer. From the recorded ratio of ion counts in the labeled and unlabeled molecular ions and the amount of labeled material added to the sample bulb and the volume of the sample, the equilibrium vapor pressure of the unlabeled explosive could be calculated. RDX was sampled at three elevated temperatures and its room temperature vapor pressures calculated

from the Clausius-Clapeyron equation. The vapor pressures determined for all six explosives by this method are given in Table 1.

Table 1

ROOM TEMPERATURE ($25^{\circ} \pm 2^{\circ}C$) VAPOR PRESSURES OF EXPLOSIVE COMPOUNDS OBTAINED BY THE ISOTOPE DILUTION METHOD

Compound	Concentration (g/cc)	P(torr)	Moles/Mole
EGDN	2.5×10^{-7}	2.8×10^{-2}	37 ppm
DNT	1.3×10^{-9}	1.4×10^{-4}	184 ppb
NG	3.2×10^{-10}	2.4×10^{-5}	31 ppb
PETN	1.0×10^{-10}	5.3×10^{-6}	7 ppb
TNT	4.0×10^{-11}	3.0×10^{-6}	4 ppb
RDX	8.0×10^{-12}	6.1×10^{-7}	0.8 ppb

A similar technique has been used to measure the vapor pressures of additives used in a number of smokeless powders. Fig. 2 shows the field ionization spectra of five different smokeless powders integrated over a probe temperature of $0-25^{\circ}C$. In the case of smokeless powders the basic explosive, nitrocellulose, has no measurable vapor pressure.

A vapor detection system for this type of explosive would consequently have to detect one or more of the stabilizing ingredients or deterrent coatings represented in the spectra shown in Fig. 2. The equilibrium vapor pressure of diphenylamine, the most common additive in smokeless powders, is found to be 10 ppb by this technique. The results of this study and their implications will be published in Forensic Science.

References

1. A. C. Scott, J. H. McReynolds, and M. Anbar, submitted to J. Labelled Compounds.

2. M. Anbar and W. H. Aberth, Anal. Chem. 46, 59A (1974).

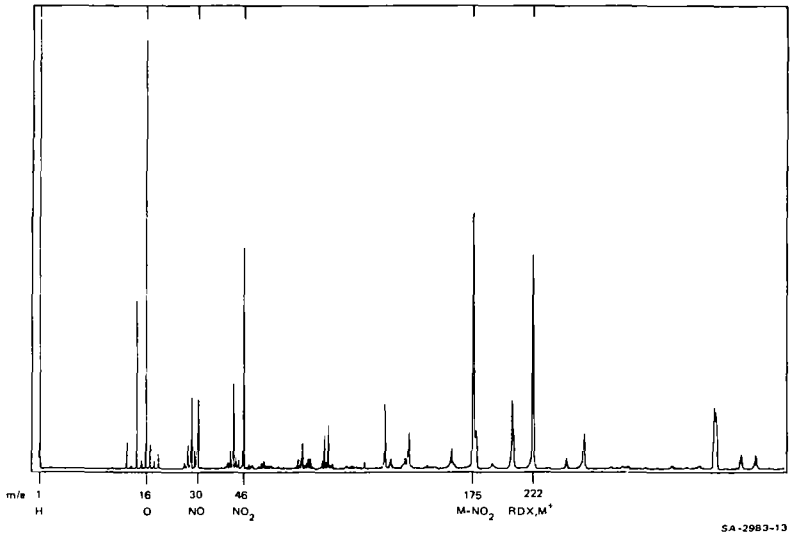

FIGURE 1 FIELD IONIZATION SPECTRUM OF UNLABELED RDX

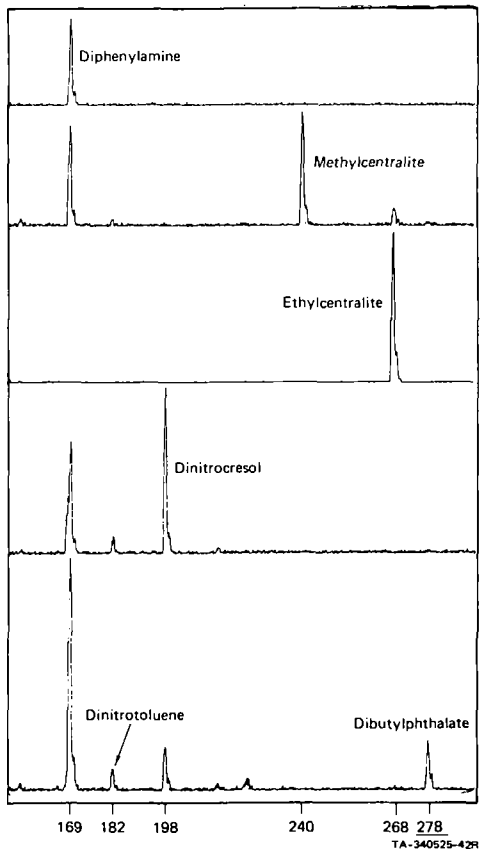

FIGURE 2 VOLATILE EFFLUENTS OF SMOKELESS POWDERS AT ROOM TEMPERATURE

Thermal Stability of Thin Films by Modulated Beam Mass Spectrometry. Margaret A. Frisch and Wilhad Reuter, IBM Research, Box 218, Yorktown Heights, N.Y. 10598

We have developed a technique in which the thermal decomposition of thin films can be examined, leading to the determination of reaction order and activation energy. The volatilization of impurities, even at low nanogram levels, can also be studied enabling one to distinguish between surface vaporization and bulk diffusion. The method involves the controlled heating of the sample at a precise linear rate usually in the range of 1 to 100 degrees/min. The molecular beam after modulation at 20 c/s is analyzed by repetitive scans in an automated quadrupole mass spectrometer. Kinetic data on non-equilibrium processes can be derived from the shape of the time-intensity curve, employing the analytical methods derived by P. A. Redhead.(1) We have applied this method to the properties of dicyan films, deposited by RF sputtering. Based on these mass spectrometric data and other supporting measurements, a description of the carbon-nitrogen bonding sequence in the film is suggested.

(1) P. A. Redhead, Vacuum, 12, 203.

QUANTITATIVE ANALYSIS OF COMPLEX SAMPLES BY COMPUTER CONTROLLED MASS SPECTROMETRY

D. Schuetzle and T. J. Prater, Research Staff, Ford Motor Co., Box 2053, Dearborn, MI. 48121, D. E. Hagge, Incos Corp., Berkeley, CA. 94710 and R. L. Knights, University of Washington, Seattle, WA. 98105.

The quantitative analysis of complex mixtures is subject to many problems. First of all there is a large dynamic range of concentrations for individual components. The presence of a complex matrix, including hundreds of compounds within this dynamic range, may lead to errors in quantitation since overlapping fragments may contribute to the total intensity of the ion peak used for quantitative work. High resolution accuracy to within $\pm$ 0.003 AMU is therefore needed to help eliminate this problem. High source pressures up to 10^{-5} Torr are generally incurred if trace components (< 1ng) are to be detected. The presence of high concentrations of water in addition to high source pressures may lead to source defocusing. The use of a computer system for this type of analysis is necessary for calculations of high resolution spectra and determinations of the concentrations of the desired peaks in the spectra.

Computer techniques for the quantitative analysis of complex hydrocarbon mixtures by high resolution mass spectrometry was first reported by Aczel et al.(1). Up to three hundred components for each sample were analyzed quantitatively. Schuetzle(2-5) and Knights(6) have used computer controlled mass spectrometric techniques for the qualitative and quantitative analysis of up to two hundred components in complex environmental mixtures. Precisions and accuracies of from 1 to 2% have been obtained on simple mixtures using several techniques(7-9). However, it is obvious that this represents a higher degree of quantitation than could be possible for complex samples.

Little data exists, concerning the factors which affect the quantitative accuracy and precision of such an analysis, and it has become increasingly obvious that a systematic study is needed. In addition, results from independent laboratories need to be compared on standard and unknown samples. Another important question is how much interlaboratory variation could be expected if compound response factors from one laboratory are used by another.

For this particular study, mixtures of standards were analyzed in the presence and absence of a complex mixture (atmospheric aerosols). Results obtained from the analysis of the aerosols were also compared.

Two computer controlled mass spectrometers were used for this study, one at Ford using a Varian Mat 311 mass spectrometer and a computer system developed by Incos Corporation of Berkeley, California, and the second at the University of Washington which used an AEI-MS9 mass spectrometer coupled to a PDP-12 computer.

The procedure for reduction of the mass spectral data to yield qualitative and quantitative results is summarized using the flow diagram given in Figure 1. An internal standard (2.9 μg) was added to the sample before analysis. The sample and standard were then eluted from a direct insertion probe and high resolution mass spectral data obtained every seven seconds (m/e:15-500). Major identifying masses ($\pm$ 0.003 AMU) were found for both the standard and unknown using a library reference file. Figure 2 gives the high accuracy mass chromatogram for one unknown, hexahydropyrene and the internal standard. The area under each curve was determined and the quantity of hexahydropyrene (Q) determined from the equation presented in Figure 2, where UNK was the integrated area under the hexahydropyrene peak, STD the integrated area under the standard peak, X the

quantity of standard added and R the relative response factor of the unknown to the standard. Peak deconvolution was performed on overlapping mass chromatograms.

The most serious problems affecting quantitative results were found to be source defocusing, electronic and vibrational noise and compound decomposition or oxidation. Changes in source focusing have been found to be responsible for gross errors in quantitative accuracy. An inert gas was mixed with the sample stream, and used to monitor any changes which occurred during the analysis. If deviations occurred, corrections were made to the spectra. Electronic or vibrational noise will cause variations in ion intensity and can be reduced by proper grounding and vibrational isolation of the mass spectrometer. Variations in the Ford system due to these effects were found to be 50 parts in 10,000 (full scale) and reduced to 1 part in 10,000. It has been found that even low concentrations of air (oxygen) in the source can cause oxidation and loss of many organic compounds. Flushing of the source with argon or helium greatly reduced this problem. Gold and treated glass surfaces minimized decomposition. Once these major problems were eliminated, the theoretical limit for quantitative accuracy was only a function of ion statistics as given by the equation:

$$IS = \pm \sqrt{1/N}\,(100)$$

where N was the number of ions represented under each ion peak and the factor 100 given to express the variation in %. The electron multiplier was set such that the amplitude of one ion was a minimum. The details of this experimental procedure is quite lengthy and details may be obtained from the author. By setting the intensity of one ion to a minimum, it was possible to maximize the dynamic range of the system. The average area of one ion was found to be 16 and this was used to calculate the theoretical precision as determined by ion statistics. A dynamic range of greater than 1000/1 was thus achieved. The table given below shows that the % variation in area obtained experimentally was very close to the theoretical value given by ion statistics.

			% Variation in Area (1σ)	
Mass	Area	No. of Ions	Experimental	Theoretical
63.027	27	2	100.0	81.0
77.020	50	3	69.0	56.0
70.003	548	34	18.2	17.1
118.992	7681	480	5.1	4.6
68.995	39570	2473	2.2	2.0

Five standards were analyzed in the absence and presence of a complex matrix using computer techniques. The matrix was also analyzed and the intralaboratory and interlaboratory results compared. All of the integrated mass chromatograms were comprised of more than 1000 ions, thus the % variation due to ion statistics was 2% or less. For the five standards there was a 7.8% (Ford) and 8.9% (UW) variation in results in the absence of a matrix and 12.9% (Ford) and 11.6%(UW) with matrix. Standards with matrix were 12.9% (Ford) and 11.6% (UW) higher than those of the standards without matrix. This data suggests that interfering ions were not resolved from the high accuracy mass chromatograms. A resolution of greater than 10,000 appears to be necessary to increase accuracy. Five unknowns were analyzed within a 11.2 to 12.1% precision. Results averaged from 10.2 to 19.6% higher at Ford than the UW, and was probably the result of instrumental differences.

In conclusion, quantitative results of accuracies better than ± 15% can be obtained for the analysis of complex samples using computer controlled high resolution mass spectrometry. If one laboratory uses response factors derived from another, then an average error of 30% may be expected.

REFERENCES

1. T. Aczel et.al., Anal. Chem. 42, 341(1972).
2. D. Schuetzle, A. L. Crittenden and R. J. Charlson, JAPCA, 23, 704 (1973).
3. D. Schuetzle et.al., Env. Sci. Tech. (August 1975).
4. D. Schuetzle, Ph.D. Dissertation, Univ. of Washington (1972).
5. D. Schuetzle, Biomed. Mass Spec. (Sept. 1975).
6. R. S. Knights, Ph.D. Dissertation, Univ. of Washington (1973).
7. L. Bertilsson et. al., Anal. Chem. 44, 1434, (1972).
8. N. Frew et. al., Anal. Chem. 44, 665 (1972)
9. N. M. Frew and T. L. Isenhour. 44,659 (1972)

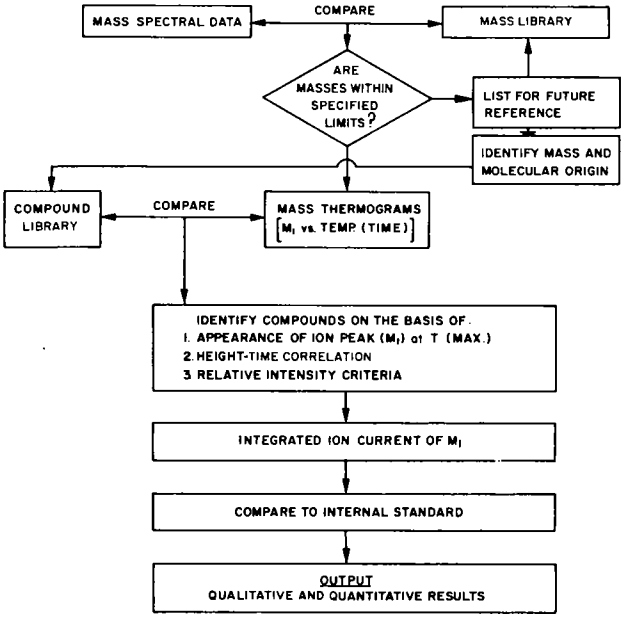

Figure 1. Computer Flow Diagram for Quantitative Analysis

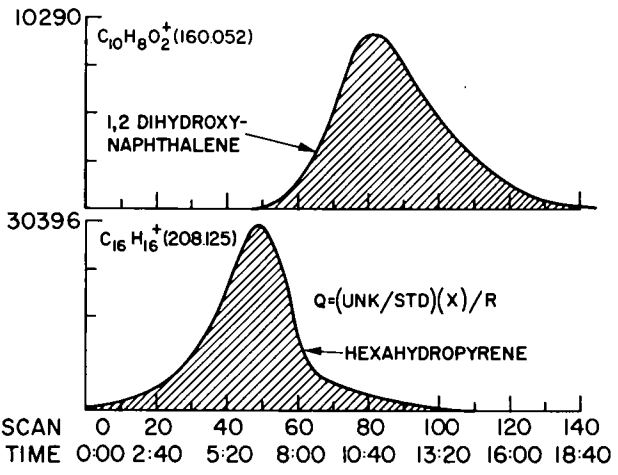

Figure 2. High Accuracy Mass Chromatograms

SIMULTANEOUS ION SCATTERING AND SECONDARY ION MASS SPECTROMETRY

by

Michael J. Vasile and Donald L. Malm
Bell Laboratories
Murray Hill, New Jersey 07974

This paper describes the addition of secondary ion mass analysis capabilities to a commercially available ion scattering spectrometer. Particular attention has been payed to optimizing both signals in simultaneous operation. The primary ion beam profile and the contribution from the sample holder to the secondary ion signals have been examined. The combined technique has been found to work well for insulators, semiconductors or conductors. The results of surface analyses for fluorocarbon and organosilicon coatings on quartz are given. Molecular species indicative of chemical bonds at the interface of the coating and the substrate were found by SIMS. Both ISS and SIMS agree in the approach to steady state with sputtering time. The system was also applied to study of sodium profiles in glass. In this case, the sodium concentration with depth could not be followed by ISS, but was easily detected with SIMS.

Identification of Bacteria by Pyrolysis Mass Spectrometry Combined with Multivariate Analysis. Henk L.C. Meuzelaar Piet G. Kistemaker and Wim Eshuis, FOM-Instituut voor Atoom-en Molecuulfysica, Amsterdam, The Netherlands.

Microgram quantities of whole bacteria are taken directly from solid culture media and introduced into a special pyrolysis mass spectrometry system.[1] The method is based on Curie-point pyrolysis, low voltage electron impact ionization, fast repetitive mass scanning (quadrupole), ions counting, and multichannel signal averaging. Computer processing of the data by means of multi-variate analysis allows matching of unknown bacteria against reference strains, monitoring of epidemic outbreaks in hospitals, and taxonomical studies. Bacterial species studied thus far, include Klebsiella, Mycobacterium and Streptococcus. The results seem to suggest a whole range of new mass spectrometric applications in biology and medicine.

[1] H.L.C. Meuzelaar, P. G. Kistemaker and M. A. Posthumus, Biomedical Mass Spectrometry, December issue, 1974.

MASS SPECTROMETRIC DETERMINATION OF WATER DESORBED FROM SOLIDS

George M. Wood, B. T. Upchurch,[a] and David B. Hughes[b]
NASA Langley Research Center, Hampton, VA 23665

Trace quantities of water thermally desorbed from teflon-FEP copolymer insulation were suspected of initiating electrolytically-induced failure of hermetically sealed microcircuitry developed for the Viking-Mars program. In order to establish the pressure of water at the ppm level, determinations of total water content of less than 1 gram samples of the copolymer were accomplished using a measurement technique recently developed at the Langley Research Center for this purpose. In this paper we discuss the salient features of the method, and present supportive data verifying performance. It is also shown that the method is usable over a wide range, and that an analysis can be completed in 2-4 minutes.

The technique is shown in figure 1. The mass spectrometer used in these studies is a modified DuPont 21-104 12.70-cm radius analytical instrument. The spectrometer includes a heated leak cavity, previously described by one of us,[1] which contains an unbonded strain gage absolute pressure transducer and a gold foil molecular leak. Gaseous species desorbed from a solid material in a thermally controlled pyrex cell are carried by a dry nitrogen gas stream through a heated 0.025-cm (0.010 in.) capillary to the leak cavity. A representative sample is therefore continuously introduced into the mass spectrometer ion source for analysis. Since the entire system including the mass spectrometer is maintained above 100° C, loss of sample to any surfaces is eliminated. The ion current from the mass spectrometer is plotted on an x-y recorder as a function of time or of programed sample cell temperature. Simultaneously, the ion current is also totaled with an integrating digital voltmeter for quantization of the data.

To prepare the system for operation the dry nitrogen flow is adjusted to 25 cc/min, resulting in a cell pressure slightly above atmosphere. With the capillary and mass spectrometer maintained at 150° C, the cell is heated to above 200° C to desorb gases from the surfaces. The cell temperature can then be adjusted to the desired value and a weighed sample inserted for analysis. The mass spectrometer is adjusted to monitor a m/e ratio specific to the species being observed, e.g., m/e 18 for the water analysis.

In the isothermal mode, the cell is preheated to a selected (normally 150° C) value sufficient to assure total desorption. Counting is initiated when the sample is inserted, and the ion current recorded on the x-y plotter as a function of time. When the trace has returned to baseline, which normally occurs in 2-4 minutes, all available water is considered to have been desorbed, and the run is terminated. Total water content is then computed using the mass spectrometer calibration described below.

In the temperature programed mode, the cell temperature increases ballistically from ambient to a predetermined value sufficient to assure total

---

[a]Dept. of Chemistry, Old Dominion Univ., Norfolk, VA 23508
[b]E. I. DuPont de Nemours, Wilmington, DE 19898

desorption. Counting is initiated coincident with the application of cell heater power, and ion current is recorded on the x-y plotter as a function of cell temperature.

The principal differences between the isothermal and temperature programed modes lie in the information contained in the data. While total water content is obtained in both cases, the trace obtained in the isothermal mode is a single peak, increasing rapidly to a maximum and then returning to baseline as the amount of adsorbed water diminishes. In the temperature programed mode, on the other hand, repeatably obtainable multiple peak structure consisting of two or more peaks are observed at discrete temperatures. These are thought to be the result of desorption from dissimilar absorption sites, with the temperature of peak maxima being indicative of heats of adsorption.

Quantitative calibration of the mass spectrometer is accomplished through the thermal dehydration of measured quantities of disodium tartrate dihydrate which contains 15.66% water by weight. Milligram samples of the dihydrate are placed in aluminum foil boats and inserted into the cell. The procedures for measuring the water desorbed are the same as described above. Results of the calibrations are listed in figure 2 in counts per milligram of water as obtained from the integrating digital voltmeter.

In order to verify system performance, a series of tests on measured quantities of barium chloride dihydrate, which contains 14.75% water by weight, were performed. Data were obtained in both the isothermal and temperature programed modes of operation. A curve depicting ion current as a function of time is shown in figure 3, where it is seen that the curve essentially returns to baseline in approximately 150 seconds. In figure 4, programed temperature data clearly indicates the presence of multiple peaks, which, as stated above, is presently believed to be a function of different adsorption sites. These may be indicative of surface and bulk desorption processes, however we have not at this time completed the studies to verify that this is the case. Total water content data are shown in figure 5 for several experiments; from these data it is seen that agreement of the measured value with the theory is very good.

Total water content in a number of teflon-FEP copolymer samples were determined with the system operating in the isothermal mode. The samples were approximately 2.54 cm^2 patches cut from 0.013-cm (0.005 in.) sheet similar to that used in construction of the hermetically-sealed microelectronic circuitry. Data from these tests are tabulated in figure 6. From these measurements it was determined that the samples contained from 10 to 16 ppm water by weight. As a matter of interest, samples of pure teflon tape were also examined, and were found to contain an average of 8 ppm water by weight.

The present limit of detectability is approximately 300 ng of water as determined from background measurements in the system. Prior to initiating a run, these background signals are surpressed by adjustment of the mass spectrometer ion current amplifier zero control until the counting observed on the integrating digital voltmeter ceases. Background counts arising from desorption from the aluminum boat obtained by running blanks are subtracted from total counts before calculating water content. This step becomes important when determinations at the ppm level are made; however, errors due to background at the higher levels, such as in the

$BaCl_2 \cdot 2H_2O$ analyses were calculated to be less than 1%. The relative precision of the measurement at the ppm level has been calculated to be better than 15%.

Finally, desorbed species other than water may be analyzed with the system, provided only that a suitable standard exists and an unambiguous mass peak specific to the species can be found.

1. Hughes, D. B. and Nowlin, T. D., Trace Gas Analysis, paper P7, 19th Annual Conference on Mass Spectrometry, Atlanta, GA, May 1971.

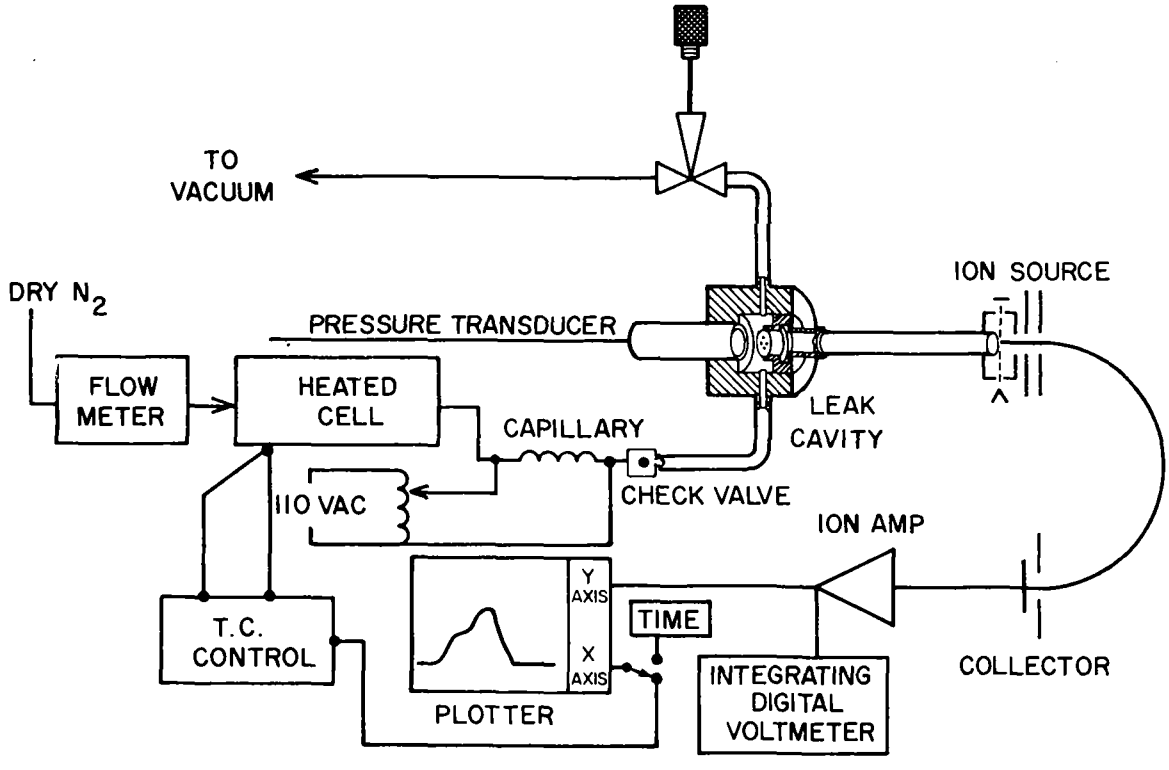

SCHEMATIC DIAGRAM—WATER ANALYSIS SYSTEM

FIGURE I

PROGRAMMED CALIBRATION DATA, 30–180° C

SAMPLE WT, mg	H_2O, mg	AREA COUNTS VOLT–SEC	BACKGROUND VOLT–SEC	VOLT–SEC/ mg H_2O
20.8	3.26	624.962	6.820	189.614
13.9	2.18	423.050	6.478	191.088
12.6	1.97	381.424	7.234	189.944
12.0	1.88	365.678	6.448	191.080
12.6	1.97	387.346	6.922	193.108
14.3	2.24	433.120	6.352	190.521
10.2	1.60	308.480[a]	2.646	191.146
10.7	1.68	325.260[a]	3.232	191.683

MEAN 191.023 VOLT–SEC
s = ±6 ppt

[a] ISOTHERMAL, 150° C

FIGURE 2

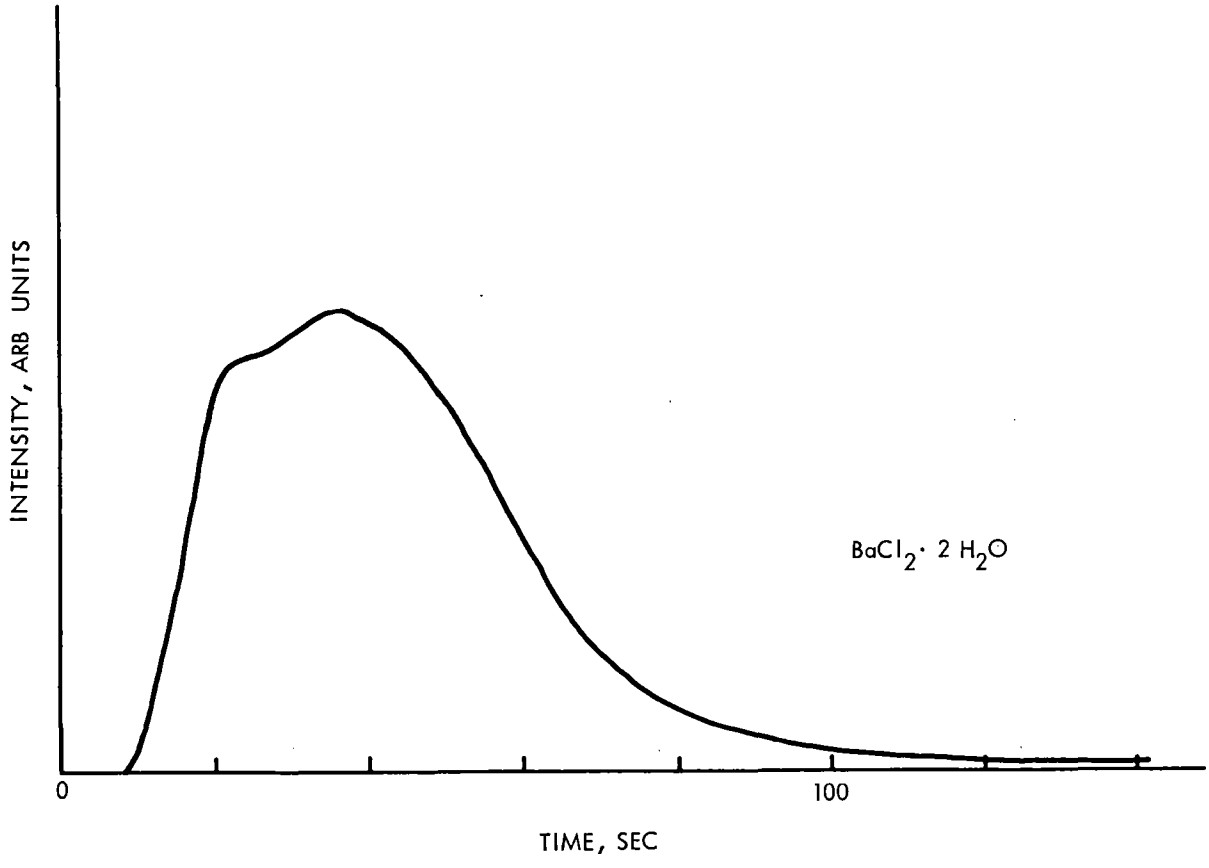

FIGURE 3

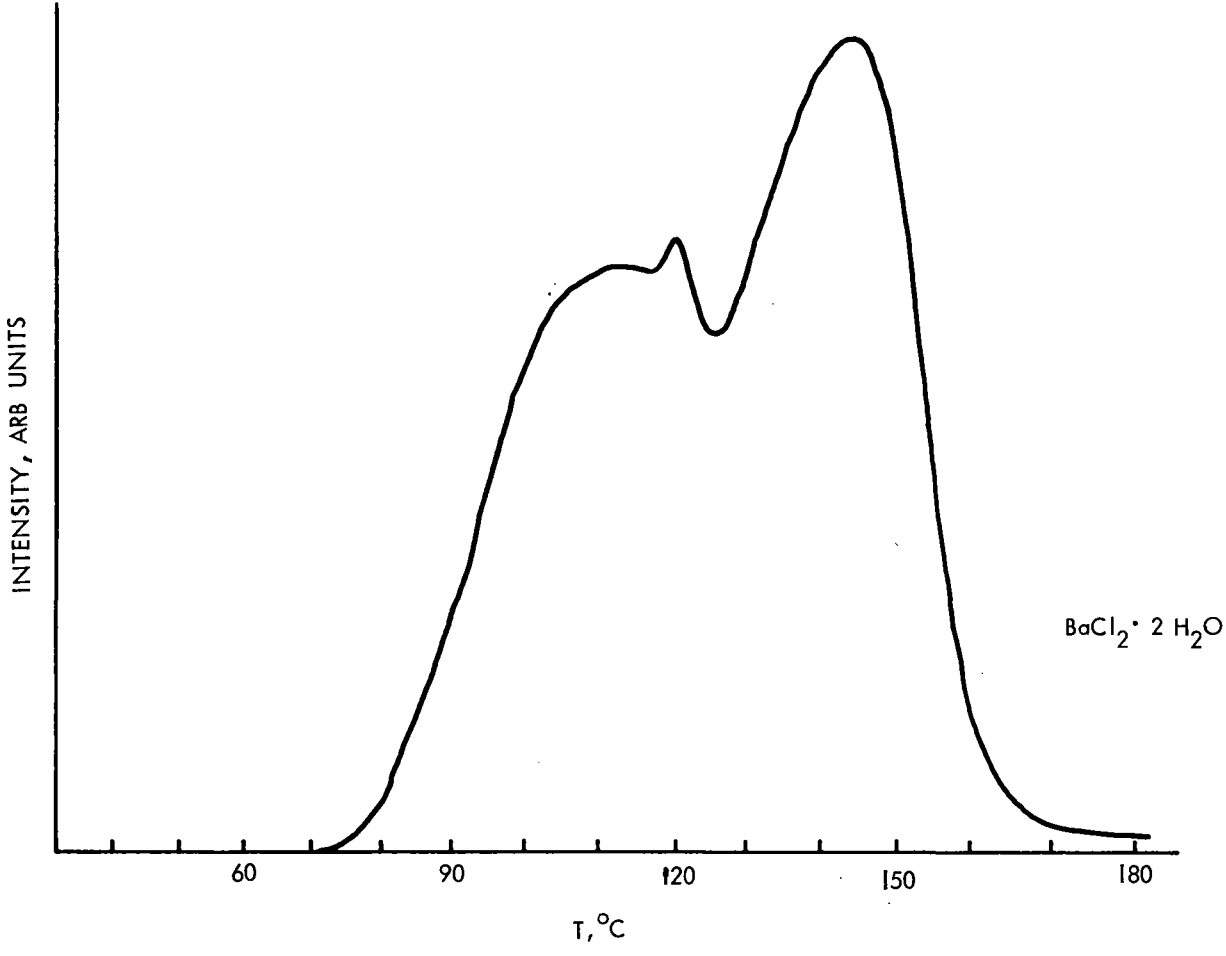

FIGURE 4

$BaCl_2 \cdot 2H_2O$ DATA

$BaCl_2 \cdot 2H_2O$ mg	VOLT–SEC	VOLT–SEC CORRECTED	Mg H_2O	% H_2O
24.9	699.698[a]	693.100	3.63	14.58
21.7	624.086[a]	618.016	3.24	14.93
10.1	283.159[b]	280.896	1.47	14.55
25.1	718.473[b]	715.669	3.75	14.94

MEAN 14.75%
THEORY 14.75%

[a]TEMP PROGRAM: 25–180° C BALLISTIC
[b]ISOTHERMAL: 150° C

FIGURE 5

TEFLON DATA, ISOTHERMAL 150° C

TEFLON-FEP, mg	VOLT-SEC	VOLT-SEC, CORRECTED	H_2O, µg	% H_2O
280.9	0.676	0.706	3.7	0.0013
262.9	0.491	0.521	2.7	0.0010
248.7	0.531	0.561	2.9	0.0012
280.8	0.718	0.748	3.9	0.0014
262.8	0.748	0.778	4.1	0.0016
248.6	0.612	0.642	3.4	0.0014
TEFLON TAPE, mg				
276.3	0.415	0.445	2.3	0.0008

FIGURE 6

USE OF AUTOMATIC DATA ACQUISITION/REDUCTION WITH EI/FD MASS SPECTROMETRY IN ANALYSIS OF CRUDE EXTRACTS OF BIOLOGICAL SAMPLES*

W. D. Jamieson and F. G. Mason

Atlantic Regional Laboratory, National Research Council of Canada,

Halifax, Nova Scotia, B3H 3Z1

Photographically recorded high resolution mass spectra have proved useful in qualitative/"semi-quantitative" direct analyses of crude extracts of biological materials and also in the design of other procedures for mixture separation followed by quantitative analysis which do not depend on routine use of mass spectrometry (1,2,3). When used as a "screening" procedure, this method is comprehensive and also not likely to suffer from introduction of artifacts (e.g. silicones, phthalates). In favourable cases (e.g. halogenated aromatics), residues and metabolites at levels as low as 10 ppb. can be identified in microgram range samples. An instrumentation system has been developed to aid in interpretation of data from photoplate records of the mass spectra of complex mixtures. Field-desorption ionization techniques augment electron-impact ionization methods and these FD data also aid in interpretation.

The Data Acquisition System

Spectra obtained using a Dupont/CEC 21-110B instrument are recorded on vacuum-deposited silver bromide type photoplates (Ionomet Co., P.O. Box 56, Waban, Mass., 02168) with the object slit adjusted usually to yield a resolution of about 15 000. The photoplate records are measured using a comparator-densitometer (Model M-1205-PC, Gaertner Scientific Corp., 1201 Wrightwood Ave., Chicago, Ill., 60614) fitted with an optical shaft angle encoder (Model 29-10-A12-2000, Dynamics Research Corporation, 50 Concord St., Wilmington, Mass., 01887) from which were available 4000 pulses and a zero reference pulse for each turn of the lead screw — for each millimetre of plate travel past the fixed optical axis of the densitometry system. This plate position data is acquired through the priority interrupt module of the computer system by way of an interface which includes a divider circuit so that pulses can be presented to the computer at either 0.25, 0.50, 1.0 or 2.0 micron intervals of plate travel. The zero reference pulse allows software counters to be reset so errors in plate travel measurement will not accumulate over more than one millimetre. Data from the densitometry system is acquired by the computer through a 13-bit analog/digital converter module which can operate at a maximum conversion rate of 50 kHz.

The computer system and standard peripherals were purchased from Varian Associates of Canada, Ltd., 3860 Cote Vertu Rd., Montreal, P.Q., H4R 1P6. The computer is a Varian 620/L-100 type, having 8K core, 16-bit word length and a 950 nanosecond cycle time. A dual-drive cassette magnetic tape system provides for storage of program and data files. The paper tape punch on the associated teletype provides for final output of the reduced data so that these can be processed further by remote-terminal input to a time-shared computer (CDC 6400; KRONOS 2.1, Level 7).

Software written in Varian 620 Assembler has been developed to modify

---

*Issued as NRCC 14729.

and augment that available from the manufacturer so that the purchased equipment could operate as a system. Other software has also been written in Varian 620 Assembler so this system could be used for this data acquisition/reduction application. The data acquired is reduced by a routine which senses record lines on the basis of optical density change and rejects baseline values while updating the average baseline to be used in this line-sensing routine. Optical density and associated distance information is stored for each line profile as is the integral of the profile and these data are later processed further or output.

A library of programs for data reduction and interpretation using the CDC time-shared computer has been developed or adapted. Some are written in FORTRAN IV, some in BASIC. The major such adaptation has been to modify the set of FORTRAN IV programs developed by M. P. Romiez (4). These programs provide for such usual tasks as automatic recognition of lines due to reference compounds, deconvolution of doublet and triplet line profiles, calculation of relative abundances, m/e's (error usually <4 ppm) and elemental formulae corresponding to lines due to ions from unknown compounds. Programs to aid in interpretation of particular types of spectra, such as those of crude extracts of biological samples, are under development.

Further development of this data acquisition system is in progress, and will provide for automatic operation of the comparator-densitometer, the use with the minicomputer of FORTRAN IV programs in concert with routines written in Varian 620 Assembler and operating system software which will allow more efficient use of the system in this and such other applications as real-time data acquisition from a low resolution mass spectrometer (Dupont/CEC 21-491) and from gas chromatography experiments. To provide for these further developments, the core memory of the system has been expanded to 16K and a third cassette magnetic tape drive has been added (Compucorder 120, Sykes Datatronics, Inc., 375 Orchard St., Rochester, N.Y., 14606).

The EI/FD System

The system developed in this laboratory (5) based on a combined EI/FD source for use with a CEC 21-110B mass spectrometer has been modified further. "Mycalex" plates used to insulate the "draw-out" (cathode) plate from the rest of the source have not been durable for more than one or two use-clean cycles. Dupont "VESPEL" polyimide insulating plates have been more satisfactory and are easier to make, although the source in EI mode cannot be used regularly above 250° and 300° seems to be a service limit. Insulating plates made from high-purity alumina by slip-casting and sintering should be superior and will be assessed. Minor source improvements have included directly linking the intra-source emitter positioning rod to the bellows-sealed drive used to adjust it.

The FD emitter probe design has been altered. The vacuum seal at the tip (intra-source end) of the probe is now made by fitting an insulating sleeve of high-alumina porcelain into the end of the hollow probe shaft (0.25 inch o.d. stainless steel tubing) and using a special epoxy resin ("TORR SEAL", Varian Associates, Vacuum Division, Palo Alto, Calif.) for assembly and as a vacuum sealant.

With the earlier system, intra-source arcs had often damaged emitters or other system components external to the source. These problems have been effectively eliminated by installation of a 100 megohm resistance and 30 henry choke in series with the circuit lead to the source cathode plate and also with the lead to the emitter probe.

The technique used to activate emitters (high-temperature graphitized type) has been modified slightly. Details will be provided on request.

Introduction of very small samples (about 50 nanograms) for EI mass spectrometry can be done using the FD probe and FD sample-handling techniques if the FD "emitter" (in this mode, merely the sample probe) does not seriously affect the electron beam geometry. Cathode to emitter distances of 3-4 mm. are suitable.

We acknowledge gratefully the assistance of C. A. Collings, H. A. Dawson, D. J. Embree, G. K. Morstatt, D. E. Webber and M. P. Wingham at this Laboratory and helpful discussions with C. N. McEwen, C. R. McKinney and H.-R. Schulten.

REFERENCES

1. O. Hutzinger and W. D. Jamieson. Pesticide Chemistry, Proc. 2nd International IUPAC Congress, ed. A. S. Tahori. 4, 7 (1971).

2. W. D. Jamieson, O. Hutzinger, S. Safe, J. F. S. Crocker and V. Zitko. 21st Annual Conference on Mass Spectrometry and Allied Topics, San Francisco, 1973. p. 486.

3. O. Hutzinger, W. D. Jamieson, S. Safe, L. Paulmann and R. Ammon. Nature, 252, 698 (1974).

4. M. P. Romiez. Conversational High-Resolution Mass Spectrographic Data Reduction. NASA Technical Report TM X-2847. National Technical Information Service (1973).

5. W. D. Jamieson, F. G. Mason and R. D. Grigsby. 22nd Annual Conference on Mass Spectrometry and Allied Topics, Philadelphia, 1974. p. 75.

Mass Spectral Study of a High-Boiling Saturate Fraction from Petroleum. F. D. GUFFEY and J. H. WEBER, Energy Research and Development Administration, Laramie Energy Research Center, Laramie, Wyoming 82071

Characterization of high-boiling saturate fractions from petroleum is difficult. Gel permeation chromatography (GPC) has been used to separate a saturate distillate into fractions based on the number of fused rings.[1] Four GPC fractions, obtained from a 450-475° C distillate, were analyzed by high and low-resolution mass spectrometry. The low-resolution method of Hood and O'Neal indicated that the GPC separation follows the pattern predicted by model compounds. The high-resolution mass spectral study of these GPC fractions confirmed the separation and provided further information as to the type and distribution of compounds present.

[1]J. H. Weber and H. H. Oelert, Separation Science, 5, 699 (1970).

Mass Spectrometric Analysis of the Hydrocarbons-Ethers from Coal Liquids and From the Products Obtained Upon Their Hydrogenation-Hydrogenolysis.

S. E. Scheppele, G. J. Greenwood and B. L. Crynes, Departments of Chemistry and Chemical Engineering, Oklahoma State University, Stillwater, OK 74074.

Raw anthracene oil and four product mixtures obtained from its hydrogenation-hydrogenolysis (1) were subjected to separation (2). For each sample the weight percents of the various fractions, catalysts, and reaction conditions are given in Table I. Table I shows that the acidic components suffer extensive degradation during hydrogenation-hydrogenolysis. The conclusion concerning the acidic components is supported by the 12 eV mass spectra of the feedstock and reactor sample 1. The former shows the presence of appreciable numbers of compounds having molecular weights ranging from 94 to 250, whereas the latter is characterized by the presence of ions whose nominal and exact masses are consistent with carbazole and methylcarbazoles. Although the available data are insufficient to permit a detailed mass balance, the decrease in the weight precent of the acidic fractions accounts for (actually exceeds somewhat) the increase in the weight percent of the hydrocarbon + ether fractions.

Consideration of the effective use of hydrogen in the reduction process lead us to analyze the hydrocarbon + ether fractions first. High resolution data were acquired from spectra recorded on photographic plates; the experimental masses and the masses for the assigned compositions agreed to ≤ 3 mmu. Quantitative information was obtained using GC/MS in conjunction with GC and low-voltage MS. Table II lists major components which account for ca. 84 and 74% of the total hydrocarbons + ethers present in the feedstock and reactor samples, respectively. High resolution data, ion fragmentation patterns, and GC/MS data provide no evidence for the presence of saturated aliphatic hydrocarbons or ethers in either the feedstock or reaction mixtures. The only oxygenated species identified were molecular ions corresponding to dibenzofurans; no evidence was obtained for the presence of aryl, alkyl or diaryl ethers. The hydrocarbon fraction of the feedstock is essentially composed of 2, 3 and 4 fused-ring aromatics. For the hydrocarbons and ethers present in anthracene oil our composition data in general agrees with the results previously obtained by Shultz, Friedel, and Sharkey (3). Hydrogenation-hydrogenolysis reduces the molecular weight range but increases the complexity of the hydrocarbon mixture. Tables I and II and nmr data support the occurrence of both catalytic hydrogenolysis of the heteroatom components to hydrocarbons and catalytic hydrogenation-hydrogenolysis of hydrocarbons, e.g., dibenzothiophene and carbazole are two precursors to biphenyl. The distribution of hydrocarbons and ethers is catalyst and reaction-variable dependent; analysis of the heteroatom containing components will more clearly delineate this dependence.

This research was supported in part by the Pittsburg and Midway Coal Mining Company, the Office of Coal Research, and the Oklahoma State University.

(1) B. L. Crynes, "Special Catalyst Tailoring for Coal Liquids", Proceedings 41st Annual Chemical Engineering Symposium, I&EC Division ACS and Pittsburg Catalyst Soc., Pittsburg, PA, 1975.

(2) D. M. Jewell, J. H. Weber, J. W. Bunger, H. Plancher, and D. R. Latham, Anal. Chem., 44, 1391 (1972).

(3) J. L. Shultz, R. A. Friedel, and A. G. Sharkey, Jr., U. S. Department of Interior, Bureau of Mines, R.I., 7000(1967).

Table I. Weight Percents of Various Fractions Obtained From Separation

Component	Weight Percent in				
	Feedstock	Reactor Sample[a,b]			
		1	2	3	4
Acid	14.9	2.5	4.3	3.0	2.8
Base	9.5	7.5	6.1	10.1	8.6
Neutral Nitrogen	1.7	2.6	2.3	1.1	0.9
Neutral Sulfur	2.7	2.3	2.4	2.6	1.2
Compounds					
Hydrocarbon + Ether	71.2	80.2	79.9	78.3	81.5

[a]For the reactor samples the variables in order of entry are: Catalyst: Nalco Spherecat 474, Nalco Spherecat 474, Harshaw HT 400, Harshaw HT 400; Pressure (PSIG): 1000, 1000, 1020, 507; Space Time: 1.48, 2.50, 0.75, 0.75; Temperature (^{o}F): 700, 600, 700, 700.

[b]Assumes 5% weight loss to formation of gaseous products.

Table II. Weight Percents of Various Compounds Obtained from Hydrocarbon-Ether Fraction

Component	Weight Percent in				
	Feedstock	Reactor Sample			
		1	2	3	4
Indane	0.4	1.2	0.9	1.0	1.2
Tetrahydronaphthalene	0.0	4.5	2.5	6.4	3.2
Naphthalene	8.5	5.8	5.5	3.1	6.3
Alkylnaphthalenes	5.0	5.9	5.5	5.1	5.1
Biphenyl, Tetrahydroacenaphthene	0.5	5.2	2.6	6.7	3.0
Acenaphthene	8.1	4.3	5.5	2.8	4.5
Dibenzofuran	3.4	3.2	3.2	2.4	3.3
Fluorene	3.9	3.5	3.6	3.7	3.7
Perinaphthane	2.3	0.3	1.1	0.8	1.2
Dihydroanthracenes	0.8	3.6	4.2	3.0	2.0
Methylanthracenes	2.0	4.2	2.4	4.8	4.0
Anthracene	21.0	11.0	13.0	10.6	12.9
Tetrahydrofluoranthene	0.7	5.2	6.7	4.7	2.3
Fluoranthene	14.6	4.8	3.8	3.7	8.0
Dihydropyrenes	0.0	0.3	2.3	0.2	0.9
Pyrene	9.2	5.1	5.0	5.9	6.6
Methylpyrenes	2.1	1.2	2.4	1.3	1.8
Benanthrene, Chrysene	1.6	0.8	0.6	0.6	0.6
Benzophenanthrene, Benzpyrene					

MS ANALYSIS OF COAL LIQUEFACTION PRODUCTS

Thomas Aczel and H. E. Lumpkin

Exxon Research and Engineering Company
Baytown Research and Development Division
Analytical Research Laboratory
Baytown, Texas

Development of coal liquefaction technology requires detailed analyses of the composition of both intermediate and final products. This requirement is satisfied to a great extent by mass spectrometric methods developed in our laboratories in the past several years. The main features and applications of these procedures are summarized in this paper.

Selection of the analytical approach is based on the nature of the sample. High voltage-low resolution methods are used for the analysis of light distillates in the C_6 to C_{12} range and for the determination of total saturates in heavier materials up to C_{50}. High resolution-low voltage methods are used for the analysis of the predominant aromatic and polar components in middle and heavy distillates, tars and residues. Most analyses are carried out without preliminary separations or sample treatment. Chromatographic separations as well as other analytical methods, such as GC, NMR, UV, hydrogenation/dehydrogenation are used occasionally, mainly for calibration purposes and for structural assignments.

Analysis of a light distillate is shown in Figures 1 and 2. A 42 x 42 parent peak inverse is used. Calibration is based on pure aromatic compounds and on individual C_5 to C_{11} paraffinic and naphthenic fractions separated from typical samples on a GC 13X molecular sieve column. These fractions were preferred to blends of pure compounds because they furnished a representative isomeric distribution within each saturate homolog and thus allowed us to correct for the significant interferences between components. The fractions were obtained through the courtesy of Messrs. R. B. Williams and J. B. Beaugh of our laboratories. Mathematical combination of capillary GC and MS data provide an even greater detail. A large number of individual isomers, amounting to 80 percent of the total sample, were determined in the sample shown. A list of these is available from the authors.

Total saturate content of middle and heavy distillates is determined on unseparated samples with a high voltage method based on calibrants from clay-gel percolations. Accuracy of this fast method is 0.3 percent, reproducibility 0.1 percent. Semiquantitative data on the saturate type distribution are also obtained.

A more detailed characterization of the saturates in this boiling range is obtained on narrow distillate or GC fractions from clay-gel saturates. Homologs identified in middle distillates include C_{10} to C_{25} paraffins and perhydroderivatives of benzenes and naphthalenes, acenaphthenes, fluorenes, phenanthrenes, pyrenes and chrysenes. Minor amounts of tricyclodecanes, possibly adamantanes are also found. Boiling points determined from the MS carbon number distribution in narrow distillate fractions agree well with the average boiling points calculated for some of these components from literature data, thus confirming our identifications and analyses (Figure 3). Several individual isomers have also been identified.

Aromatic and polar components comprise most of the 400-1200°F portion of coal liquefaction products. Our computerized high resolution-low voltage method provides a routine quantitative carbon number-compound type distribution for as many as 3000 homologs in 100 aromatic hydrocarbon, S, N and O compound types per sample. Semiroutine methods cover additional compound types. Major types determined include one to eight ring aromatic hydrocarbons and heterocompounds, prevalently hydroxy-aromatics, aromatic thiophenes, and both pyridinic and pyrrolic type N compounds. Analysis of a middle distillate is summarized in Figures 4 and 5.

Although the MS data provide only a formula distribution, structures are assigned to all major types. These assignments are based on the combination of MS, GC, UV, NMR, hydrogenation and dehydrogenation techniques. Isomeric aromatic structures, such as phenanthrenes and anthracenes, or isomeric alkylaromatic and hydroaromatic structures, such as C_2-acenaphthenes and tetrahydrophenanthrenes can thus be determined separately. A list of the more than 200 compound types identified in the thousands of samples analyzed is available from the authors.

User oriented computer programs handle the data obtained for saturate, aromatic and polar components. In addition to wt. pct. for each homolog, these also calculate elemental analysis, distillation, density, etc. from the MS composition. (Figure 6). These computations make the MS method particularly attractive for exploratory samples available only in mg. quantities, as the above properties could not be determined otherwise. Agreement with conventional data, where available, is very good, as shown in Figure 6 for H and O calculated from MS composition and conventional methods in a series of distillation fractions.

In conclusion, we found that our MS methods are uniquely suitable for the detailed analysis of a great variety of coal liquefaction products. They have been used for the analysis of literally thousands of samples with good success.

GC - MS DATA ON A COAL NAPHTHA

A. Saturates (71.91 pct)

C No.	Weight Per Cent				
	Paraffins		Naphthenes		
	Iso	Normal	CH	CP	2-Ring
1-4	-	0.14	-	-	-
5	0.36	0.68	-	0.62	-
6	0.93	1.38	6.09	1.90	-
7	1.39	1.26	10.55	1.22	-
8	2.07	0.87	8.29	2.66	-
9	1.17	0.95	7.30	1.83	0.39
10	0.86	0.24	4.94	1.24	6.91
11	1.05	0.07	2.74	0.64	1.14
Totals	7.83	5.59	39.94	10.11	8 44

1

GC - MS DATA ON A COAL NAPHTHA

B. Aromatics and Polars (28.09 pct)

C No.	Weight Per Cent				
	Benzenes	Indans + Tetralins	Indenes	Phenols	H_2O
0-5	-	-	-	-	
6	0.50	-	-	Traces	
7	3.80	-	-	0.32	
8	4.83	-	-	0.83	
9	3.67	3.25	0.17	Traces	
10	3.94	5.40	0.00	0.00	
11	0.80	0.51	0.00	0.00	
Totals	17.54	9.16	0.17	1.15	0.07

2

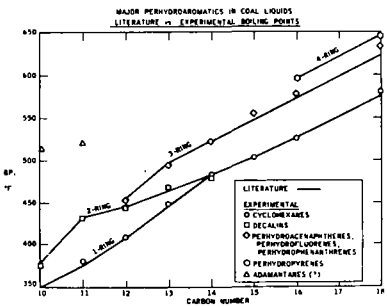

3

DISTRIBUTION OF AROMATICS IN A MIDDLE DISTILLATE. I

Aromatic Rings	Saturates	Aromatics	Furans	Phenols (1 or 2 OH Groups)
1	-	26.7	0.2	1.2
2	-	40.4	4.1	0.8
3	-	11.2	0.5	0.2
4	-	4.9	0.2	0.2
5	-	0.4		0.1
6	-	0.1		0.1
	5.5	83.7	5.1	2.6

4

DISTRIBUTION OF AROMATICS IN A MIDDLE DISTILLATE. II

Aromatic Rings	Thiophenes	Pyridines + Pyroles	Hydroxy-N Compounds
1	<0.1	1.1	<0.1
2	0.1	0.7	<0.1
3	<0.1	0.4	<0.01
4	<0.1	0.4	<0.01
5	-	0.1	-
6	-	<0.1	-
	0.2	2.8	0.1

More than 100 aromatic, hydroaromatic and heteroaromatic compound types in this sample.

5

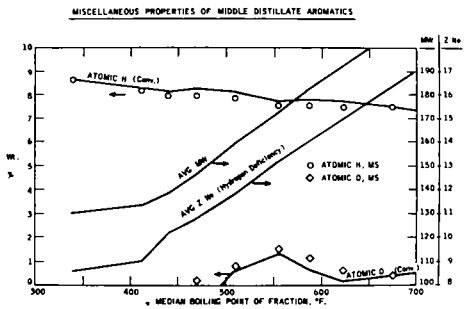

6

Coal Gasification Studies by Field Ionization Mass Spectrometry,
Eric J. Kempster, Rafael Schnitzer, and Michael Anbar, Stanford Research Institute, Mass Spectrometry Research Center, Menlo Park, CA 94025

Field ionization mass spectrometry (FIMS) is being applied to study the kinetics of coal gasification processes. FIMS has been successfully applied to the analysis of complex multicomponent mixtures because of the nonfragmenting nature of the ionization process. Therefore, the method is adequate for studying the kinetics of coal gasification, which yields a complex gaseous mixture.

The instrument used for the kinetic studies is a directly coupled micro gasification chamber with a commercial quadrupole mass spectrometer (Fig. 1). The reaction chamber and inlet system are made of inert materials, Al_2O_3 and glass, to avoid catalysis by metal walls. The reaction chamber made of Al_2O_3 is designed to hold temperatures up to 1000°C and pressures up to 150 atm. The gas sample for analysis is leaked through a capillary extended to the coal sample region. After discarding the contents of the capillary and the dead volume of the valve, the sample is introduced into a glass expansion chamber where it becomes kinetically "frozen" (relative to temperature and pressure in the reaction chamber). From the expansion chamber a sample is fed into the mass spectrometer through a molecular leak. The system is designed to operate automatically since accurate timing is required for the sample handling. As the kinetics studied have halflives of the order of one hour, several reaction chambers are connected in parallel to facilitate more effective use of the mass spectrometer. In the preliminary studies a single manually operated chamber was used to study coal gasification up to 800°C and 1 atm.

At the initial stages of a kinetic run the analyzed gas contains low concentrations of products. These concentrations increase with time and the composition of the gas phase changes. Using our technique we do not separate the reactant gas and the crude gas sample is analyzed.

Our first experiments were carried out by electron impact ionization. Fig. 2 illustrates the products of the coal-steam reaction at different temperatures. Since the spectra are mainly of fragmented ions, the interpretation is rather difficult.

The coal-steam reaction spectra utilizing FIMS are illustrated in Fig. 3. Since this is a molecular weight profile rather than a fragments spectrum, we can identify various products by their mass numbers and follow the changes in their concentration with change of temperature. Many of the constituents are due to volatilization of the coal. For example, the yield of benzene (78) and toluene (92) increases with temperature.

Directly associated with the coal-water reaction is the shift reaction

$$CO_2 + C \rightarrow 2CO$$

at 300°C the mass 44 signal is much bigger than that of mass 28 whereas at 800°C the mass 44 signal is largely reduced and 28 increased.

The advantage of FIMS in the analysis of even such relatively simple mixtures can be demonstrated in the interpretation of the mass 16 peak. Mass 16 in the electron impact spectra could be interpreted to be that of methane. But this mass peak does not appear in the field ionization spectrum and therefore, it has to be attributed to a fragment ion, most probably O^+.

The same multicomponent field ionization analysis is being applied to the products of coal liquefication. Fig. 4 is a molecular weight profile of a complex fraction of coal liquefication,demonstrating the usefulness of this technique to the analysis of products of higher molecular weight.
We are analyzing at present molecular weight profiles of mixtures with an average molecular weight of over 500, but with a lower resolution than the spectrum shown in Fig. 4.

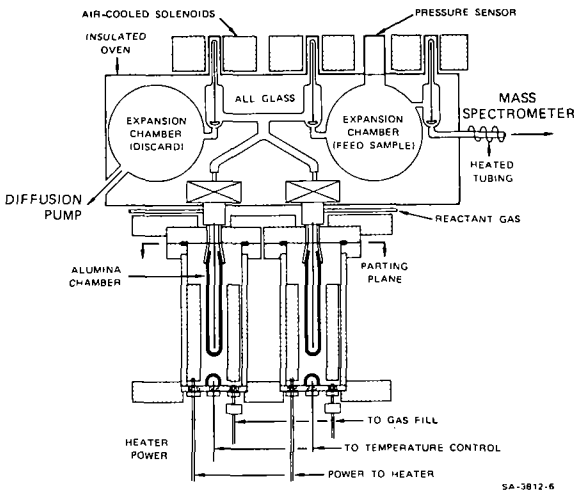

FIGURE 1 COAL GASIFICATION, MASS SPECTROMETER COUPLING
Reaction Chamber and Glass Inlet.

Figure 2: Electron Impact Spectra of Coal Gasification Products (North Dakota Lignite + Steam)

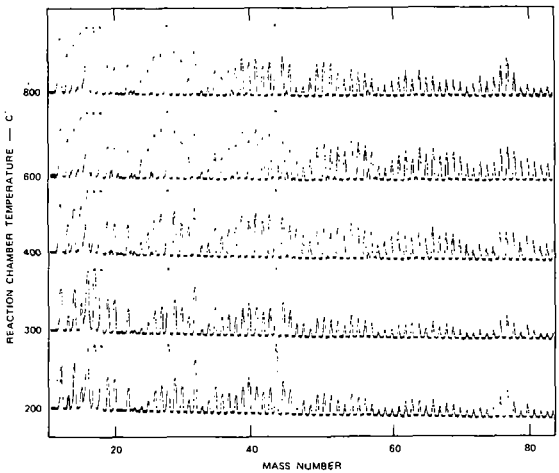

Figure 3: Field ionization spectra of Coal Gasification Products (North Dakota Lignite + Steam)

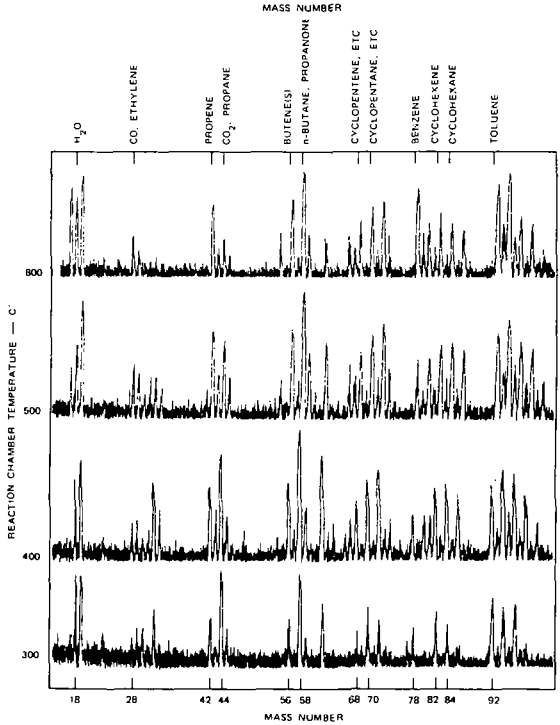

Figure 4: Field ionization spectrum of eluted fraction No. 1A from ARCO "H" Coal Liquid

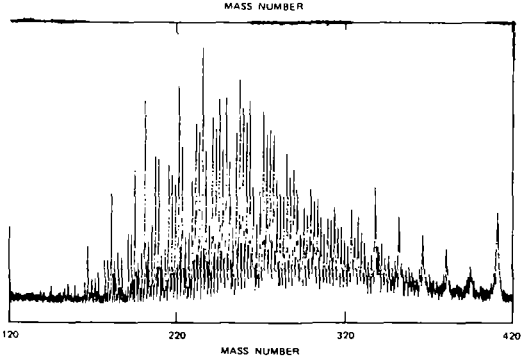

ANALYSIS OF VOLATILES FROM FRESH COAL SURFACES USING HIGH RESOLUTION MASS SPECTROMETRY AND COMPUTER PROCESSING OF DATA

By
M. C. Hamming, F. J. Radd, and A. B. Carel
Continental Oil Company
Research and Development Department
Ponca City, Oklahoma 74601

The release of volatile coal components into mine air and water systems from fresh coal surfaces is important to the mine environment. (Eventually, such components find their way into the atmosphere and surface waters and are investigated.)

In this study, the particular coal samples were selected CONSOL Blacksville (W. Va.) No. 2 Mine of the Pittsburgh No. 8 coal seam, but this Blacksville coal is in general fully representative, within certain limits, of the behavior of any high-methane, deep bituminous coal seam in the West Virginia-Pennsylvania lithology.

The composition and concentration of the released gaseous materials and residues from the Bleuler mill grinding of Consol-Blacksville, Pittsburgh No. 8 seam coals and the incremental volatiles and residues from these coal samples obtained with a thermogravimetric analyzer were studied by mass spectrometry using computer techniques.

The high resolution data on photoplates were reduced via the photodensitometer and the Supernova computer, with final processing being performed on the 370/155 computer system. Peak intensities and line positions were processed by program HIRES-1 (modified version of a program by Tunnecliff and Wadsworth, 1968). Accurate masses were found by program MASSCAL developed by Rosenberg (1973). This work was different from that of others in two respects. Fragment peaks were used as candidate peaks to guide the computer along a high resolution spectrum rather than PFK peaks, and small computer programs were used to search a complete spectrum for various groups of selected peaks such as CH, CHO, CHN ions.

These new data indicate quite clearly why these high-methane Blacksville coals are so easily ignited: they have highly combustible gaseous and liquid hydrocarbon-based films upon their new, unstable surfaces, and these new studies present some of the primary components in these inflammable films.

Such experimental and computer analyses are useful for increasing the safety of underground coal mines and for understanding coal surface chemistries with high-methane, fresh bituminous coal surfaces. The most unique contributions of this research are: (1) a full detailed definition of methane-emitting coal surface chemistries; (2) an experimentally-based understanding of the various reactions of coal surfaces with air (oxygen) exposures versus time; and (3) a prototype apparatus and a new procedure for the analysis of gas phase reactions upon or at solid surfaces and of methods for such gas-solid reactions upon catalytic templates.

REFERENCES

Rosenberg, A. S. (1973), Unpublished Computer Program, MASSCAL, Continental Oil Company, Ponca City, Oklahoma.

Tunnecliff, D. D., and Wadsworth, P. A. (1968), Anal. Chem. 40, 1826.

The Application of Ultra High Resolution Dynamic Scanning to the Analysis of Sulfur-Containing Petrochemicals

H.E. Lumpkin, Exxon Research and Engineering Co., Baytown, Texas
R.M. Elliott, S. Evans, D. Hazelby and W.A. Wolstenholme*
AEI Scientific Apparatus Ltd., Manchester, England
*AEI Scientific Apparatus Inc, Elmsford, New York

Introduction

One of the earliest analytical applications of mass spectrometry was the analysis of complex petroleum fractions and the technique is still employed for this purpose. In 1964, the first results involving high resolution combined with low ionizing voltage were published(1). Spectra were recorded at a resolution of 10,000. Since then, the method has been extended to more complex, wider boiling samples. Furthermore, the very large amount of data generated led to the development of computerized data processing techniques (2).

The use of a resolution of 10,000 allows easy separation of some of the multiplet peaks which occur in the spectra of complex fractions. Typical doublets are due to $C-H_{12}$, CH_4-0, C_2H_8-S. However, a continuing difficulty has been in the inability to determine the sulfur compound content accurately. This is due to the presence of compounds giving rise to the C_3-SH_4 doublet in the spectra of these mixtures.

The C_3-SH_4 doublet represents a mass difference of 0.0034 amu and requires a resolution of 70,000 for separation at mass 240. In practice, for high sulfur fractions these doublets can occur above mass 190 at every even mass number. For good results to be obtained it is necessary to be able to separate these doublets at as high a mass number as possible and to record them with sufficient signal-to-noise ratio to make quantitative measurements meaningful.

The mass spectrometer conditions necessary for the analysis are:

1. Resolving power 70,000 (10% valley) whilst scanning a wide mass range.
2. Operation at low ionizing voltage.
3. Sensitivity sufficient for detection and measurement of peaks as small as approx. 0.03% of total ionization.
4. Reservoir inlet system
5. Slow scan speed (typically 1000 seconds/decade).
6. High system stability.
7. Multiplet detection facility.

The first three of the above requirements represent a very high level of performance and in order to achieve these a mass spectrometer with very high performance characteristics is essential. For example, in order to achieve a resolution of 70,000 with good sensitivity whilst scanning a wide mass range, an instrument capable of a resolution considerably in excess of 70,000 is required.

Experimental

A high sulfur content (4% total S) fraction has been analyzed using the AEI MS5074 mass spectrometer. This instrument has a static resolving power of 150,000 and

employs a hexapole focusing system to enhance sensitivity at high resolution (3). The sample was admitted together with a low voltage reference mixture of halogenated aromatics and spectra were scanned at 1000 secs/decade and a resolution of 70,000. The ionizing voltage was set at 14eV.

Spectra were acquired by the AEI DS50 data system. The data acquisition routines employed in this system include a multiplet detection routine. Since the C_3-SH_4 doublet required 70,000 resolution for separation at mass 240, correspondingly higher resolutions are needed in higher mass regions of the spectra of interest. However, the multiplet detection routine allows measurement of the doublet components at higher masses where the valley between the peaks is greater than 10% of the mean height of the individual components.

The time and intensity data recorded by the DS50 system were later fed as data into an Exxon Research program which calculates masses and determines molecular formulas.

Results

Figure 1 shows part of a slow voltage scan over the mass 232 region. The various peaks have been identified from precise mass determination made from the chart. This type of voltage scan on the MS5074 is very precise in terms of ppm of mass per second. The linear trace at the top of the chart can, therefore, be used to determine the mass by comparison with the reference peak (s).

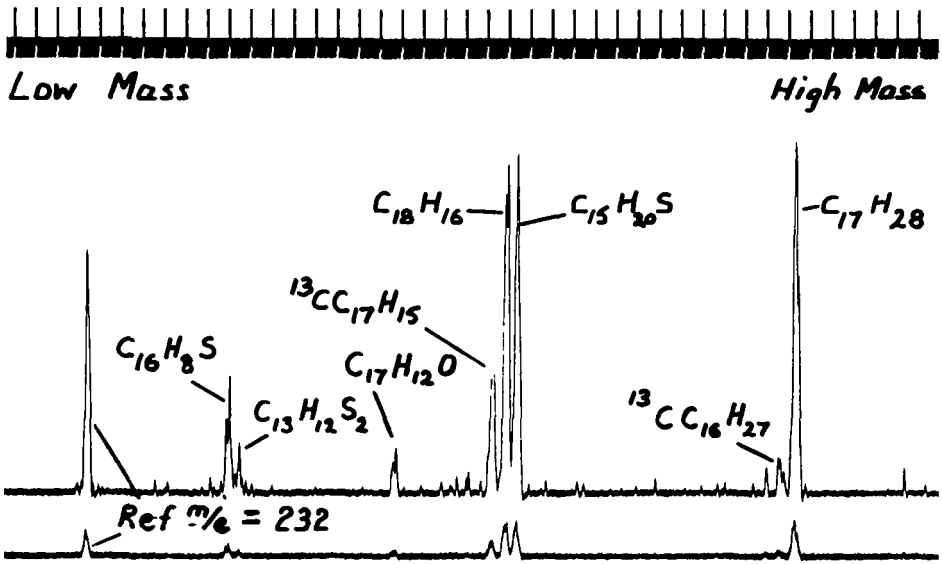

For analytical purposes the faster wide scans are essential and 1000 secs/~~decade~~ scans covering a factor ten in mass were used for the analytical runs. Table 1 shows a summary of some of the results obtained on peaks involving the C_3-SH_4 doublet. It should be noted that throughout the run, the attained mass measurement accuracy was excellent, most values being less than 1 mmu from theoretical.

TABLE I

	C_2H_8-S ΔM= .0905			SH_4 -C_3 ΔM= .0033		
	C_nH_{2n-6}		$C_nH_{2n-10}S$		C_nH_{2n-20}	
Nominal Mass	Intensity	Error MMU	Intensity	Error MMU	Intensity	Error MMU
246	232	-0.1	78	-0.7	7	0.1
260	221	0.0	132	0.2	96	-0.2
274	60	-2.4	58	0.5	36	1.5
288	73	-1.7	65	-2.0	45	-1.5

TABLE II

Intensity	Meas. M/E	MMU Error	C12	H	016	S32
1630	258.2339	-0.7	19	30	0	0
830	258.1443	0.2	17	22	0	1
1090	258.1443	-0.5	20	18	0	0

TABLE III

Intensity	Meas. M/E	MMU Error	C12	H	016	S32
780	272.2495	-0.7	20	32	0	0
810	272.1589	2.7	21	20	0	0
810	272.1589	-0.7	18	24	0	1
530	272.1569	0.2	21	20	0	0

Table II is a reproduction of the computer printout for mass 258, where the three components are unambiguously identified, and TABLE III shows the output for mass 272 with correct assignments underlined. Data consistent with C_3-SH_4 doublets was obtained at masses as high as 386, indicating an effective resolution of greater than 100,000.

Conclusions

This preliminary work on sulfur containing petroleum fractions has shown that the MS5074 mass spectrometer can be scanned at ultra high resolution (>70,000) over a wide mass range and with sufficient sensitivity at low ionizing voltages to give good analytical data for the minor constituents of complex petroleum fractions.

Still more sensitivity is desired and since this work was carried out, modifications to the electron gun in the ion source have improved the low voltage performance giving an increase in sensitivity of at least a factor of 3. It is believed, therefore, that in the near future, even lower level components will be detected and measured quantitatively using these techniques.

References

1. H.E. Lumpkin, Anal. Chem 36, 2399 (1964)

2. Thomas Aczel, D.E. Allan, J.H. Harding and E.A. Knipp, Anal. Chem. 42, 341 (1970).

3. S. Evans and R. Graham, "Advances in Mass Spectrometry", Vol 6, Applied Science Publishers, p. 429.

SOME OBSERVATIONS ON THE APPLICATION OF GROUPS OF MASS CHROMATOGRAMS TO THE CHARACTERIZATION OF VERY COMPLEX UNRESOLVED MIXTURES: PETROLEUM OILS

Woodfin V. Ligon, Jr. and Robert L. Johnson, Jr.

General Electric Corporate Research & Development

Schenectady, New York 12301

Mass chromatograms have been applied to the analysis of narrow boiling fractions of crude oils. GC columns of relatively high selectivity but having small numbers of theoretical plates have been used for the analyses. This combination results in partial separation of these highly complex mixtures into discrete classes of materials but gives very little separation of individual components. The GC traces therefore appear as broad distributions of unresolved components. Due to the large number of contributors to each ion and the low GC resolution, the mass chromatograms obtained also appear, in general, as broad curves rather than sharp peaks corresponding to individual components. The separation into classes is not readily apparent in a simple gas chromatogram because the large number of classes in an oil results in severe overlap. When single ions are observed, however, the situation is much simplified because only a limited number of classes can contribute to any single mass. For example at mass 197, hydrocarbon ions of only two elemental compositions are likely to occur: $C_{14}H_{29}$ and $C_{15}H_{17}$. If one recorded a mass chromatogram for this ion, one might expect to detect resolution of the distributions of precursors of these two contributors since one set of precursors must be saturated and the other highly aromatic. It is important however that the ion be observed in an oil for which mass 197 falls in or near the parent ion region since the contributing ions <u>must</u> have been formed via a minimum of fragmentation if they are to closely resemble their precursors. Obviously given sufficient opportunity for fragmentation even a relatively saturated precursor can produce relatively aromatic daughter ions. High resolution mass chromatograms of the components of mass 197 in such an oil are shown in Figure 1. This result demonstrates that a separation is indeed observed. The "SUM" trace at the top of the figure simulates the data that would be obtained under the same conditions at low MS resolution and indicates that a clean separation of the two classes of precursors should be observed at low resolution. It is important to note that the areas under the two curves are related to each other in exactly the same way as the peak heights which would be found for the components of this same ion if the ion was examined in the unfractionated oil at high MS resolution. In

other words, for this ion under these conditions it is possible to use low resolution mass chromatograms to obtain the same information that would be obtained by running the oil in a high resolution mass spectrometer.

A group of low resolution mass chromatograms arising from an oil run on a very selective column (Apolar 10C) is shown in Figure 2. The oil is an 80-110° (0.05 Torr) boiling fraction of Sumatra crude. A separation of classes is clear in the vicinity of mass 197 and again around mass 183. From mass 177 ($C_{14}H_9$) to mass 197 ($C_{14}H_{29}$), a progression of related distributions can be observed; all consisting of 14 carbons and differing from their nearest neighbors by two hydrogen atoms. The progression proceeds smoothly to the left (shorter retention time) as the respective ions and therefore, their precursors become increasingly saturated. Partial progressions of 15 carbon and 13 carbon species are also present in the data. The distribution at mass 175 which is not part of the C-13 progression (displaced to right) has been shown to be $C_{11}H_{11}S$. It is possible in some cases therefore, to resolve heteroatom contributions to a given mass as well as the various hydrocarbon contributions.

This technique provides therefore, a method for obtaining information about the composition of a total oil which has previously been available only via high resolution mass spectrometry. In addition, the appearance of a group of these curves such as those in Figure 2 clearly suggests their possible application as very informative "fingerprints" of a given oil.

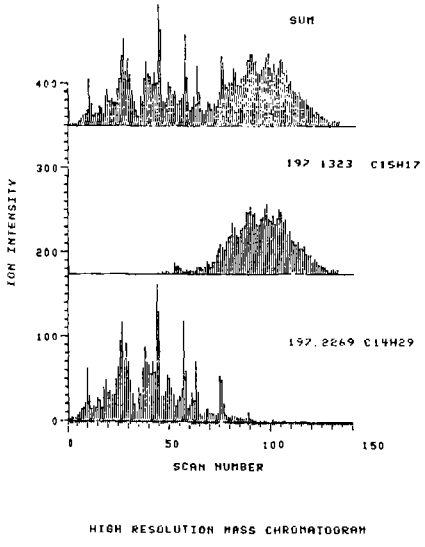

Figure 1. Components of Mass 197.

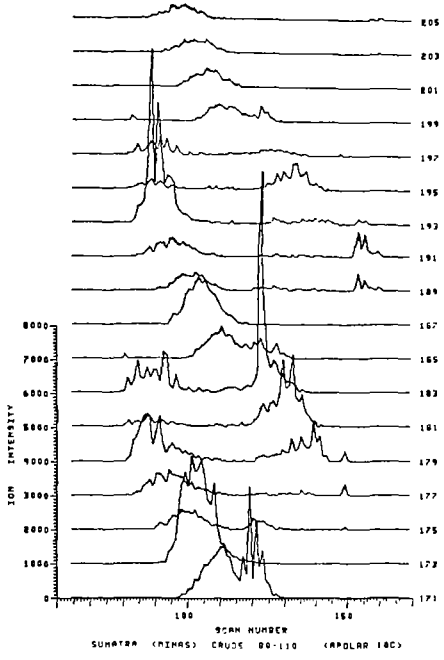

Figure 2. Group of Mass Chromatograms for Crude Oil Fraction.

Mass Spectrometry Investigation of Catalyst Deactivation

A. G. SHARKEY, JR., R. G. LETT and J. L. SHULTZ, U. S. Energy Research and Development Admin., Pittsburgh Energy Research Center, 4800 Forbes Ave., Pittsburgh, Pa. 15213

Economic feasibility of processes for making substitute liquid fuels from coal, such as the Bureau of Mines SYNTHOIL process, will be increased if the catalyst lifetime is extended as long as possible. Three functions of the catalyst that deteriorate with aging during operation are: (1) The cracking function, (2) the hydrogenating function and (3) the desulfurization function. Mass spectrometry has given insight into the factors contributing to catalyst deterioration by providing data relating to the trace elements on the catalyst surface, changes in the composition of the product, particularly the increase in sulfur and oxygen compounds, and also the composition of products associated directly with the catalyst surface.

High-resolution mass spectrometry indicated that the oxygen and nitrogen compounds extended to higher carbon numbers as the coal liquefaction run progressed. Product vaporized directly in the ion source from the surface of used catalyst indicated large, highly condensed ring systems having up to 32 carbon atoms. Highly-condensed, aromatic ring systems showed higher concentrations where less severe hydrogenation conditions were used. Over 65 trace and minor elements have been identified in SYNTHOIL liquids and on the surface of used catalysts. Spark-source mass spectrometry and DIMA are being used to determine if there is a preferential build up of certain elements on the catalyst surface.

RAPID SURVEY ANALYSIS OF COMPLEX ENVIRONMETAL SAMPLES USING HIGH ACCURACY MASS CHROMATOGRAPHY

T. J. Prater, D. Schuetzle, Research Staff
Ford Motor Company, Dearborn, Michigan 48121 and
D. E. Hagge, Incos Corporation, Berkeley, CA. 94710

A computer/mass spectrometer system, for elucidating complex samples, as previously reported by D. Schuetzle, et al. (1-5) has been expanded for use with rapid and repetitive scanning mass spectrometry. High accuracy mass values have been obtained without the use of continuous reference material such as PFK. The absence of the reference material facilitates rapid computer routines and eliminates an enormous amount of data storage. Accuracies of thirty ppm have been routinely obtained for the mass range: 15-600, resolutions from 1000 to 10,000, and scan times as low as five seconds for periods in excess of 60 minutes. The instrument stability necessary to achieve this accuracy was accomplished by removing vibrational noise with a Barry Control System isolation pad, by filtering nearly all instrument noise and removing 60 Hz ground loops. The system consisted of a Data General computer, provided by the Incos Corporation that was interfaced to a Mat 311 mass spectrometer. The computer was programmed with instrument diagnostics, which indicated the readiness of the instrument prior to analysis. The change in mass with time for a CHF_2 fragment with a 51.005 accurate mass value is shown in Figure 1. The accuracy is $\pm$ 40 ppm at a resolution of 1500 without PFK. Since this degree of accuracy can be obtained in low as well as high resolution, it is expected that high accuracy mass values can be obtained with both time of flight and quadrupole instruments.

The use of high accuracy mass values eliminates much of the need for high resolution gas chromatographic columns, used with mass spectrometry, and laborious separations of samples prior to analysis, since compounds can be identified on the basis of accurate mass values and relative elution times. Compounds present in complex mixtures were identified by comparison with a mass library search system containing compound classes and condensed high accuracy MS data for individual compounds. The individual compounds were stored according to: (1) three major identifying masses, (2) their relative intensities and (3) the relative elution time of the compound from a direct insertion probe or column.

Polycyclic aromatic compounds identified from an air particulate sample (Fig. 2) demonstrate how high accuracy mass chromatograms were used. The atmospheric concentration of these compounds was approximately 3 ng/M^3. Although, several of these compounds have the same parent mass, they have been identified by their relative elution times. High accuracy mass chromatography relies heavily on high accuracy mass values due to the existence of several different ions possible at most unit masses. For example, at unit mass 64 the presence of either SO_2^+, $C_5H_4^+$ or $C_2H_5Cl^+$ is possible. Ammonium sulfate has been identified as a constituent of air particulates in Figure 3. The $C_5H_4^+$ and SO_2^+ have been found as distinct peaks and no $C_2H_5Cl^+$ was found. Two peaks appear in the SO_2 curve; the first is probably an organic sulfate which has not been identified and the second is ammonium sulfate which was identified from the library. The Mat 311 double focusing mass spectrometer was modified for this study using the computer to control the scan cycles. Computer control of the mass spectrometer affords accurate and repeatable scans, which were necessary for high accuracy mass values, obtained from a calibration run prior to the sample analysis. The calibration run was used to create a mass/time scale from which accurate masses for subsequent mass spectra were obtained.

It is expected that the 40 ppm accuracy achieved in this study can be improved by eliminating some residual electronic noise that remains in the

magnet power supply. One of the greatest needs to facilitate high accuracy mass chromatography is a more extensive compound library. Presently 300 compounds and 20 compound classes found in atmospheric particulate samples are on file.

REFERENCES

1. D. Schuetzle, A. L. Crittenden, and R. J. Charlson, "Application of Computer Controlled High Resolution Mass Spectrometry to the Analysis of Air Pollutants", J. Air Poll. Control Assoc., 23, 704(1973).

2. D. Schuetzle, D. Cronn, A. L. Crittenden, and R. J. Charlson, "Molecular Composition of Secondary Aerosol and Its Origin", presented at the 172nd National ACS Meeting Symposium on Surface and Colloid Chemistry in Air Pollution Control, (Environmental Science and Technology, August 1975).

3. D. Schuetzle, "Computer Controlled High Resolution Mass Spectrometric Analysis of Air Pollutants", Ph.D. Dissertation, University of Washington (1972).

4. D. Schuetzle, "Analysis of Complex Mixtures by Computer Controlled High Resolution Mass Spectrometry - I. Application to Atmospheric Aerosol Composition", Biomedical Mass Spectrometry, Sept., 1975.

5. R. L. Knights, "Computer Controlled Fast Cyclic Scan Mass Spectrometric Thermal Analysis - II. Inorganic Air Pollutants", Ph.D. Dissertation, University of Washington (1973).

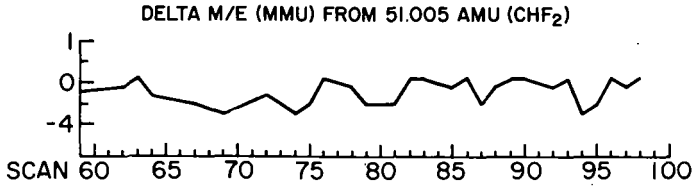

Figure 1

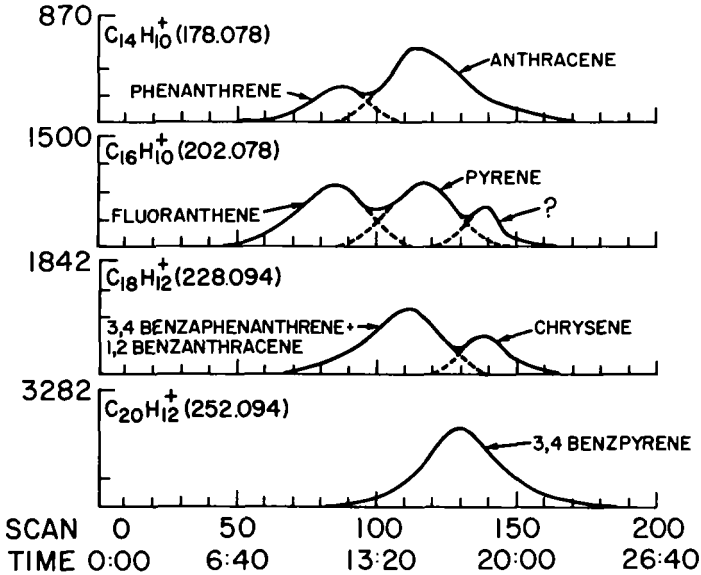

Figure 2 - High Accuracy Mass Chromatograms of Several Polynuclear Aromatics

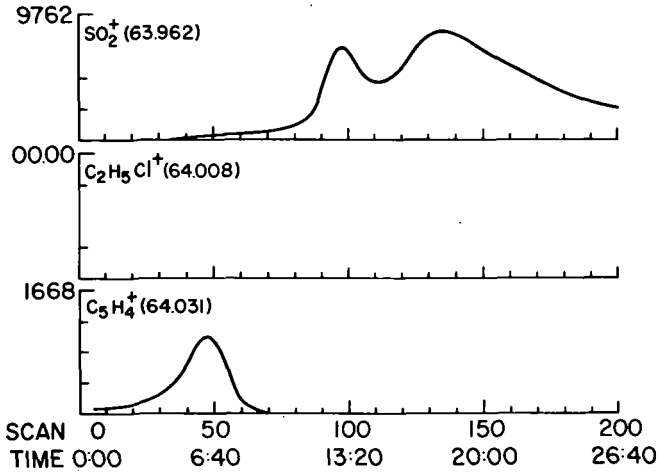

Figure 3 - High Accuracy Mass Chromatograms at Mass 64

A MODULAR ELECTRONIC OUTPUT SYSTEM FOR IMPROVED FAST-RESPONSE TIME-OF-FLIGHT MASS SPECTROMETRIC MEASUREMENTS

Kenneth A. Lincoln
Ames Research Center, NASA, Moffett Field, Calif. 94035

Extending the mass spectrometric capabilities for the dynamic sampling of vapor plumes produced by the pulsed laser heating of various materials has necessitated overcoming some limitations in the state-of-the-art of the electronic output system. This paper pertains only to the innovations in signal conditioning prevailing between the multiplier output of the time-of-flight mass spectrometer and the display and/or data processing devices employed.

Most commercial time-of-flight mass spectrometers utilize a Bendix continuous-strip dynode, magnetic electron multiplier containing several post-dynode, electron beam-switching channels; these are used for scanning (via sampling) the spectra onto a strip chart recorder or for monitoring individual mass peaks vs. time in the spectra. Accordingly, each mass spectrum is comprised of packets of electrons, which correspond to discrete m/e values, emerging from the dynode; if these electrons are not gated from the stream into one of these channels, they arrive at the final or "scope" anode producing a complete mass spectrum on each cycle of the instrument as it operates at a repetition rate of 20-50 kHz. Each spectrum is thus made up of a group of pulses (mass peaks) nominally triangular in shape and varying in amplitude; they have fairly uniform base widths of approximately 30 nanosec and are spaced about 100 nanosec apart at the lower mass ranges.

A technique for time resolving the intensities of several mass peaks simultaneously has been described previously[1] and may be briefly outlined as follows: The gating pulses to the individual multiplier channels are positioned (in time delay) to the locations of the preselected mass peaks in the spectrum, and they are adjusted in a wide enough time window (about 50 nanosec) to divert to its respective anode the entire electron packet corresponding to each selected mass peak.

The outputs from the anodes are fed to the vertical inputs of a multitrace oscilloscope with its horizontal sweep triggered by the laser (or other event under study). Although this technique has been very fruitful, some of the drawbacks encountered are 1) those mass peaks gated out of the electron stream into multiplier channels ahead of the scope anode are missing from the spectrum displayed on the scope; 2) the sharp rise and fall of the 100 V gating pulses inside the multiplier induce severe "ringing" in the scope anode which interferes with the display of the total spectrum; they also produce enough interference between multiplier channels to restrict amplification of those signals; and 3) the number of mass peaks that can be monitored simultaneously without multiplexing is limited to the number of channels built into the multiplier.

The system presented here uses the same approach to time resolving mass spectra, but achieves it without these drawbacks by performing all gating and other operations entirely external to the multiplier. As shown in Fig. 1, the total signal at the scope anode is fed from the mass spectrometer to a series of nuclear instrument modules (NIM) which are all "off the shelf" items; therefore, no new electronic equipment development is required. One key element in the system is the fan-out amplifier: the total mass spectra fed into it appear simultaneously at 16 separate, isolated outputs (only 5 are shown in the diagram) and an operation performed at one has no influence on the signal appearing at the others. This feature provides many options for displaying and further conditioning the mass spectra. As can be seen from the block diagram, the

conventional method of continuously displaying TOF mass spectra on an oscilloscope is retained, and a circuit for z-axis brightening of the mass peaks in this display is also included. For measuring the dc component of the multiplier current, any one of many types of microammeters may be used; this measurement provides a very convenient gauge of the total ion current in the spectrometer.

In the present system the gated integrators are used to sort out the preselected m/e values from the spectra. (We are using EG&G Model LG 105 Linear Gate and Stretcher for this purpose.) These accept signals only for the duration of an externally applied gating pulse. Thus, the time delay from the reference trigger is adjusted to position the gate pulse at the desired m/e peak and the gate time-width is set at approximately 50 nanosec (as in the earlier method) to bracket completely the mass peak. The gated integrator then produces a 3 microsec output pulse with an amplitude directly proportional to the area of the preselected mass peak rather than its height, a factor which can improve the accuracy of the data. The net result is a conversion of the somewhat poorly defined shape of the 30 nanosec mass peaks to clean, flat-topped, 3 microsec pulses. Figure 2 is an example of such a pulse corresponding to a single mass peak in the spectrum occurring at a repetition rate of 50 kHz. These stretched pulses are now in a form much more amenable to further signal conditioning. For example, they are readily accepted by a transient recorder for storage or a multichannel analyzer for signal averaging, or are easily digitized for computer handling.

An entire spectrum can be scanned in the conventional manner for strip chart presentation by first narrowing the gate width (to 5-10 nanosec) and then slewing across the spectrum with the delay and gate generator as the output of the corresponding gated integrator is fed to a chart recorder. With this present arrangement, scanning of spectra will not interfere with the continuous monitoring of mass peaks on which other gated integrators are set. When damping of the output signal is required, a dc amplifier with limited bandpass can be inserted ahead of the recorder. As an optional substitute for the delay and gate generators, we have utilized the analog scanners that were a part of the original spectrometer by attenuating their -100 V pulses (normally fed to the multiplier) to the -750 mV level required by the gated amplifiers.

The salient features of this instrument may be summarized:

1) All signal conditioning is external to the mass spectrometer. This feature has the added quality of facilitating remote operation.
2) No interference is coupled between the many types of output displays.
3) The number of mass peaks monitored is not limited by the multiplier. This feature permits the use of a less complicated electron multiplier.
4) The speed and sensitivity of measurements for fast events are improved.
5) Output pulse height is proportional to the area of corresponding mass peak.
6) The stretched mass peaks enhance further data handling.

[1]Lincoln, K. A., J. Mass Spectrometry and Ion Phys., 2 (1969) 75-83.

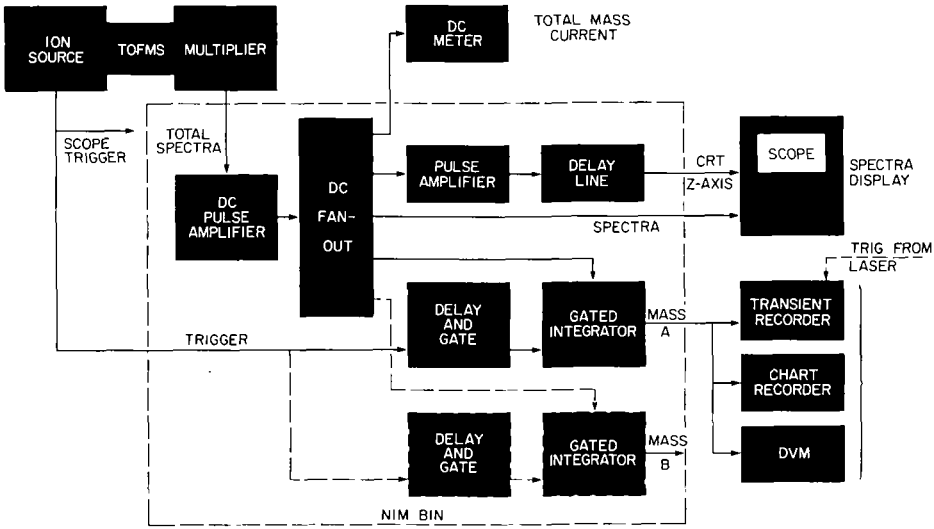

Fig. 1. Block diagram for gating and displaying TOFMS spectra.

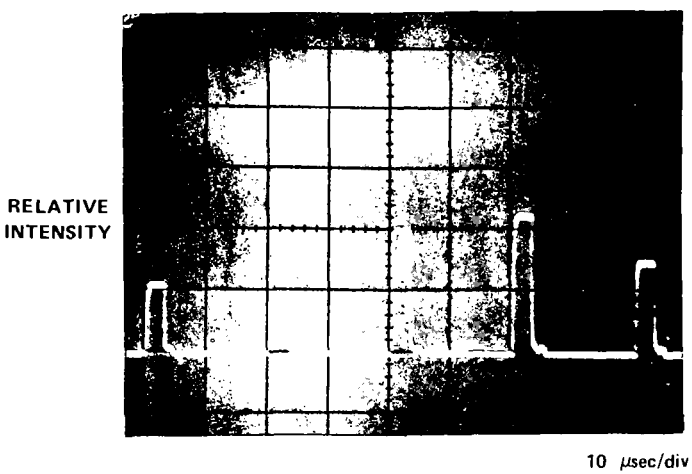

Fig. 2. Mass 28 peaks after transiting gated integrator.

An Intracavity Dye-Laser Technique for the Study of Laser-Induced Ionic Processes.*

JOHN R. EYLER
University of Florida, Department of Chemistry
Gainesville, Florida 32611

As part of a continuing study of laser-induced ionic processes, we found it desirable to increase the sensitivity of the pulsed dye laser-pulsed ion cyclotron resonance (icr) detection method. Our early work[1], in which SH^- photodetachment had been investigated, was not hampered by low sensitivity because the cross-section for this process ($SH^- + h\nu \rightarrow SH\cdot + e^-$) is quite high[2]. However, in studying positive ion photodissociation and in examining the threshold behavior of any laser-induced process, increased sensitivity is quite desirable. As one means of gaining this improvement in sensitivity, a technique which places the icr cell inside the flashlamp-pumped dye laser cavity was developed[3].

Figure 1 gives a schematic representation of the experimental arrangement used. The laser cavity is defined by mirrors M_1 and M_2, and by the coaxial flashlamp and dye cell (E). The mirror M_1 is located inside the vacuum chamber (B), and the icr cell (A) is located inside the laser cavity, between the mirrors M_1 and M_2.

The intracavity technique was tested by observing the photodetachment of OH^- ($OH^- + h\nu \rightarrow OH + e^-$). Using Rhodamine 6G in the dye laser, at a wavelength of ca. 600 nm., 93% of the OH^- ions trapped in the icr cell underwent photodetachment. This represents an improvement by a factor of 6.8 over a conventional, double-pass experiment. The intracavity technique has also been applied in a study of $C_7H_8^+$ photodissociation in gaseous toluene[4] and has given quite reliable and reproducible results which are in excellent agreement with earlier lower-resolution studies.

*Research performed at the National Bureau of Standards, Gaithersburg, Md.

1. J.R. Eyler and G.H. Atkinson, Chem. Phys. Lett., 28, 217 (1974).
2. B. Steiner, J. Chem. Phys. 49, 5097 (1968).
3. J.R. Eyler, Rev. Sci. Instrum. 45, 1154 (1974).
4. J.R. Eyler, submitted for publication.

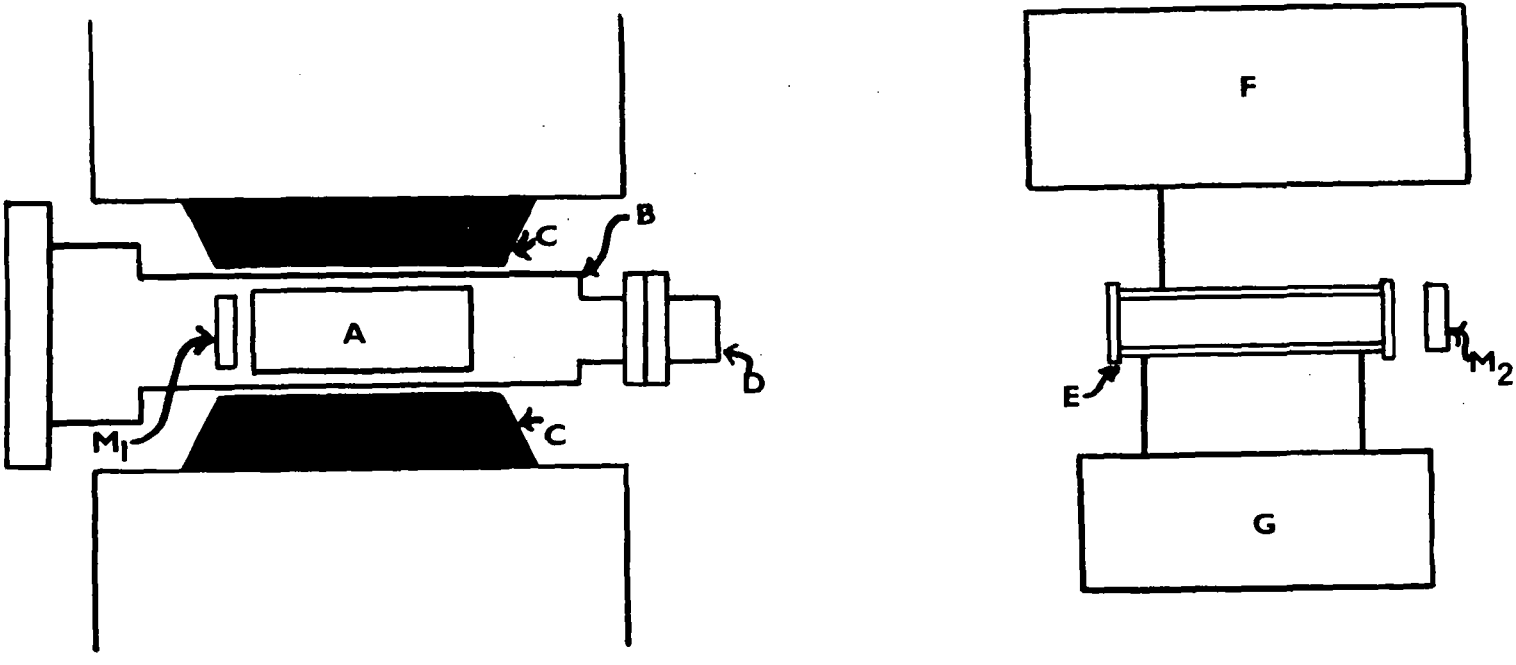

FIGURE 1

DESIGN MODIFICATIONS ON A VARIAN ATLAS CH-4B MASS SPECTROMETER FOR CHEMICAL IONIZATION

Robert S. Ampulski
The Procter & Gamble Company
Miami Valley Laboratories
Cincinnati, Ohio 45247

ABSTRACT

Design modifications of a CH-4B mass spectrometer for chemical ionization are described. The CI source is easily interchanged with the standard electron impact source. The sensitivity for observing the "molecular ion" of methyl stearate is 2×10^{-11}g/sec (S/N = 10/1), a 100x increase over the normal EI mode of operation. Resolution is maintained at $m/\Delta m = 550$ (10% valley). Except for the source and pumps, the system uses standard Varian replacement components. CI mass spectra are as easy to record as normal electron impact spectra.

Several extensive modifications to the CH-4 mass spectrometer were made to allow chemical ion mass spectra to be obtained.

MODIFICATIONS

The pumping capacity was increased by connecting a 1400 lps 6" TM Products oil diffusion pump to the source housing at the probe inlet flange as shown in Fig. 1. The original mercury source pump was closed to the source and opened to the analyzer region. The effective pumping speed at the source was calculated to be approximately 135 lps. The source pressure was less than 4×10^{-4} torr and the analyzer pressure was less than 2×10^{-5} torr.

The probe lock inlet system was rotated 90° with respect to the ion beam, such that the inlet system was parallel to the floor (Fig. 2).

The standard Varian EF04B EI ion source and lens system were used as a basis for the source design. The source was machined from a single blank of stainless steel having the overal dimensions of the original combination of the extraction plate, filament support block and backing plate (Fig. 3). The relationship of the reagent gas inlet, probe inlet electron entrance slit and ion exit slit is shown in Fig. 4. The source slit dimensions are listed in Table 1.

Table 1

Slit Dimensions

Electron entrance (2)	.033 cm diameter
Ion exit	.0051 x .51 cm
Gas inlet	.01 x 1 cm capillary
Conductance	~50 ml/sec

The Power Supply #86 modifications are shown in Fig. 5. The standard CH-5 pushrod inlet probe was fitted with a small male Luer tip constructed of Teflon (Fig. 6).

RESULTS AND DISCUSSION

The standard operating conditions are listed in Table 2.

Table 2

Operating Conditions

Source pressure	.5 torr
Source housing	.8-2 x 10^{-5} torr
Electron emission	1 ma
Electron energy	230 V
Repeller, trap	0 V
Accelerating voltage	2-8 KV
Ion current	2 x 10^{-11} amps

A comparison of the sensitivity of the standard EI source with the CI source is shown in Table 3, using i-butane and the conditions listed in Table 2.

Table 3

EI-CI Specifications

Sensitivity	EI	CI
Methyl Stearate	1.5 x 10^{-9}g/sec	2 x 10^{-11}g/sec
S/N	10/1	10/1
Resolution ($M/\Delta M$ - 10%)	>500	>500
m/e 40-550		
.1/.3 mm slits		

Mass spectra of hexanoic acid, n-docosane, and tetradecanol (Figs. 7-9) are included to show the ability of this system to produce "Parent ions" as compared to electron impact spectra.

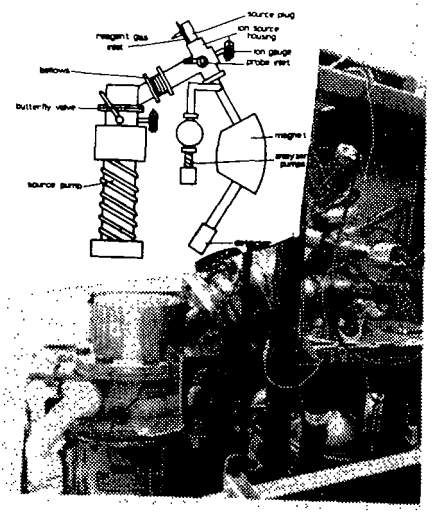

Fig. 1

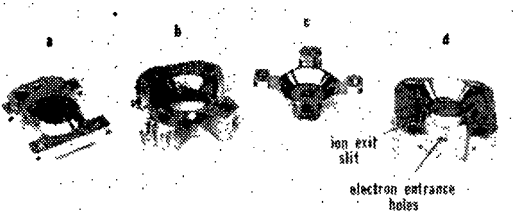

Fig. 2

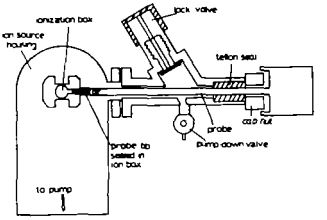

Fig. 3

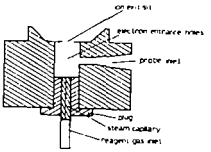

Fig. 4

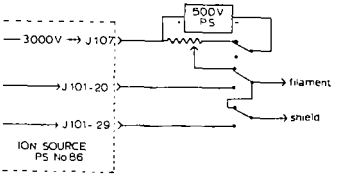

Fig. 5

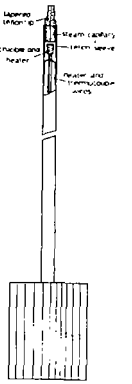

Fig. 6

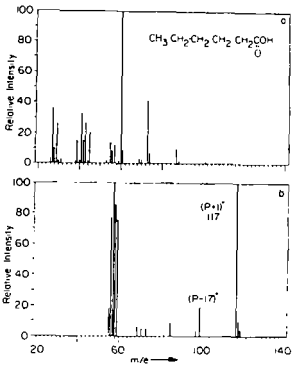

Fig. 7

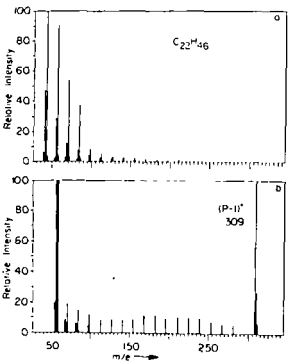

Fig. 8

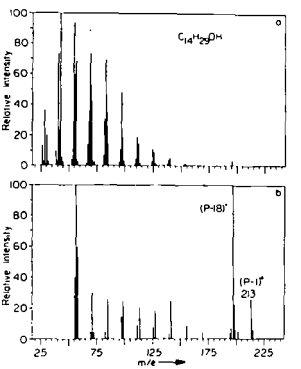

Fig. 9

A Cold Cathode Sampling Orbitron Ionization Gauge

by

K. M. Jackson, P. C. McLeod, and M. K. Testerman
Department of Electronics and Instrumentation
University of Arkansas Graduate Institute of Technology
Little Rock 72203

A cold electron-emitting source, suitable for mass spectrometry and fabricated by generation of a micron-sized, high-resistance gap in thin films of tin oxide on quartz substrates, was reported at the 18th and 19th Annual Conferences on Mass Spectrometry and Allied Topics.[1,2] Since those reports, this electron source has been married to an orbitron arrangement to produce a low-power, efficient ionization vacuum gauge. The gauge is operated in a pulsed, or sampling, mode by energizing the emitter for a short period of time (~ 1 sec) for each pressure reading. To avoid inducing changes in the energy of the emitted electrons, "emission control" is accomplished by regulating the number of electrons emitted during each pulse (if the integral of the electron current is maintained constant, the integral of the ion current is directly proportional to the pressure). Linear response has been obtained from 10^{-5} torr (~ 10^{-3} Pascal) down to the present system limit of 8×10^{-10} torr. With only 4 mW of power dissipated in the gauge and with 1 μA of electron emission, 0.01 amp/torr (nitrogen) of ion current has been obtained.

The electron emitter is shown in Figure 1. The device is fabricated on a quartz slide that is 1" long by 0.2" wide by 0.04" thick (comparable in size with a tungsten hairpin filament). The emitting region is formed on the edge of the slide, where the 0.1"-wide tin oxide film and gold electrical contact overlap. Electron emission occurs upon application of a voltage (typically 300 V) across the device. The electrons are emitted directionally with a broad energy distribution. The length of each arrow in Figure 1 is proportional to the number electrons emitted in that direction.

Figure 2 shows the electron emitter married to an orbitron. This electrostatic arrangement, first introduced by Herb et al.[3] in 1963, consists of two concentric electrodes. The inner electrode serves as the electron collector; the outer electrode serves as the ion collector. Electrons with sufficient angular momentum are injected into orbit about the central electrode. They remain in orbit until they lose sufficient

angular momentum by collision with a gas molecule or through interaction with perturbations in the radial field caused by the presence of the electron emitter. This results in very long electron path lengths and a high probability of an ionizing collision as the electrons travel from the emitter to the collector. Improvements in sensitivity of over 1000 times that of a Bayard-Alpert gauge have been obtained.

Figure 3 shows the response of the cold-cathode orbitron from 8×10^{-10} torr to 8×10^{-6} torr. The points shown are not average values of several samplings of the pressure; the electron emitter was pulsed only once at each pressure. The lower limit of linear response has not been determined because 8×10^{-10} torr is the present lower limit of the vacuum system. The sensitivity of the cold-cathode orbitron was 12,500 $torr^{-1}$.

Figure 4 illustrates the advantage of the low power consumption of the cold source of electrons and the sampling capability of the cold-cathode orbitron. A VAC-ION system was operating at a pressure of 1.1×10^{-9} torr, as indicated by the orbitron and by the Bayard-Alpert reference. Nitrogen was introduced into the system until the pressure was increased to 10^{-6} torr. The system was allowed to remain at this pressure for about 1 min, both gauges were turned off, and the system was allowed to recover for 2 hr. The orbitron was pulsed once and indicated a pressure of 2.1×10^{-9} torr. The initial indication on the Bayard-Alpert gauge was 4×10^{-7} torr. Even after 20 min of continuous operation, the Bayard-Alpert gauge indicated a pressure much higher than that indicated by sampling with the orbitron.

Possible applications of the cold-cathode orbitron include pressure monitoring in deep-space probes and in static vacuum systems. Its low power consumption and sampling capability should be advantageous in space probes; the extremely small amount of outgassing associated with the pulsing of the electron emitter makes it ideal for sampling the pressure in a static system.

---

[1]Sprouse, J. F., et al., 18th Ann. Conf. M.S. and Allied Topics; San Francisco, 1970.

[2]McLeod, P. C., et al., 19th Ann. Conf. M.S. and Allied Topics; Atlanta, 1971.

[3]Herb, R. G., Pauly T., Fisher, K. J., Bull. Am. Phys. Soc. 8, 336 (1963).

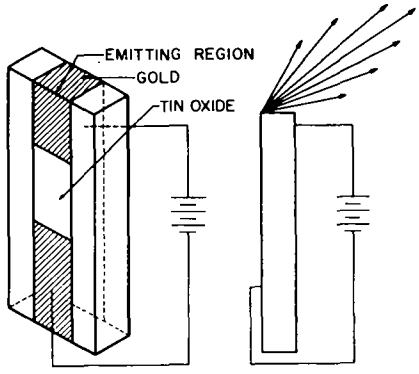

Figure 1 Cold Electron Emitter

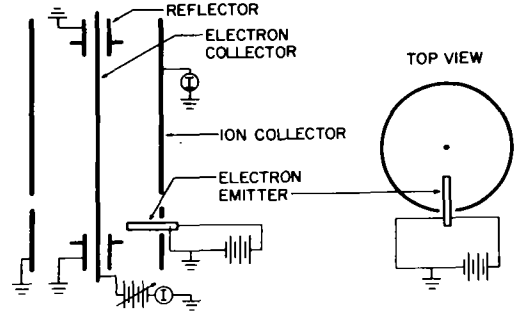

Figure 2 Emitter Married to Orbitron

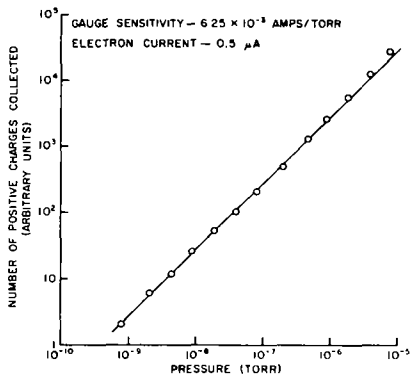

Figure 3 Response of Cold-Cathode Orbitron

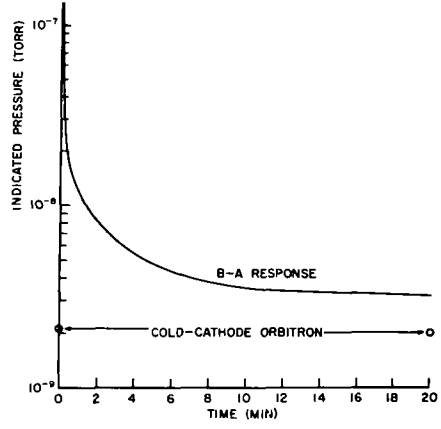

Figure 4 Recovery of Gauges from Pressure Increase

A Digital Mass Readout for Magnetic Sector Mass Spectrometers

A.M. Hogg, Department of Chemistry, University of Alberta
Edmonton, Alberta, Canada T6H 2E1

A device which can give an accurate mass readout on magnetic sector mass spectrometers can be of immense value but many instruments in current use lack such a readout and many commercial devices supplied in the past have proved expensive or unreliable.

For a little more than one year a mass readout based on a commercial high linearity, temperature compensated Hall Probe and a microcircuit which can produce the transfer function X^2/Z has been in continuous use in this laboratory on an AEI MS9 high resolution instrument where it has greatly increased the speed with which mass measurement by the peak matching technique can be carried out. It allows reference or sample peaks to be located at high resolution, compensating for electrostatic sector battery drift and permitting accurate mass readout in both the high and low mass positions as the accelerating voltage is alternated.

A Bell HTJ8-0603 Hall Probe is mounted in an aluminum holder in the pole gap of the MS9 so that it contacts the flight tube and is powered by a Bell 810H Field Monitor. The accelerating voltage is sampled from an existing resistor chain in the source chassis at a level of about 6v (lead 133). These two inputs are fed to the circuit shown in Fig. 1 which squares the Field Monitor input and divides by the accelerating voltage input. The AD531L monolithic multiplier/divider, together with a voltage to current converter using a 741C operational amplifier, provides the function X^2/Z while a second 741C voltage follower prevents loading of the high voltage resistor chain. A reed relay disconnects the inputs to protect the microcircuits when the ±15v supplies are removed and a 12v zener prevents overload of the voltage follower. The ±15v rails are obtained from a power supply in the Field Monitor. The output is fed to a 4½ digit digital panel meter capable of 30 conversions/second.

Three 10 turn precision potentiometers labelled "Curvature", "Offset" and "Slope" are required for setting up the circuit and Fig. 2 shows the effect of maladjusting each separately. A further unlabelled potentiometer shown in dotted lines in Fig. 1 helps in linearising the dividing circuit for wide voltage ratios but is not necessary for all 531L's. Setting up must be done on the mass spectrometer with a reference compound and the three potentiometers adjusted for best linearity. Attempting to tune the circuit to give accurate squaring and dividing using bench supplies does not give the best overall linearity because it is necessary to compensate for non-ideality in the relation of field to mass through offsetting the squaring circuit. The set-up procedure is as follows: (a) The Field Monitor is zeroed on its 10 kilogauss range with the probe in a zero gauss chamber and set to give about 10 volts output at the maximum field of the magnet. (b) With the Field Monitor input to the squaring circuit grounded, the output is set to zero volts with the Offset control. (c) By means of the Slope control, some high mass peak (eg. m/e 614 in perfluorotributylamine) is set to read correctly on the panel meter (10 mV per a.m.u. on a 10 volt f.s.d. meter). (d) A low mass peak (eg m/e 28) is now set to read correctly by readjusting the Offset. Steps (c) and (d) are then repeated until both high and low masses are correct. (e) The instrument is now tuned to some intermediate mass (eg m/e 219) and the error noted. (f) The Curvature Control is now moved by some measured amount (a turns - counting dial helps), steps (c) and (d) repeated and the error at the intermediate mass again noted. By repeating steps (f), (c) and (d) several times it is possible to set up for zero readout error on any three chosen peaks.

An error of ±0.1 a.m.u. can be maintained from m/e 28 to about m/e 700 while above that a roll-off in error is found which is either positive or negative depending on probe position. Similar results are found with both an AEI MS12 (12" radius, single focussing) and an AEI MS2 (6" radius, single focussing). Long term stability is very good with only the Slope being adjusted occasionally to bring high masses back on line. Over a 3½ month period where only the Slope was adjusted, a maximum error of 0.3 a.m.u. developed. A change of temperature of the pole gap of 10.0°C produced a shift in the error curve of a further 0.3 a.m.u. The BCD output of the panel meter drives a marker galvanometer on the U.V. recorder which is accurate for scans no faster than 50 secs/decade being limited by both the sampling rate and magnetic field distortion.

Bell Model 810H Field Monitor (10v output)	$1250.00
Bell Model HTJ8-0608 Hall Probe	209.00
Bell Model YA-111 Zero Gauss Chamber	10.00
Analog Devices AD531L Monolithic Multiplier/Divider	45.00
Weston Model 1234 4½ Digit D.P.M. (30 conversions/sec)	312.00
Electro-numerics Corp Model 375 4½ Digit D.P.M. (30 conversions/sec)	[$ 353.00]
	$1826.00

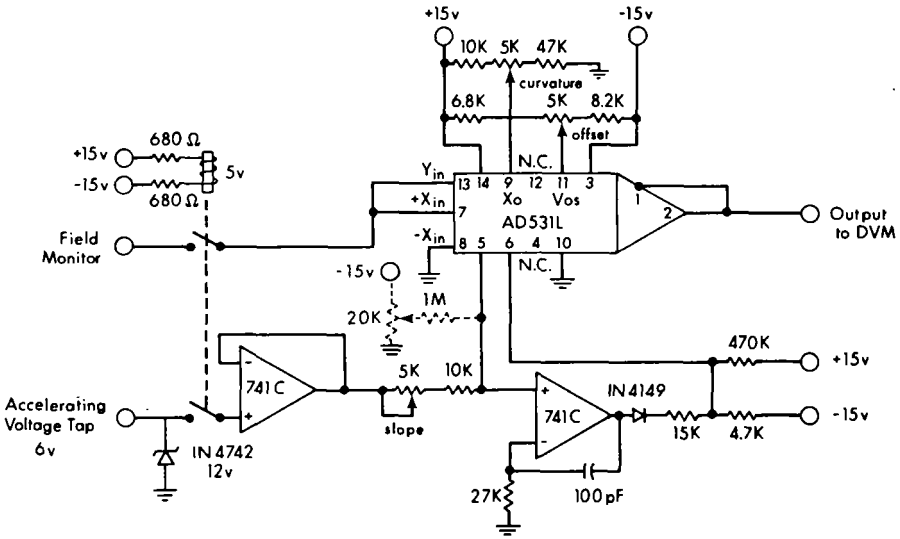

Figure 1

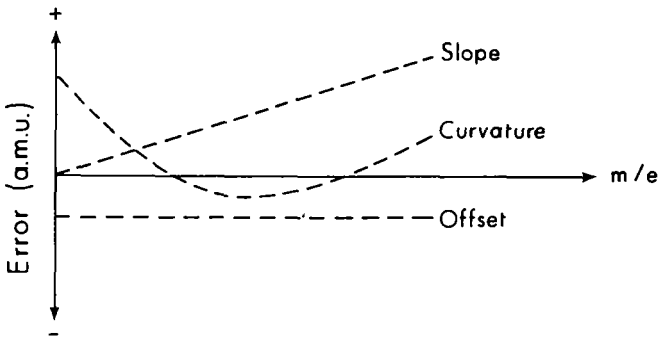

Effect of H^2/V Potentiometer Adjustments

Figure 2

DYNAGRAPH RASTER GRAPHICS DISPLAY SYSTEM

Gilbert L. Brezler
Nuclide Corporation
642 East College Avenue
State College, PA 16801

Today a GC/MS data acquisition system without a CRT display is considered by most analysts to be incomplete. Nuclide has developed its own GC/MS CRT display unit, designated Dynagraph MK-III, which meets the following design requirements: (1) the display is not an alpha-numeric-only terminal that only presents a small number of mass peaks on one horizontal line (usually 80); (2) it plots a spectrum of at least 500 peaks in less than one second so that the spectrum can be displayed between every scan. This allows the system sufficient time to perform the time-to-mass conversion and store the spectrum on disc; (3) it is not a storage device since we desired to selectively edit the display; and (4) the display has an instruction set that allows rapid picture movement. (The thought here was that some chemists might want to do molecular modeling which could involve rotation of the molecule.)

Slide 1 shows a simplified block diagram of the Dynagraph MK-III. The central processing unit and teletypewriter are customer-supplied or optionally available from Nuclide. The interface block represents the hardware required for the particular brand of CPU to communicate with the Dynagraph (another slide presented later shows the simplicity of this module). The timing and decoding circuits are those parts of the system which decode the operation code portion of the instruction received from the CPU and direct the information flow to the proper section of the Dynagraph.

The CRT supplied as a standard item in the Mark-III is a 12-inch diagonal video monitor. The information supplied to the video monitor is compatable with optional, off-the-shelf hard-copying units.

The character generator is a read-only memory which produces a 5 x 7-dot matrix character to the monitor. A set of 64 ASCII characters is standard. The display memory is a 256 x 256-bit random access semiconductor memory in which the picture presently being displayed is stored. Tha refresh rate of 60 frames per second provides a flicker-free display. The processor memory is a 1024 x 16-bit random access semiconductor memory expandable to 4096 x 16-bits; this section allows construction or modification of stored picture sets without interruption of the picture being displayed. This new or modified picture is then transferred to the display memory with a single instruction. Transfer from processor memory to display memory occurs at the rate of 1 vector every 100 microseconds or 1000 vectors in 100 milliseconds.

The internal command instructions are stored in the processor memory and executed at a later time, whenever the CPU issues an Execute instruction. Each instruction is one 16-bit computer word. There are eight internal commands. These commands provide the user with ability to move the cursor with the beam on or off in any direction and at any angle for a maximum relative dot movement of ± 63. The best straight line is calculated by the Dynagraph. One can also, of course, generate alphanumeric characters. The jump-to-processor address instruction allows the user to store subroutines in the processor memory and be repetitively displayed on the monitor. For example, the axis for a mass spectrum can be built as a sub-

routine in the processor memory. Whenever the user wishes to display this axis he must issue a jump-to-subroutine command which initiates the transfer of the axis to the display memory and thus to the monitor.

There are also commands to move the beam — on or off — any length in the X or Y direction or on a 45° diagonal.

There are five external commands which are not stored in the processor memory but are executed immediately. These instructions can reset the entire screen to black or white, they can translate the processor memory instructions to display black-on-white pictures or white-on-black pictures. Selective erasing occurs if a picture previously displayed in a white-on-black pattern, for example, is translated using the black-on-black instruction.

Slide 2 shows a mass spectrum taken with a DuPont 21-491 using a Nuclide model DA/CS-I.2 GC/MS data acquisition system. It is a spectrum from a GC analysis of a sample of Green River oil shale.

This spectrum is number 152 of the GC run. The time taken to present the spectrum on the video monitor is less than 300 milliseconds after pressing the return key on the keyboard (this includes the time required to retrieve the spectrum from the disc as well).

Slide 3 shows the same spectrum scrolled by 250 mass units. This is accomplished by simply pressing the space bar on the keyboard and the change takes less than 200 milliseconds for the spectrum to be displayed.

But how can the Dynagraph be interfaced for use in your lab? Slide 4 shows an interface unit built for use with a PDP-8 minicomputer. The "Device No. 20" name was arbitrarily chosen. Because the PDP-8 is not a 16-bit machine, we have designed the interface to transfer 2 bytes of data to the Dynagraph. Bits 4 through 11 of the accumulator are shown connected directly to the Dynagraph. The first byte is strobed into the graphics unit with a 6201 instruction which generates an IOP 1 pulse. The second byte is transferred with a 6202 which generates an IOP 2 pulse. The last I/O command, 6204, permits testing of the ready line which allows the PDP-8 to identify when the Dynagraph is ready to accept more information. Testing of the ready line is only necessary for the external instructions Execute and Reset, since the Dynagraph can process all other instructions at a data rate which is faster than the computer's input/output rate.

Color may be added so that the Dynagraph may be used with multiple ion detection systems, etc. This is simply done by first replacing the standard video monitor with a color monitor, and by then adding two more 256 x 256 display memories. This will yield one memory for each color gun and allow presentations of eight colors, including black. The color system is ideal for keeping track of overlapping graphics.

Copies of the complete paper as given at the ASMS meeting are available from the author upon request.

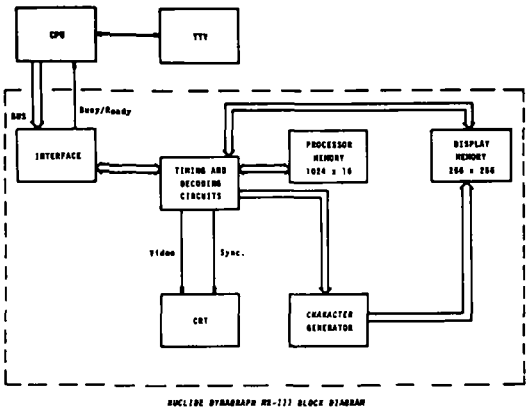

SLIDE 1

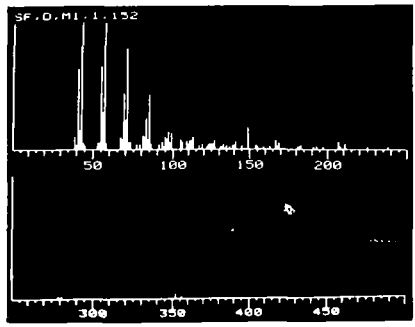

SLIDE 2

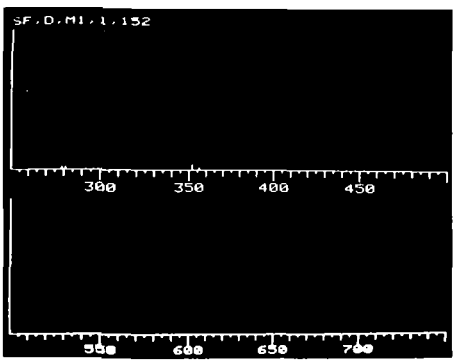

SLIDE 3

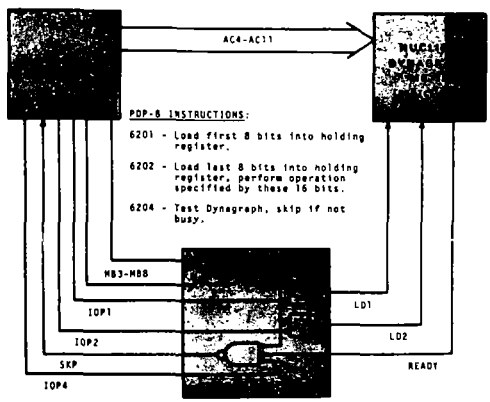

Figure 1 shows a typical Dynagraph interface to a PDP-8. In this example, the computer transfers the 16-bit word as two bytes. The Dynagraph device number has been arbitrarily chosen to be 20. The two I/O commands 6201 and 6202 load a 16-bit word (instruction) which the Dynagraph then processes. The last I/O command, 6204, permits testing of the READY line which allows the PDP-8 to identify when the Dynagraph is ready to accept more information. Testing of the READY line is only necessary for the instructions EXECUTE and RST DISPLAY MEMORY, since the Dynagraph can process all other instructions at a data rate which is faster than the computer's rate.

SLIDE 4

VOLTAGE COEFFICIENTS OF HIGH VALUE RESISTORS

L. F. Herzog and T. J. Eskew
Nuclide Corporation
642 East College Avenue
State College, PA 16801

Certain applications of mass spectroscopy require high accuracy in ion current measurement. An example is the measurement of small differences in isotope ratios in natural samples of different origins, and nuclear materials.

The "classical" system for measuring ion current intensities involves converting these small currents into voltages by passing them through a resistor. The conversion resistors have to be large — typically 10^9-10^{12} ohms.

By 1950, a class of glass-encapsulated carbon resistors (e.g., the Victoreen RX series) had been developed for this purpose. Their temperature coefficients are small, but they depart from Ohm's law increasingly with voltage. Consequently, resistor manufacturers usually include a "typical" voltage coefficient in their data sheets.

Today the more extensive use of electron multipliers has made it easily possible to produce higher MS output voltages, and the availability of electrometer amplifiers with 50 to 100-V capabilities makes it possible to measure voltages for which the correction is significant, while minicomputer control and data processing has made it possible to achieve internal measurement precisions of ± 0.01%. Anomalies in high precision analyses led us to reinvestigate the voltage coefficient correction, especially since, while "voltage coefficient," 1/R x (dR/dV), implies that resistance changes linearly with voltage, Whittles had shown in 1960 that the relationship was not linear.

To calibrate hi-meg resistors for more exacting work, devices known as "ramp generators" (R.G.s) were developed in the 1950s. These produce a constant current that can be varied over a range simulating that of the ion currents of interest.

We decided to use such a precision current source rather than a Wheatstone bridge (1). Slide 1 shows the system. When a control voltage, V_0, is applied as shown, the capacitor C_1 charges at a constant rate:

$$C_1 \frac{dV_1}{dt} = \frac{V_0}{R_1}$$

V_0 is obtained from a highly stable supply. The voltage generated, V_1, is applied to a coupling capacitor, C_2.

At equilibrium, C_2 remains at a constant voltage, so the current injected into the electrometer input is:

$$i = C_2 \left(\frac{dV_1}{dt}\right)$$

The resistor under test, R_3, in a shielded box, is connected as the electrometer feedback resistor. Hence,

$$R_3 = R_1 \frac{C_1}{C_2} \frac{V_3}{V_0}$$

We only need relative values of R_3, so it is only necessary to measure V_3 and V_0, and to be sure that R_1, C_1, and C_2 remain constant during the measurement. A Cary 31 VRE was used for some measurements, and a Nuclide EA-11/EAH-300 for others.

The resistances of several carbon resistors were determined at several voltages. The results were plotted as correction factor vs. voltage curves, from which one can read off the correction at a given voltage for a given resistor. The curves can also be represented well by an empirical formula.

If the shapes of the curves $R = f(V)$ were similar for all resistors, it might be sufficient to make only one determination of resistance for each resistor, and if the voltage coefficients were approximately proportional to the applied voltage, a single constant, ("k" of Slide 2), could characterize a resistor.

When k is small, the Slide 2 formula can be rewritten as:

$$R = R_0 \ (1 + kV^2)$$

Slide 3 shows our measurements of a typical 10^{11}-ohm carbon resistor, plotted as R_0/R, which is the factor by which intensities have to be multiplied. At 50 V the correction exceeds 2%. None of the resistors we tested have voltage coefficients small enough at 50 V to be classed as "typical" in terms of the manufacturers' figure.

To obtain k, one determines the slope of the straight line best least-squares fit to the points. This is of course an approximation. A formula such as $1 + k_1V^2 + k_2V^2$ gives a better fit.

Slide 4 shows data for a 2×10^{11}-ohm resistor. An e^{-kV^2} curve does not fit as well in this case, but the error of about 0.08% near 20 volts is the highest discrepancy noted for the 11 carbon resistors that we have thus far tested. The scatter in the data points (± 0.1% at 1 V) results from about 3×10^{-14} A of "noise" on the R.G. output. This resistor was tested on three days, and the 0.08% departure from e^{kV^2} at 20 V was always reproduced.

Slide 5 shows the values of k, calculated by linear regression, for this resistor on three days. This much uncertainty in k results in a negligible uncertainty in a corrected isotope ratio, compared to the uncertainties resulting from other causes.

Slide 6 shows the k values for the 11 carbon resistors tested. Each value in this table was obtained from just a pair of readings made at 1 and 30 volts, rather than by plotting curves - the value "8.18" is for the 2×10^{11}-ohm resistor for which the least-squares treatment gave 7.59.

The spread in these values is sufficiently great that, if one wishes to measure isotope ratios to better than 0.1% with one signal being above 10 volts, one cannot expect to find a typical value and use it for all resistors. Further, we found no correlation of "k" with resistance.

Recently, tin oxide film resistors have also been advertised as having very small voltage coefficients. We tested some of these in the same system. We found they exhibit several characteristics which will seriously limit their usefulness in mass spectrometry. Some of these are illustrated in Slide 7, showing recorder traces. The electrometer was "zeroed" with the shorting switch closed. First, for a carbon resistor, when the shorting switch is opened, the trace shifts less than 2 millivolts, and shows about 3×10^{-14} A noise on the ramp generator output. The R.G. was set to produce 20×10^{-11} A. The resulting 20-V signal was bucked out with the differential voltmeter and displayed at 20 mV/small division, or 0.1%/div. After about 50 seconds both the range and the DVM were reversed: the trace returned to the same level within 5 or 10 seconds. These traces are flat within 0.03%.

This procedure was repeated with a tin oxide resistor. Note first the 35-mV shift in zero - the resistor generates an e.m.f. of this magnitude. Then, when the test current is applied, the resistor's voltage-drop changes with time. Further, the resistance appears to be different for the two directions of current flow. Hence, we were not able to measure the resistances of tin oxide resistors with the precision of interest.

Conclusions

1. Present tin oxide resistors are not satisfactory for high-precision current measurements.

2. For carbon resistors such as the Victoreen RX-1s, the correction reaches 0.1% at roughly 10 V and 2% at about 50 V. However, it varies by at least a factor of 4 from resistor to resistor. The correction curve can be approximated by the formula $R/R_0 = e^{kV^2}$.

3. Decreases in the required correction can be achieved by selecting resistors, or by replacing a single resistor by several having the same total resistance, or by switching resistors so as to keep all voltages under, say, 2 V, where the average resistor we tested deviates by less than 0.004%.

4. Since high-quality capacitors introduce no equivalent problems, measuring ion current by measuring the rate at which charge accumulates on a capacitor should be more accurate than any technique in which current is converted to a voltage by passing it through such a resistor.

Copies of the complete paper as given at the ASMS meeting are available from the authors upon request.

Notes

(1) A commercial R.G. available from Nuclide is the model CCS-1 constant current source.

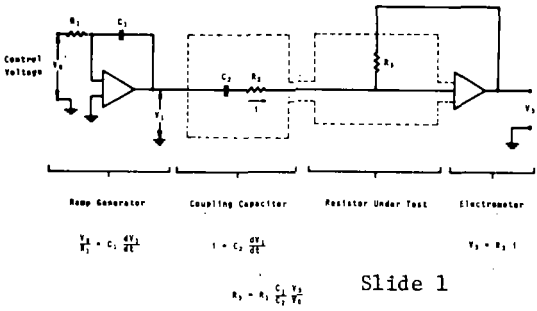

Slide 1

$$\text{Voltage Coefficient} = \frac{1}{R}\frac{dR}{dV}$$

$$\text{If } \frac{1}{R}\frac{dR}{dV} = 2 \text{ kV},$$

$$\text{then } \ln R = kV^2 + \ln R_0,$$

$$\text{or } R = R_0\, e^{kV^2}.$$

Slide 2

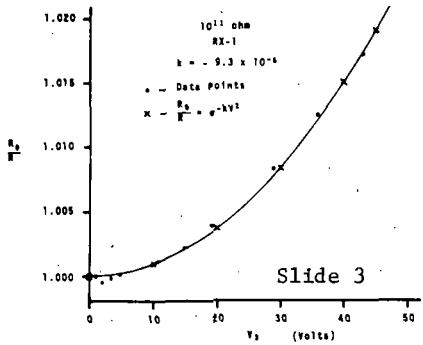

Slide 3

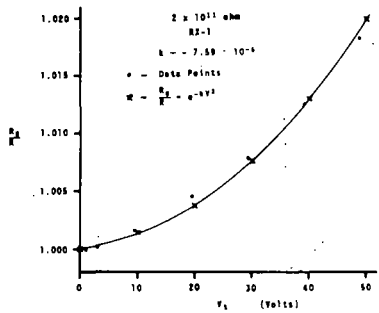

Slide 4

Day	REPEATABILITY OF k	Detector
Monday	7.68×10^{-6}	Cary Model 31
Wednesday	7.67×10^{-6}	Nuclide EA-11
Friday	7.64×10^{-6}	Nuclide EA-11

← Slide 5

If $k = -5 \times 10^{-6}$, $\frac{R_0}{R} = 1.0045$ at 30 volts.

If $k = -10 \times 10^{-6}$, $\frac{R_0}{R} = 1.0090$ at 30 volts.

k VALUES FOR 11 RESISTORS

Resistance	-k
10^{11}	7.66×10^{-6}
10^{11}	8.18×10^{-6}
10^{11}	8.86×10^{-6}
10^{11}	9.30×10^{-6}
10^{11}	20.50×10^{-6}
2×10^{11}	3.40×10^{-6}
2×10^{11}	8.18×10^{-6}
2×10^{11}	10.40×10^{-6}
5×10^{11}	7.41×10^{-6}
10^{12}	4.48×10^{-6}
10^{12}	5.13×10^{-6}

Slide 6

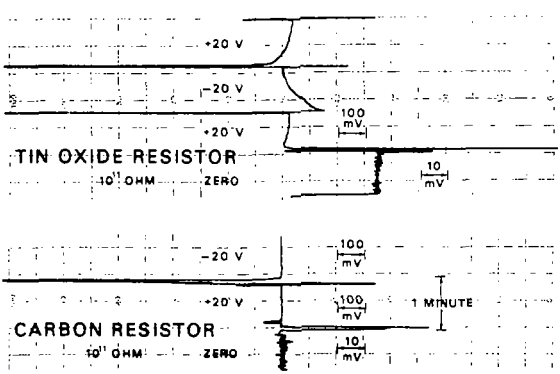

← Slide 7

Fast Switching of Ion Accelerating Potential: Some Limitations and a New Circuit. T. J. Eskew, Nuclide Corp., 642 E. College Ave., State College, PA 16801.

A magnetic deflection MS can monitor several peaks quasi-continuously and hence follow rapid changes in species abundance if the HV potential is switched among the several values with sufficient speed and precision. However, speed and precision tend to be mutually exclusive in electronic circuits. An approach to resolving this conflict will be described. This circuit uses a pair of HV tubes to rapidly charge and discharge the capacitance associated with the ion source, its power supply and isolation transformer. The circuit can switch between 1000 and 12,000 V with a slewing rate in excess of 10^8 V/sec and a settling-time of 50 μsec to within ± (1 V + 0.1%) peak-to-peak. With rate set at 10^7 V/sec and settling-time 300 μsec, it is straight-forward to achieve noise and regulation within ± (0.03 + 0.003%). Peaks can be located "blindly" at a resulution of 2000, hence with the MS under computer control it is possible to monitor, say, 100 peaks quasi-continuously, in a total cycle time of about 300 μsec. Ion counting is required to take full advantage of such switching speeds.

Pharmacokinetic Studies Using CI Mass Spectrometry. JEAN NOWLIN, GOTTFRIED KELLERMANN, REBA M. HILL and MARJORIE G. HORNING, Baylor College of Medicine, Houston, Texas 77025

Pharmacokinetic studies were carried out by selective ion detection (SID) with a Finnigan 1015-PDP 8/I system operated in the chemical ionization mode. The half life of antipyrine, mephobarbital, caffeine and secobarbital were studied in normal adults. Analyses were carried out on 200 µl-1 ml of plasma and on 200 µl of breast milk. Stable isotope labeled drugs were added to the biological samples as internal standards. The plasma half life of antipyrine varied from 5 to 22 hr. The half life of diphenylhydantoin in plasma and breast milk measured in the same individual was found to be longer in breast milk (7 hr) than in plasma (6 hr). The plasma half-life of mephobarbital varied from 35 to 45 hr. It was also possible to measure the change in concentration of three of the metabolites of mephobarbital (phenobarbital, hydroxyphenobarbital and the glucuronide of hydroxyphenobarbital). Because of the sensitivity and specificity of detection and the small quantities of plasma and other biological fluids that can be used, GC-MS-COM methods may be the method of choice for pharmacokinetic studies.

Pharmacokinetic Studies of Methaqualone Using Isotope Dilution Analysis and Field Ionization Mass Spectrometry. Henry d'A. Heck, James H. McReynolds, and Michael Anbar, Stanford Research Institute, Mass Spectrometry Research Center, Menlo Park, CA 94025

Methaqualone, originally introduced on the market as a non-barbituate, non-addictive sedative, has become subject to widespread abuse. The purpose of this study was to follow the long term excretion profile of this drug using stable isotope internal standards and field ionization mass spectrometry for detection and quantitation. The lack of fragment ions and a low probability of background interference at a given mass results in a high signal-to-noise ratio allowing a wide dynamic range in quantitative measurements. The fact that molecular ions are obtained from underivatized samples makes this a highly universal technique.

Methaqualone and 6-hydroxymethaqualone were quantitated using d_7 analogs of the drug and metabolite as internal standards. These materials contained less than 0.01% undeuterated material. Urine samples were processed either directly or following enzymatic hydrolysis to measure free or conjugated drugs, respectively. After spiking with a known amount of d_7-MTQ and d_7-HOMTQ, the samples were filtered onto XAD-2 columns and the drugs eluted with ethyl acetate and methanol.

The eluates were purified by thin-layer chromatography in four separate solvent systems. The final purified spots were eluted and transferred to the solid probe for mass analysis. The mass spectrometer consisted of a 10-inch radius 90° magnetic sector equipped with a multipoint field ionization source and channeltron multiplier used in the pulse counting mode. During heating of the probe the molecular ion regions were repetitively scanned electrostatically while integrating the detector output on a multichannel analyzer. Urine blanks spiked with d_7-standards and processed as described had ratios corresponding to 300 pg/ml for MTQ and 200 pg/ml for HOMTQ.

A calibration curve made by spiking urine with unlabeled methaqualone at concentrations ranging from 0.4 ng/ml to 20 ng/ml is shown in Fig. 1.

A volunteer subject collected urine samples for 11 days following a single 300 mg oral dose. These samples were analyzed to determine the concentration vs time of the unchanged drug, the conjugated 6-hydroxy-MTQ and free 6-HO-MTQ. Fig. 2 shows the integrated molecular ion spectrum of HOMTQ after 11 days. The results of the entire experiment are plotted in Fig. 3. The various components of the drug are seen to be one to two orders of magnitude above the background levels at the end of 11 days, indicating that the concentration of this drug in urine could be followed for a longer period of time.

A complete report of this work will be submitted to Biomedical Mass Spectrometry.

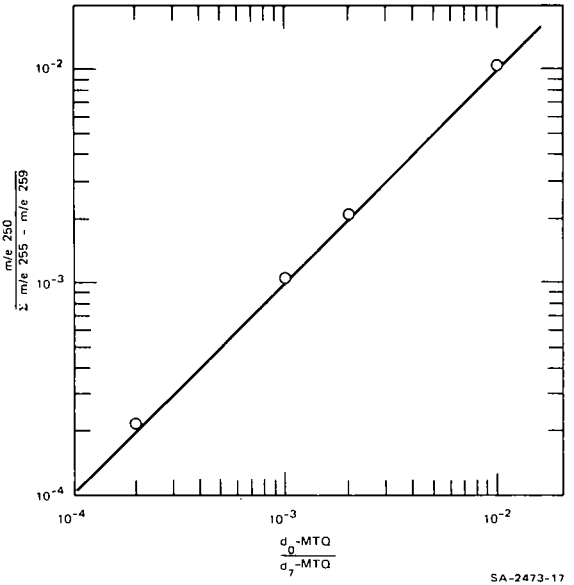

FIGURE 1 CALIBRATION CURVE FOR STANDARD MIXTURES OF d_0- AND d_7-MTQ ADDED TO URINE SAMPLES

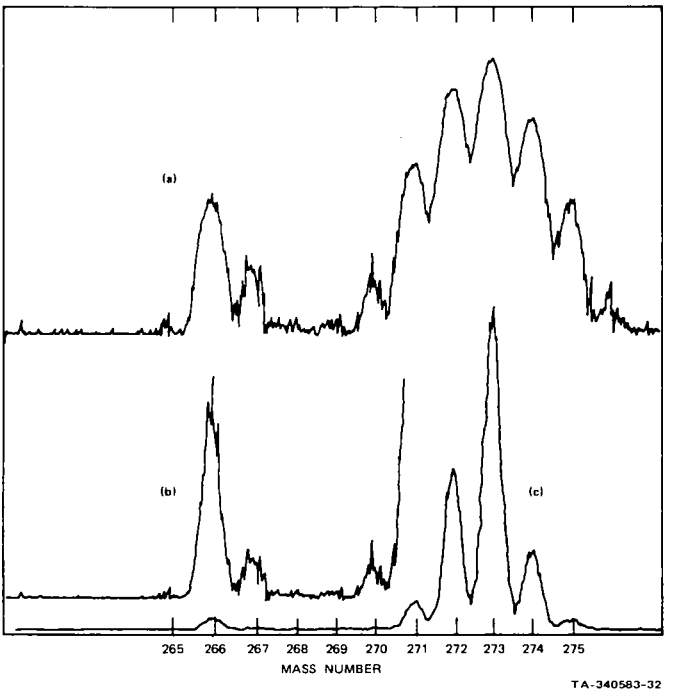

FIGURE 2 FIELD IONIZATION MASS SPECTRA OF MTQOH AND MTQOH* EXTRACTED FROM HYDROLYZED URINE SAMPLE COLLECTED 261.5 HR AFTER DRUG INGESTION

(a) logarithmic scale; (b) linear scale, 256 counts/channel full scale; (c) linear scale, 4000 counts/channel full scale.

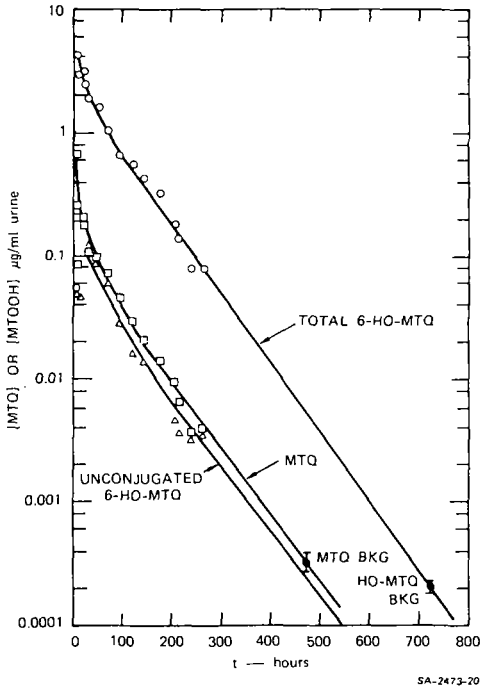

FIGURE 3 ELIMINATION KINETICS OF MTQ AND MTQOH FOLLOWING A SINGLE 300 mg DOSE

Mass Spectrometric Studies on Drug Metabolism Using Stable Isotopes ---A New Quantifying Method--- [1)]

Yuzo Nakagawa, Kouji Iwatani, Shin'ichiro Hashimoto, and Shiro Takahashi
Shionogi Research Laboratory, Fukushima-ku, Osaka, 553 Japan

Since it is undesirable to use the radio isotopes in human, to use stable isotopes for the study of drug metabolism has been paid much attention. Utilization of GC-MS for the quantitative analysis of the metabolites labelled with stable isotope do not require the usual laborious isolation and purification. Our new method for quantitative analysis will be described with using our example, the metabolites of a compound 31252-S.

In our case, instead of using mass fragmentography, GC-MS scanning method was used. Before establishing this method, we had been very careful for the following problems: (1) Keeping the vapour pressure at constant in the ion source during the mass scanning. (2) To discriminate two or more metabolites of the same retention time. (3) The retention times of both the labelled and unlabelled compounds should be the same. All these problems, however, have been resolved in our case.

In the GC (TIM) of our example (Fig. 1) each peak includs labelled (the carbon atoms of the benzene ring were deuterated) and unlabelled compounds. As shown in the Fig. 2, known amount of each unlabelled authentic compound was added to the urine which contained the metabolites of the labelled compound. The mixture was processed to give samples which was injected to GC-MS. And mass spectra were measured at the TIM-peak top. The scanning range is, for example, M-2 to M+7, where M means molecular ion mass number of the unlabelled compound. It is very important to select which ion peak top is to be measured. The peak heights of lower mass numbers are not always in proportion to the number of molecules because those peaks may contain other ion species caused by unexpected fragmentations. Therefor, the molecular ion peak is the most suitable for this purpose, unless the peak is too small.

The scanning period for the full mass range in GC-MS is usually a few seconds, but with such rapid scanning, the peak height of the mass spectrum does not precisely correspond to the amount of the ion. On the hand, where the scanning is too slow, the amount of eluate varies greatly over the scanning period. To correct for the variation of the vapour presure of samples during mass scanning, the peak height measurements were carried out with both increase- and decrease-scanning as shown in the Fig. 2 and both the data were averaged, and the mole ratio of D-compound to H-compound was calculated. Actually the scanning period of this case is about one second, and the difference of both the rate were negligible.

Although the M^+ is small, we selected this molecular peak for the quantitation. By using this M^+ ion we measured standard samples and obtained the calibration curve as Fig. 3, which shows straight line with a slope of $\theta = 45°$. This indicates no chemical isotope effect exists.

For unresolved TIM peak (as seen in Fig. 1), we could resolve it with using the specific mass number peak. M_2 and M_5 still formed an unresolved peak in this condition. M_2 has one less deuterium atom than M_5, so they can be determined from the intensities of their molecular ion peaks. But the protium-molecular ion peak (same m/e) should be alloted for their components. For this allotments we did direct comparison of the M^+ abundance derived from the exactly same amount of both the

compounds, and gave 1.20/1.00.

Next, in case the metabolite decomposes in GC, for example, as shown Fig. 4, we should be very careful to select the TIM-peak.

Deuterium labelled compounds elute a little faster than the corresponding protium compounds on GLC in usual conditions. We found the retention times in our example, 31252-S, have negligible difference, which was checked by single ion monitoring.

A possibility for Deuterium/Protium exchange during conjugate formation was examined as shown in the Table 1, which did not show any significant difference.

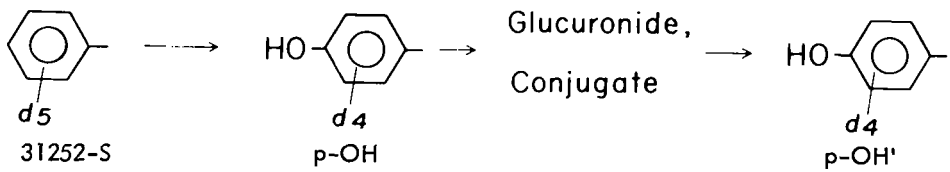

Table 1

	$(M - 1)^+$	M^+
p-OH (in vitro-Rabbit)	16.12 ± 0.97	100
p-OH' (Gluc.-Rabbit)	14.52 ± 1.03	100
p-OH' (Conj.-Man)	15.78 ± 0.86	100

The result of our example was shown in the Table 2. To confirm the result the GLC data and our GC-MS data were compared and gave good agreement.

In conclusion, I will summarize the special feature of our quantitation method. Our method has a good reliability as: (1) A straight calibration line (θ = 45°) was superimposed with a theoretical line. (2) GLC-data and GC-MS data well agreed. Our method has the following advantages: (1) No radiation hazard. (2) Small sample size. (3) No error by sample losses during isolation, derivatization, and running through gas chromatograph. (4) Same GC-retention time components can be resolved. (5) Quantitation can be done without using special additional instruments such as AVA. (6) Many metabolites can be measured with one injection to GC-MS.

Finally, with using stable isotopes and such as our quantitation methods, drug metabolism work will be greatly developed soon.

Table 2

Metabolite \ Animal		Rabbit 20mg/kg		Human 100mg/body	
		1	2	0~4 hr	4~8 hr
(recovered)	Free	(0)%	0	<0.1	0
	Gluc	2.6	4.2	4.3	0.6
	Conj	1.4	1.6	1.0	<0.1
	Free				
	Gluc				
	Conj	0.3		~0.1	
	Free	(<0.1)	<0.1	<0.1	0
	Gluc	<0.1	0	0.1	<0.1
	Conj	0	0	0.2	<0.1
	Free	(<0.1)	<0.1	<0.1	<0.1
	Gluc	0	0	<0.1	0
	Conj.	0	0	0.1	0

Metabolite \ Animal		Rabbit		Human♂	
		1♀	2♀	0~4 hr	4~8 hr
	Free	(<0.1)	<0.1	<0.1	0.1
	Gluc	<0.1	0	<0.1	~0
	Conj	0	0	0.2	0
	Free	(<0.1)	0.1	<0.1	<0.1
	Gluc	3.3	4.7	<0.1	0
	Conj	0.2	0.4	0.4	<0.1
	Free	(0.5)	0.5	<0.1	0
	Gluc	4.8	6.9	2.2	0.4
	Conj	0.7	0.8	4.8	0.2
	Free	0	0	0	0
	Gluc	0	0	0	0
	Conj	0	0	0	0
Total		13.8	19.2	13.3	1.3

Fig. 1

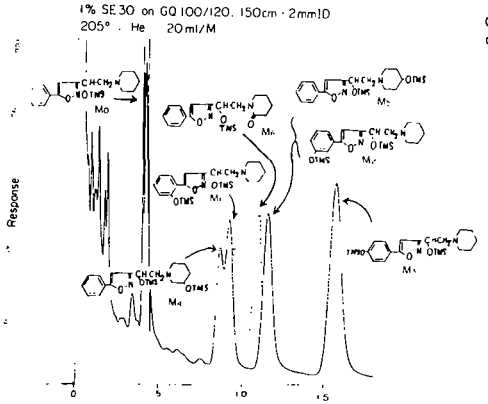

Fig. 3

Calibration curve derived from standard mixtures of the 031252-S and its d_5-derivative

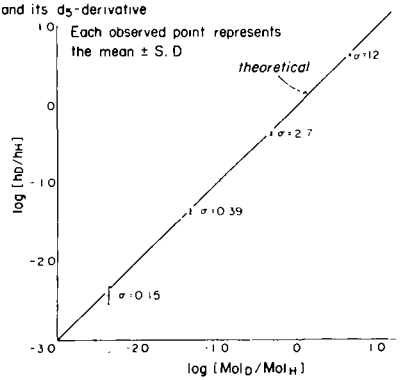

Fig. 2

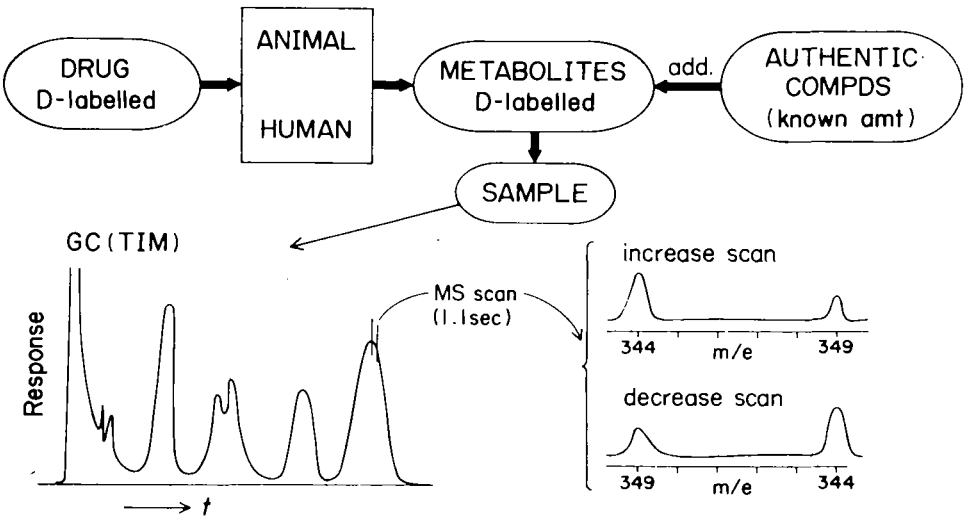

Fig. 4

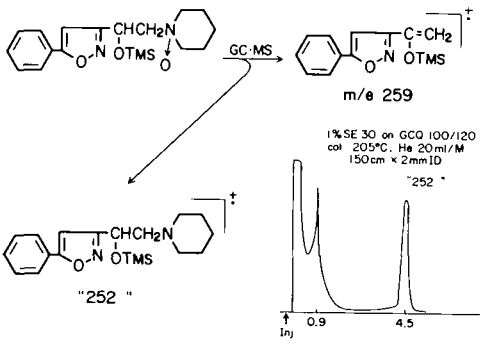

1) This work will be submitted probably to Biomedical Mass Spectrometry.

J-4

Studies of Drug Metabolism by GC-MS-Computer Methods. WANDA G. STILLWELL, PATRICIA GREGORY, NORMA BOOHER and RICHARD N. STILLWELL, Baylor College of Medicine, Houston, Texas 77025

The metabolism of several aromatic compounds was studied by means of gas chromatographic-mass spectrometric-computer systems. Spectra of TMS derivatives were obtained by rapid repetitive scanning on an LKB-9000 GC-MS instrument with data acquisition by a PDP 12 computer. Data from the PDP 12 were transferred to a PDP 11/45 and analyzed with the aid of the LEXER interactive data analysis system. Reconstructed single-ion chromatograms were generated and studied to determine the presence of classes of related compounds (for example, the single-ion chromatogram for m/e 191 reveals the presence of vicinal di-OTMS ethers). All of the compounds studied, including naphthalene, methaqualone and glutethimide, contain vicinal di-OTMS ethers among the derivatized metabolites, indicating that they are metabolized through the epoxide-diol pathway. Further metabolism of the dihydrodiols in most cases leads to the formation of phenols and catechols, whose derivatives are also detected.

J-5

Use of Mass Spectrometry in the Chemical Ionization Mode for the Study of in vitro Drug Metabolism. KATHLEEN R. SOMMER, MARJORIE G. HORNING and JEAN PAUL THENOT, Baylor College of Medicine, Houston, Texas 77025.

A gas chromatograph-mass spectrometer-computer (GC-MS-COM) system operated in the chemical ionization mode was used for the study of *in vitro* metabolism of various drugs. Microgram quantities of drugs, including antipyrine, methsuximide, caffeine, methaqualone, phensuximide, pentobarbital, secobarbital and warfarin were added to a liver homogenate system. This homogenate contained a 10,000 g rat liver supernatant, an NADPH generating system and O_2. After incubation at 37°, the homogenates were analyzed on a Finnigan 1015-PDP 8/I system operated in the chemical ionization mode, using repetitive scanning, multiple ion and/or single ion detection. Drugs and their metabolites were identified and quantified and rates of metabolism determined. Since the results were in good agreement with *in vivo* drug metabolism analyses, it is now possible to study drug metabolism at the microgram and submicrogram level.

Determination of 6-Acetyl Morphine in Biological Fluids by GC-MS-COM Techniques.

J-P Thenot and E.C. Horning, Baylor College of Medicine, Houston, TX 77025.

Heroin (diacetylmorphine) is rapidly deacetylated *in vivo* to form morphine. The biological role of the monoacetyl intermediate is not fully understood. For our study, aimed at the detection and measurement of monoacetyl morphine in biological fluids by GC-MS-COM techniques, both monoacetyl morphine isomers were prepared. Under CI (methane) conditions the allylic (and not the phenolic) oxygen of morphine is protonated followed by the loss of water. If the hydroxyl group is derivatized, with $R=CH_3$, $Si(CH_3)_3$ or CH_3CO, loss of ROH occurs. The chief fragment ion is $\{M+H-ROH\}^+$. Thus, 3- and 6-acetyl morphine give different fragment ions. The trimethylsilyl derivatives of monoacetyl morphines have good GC properties. 6-Acetyl morphine can be measured in nanogram quantities as the TMS derivative by selective ion detection with 6-acetyl morphine-$(N-CD_3)$ as an internal standard using the ion pairs at 340-343 and 400-403 amu.

This work was supported by Contract DAMD-17-74-C-4052.

APPLICATION OF GC-MS TECHNIQUES TO METABOLISM STUDIES ON NOVEL URICOSURIC-SALURETIC AGENTS

A.G. Zacchei and T. Wishousky
Merck Institute for Therapeutic Research
West Point, Pennsylvania 19486

Recent publications from our laboratories have disclosed several series of new orally active indanyloxy acetic acids with saluretic and uricosuric activity. The metabolism of two of these compounds (figure 1) will be presented. In all metabolic studies where radioactivity was employed, the tracer was on the methylene carbon of the side chain. Clinical studies have been performed on both compounds. Compound I was absorbed rapidly and extensively in all species studied. In the rat and dog the major route of ^{14}C elimination was via the feces (∿80%). In these species, essentially all of the dose was recovered as unchanged drug (70-80%) and its glucuronide conjugate (∿20%). In contrast, man, monkey and chimpanzee excreted the majority of the dose via the urine (60-70%) and showed extensive metabolism in urine, feces and plasma. The major metabolite resulted from p-hydroxylation and represented ∿70% of the urinary radioactivity in man, 50-60% in chimpanzee. Intact drug accounted for 5-40% of the dose in these species.

Solvent extraction, column chromatography, TLC, GLC, GC-MS, MS and NMR techniques were employed in the isolation and identification of the metabolites of compounds I and II. The metabolites were initially characterized by GC-MS techniques before and after derivatization with a variety of reagents. However, isolation of the metabolites was essential to obtain sufficient material to determine the orientation and position of the various substituents by NMR techniques. Final identity was made when the postulated metabolites were chemically synthesized and their physical properties (TLC, GLC, GC-MS, NMR) compared with the metabolites.

Comparisons of mass spectral data for the metabolites of compounds I and II and synthetic compounds were presented. Figure 2 summarizes the metabolites identified for compound I. A typical GC tracing of a urine isolate of compound II as the methyl esters is presented in figure 3. The four metabolites (A, B, C and D) were identified and the structures are shown on Figure 4. The position and orientation of the various hydroxyl groups on the cyclopentyl moiety were established by NMR analysis.

In general, the mass spectra of compound I and its metabolites (the p-hydroxy, p-methoxy, x-hydroxy-x methoxy compounds) all gave rise to intense molecular ions (base peak) with little fragmentation. Characteristic minor fragment ions arose from loss of the substituent at C-2. However, in the case of compound II and its metabolites (hydroxyl on cyclopentyl group), extremely weak (usually $\leq$ 1% of base peak) molecular ions were observed. Under low voltage conditions we were able to increase this value several percent. Appropriate derivatives further increased the intensity of the molecular ion region. The base peak in the spectra occurred at 302 m/e and resulted from the loss of the 2-cyclopentyl moiety via a McLafferty rearrangement mechanism.

The details of this work will be published in the near future.

FIGURE 1.

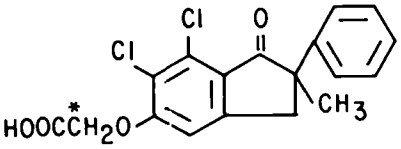

I

(6,7-dichloro-2-methyl-1-oxo-2-phenyl-5-indanyloxy) acetic acid

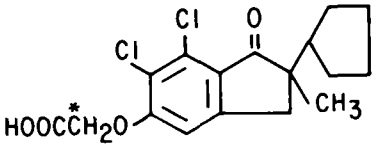

II

(6,7-dichloro-2-cyclopentyl-2-methyl-1-oxo-5-indanyloxy) acetic acid

FIGURE 2.

SUMMARY OF IND METABOLISM IN VARIOUS SPECIES

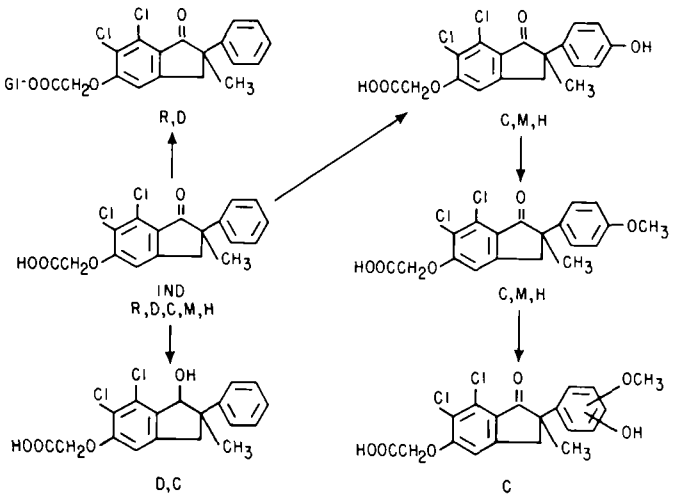

R - RAT
D - DOG
C - CHIMPANZEE
M - MONKEY
H - HUMAN

SUMMARY OF HUMAN AND CHIMPANZEE METABOLITES OF COMPOUND II

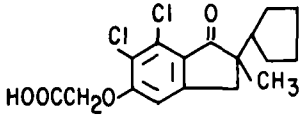

II

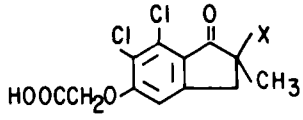

R

METABOLITE A

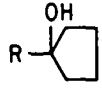

METABOLITE B

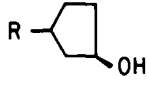

METABOLITE C

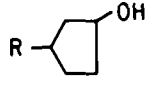

METABOLITE D

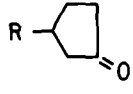

TYPICAL GC TRACING OF MK-473 URINE EXTRACT
(SUBJECT # 2, 6 hr. URINE)

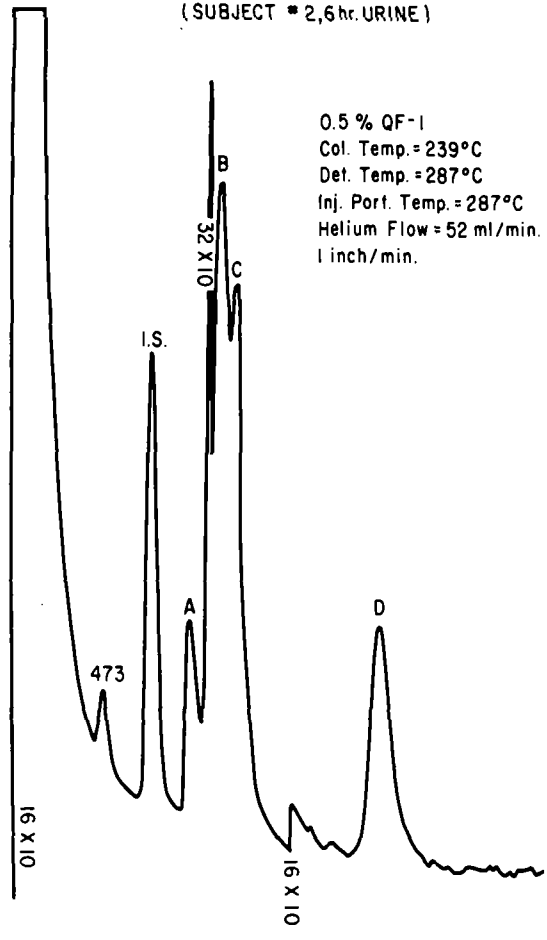

Quantification of Phencyclidine (PCP) in Body Fluids and Identification of Major Metabolites*. DENIS C.K. LIN and RODGER L. FOLTZ, Battelle Columbus Laboratories, Columbus, Ohio 43201, and R. D. FORNEY, JR. and I. SUNSHINE, Cuyahoga County Coroner's Office, Cleveland, Ohio 44106

Phencyclidine-d_5, 1-(1-phenyl-d_5-cyclohexyl)piperidine was synthesized and used as an internal standard for the quantification of phencyclidine, a common component of "street drugs". Using methane as the carrier gas and the chemical ionization reagent gas, the ions selected for recording were m/e 159 and 243 for phencyclidine and m/e 164 and 248 for phencyclidine-d_5. The amount of phencyclidine that can be determined by this technique using 1 ml samples ranges from 1 ng/ml to 5 μg/ml. In the analysis, two important factors have to be considered: (1) the basic compound, phencyclidine, can be extracted at an acidic pH (especially in hydrochloric acid) by chloroform and methylene chloride and (2) phencyclidine starts to decompose at temperatures above 200°C, producing 1-phenyl-1-cyclohexene. In human urine, after enzymatic hydrolysis, two metabolites were discovered. They were identified as 4-phenyl-4-piperidino-cyclohexanol and 1-(1-phenylcyclohexyl)-4-hydroxy-piperidine by spectroscopic techniques and comparison with authentic material.

* Complete manuscript submitted to Biomedical Mass Spectrometry.

Determination of Ribavirin and Pyrazofurin in Serum by Gas Chromatography-Chemical Ionization-Selected Ion Monitoring Technique.

John Roboz, Robert Suzuki, Marjorie Perloff and Takao Ohnuma; Mount Sinai School of Medicine of City University of New York; New York, New York 10029.

Ribavirin (1-β-D-ribofuranosyl-1,2,4,-triazole-3-carboxamide, formerly known as Virazole) is a synthetic nucleoside which is active in tissue culture and in animals against some 25 DNA and RNA viruses. The drug is now in Phase I and pharmacokinetic studies for use in tumors of possible viral etiology to prevent reinduction. Pyrazofurin (1-β-D-ribofuranosyl-4-hydroxypyrazole-5-carboxamide) is a fermentation product from streptomyces candidus; its activity is probably due to inhibition of the conversion of orotidylic acid to uridylic acid. This drug is also in Phase I and pharmacokinetic studies with patients having a variety of tumors. The two drugs are discussed together because the same methodology may be used for the quantification of both in human serum.

After removing proteins by molecular filtration (M.W. exculsion=20,000, drug recovery≈85%), lipids by solvent extraction (methylene chloride), and purifying by ion exchange resins (Dowex 50 to protonate and retain a variety of interfering serum nucleosides followed by Biorex 5 to neutralize) circulating free drugs are quantified as trimethylsilyl derivatives; added Ribavirin serves as the internal standard when Pyrazofurin is analyzed and vice-versa.

Concentration range covered is from 5 ng/ml to 5 ug/ml. For levels <300 ng/ml chemical ionization (methane) and selected ion monitoring are used. When Pyrazofurin is silylated 6 trimethylsilyl groups are incorporated incidating that all hydroxy groups as well as the NH_2 groups are silylated. When Ribavirin is silylated 4 trimethylsilyl groups are incorporated but the compound formed is stable only when introduced via the direct probe. When introduced via gas chromatograph decomposition occurs and a stable cyano compound is formed; the composition of this compound was determined by high resolution mass spectrometry (electronic ionization) as $C_{17}N_{34}N_4O_4Si_3$ (m/e 442.1974). The M+1 ions of both Pyrazofurin and Ribavirin are stable and intense when chemical ionization is employed and are used for selective ion monitoring.

Drug levels peak at 1-2 hr for Ribavirin (oral) and 5-15 min for Pyrazofurin (i.v.). Serum concentration is approximately linear with dosage (single dosage); with multiple doses it is possible to maintain relatively high blood levels (ug/ml level) for extended periods.

(Details of analytical methodology and results of the Phase I studies will be published separately for the two drugs).

Identification of L-DOPA Metabolites in CSF of Parkinsonian Patients by GC-MS

S.E. Hattox and R.C. Murphy

Department of Pharmacology
University of Colorado Medical Center
Denver, Colorado 80220

Parkinson's disease is a relatively common neurological disorder occurring in one out of every 1,000 persons. It is biochemically characterized by a depletion of 3,4-dihydroxyphenylethylamine (dopamine) in the basal ganglia area of the brain[1]. Recent treatment of Parkinson's disease has centered around the concept of replacement therapy. Dopamine itself will not pass through the blood-brain barrier to enter the brain. Therefore the dopamine 1-amino acid precursor, 3,4-dihydroxyphenylalanine (L-DOPA) is employed. This molecule is able to pass through the blood-brain barrier into the brain where it is metabolized to dopamine and subsequently into other metabolites.

It is not known whether the therapeutic effects of L-DOPA are due to a direct or an indirect mechanism, and three differing theories are currently being put forth to explain these effects. The three theories postulate that the beneficial effects are (1) due to direct replacement of dopamine as a major metabolite of L-DOPA[2] or (2) due to the accumulation of a small molecule minor metabolite of dopamine or L-DOPA[3] or (3) due to the accumulation of a tetrahydroisoquinoline-type compound formed by condensation of dopamine or one of its amine metabolites with biologically available aldehydes[4].

The purpose of our work has been to compare metabolic profiles of cerebrospinal fluid (CSF) from three groups of people: (1) normals (2) Parkinsonian patients prior to L-DOPA treatment and (3) Parkinsonian patients after neurological improvement on L-DOPA therapy. The final goal is to correlate that neurological improvement with biochemical changes. Cerebrospinal fluid was chosen as the biological fluid most appropriate to examine in the hopes that it might reflect events occurring in the brain more closely than plasma or urine. This is essential since the disease state being examined is of neurological involvement. The instrument used is a Finnigan 3200 GC/MS system with a model 6000 data system.

The development of methodology to carry out the study involved three areas. First the fragmentation patterns of the TMS derivatives of typical catecholamine metabolites were determined and their gas chromatographic characteristics in terms of methylene unit (MU) values[5] were examined. Secondly, a new method of limited mass scanning was developed to allow increased sensitivity and resolution of the complex mixtures. Finally, this methodology was applied to the analysis of cerebrospinal fluid.

The mass spectra of the TMS derivatives of over fifty compounds related in structure to L-DOPA and its known metabolites have been examined in an effort to correlate fragmentation patterns with variations in structural features. In addition, the methylene unit values of over fifty catecholamine related compounds have been determined and correlated with molecular weight as an aid in structural determination of unknown metabolites. General correlations were found with respect to the number of TMS groups, the extent of methylation of the hydroxyl groups and whether the compound is an acid, an amine or an amino acid.

In analyzing the spectra of the catecholamine-related compounds, certain ions such as those due to benzylic cleavage were seen to occur repeatedly and usually in high intensity. A technique of limited mass scanning

was developed to take advantage of these characteristic ions. Our limited mass scanning method involves injecting a series of straight chain hydrocarbons with the sample. A predetermined series of ions is scanned which includes only those ions characteristic of either hydrocarbons or of the catecholamine-type compounds. Figure 1 shows a comparison of the spectrum of homovanillic acid from CSF using total mass scanning and limited mass scanning. The upper spectrum was obtained in 3 sec with integration times per amu ranging from 2-6 msec. The lower spectrum was obtained in 0.8 sec. thereby resulting in a 3.5-fold increase in time-resolution of components. The dark bands indicate the masses actually scanned, and the number below each set of scans indicates the integration time in msec per amu within that set. Experiments have shown that the higher integration times employed with the limited mass scanning technique result in a 5-10 fold increase in sensitivity, depending on the particular compound.

The use of limited mass scanning also allows determination of MU values with a precision of ±0.1 MU while programming the gas chromatographic inlet system at a rapid rate of 12°C/min. Table 1 shows the standard deviation for 11 determinations of the MU values of six acids and neutrals whose gas chromatographic behaviors are characteristic of the CSF components.

TABLE 1

	Lactic Acid	Oxalic Acid	Pyroglutamic Acid	Citric Acid	Homovanillic Acid	Cholesterol
Mean	11.08	12.46	16.73	18.93	19.32	32.42
SD	±.133	±.05	±.04	±.04	±.03	±.12
SE	±.040	±.01	±.01	±.01	±.01	±.03

The limited mass technique was used in conjunction with total mass scans for precise and positive identification according to MU value plus unique mass spectrum. The technique has been applied to the analysis of neutral and acid fractions of CSF from Parkinsonian patients and to fractions of hydrolyzed CSF. Table 2 shows the components identified in the neutral, acid and acid hydrolysate fractions of post-DOPA Parkinsonian patients. The most pertinent of these results include the identification of methoxyhydroxyphenylethanol, homovanillic acid, p-hydroxyphenyllactic acid, dihydroxyphenylacetic acid, and the conjugated forms of homovanillic acid and dihydroxyphenylacetic acid in increased amounts in post-DOPA patients. The two conjugated acids have been identified here for the first time.

These experiments have indicated that the limited mass scanning technique is an invaluable aid in examining metabolic profiles of extremely complex mixtures, giving increased sensitivity and resolution of components with a minimum decrease in structural information.

References

(1) Ehringer, H. and Hornykiewicz, O., Klin. Wschr., 38, 1236 (1960).

(2) Birkmayer, W. and Hornykiewicz, O., Wien. Klin. Wschr., 73, 787 (1961).

(3) Calne, D.B. and Sandler, M., Nature, 226, 21 (1970).

(4) Sourkes, T.L., Ibid., 229, 413 (1971).

(5) Dalgliesh, C.E., Horning, E.C., Horning, M.G., Knox, K.L. and Yarger, K., Biochem. J., 101, 792 (1966).

FIGURE 1

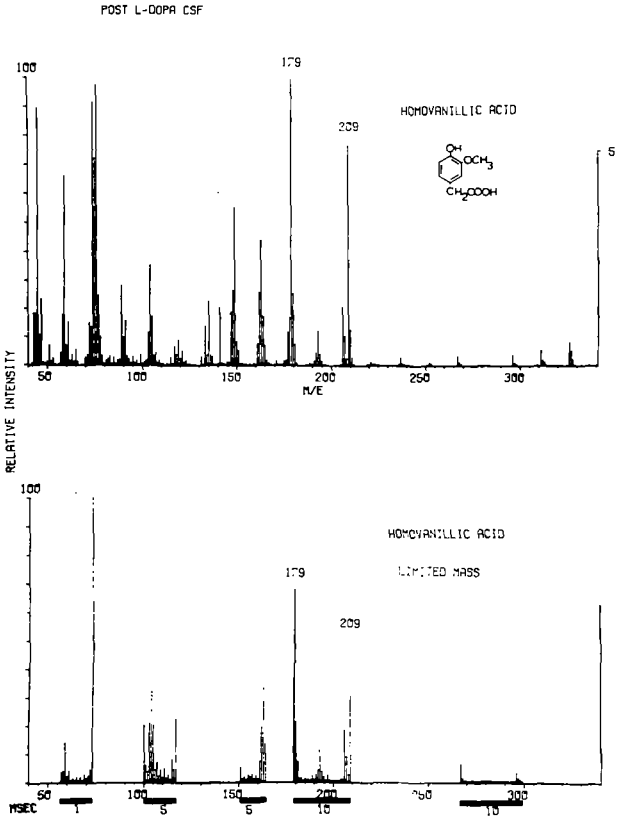

TABLE 2

Components Identified in CSF of Post-DOPA Parkinsonian Patients

Acids		Conjugated Acids and Neutrals	Neutrals
Acetoacetic acid	Lactic acid	Fatty acids	Cholesterol
Aconitic acid	Oleic acid	Glycerol	Fatty acids
γ-Aminobutyric acid	Oxalic acid	Glycolic acid	Glycerol
Benzoic acid	Oxaloacetic acid	Homovanillic acid	Hydroxymethoxyphenylethanol
Citric acid	Palmitic acid	3,4-Dihydroxyphenylacetic acid	Urea
Glycolic acid	Phosphoric acid	Lactic acid	
Homovanillic acid	Probenecid	Oxalic acid	
β-Hydroxybutyric acid	Pyroglutamic acid	Phosphoric acid	
5-Hydroxyindoleacetic acid	Pyruvic acid	Pyroglutamic acid	
p-Hydroxyphenylacetic acid	Stearic acid		
3,4-Dihydroxyphenylacetic acid	Succinic acid		
p-Hydroxyphenyllactic acid			
3,3'-indoleacrylic acid			

Identification of Metabolites of Monensin from Rats

Alvin L. Donoho and John L. Occolowitz, Lilly Research Laboratories, Indianapolis, Indiana 46206

Using a combination of chromatographic techniques, field desorption, chemical ionization, and high and low resolution mass spectrometry, the following three metabolites were identified from the metabolism of monensin in rats:

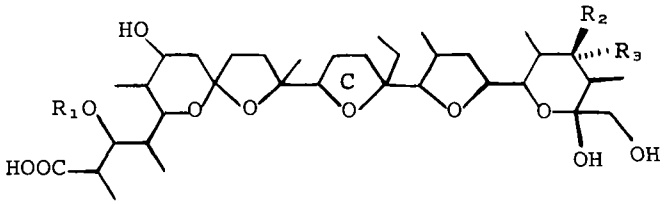

$R_1 = CH_3$, $R_2 = R_3 = H$; Monensin
$R_1 = H$, $R_2 = R_3 = H$
$R_1 = H$, $R_2 = OH$, $R_3 = H$
$R_1 = H$, $R_2 = H$, $R_3 = OH$

A fourth metabolite was found where $R_1 = H$, $R_2 = R_3 = H$, and having an additional hydroxyl group in the vicinity of the C ring.

KINEMATICS OF ION-MOLECULE COLLISIONS

Zdenek Herman

J. Heyrovský Institute of Physical Chemistry and Electrochemistry, Czechoslovak Academy of Sciences, Prague

1. INTRODUCTION

The decade of studies of the kinematics of ion-molecule collisions, namely of chemical reactions of ions, by beam techniques has witnessed a development from the basic question of deciding whether the reaction proceeded by a direct mechanism or via a complex formation to a deeper insight into the details of the collision mechanism and its characteristics and into the question of interchange of various forms of energy in a reaction. Ion-molecule studies parallel studies of neutral-neutral reactions and their results are of general importance for reaction kinetics; the differences between the two groups of studies can be usually reduced to the differences in the interaction potentials between the colliding species. Ion-molecule processes can be studied rather easily over a wide range of collision energies, universal detection of ionic species by mass spectrometers has not been a problem and combination of angular and energy (velocity) analysis was soon achieved. On the other hand, achieving very low (thermal) beam energies, control over internal energy of reactant molecular ions and analysis of internal states of products represent considerable experimental problems.

Achievements of experimentalists have soon attracted the attention of theoreticians and this interaction has been very fruitful. As a result, we know much more about potential energy surfaces for ion-molecule systems, valuable electronic state correlations have been made, the problem of non-adiabatic transitions (so frequent in ion-molecule processes) has been tackled, statistical theories have been applied and developed for ion-molecule processes, and - quite significantly- quasiclassical trajectory studies have been carried out which have provided dynamical characteristics of the processes directly comparable with results of beam experiments.

This paper reviews some of the work on ion-molecule kinematics that has been done in Prague during the last three years. Results on both experimental and theoretical description of a simple impulsive process, on the problem of energy equilibration in intermediate complexes, and on the kinematics of a charge-transfer process will be shortly discussed.

2. APPARATUS

The schematics of the crossed beam apparatus (EVA II) is shown in Fig.1.[1] It uses an electron-impact ionization source (2) and the mass selection of the primary ion beam (3). Usable beamsof energies from 0.5 eV up are produced by the deceleration lens (4), of energy spread typically 0.2 eV (FWHM) and angular spread about 1^{o}(FWHM). The crossed neutral

thermal beam (5) is modulated (6) and locked-in detection is employed. Angular distribution can be usually measured between -15° and $+90^{o}$(LAB) by rotating the beams. Energy analysis is carried out behind the detection slit (8) in a stopping potential energy analyzer (9) whose performance for low-energy ion detection was carefully checked. A magnetic mass spectrometer (10) with a multiplier (11) is used for detection and a signal averager is employed to improve the signal-to-noise ratio for weak product ion signals. Laboratory angular distributions and a series of energy profiles at various angles provide the primary data which are then processed in the usual way to obtain scattering contour diagrams; CM-angular distributions and distributions of product relative translational energy, $P(T')$, are then obtained from the contour diagrams[1,2].

3. REACTION $H_2^+(He,H)HeH^+$

We studied[3,4] the ion-molecule reaction

$$H_2^+ + He \rightarrow HeH^+ + H \qquad (1)$$

both experimentally in a crossed beam experiment and theoretically using the quasiclassical trajectory method (the calculations were carried out by our colleagues in the Central Institute for Physical Chemistry, Berlin). The reaction occurs at low collision energies on one potential energy surface only, and its energetics shows that it is endoergic with ground state reactants by 0.8 eV; vibrational energy is known to be more efficient in overcoming the energy barrier than translational energy[5]. In our experiments the reactant beam contained H_2^+ ions in various vibrationally excited states whose population was given by Franck-Condon transition factors. The calculated results, obtained originally for specific vibrational states of H_2^+, were subsequently averaged over the state distribution to be compared with the experiments.

Fig. 2 shows the scattering contour diagram of HeH^+ at the relative collision energy 2.70 eV (CM)("Cartesian" intensity is plotted). The product ion is distributed asymmetrically about the center-of-mass with a prominent peak forward with respect to the direction of the incoming He atom; then there is considerable intensity scattered all-around the center-of-mass. The position of the peak and the asymmetrical intensity distribution with respect to the center-of-mass are consistent with the impulsive, stripping[6] mechanism of the process. The crater at the center-of-mass results from the dissociation of HeH^+ excited above the dissociation limit. The stripping mechanism governs the reaction over the entire collision energy region studied (0.5 - 3.5 eV,CM)

Fig. 3 compares experimental and calculated CM-angular distribution data at several collision energies. The agreement is very good. The pictures show a prominent, narrow "stripping" intensity peak whose width is practically independent of collision energy, and a large-angle contribution whose relative importance seems to increase with increasing collision energy. Also, the comparison of product relative translational energy distribution, $P(T')$ is very satisfactory. The curves show a fairly broad distribution peaking close to

to T´expected for stripping (SS-arrow). The agreement between experiment and theory in these characteristics of the reaction can serve as a check of the validity of the theoretical procedures used. The theory can be then used to predict other characteristics of the process which are not directly accessible experimentally. Thus, Fig. 5 shows predictions of the distribution of vibrational and rotational energy of HeH^+ at several collision energies. Finally, Fig. 6 summarizes the data on partition of energy available in the reaction into product translation, vibration and rotation (average values of the distributions are shown). It can be seen that with increasing collision energy the portion of energy in translation increases from about 20% to about 50% at T = 4 eV (CM), while the fraction of energy in vibration remains about constant (20%), and the fraction in rotation accordingly decreases.

Preliminary experiments with a selected beam of H_2^+ containing only vibrational states v=0,1 have been made. Thus, only endoergic channels of the reaction can be followed. At T = 3.6 eV a dramatic change of the kinematics occurs: while the stripping contribution in the CM-angular distribution almost disappears, the large-angle scattering strongly increases and the CM- angular distribution becomes almost isotropic. This result agrees well with the theoretical prediction. It appears to be consistent with a simple picture that in the case of endoergic processes hard, impulsive collisions (giving mostly rise to large-angle scattering) are required to achieve the translational-to-internal energy transfer necessary to overcome the energy barrier.

4. ENERGY EQUILIBRATION IN AN INTERMEDIATE COMPLEX

The next two examples concern the question of energy redistribution in reactions in which an intermediate complex is formed. The reaction

$$C_2H_2^+ + C_2H_4 \longrightarrow [C_4H_6^+] \longrightarrow C_3H_3^+ + CH_3 \qquad (2)$$

was shown to proceed via an intermediate complex formation[1]. In the region of collision energies 1 -4 eV (CM) the symmetry of the scattering pattern of $C_3H_3^+$ changed from a fully forward-backward symmetrical one about the center-of-mass to a 2 : 1 unsymmetrical one. This indicates that the mean lifetime of the intermediate complex involved is of the order of several to one mean rotations of theintermediate species. The value of the mean lifetime was estimated from the ratio of the total intensity in the forward and backward hemisphere and from the mean rotational period calculated for the most probable structure of the complex in the critical configuration. The mean τ decreased from $\tau > 3.10^{-12}$ s. at T = 1.76 eV to $\tau = 0.4.10^{-12}$ s. at T = 3.75 eV. As these lifetimes are relatively short, a question arises about the extent of energy equilibration in such "osculating" complexes. The distribution of product relative translational energy showed that the amount of translational energy inthe reaction coordinate was at T = 1.76 eV about twice as large than expected for a fully equilibrated ten-atom complex. Hence, it appears that only some degrees of

freedom are "active" in the intermediate species.

Investigation of the reaction[1]

$$I_2^+ + C_2H_4 \rightarrow C_2H_3I^+ + HI \qquad (3)$$

revealed the formation of an intermediate complex, besides a direct mechanism, too. The decreasing part of the product translational energy distribution curve pertinent to the complex formation is determined in this case by the statistical level-density factor whose exponent is related to the number of degrees of freedom of the complex involved.[7] A proper plot of the P(T´) curve reveals an involvement of a loose, four-atom complex. Therefore, it appears that only the heavy-atom skeleton is the structure involved actively in the energy equilibration. Further information on this intermediate species comes from the investigation of the I_2^+ scattering on ethylene: beside the elastic and inelastic processes one can distinguish a very inelastic peak at the center-of-mass which can be ascribed to an efficient energy exchange in the complex which decomposes backwards reforming the reactants. The mean energy estimated from the width of this peak indicates again that 4 - 6 atoms are involved in the energy interchange in the intermediate species.

5. KINEMATICS OF CHARGE TRANSFER

As an example, kinematics of the charge-transfer process[8]

$$Ar^+ + NO \rightarrow Ar + NO^+ \qquad (4)$$

will be discussed. Fig. 7 shows the scattering contour diagram of NO^+ at the collision energy 0.65 eV. Besides the intensity peak at the CM-scattering angle 180° which corresponds to NO^+ ions with thermal LAB-velocity, there is considerable intensity spread in all directions with a crest close o slightly inside of the "resonant charge-transfer" circle and a peak at $\chi = 0°$ (backward with respect to the original movement of NO). Two essential kinematic informations can be drawn from this scattering experiment: on the mechanism and on the energetics of the process.

The CM-angular distribution (Fig. 8) shows a strong intensity peak which can be ascribed to the simple electron exchange mechanism in which the particles preserve their rectilinear trajectories. The other contribution, the large-angle scattering of NO^+, results from intimate collisions governed by the ion-induced dipole attraction. The shape of the angular distribution, symmetrical about $\chi = 90°$, suggests that an intermediate complex is formed. As the species $ArNO^+$ is stable and was observed earlier in associative ionization reactions, the formation of the complex is not surprizing. From the intensity distribution in 3D the relative importance of the two mechanisms can be estimated. The conclusion is that at this collision energy more than 90% of the charge-transfer encounters proceed via the intermediate complex formation, in agreement with the information extracted from the energy dependence of the total cross-section for this process[8,9].

The other piece of information concerns the energetics. The molecular product NO^+ can be formed at the collision energy 0.65 eV either in the ground state $^1\Sigma^+$ via a very exoergic (6.5 eV) process or in the excited $^3\Sigma^+$ state in a near-resonant charge-transfer. The formation of the ground state would require either a large distortion of the NO bond during the reactant ion approach in order to accomodate the exoergicity as the vibrational excitation or a very superelastic process with large reaction heat-to-translation transfer. The former case is rather improbable and the latter is not born out by the experiment. The distribution of relative translational energy of the products (Fig. 9) from the complex formation mechanism (curve 1) suggest the formation of the excited $^3\Sigma^+$ state in a near-resonant, slightly inelastic process. Indeed, the distribution is very similar to the envelope curve of the Franck-Condon factors from photoionization transition NO-NO^+ ($^3\Sigma^+$) in the gas phase. It thus appears that the approach of Ar^+ to NO does not perturb the N-O internuclear distance and the electron jump occurs as in the free NO. This may be understood,if one realizes that the NO distance in the isoelectromolecule NOCl is the same as in NO (1.15 Å) and, moreover, recent calculations show that the same is the case in the ion Ar^+-NO. The P(T´) corresponding to the electron exchange process (curve 2) is less reliable because of the spread in the crossed beam and difficulties encountered in measuring thermal ions (energy analyzer resolution). However, it indicates a shift towards a slight endoergicity and towards the Franck-Condon factors envelope curve. Another experiment, carried out at T = 1.57 eV gave analogous results. In addition, even higher-lying states of NO^+ were formed here via the intermediate complex formation in very inelastic processes.

Acknowledgement: The author wishes to express his thanks to the American Society for Mass Spectrometry, in particular to the Program Vice President Professor J.H. Futrell,for the invitation to present this paper at the 23rd Annual Conference, and for making the participation possible. It was a pleasure to have in this research the cooperation of Dr. V.Pacák (all experiments), Dr. K.Birkinshaw (experiments HeH_2^+), Drs. L. Zülicke, U. Havemann and F. Schneider (theory HeH_2^+), Dr. J.H. Futrell and Dr. A.J. Yencha ($ArNO^+$) and the author is indebted to all of them for the valuable contribution they made to this work.

REFERENCES

1. Z. Herman,K. Birkinshaw: Ber. Bunsenges. Phys.Chem. 77, 566 (1973).
2. K. Birkinshaw, V. Pacák, Z.Herman: in "Interactions between Ions and Molecules", P.Ausloos Ed.,Plenum Press, New York, 1975, p. 95.
3. V. Pacák, K. Birkinshaw, Z. Herman: to be published.
4. F. Schneider, U. Havemann, L.Zülicke, V.Pacák, K. Birkinshaw, Z. Herman: Chem.Phys. Letters (in press).
5. W.A.Chupka, J. Berkowitz, M.E.Russel: Papers of 6th ICPEAC, M.I.T., Cambridge, Mass. (1969), p.71.
6. A.Henglein, K.Lacmann,G.Jacobs: Ber. Bunsenges. Phys. Chem. 69, 279 (1965).

7. A.S. Safron, N.D. Weinstein, D.R. Herschbach, J.C. Tully: Chem.Phys. Letters 12, 564 (1972).
8. Z.Herman, V.Pacák, A.J. Yencha, J.H. Futrell: Chem.Phys. Letters (to be published).
9. N. Kobayashi: J.Phys. Soc.Japan 36, 259 (1974).

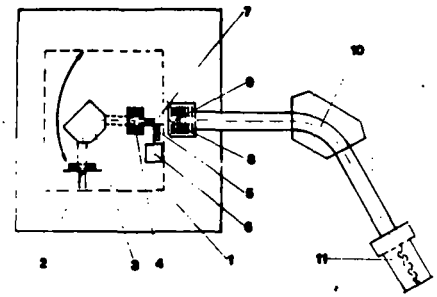

Fig. 1

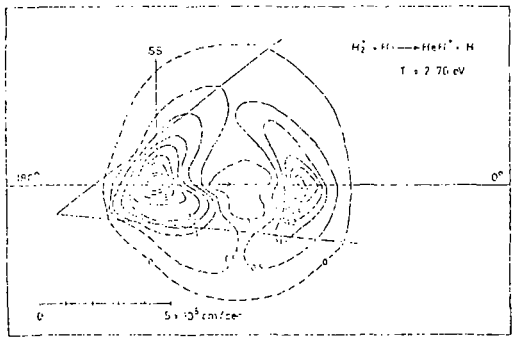

Fig. 2

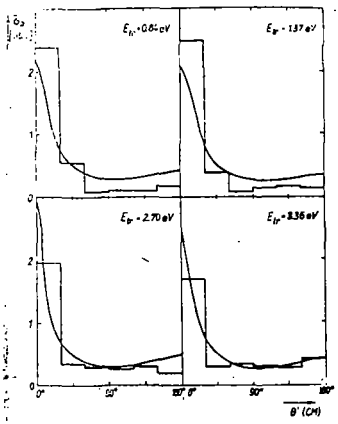

Fig.3

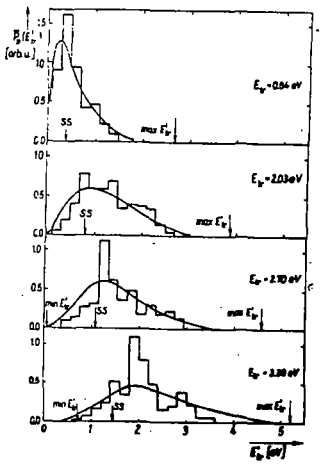

Fig. 4

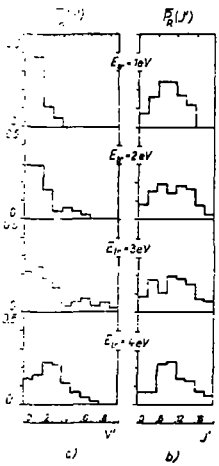

Fig.5

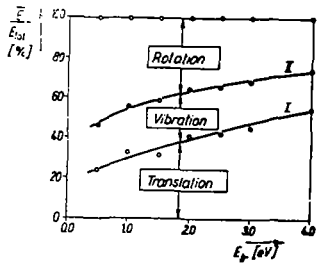

Fig. 6

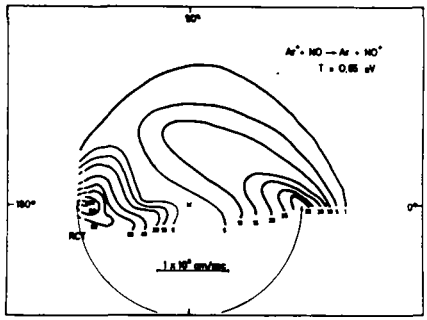

Fig. 7

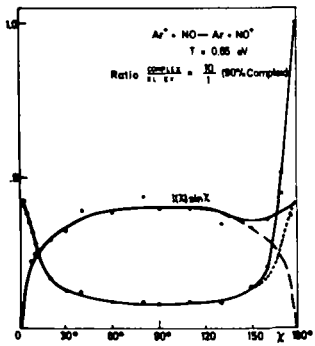

Fig. 8

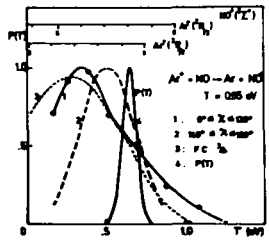

Fig. 9

Crossed-beam Studies of the Reactions of Ar^+/Kr^+ with CH_4.

S.Y. Tang, R.L.C. Wu, E.G. Jones and T.O. Tiernan, Aerospace Research Laboratories (LJ), Wright-Patterson AFB, Ohio 45433

The angular distributions of the product ions, CH_3^+ and ArH^+/KrH^+ from the reactions of Ar^+/Kr^+ with CH_4 have been determined using a crossed-beam apparatus in the range of Ar^+ ion energies from 0.5 to 15 eV. The Ar^+/Kr^+ ions are produced by electron impact, accelerated to about 170 eV, energy-analyzed by a 90° electric sector, mass-analyzed by a 60° magnetic sector, and finally decelerated to the required energy. The FWHM for the Ar^+ ions is about 5° at 2 eV and 1.3 at 6 eV or above. The molecular beam (CH_4) is produced by the effusive flow through a capillary array, and the beam is chopped at a frequency of 9 Hz and collimated by a narrow slit near the interaction region. Product ions are mass-analyzed with a quadrupole mass filter and detected with a channel-type electron multiplier operated in pulse-counting mode. The entire detector assembly can be rotated about the collision center. The measured angular distribution of CH_3^+ ions was found to be very broad at low energy, but shifts as the energy increases. These results will be compared with beam data from other laboratories.

DYNAMICS OF THE $Kr^+ + H_2$ REACTION

S. Chivalak and P. M. Hierl
Department of Chemistry
The University of Kansas
Lawrence, Kansas 66045

The exothermic ion-molecule reaction $Kr^+(H_2,H)KrH^+$ has been studied in recent years by a variety of techniques, including trapped-ion mass spectrometry[1], flowing afterglow[2], photoionization[3], and chemical accelerator techniques[4,5]. A rather unusual intramolecular isotope effect has been reported[5] for the reaction of Kr^+ with HD, and the present study provides additional information concerning the deuterium isotope effect upon both the reaction yield and the reaction dynamics for this system.

The instrument used in this study is a single beam - collision chamber type of chemical accelerator with product velocity and angular analysis[6]. Krypton ions, formed by electron impact, are collimated into a nearly monoenergetic beam whose energy can be varied from 0.5 to 100 eV (LAB). This beam passes through a collision chamber containing the neutral target gas at a temperature of 85° C. and a pressure of about 10^{-3} torr. Reactively scattered ions are energy analyzed by a retarding potential analyzer, mass analyzed by a 12", 90° sector instrument, and detected by an electron multiplier. Angular distributions are measured by rotating the primary ion gun about the center of the collision chamber.

Integral reaction cross sections for the reaction $Kr^+(H_2,H)KrH^+$ have been measured as a function of the collision energy over the range 0.04 to 2.96 eV (CM). The results (Table I) show that, at the lowest energies, the cross section for this reaction is about 1/3 of that for the corresponding reaction of Ar^+ with H_2; at the higher energies the ratio is more nearly 1/10. The values reported here are in good agreement with those previously reported by Henchman and co-workers[5].

Velocity vector distributions for the KrH^+ show that the product ion is nearly isotropically scattered about the center of mass at the lower collision energies. With increasing collision energy, however, the peak in the KrH^+ intensity shifts towards the forward direction, approaching the velocity expected on the basis of the spectator stripping model at collision energies of 2 - 3 eV (CM). Similar results were reported by Henglein[4] for the reaction of Kr^+ with D_2.

Integral cross sections and velocity vector distributions have also been measured for the reactions of Kr^+ with HD at various collision energies in the range 0.08 to 3.04 eV (CM). The kinetic isotope effect, calculated as the ratio of the cross section for KrH^+ formation to that for KrD^+, is listed in Table II. Particularly striking is the observation that this ratio passes through a maximum at low collision energies and then decreases to less than unity at the higher energies studied. This contrasts sharply with the kinetic isotope effects reported for the reactions of Ar^+, F^+, N_2^+, CO^+ and other simple ions with HD[7,8]. In these cases, the yield ratio remained nearly equal to unity at low and medium collision energies, increasing to large values only at rather high (> 4 eV) collision energies.

The product velocity vector distributions measured for the Kr^+ + HD system are summarized in Table III. Two features are worth noting: (1) At the lowest collision energy, where KrH^+ is 2.5 times as abundant as KrD^+, there is no discernable difference in the product velocity vector distributions. (This, however, may partially result from the rather poor resolution in the CM system arising from the unfavorable kinematic factors for this reaction.) (2) At the higher collision energies, KrH^+ is forward scattered (implying formation in large impact parameter collisions) whereas KrD^+ is back scattered (small impact parameter collisions). Although large impact parameter collisions are more probable, KrD^+ is the dominant product at these collision energies.

At this time, we have not found an explanation for the unsual isotope effects observed for this reaction. It is difficult to contruct a simple kinematic model that does not predict identical results for the Ar^+ + HD system, which does not show these same effects. Trajectory calculations on a realistic potential energy surface would hopefully provide an explanation, but such calculations have not yet been performed.

A more detailed account of this work will be submitted to The Journal of Chemical Physics.

References

1. K. R. Ryan and I. G. Graham, J. Chem. Phys. 59, 4260 (1973).

2. P. F. Fennelly, J. D. Payzant, R. S. Hemsworth and D. K. Bohme, J. Chem. Phys. 60, 5115 (1974).

3. W. A. Chupka, Interactions Between Ions and Molecules, Pierre Ausloos, Ed., Plenum Press, New York (1975), p.259.

4. G. Bosse, A. Ding and A. Henglein, Z. Naturforsch. 26a, 932 (1971).

5. P. Fennelly, Ph. D. Thesis, Brandeis University, 1972.

6. P. M. Hierl, L. W. Strattan, and J. R. Wyatt, Int. J. Mass Spectrom. Ion Phys. 10, 385 (1973).

7. A. Hengelin, Adv. Chem. Ser. 58, 63 (1966).

8. K.-c. Lin, R. J. Cotter and W. S. Koski, J. Chem. Phys. 61, 905 (1974).

TABLE I. Integral Cross Sections for the Reaction $Kr^+(H_2,H)KrH^+$.

Collision Energy in CM (eV)	Cross Section ($Å^2$)
0.04	9.77
0.06	10.5
0.07	9.62
0.11	7.65
0.14	6.36
0.18	6.44
0.23	5.27
0.28	3.23
0.29	4.07
0.32	4.21
0.39	3.81
0.46	3.23
0.48	3.33
0.58	1.96
0.70	1.82
0.94	0.73
1.17	0.98
1.19	0.47
1.42	0.50
2.13	0.59
2.37	0.56
2.96	0.49

TABLE II. Yield Ratio KrH^+/KrD^+ for the Reaction of Kr^+ with HD.

Collision Energy in CM (eV)	Yield Ratio KrH^+/KrD^+
0.08	1.28
0.24	1.60
0.33	1.77
0.51	2.00
0.52	1.96
0.67	2.45
0.70	2.24
0.86	2.21
1.04	1.90
1.08	1.80
1.26	1.60
1.35	1.25
1.47	1.18
1.75	0.86
2.02	0.58
2.39	0.65
2.72	0.27
3.04	0.27

TABLE III. Summary of Product Velocity Vector Distributions for the Reaction of Kr^+ with HD.

Collision Energy in CM (eV)	Product Distribution with Respect to CM	
	KrH^+	KrD^+
0.68	Nearly isotropic	Nearly Isotropic
1.41	Slightly forward	Slightly forward
2.07	Strongly forward	Slightly backward
2.72	Strongly forward	Backward

ENERGY DISPOSAL IN PARTIAL CHARGE TRANSFER REACTIONS

C. Cole and P. M. Hierl
Department of Chemistry
The University of Kansas
Lawrence, Kansas 66045

We have recently begun kinematic studies of partial charge transfer reactions of the general type

$$A^{++} + B \rightarrow A^{+} + B^{+}. \qquad (1)$$

The instrument employed, a single beam - collision chamber type of chemical accelerator, is described in the preceding paper [K-3]. A beam of doubly charged ions, accelerated to a given translational energy, interacts with the target molecules under single collision conditions, and the velocity and angular distributions of the reactively scattered A^{+} ions are then measured. Conservation of energy permits one to write

$$RE(A^{++}) + E_T = IP(B) + E_T' \qquad (2)$$

where $RE(A^{++})$ is the recombination energy of A^{++} (*i.e.*, the energy rereleased in the transition $A^{++} + e \rightarrow A^{+}$), E_T is the initial relative translational energy, IP(B) is the ionization potential of species B, and E_T' is the relative translational energy of the products. Rearrangement of Equation (2) yields

$$IP(B) = RE(A^{++}) - Q \qquad (3)$$

where $Q = E_T' - E_T$, the translational exoergicity. The analogy with photoelectron spectroscopy is obvious: if one employs reactant ions of known recombination energy, ionization potentials are readily obtained by measuring the translational energy of reactively scattered ions at a given collision energy.

The reaction

$$Ar^{++} + CH_4 \rightarrow Ar^{+} + (CH_4^{+}) \qquad (4)$$

was studied at several collision energies in the range 0.99 to 18 eV (CM). The parentheses around the CH_4^{+} are in recognition that the internal excitation may be sufficient to produce subsequent dissociation of the ion. It is assumed, however, that such dissociation occurs sufficiently long after the primary ionization that the kinematic analysis may be treated as a 2-body problem.

The product velocity vector distributions were found to be asymmetric with respect to the center-of-mass, with the Ar^{+} being strongly forward scattered. This asymmetry clearly shows that the charge transfer process occurs by a direct mechanism over the energy range studied. This, of course, is to be expected in view of the strong Coulombic repulsion between the ionic products. Moreover, the Ar^{+} velocity distribution was found to consist of two clearly resolved components, indicating the occurrence of two different reactions. One component (I) was characterized

by the release of considerable translational energy in the products, with the most probable value of the translational exoergicity being about 4.5 eV. The second peak in the Ar^+ velocity distribution (Process II) corresponded to a net release of about 1.5 eV of translational energy. At the lowest collision energy, the two processes were about equally intense, but the relative importance of Process II decreased with increasing collision energy. At the highest collision energy studied (18 eV CM), Process I accounted for about 90% of the Ar^+ intensity.

We have interpreted Process I as being the reaction

$$Ar^{++}(^3P) + CH_4 \rightarrow Ar^+(^2P) + CH_4^+(2a_1)^{-1} \qquad (5)$$

where the term $(2a_1)^{-1}$ signifies ionization occurs by the loss of an electron from the $2a_1$ molecular orbital of CH_4. Conversion of the measured Ar^+ energy distribution to an "ionization distribution" via Equation (3) yield results that are in excellent agreement with the He II photoelectron spectrum of CH_4 [1]. Although the energy resolution in the present experiment is not adequate to resolve the vibrational structure, the present data form an envelope that fits over the PES data.

We ascribe Process II to the reaction

$$Ar^{++}(^3P) + CH_4 \rightarrow Ar^+(^2S) + CH_4^+(1t_2)^{-1}. \qquad (6)$$

The comparison with photoelectron data on methane is somewhat more difficult in this case as the recombination energy for the $^3P \rightarrow {}^2S$ transition is not great enough to permit observation of the full range of IP's displayed in the He I PES data. Nevertheless, the relative simplicity of the present system so restricts the number of possible transitions that this interpretation is probably correct. Especially interesting is the fact that this is a two-electron process and might, therefore, be expected to occur with considerably lower probability than Reaction (5). The more extensive interaction required for this two-electron process may account for its occurrence at low collision energies (where collision times are longest) and its rapid decrease in importance with increasing collision energy.

A more detailed account of this work will be submitted to The Journal of Chemical Physics.

References

1. C. R. Brundle and M. B. Robin, J. Chem. Phys. 53, 2196 (1970).

KINEMATICS OF THE REACTION: $H_2O^+ + H_2 = H_3O^+ + H$†

Andrew J. Yencha*, V. Pacák, and Z. Herman

The J. Heyrovský Institute of Physical Chemistry and Electrochemistry
Czechoslovak Academy of Sciences
Prague, Czechoslovakia

The ion-molecule reaction $H_2O^+ + H_2 = H_3O^+ + H$ is the simplest process in which the hydronium ion is formed. An earlier single-beam study of Ding (1) revealed that the analogous perdeutero reaction obeys the spectator stripping mechanism above the relative collision energy 0.5 eV, but suggested a transition to a complex formation below this energy.

We investigated the kinematics of the above reaction in more detail using the crossed-beam apparatus EVA II, namely with regard to the low energy region. The arrangement was as usual and is described elsewhere (2): the beam of H_2O^+ reactant ions (energy spread 0.25 eV FWHM, angular spread about 1° FWHM) produced by electron impact crossed perpendicularly with the beam of thermal hydrogen molecules. Angular distributions and energy profiles at a series of LAB angles were measured for the reactant and product ions. These provided the data set for constructing complete scattering diagrams of H_3O^+ over the energy range 0.1-2.0 eV (CM).

The calculated exoergicity of the reaction, with all particles in ground states, is 1.83 eV. We estimate that reactant H_2O^+ ions, produced by electron impact, are mostly (40%) in the ground electronic and vibrational state (n_i = 0,0,0). The rest are vibrationally excited, ground state ($^2B_1$) ions (the first excited state, $^2A_1$, radiates to the ground state (3), the second excited state, $^2B_2$, is presumably mostly dissociative (4-6)), and the average internal energy of H_2O^+ was estimated to be 0.5 eV.

Fig. 1 shows an example of the scattering diagrams obtained; as usual in this type of experiments, the Cartesian intensity is plotted. In the order of decreasing energy, the results show that:

1. The distribution of product ion intensity about the CM is asymmetric with a prominent forward peak.
2. The forward peaking occurs at the velocity predicted by the stripping mechanism, or slightly forward to it.
3. At the lowest energy (0.11 eV-CM) the forward shift of the peak is quite pronounced (about twice the stripping velocity).

This behavior is consistent with the prevailingly impulsive, stripping mechanism of the reaction over the entire collision energy range studied.

The angular resolution in the CM-coordinates for this process (peaked strongly forward in the LAB coordinates) is about 10°. The CM-angular distribution (Fig. 2) is typical for a direct, stripping process: a strong, narrow intensity peak at χ = 0° and a low intensity over the other angles, with small increases in the backward direction. It is worth noting that

†Study conducted under the joint auspices of the Czechoslovak Academy of Sciences and the National Academy of Sciences of the United States.

*Permanent Address: Department of Chemistry, State University of New York at Albany, Albany, New York 12222.

the angular distribution appears to be, within the accuracy of the experiment, independent of the collision energy which changed four times (the lowest collision energy is not shown - the spread in the reactant beams slightly distorts it). The distribution of product translational energy P(T') was obtained from the scattering data by the 3D integration. Note that the x-axis shows a "reduced" quantity T'/T'_{ss} so that peaking occurs for spectator stripping at 1. It can be seen that the peaking indeed occurs in the vicinity of 1, however, the distribution stretches more to the higher values so that the mean energy is higher than T'_{ss} (Fig. 3).

Fig. 4 shows the translational exoergicity, Q = T'-T, plot (the data were mostly obtained by measuring the energy profiles of H_3O^+ at the LAB angular maximum, full points refer to the values read from the scattering diagrams). The plot indicates, as in many other H-transfer reactions, a positive deviation from the spectator stripping expectation. The data can be accounted for by the polarization stripping model (7) with the transfer of H occurring at about r_c = 1.3 Å (a somewhat outstretched O^+-H bond). In the isoelectronic molecule NH_3 r = 1.014 Å. For this transfer distance Q_0 should be much higher at 0.36T.

Another model by Connaly and Gislason (8) which assumes that the deviation is due to the movement of H atoms in H_2 due to the zero-point energy in the moment of spectator transfer, fits the data quite well, too. The potential energy of vibration transferred into translation should be between $h\nu_0/4$ and $h\nu_0/2$.

REFERENCES

1. A. Ding, Z. Naturforsch., 21A, 856(1969).
2. Z. Herman and K. Birkinshaw, Ber. Bunsenges. physik. Chem., 77, 566(1973).
3. H. Lew and I. Heiber, J. Chem. Phys., 58, 1246(1973).
4. M. Cottin, J. Chem. Phys., 56, 1024(1959).
5. V. H. Dibeler, J. A. Walker, and H. M. Rosenstock, J. Res. Nat. Bur. Std., A, 70, 459 (1966).
6. K. E. McCulloh and V. H. Dibeler, Abs. of Papers, 23rd Annual Conference on Mass Spectrometry and Allied Topics, Houston, Texas, May, 1975, p. 41.
7. P. M. Hierl, Z. Herman, and R. Wolfgnag, J. Chem. Phys., 53, 660(1970).
8. C. M. Connaly and E. A. Gislason, Chem. Phys. Letters, 14, 103 (1972).

FIGURE CAPTIONS

Fig. 1. Contour intensity diagram of H_3O^+.
Fig. 2. Center of mass angular distribution of the ion product, H_3O^+.
Fig. 3. Distribution of product translational energy.
Fig. 4. Translational exoergicity Q vs. initial relative energy T_1.

Fig. 1

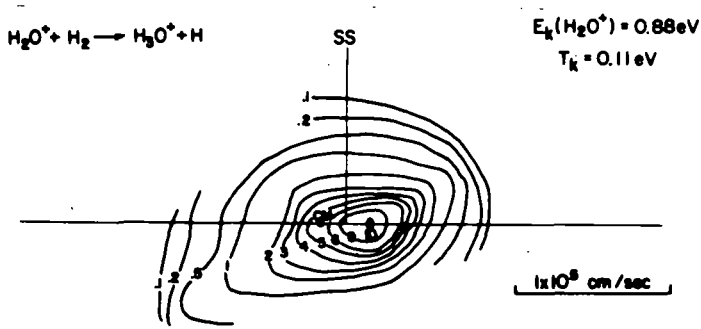

Fig. 2

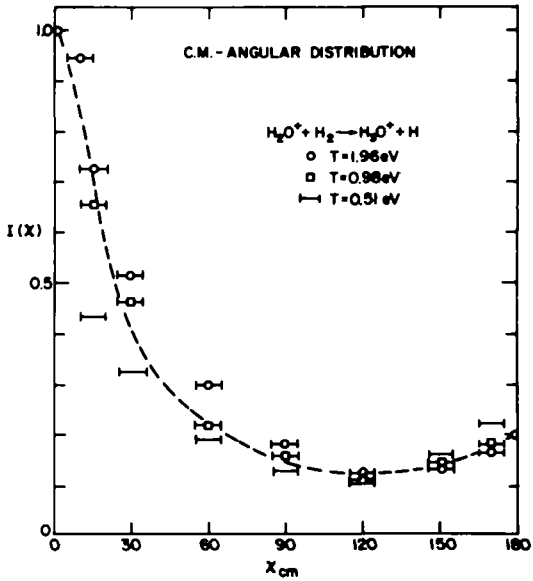

Fig. 3

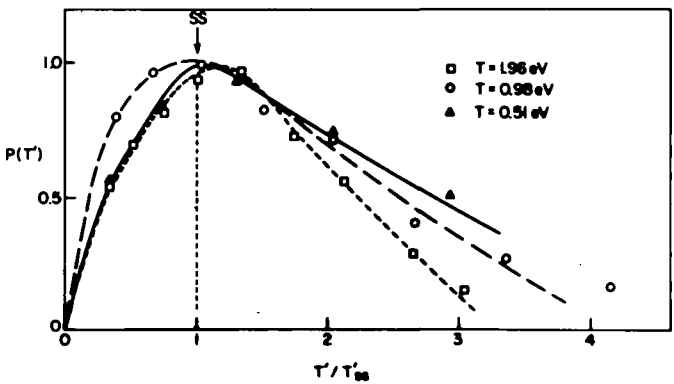

Fig. 4

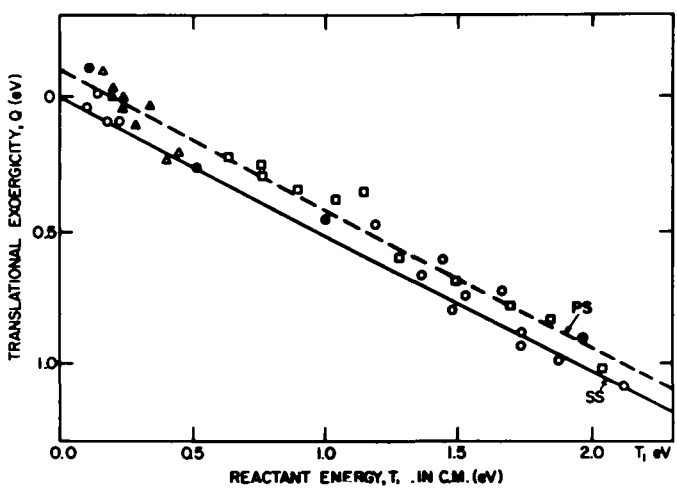

CROSSED-BEAM STUDIES OF CHARGE EXCHANGE AND ELASTIC SCATTERING IN RARE GAS ION-ATOM COLLISIONS

M. L. Vestal, C. R. Blakley, and J. H. Futrell
Chemistry Department
University of Utah, Salt Lake City, Utah 84112

Relative differential cross sections for the combination of elastic scattering and charge exchange with elastic scattering have been measured for collision of He^+ with He using the Utah crossed-beam apparatus.[1-3] Prior to these studies the instrument was modified by replacing the retarding potential integral energy analyzer with a 15 cm radius, 90 degree deflection, differential analyzer. With the modified apparatus the angular resolution of the detector is 1 degree FWHM and the energy resolution is 2% FWHM. An important feature of the apparatus for these studies is the supersonic molecular beam source which produces a molecular beam with a narrow spread in velocity thus minimizing the loss in resolution at low ion energies due to random thermal velocities of the target neutrals.

The He^+ + He system has been previously investigated by Lorents and Aberth[4] at relative translational energies from 10 to 300 eV in the angular region in which elastic scattering is predominant. In the present work the energy range studied has been extended downward from 10 eV to 1 eV relative translational energy. In addition we have measured the differential scattering cross sections for the full range of CM scattering angles from 0 degrees to 180 degrees relative to the incident ion direction.

The results obtained at a relative translational energy of 10 eV are summarized in Figure 1. At scattering angles less than 20 degrees CM the present results are in good agreement with the earlier work.[4] The details of the scattering at large angles and low energies has apparently not been investigated previously.

The theory of He^+ + He scattering at low energies has been developed by Marchi and Smith.[5] While their numerical results do not extend down to the energy range covered in this work, their results can be extrapolated to qualitatively interpret our results. In Figure 1, the peak at 15 degrees apparently corresponds to the classical rainbow maximum for elastic scattering and the peak at 162 degrees to the classical rainbow maximum for elastic scattering with charge exchange. The oscillations at angles smaller than 15 degrees and larger than 162 degrees are apparently due to supernumerary rainbows. The major oscillations between 20 degrees and 160 degrees, which occur with a period of about 7 degrees, are attributed to interference between the waves scattered from the gerade and the ungerade potentials describing the He_2^+ molecular ion. The smaller, higher frequency oscillations observed between 50 and 130 degrees are attributed to interference between the direct scattering of the incident ion at an angle χ and scattering with charge exchange at angle $\Pi - \chi$.

The complete results of these experiments will be published elsewhere. These low energy results, which probe primarily the long range portion of the potential, should provide important new data for testing theoretical calculations. It is hoped that these results will stimulate the extension of the theoretical calculations on elastic scattering and charge exchange into this lower energy regime.

References

1. M. L. Vestal, C. R. Blakley, P. W. Ryan, and J. H. Futrell, Advances in Mass Spectrometry, Vol. 6, J. R. West Ed., pp 781-787, Applied Science Publishers Ltd., London (1974).

2. M. L. Vestal, Ph.D. Dissertation, University of Utah (1975).

3. A paper describing the appartus has been submitted to Review of Scientific Instruments.

4. D. C. Lorents and W. Aberth, Phys. Rev. 139A, 1017 (1965).

5. R. P. Marchi, and F. T. Smith, Phys. Rev. 139A, 1025 (1965).

6. To be sumbitted to Physical Review.

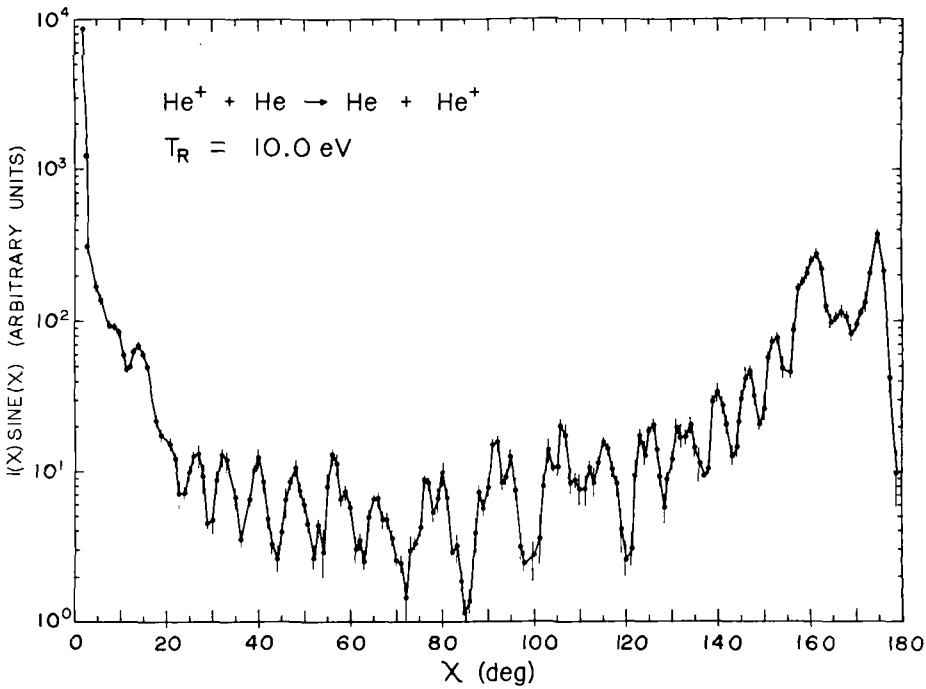

Figure 1

A CROSSED BEAM STUDY OF PROTON TRANSFER FROM HYDRONIUM IONS TO WATER MOLECULES

P.W. Ryan, M.L. Vestal, C.R. Blakley and J.H. Futrell
Department of Chemistry
University of Utah, Salt Lake City, Utah 84112

The technique of crossed ion and neutral beams has been applied to the study of several proton transfer reactions. This paper discusses the reactions

$$H_3O^+ + D_2O \rightarrow HD_2O^+ + H_2O \qquad [1]$$

$$H_3O^+ + D_2O \rightarrow H_2DO^+ + HDO \qquad [2]$$

The Utah crossed beam instrument has been described previously[1], but several of its unique features are relevant to this discussion. The ion beam is produced in a high pressure chemical ionization source. Once formed, the hydronium ions suffer ca 10^5 collisions before diffusing out into the ion optics, so their internal energies are described by a Boltzman distribution.

Neutral reactant is delivered through a supersonic nozzle and skimmer, which leads to extremely low internal energies. By seeding a helium beam with D_2O, the neutral translational energy is enhanced to provide favorable kinematic conditions.

At relative energies greater than 1 eV, only reaction [1] is observed. In contrast to the similar symmetric proton transfer reaction, [3],

$$H_3^+ + D_2 \rightarrow HD_2^+ + H_2 \qquad [3]$$

which was studied in the same instrument[1], the product is scattered exclusively through very small angles (figures 1,2 and 3). Reaction [3] had shown a significant amount of large angle scattering which could be attributed to elastic scattering of the reactant and product particles.

The implication is that [1] proceeds at much larger impact parameters than [3], so that its scattering pattern is determined mostly by the long-range attractive potential, while [3] requires smaller impact parameters and harder collisions so that scattering occurs predominantly from the short-range repulsive potential.

At relative energies below 1 eV, reaction [2] is also observed. Figures 4 and 5 give the differential scattering cross sections at 0.7 eV. Significant amounts of back-scattering are observed, which implies a much stronger coupling of the collision complex. The long-range, loosely coupled, spectator stripping mechanism which successfully described [1] at higher energies is no longer the dominant mode of reaction. It is interesting to note that the isotopically scrambled product of [2] does not appear to arise from a separate, low energy process in competition with the reaction which gives non-scrambled product at higher energies. The scattering patterns for the two products are identical, and thus are presumably produced by the same mechanisms.

Reference

1. F.D. Hileman, T.A. Elwood, M.L. Vestal and J.H. Futrell, presented at the Twenty-Second Annual Conference on Mass Spectrometry and Allied Topics, Philadelphia, Pennsylvania, May 19-24, 1974.

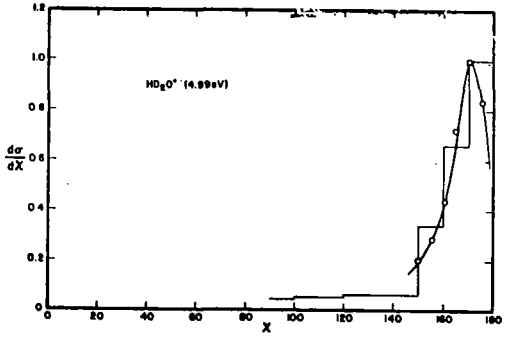

Fig. 1. Differential cross section vs center of mass cross section for reaction 1 at 5.0 eV (relative)

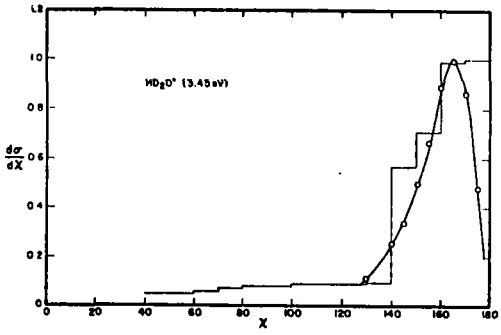

Fig. 2. Differential cross section vs center of mass cross section for reaction 1 at 3.5 eV

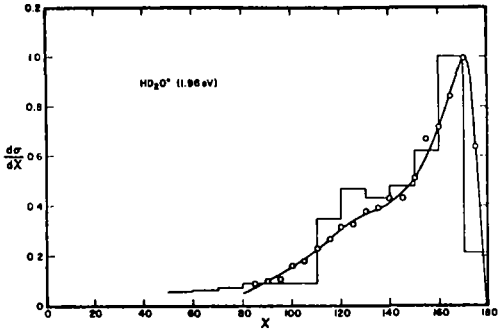

Fig. 3. Differential cross section vs center of mass cross section for reaction 1 at 2.0 eV

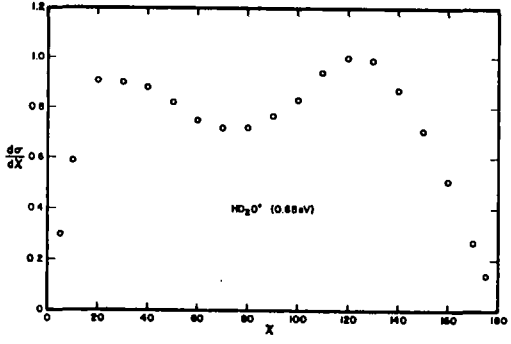

Fig. 4. Differential cross section vs center of mass cross section for reaction 1 at 0.7 eV

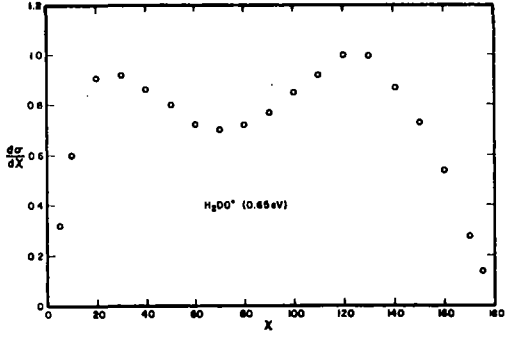

Fig. 5. Differential cross section vs center of mass cross section for reaction 2 at 0.7 eV

Low Energy He^+/H_2 Interactions

E. G. Jones*, B. M. Hughes**, D. G. Hopper** and T. O. Tiernan**, Aerospace Research Laboratories (LJ), Wright-Patterson Air Force Base, Ohio 45433

The reaction systems He^+/H_2 and He^+/D_2 have been investigated emphasizing the dependence of the product species on the kinetic energy of the reactants. Ionic products were detected using an in-line tandem mass spectrometer; excited neutral products were detected using an optical excitation apparatus viewing the radiation along the ion beam axis. Kinetic energy thresholds for the He^+/H_2 system are summarized in Table I. The thresholds are interpreted in terms of the adiabatic correlation diagram for (HeH_2^+). The magnitude of the threshold for H(n = 2) formation is in good agreement with the calculated reaction barrier involving the $2^2\Sigma^+$ state of HeH_2^+. Further calculations of reaction barriers for H(n> 2) formation are currently in progress.

Table I

Kinetic Energy Thresholds, $He^+ + H_2$

Species Detected	Threshold Energy (eV)
H^+	7.6 ± 0.5
H(2); Lyman α	9.0 ± 0.5
H(3); Lyman β	12.8 ± 1.0
H(3); Balmer α	12.2 ± 1.0
H(4); Balmer β	14.4 ± 1.5

*Systems Research Laboratories Inc., Dayton, Ohio

**Present address Chemistry Department, Wright State University Dayton, Ohio 45431

KINEMATICS OF CHARGE TRANSFER $Kr^+ + CH_4$ AT LOW COLLISION ENERGIES

Z. Herman, V. Pacák and K. Birkinshaw[+]

J. Heyrovský Institute of Physical Chemistry and Electrochemistry, Czechoslovak Academy of Sciences, Prague

Collision dynamics of the non-dissociative charge transfer

$$Kr^+ + CH_4 = Kr + CH_4$$

was investigated in a crossed-beam experiment with the aim of obtaining information on its mechanism and on energy interchange in this ion-polyatomic molecule system. Earlier important study was made in Dr. Henchman's laboratory(1) in which the rare gas ion - methane systems were investigated using a short-pulse techniques and the time-of-flight velocity analysis along the direction of the reactant ions movement. Two processes could be distinguished: an electron-jump process giving rise to presumably thermal products and an impulsive scattering process giving rise to "fast" products.

The crossed-beam apparatus EVA II (2) was used. The Kr^+ beam was produced by 120 eV electron impact and contained both the $^2P_{3/2}$ and the $^2P_{1/2}$ states of the ion. Experiments at collision energies T =0.75 eV and T = 0.48 eV provided complete scattering contour diagrams from which the center-of-mass angular distributions and product relative translational energy distribution were obtained. The higher state, $^2P_{1/2}$, (IP= 14.67 eV) leads presumably mostly to dissociative charge-transfer ($CH_3^+ + H$); the lower-lying state (IP=14.00 eV) gives rise to CH_4^+, though at collision energies above 0.25 eV the dissociative process in inelastic collisions is a possibility, too (at T = 0.48 eV it should play a minor role, though).

Fig. 1 shows the contour diagram of CH_4^+ at 0.75 eV. It is characterized by a prominent peak of the ion product at the CM-scattering angle 180° (thermal CH_4^+) and by a small, practically isotropic contribution all-around the center-of-mass. A weak crest of the distribution falls closely to the "resonant charge-transfer" velocity circle, though there is some intensity both inside and outside of this circle. The scattering diagram at 0.48 eV exhibits the same general features.

The CM-angular distribution (Fig. 2) reflects these features of the scattering diagram: there is a strong, narrow intensity peak at χ= 180°, and a small, practically isotropic distribution at all scattering angles. The peak can be ascribed to ions formed by the simple electron-jump mechanism in which the rectilinear trajectory(3) of the colliding particles was preserved (product ions are then thermal in the

---

[+]) Permanent address: Department of Physics, University College London, London WC1.

LAB coordinate system). On the other hand, the large-angle scattering of CH_4^+ results from intimate collisions. Its isotropic character suggests that these intimate collisions are of an impulsive, short-duration type, giving rise to hard-sphere-like scattering. It does not seem probable that a long-lived intermediate could be formed (as, e.g., in another charge-transfer system, Ar^+ + NO (4)) or that the intimate collisions lead to another product (the sum of cross sections of chemical processes does not exceed several percent of the charge-transfer cross section (5)). Similar conclusions can be drawn from the lower-energy experiment, too, though the intensity of the large-angle scattering is somehigher. From the angular intensity distribution in 3D (function $I(\chi)\sin\chi$ in Fig. 2) one can estimate the relative importance of the two mechanisms, intimate collision vs. electron exchange, which is 1 : 1 at 0.75 eV and 5 : 1 at 0.48eV.

Further kinematic information can be obtained from the distribution of product relative translational energy, $P(T')$. That part of the scattering diagram pertinent to the electron exchange mechanism (Fig.3, curve 2) was analyzed separately from the intimate-collision, large-angle portion (curve 1). The $P(T')$ curve corresponding to the latter process at 0.75eV shows that the most probable energy transferred is that one which corresponds to the "resonant charge transfer" giving rise to vibrationally excited ions CH_4^+. However, up to about 0.5 eV can be transferred in inelastic or superelastic collisions. The $P(T')$ curve for the simple electron-exchange process is very similar to that one of the intimate-collision mechanism. Again, the most probable energy transferred is that one of the resonant charge-exchange. However, this curve is less reliable as far as it width is concerned, as it may be appreciably broadened by the angular (20° FWHM) and energy (Boltzmann) spread of the crossed beam. The actual translational energy distribution curve corrected for this effect may be slimmer.

REFERENCES

1. A.J. Masson: Thesis. Brandeis Univesity, 1970.
2. Z. Herman, K.Birkinshaw: Ber. Bunsenges. Phys. Chem. 77, 566 (1973).
3. D. Rapp, W.E. Francis: J.Chem.Phys. 37, 2631 (1962).
4. Z. Herman, V.Pacák, A.J. Yencha, J.H. Futrell: Chem.Phys. Letters (to be published).
5. F.H. Field, H.N. Head, J.L. Franklin: J.Am.Chem.Soc. 84, 1118(1962).

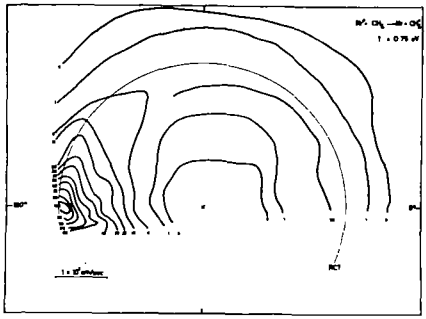

Fig. 1

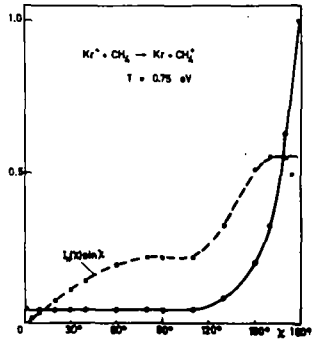

Fig. 2

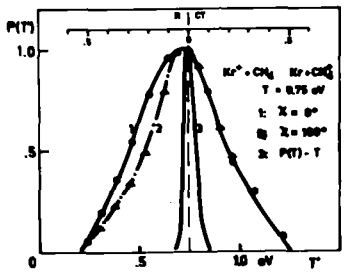

Fig. 3

Wavelength Dependence of the Branching Ratio for Competitive Photodissociation of Butene Cation

M. Riggin[‡], R. Orth, and R. C. Dunbar[+]

Department of Chemistry, Case Western Reserve University
Cleveland, Ohio 44106

ABSTRACT

The competitive photodissociation of butene parent cations according to the scheme

$$C_4H_8^+ \xrightarrow{h\nu} C_4H_7^+ + H$$
$$C_4H_8^+ \xrightarrow{h\nu} C_3H_5^+ + CH_3$$

has been examined quantitatively as a function of wavelength. The ratio of $C_4H_7^+$ to $C_3H_5^+$ increases with decreasing photon energy. The branching ratio curve is in acceptable agreement with quasiequilibrium theory calculations if activation energies of 2.17 eV and 2.22 eV are taken for formation of $C_4H_7^+$ and $C_3H_5^+$, respectively. This supports the assumption that the process is a true unimolecular competition on the ground electronic state potential surface, and moreover gives precise and reliable data for the difference in activation energies for the two channels.

The full paper has been submitted for publication in the journal of Chemical Physics.

[‡]Present address, Institute for Chemical Physics, Department of Physics, University of Western Ontario, London, Canada.

[+]Alfred P. Sloan Fellow, 1973-75.

Dye-Laser Induced Photodetachment of Electrons From Gaseous SH^- Ions.*

JOHN R. EYLER
University of Florida, Department of Chemistry
Gainesville, Florida 32611 and GEORGE H. ATKINSON
Syracuse University, Department of Chemistry
Syracuse, New York 13200

A flashlamp pumped tunable dye laser has been coupled to a pulsed ion cyclotron resonance (icr) mass spectrometer to study various laser-induced ionic processes. The high energy resolution of the dye laser combined with the ability of the icr spectrometer to produce ions of low internal energy allows, in favorable cases, fine structure related to various energy levels of the ions and neutrals involved in these processes to be observed.

Our initial experiments using this technique involved the photodetachment of SH^- ions ($SH^- + h\nu \rightarrow SH\cdot + e^-$).[1] The SH^- ions were formed by dissociative attachment of electrons to H_2S at a pressure of 3×10^{-5} torr, trapped in the icr cell for 32.5 msec, and then irradiated by a pulse of tunable laser photons lasting less than one microsecond. The number of SH^- ions remaining in the cell (those which had not undergone photodetachment) was then determined, and compared to the number contained in the cell under identical conditions when the laser was not flashed. From comparisons of this sort the results shown as closed circles in Fig. 1 for the relative cross-section for SH^- photodetachment as a function of wavelength were obtained.

The energy onset of the photodetachment process, corresponding to a wavelength of 538.7 ± 0.3 nm can be directly related[1] to the electron affinity of SH·, E.A.(SH·), which is determined in this work to be $2.301_6 \pm 0.001_3$ eV. The arrows in Fig. 1 are the upper and lower bounds to E.A.(SH·) reported in an earlier study[2]. Closer inspection of the closed circles in Fig. 1 reveals two regions of greater slope, separated by a region of lesser slope (526-534 nm). The two regions of greater slope represent the onset of photodetachment to two final states of the SH· radical, which are split by the spin-orbit coupling in the radical.

To determine more exactly the magnitude of the observed splitting, a five-point numerical differentiation of the data represented by the closed circles was performed; the results are plotted as open circles in Fig. 1. The two largest maxima in the first derivative are separated by about 11.8 nm (422 cm^{-1}, 0.052 eV). This is to be compared with a value for the spin-orbit coupling constant of 10.7 nm determined spectroscopically.[3] The first derivative of the cross section curve also shows periodic oscillations as a function of wavelength, with a period of about 2.5 nm. No explanation for the origin of these oscillations can be given at this time.

A computer simulation of the expected SH^- photodetachment spectrum, similar to that reported for OH^-[4], is currently underway. Preliminary results indicate that the true E.A. (SH·) corresponds to an energy quite close to the initial sharp rise (ca. 537 nm) in Fig. 1. Results of this detailed analysis should thus yield a value for E.A.(SH·) quite close to the upper wavelength (lower energy) limit reported earlier.[2] Preliminary results also indicate that the splitting of 11.8 nm observed in this work may not be reconciled with the earlier reported value of 10.7 nm, even after the more detailed analysis.

*Research performed at the National Bureau of Standards, Gaithersburg, Md.

1. J.R. Eyler and G.H. Atkinson, Chem. Phys. Lett. 28, 217 (1974).
2. B. Steiner, J. Chem. Phys. 49, 5097 (1968).
3. D.A. Ramsay, ibid., 20, 1920 (1952).
4. H. Hotop, T.A. Patterson, and W.C. Lineberger, ibid., 60, 1806 (1974).

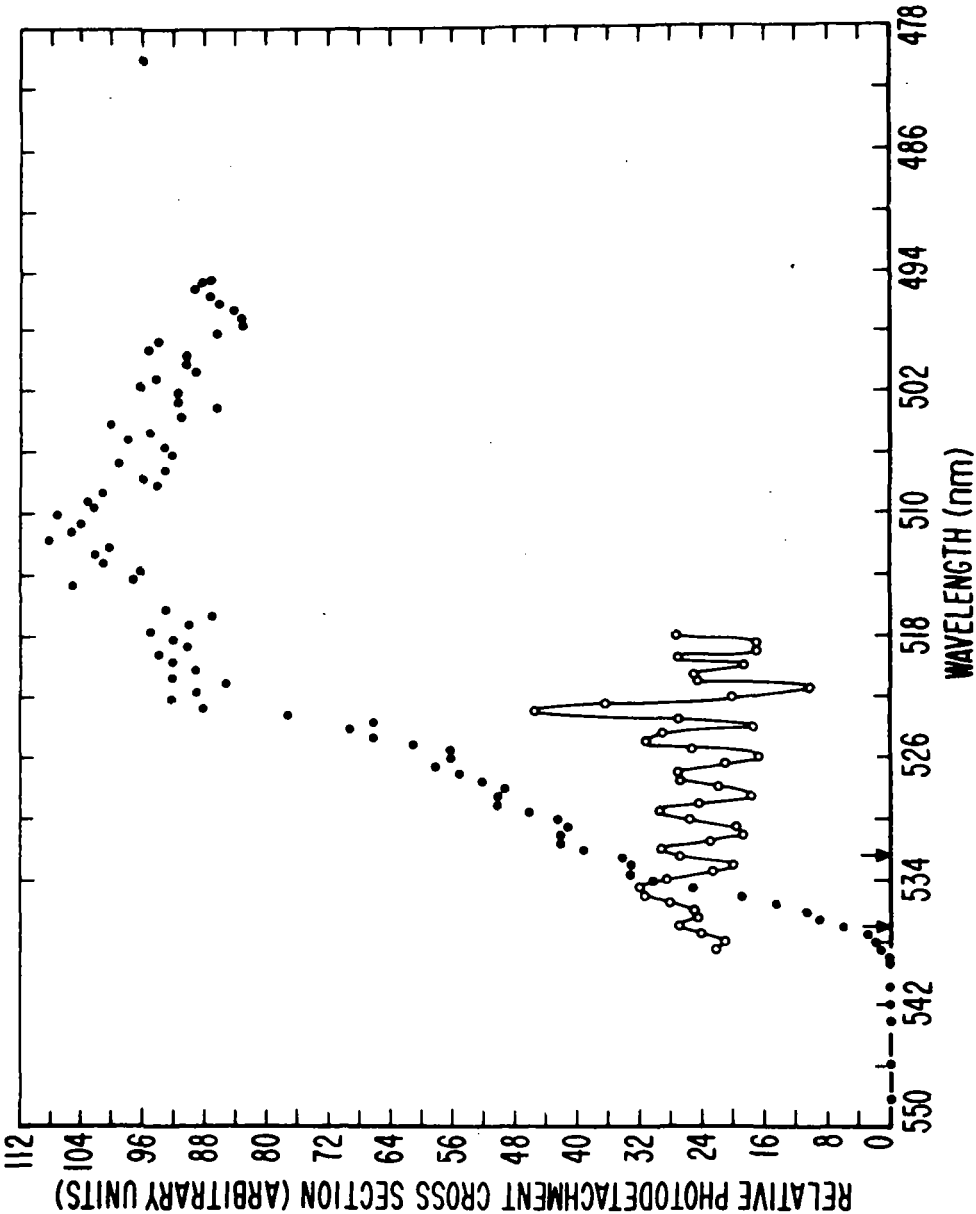
RELATIVE PHOTODETACHMENT CROSS SECTION (ARBITRARY UNITS)
112
104
96
88
80
72
64
56
48
40
32
24
16
8
0
550
542
534
526
518
510
502
494
486
478
WAVELENGTH (nm)

FIGURE 1

Dye Laser-Induced Photodissociation of $C_7H_8^+$ Ions in Gaseous Toluene.*

JOHN R. EYLER
University of Florida, Department of Chemistry
Gainesville, Florida 32611

As a continuation of our earlier studies[1,2] of laser-induced ionic processes, the pulsed ion cyclotron resonance (icr)- intracavity dye laser technique[2] was applied to a study of positive ion photodissociation. Photodissociation of $C_7H_8^+$ ions in gaseous toluene ($C_7H_8^+ + h\nu \rightarrow C_7H_7^+ + H\cdot$) was chosen as an initial system for study.[3] Earlier investigations[4] using a conventional light source for ion irradiation had shown that the energy threshold for this process corresponded to photon wavelengths easily accessible using flash-lamp-pumped dye lasers, and that the cross section for the process was high relative to that for many other positive ions.

Gaseous toluene at pressures of 5×10^{-6} Torr was subjected to a 20 msec. electron beam pulse, of nominal energy 10 eV. The $C_7H_8^+$ ions formed were trapped for an additional 156 msec, and then subjected to a pulse of tunable laser photons of approximately 1 μsec duration. After 4 msec., the number of photoproduced $C_7H_7^+$ ions was monitored. Experiments of this nature, carried out at many different wavelengths, after normalization with respect to photon intensity and parent ion intensity, gave rise to the data plotted as closed circles in Figure 1 for the relative cross-section for $C_7H_7^+$ appearance as a function of wavelength. The error bars represent the standard deviation of several values for the cross-section determined within ± 5 Å of the wavelength shown.

The open circles shown in Fig. 1 are the results of a previous study[4] of $C_7H_8^+$ photodissociation of much lower resolution. Agreement with the present investigation is seen to be quite good. The apparent threshold for this process, taken to be that point where the error bars begin to consistently contain a zero value for the relative cross-section, is found to be 538 ± 2 nm (2.31 ± 0.01 eV). This is also in quite good agreement with the previous study. Although fluctuations in the photodissociation cross-section curve suggestive of fine structure do appear, the large error bars dictate that these fluctuations cannot be considered statistically significant.

A comparison of the cross section for $C_7H_8^+$ photodissociation to that for SH^- photodetachment was made at a laser output wavelength of 490 nm under experimental conditions as nearly identical as possible for the two different systems. The results indicate that the absolute cross section for $C_7H_8^+$ photodissociation at 490 nm is $1.01 \pm 0.24 \times 10^{-18}$ cm^2. This value can be used to obtain an estimate of $5.1 \pm 1.6 \times 10^{-18}$ cm^2 for the process $C_7H_8^+ + h\nu \rightarrow C_7H_7^+ + H$ at its observed[4] lower energy maximum near 400 nm.

This study demonstrated that the pulsed icr - intracavity pulsed laser technique can be used to obtain reliable information about various laser-induced ionic processes. The technique gives rise to improved sensitivity when compared to single- or double- pass experiments; from Fig. 1 it is seen that near threshold the photodissociation process with a cross-section of ca. 3×10^{-20} cm^2 was still able to be monitored.

*Research performed at the National Bureau of Standards, Gaithersburg, Md.

1. J.R. Eyler and G.H. Atkinson, Chem. Phys. Lett., 28, 217 (1974).
2. J.R. Eyler, Rev. Sci. Instrum., 45, 1154 (1974).
3. J.R. Eyler, submitted for publication.
4. R.C. Dunbar, J. Amer. Chem. Soc., 95, 472 (1973).

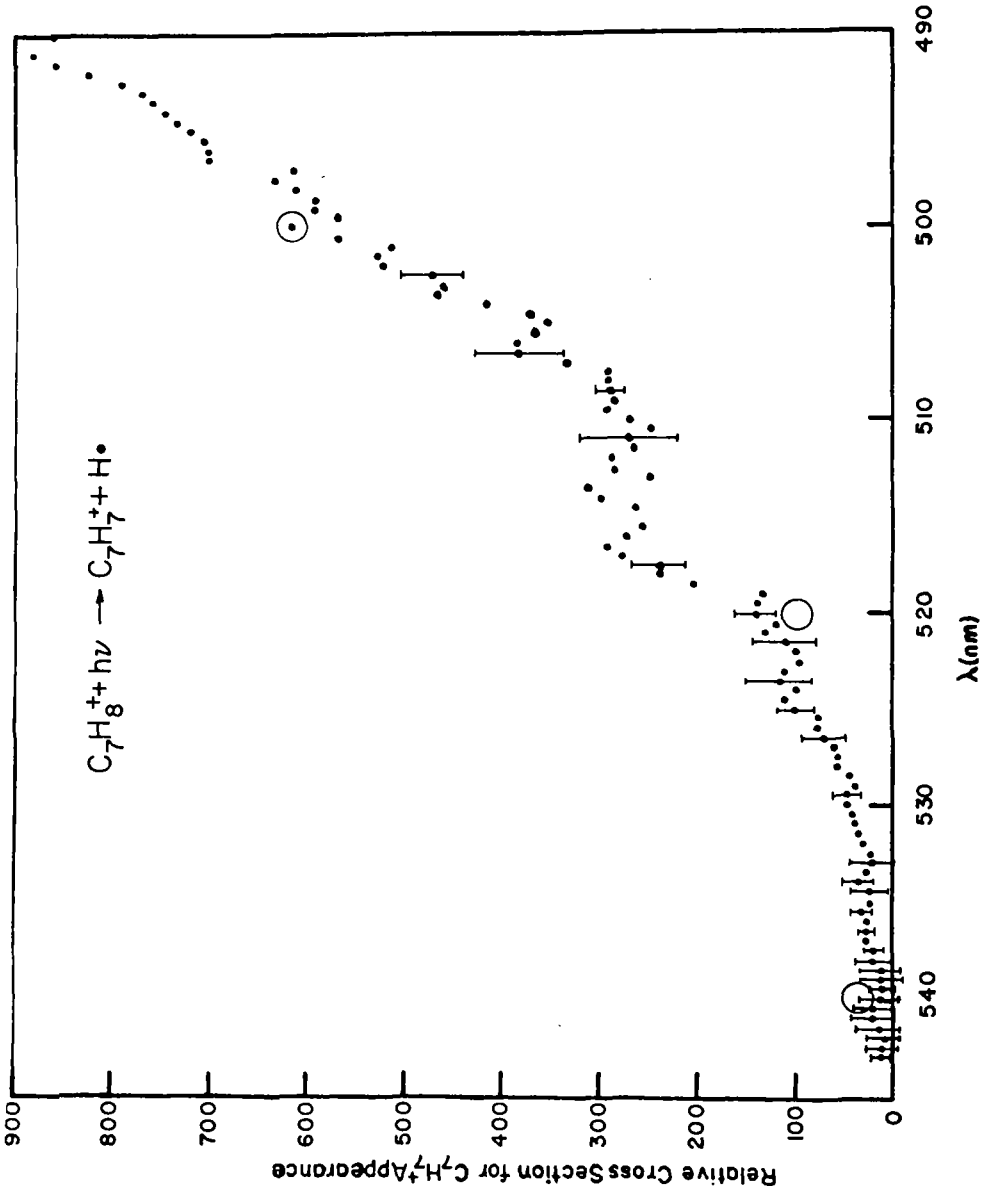
$C_7H_8^+ + h\nu \rightarrow C_7H_7^+ + H\bullet$
Relative Cross Section for $C_7H_7^+$ Appearance
λ(nm)
0
100
200
300
400
500
600
700
800
900
490
500
510
520
530
540

FIGURE 1

APPLICATION OF ATMOSPHERIC PRESSURE IONIZATION TO MONITORING OF ORGANIC CONTAMINANTS IN AIR

D.I. Carroll and Ismet Dzidic,
Baylor College of Medicine
Houston, Texas 77025
and
W.H. McFadden and J.R. Reeher
Finnigan Corporation
Sunnyvale, California 94086

This paper describes an attempt to utilize an API source for direct monitoring of a specific atmospheric contaminant, in this case, acetic anhydride. The ionization source used was of the same basic design as described in previous publications (1,2). A high voltage (2500-2800V) corona discharged produced the ion plasma. Atmospheric air was drawn through the source at a rate of 400 standard cc/min. The API source was retrofitted into a chemical ionization mass spectrometer that had been ruggedized and mounted for mobile operation.

The background spectrum obtained from an API source when normal atmospheric air is monitored is dominated by ionic water clusters (Figure 1). In Figure 1, the most abundant ion is $H(H_2O)_4$, but the intensity distribution of the cluster ions will be changed by water concentration, corona discharge conditions, and temperature.

Sample molecules or trace contaminants present in the discharge compete with the water ions for the available charge on a kinetic basis. The abundance of sample ions thus depends upon the relative proton affinity of the molecule and the relative reaction rates of the competing processes. Consequently, the sensitivity for a specified molecule will depend upon the nature of the environment. Molecules of high proton affinity may dominate the charge distribution and completely eliminate ion current due to other compounds of lower proton affinity.

The most common organic ions observed from an API source are MH^+ and $MH(H_2O)_n^+$, but fragment ions and addition ions can also be formed. The following tabulation of positive ions that can be formed suggests that the spectrum of an unknown must be interpreted cautiously.

1) Background peaks, eg. series of H_2O clusters, NO/H_2O, etc.
2) Molecular ion plus H
3) Molecular ion minus H
4) Molecular ion plus $H(H_2O)_n$ series
5) Molecular ion plus NO or other impurity addition
6) Dimers (P_2 ions)
7) Fragment ions
8) Rearrangement fragments
9) Molecular ion plus fragments

Figure 2 shows the API spectrum of 3-heptanone predominantly due to the $M+H^+$ ion (mass 115). The signal level of 0.87 volts for $3x10^{-9}$ gms/cc of air would give a positive detection of the mass 115 ion at a level 2-3 picograms/sec. Figure 3 gives the API mass spectrum of n-butyl acetate. Ions are observed due to MH^+ and $MH(H_2O)_n^+$ but in addition, significant ion current occurs as the fragment ion $C_4H_9^+$ and the rearrangement ion $CH_3COOH_2^+$. The sensitivity is about one order of magnitude less than that of 3-heptanone. Figure 4 shows an API mass spectrum for cyclohexene. The sensitivity for cyclohexene was about three orders of magnitude less than that of 3-heptanone, but the spectrum showed peaks that can be attributed to MH^+, $M-H^+$, $M-3H^+$ and to H_2O clusters on thes ions. Thus, a mixture of unsaturated hydrocarbons such as may be encountered in some smog conditions could give interfering peaks over a large mass range.

An analytical method for trace amounts of acetic anhydride was developed capable of detecting down to 10^{-12} gms/cc of air (less than 1 ppb v/v). Figure 5 shows a system test in which the mobile API mass spectrometer unit was driven in the test area for 1 hour, allowed to stand for 1 hour about 600 meters up wind from the source site, and then continued to monitor in a stationary mode with acetic anhydride vaporizor in operation. No detection of an acetic anydride plume is observed until the vaporizor is started. The plume "hits" correspond to approximately $2-5x10^{-12}$ gms/cc of air. (Maximum plume concentration calculated: $10-15x10^{-12}$ gms/cc of air).

The above results were typically obtained on consecutive days. Unfortunately, the zero control results are dependant on particular atmospheric conditions and further testing showed that the results were not reliable. An example of extreme interference obtained during a period when auto exhaust emissions were high and wind dispersion minimal is given in Figure 6. (Instrumental conditions same as Figure 5). Such interference suggests that direct monitoring of an uncontrolled environment using an API mass spectrometer system will be very difficult unless a highly specific method can be developed.

1. D.I. Carroll, I. Dzidic, R.N. Stillwell, M.G. Horning, and E.C. Horning, Anal. Chem. 46, 706 (1974).

2. E.C. Horning, M.G. Horning, D.I. Carroll, I. Dzidic, and R.N. Stillwell, Anal. Chem. 45, 936 (1973).

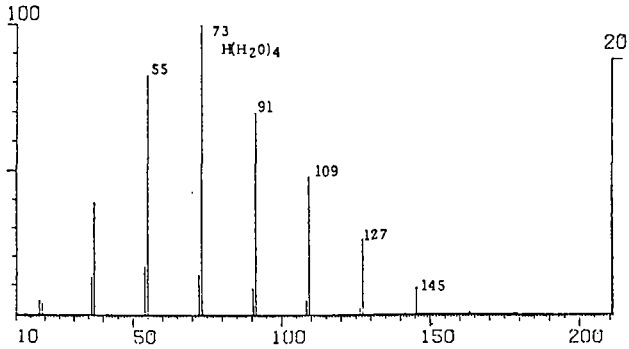

Figure 1. API Background Spectrum of Normal Atmosphere.

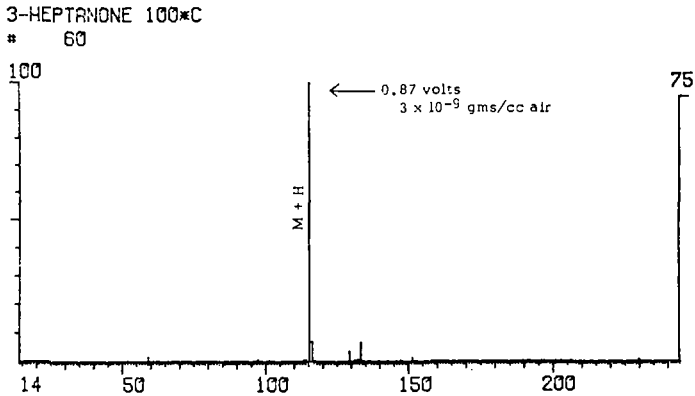

Figure 2. API Spectrum of 3-Heptanone

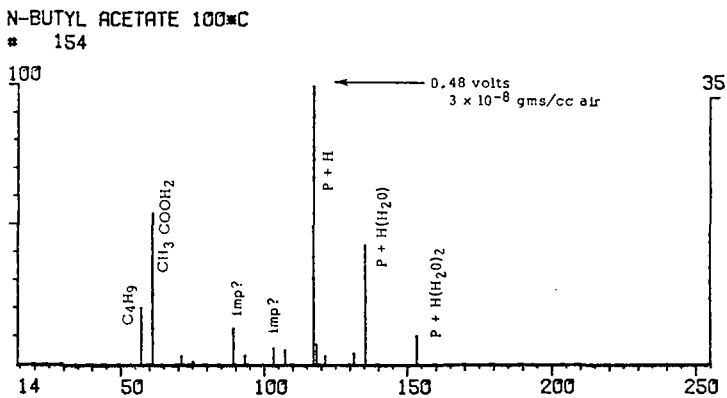

Figure 3. API Spectrum of n-Butyl Acetate

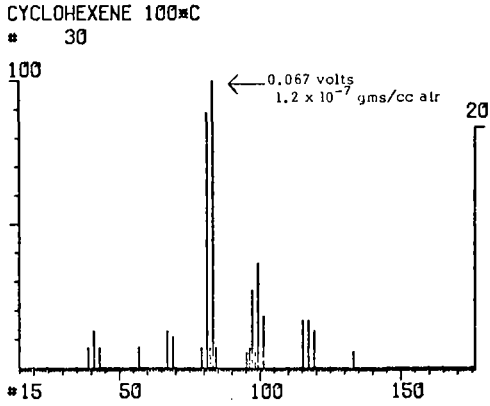

Figure 4. API Spectrum of Cyclohexene

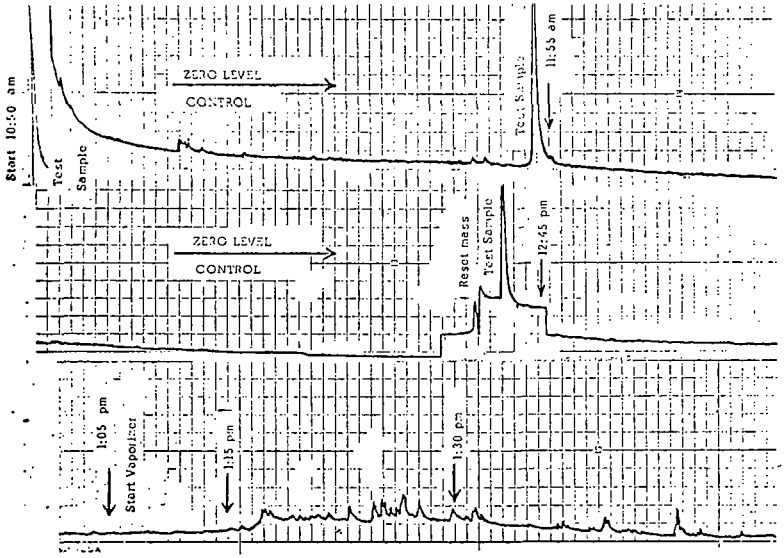

Figure 5. Stationary System Test, 1/3/75. Van parked on Pastoria Ave., 600 meters from source.

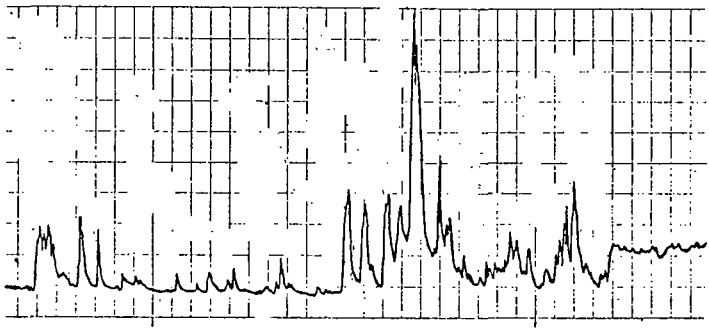

Figure 6. Thirty Minute Section of Background Run
Region of Maude and Pastoria.

DETERMINATION OF CARCINOGENIC POLLUTANTS IN AMBIENT AIR USING A GC- MS- COMPUTER SYSTEM by R. C. LAO, R. S. THOMAS and J. L. MONKMAN, Chemistry Division, Air Pollution Control Directorate, Environmental Canada, Ottawa, Canada, K1A 0H3

Increasing concern about analysis of the organic constituents of polluted air has focussed attention on polycyclic organic matter (POM) because of the carcinogenic potential of many of these compounds. A steadily increasing incidence of lung cancer in industrial and polluted areas has provoked a deep concern about the control of air pollution generally and the identification of sources of contaminants hazardous to health.

In terms of composition al complexity, POM mixtures cover the spectrum of simple to extremely complex. With increasing use of fossil fuels and the growing importance of coal and oil shale, the pyrolysis products of which are a rich blend of aromatic hydrocarbons, raise many environmental and health questions.

Environmental samples may contain POM from many of these sources. This implies that there is a need for analytical techniques which will adequately resolve the numerous POM series from any combustion of fossil fuels.Techniques such as spectrophotometry and GC have been used in determining relatively simple environmental samples. However, these methods alone cannot be used to determine the entire POM fraction on a submicrogram basis and of samples which contain numerous heterocyclic hydrocarbon compounds.

During the past two decades, this laboratory has maintained a major effort to elucidate the measurement of polynuclear aromatic hydrocarbon (PAH) contant in a variety of environmental samples. The development of rapid screening methods without tedious pre-separation and clean-up procedures was seen as necessary to establish straightforward standardized analytical procedures for identification and measurement of the POM in all samples whether from urban atmospheres, engine exhaust, coke oven emission or other environmental sources.

Three years ago, we initiated a programme to develop a rapid and reliable approach to PAH analysis by the application of GC-MS Computer technique. The approach has been adapted to measure PAH in various samples .

Out of 600 odd carcinogens now listed on the toxic substance on the NIOSH listing, only scant attention is given for the mass spectra of a select few individual compounds. We have studied most of the POM by GC-MS system available from our POM standard catalogue. The instrumentation used is a combination of Finnigan 9500 GC-1015D MS and 6000 data system. This is properly calibrated by FC-43 and DFTPP following the standard procedure. Seven of the aromatic nitrogen compounds available from our POM stock were investigated. The chemicals obtained from Koch-Light Laboratories, England were purissima and required no further purification. A small amount of standard compound was dissolved in spectro grade methylene chloride which had been distilled from glass. Of this sample solution, 0.5 microliter was injected into the GC and an average mass

spectrum was obtained from 5 to 10 runs with a standard deviation of 5%. The compounds investigated in this work were:

1. 4-nitrobiphenyl
2. 6,9-dimethyl benzacridine
3. 5,7-dimethyl benzacridine
4. 3,4-benzacridine
5. 6-aminochrysen
6. 1,2,7,8-dibenzcarbazole

and

7. 6,12-diazaanthanthrene

Each of the compounds investigated is a known carcinogen and each has been reported to be present in the environment. The significance of the mass spectra of these compounds is the abundant parent ion peaks and simple fragmentation patterns which readily establish their identity and presence in any sample.

The detailed spectra and analytical procedures will be published in the Journal of Canadian Spectroscopy.

Development of a Cryogenic Separator for CI Analysis of Environmental Air Samples

H. S. Swofford, Jr., I. C. Wang, D. P. Martinsen and S. E. Buttrill, Jr.

Dept. of Chemistry, Univ. of Minnesota
Minneapolis, Minnesota

Cryogenic preconcentration of volatile trace components in air samples is known to be an efficient, although nonselective method of isolation (1). This separation technique has been applied to both gas chromatography and EI mass spectrometry in the past (2-7). Limits of detection reported are nominally at the 1-ppm level with the presence of appreciable water being a serious problem in environmental applications. Since water vapor is trapped coincidently with many volatile compounds, the advantages of cryogenic preconcentration can be exploited in chemical ionization mass spectrometry using water as the CI reagent gas.

The chemical ionization mass spectrometer used in this work was a DuPont 21-490B, 90° magnetic sector, single-focusing, low resolution instrument modified in our laboratory for chemical ionization. These modifications involved 1) the electron production system, 2) the original EI source, and 3) the inlet system. Following the fitting of a high capacity differential pumping station, the instrument was operated at elevated source pressures.

The new gas sample inlet system designed and installed on our instrument is shown in Figure 1. For this work methane gas, which served as a sweep gas and low temperature CI reagent gas, was connected at Valve #1. A 12.3 liter (calibrated) carboy, used as the control environment, was connected at Valve #2. The cryogenic trap was connected between Valves #2 and #3. Valve #4 is connected to system vacuum while Valve #5 is connected to the CI mass spectrometer source.

The cryogenic trap consisted of a Pyrex trap (15.2 cm x 2.54 cm O.D.) with two vacuum valves as shown in Figure 1. Nichrome heating wire was wound around the bottom of the trap, which was previously wrapped with asbestos insulating material. Temperatures were read on a digital voltmeter using a thermocouple embedded in the asbestos; the temperatures were controlled with the aid of a variable transformer connected to the Nichrome wire heater. Cryogenic temperatures were reached using dry ice contained in a dewar surrounding the trap. An individual sample (present at 1 atmosphere in the control environment) was drawn through the trap and frozen out using system vacuum.

Prior to the introduction of a test sample into the control environment, the carboy was first flushed with a nitrogen-water mixture (the water vapor pressure was controlled at water/ice temperature by passing the nitrogen stream through a bubbling tower containing a water/ice mixture) at 1-atmosphere for 3-minutes. A test sample was then injected using a microliter syringe and allowed to equilibrate (10 minutes was found to be optimum). Valves #2 and #4 were then opened and the water vapor, nitrogen gas and sample mixture was pulled through the trap at a flow rate of ~400 ml/min for 1-minute (found to be optimum) using system vacuum.

Following test sample collection in the cryotrap (for a 1.5 ppb injection of ethyl butyrate in the 12.3ℓ control environment withdrawn at a 400 ml/min flow rate for 1-minute, this corresponds to ~3-ng of sample frozen out), valve #2 was closed, the inlet system was pumped down and then opened to the CI source (valve #5), methane gas flow was adjusted (valve #1) to give a source pressure of ~0.2 torr at 120°C and a background spectrum was recorded (see Figure 2) with the cryotrap held at -80°C. The dry ice was then removed from the dewar surrounding the trap and the trap was heated in stages to room temperature. The maximum signal for the M+1 (117) peak in the ethyl butyrate (MW = 116 and chosen as the model "air pollutant") CI mass spectrum was -3°C (see Figure 3).

Low concentrations of ethyl butyrate for injection were prepared by dissolving the test compound (0.02 ml) in methyl alcohol (9.98 ml). A 5-µl injection of this stock solution (after additional dilution x 100) produced a 1.5 ppb concentration of test sample in the test environment (when allowed to volatilize and equilibrate) which we report as our present limit of detection (signal to noise ~2:1). The presence of the methyl alcohol deluant is also noted in the CI mass spectrum.

Further refinements in the cryogenic trap and heater system should produce lower detection limits.

Literature cited

1. Rasmussen, R. A., Amer. Lab. 4, 19 (1972).
2. Tyson, J., and Carle, G. C., Anal. Chem. 46, 610 (1974).
3. Pebler, A., and Hicham, W. M., Anal. Chem. 45, 315 (1973).
4. Schubert, R., Anal. Chem. 44, 2084 (1972).
5. Rasmussen, D. V., Fisher, I. P. and Rowan, J. R., Can. Spectro. 17, 79 (1972).
6. Snyder, R. E., J. Chromatogr. Sci. 9, 638 (1971).
7. Mignano, M. J., Rony, P. R., Grenoble, D., and Purcel, J. E., J. Chromatogr. Sci. 10, 637 (1972).

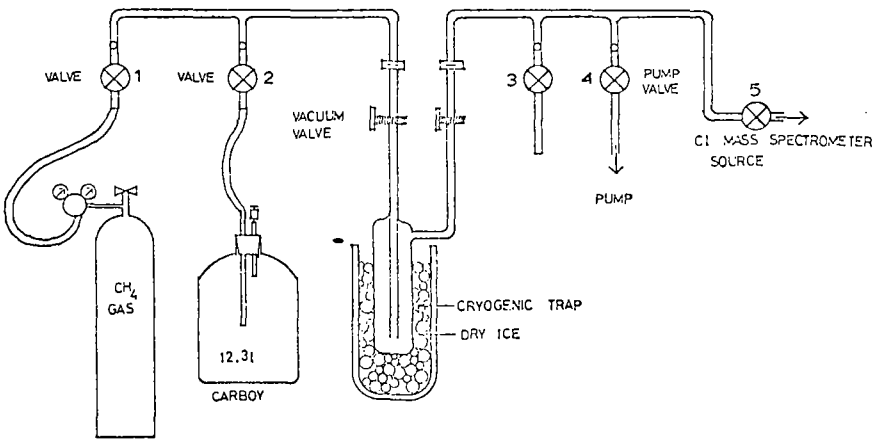

Figure 1. Gas Sample Inlet System

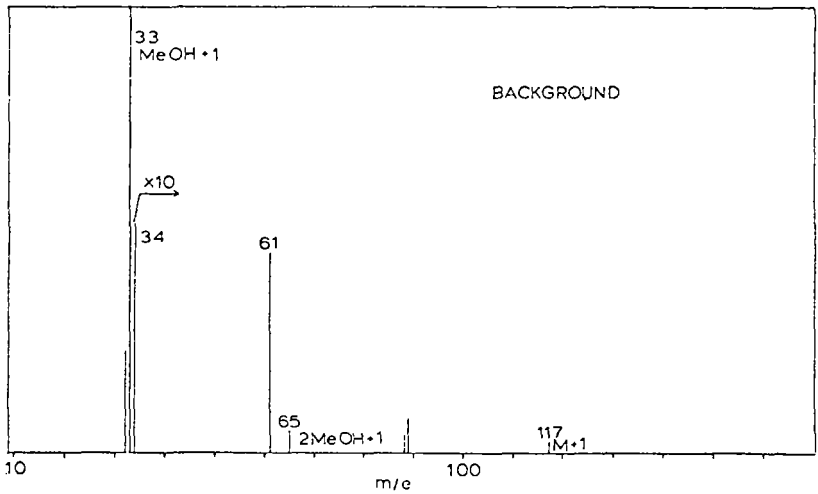

Figure 2. Background CI Mass Spectrum

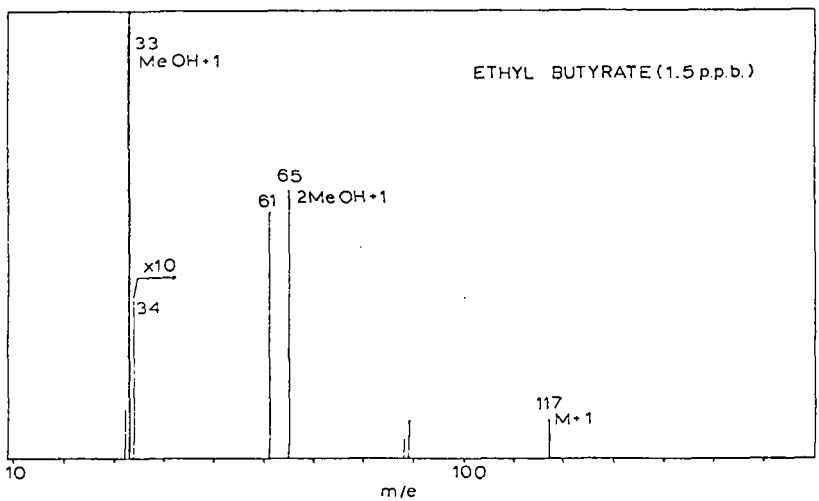

Figure 3. CI Mass Spectrum for Ethyl Butyrate

The Analysis of Halocarbons in the Atmosphere by GC-MS.

E. P. Grimsrud and R. A. Rasmusson, Air Pollut. Res. Div., Col. of Eng., Wash. St. Univ., Pullman, WA 99163

Recent reports suggest that halocarbons in the atmosphere, particularly $CFCl_3$ and CF_2Cl_2, may in the future cause a significant depletion in the ozone content of the stratosphere. The only direct method to be utilized to date for halocarbon analyses is GC with an electron-capture detector. While this method has proved to be adequately sensitive to $CFCl_3$, CCl_4, CH_3CCl_3 and other highly chlorinated molecules, its lack of sensitivity to other simple halocarbons, often including CF_2Cl_2, has severely limited its use for the accurate determination of these compounds in non-urban air masses.

We wish to report an investigation of the use of a GC directly linked (no separator) to a mass spectrometer equipped with high-speed pumping and operating in the single-ion mode for the quantitative analysis of $CFCl_3$, CF_2Cl_2 and other simple halocarbons thought to be possibly present in background rural air. Samples contained in pressurized stainless steel cans were flushed through a 20-ml sample loop. The loop valve was then switched so that the carrier gas (helium, 10 ml/min) swept the contents of the loop onto the head of the GC column (20-ft x 1/16 in stainless steel Durapak n-octane/Porasil c, 100-120 mesh) held at -60°. Three minutes later, after the nitrogen and oxygen had passed through the column, the oven temperature was temperature programmed from -60 to 100° C at 32°/min. The mass spectrometer was set manually to monitor the nominal mass (or masses) characteristic of a sought-for halocarbon during its known GC retention period.

A summary of the results obtained from the application of the above procedure to an analysis of background (rural and aircraft sampling) air of southeastern Washington State is given in Table I. The detection limit of the method is estimated to be 5 parts per trillion (v/v) or about 0.5 picograms in the 20-ml samples. The two chlorofluorocarbons and five chlorocarbons were found in concentrations above the detection limit. Of these, methyl chloride had been previously unreported as a trace halocarbon in the atmosphere even though its concentration is the greatest. These data indicate that the chlorofluorocarbons carry a smaller portion of the organic chloride in the troposphere than do chlorocarbons. In assessing significance of these data as related to the stratospheric ozone question, the obvious question is what are the sources of the chlorocarbons?

Another interesting result of the GC-MS air analyses is that the concentration of CF_2Cl_2 was found to be much higher (230 ± 10 ppt) than previously expected. Earlier studies by others using the electron-capture detector reported estimates of CF_2Cl_2 to be only slightly above 100 ppt. Considering demonstrated detection levels for CF_2Cl_2 and the inherent simplicity of electron-impact mass spectrometry versus the electron-capture detector, we are hesitant to regard the higher value reported here as being in error (even though 230 ppt of CF_2Cl_2 appears to exceed "reasonable" estimates of CF_2Cl_2 concentration based on reported total production amounts diluted into the total troposphere).

The GC-MS method offers an independent check of the accuracy of the calibration methods used. It was found that relative sensitivity factors for different compounds could be obtained simply from the mass spectra of equimolar mixtures of pure materials. This valuable addition to these

ppt. level analyses is possible only because the entire GC effluent enters the ion source. A more complete description of this work is given elsewhere.[1,2]

The high sensitivity reported here represents an invasion by mass spectrometry of an analytical domain previously held solely by the electron-capture detector. It should be recognized, however, that our analog system is operating on the fringe of its detection capability and its performance is, therefore, annoyingly dependent on the quality of the electron multiplier. The use of an ion-counting detection system is, therefore, suggested to remove this dependence and also to attain still improved signal-to-noise ratios during analyses.

1 & 2. Atmos. Environ., E. P. Grimsrud and R. A. Rasmussen. In Press (two articles).

TABLE I. Halocarbons Sought in the Atmosphere of the Rural Northwest (Dec. 1974 to Feb. 1975).

Halocarbon	Conc. (ppt)
Dichlorodifluoromethane	230 ± 10
Fluorotrichloromethane	128 ± 8
Methyl chloride	530 ± 30
Dichloromethane	< 5
Chloroform	20 ± 10
Carbon tetrachloride (by ECD)	120 ± 15
Ethyl chloride	< 5
1,1- and 1,2-dichloroethane	< 5
1,1,2-trichloroethane	< 5
1,1,1-trichloroethane	100 ± 15
Vinyl Chloride	< 5
cis, *trans* and 1,1-dichloroethylene	< 5
Trichloroethylene	< 5
Tetrachloroethylene	20 ± 10
Methyl bromide	< 5
Methyl iodide	< 5

GC/MS Techniques, Including Interscan Display, in the Analysis of Trace Contaminants in Great Lakes Fish

by

Douglas W. Kuehl
Gilman D. Veith
Gary E. Glass

U.S. Environmental Protection Agency
National Water Quality Laboratory
6201 Congdon Blvd
Duluth MN 55804

Advances in methodology of tissue residue analysis of environmental samples at the National Water Quality Laboratory were presented at the 1974 ASMS meeting. This work centered around the lowering of compound detection levels and was based upon two points. The first was an improvement in the GC/MS interface system[1] and the second an improvement in tissue clean-up procedures designed specifically for GC/MS analysis[2]. The combination of these two developments allowed the possibility of analysis of hazardous synthetic organics at sub ng/gm concentrations in fish tissue.

This paper presents two additional instrumental advances that allow for rapid analysis of residues. The first is the development of software for a Varian MAT spectrosystem 100 MS data system to allow interscan spectrum display on a Tetronix 611 scope[3]. A time-based spectrum is automatically displayed on the scope at the end of a scan and held until the completion of the next scan. This feature allows an immediate evaluation of the quality of a GC/MS run. Another improvement is the addition of a second computer to our existing MS data system. The original computer, a 12K Varian Data System 620-i serves as the acquisition computer and is equipped with a magnetic tape drive unit for data storage and a Tetronix 611 scope for the interscan display. Software has been developed to transfer the data from the acquisition computer to the data processing computer, a 16K Varian Data System 620-L-100, with mass conversion. The processing computer is equipped with a magnetic tape drive unit for permanent storage of mass converted data, high speed peripherals for data handling and a phone modem for automated spectrum library searching. This system has allowed up to 10,000 spectra to be gathered and processed per week.

An interesting series of polychlorinated compounds have been isolated and tentatively identified using these new techniques during a study of Great Lakes fish. The series is believed to be polychlorinated phenylphenols which may arise from the metabolism of polychlorinated biphenyls or the use of chlorinated phenylphenols as pesticides in the watershed. The five, six and seven chloro isomers have been identified in various species of fish from all of the Great Lakes.

A comparison of residues of the Great Lakes fish show that only Lake Ontario fish contain a $C_{10}Cl_{12}$ chlorocarbon. This compound has been used as a pesticide, Mirex®, as a flame retardant and has been found to be carcinogenic.

Also, during the study of Great Lakes fish an octachloro compound was observed at the same retention time in the Lake Huron, Lake Ontario and Lower Detroit River (Lake Erie) fish extracts. This compound was confirmed as octachlorostyrene (OCS) by comparison of mass spectra and GC retention time to a synthesized standard[4]. OCS has a relative retention time to aldrin of 1.29 and to p,p'-DDE of 0.67 on a six-foot, three percent OV-101 glass column operated at 180°C with a column flow of 20 ml/min. A series of hepta and hexachlorostyrenes have also been identified. Work will continue on the quantitation of OCS and the determination of its source of origin.

1. Kuehl, D.W., Glass, G.E., and Puglisi, F.A., Anal. Chem. 46, 804 (1974).
2. Veith, G.D., Kuehl, D.W., and Rosenthal, J., JAOAC, 58, 1 (1975).
3. The authors wish to acknowledge the programming contribution of Mr. M. Schmidt of Varian MAT.
4. Kuehl, D.W., Kopperman, H.K., Veith, G.D., and Glass, G.E., "Isolation and Identification of Polychlorinated Styrenes in Great Lakes Fish", submitted for publication.

Identification of Plant Metabolites of "Vydate" Oxamyl Insecticide/Nematicide by Mass Spectrometry

By Robert W. Reiser and John Harvey, Jr.
Biochemicals Department
Research Division
E. I. du Pont de Nemours and Co., Inc.
Wilmington, Delaware 19898

Figure 1 shows the mass spectrum of oxamyl, which is the active ingredient in Du Pont's "Vydate" L oxamyl insecticide/nematicide. "Vydate" is currently registered in the United States for use on tobacco and ornamentals.

Highly polar metabolites of oxamyl are obtained in tobacco and peanut plants. These polar metabolites were purified by liquid chromatography and identified by GC/MS analyses of their T.M.S. derivatives. For metabolism studies, oxamyl was labeled with ^{14}C in the position shown with an asterisk in Figure 1.

The first step in the metabolism of oxamyl is hydrolysis to form the oxime, whose spectrum is shown in Figure 2. By about 1 month after treatment of the plants, the oxime is completely metabolized to more polar compounds.

The gas chromatogram of the T.M.S. derivative of the major polar metabolite from tobacco plants is shown in Figure 3. The mass spectrum of the metabolite peak is shown in Figure 4. The molecular ion is extremely weak, but a significant M-CH_3 fragment is obtained. The fragments marked "s" are characteristic of T.M.S. sugars. The base peak at m/e 72 is due to the dimethylcarbamoyl fragment. An unusual fragment ion was obtained at m/e 234 due to rearrangement of a T.M.S. group back onto the oxime. The identity of the 234 and 72 ions were confirmed by high-resolution mass measurements. These data led to the identification of the metabolite as the glucose conjugate of the oxime - Figure 5 shows the structure. This compound was synthesized, and the GC retention time and mass spectrum of the synthetic compound were identical to those of the isolated metabolite.

This same polar metabolite was also identified by GC/MS in extracts of peanut plants. In addition, liquid chromatographic analyses showed the presence of a second ^{14}C-containing polar metabolite in the peanut plant extract. This second metabolite was isolated by LC, and the T.M.S. derivative was analyzed by GC/MS. Figure 6 shows the gas chromatogram obtained. The other components in the sample are mainly T.M.S. derivatives of various sugars from peanut plants. Figure 7 shows the mass spectrum of the metabolite peak. It was identified as the N'-demethylated structure shown in the figure. This identification was also confirmed by synthesis.

Additionally, we prepared the trifluoroacetyl (TFA) derivatives of these compounds using the synthetic samples. These derivatives eluted from the GC several minutes earlier than the T.M.S. derivatives, and their mass spectra showed significant molecular ions (rel. int. ~ 2%). In view of the increased volatility and more easily interpretable spectra, it appears that the TFA derivatives would be preferred over the T.M.S. derivatives for identification of unknown sugar conjugates.

A more detailed presentation of this work will be submitted to J. Agr. & Food Chem.

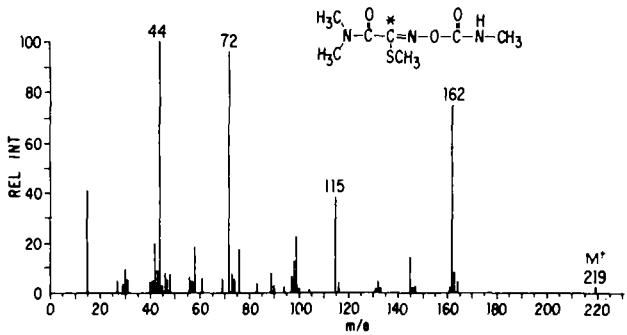

FIGURE 1 MASS SPECTRUM OF OXAMYL (DIRECT PROBE)

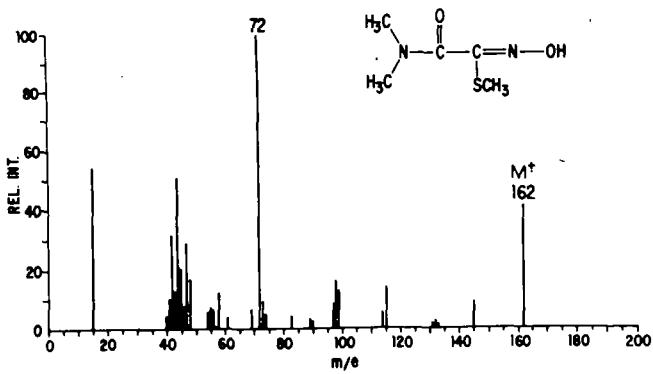

FIGURE 2 MASS SPECTRUM OF OXAMYL METABOLITE

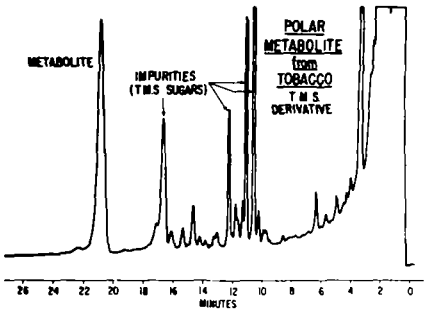

FIGURE 3

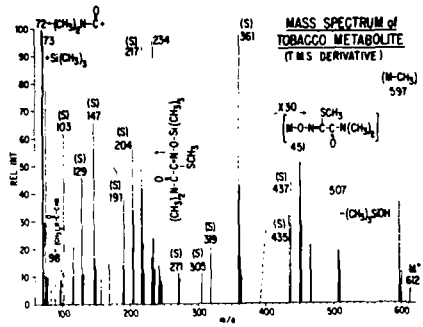

FIGURE 4

POLAR PLANT METABOLITE OF OXAMYL

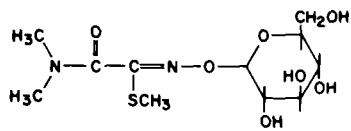

FIGURE 5

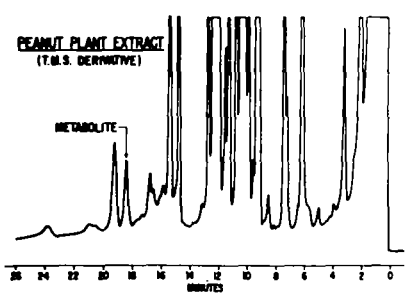

FIGURE 6

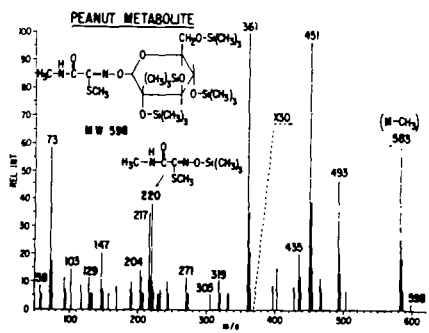

FIGURE 7

NEGATIVE CHEMICAL IONIZATION MASS SPECTROMETRY SCREENING FOR ENVIRONMENTAL CONTAMINATION: APPLICATION TO HUMAN URINES

Ralph C. Dougherty and Krystyna Piotrowska

Department of Chemistry
Florida State University
Tallahassee, Florida 32306

A screening procedure based on negative chemical ionization mass spectrometry has been developed for organochlorine pesticides and related compounds with masses greater than 130 daltons. A limited survey of human urines indicated extensive contamination of the subjects studied at ppb and higher levels with pentachlorophenol, polychlorophenoxy acids and numerous unknown compounds. In an attempt to define the source of the contamination the screening procedure was applied to samples of environmental substrates. The results suggest the food chain as one significant source of the contamination. A preliminary study of mutagenic organochlorine compounds in human seminal fluid suggests that this area may merit additional monitoring.

This paper has been submitted for publication in Science.

A NEW DEVICE FOR THE VAPOR PHASE TRANSFER OF ADSORBED ORGANICS DIRECTLY FROM AN ADSORBENT TO A GAS CHROMATOGRAPH-MASS SPECTROMETER

Woodfin V. Ligon, Jr. and Robert L. Johnson, Jr.

General Electric Corporate Research & Development

Schenectady, New York 12301

ABSTRACT

We will describe a device which provides a means for rapidly and quantitatively transferring adsorbed organics from an adsorbent to the head of a gc column. The device consists of a probe designed for holding a conventional adsorbent tube and a heated barrel into which the probe and enclosed tube are inserted. The device provides rapid sample exchange since demounting or cooling of the heated region is not necessary and it also causes minimum disturbance of the normal carrier gas flow. In addition air is automatically flushed from the system as the probe is inserted preventing its reaching the mass spectrometer. The device has been used for the transfer of materials as diverse as 4,4'-isopropylidenediphenol (BPA) and permanent gases. A linear relationship has been obtained for transfer of samples of phenol in the 1-5 μg range. A schematic of the device appears in Figure 1.

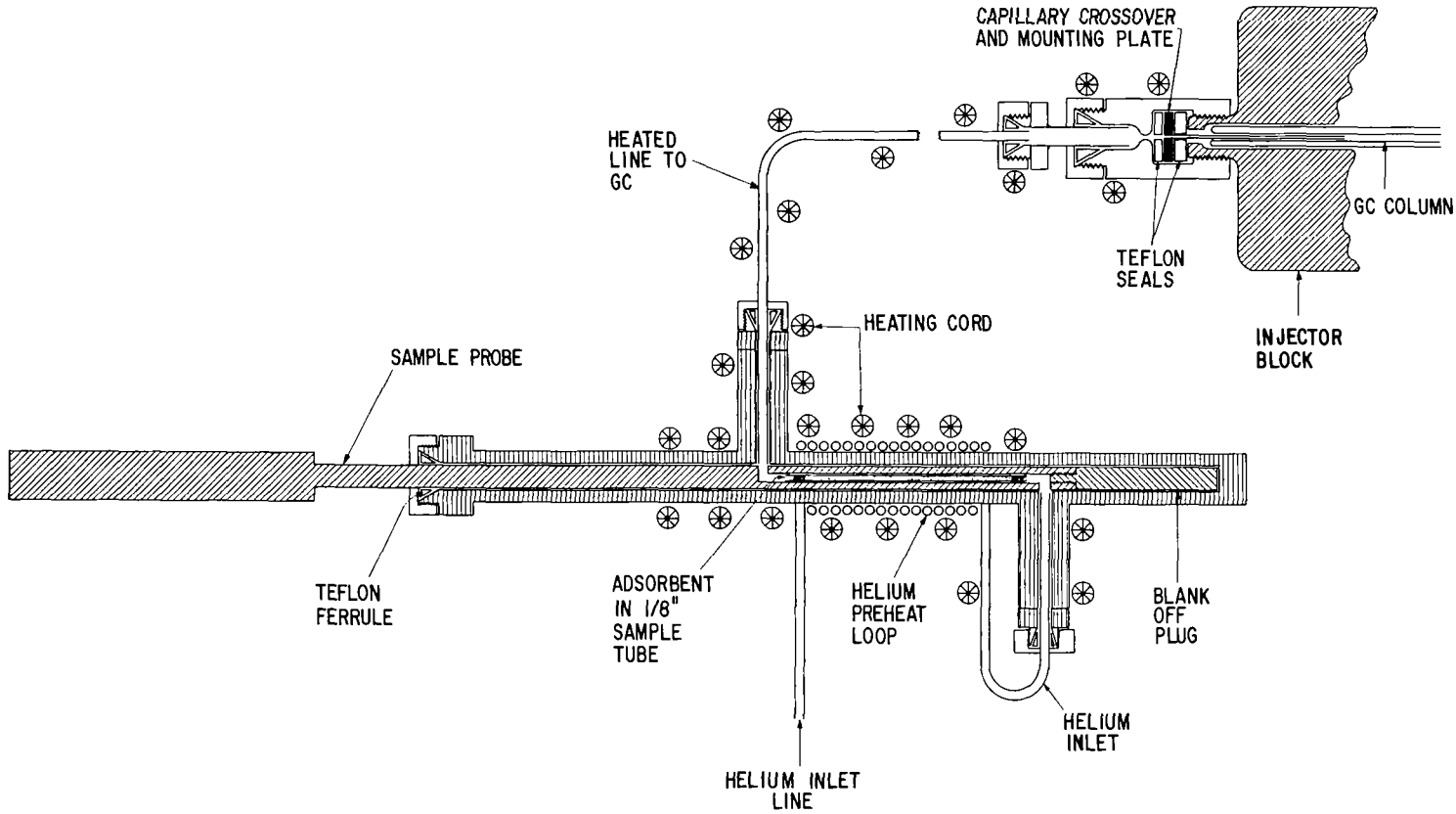

Figure 1. Thermal Desorption Device

Characterization of Polycyclic Aromatic Hydrocarbons in Diffusion Flames by GC/MS

Ping-Huang Lin and Ronald A. Hites
Department of Chemical Engineering
Massachusetts Institute of Technology
Cambridge, Massachusetts 02139

Polycyclic aromatic hydrocarbons (PCAH) have received considerable attention because of the carcinogenic nature of certain members of this class (1). Incomplete combustion, associated with soot formation, is one of the most prominent sources of PCAH in the air; however, the formation mechanism of PCAH in such processes is not fully understood. As a first step in elucidating this mechanism we are obtaining detailed identifications of the PCAH produced in several well-defined diffusion flames using GC/MS.

A Perkin-Elmer model 990 gas chromatograph coupled via a Watson-Biemann type separator to an Hitachi Perkin-Elmer RMU-6L, single focusing, magnetically scanning mass spectrometer has been used for this study. In general, soot and organic matter were collected on a water-cooled stainless surface or with a water-spray sampling probe (2) held in a one atmosphere methane, alkane, or kerosene -air diffusion flame. The deposit coated crucible or filter (containing ca. 100 mg soot) was placed into an ultrasonic bath and extracted with 150 ml Nanograde methylene chloride. The extract was filtered and concentrated by evaporation at reduced pressure, and a 2 µl aliquot was injected into the GC/MS system. The mixture of PCAH was separated on a OV-17 GC column, and components were identified by mass spectrometry and GC retention times. A typical GC of an extract from a methane-air diffusion flame is shown in following figure.

In summary, we have concluded: First, vastly different fuels and flame conditions give very similar product distributions; therefore, acetylene may act as a key intermediate in all cases. Second, PCAH species with 5-member rings (AN, 45MP, and BAN) are abundant in flames but not in air particulates (3), thus these compounds may be readily decomposed in the atmosphere.

This work is supported by the Environmental Protection Agency (grant number R803242).

References

1. National Academy of Sciences, "Particulate Polycyclic Organic Matter," Washington, D.C., 1972.
2. G. P. Prado, M.I.T. (1975), private communication.
3. R. C. Lao, et al., Anal. Chem., 45, 908 (1973).
4. L. Wallcave, et al., Environ. Sci. Tech., 9, 143 (1975).

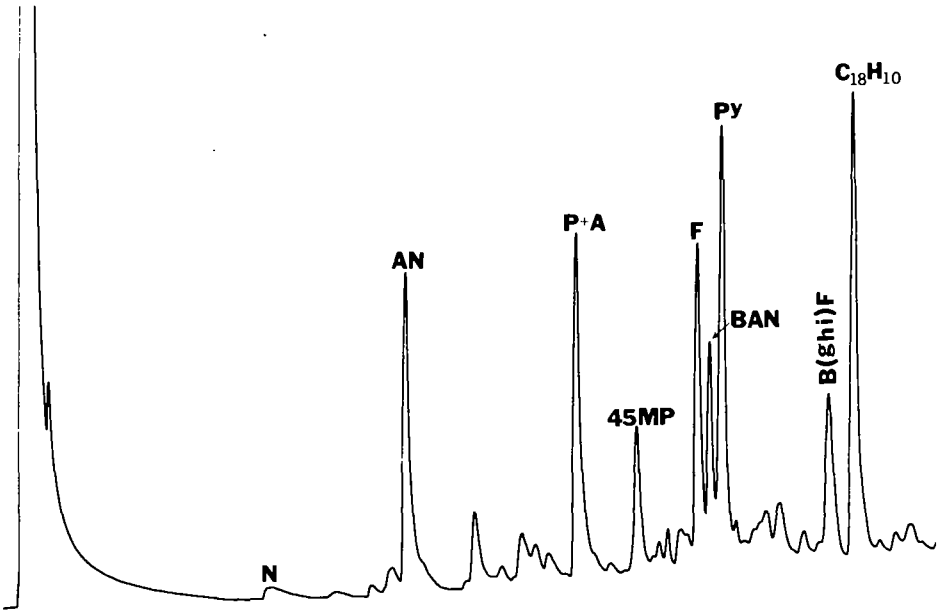

Figure:

Typical gas chromatogram of an extract of PCAH produced in a methane-air diffusion flame. GC Column: 3% OV-17 on 100/120 mesh Gas-Chrom Q, 5 ft. x 1/8 in. OD. Temperature: 70° to 250° at 12°/min. Abbreviations: N, naphthalene; AN, acenaphthylene; P+A, phenanthrene and anthracene; 45MP, 4,5-methylenephenanthrene; F, fluoranthene; BAN, benzo[d or e] acenaphthylene; Py, pyrene; B(ghi)F, benzo[ghi]fluoranthene. The peak labeled $C_{18}H_{10}$ may be cyclopenta(c,d)pyrene (4).

DETERMINATION OF TETRACHLORODIBENZO-p-DIOXIN IN CHEMICAL AND ENVIRONMENTAL MATRICES

M. L. Taylor*, B. M. Hughes*, T. O. Tiernan*, R. L. C. Wu*, and D. T. Terwilliger*

Aerospace Research Laboratories (LJ)
Wright-Patterson AFB, Ohio 45433

The potent toxicity of 2,3,7,8-tetrachlorodibenzo-p-dioxin(2,3,7,8-TCDD)

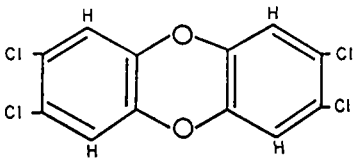

2,3,7,8-TETRACHLORODIBENZO-p-DIOXIN

has been described in recent review articles (1.2). The awesome LD_{50} of this compound in guinea pigs - 0.6 μg 2,3,7,8-TCDD per kilogram of body weight - together with its embryotoxic and acnegenic properties has prompted great concern in certain sectors of the scientific community. Some chlorophenoxy herbicides containing or derived from 2,4,5-trichlorophenol have been found to contain traces of 2,3,7,8-TCDD most probably because contaminated 2,4,5-trichlorophenol was used in the synthesis of the herbicide constituents. Because of the potent toxicity of 2,3,7,8-TCDD, use of certain chlorophenoxy herbicide formulations for defoliant purposes was abruptly discontinued by the Department of Defense late in the 1960's. Several thousands of barrels of the herbicide are now in storage pending a decision whether to reclaim the material or destroy it. In our laboratory the need to determine the levels of 2,3,7,8-TCDD in large numbers of herbicide samples prompted the development of an automated gas chromatograph quadrupole mass spectrometer (GC-QMS) system which was used in conjunction with a simple, rapid sample preparation method. Furthermore, in order to assay soil samples for 2,3,7,8-TCDD, an ultrasensitive analytical mass spectrometric method was devised and implemented. These two analytical mass spectrometric techniques are summarized in the sections following.

Method for Determining 2,3,7,8-TCDD in Chlorophenoxy Herbicides

An automated system capable of unattended operation for periods up to 24 hrs. was designed and assembled in our laboratory. The system, shown schematically in Fig. 1, includes the following:

A Varian 2740 Gas Chromatograph equipped with a Varian Model 8000 Autosampler, flame ionization detector, and special switching manifold†.

An Extranuclear Quadrupole Mass Spectrometer housed in a 6" stainless steel "T" fitted with a Teflon collar to permit differential pumping of the source and analyzer regions which were pumped respectively by a Bendix PMV-100 6" Oil diffusion pump and a Varian/NCR 161-2 4" oil diffusion pump. No helium separator was required - the effluent from the gas chromatograph (when carrier gas flows of up to 30 cc/min were used) was routed directly into the mass spectrometer source.

The instrumental conditions for analysis were as follows:

Gas Chromatography
Column-6' x 1/8" glass coiled column packed with 10% OV-17 on Chromosorb W/HP
Carrier gas-Helium at 30 cc/min.
Temperatures-Injection Port, 240°
Column, 240°
FID, 240°
Transfer line into mass spectrometer, 310°

Mass spectrometer
Ionizing voltage, 23 eV
Multiplier voltage, 3500 V
Source envelope pressure, 2.3×10^{-4} torr
Analyzer pressure, 3.5×10^{-6} torr

Selected ion monitoring was used in these studies; i.e., the mass spectrometer was tuned to monitor either m/e 320 or m/e 322. Data was acquired on a 1 mv strip chart recorder and simultaneously on an Autolab System IV Computing Integrator equipped with an ASR-33 Teletype with punched paper tape accessory. The data on punched paper tape was automatically reduced using a Hewlett-Packard 2116 C minicomputer.

The samples of chlorophenoxy herbicide were prepared for analysis using a simple column chromatographic clean-up procedure which can be completed in about 30 min.† In the automated mode the precision of the overall method is shown by the following:

Number of samples of herbicide: 5
Concentration of 2,3,7,8-TCDD: 0.22 μg/g
% Standard deviation for n = 5: 6.3

The lower limit of 2,3,7,8-TCDD which could be quantitatively determined was 0.02 μg 2,3,7,8-TCDD/g.

Ultratrace Analytical Method for Estimating 2,3,7,8-TCDD in Soil

For determination of picograms/g concentrations of 2,3,7,8-TCDD in soil an AEI Scientific Apparatus, Inc. MS-30 double beam mass spectrometer was employed. The MS-30 was coupled through an AEI silicone membrane separator to a Varian 1400 Gas Chromatograph. Instrumental conditions for the analysis are listed below:

Gas Chromatograph-Column-1.5% OV 101 on Chromosorb G/HP packed in 5' x 1/8" O.D. stainless steel tubing.
Carrier gas - Helium at 60 cc/min.
Temperatures - Injection port, 230°
Column oven, 231°
Separator, 184°

Mass Spectrometer
Selected Ion monitoring - At a resolution of 1000 either m/e 320 or m/e 322 was minitored; data was acquired by routing the multiplier output from the sample beam to a 1 mv strip chart recorder.
Source temperature - 250°
Ionizing Voltage - 70 eV

Soil samples received from the field were kept frozen until just prior to analysis at which time approximately 20 g was allowed to thaw and air dry. Exactly 10 g of dry soil were weighed and extracted as follows:

1. To 10 g of dry soil contained in a 50 ml glass stoppered erlenmeyer flask add 15 ml 20% (V/V) benzene in hexane. Shake for 2 hrs.
2. Decant the organic extract into a 60 mm x 6 mm glass tube, rinse soil with an additional 5 ml of 20% benzene in hexane and concentrate the combined extracts to about 0.5 ml in a stream of air.
3. Transfer the 0.5 ml residue using an additional 0.1 ml 20% benzene in hexane to rinse the glass tube and concentrate to dryness in a 0.1 ml cone-shaped vial.
4. If analysis is to be effected immediately, add 0.1 ml o-Xylene to dissolve the residue. If storage of the sample is necessary, delay addition of the o-Xylene until immediately prior to analysis.

Results of analyses of soil samples are shown in Table 1. The values shown in the table which were obtained at a resolution of 400 were obtained by an independent laboratory.

---

†-The methodology and instrumentation for determining 2,3,7,8-TCDD are described in more detail in a paper which has been submitted to Analytical Chemistry.

*Present Address: Chemistry Department, Wright State University, Dayton, Ohio 45431

ACKNOWLEDGEMENTS

Mr. C. D. Miller is gratefully acknowledged for his assistance in design and fabrication of the GC-QMS. Portions of this study were funded by Air Force Logistics Command.

LITERATURE CITED

1. "Chlorodioxins - Origin and Fate," E. H. Blair, Ed., Advances in Chemistry Series No. 120, American Chemical Society, Washington, D. C., 1973.
2. Environmental Health Perspectives, Experimental Issue No. 5, G. W. Lucier, Ed., DHEW Publication No. (NIH) 74-218, U. S. Department of HEW, USPHS, NIH, Sept., 1973.

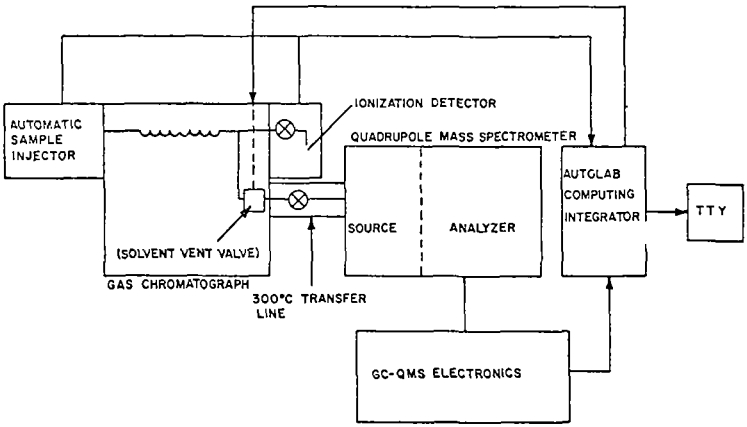

Fig. 1 SCHEMATIC REPRESENTATION OF AUTOMATED GC-QMS SYSTEM

TABLE I

Determination of TCDD in Soil

Sample No.	Mass Spectrometer Resolution	TCDD Found Picograms per gram
A	400	1,100
	1,000	1,549
	10,000	1,241
B	400	1,000
	1,000	1,237
	10,000	1,261
C	400	640
	1,000	262
D	400	810
	1,000	293

Development of Solid Sorbent-Mass Spectrometeric Techniques for Low Level Monitoring of NO and NO_2 in Air

C. Chang*, T. O. Tiernan*, B. M. Hughes*, and M. L. Taylor *

Aerospace Research Laboratories (LJ), Wright-Patterson AFB, Ohio 45433

The National Institute for Occupational Safety and Health (NIOSH) is currently evaluating a work-place air monitoring system which consists of a small sampling tube through which air is drawn from the breathing zone of the individual worker by means of a small belt-mounted pump worn by the individual worker. The tube is fitted with a small removable section containing an appropriate sorbent which quantitatively sorbs the toxic gas(es) of interest. For analysis, the sorbed gases are desorbed from the solid and analyzed at a laboratory remote from the sampling site. We describe here a mass spectrometric method developed for use in studying the quantitative aspects of sorption-desorption phenomena as well as the solid sorbent technique developed for quantifying nitrogen dioxide (NO_2) and nitric oxide (NO) present in air at concentrations at or near the Threshold Limit Value for these materials (1-25ppm).

The mass spectrometer used in these studies was a modified CEC 21-103C instrument which was used in the selected ion monitoring mode. Data was acquired using a IMV strip chart recorder and a Datex DIR-1 Integrator. Gas samples were admitted into the mass spectrometer by means of a special test apparatus which was constructed for these studies. The apparatus is actually a combined gas dilution apparatus and solid sorbent test system. Dilutions of the gas of interest were obtained by metering the gas into a stream of air to achieve the desired concentration which was determined mass spectrometrically by sampling the effluent from the test apparatus through a Granville Phillips Leak. In the case of NO_2, m/e 30 corresponding to NO^+, was monitored as a function of time. Changes in flow or other instrumental parameters were checked by monitoring the intensity of the air peak (actually m/e 29 corresponding to $^{14}N^{15}N^+$). Thus dilutions of NO_2 in the 1-25ppm range were generated and passed through various solid sorbents. By determining the intensity of the m/e 30 signal in the air stream before and after the sorbent, the time course of the sorption process was determined. The amount of NO_2 sorbed was determined by desorbing the gas by heating the sorbent tube to 240°C while purging the tube with air (typically at flow rates on the order of 100 cc/min), while monitoring the NO_2 level in the effluent.

The adsorption of NO_2 on molecular sieve 5A sorbent at ambient temperature was found to be quantitative over the 1-25ppm concentration range. The recovery of NO_2 upon desorption was independent of the amount of NO_2 sampled with accuracy better than 5%. However, it was found that the moisture in ambient air can strongly interfere with the adsorption of NO_2 and consequently cause a substantial loss in the NO_2 recovery. This was remedied by using a P_2O_5 precolumn which quantitatively retains all the moisture from the air sample while allowing NO_2 pass through with negligible loss.

Although NO gas cannot be adsorbed at room temperature by most solid sorbents commonly available it was found that NO in air at concentrations as high as 40 ppm can be quantitatively and catalytically converted to NO_2 and adsorbed on the surface of molecular sieve 5A. The desorption of the NO_2 obtained from this catalytic conversion of NO achieved in the

similar fashion as in the NO_2 analysis with equal accuracy. The differentiation between NO and NO_2 is accomplished by using a precolumn filled with molecular sieve 13 X coated with a solution of triethyleneamine (tea).[1] Extensive tests show that this precolumn can quantitatively adsorb NO_2 while having no effect on NO in the air stream. A complete analysis of NO and NO_2 can be achieved by running parallel experiments where in one case a simple P_2O_5- molecular sieve 5A column is used and in the second a P_2O_5- molecular sieve 5A column attached with a TEA precolumn is employed. After sample collection the analysis of the single column should yield the total amount of NO and NO_2 and the latter one the amount of NO alone. The difference between the two columns is equal to the amount of NO_2 sampled.

A full account of this work will be submitted for publication in the American Industrial Hygiene Association Journal.

* Present Address - Chemistry Department, Wright State University, Dayton, Ohio 45431.

References

1. D. A. Levaggi, W. Sin, and M. Feldstein, J. Air Poll. Control Assoc. 23, 30 (1973).

Quantitative Analysis of the Major Urinary Metabolite of Prostaglandin E in Man by Selected Ion Monitoring. B. J. Sweetman, H. W. Seyberth, J. C. Frolich and J. A. Oates, Department of Pharmacology, Vanderbilt University, Nashville, Tennessee 37232.

Prostaglandins occur in only minute amounts in most tissues and biological fluids. They are metabolized extremely rapidly and their metabolism is complex leading to a variety of compounds.

The prostaglandins and their metabolites have chemical similarities to many other naturally-occurring compounds, and so their isolation from biological samples in a state suitable for analysis by mass spectrometry often requires exhaustive purification.

We have been interested in developing a method similar to that used by Hamberg (Biochem. Biophys. Res. Comm., 49:720 (1972)), based on selected ion monitoring (SIM) to analyze the major urinary metabolite of prostaglandins E_1 and E_2 (7α-hydroxy-5,11-diketotetranorprostane-1,16-dioic acid) (PGE-M), in the hope that such a method might be useful in clinical pharmacology and other areas for assessing changes in total body biosynthesis of prostaglandin E (PGE). The major urinary metabolite represents about 15% of the total body production of PGE.

The derivative used as the basis for the SIM method is the bis-methoxime, bis-methyl ester-TMS ether, formed by reaction of PGE-M, in sequence, with diazomethane in diethyl ether-methanol, 2% methoxyamine hydrochloride in pyridine and bis-trimethylsilyl acetamide in pyridine (1:1). The internal standard-carrier used in this method is the analogous bis-^2H_3C-oxime derivative. This compound was synthesized partially by a chemical synthesis and partially by a biochemical synthesis. Tritiated (5, 6)-PGE_2 was oxidized to the 15-keto compound using activated MnO_2 in $CHCl_3$, and the product was reduced using Rd-C in C_2H_5OH. The resultant 15-keto-tetrahydro compound was infused into a rabbit. Following collection of the urine and purification through a number of steps including methylation, the sample was treated with ^2H_3C-oxime hydrochloride to produce the internal standard, labeled with both tritium and deuterium atoms. For analysis by SIM, 1 μg of this internal standard was added typically to about 1 or 2% of a 24 hr urine collection. Usually, about 10% of the total sample is needed for the analysis by SIM (duplicate injections within ± 5%). The purification scheme for urine samples is lengthy and involves adjustment of urine to pH4, chromatography on XAD-2, methylation, methoxime formation, extraction by diethyl ether, addition of internal standard, reversed phase partition chromatography, thin-layer chromatography and formation of the TMS ether.

Analysis by SIM was performed using an LKB-900 GC-MS instrument, interfaced with a PDP-12A computer. In the SIM mode, one power supply is programmable - so that when the correct values of the accelerating voltage (ca. 3.5 kV) corresponding to the ions-of-interest are established, the computer cycles the accelerating voltage between the predetermined reference points. Stability of the mass scale is assessed by a voltage scan of a calibration compound about once per hour and, if needed, appropriate adjustment of the accelerating voltage is made. Routinely, the magnet is kept at the required value for the analysis overnight prior to the run. When this is done, magnetic field drift does not represent a major problem.

The mass spectrum of derivatized PGE-M has two intense ions at m/e 455 and m/e 365 - due respectively to loss of - OCH_3 (methoxime) alone or together with loss of trimethylsilanol. The mass spectrum of the hexa-deutero internal standard has corresponding ions at m/e 458 and 368, the formation of these involving loss of one of the - OCD_3 groups. We routinely use the m/e 365/368 pair for analysis but the m/e 455/458 pair can also be used, with a little less sensitivity, but, in general, with slightly higher specificity. Linear standard curves were obtained for either ion pair for protium form/deuterium form ion ratios between 0.01 and 1.0. There was an excellent correlation for SIM analyses on levels of PGE-M found in urine samples between the two ion pairs.

For a group of normal females (n=9), output of PGE-M in urine was 3.42 ± 1.36 μg/24 hr (range 1.18 - 5.20), while in a group of normal males (n=14), the corresponding output of PGE-M was 15.67 ± 8.17 μg/24 hr (range 6.74 - 30.41). These results are in excellent agreement with the results of Hamberg (loc. cit.) for normal Swedish groups.

This SIM method for PGE-M is being used in many on-going studies in our laboratory in the area of clinical pharmacology, including the effects of various drugs on PGE production, fatty-acid precursor feeding experiments, PGE production in pathological states and in response to various physiological stimuli. The method has been applied to nearly 1000 urine samples, to date, and has shown a high degree of reliability.

We are grateful to Dr. J. Pike, The Upjohn Company, Kalamazoo, Michigan for supplies of PGE_2 and to Mr. Lee Morgan for skillful technical assistance and to Dr. J. Throck Watson for helpful discussions. This work was supported by an NIH Grant, GM-15431.

POLYHYDROXYBUTYRIC ACIDS DETECTED IN URINE EXTRACTS BY GC-MS

J.A. Thompson, P.V. Fennessey and S.P. Markey,
University of Colorado Medical Center,
Department of Pediatrics,
Denver, Colorado

Screening for metabolic disorders by gas chromatographic or gas chromatographic-mass spectrometric (GC-MS) analysis of urinary organic acids involves preliminary isolation and conversion to volatile derivatives. These acids are normally isolated by one or a combination of solvent extraction techniques which require very little time or effort to perform. While these methods are sufficient to detect gross metabolic errors, there are several inherent problems which preclude the use of solvent extraction for the study of more subtle changes in metabolism: (a) Non-acidic compounds, especially urea, are removed and interfere with analysis; (b) the more water-soluble-polyfunctional acids are very inefficiently extracted; and (c) acid recoveries are in general, highly variable.

DEAE-Sephadex anion exchange columns have been successfully employed in several laboratories for the efficient isolation of urinary acids (1,2). Extracts produced in this way are essentially free of non-acidic compounds, but do contain copious amounts of inorganic acids, specifically sulfate and phosphate. These form trimethylsilyl derivatives, and because the concentrations in urine are much higher than the organic acids of interest, large portions of gas chromatograms are obscured. After attempting several methods of eliminating these ions from anion exchange extracts, we selected a barium precipitation procedure as the most successful with regard to selectivity and simplicity (3). An acid standard and a barium hydroxidy solution are added to an aliquot or urine, and the precipitated barium sulfate and phosphate removed by centrifugation. Hydroxylamine is added to the supernatent and this is heated at 60° for 30 min., which affects oxime derivation of keto acids and hydrolyses lactones so that they are not lost during anion exchange. After adjustment to pH 8, the solution is added to a DEAE-Sephadex column in the acetate form, the neutrals and bases are washed out with water, and the acids are eluted with pyridinium acetate. The effluent is lyophylized, a chromatographic standard added, and the residue silylated directly.

Using this procedure, we have been able to identify a series of very water soluble di- and trihydroxybutyric acids by GC-MS. These are the two diastereomers, as well as the 2-deoxy- and 3-deoxytetronics. Glyceric and 2-methylglyceric acids were also identified. To our knowledge, the 4-deoxytetronics and 2-methylglyceric have not previously been reported to be normal urinary constituents. Authentic samples of these 4-carbon acids were synthesized in order to substantiate preliminary identifications and to assign diastereomeric configurations. Standard aqueous solutions of these acids containing the appropriate inorganic ions were extracted by precipitation-anion exchange to determine recoveries. These were high, in the 78% to better than 90% range.

The mass spectrum of the TMS derivative of 4-deoxyerythronic acid is illustrative of some fragmentation pathways of these compounds. A small M-15 peak appears at m/e 321 for the loss of a TMS methyl group. A peak at m/e 292 has been established to be characteristic of 2,3-dihydroxy acid-TMS derivatives (4). The 3-TMS group shifts to the carbonyl oxygen, with elimination of a neutral molecule, in this case, acetaldehyde. A McLafferty rearrangement of the 3-hydrogen results in an ion at m/e 220.

Although lactones are hydrolyzed prior to our extraction procedure, some lactonization reoccurs during a later step, as small amounts were identified by GC-MS. Therefore, lactones were prepared from those acids with a hydroxyl group in the 4-position, and mass spectra of their TMS derivatives recorded for comparison purposes.

Those acids were quantitated in the urine of groups of normal adults and normal newborn infants in their first week of life, by gas chromatography on OV-22. Erythronic and threonic acids are relative major constituents in both urines. Several differences are apparent, including the fact that 2-deoxytetronic acid contributes considerably more to the infant acid content than to the adult. The diastereomeric pair, 4-deoxyerythronic and 4-deoxythreonic acids are obscurred by a large phosphate-TMS peak when barium precipitation is omitted from the extraction procedure. 2-Methylglyceric and 3-deoxytetronic acids are either tract constituents or are undetected in both groups. The technique of GC-mass fragmentography was helpful in locating the latter two acids in the complicated gas chromatogram. Both have an abundant 219 ion. The more concentrated acids could normally be located by monitoring the 321 ion, which is the M-15 ion of the deoxytetronics, and is a weak ion associated with the tetronic acids. Glyceric acid was found to contribute to the GC peak containing 4-deoxyerythronic acid.

GC-chemical ionization MS with methane as the reagent gas did not produce M+H ions of insufficient intensity to be of diagnostic value in dilute solutions. Fragmentation to M-15 and M+H-TMSOH ions was prominent in the case of the TMS derivative of 2-deoxytetronic acid. With isobutane as the reagent gas, the M+H ion corresponded to 12% of the total ionization of this acid. GC-chemical ionization mass fragmentography of an adult urine extract demonstrated the value of C.I. analyses of TMS-acids. All five of the deoxytetronics are clearly demonstrated when m/e 337 (M+H) is monitored. Similarly, both tetronics show up at m/e 425 (M+H), and glyceric at m/e 323 (M+H).

References:

1. E.C. Horning and M.G. Horning, J. Chromatog. Sci., 9, 129 (1971).
2. F.A. Chalmers and R.W.E. Watts, Analyst, 97, 958 (1972).
3. J.A. Thompson and S.P. Markey, Anal. Chem., 47, 1313 (1975).
4. G. Petersson, Tetrahedron, 26, 3413 (1970).

Molecular Weight Profiles of Carboxylic Acids in Urine Obtained by Field Ionization Mass Spectrometry and Their Clinical Applications, Robert L. Dyer, Martin E. Scolnick, Russell R. Sperry, and Michael Anbar, Stanford Research Institute, Mass Spectrometry Research Center, Menlo Park, CA 94025.

The nonfragmenting nature of field ionization mass spectrometry lends itself ideally to the analysis of complex mixtures with minimal pretreatment. We have applied this technique to crude urine extracts (pH = 9 following removal of urea by urease) and the spectra, obtained using an Extranuclear Model 270-9, 3/8-inch quadrupole mass analyzer, are highly informative (Figure 1) and reproducible. However, the variability between the urines of different individuals is very high and only by analysis of many samples from normal and "abnormal" individuals may a diagnostic pattern be established. Such was the case for a series of non-fasting and fasting subjects examined by us in collaboration with Drs. Pauling and Robinson. In the same study, a series of multiple sclerosis patients was examined and indications for a diagnostic pattern have been found.

Hoping to obtain less biologically "noisy" results, we have analyzed a single family of metabolites in urine, namely carboxylic acids. These were separated by acid extraction (pH = 1) of all neutral and acid constituents from urine (which were first freed of urea by treatment with urease) into ethyl acetate. The carboxylic acids were then extracted back into the aqueous phase at pH = 9 (bicarbonate) and the back and forth extraction procedure was repeated twice to ensure complete removal of all non-acidic constituents as well as those with pH < 1. The last extraction was with ethyl acetate to facilitate easy removal of the solvent without loss of acids.

The molecular weight profiles obtained contain a large number of constituents (Figure 2) and the extraction technique and mass analysis are highly reproducible (Figure 3). Still there is considerable redundancy in these spectra due to the existence of isomers and isobars sharing the same nominal mass number. This problem is presently being alleviated by collisional fragmentation of the mass separated ions and before long we hope to be able to identify the chemical nature of each constituent. The individual variability is still very high among normal subjects and even higher between pooled morning and evening urines of the same subjects. It seems that even after separation of a single family of metabolites, there is still the need for dozens of samples to establish new diagnostic procedures based on multi-component analysis. Field ionization mass spectrometry offers a preferred analytical method for this purpose, being reproducible, highly sensitive (a complete analysis of a multicomponent analysis can be carried out on a few μg samples), having a wide dynamic range (about four orders of magnitude--allowing routine determination of constituents present in the sample in an amount of 1 nmole

with 10% precision). It is universal (unlike chromatographic techniques, the mass peak assignment is not dependent on the instrumentation used) and reasonably rapid (a complete multi-component analysis can be carried out in 15 to 20 minutes). It also does not require elaborate pretreatment and derivatization which limit the reproducibility of other procedures, and it produces meaningful results--the constituents of a pathological *urine can be identified by molecular weight and their structures* determined by secondary collisional fragmentation.

In short, if multicomponent analysis of biological fluids will prove to have significant clinical diagnostic value, field ionization mass spectrometry, which can reproducibly handle more samples than competing analytical methods, will undoubtedly be the method of choice to establish meaningful diagnostic patterns.

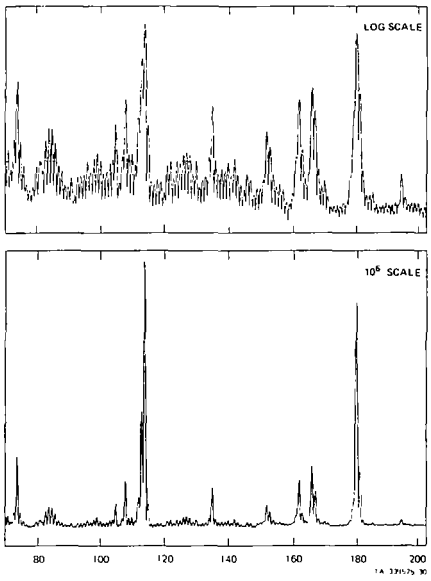

FIGURE 1 INTEGRATED MASS SPECTRUM OF HUMAN URINE
Two aliquots from same sample

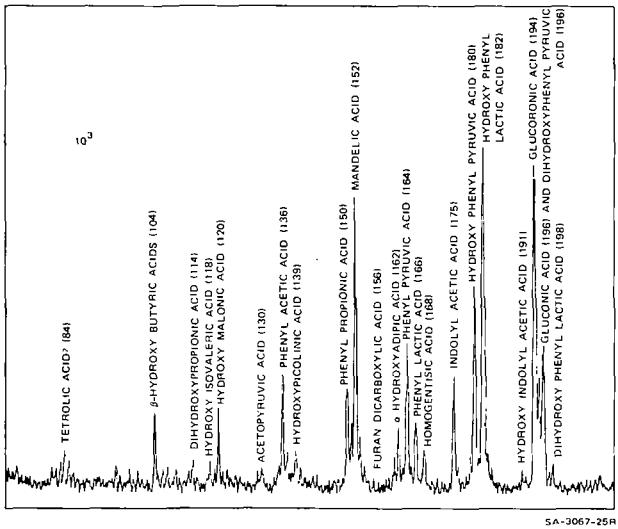

FIGURE 2 CARBOXYLIC ACIDS EXTRACTED FROM NORMAL HUMAN URINE

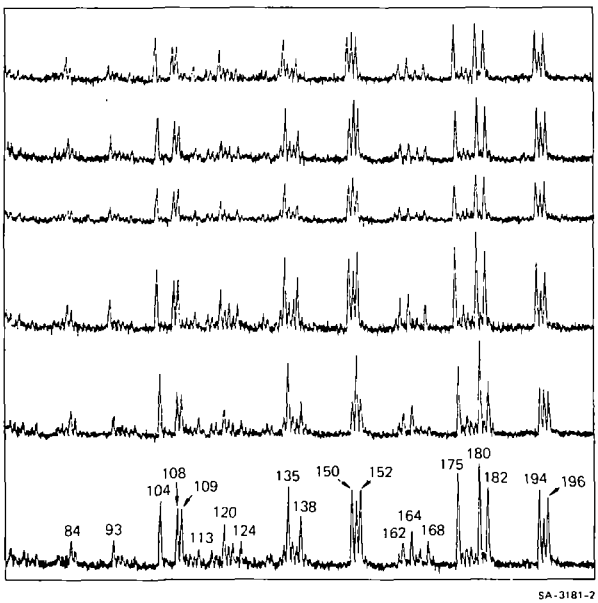

FIGURE 3 REPLICATION OF CARBOXYLIC ACID EXTRACTS FROM HUMAN URINE

MASS SPECTROMETRIC CHARACTERIZATION OF HUMAN URINARY METABOLITES OF CYPROHEPTADINE

W. J. A. VandenHeuvel,* V. F. Gruber,* B. H. Arison,*
D. C. Titus** and C. C. Porter**

Merck Sharp & Dohme Research Laboratories
Rahway, New Jersey 07065* and West Point, Pennsylvania 19486**

Direct probe mass spectrometry, combined gas-liquid chromatography-mass spectrometry, heavy isotope labeling and derivatization techniques have been employed to characterize the human urinary metabolites of cyproheptadine, 1-methyl-4-(5H-dibenzo[a,d]cycloheptenylidene)piperidine. The mass spectra of this and related compounds show extensive fragmentation of the heterocyclic ring and relative stability of the tricyclic nucleus, facilitating metabolite structure determination. Aromatic ring hydroxylation, N-demethylation and heterocyclic ring oxidation of cyproheptadine occur to a minor extent in man. The major metabolite found in human urine is a glucuronidase-sensitive "conjugate" involving only the nitrogen atom of cyproheptadine. This unique quaternary ammonium compound is thermally labile, being transformed to parent drug and glucofuranurono-(6→1)-lactone (identified as its trimethylsilyl derivative) during direct probe heating and upon injection into a heated GLC column.

APPLICATION OF GC-MS IN THE ANALYSIS OF VOLATILE COMPOUNDS IN URINE AND ASCITIC FLUID OF NORMAL AND TUMOR BEARING MICE.

A.M. Lovett, E. Sherwood and J. Oro , Departments of Biophysical Sciences and Chemistry, University of Houston, Houston, TX 77004, and D. A. Flory, Spectrix Corporation, Houston, TX 77027.

The analysis of urine as an index for the presence of a pathological condition is a standard medical procedure. Little attention has been paid to the volatile metabolites of urine, except in a study of patients suffering from diabetes mellitus (1). The major volatile compounds present in the urine of female Swiss Albino mice is shown in Table I. Those compounds indicated by an asterisk have been reported to be present in human urine (1). Mice could therefore make a useful model for investigating abnormal volatile compounds resulting from the presence of tumor cells. A study has been made comparing the GC and GC-MS profiles of the volatiles from the urine of normal female Swiss Albino mice and the urine and ascitic fluid from mice innoculated in the intraperitoneal cavity with 4 x 10^6 Ehrlich Ascites tumor cells. These mice survive approximately 14 days after injection.

Urine from 10 normal or 10 tumor bearing mice housed in an all glass metabolic cage, was collected in an ice cooled test tube over a 24 hour period. The volatile compounds were extracted immediately after collection using the headspace sampling technique of Zlatkis et al., (1), heat desorbed at 200°C for 20 min. onto a precooled 10 ft. x 0.02 in.i.d.nickel precolumn. Chromatography was performed on a 300 ft. x 0.02 in. i.d. nickel column using a Varian 1400 GC equipped with a FID detector. Both columns were coated with Emulphor ON-870 and the helium flow rate was 4.25 ml/min. After 16 min. at room temperature the column temperature was increased to 60°C for 8 min. and then programmed at 2°/min. to 175°C.

Approximately 25 urine samples have been studied, and in all cases the gas chromatograms were very reproducible with respect to general appearance, although differences in the retention times of the various peaks were unavoidable due to the technique of introducing the samples into the GC. Figure I shows a comparison of a typical gas chromatogram of the volatile compounds obtained from a 24 hr urine sample of 10 mice prior to injection, and 3 and 7 days after injection with 4 x 10^6 Ehrlich Ascites tumor cells. The major peaks ('a' through 'k') in these chromatograms have the same retention times relative to peak 'u'. The peak 'u' is present in all chromatograms, including the blanks, and is probably a product resulting from the decomposition of the column at higher temperatures. This peak has therefore been used to substitute for an internal standard. An examination of these GC profiles will show that the relative peak heights of the doublet 'k' changes with the onset of the disease. As the disease progresses the peak 'g' increases considerably in height, and this difference is not due to higher sample concentrations. A comparison has also been made of profiles from normal urine and urine from

mice injected with 4 x 10^6 dead tumor cells. The latter profiles were very similar to the profile shown for normal urine, indicating that the differences observed in the urine profiles of tumor bearing mice were not due to the introduction of a foreign material into the abdominal cavity. Figure II shows a gas chromatogram of the volatile compounds present in the Ascites fluid from the abdominal cavities of the above 10 mice. This profile is consistent with similar profiles obtained from other groups of mice. The four peaks labelled a,b,c and d were the only peaks found in a saline wash of the abdominal cavities of normal mice, the control used for these experiments. It has not been possible to draw sufficient blood from mice to obtain GC profiles of the volatiles present in the blood plasma. Such a study would enhance this work.

A comparison of normal and abnormal profiles of urine obtained using the same column and programming times as described for the GC work, but using an LKB 9000 GC-MS is shown in Figure III. This figure shows only the section of the chromatogram above 100°C, the area judged to be important from the GC work. Major constituents present in both normal urine and urine from tumor bearing mice are listed in Table I. Highly constant and reproducible results are also obtained from these analyses. Two compounds, so far unidentified, have been detected in the cancer urines only. An extension of this work to mice bearing other tumor lines will indicate whether the differences we are observing in the GC and GC-MS profiles from urine are significant or not.

(1) Zlatkis, A., Bertsch, W., Lichtenstein, H.A., Tishbee, A., Shunbo., Leibich, H.M., Coscia, A.M. and Fleischer, N., Anal. Chem., 45, 763-767 (1973).

*Acetone	*4-Heptanone
*2-Butanone	*2-Heptanone
*3-Methyl-2-butanone	*3-Octanone
Benzene	Ethylmethylbenzene
*2,3-Dimethylfuran	*Pyrrole
*2-Pentanone	*Benzaldehyde
*Toluene	Linalool
*Dimethyldisulfide	Acetophenone
*3-Penten-2-one	Phenyl-2-propanone
*C_4-Furan	Naphthalene

TABLE I

The major volatile compounds found in mouse urine
(*)Indicates compounds also found in human urine.

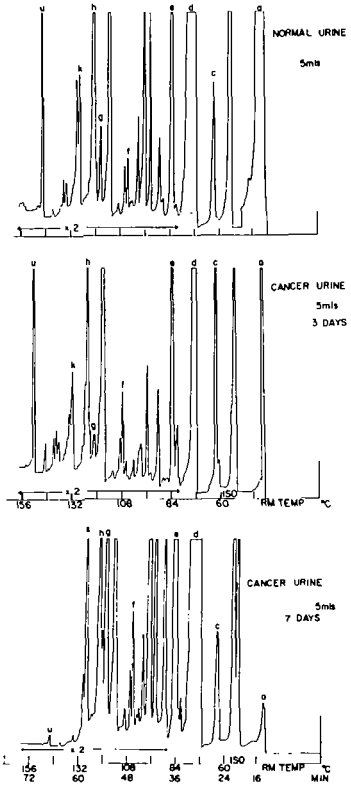

Figure I. GC-FID profiles of the volatiles in 5 ml, 24 hr urine samples from 10 mice, before and after injection with 4 x 10^6 Ehrlich Ascites tumor cells.

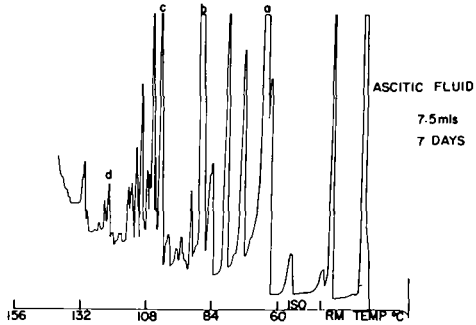

Figure II. GC-FID profile of the volatiles from ascitic fluid from the same 10 mice, 7 days after injection with Ehrlich Ascites tumor cells. Peaks a, b,c and d were the only peaks found in a saline wash of the abdominal cavity of normal mice.

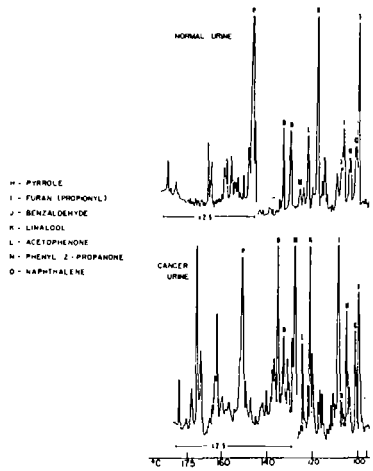

Figure III. GC-MS profiles of the volatiles from a 9ml, 24 hr urine sample from 10 normal mice (top) and 5 ml, 24 hr urine sample from 10 mice 7 days after injection with 4 x 10^6 Ehrlich Ascites tumor cells.

THE ANALYSIS OF EPITAXIAL FILMS BY SPARK SOURCE MASS SPECTROMETRY

G. G. Sweeney and H. B. Kim
Westinghouse Research Laboratories
Pittsburgh, Pennsylvania 15235

Spark source mass spectrometry as an analytical technique is characterized by two features; high sensitivity for trace elements and the ability to provide quantitative information on a wide variety of materials. By systematically scanning a sample, the advantages of conventional SSMS are retained while the analysis can be restricted to that of the surface or thin film. The experimental work to be reported is concerned with a modified scanning technique which has been applied to the analysis of epitaxial films on gallium arsenide. A dendrite of GaAs is used as the counter electrode. High purity dendrites are grown in the epitaxial reactor by self-nucleation on the quartz substrate holder and the quartz reactor tube wall. Analytical results are discussed together with detection limits to be expected with various scanning techniques.

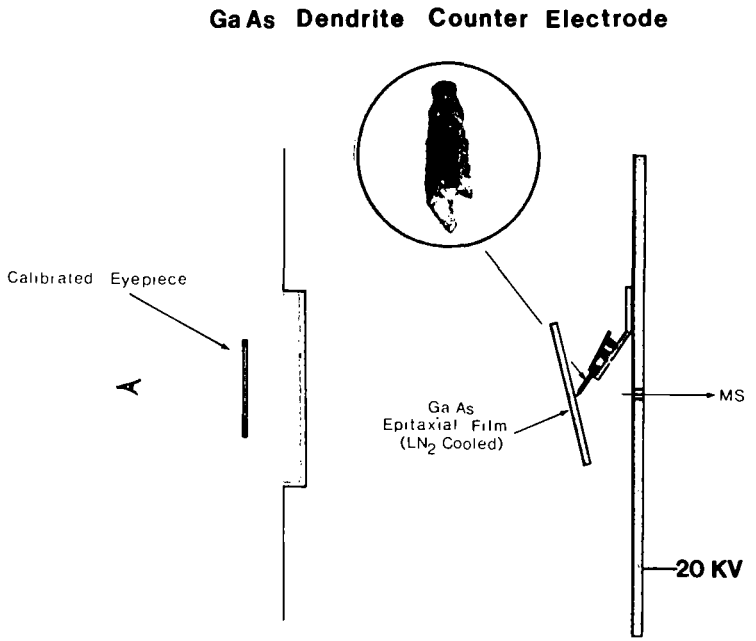

MULTI-ELEMENT ISOTOPE DILUTION SPARK-SOURCE MASS SPECTROMETRY*

J. C. Franklin, J. A. Carter, D. L. Donohue, and R. W. Stelzner

Analytical Chemistry Division
OAK RIDGE NATIONAL LABORATORY
Oak Ridge, Tennessee

Multi-element isotope dilution by spark-source mass spectrometry is an extension of single element isotope dilution. A number of enriched stable isotopes are added to a sample solution and equilibrated. After the spike and sample isotopes are equilibrated, any concentrations or separations required are performed.

In spark-source mass spectrometry, the equilibrated solution is loaded on support electrodes, usually graphite or silver, and sparked with standard operating parameters. The primary requirement for isotope dilution is that the ratio of spike and sample isotope be measured as accurately and precisely as possible.

We have assembled a data system for collecting the ratio data. The lines are scanned on a microphotometer that has been converted to a single beam instrument. The output of the photomultiplier is amplified and stored in core of a PDP-8/E computer. The computer, with dual Dec-Tape storage, collects the data, converts to ion intensity, subtracts background and calculates elemental concentration from standard isotope ratio calculations. The data system has software for 42 isotope pairs, as well as emulsion calibration curves for several emulsions.

The combination of isotope dilution and the data system provides an analytical precision and accuracy that is limited only by the reproducibility of the emulsion. The process of converting %T to ion intensity has a precision of less than 2% RSD at any %T range. We have measured a 105 ppm iron impurity in U_3O_8 with an RSD of 3.3% over a period of three months.

We have prepared isotope spikes containing as many as 21 enriched stable isotope spikes for use in samples of various types. The most useful spike solutions have natural erbium, as well as the enriched isotopes. Table 1 summarizes the sample types and concentration ranges analyzed.

Table 1. Sample Types Analyzed by Spark-Source Multi-Element Isotope Dilution

Sample Type	Concentration Range
Gasoline	10^{-9}-10^{-6} g/ml
Water	5×10^{-11}-10^{-5} g/ml
$^{233}UO_2$	2×10^{-5}-1×10^{-4} g/g
Cigarette Tars	$\sim1\times10^{-6}$ g/g
Fish, Frogs, etc.	10^{-7}-10^{-5} g/g
Pt, Rh, W Alloy	1×10^{-1}-6×10^{-1} g/g

*Research sponsored by the U. S. Energy Research and Development Administration under contract with the Union Carbide Corporation.

The gasoline samples have presented problems in equilibration of the spike isotope and the sample elements. The metallic elements in gasoline are present as unknown organo-metallic compounds. The spike isotope solutions were prepared from pure elements or oxides in acid solutions so that addition to gasolines were made as acetone/water solutions. To confirm the analysis, synthetic samples were made from alkyl metal sulfonates obtained from Continental Oil Company and from NBS organo-metallic standard reference materials.

The method being used now requires that the spike isotopes be added to one ml of HCl. Ten ml of gasoline are added to the HCl spike solution; the two-phase system is refluxed for 4-6 hours. The aqueous phase is removed and dried on graphite electrodes for sparking.

Table 2 is a summary for selected elements determined in gasolines by multi-element isotope dilution.

Table 2. Selected Elements in Gasoline Samples Determined by SSMS-ID

Element	Concentration Ranges μg/ml
Ba	0.005 - 0.6
Cd	0.003 - 0.1
Mo	0.001 - 0.1
Se	0.001 - 0.02
Cu	0.05 - 0.2
Ni	0.005 - 0.05
Fe	0.05 - 2.0
Cr	0.01 - 0.5

The recovery rate for most metallic elements in the synthetic samples is good by the reflux method. The precision at the 0.5 - 1.0 μg/ml level is about 10%. The multi-element isotope dilution technique adds dimensions of precision and accuracy to the high sensitivity and broad elemental range of spark-source mass spectrometry.

Evaluation of the Joyce-Loebl Automated Microdensitometer for Spark Source Mass Spectra. M. A. Haney, FBI Laboratory, Washington, D.C. 20535.

Several laboratories have reported adaptations of microdensitometers for computerized acquisition of spark source mass spectral data.[1,2,3] The Joyce-Loebl Autodensidater is the first fully integrated package commercially available. The specimen table is driven by computer-controlled x and y stepper motors. Data is collected and analyzed by the DEC PDP/8 mini into mass spectral peaks. Their relative position, maximum density, integrated density, and width are printed on teletype and punched on paper tape. The peak data may then be further processed by a larger remote computer to yield a complete elemental analysis. The results of automated runs are compared with manual data acquisition on the same instrument. Further comparisons are made with other design.

[1] Frisch & Reuter, Anal. Chem. 45, 1889 (1973).

[2] Burdo, et.al., ibid 46, 701 (1974).

[3] Millet, et.al., Int. J. Mass Spec. & Ion Phys. 13, 1 (1974).

MOLECULAR BEAM MASS SPECTROMETRIC STUDIES OF LASER PLUMES FORMED AT ATMOSPHERIC PRESSURE*

Frank T. Greene and Gil Radolovich

Midwest Research Institute
Kansas City, Missouri 64110

The interaction of 10.6 micron laser radiation with polycarbonate, polyacrylic and composite materials in air at atmospheric pressure has been investigated. Plume composition measurements were made using molecular beam mass spectrometry. Plume temperatures were measured by molecular beam velocity analysis, optical pyrometry, sodium line reversal, and thermocouples. Plume structure and general behavior were determined by means of conventional and schlieren photography.

The general features of the molecular beam sampling system have been described previously.[1/] For this work the hot gases from the laser plumes were sampled through a 0.025 cm diameter orifice in the tip of a water-cooled conical Pt probe, expanded as a free jet, collimated into a molecular beam, and chopped by a rotating sector prior to introduction into the ion sources of the mass spectrometers. Two mass spectrometers were used: a Nuclide Model 12-90 HT single focusing magnetic mass spectrometer and a modified EAI Model 200 quadrupole mass spectrometer. The Nuclide spectrometer was equipped with ion counting apparatus and a fast data acquisition system and was used to follow individual ions as a function of time and to make time-of-flight velocity analysis measurements. The EAI quadrupole was equipped with a data acquisition system in which the scan was synchronized with the molecular beam chopper. This novel arrangement permits a complete spectrum to be obtained in 20 milli-seconds while still utilizing phase-sensitive detection. The high sensitivity of the quadrupole mass spectrometer allows statistically significant scans to be obtained in this short time interval. When atmospheric pressure nitrogen was sampled, the signal from the molecular beam at m/e = 28 was found to be 2×10^8 ions/sec. Consequently, if a mass range covering 100 amu is scanned in 20 milliseconds, it is possible to measure a species present at a partial pressure of .01 atmospheres to within about $\pm$ 10%. The two mass spectrometers can be operated simultaneously. This permits the quadrupole to be used to obtain complete, time-resolved spectra while the single focusing spectrometer can be used for time-of-flight velocity analysis or to monitor a single ion.

Lexan,[2/] Plexiglas,[3/] graphite-epoxy composites, and a boron-epoxy composite were irradiated using a Coherent Radiation Model 41 continuous CO_2 laser capable of producing over 250 watts of TEM_{00} power. Electron impact spectra of the plume gases were obtained at both 70 eV and 20 eV and the major ions in these spectra have been assigned to neutral

* This work was supported by the Air Force Materials Laboratory, WPAFB.

species in the plume. Lexan plumes produced by irradiation with a flux of 10^3 watts/cm^2 were found to consist primarily of CH_4, H_2O, C_2H_2, CO, and C_6H_6. Minor ions corresponding to much larger species were also observed. Evaluation of the measured species concentrations using well-known thermochemical data indicate that the Lexan plume gases are not in chemical equilibrium. Plexiglas plumes were found to consist principally of methyl methacrylate. The spectra from the composite plumes indicated that significant combustion had occurred during the irradition. These plumes were also found to not be in chemical equilibrium.

1. Milne, T. A., J. E. Beachey, S. L. Bennett, and F. T. Greene, paper presented at the Twenty-First Annual Conference on Mass Spectrometry and Allied Topics, San Francisco, California, May 20-23, 1973.

2. Lexan is a polycarbonate material produced by the General Electric Company.

3. Plexiglas is a polyacrylic material produced by the Rohm and Haas Company.

TIME RESOLVING MASS SPECTRA PRODUCED BY LASER VAPORIZATION OF SOLIDS

Edmund J. Rolinski, AFML, WPAFB, Ohio
Charles J. Oblinger, Univ. of Cincinnati, Cincinnati, Ohio
Charles R. Thomas, Capt, USAF, AFIT, WPAFB, Ohio

Abstract

The identification of species emanating from a solid material subjected to laser irradiation power densities between 10^2 w/cm and 10^4 w/cm was attempted. A method was developed to time resolve species which constitute the vapor produced in a vacuum. A Bendix Model 12-107 TOF mass spectrometer was used in this study. An experimental windshield material (vinyl siloxane cured with peroxide and a formulation of diglycidyl ether of bisphenol-A epoxy resin cured with trimethoxy boroxine) was investigated. Mass peaks of H_2, C_2H_2, CN, N_2 and C_2H_4 were plotted of ion intensity vs. time. Results of this study indicate that the rate of evolution of all species observed in the laser induced vapor plume reaches a maximum 150 msec after laser irradiation and m/e 26 species is the predominent vapor species. Varying amounts of char formed around the vaporization area indicating that further laser interaction was being blocked reducing further vaporization of the surface.

Introduction

In developing materials which are expected to withstand high energy laser radiation, it is necessary to understand the underlying causes for failure and burnthrough. In order to determine the various modes of energy dissipation in materials, an experimental program should be coupled to a parametric analysis of the problem. The most comprehensive analysis of such a predictive treatment makes use of computational techniques developed for the reentry problem, but modified to simulate laser radiative effects. The analytic procedures make use of coupling coefficients in the laser beam interaction area and hence plume chemistry and thermochemical species are important features which require identification. The surface energy balance can then be attempted assuming chemical equilibrium. The details of this computational procedure are reported in Ref. 1. Typical computational results are shown in Fig. 1, which shows the energy flux dissipation modes for a graphite-epoxy composite material as a function of time for a thickness of 0.100 inch. The chemical generation term shown in Fig. 1, represents the net energy transfer caused by a number of chemical energy fluxes. These include the transport of chemical energy associated with chemical reactions at the wall, the energy fluxes arriving at the surface from within the solid, and the gross motion of gases near the surface. The unusual dip is attributed to the char being penetrated to the backwall. As can be seen from Fig. 1, the chemical concentration changes predicted occur in the time from 0 to about 200-300 msec. The purpose of this study is to qualitatively measure the time rate of change of species evolution. In Fig. 2, the dissipation rates are integrated over 0.4 sec., normalized and shown as a bar graph (this corresponds to a quasi-steady state condition). As shown in Fig. 2, the chemical generation term represents almost 1/2 the energy flux dissipation as a result of chemical generation term.

Experimental

The vapor plume was generated by material irradiation using a Sylvania Model 971, one kilowatt infrared (10.6μ) carbon dioxide laser operating in the continuous wave, TEM_{00} mode. Vapor species evolving from the surface

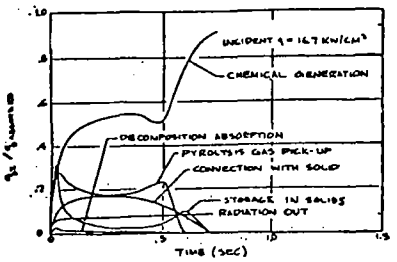

Fig. 1 FLUX DISSIPATION MODES FOR GRAPHITE-EPOXY

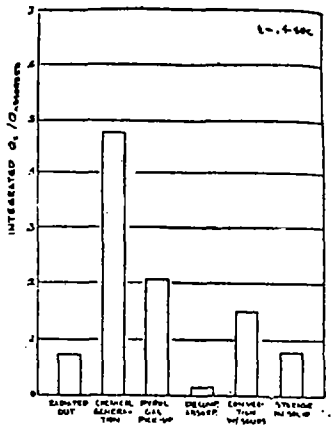

Fig. 2 ENERGY DISSIPATION MODES FOR GRAPHITE EPOXY

of the solid were analyzed using a Bendix Model 12-107-time of flight (TOF) mass spectrometer. The experimental arrangement is shown in Fig. 3. The object of this experiment was to measure real time rate of species evolution from the surface. The method used was a variation of the multiple trace raster display technique and is described in Ref. 2. Briefly the method makes use of a sawtooth or "ramp" voltage applied to the vertical and horizontal amplifiers of the oscilloscope which displays the mass spectrum.

The materials chosen for this study were those which exhibit interesting chemical generation behavior, and the experiments were done on a comparative basis. The first sample was a formulation of vinyl siloxane cured with peroxide, and the second was a formulation of diglycidyl ether of bisphenol-A epoxy resin cured with trimethoxy boroxine. All sample vaporizations were done at a power level of 50 watts which provided a power density of 5 kilowatts/cm^2 at the sample surface; the total sample interaction times were 780 msec and the electron beam energy was 23 eV.

Results and Discussion

Data points for the ion intensity (peak height) vs. time plots were obtained by measuring the vertical position of the oscilloscope trace and knowing the vertical deflection sweep rate. An ion intensity plot for m/e = 2 for hydrogen is shown in Fig. 4. Similar plots were obtained for

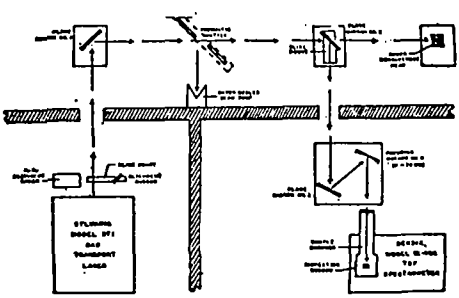

Fig. 3 Schematic Diagram of Experiment

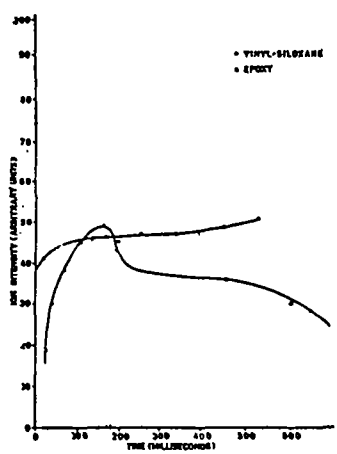

Fig. 4 ION INTENSITY VS. TIME (M/E = 2)

m/e ratios of 26 and 28. In comparing the results of the two samples, it was found that the rate of evolution of the measured species in the laser induced vapor plume reaches a maximum in the first 150 msec. This seems to confirm the assumptions of the computational procedure. Further, the ion intensity of species resulting from the vaporization of the epoxy decreases, whereas the vinyl siloxane is approaching a steady state condition. A visual inspection of the two samples showed that there was a much greater degree of charring on the epoxy resin sample. Thus, it may be postulated that large amounts of char formed around the vaporization area of the epoxy can interact with the laser beam to effectively block further vaporization.

Another experimental observation was that m/e of 26 was the predominant species emanating from the laser heated samples. This could either be the result of acetylene (C_2H_2) or CN both of which may be present in large amounts.

References

1. H. Tong, K.E. Suchsland, W.S. Bonnett, L. Cooper, C.B. Moyer, G.J. Neuner, "Radiant Heating of Aerospace Materials," AFML-TR-73-190, Part 1, WPAFB, Ohio 45433, September 1973.
2. C.R. Thomas, "A Method of Time Resolving the Mass Spectra Produced by Laser Vaporization of Solids," AFIT Thesis GNE/PH/75-12, WPAFB, Ohio 45433, March 1975.

N-6

Laser Source Mass Spectroscopy of Inclusions in Solids.

Kenneth R. Thompson, Eng. Phys. Lab., Eng. Dept., DuPont, Wilmington, Del. 19898

The use of laser source mass spectrometer for the qualitative analysis of inclusions in solids is outlined. The technique has been used to determine the identity of foreign materials in polymers, on metals and to detect three dimensional structures in polymers.

Evaporation of Solids by Laser Pulses

DONALD R. OLANDER, Univ. of California, Dept. of Nuclear Engr., Berkeley, CA 94720

The vaporization of solids by laser pulses was studied using the apparatus shown in Fig. 1. The nature, quantity and velocity distribution of the emitted particles was determined by a quadrupole mass spectrometer which directly viewed the irradiated solid target. Neutral atoms emitted by thermal processes at the surface were of interest; energetic ions produced by a plasma near the surface were not. The laser pulses served as a heat source and the characteristics of the pulses of vaporized atoms reaching the mass spectrometer were determined by time-of-flight analysis of the output signal from this device. The data were compared with the predictions of an equilibrium model, in which transient surface vaporization is treated as a sequence of equilibrium stages at each of which Langmuir vaporization with unit condensation coefficient occurs.

For pure iron, the equilibrium model adequately predicted the measurements from conventional mode pulses at low laser energies. Agreement between theory and experiment failed at high laser energies because of the outward flow of molten iron from the spot struck by the laser. This cratering phenomenon invalidated the temperature calculation from which the vaporization rate was calculated.

The vaporization of hydrogen from the binary solid compound zirconium hydride induced by pulses from a Q-switch ruby laser was studied. The rate of vaporization of H and H_2 during the rapid temperature transient was determined from the measured mass spectrometer signals. Application of an equilibrium model to the vaporization process predicts that predominantly H_2 (rather than H atoms) should be emitted. The vaporized hydrogen should have a Maxwellian velocity distribution characteristic of the instantaneous surface temperature, and the rates of vaporization should be related to the equilibrium H_2 and H pressures by the Langmuir equation. Since the equilibrium pressure is a function of both surface temperature and surface hydrogen concentration, it was necessary to solve simultaneously the time-dependent heat conduction and hydrogen diffusion equations in the heated zirconium hydride in order to predict the vaporization rates. It was found that H atoms and H_2 molecules were emitted at thermal equilibrium with the surface. At low laser power density, the magnitude of the H_2 signals was less than predicted, possibly because of a diffusion barrier at the surface. The H atom signals were much larger than predicted, indicating that they were produced by a nonequilibrium surface process which favored direct vaporization of adsorbed hydrogen atoms rather than recombination followed by H_2 desorption.

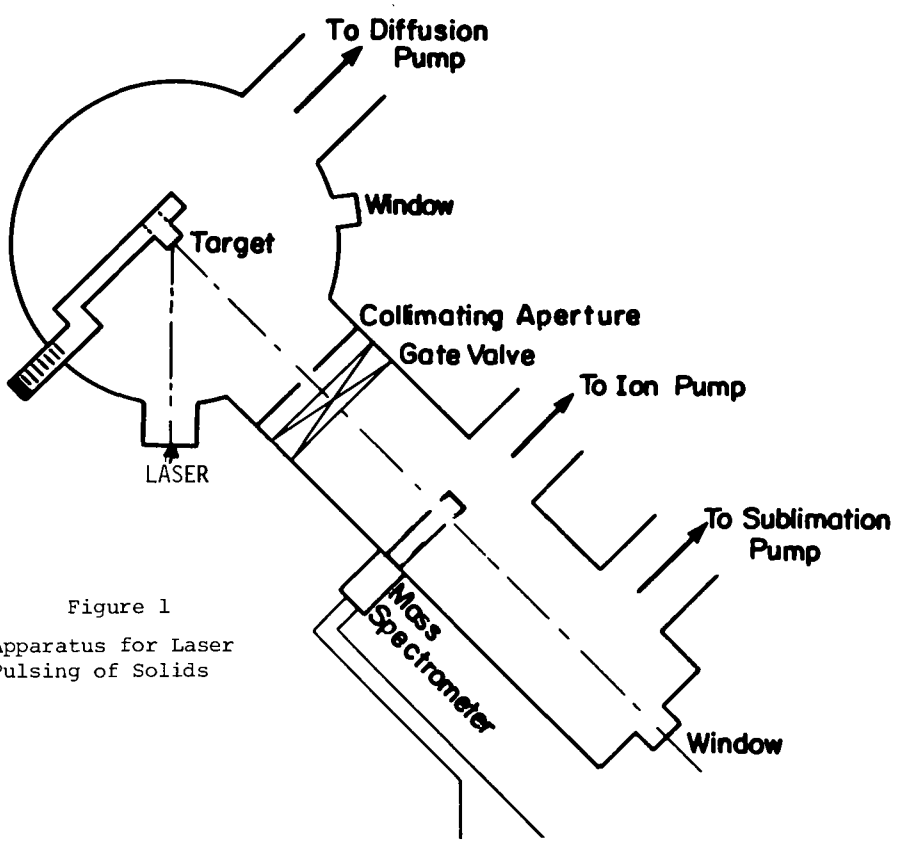

Figure 1

Apparatus for Laser Pulsing of Solids

Initial Energy Distributions of Secondary (+) Ions from the Sputtering of Non-Metallic Solids with Ar^+ (3KeV to 10KeV)*

Frank G. Satkiewicz
Applied Physics Laboratory
The Johns Hopkins University
Laurel, Maryland 20810

In order to provide meaningful, quantitative, fragmentation data on the sputtering of solids, account must be taken of the portion of the initial energy distribution of secondary ions transmitted in a given spectrometer arrangement. This is of particular importance in cases where the energy band acceptance is limited and variable (double focusing instruments such as the GCA IMS 101B). In prior work[1,2,3], Poschenrieder, et al., found differences in secondary distributions for species arising from the sputtering of Pt and Al with 10-12KeV Ar^+ and Xe^+. An energy band width of 4eV was used.

In this present study, a broader bandwidth (50eV), a defocused beam for minimizing thermal effects, and a charge compensation filament[2] was used. Distribution curves were obtained for atomic species from a kaolin "paint" (an aluminosilicate calcined with potassium silicate) and for polyatomic as well as atomic species from fused silica. Experimental data from both substances was found to fit the following distribution expression:

$$\frac{I}{I_m} = \frac{\eta^b}{|E_s-(E_s)_m|^b + \eta^b} \qquad (1)$$

where I = ion species intensity at initial energy E_s; I_m = maximum intensity in the distribution curve at initial energy $(E_s)_m$; η = value of E_s at $I/I_m = 0.5$; and b = a number ranging from 1.5 - 3.

The distribution curves for species from sputtering kaolin are shown in Figure 1. The elements in parentheses have curves similar to Ca^+. It was observed that O^+ which has a high ionization potential exhibited a very broad distribution, while potassium which has a low ionization potential had a narrow distribution. The first ionization potential was compared with the area, A_d, under the curves in the range 0-500eV, which in most cases includes the majority of the ions. The results are shown in Table I. Table I also contains the values of the parameters in the distribution equation. As can be seen, with the possible exception of hydrogen, the normalized distribution areas are (within experimental error) in direct proportion to the ionization potential; thus the higher the ionization potential, the higher the population of more energetic ions.

The results for fused silica are summarized in Table II. The last three columns show the calculated ionization potentials for all the species, assuming a direct relation to the distribution areas and the ionization potential of Si^+. As

can be seen, there is fair agreement with the measured potentials.

The difference in positive ion spectra from applying 0-50eV or 0-500eV distributions to the fragmentation pattern of fused silica is shown in Table III. The figures include contributions of all isotopes. For species containing two Si atoms, isotope mixing was taken into account. It is evident that a detailed knowledge of the energy distribution of polyatomic ions from a material enables an analyst with any solids mass spectrometer to determine detection limits for impurities at masses where isotope ratio measurements are not possible and where instrument resolution is insufficient to decouple interfering species.

Further work is being carried out with other substances to confirm the observed relation between ionization potential and distribution area.

1. Herzog, R.F.K., Poschenrieder, W.P., Rüdenauer, F.G. and Satkiewicz, F.G., 15th Annual Conference on Mass Spectrometry and Allied Topics, Denver, Col., 1967, pp 301-308.
2. Herzog, R. F.K., Poschenrieder, W.P., Satkiewicz, F.G., NASA Contract No. NAS5-9254, Final Report (1967).
3. Ibid, Radiation Effects 18, 195-205 (1973).

*Work supported in part by Naval Sea Systems Command, Contract No. N00017-72-C-4401, X81V.

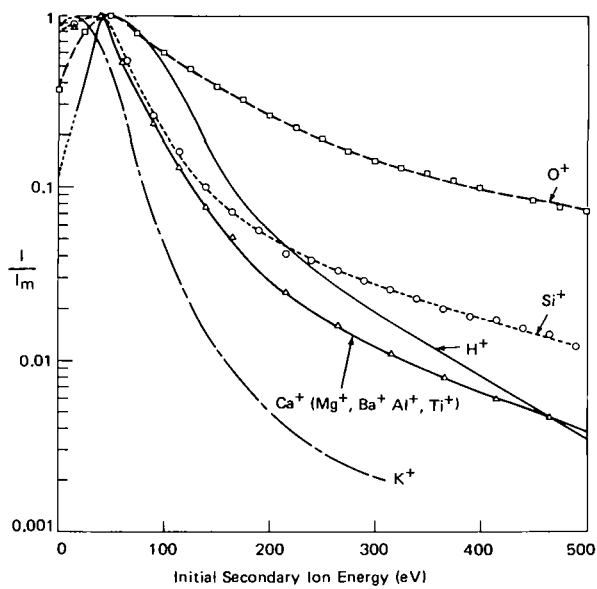

Fig. 1 ENERGY DISTRIBUTION OF ELEMENTAL SPECIES FROM SPUTTERING KAOLIN WITH 10 KeV Ar^+

TABLE I
COMPARISON OF ENERGY DISTRIBUTIONS OF ELEMENTAL IONS FROM SPUTTERING KAOLIN WITH 10 KeV Ar^+

SPECIES	$(E_s)_m$,(eV)	η,(eV)	b	V_I,(eV)	A_d
O^+	40	80	1.5	13.60	178
H^+	50	50	2.5	13.61	101
Si^+	40	30	1.75	8.15	100
Mg^+	30	31	2.0	7.64	86
Ti^+	33	34	2.0	6.83	81
Ca^+	34	34	2.0	6.11	84
Al^+	29	29	1.8	5.98	72
Ba^+	30	30	2.1	5.81	78
K^+	23	23	2.5	4.34	52

TABLE II
ENERGY DISTRIBUTIONS OF (+) IONS FROM SPUTTERING FUSED SILICA WITH Ar^+

SPECIES	AREA UNDER CURVE, A_d			CALCULATED IONIZATION POTENTIAL, (eV)*			REPORTED IONIZATION POTENTIAL (eV)
E_p, KeV	10.8	5.4	3.1	10.8	5.4	3.1	
Si^{2+}	281	272	161	19.6	20.9	13.4	16.3
O^+	172	162	153	12	12.5	12.7	13.5
Si^+	117	106	98	(8.15)	(8.15)	(8.15)	8.15
SiO^+	96	76.8	76.8	6.7	5.9	6.4	—
Si_2^+	86	78	84	6	6	7	—
SiO_2^+	47	59	55	3.3	4.5	4.6	—
Si_2O^+	42	61	57	2.9	4.7	4.7	—
$Si_2O_2^+$	41	48	64	2.9	3.7	5.3	—

*BASED ON $(V_I)_{Si^+} = 8.15$ eV

TABLE III
RELATIVE CONCENTRATION OF (+) IONS FROM SPUTTERING FUSED SILICA WITH 10 KeV Ar^+

SPECIES	FRACTION (+) IONS	
	0–50 eV	0–500 eV
Si^{2+}	0.00078	0.0023
O^+	0.0023	0.0055
Si^+	0.95	0.96
O_2^+	0.00009	0.00018
SiO^+	0.030	0.022
Si_2^+	0.0031	0.0025
SiO_2^+	0.00019	0.000093
Si_2O^+	0.0071	0.0026
$Si_2O_2^+$	0.0015	0.00052
$Si_2O_3^+$	0.00011	0.000039

IMPROVEMENTS IN QUANTITATIVE ANALYSIS OF SOLIDS BY SIMS

K. Kusao, Y. Yoshioka, N. Nakamura and F. Konishi
Central Res. Labs., Matsushita Elec. Ind. Co., Ltd.,
Kadoma, Osaka, Japan

In the case of the analysis of the solid surface by SIMS, it is well known that the yield of secondary ions increase when using oxygen as a primary ion species. It also increases when introducing oxygen into a specimen chamber. We have developed a SIMS apparatus which is provided with a quadrupole type mass analyzer. This report is related to the improvement of reproducibility for determining the composition of an alloy. In this study, we have attempted to determine the optimal oxygen pressure in the specimen chamber for the iron-nickel alloy.

Fig. 1 shows the SIMS apparatus developed and used for the study. This apparatus consists of two main parts; first, the primary ion beam was created from a PIG ion source. Ions formed were extracted and focused on, by three cylindrical lens and electrostatic quadrupole lens on the sample surface in a beam diameter of 0.1 mm.

Second, secondary ions from the specimen were extracted by extractor electrodes, deaccelarated by the retarding electrodes, and filtered out by a deflection type energy analyzer. Thus, only ions that have an optimal energy width were analyzed by the quadrupole mass spectrometer. Oxygen could be introduced into the specimen chamber through the gas inlet valve, which controls the oxygen pressure up to about 10^{-3}Torr but the pressure in the entire system, except the specimen chamber is maintained though the aid of differential pumping system, even if the pressure in the specimen chamber reaches 10^{-3}Torr. Experimental conditions were as follows: The primary ion species was argon, the primary ion accelerating voltage was 12kV and the primary current was 1 mA/cm^2. The angle of incidence is 45 degrees.

In order to study the linearity of the calibration curve, four kinds of iron-nickel alloys have been tested. Compositions of the test samples ranged from 0.56 to 3.53. All samples were polished with alumina powder with granular size of 0.06μm, prior to being set on the sample holder.

Fig. 2 shows effect on the secondary ion intensity of the oxygen

pressure. When increasing oxygen pressure in the sample chamber, secondary ion intensities indicate a steep increase until the oxygen pressure reaches around $5x10^{-5}$Torr, at which point the secondary intensities level off at a constant value. The tendency of the intensity increase of nickel ions in somewhat different from that of iron ions.

Fig. 3 shows the change of the secondary ion intensity ratio vs. the oxygen pressure. The intensity ratio of nickel ions to iron ions changes considerably with the oxygen pressure. Especially, in the low pressure range, the behavior of this ratio is remarkable, but it rises to a steady region in the pressure range beyond $5x10^{-5}$Torr. Similarly, the behavior of the chromium ions, that is obtained from the test sample as an impurity, is shown in this figure. The ratio of chromium ions to iron ions decreases if the oxygen pressure increses and it also approaches a constant value when the oxygen pressure is about $5x10^{-5}$Torr or above. Anyhow, both cases show the saturation effects in the range of oxygen pressure of $5x10^{-5}$Torr or higher. Accordingly when the SIMS analysis is done in a pressure range of $5x10^{-5}$Torr or higher, variations of data obtained is not expected to be so large.

As shown in Fig. 4, when the primary current density changes, the curve of the secondary ion intensity of nickel vs. the oxygen pressure become parallel. The smaller the current density, the point at which the nickel intensity levels off to a constant value is at a lower oxygen pressure. However, the nickel ion intensity does not vary beyond the point at which the largest current density levels off, even if the current density varies. The secondary ion intensity ratio is not affected by a change in the angle at which the ion beam strikes the sample at an oxygen pressure of $5x10^{-5}$ Torr, but at an oxygen pressure of $1.9x10^{-7}$Torr the ion intensity ratio is greatly affected.

As was expected from previous data, the precision of the data will be greatly dependent on the oxygen pressure. Fig. 5 shows the aspects of change in the precision of the data obtained. The coefficient of variation at a pressure of 10^{-6}Torr indicates about 6%, while that of about 1.6% could be obtained in the pressure range $5x10^{-5}$Torr or above.

Fig. 6 shows the calibration curve of the iron-nickel alloy at the oxy-

gen pressure of 5×10^{-5} Torr. At this pressure, the secondary ion intensity ratio shows the linear relation of the iron-nickel alloy composition ratio through zero point. The accuracy obtained from the method reported here is better than 2%.

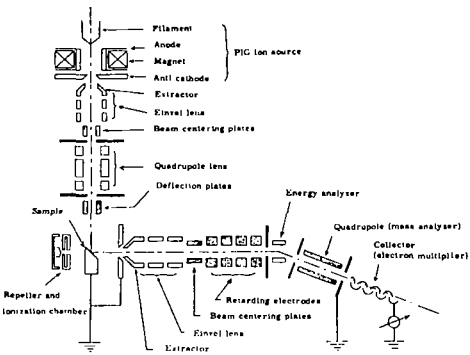

Fig. 1

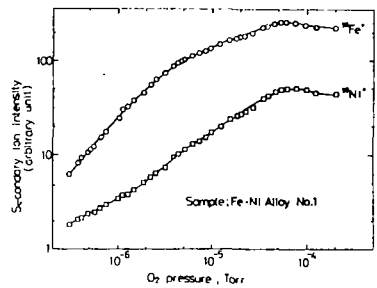

Fig. 2

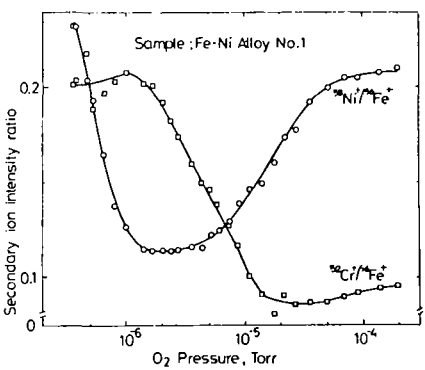

Fig. 3

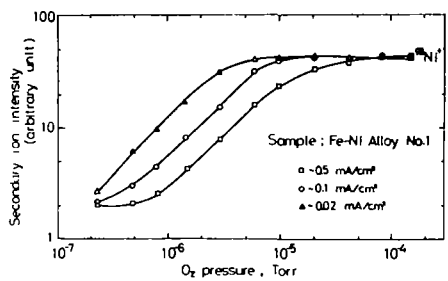

Fig. 4

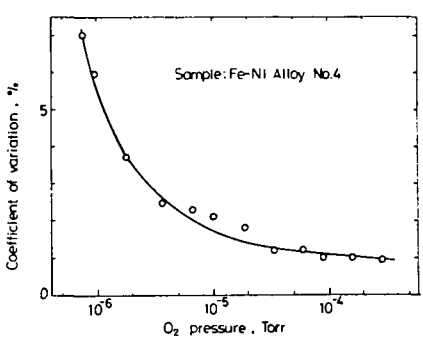

Fig. 5

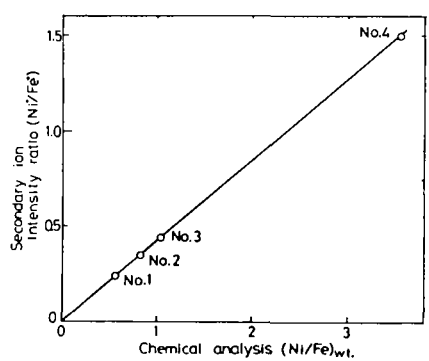

Fig. 6

N-10

A Coaxial Cathode Gas Discharge Source for Solids Analysis

W. A. MATTSON and W. W. HARRISON, University of Virginia, Department of Chemistry, Charlottesville, Virginia 22903

A hollow metal anode coupled with a coaxial sample cathode allows a gas discharge, usually of argon, to be struck at approximately 1-5 torr with ion extraction from an anode slit. The sputtering of the cathode allows analysis of conducting solids or of solution residues dried to a surface film on an appropriate cathode. Metal rods or wires may be used as cathodes directly. Solutions can be applied to metals or high purity graphite electrodes. Sensitivities to the sub-ppm level can be obtained. Average currents of less than 10 ma by dc operation and less than 3 ma by pulsed discharge operation can be used to minimize heating effects. Operation using the high voltage rf available on a commercial spark source mass spectrometer has also been examined.

N-11

A Pulsed Mode Hollow Cathode Ion Source for Solids Analysis

W. W. HARRISON and W. A. MATTSON, University of Virginia, Department of Chemistry, Charlottesville, Virginia 22903

The hollow cathode ion source (HCIS) is operated in a pulsed configuration at 10-500 Hz repetition rates and variable pulse lengths. Peak pulse conditions of 1200 v and 200 ma yield average currents of 10 ma or less, thus producing little net heating effect. Comparison to dc operation of the HCIS for the same average current shows a more stable response from the pulsed mode and a more efficient current utilization. Light emission is much higher in the pulsed state. Sensitivity and precision studies are compared for NBS metal samples and also for solution residue samples dried onto a matrix cathode.

Measurement of In Vivo Incorporation of Multilabeled Thymidine into DNA using Field Ionization Mass Spectrometry. James H. McReynolds, Henry d'A. Heck, and Michael Anbar, Stanford Research Institute, Mass Spectrometry Research Center, Menlo Park, CA 94025.

Information about the rate of DNA synthesis in normal and malignant cells is vital in many areas of cancer research and therapy. As an alternative to the use of tritiated thymidine, which is not applicable for tracer work in human subjects, we have synthesized and measured the in vivo incorporation of thymine labeled with stable isotopes.

In preliminary experiments, Sprague-Dawley rats were administered intraperitoneal doses of both tritiated thymidine and multilabeled thymine synthesized using stable isotopes.

DNA was isolated from various tissues and field ionization mass spectrometry used to measure the ratio of normal to multilabeled thymine. In order to achieve a wide dynamic range and measure low levels of incorporation we synthesized thymidine from thymine ($1,3\text{-}^{15}N_2\text{-}5,5,5\text{-}d_3\text{-}6\text{-}^{13}C$).[1]

For each selected tissue 1 to 10 mg were homogenized, hydrolyzed in KOH and extracted with TCA to recover the DNA. The DNA was hydrolyzed and the thymine isolated by tlc. Thymine eluted from the plates was introduced underivatized by solid probe into a mass spectrometer using a multipoint field ionization source.

The relative abundances of the two molecular ion beams were measured by repetitively scanning from m/e 125 to 135 electrostatically and integrating the multiplier output on a multichannel analyzer. Fig. 1 shows the integrated spectra from several samples and control tissues analyzed in these experiments. The relative levels of incorporation are given in Table 1. The values measured are consistent with the amount of tritiated

Table 1
IN VIVO INCORPORATION OF ^{132}TdR INTO DNA OF RAT TISSUE
Injected with 5 x 0.5 μM of ^{132}TdR

Tissue	$\left(\frac{^{132}T}{^{126}T}\right) \times 10^3$	$\frac{\mu g\ ^{132}T}{gm\ DNA}$
Brain	<0.01	<1
Heart Muscle	0.44 ± 0.10	48 ± 10
Thymus	0.45 ± 0.03	50 ± 3
Spleen	1.70 ± 0.14	187 ± 16
Bone Marrow	4.34 ± 0.01	478 ± 1
Intestine	5.80 ± 0.07	638 ± 8

thymine incorporated in the same tissue. The sensitivity of this method would allow the determination of 0.01% of new DNA in a 1 to 10 mg tissue sample.

Since this technique does not require the use of radioactive isotopes and information can be obtained with biopsy-sized samples in less than one day, it should prove to be a valuable clinical tool.

Reference

1. J. A. Lawson, J. I. DeGraw, and M. Anbar, submitted to J. Labelled Compounds.

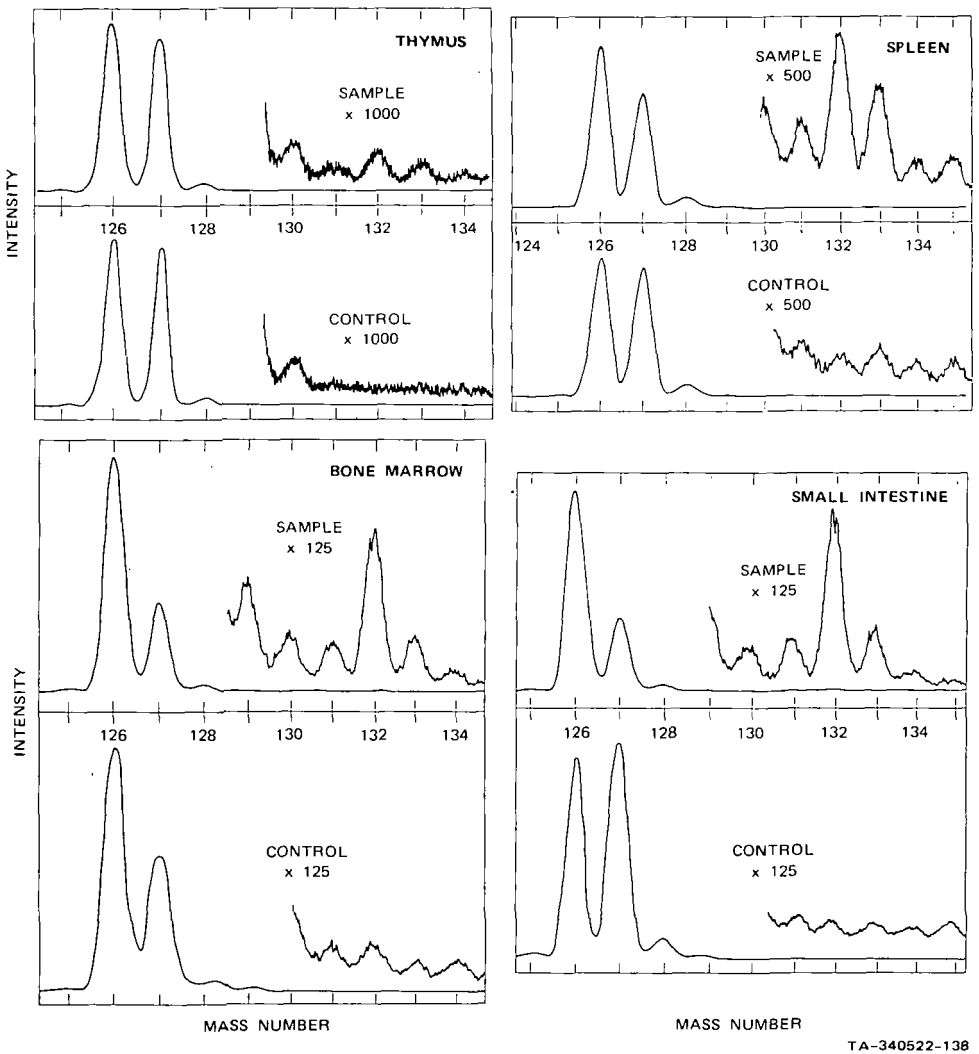

FIGURE 1

THE QUANTITATIVE DETERMINATION OF DOPAMINE IN BRAIN TISSUE BY METHANE CI-MS

M.S. Silberberg, M.E. Rennekamp, and D.V. Bowen

Department of Neurology
Albert Einstein College of Medicine

and

The Rockefeller University
New York, New York

Dopamine, or 3,4-dihydroxyphenylethylamine (DA), is thought to function as a neurotransmitter in the mammalian central nervous system. We have developed a protocol which allows us to measure picomole amounts of DA in small regions of rat brain. The method uses gas chromatographic separation of tissue constituents followed by chemical ionization mass spectrometry in conjunction with selected ion recording. The ions recorded are the protonated molecular ions of perfluoropropionyl derivatives of dopamine (PFP-DA; m/e 592) and of the internal standard, α-methyl-dopamine (PFP-αMDA, m/e 606). Methane serves both as carrier gas in the GC and as reactant gas in the ion source of a Biospect quadrupole mass spectrometer manufactured by Scientific Research Instruments, Inc., Baltimore, Maryland.

The GC derivatives were prepared by heating the amine hydrochloride for 30 minutes at 60°C in a 1:1 mixture of pentafluoropropionic anhydride: ethyl acetate (PFPA:EtOAc).

A calibration curve was obtained by simultaneously injecting varying amounts of PFP-DA and a fixed amount of PFP-αMDA. The mass spectrometer is first focussed on the ion from PFP-αMDA, since this material has the shorter GC R_T, and then manually switched to focus on the ion from PFP-DA. A plot of the ratio of the integrated ion intensities ($I_{DA}/I_{\alpha MDA}$) versus the amount of PFP-DA injected is linear between 0.06 and 6.0 picomoles and shows a relative standard deviation of 10%.

Occasionally a standard run will show a much larger deviation (as

much as 40%). This usually occurs with increasing GC-column age and is probably due to sites which adsorb PFP-groups. When PFP-standards are injected, these sites become filled thereby decreasing the amounts of standard entering the mass spectrometer and producing a smaller-than-expected response. A blank injection of PFPA-EtOAc then displaces some adsorbed standard and produces a greater-than-expected response. We have successfully alleviated this problem by "priming" the column with repeated injections of PFPA prior to collecting data.

Before injection into the GC, a brain sample is prepared as follows: White male rats weighing 250-300 grams are anesthetized, killed by decapitation, their brains rapidly removed and dissected at 4°C. The specific brain region weighing between 10-30 mg is homogenized in 1N·HCl containing a known amount of the internal standard, α-methyl dopamine, and centrifuged. The supernatant is then extracted with ethyl acetate to remove lipids. The aqueous fraction is then dried *in vacuo*, derivatized with PFPA:EtOAc and 1-3 μl injected into the GC-MS.

Using this procedure we have measured the DA in two discrete rat brain regions: the corpus striatum which has a high endogenous DA content, and the cerebral cortex, which contains relatively little DA. These results are shown in comparison with other published analytical methods in the table below:

Comparison of Analytical Methods
for Determination of Brain Dopamine[1]

Brain Region	Spectro-fluorometric	Radio enzymatic	EIMS	CIMS
Corpus Striatum	7112 ± 1620	8070 ± 920	12460 ± 800	10253, 7529
Cerebral Cortex	84 ± 7 122 ± 7	114 ± 28	-	78, 79, 77

1. All values are expressed as ng dopamine/gm wet tissue.

To the best of our knowledge, this is the first application of CIMS

to the measurement of tissue catecholamines and in addition provides mass spectrometric confirmation for the presence of DA in the cerebral cortex.

O-3

ELECTRON IMPACT INDUCED FRAGMENTATION PATHWAYS OF MORPHINE AND ITS DERIVATIVES

K. D. Haegele
Institute for Lipid Research
Baylor College of Medicine
Houston, Texas 77025

In order to understand the metabolism of morphine and heroin, as well as for the identification and quantitation of morphine, heroin and their metabolites in blood and urine it was necessary to synthesize a number of derivatives, whose mass spectra have not been described previously.

The derivatives, whose mass spectral fragmentation pathways were studied in detail include the following compounds: morphine, $\underline{d}_1$-morphine, $\underline{N}$-CD_3-morphine, $\underline{N}$-C_2D_5-morphine, $\underline{N}$-CD_3-codeine, codeine, O,O-dimethyl-morphine, O,O-di-$\underline{d}_3$-methyl-morphine, O,O-di-acetyl-morphine, O,O-di-$\underline{d}_3$-acetyl-morphine, 6-O-acetyl-morphine, 6-O-acetyl-$\underline{N}$-CD_3-morphine, 3-O-acetyl-morphine, 3-O-$\underline{d}_3$-acetyl-morphine, normorphine and norcodeine.

To distinguish morphine, normorphine, codeine, norcodeine, etc. in biological fluids by means of GC/MS perdeutero-ethylation was used. The internal standard, added before extraction, is $\underline{N}$-CD_3-morphine. By using per-$\underline{d}_5$-ethylation all possible metabolites can be identified.

Details of this study and the fragmentation pathways of these compounds will be published elsewhere. This work was supported by US Army Contract DAMD-17-74-C-4052.

BASIC MASS SPECTROMETRIC INVESTIGATIONS OF AMINO ACID-FLUORESCAMINE DERIVATIVES

J. J. Shieh, K. L. Leung and D. M. Desiderio, Institute for Lipid Research and Department of Biochemistry, Baylor College of Medicine, Houston, Texas 77025.

Reaction products of 17 of the naturally occurring amino acids with fluorescamine (1) have been investigated by means of low resolution mass spectrometry, high resolution mass spectrometry as well as stable isotope incorporation. Five major fragmentation pathways have been observed for these products. Most of these pathways involve various combinations for loss of the stable molecules carbon monoxide and carbon dioxide in conjunction with a very interesting loss of one oxygen atom. The dominant ion in the upper mass region of these spectra corresponds to the loss of a water molecule to form a lactone ring producing the $(M-18)^+$ ion. This ion differentiates the amino acids studied. The major portion of all ions studied in this series involves the loss of either the side group of the amino acid or the entire amino acid chain. The resulting ions undergo subsequent losses of CO, CO_2 and an oxygen atom in various combinations to yield stable molecules with a spiro configuration of two 4-membered rings. The end product of these fragmentation processes involves subsequent cleavage of a molecule of phenylacetylene.

In conclusion, it has been straightforward to categorize the five major fragmentation pathways found for these reaction products by whether or not a molecule of carbon dioxide, carbon monoxide or an atom of oxygen is lost initially. These families of ions occur in each one of the mass spectra studied. In addition, there is always a peak at *m/e* 261 due to the ion drawn below as well as the usual base peak at *m/e* 102 which is due to phenylacetylene.

References

S. De Bernardo, M. Weigele, V. Toome, K. Manhart, W. Leimgruber, P. Böhlen, S. Stein and S. Udenfriend, Arch. Biochem. Biophys., 163, 390 (1974).

Ionization of Steroidal Epoxides Under Electron Impact and Chemical Ionization Conditions.

SERRINE S. LAU and EVAN C. HORNING, Baylor College of Medicine, Houston, Texas 77025

Epoxidation is now recognized as a normal mammalian pathway of oxidation for many compounds. In order to study the possible formation of steroidal epoxides from endogenous steroids, a group of epoxides was prepared (m-chloroperbenzoic acid oxidation). Mass spectra were obtained under EI and CI conditions through the use of GC-MS-COM analytical systems (LKB 9000-PDP 12 and Finnigan 1015-PDP 8/I). The degree of reactivity with respect to proton-catalyzed ring opening was also determined; the decreasing order is 5,10>16,17>5,6>4,5. Ionization reactions were studied to determine if specific types of ions could be used to identify steroidal epoxides in mixtures of human steroidal metabolites, and for purposes of comparison of ionization data with observed chemical reactivity. The results suggest that selective ion detection procedures can be used either directly or in repetitive scan search programs for detecting compounds of this kind.

Electron Impact, Chemical Ionization and Atmospheric Pressure Ionization Mass Spectra of the Tocopherols.

SHEN-NAN LIN and EVAN C. HORNING, Baylor College of Medicine, Houston, Texas 77025.

ABSTRACT

In order to develop analytical procedures based on mass spectrometry for the estimation of the tocopherols in plasma and other tissues, EI, CI and API mass spectra of derivatives of α-, β-, γ- and δ-tocopherol were compared. The derivatives included trimethylsilyl and dimethyl-t-butylsilyl ethers, and acyl and perfluoroacyl esters. In order to introduce the compounds into GC-MS-COM systems for analytical purposes, and to permit comparisons with GC procedures alone, it was necessary to develop a new separation method, particularly for β- and γ-tocopherol. This was accomplished through use of the new thermostable polar phase PZ-176 and trimethylsilyl derivatives. For human plasma studies, it is not necessary to employ a saponification step or a preliminary chromatographic separation. Selective ion detection procedures will be discussed.

Identification and Quantitation of Biogenic Phenolalkylamines in the Subpicomol Range Using a GC Coupled to a Small Double Focusing Mass Spectrometer

M. Donike
Institut für Biochemie, Universität Köln, D-5000 Köln, West Germany

K. H. Maurer, U. Rapp and A. Zune
Varian MAT GmbH, D-2800 Bremen, West Germany

Introduction

In the research field dealing with biogenic amines and related drugs, analytical methods must offer outstanding sensitivity and specificity. Indeed, these compounds are generally present at very low levels, and the samples, because of their biological origin, are of complex composition making mandatory a highly specific analytical method. These requirements are ideally met by a high quality GC/MS system. A modern spectrometer with very efficient ion source and high ion beam transmission provides the necessary sensitivity, while specificity is obtained on the basis of GC retention time and compound specific mass of the fragment ions monitored with the techniques of single ion detection (SID) or multiple ion selection (MIS). The measurements presented here below concern derivatives of the biogenic amines adrenaline, noradrenaline, isoprenaline, serotonin, and of the stimulants norephedrine and ephedrine.

Experimental

Instrumentation

The analyses were performed using a double focusing mass spectrometer Varian MAT 112 equipped with a multiple ion selection device and coupled to a Varian 1400 GC. In the case of packed column work, the GC effluent was passed through a variable slit separator adaptable to a wide flow rate range. Since the instrument features a differential pumping system with a 600 l/s diffusion pump for the ion source, a helium flow rate of more than 4 ml/min into the source can easily be dealt with.

When a capillary column was used, it was thus directly coupled to the ion source using a glass lined stainless steel capillary. This connection is an all glass inlet line which can be heated easily and in a uniform manner. The spectrometer's multiple ion selection unit gives the choice between two basically different peak jumping methods which are first, the usual accelerating voltage alternation mode, and, second, a fast magnetic field alternation device. While the first method presents well known restrictions, the latter enjoys constant and maximum sensitivity over the whole mass range. It uses the full accelerating voltage, and allows peak jumping over any mass interval within the spectrometer's nominal mass range. Its operation is straightforward since one can rely for each mass setting on the indications of an accurate mass marker. The GC was fitted with a 6 foot glass column packed with 3 % OV-17, operated at a helium flow rate of 20 ml/min. Alternatively, a 20 m, 0.3 mm ID glass capillary column was used, which was coated with OV-101. The flow rate in this case was set at 3 ml/min.

Choice of the derivative type

The limit of detection reached when monitoring a certain ionic species depends strongly on its relative intensity in the mass spectrum. In the case of biogenic amines and other compounds measured here, it has been shown that N-trifluoroacetyl-O-trimethylsilyl (N-TFA-O-TMS) derivatives are very suitable for SID or MIS (1). Indeed, their fragmentation upon electron impact leads to abundant, structure specific ionic species as can be seen from figure 1.

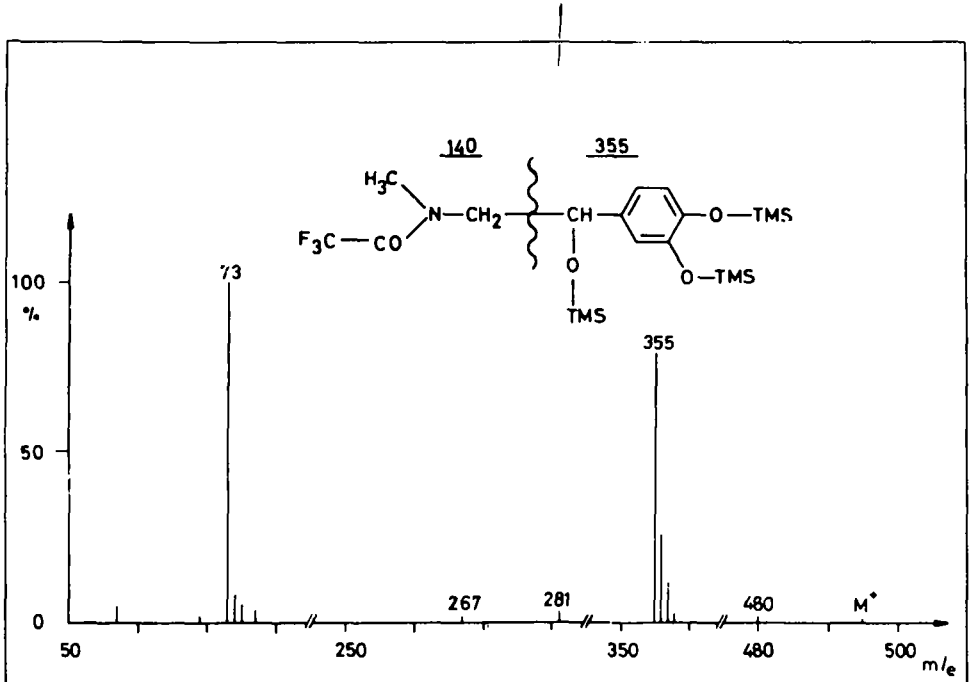

Fig. 1 EI spectrum of N-TFA-O-TMS adrenaline

Besides, they are readily prepared, and are stable for long periods of time provided moisture is excluded. When submitted to gas chromatography, they are eluted in symmetrical peaks and show no thermal decomposition or absorption. This results in linear calibration curves down to the low pg range.

Preparation of the derivatives

The derivatization of phenolalkylamines including catecholamines and hydroxyamines of the ephedrine type at the pMol level (2) was obtained as follows. A part of the solution of phenolalkylamine in 0.1 N acetic acid is added in a centrifuge tube to 0.1 ml of a freshly prepared 1 % (w/v) solution of oxalic acid in methanol. This is then submitted to the rotary evaporator, and the resulting sample is dried in a dessicator under vacuum (water aspirator) and over P_2O_5/KOH for at least 4 hours. The residue is then allowed to react at 80 °C for 30 min with 0.125 ml of a silylation mixture composed of 5 ml of acetonitrile and 1.5 ml N-methyl-N-trimethylsilyl-trifluoroacetamide (MSTFA). After cooling to room temperature, 0.01 ml of N-methyl-bis-trifluoroacetamide (MBTFA) is added to this solution. The whole is left for 10 min at room temperature, then it is heated for 5 min at 80 °C. After cooling, this solution is used as such for gas chromatography experiments.

When derivatizing serotonin, catalytic amounts (5 % w/v) of imidazole or TMS-imidazole are added to the above mentioned silylation mixture.

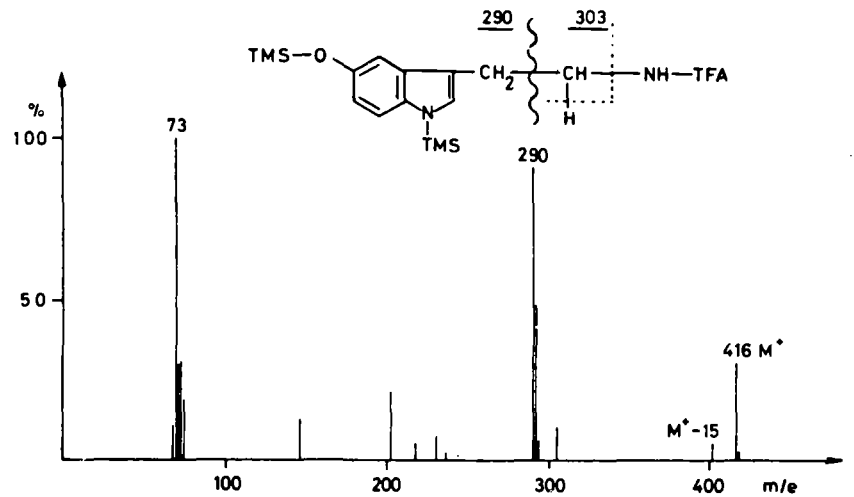

Fig. 2 EI spectrum of ^{1}N, O-TMS- $^{\omega}$N-TFA serotonin

Results and discussion

In quantitative work, an analysis calibration curve is necessary in order to check the linearity of the measurement. In the case of serotonin, for instance, in order to build up a calibration curve down to the detection limit, various volumes of a 30 pg/µl solution were successively injected in the GC. The mass spectrometer was set to monitor the GC eluate at m/e 290. This ion species is the most intense in the upper part of the mass spectrum of ^{1}N,O-TMS-$^{\omega}$N-TFA serotonin as can be seen in figure 2.

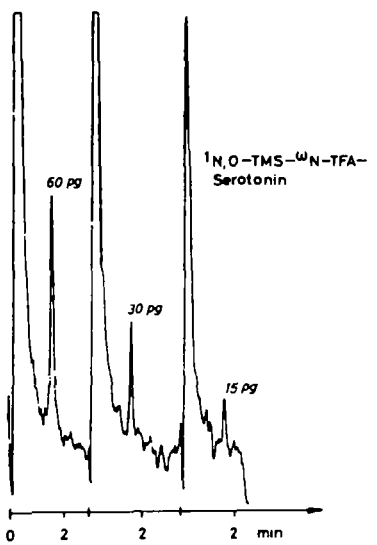

Fig. 3 Detection of ^{1}N, O-TMS- $^{\omega}$N-TFA serotonin

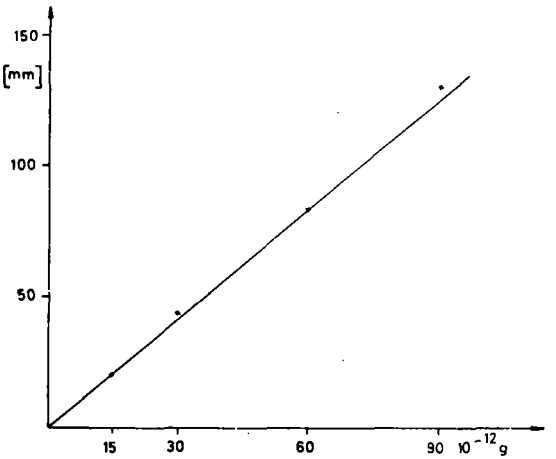

Fig. 4 Calibration curve for ^{1}N, O-TMS- $^{\omega}$N-TFA serotonin

Figures 3 and 4 represent respectively the recording of the monitored m/e 290 signal for injected volumes in the picogram range, and the calibration curve obtained when peak height values were plotted against injected amounts.

Using a similar procedure, calibration curves were built up for the catecholamines of interest.

Measure of the level of noradrenaline and adrenaline in rat tissue

The measure of catecholamines in human tissues is of general interest in the field of nervous and cardiovascular system studies. Rat tissues were here investigated in order to evaluate the analytical procedure and to determine the limit of detection in real life samples. The calibration curve at the pg level for the N-TFA-O-TMS derivatives of noradrenaline, adrenaline, and isoprenaline is shown in figure 5.

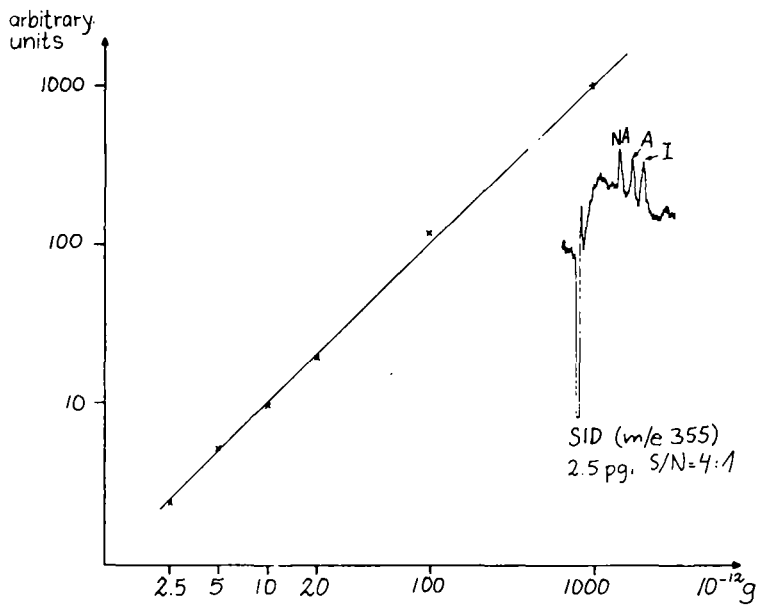

Fig. 5 **Calibration curve for N-TFA-O-TMS noradrenaline, adrenaline, and isoprenaline**

This concerns SID measurements at m/e 355. The recording of 2.5 pg per component is also shown; the S/N was measured to be 4 to 1. The extracts from rat tissues were processed and derivatized as described by Donike (2). Their content in the two catecholamines was obtained by calculation based on the signal from isoprenaline, which is added as an internal standard. It can be noted that the animals were killed under stress, which situation might have changed the catecholamine concentration in the various tissues.

In Figure 6a are reproduced recordings relative to a standard solution of N-TFA-O-TMS noradrenaline (peak number 1), adrenaline (peak number 2), and the internal standard isoprenaline (peak number 3). 0.5 ng of the internal standard per mg of tissue was added to each sample, except in the case of adrenal gland tissue, where 500 ng per mg of tissue was added.

The knowledge of the amount of internal standard per mg of tissue and the comparison of the noradrenaline and adrenaline signal with that of isoprenaline lead directly to the amount of both catecholamines per mg of tissue sample.

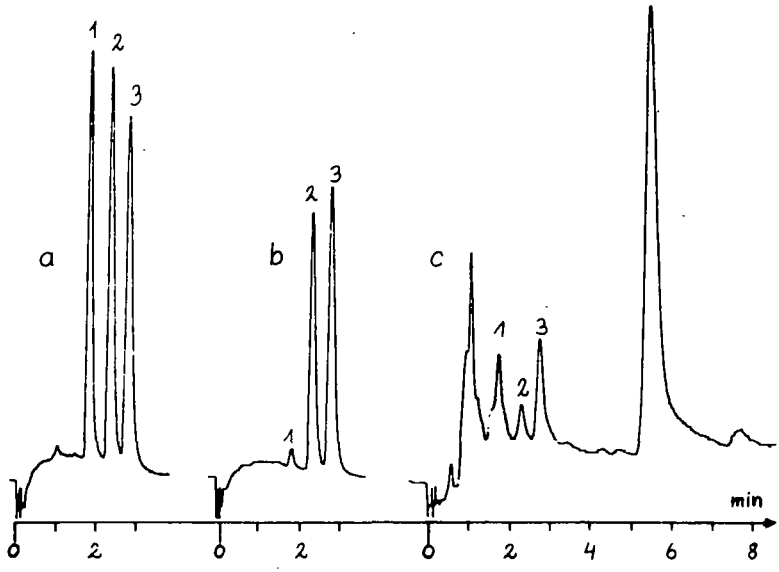

Fig. 6a: Measure of noradrenaline and adrenaline in rat tissue
(a: standard; b: adrenal gland; c: cerebellum)

Cerebellum tissue, for instance, was found to contain 0.35 ng of noradrenaline and 0.125 ng of adrenaline per g of tissue. The content in both catecholamines was also measured in the adrenal gland and, as shown in figure 6b in cerebrum, heart, and lung tissue.

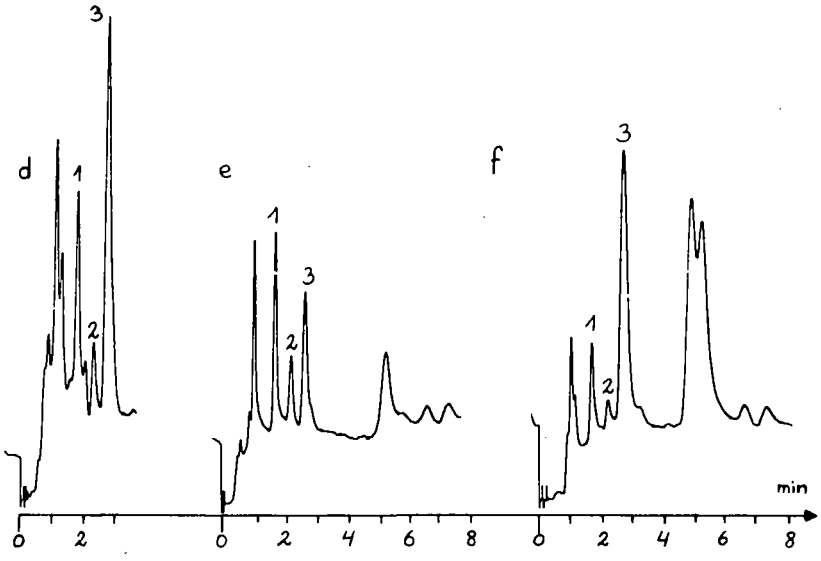

Fig. 6b: Measure of noradrenaline and adrenaline in rat tissue
(d: cerebrum; e: heart; f: lung)

Measure of norephedrine in man

Besides these measurements of catecholamines in various rat tissues, the level of a compound of a similar type was determined in man after different time periods following its intake.

The just described method of derivatization and the measure in single ion detection mode can also be used to determine the level of norephedrine in man. In our experiment, an 85 kg male subject was asked to take 50 mg of norephedrine hydrochloride. Blood samples were then drawn during a period of 14 hours, and 100 ng of ephedrine was added to one ml plasma from each sample. Each solution was extracted successively with ether, dilute hydrochloric acid, and ether, then dried, and submitted to the reagents forming the N-TFA-O-TMS derivatives of norephedrine and ephedrine. A 2 μl aliquot of each solution (i. e. about 1/50th of the sample amount) was then injected in the GC/MS system. This procedure thus leaves a large sample volume for repeated injections. The mass spectrometer was set to monitor the GC eluate at m/e 179, the most intense ion species in the mass spectra of the analyzed compounds.

Figure 7 shows the variation of the concentration of the norephedrine derivative with time. The concentration of the drug in blood was calculated by the peak height method with relation to the added internal standard. A maximum of about 200 ng/ml plasma was reached after two hours, and this level decreased to about 10 ng/ml plasma 14 hours after absorption of the drug.

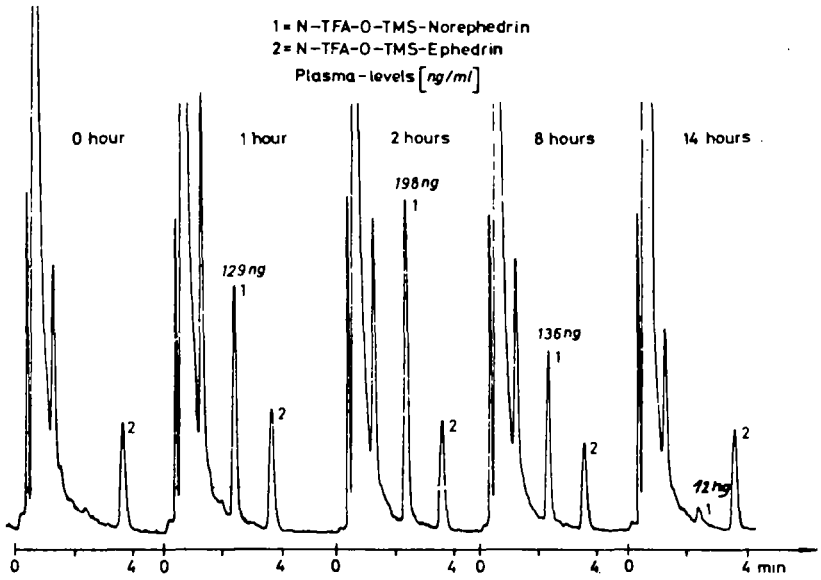

Fig. 7 Monitoring of norephedrine after intake of 50 mg norephedrine HCL

Measure of catecholamines with a directly coupled capillary column and MIS

The analysis procedure described so far for the determination and quantitation of phenolalkylamines in real life samples using packed column and SID was found to give satisfactory results. The unresolved doublet in the single ion trace obtained in the cerebrum rat tissue analysis shows, however, that more complex samples would require a higher specificity in the procedure. A higher specifity can be obtained by an increase in GC resolution (i. e. capillary column use) or by the use of multiple ion selection. Depending on the problem at hand, one might chose either of these techniques, or a combination of both. The standard solution of catecholamines and the rat cerebrum tissue sample were used to check the relevance of these techniques.

Figure 8 shows the detection of 1 pg each on column of noradrenaline, adrenaline, and isoprenaline after separation on a directly coupled OV-101 capillary column. The limit of detection is here determined by the noise at m/e 355 resulting from the column bleed.

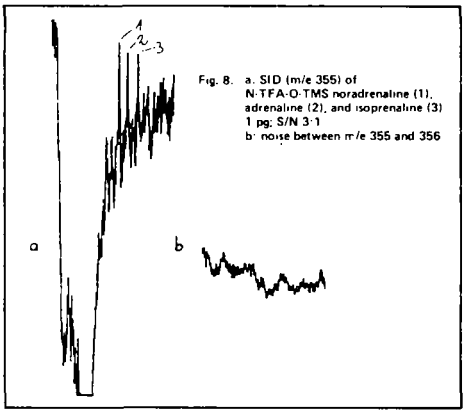

Fig. 8. a. SID (m/e 355) of N-TFA-O-TMS noradrenaline (1), adrenaline (2), and isoprenaline (3) 1 pg; S/N 3:1
b: noise between m/e 355 and 356

As shown in figure 9, the standard solution was measured in MIS mode at the low pg level. The three most intense peaks in the mass spectra were selected, i. e. m/e 73, 355, and 356. The increased resolution provided by the capillary column, and the measure of the intensity ratios of the three selected ionic species resulted in a highly increased specificity of the analysis.

Figure 10 shows the application of the method to the rat cerebrum tissue sample at a level close to the detection limit.

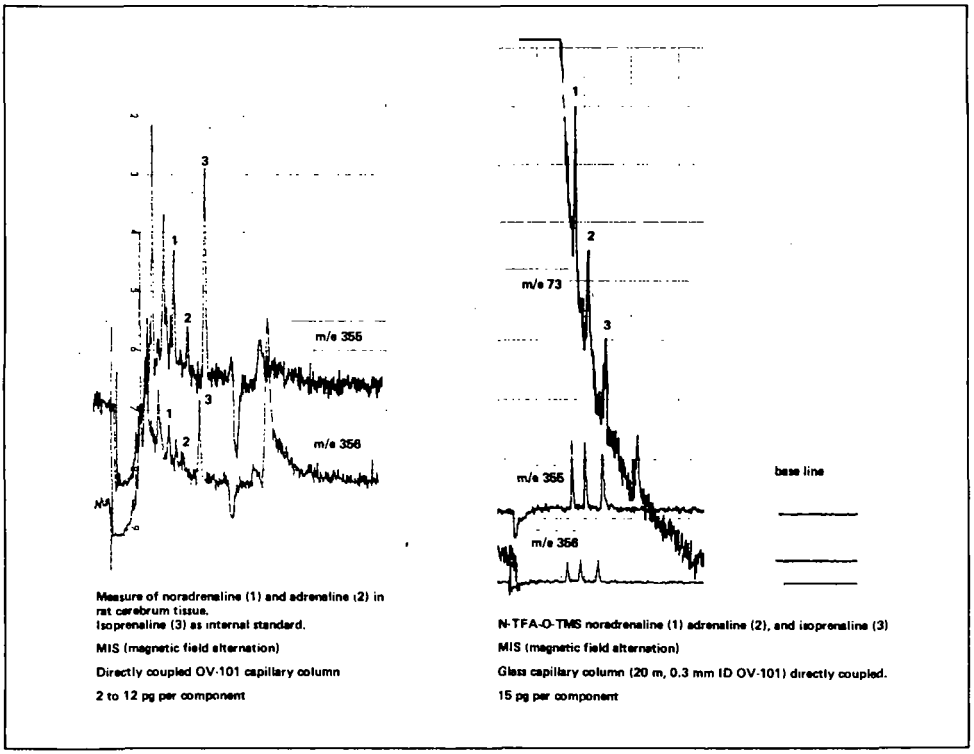

Measure of noradrenaline (1) and adrenaline (2) in rat cerebrum tissue.
Isoprenaline (3) as internal standard.

MIS (magnetic field alternation)

Directly coupled OV-101 capillary column

2 to 12 pg per component

N-TFA-O-TMS noradrenaline (1) adrenaline (2), and isoprenaline (3)

MIS (magnetic field alternation)

Glass capillary column (20 m, 0.3 mm ID OV-101) directly coupled.

15 pg per component

Conclusion

The sensitivity and specificity obtained with well designed GC/MS systems can be used to solve many detection problems in the field of biological science, as has been shown here in the case of several biogenic amines. Various possible analysis procedures have been investigated, involving the use of packed column, capillary column, SID, and MIS. The selection of the techniques which will best solve a given problem depends on the complexity of the sample, the required speed of analysis, and the required accuracy and precision of the quantitation. Capillary column overload by foreign compounds,and the concentration level of the compounds of interest have also to be taken into consideration.

References

(1) M. Donike, Chromatographia, **7**, 651 (1974)
(2) M. Donike, J. Chromatography, **103**, 91 (1975)

O-8

Fragmentation of the MO-TMS Derivatives of Cortisol and Ecdysterones. AMELIA HUNG, SERRINE S. LAU, WANDA G. STILLWELL and MARJORIE G. HORNING, Baylor College of Medicine, Houston, Texas 77025.

The MO-TMS derivatives of cortisol (M=636; 3-TMS, 2-$NOCH_3$), ecdysterone (M=941; 6-TMS, 1-$NOCH_3$) and 5β-hydroxyecdysterone (M=1029; 7-TMS, 1-$NOCH_3$) were prepared. The fragmentation pattern of the $NOCH_3$-TMS, $NOCH_3$-d_9TMS and the $NOCD_3$-d_9TMS derivatives were compared (LKB 9000). Characteristic ions were observed at m/e 361 and 246 formed by cleavage of ring D. The structures of these ions were confirmed by high resolution mass spectrometry. Because of their high molecular weight, the mass spectra of the derivatives of ecdysterone and 5β-hydroxyecdysterone were obtained with a Varian CH7. The base peaks in the spectra of ecdysterone and 5β-hydroxyecdysterone were observed at m/e 590 and 678, respectively. These ions were formed by cleavage of the side chain between C20 and C22. The concentration of cortisol in plasma and urine was quantified by selective ion detection (SID) using the ions at m/e 605. Ecdysterone was quantified by monitoring the ions at m/e 590. The response of the GC-MS-COM system (LKB 9000-PDP/12) was linear in the 1-100 ng range for cortisol and in the 32-100 ng range for ecdysterone.

O-9

Mass Spectra of Dihydrodiols. CARLA BUTLER, WANDA G. STILLWELL and MARJORIE G. HORNING, Baylor College of Medicine, Houston, Texas 77025

Most unsaturated aliphatic, heterocyclic and aromatic drugs are metabolized via epoxides to the corresponding dihydrodiols by the monooxygenase-epoxide hydrase enzyme complex. A number of these metabolites have been characterized in our laboratory by gas chromatography and mass spectrometry of the trimethylsilyl derivatives and corresponding deuterated analogs. Most aromatic drugs in which oxidation of the phenyl ring occurred had similar mass spectra characterized by an intense fragment ion at m/e 191 (80-100% RI). Pronethalol was an exception. Its mass spectrum exhibited a base peak at m/e 72 from cleavage of the side chain and an ion of low abundance at m/e 191. Also lacking the typical intense ion at m/e 191 was antipyrine. In this case the base peak at m/e 219 indicated that epoxidation of the heterocyclic ring, not the aromatic ring, had occurred. No characteristic fragment ion was found in the mass spectra of the corresponding dihydrodiols of the non-aromatic drugs but each had a unique spectrum which defined the structure. Safrole, alpha-terpineol, and several allylic barbiturates were among the non-aromatic compounds studied.

A Convincing Case for the Utilization of Electron Impact Mass Spectrometry for the Assignment of Configuration to Stereoisomers.

Mark M. Green and Jerrold L. Martin
Department of Chemistry, Michigan State University
East Lansing, Michigan 48824

As demonstrated by the classic examples in Figure 1, the spatially dependent interaction of functional groups in cyclic molecules is in the satisfying historical and time tested tradition for the assignment of configuration to stereoisomers.[1] With this in mind, one is readily convinced that the chemistry observed in mass spectrometers is of a nature to be ideally suited for such a configurational task. This is so because this chemistry is replete with now well understood spatially dependent rearrangement reactions.[2] An excellent early example of this may be found in Brion's[3] work on the isomers of 4-tertiary butylcyclohexanol (Figure 2). As suggested,[3] deuterium labelling demonstrated that the C-4 tertiary hydrogen was eliminated stereospecifically in the trans isomer.[4]

Figure 1

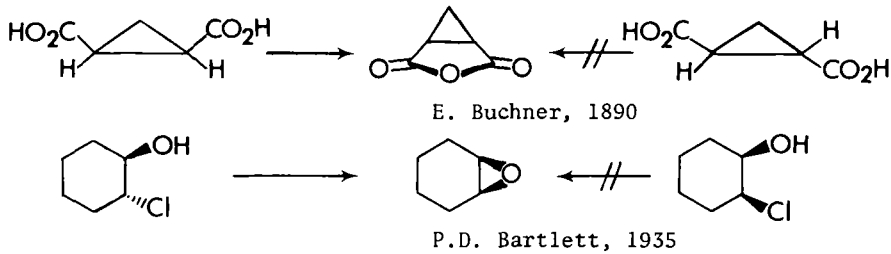

Figure 2

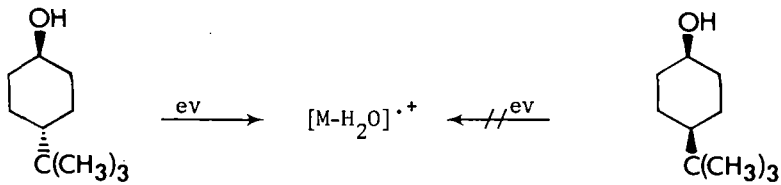

In the light of the now understood mechanism for water loss in cyclic alcohols,[4] Brion's observations constituted a stereochemical assignment of trans to the isomer which exhibited intense elimination of water on electron impact. This was, of course, already known in this system, but the principle is established.

Certain stereoisomeric alcohols do not give rise to overtly different mass spectra although the mechanism of the process strongly suggests that different hydrogen atoms are involved in the elimination. In principle, therefore, identification of the stereoisomeric hydrogen involved would allow an assignment of configuration. This may be seen in cis and trans 4-isopropyl cyclohexanol. The overt spectra are very similar and yet on deuterium labelling the elimination of water reveals itself as stereospecific (Figure 3).[5] Although again here, there is no question of the

Figure 3

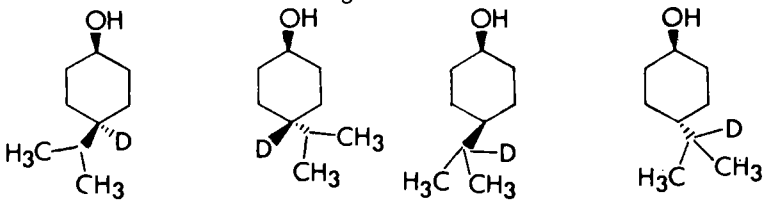

%				
M-DOH	13	81	82	17
M-HOH	87	19	18	83

isomeric assignment,[6] as seen below, these ideas do find use in systems where stereochemical questions are open.

MacLeod and Wells[7] were faced with the problem of assigning stereochemistry to the isomeric alcohols found in Figure 4.

Figure 4

A 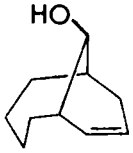 B 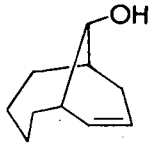

Their satisfying approach to the problem was to add deuterium to the double bond under homogeneous conditions known to lead to exo addition. The isomer in hand lost only light water (H_2O) demonstrating, based on previous understanding of the elimination mechanism,[8] that the material was (A).

This mass spectrometric approach to stereoanalytical chemistry may utilize any of a wide range of spatially dependent rearrangements.[2] Thus Lansbury was confronted by a stereoanalytical problem in an attempted synthesis of Hirsutic acid. The two isomeric possibilities are ixhibited in Figure 5.

Figure 5

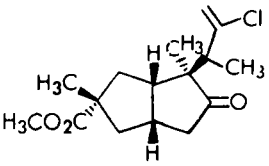

C

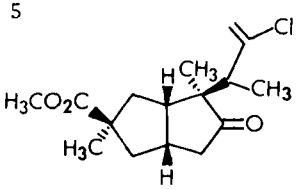

D

This otherwise stubborn stereochemical problem was solved by the observation that only one isomer lost the elements of CH_3OH (from the M-C_4H_4Cl McLafferty rearrangement ion). Only in C is the carbomethoxy group placed in proximity to the abstractable hydrogens adjacent to the carbonyl group. Replacement of these hydrogens by deuterium confirmed the stereospecific elimination and thereby the stereoisomeric assignment.[9]

A similar situation was encountered by Gray and Pryce[10] in stereochemical assignments in the gibberell in model compounds shown in Figure 6. After study of a seties of related molecules with deuterium substituted for H^*,

Figure 6

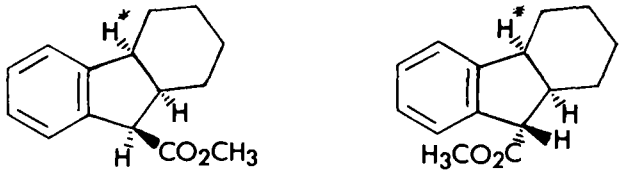

E F

these workers found that only isomers of relative configuration F (Figure 6)[10] eliminated the elements of the carbomethoxy side chain plus that hydrogen (H^*), which is, as seen, accessable only in that relative configuration.

In another area, the two stereoisomers portrayed in Figure 7 were produced as potential precursors in a synthesis of lanosterol.[11]

Figure 7

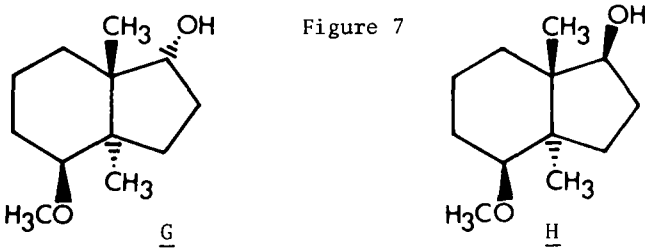

G H

Inspection of models readily demonstrates that only the carbinol configuration portrayed in G allows approach of the hydroxyl oxygen to the α-methyl group and thereby to abstraction of hydrogen through the favored six membered ring transition state.[2,12] Measurement of the mass spectra of the isomers G and H at ca 100°C and 15ev shows that loss of water is markedly more intense from one of the isomers, which we assign as G, while loss of methanol, which is in a constant configurational arrangement in G and H, is the same for both isomers. The spectra are exhibited in Figure 8. At higher temperatures and higher beam energies, the distinction continues, but is lessened. Meyerson and Weitkamp[13] have pointed out that lowering the energy input in all forms, is key to this stereoanalytical utility.

Figure 8

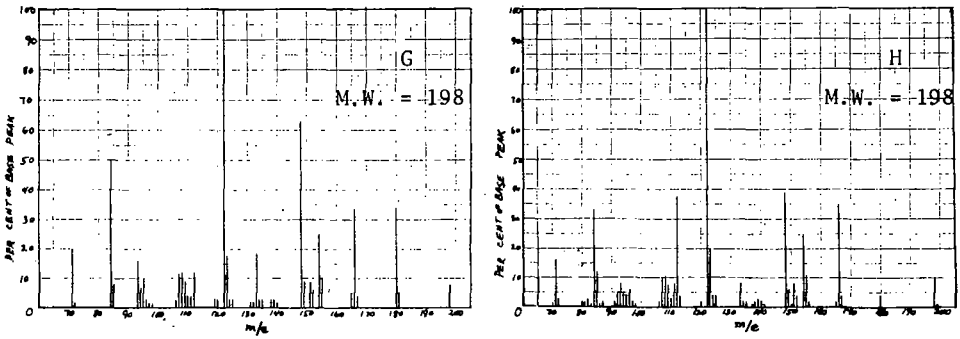

References

1. E.L. Eliel, Stereochemistry of Carbon Compounds, McGraw-Hill, 1962, p. 185, 186.

2. M.M. Green, Mass Spectrometry and the Stereochemistry of Organic Molecules, in Topics in Stereochemistry, Vol. 9, Ed. by E.L. Eliel and N.L. Allinger, Wiley-Interscience, 1975 (in press).

3. C.E. Brion, Analytical Chem., 37, 1706 (1965); C.E. Brion and L.D. Hall, J. Amer. Chem. Soc., 88, 3661 (1966).

4. Z.M. Akhtar, C.E. Brion, and L.D. Hall, Org. Mass Spectrometry, 7, 647 (1973); M.M. Green, R.J. Cook, J.M. Schwab, and R.B. Roy, J. Amer. Chem. Soc., 92, 3076 (1970).

5. M.M. Green and R.B. Roy, ibid., 92, 6368 (1970).

6. E.L. Eliel, N.L. Allinger, S.J. Anguyal, and G.A. Morrison, Conformational Analysis, Interscience Publ., 1965.

7. J.K. MacLeod and R.J. Wells, J. Amer. Chem. Soc., 95, 2387 (1973).

8. J.K. MacLeod, M. Vegar, and R.J. Wells in, Recent Developments in Mass Spectroscopy, Ed. by K. Ogata and T. Hayakawa, Univ. of Tokyo Press, 1970, 1197-1202.

9. P.T. Lansbury, N.Y. Wang, and J.E. Rhodes, Tetrahedron Lett., 1829, (1971).

10. R.T. Gray and R.J. Pryce, J. Chem. Soc., Perkin II, 1974, 955.

11. J.L. Martin and W. Reusch, unpublished work at Michigan State University.

12. W. Benz and K. Biemann, J. Amer. Chem. Soc., 86, 2375 (1964); S. Meyerson and L.C. Leitch, ibid., 86, 2555 (1964); P.J. Derrick, A.M. Falik, and A.L. Burlingame, ibid., 95, 437 (1973).

13. S. Meyerson and A.W. Weitkamp, Org. Mass Spectrometry, 1, 659 (1968).

The Comparable Low Hydrogen Deuterium Isotope Effects in Intramolecular Hydrogen Transfer Rearrangement Reactions in Mass Spectrometers and in Solution: The Reason for the Low Isotope Effect of the McLafferty Rearrangement.

Mark M. Green, J.M. Moldowan, Juan Artus, and Mark Armstrong
Department of Chemistry, Michigan State University
East Lansing, Michigan 48824

The regiospecific γ-hydrogen transfer observed in alkoxy radicals and triplet ketones are analogs in quite some depth to the formally similar hydrogen transfers observed in the molecular cation radicals of alcohols and ketones (McLafferty rearrangement) respectively.[1,2] Nevertheless, and significantly, the isotope effects for the reactions occuring in the mass spectrometer are nearly unity[3,4] while the neutral analogs exhibit high discrimination against transfer of deuterium[5,6] (Figure 1).

Figure 1.

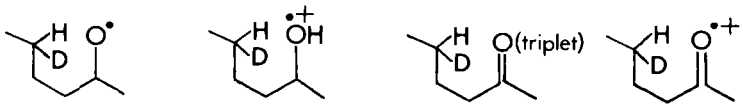

k_H/k_D	4.6[1]	1.0[1]	5.7[5(a)]	1.0[3(b)]

There exists a ready explanation for the differing isotope effects in these clearly similar intramolecular γ-hydrogen transfers (Figure 1). Free radical abstractions of carbon bound hydrogen occur with a wide range of hydrogen deuterium isotope effects. These isotope effects may be related to the energy of activation for the process and through transition state theory to the extent of carbon hydrogen bond breaking in the activated complex. Thus, highly energetic abstracting radicals, or decreased carbon hydrogen bond strength, lead to lowered isotope effects. One set of data often used to demonstrate this correlation is shown in Figure 2. There is a great deal of support for these ideas.[7,8]

Figure 2

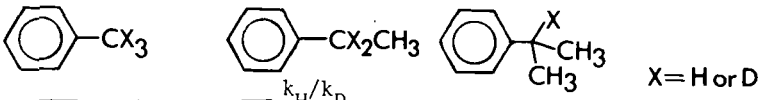

	k_H/k_D		
Br•	4.8	2.7	1.8
Cl•	1.3	—	—

Now, one may see the radical cations exhibited in Figure 1 as doubly insulted by the electron denying character of both sources of reactivity. This must lead to abstraction of carbon bound hydrogen with lowered energy of activation compared to the related neutral radicals. As seen above, this would lead to decreased isotope effects (Figure 2)[7,8] in line with the observations (Figure 1). Indeed, the electron impact induced reactions (Figure 1) show kinetic characteristics commensurate with extremely low energies of activation.[9]

If this view is correct, the decreased isotope effects (Figure 1) should be observed whatever the source of the cation radicals. The Hofmann-Loeffler-Freytag reaction[10] of chiral γ-deuterated 2-hexyl N-chloroamine in sulfuric acid gives us the opportunity for determining the isotope effect and the stereoselectivity of an intramolecular γ-hydrogen abstraction by a cation radical in condensed phase. Figure 3 exhibits the compounds utilized, the reactions studied, and the deuterium incorporation results.

Figure 3[a]

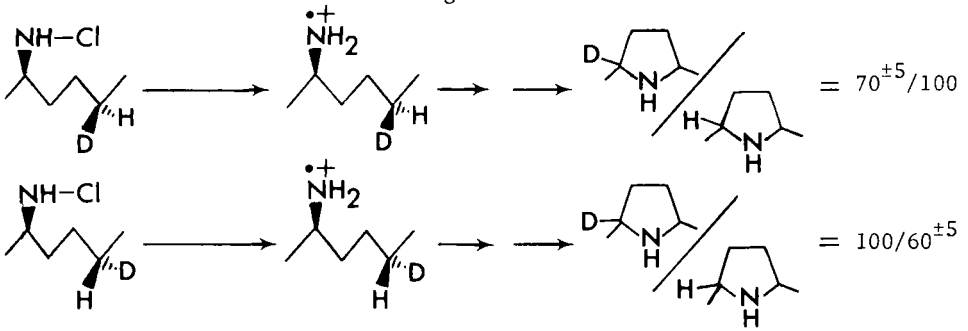

---

a. The 2,5-dimethylpyrrolidine cis and trans isomers were separated and exhibited d_0/d_1 ratios within experimental error. The values shown are averages. The pyrrolidines were obtained in ca 20% yield utilizing a 500 watt flood lamp and a few crystals of ferrous ammonium sulfate on the N-chloroamine in sulfuric acid,[11,12] at 10°C. The precursor chiral deuterated 2-hexylamines were prepared from the deuterated chiral 2-hexanols[1] by a known stereospecific route.[13]

The numerical results in Figure 3 may be transposed into both the relative rates for abstraction fo the diastereotopic deuterium atoms (by external comparison)[14] and the isotope effect (k_H/k_D).[15] The results of this calculation as well as comparable data on γ-hydrogen transfer for 2-hexyloxy radical, 2-hexanol radical cation, 2-hexyl chloride radical cation and the carbonyl systems are given in Table I.

Table I

k_a/k_b[c]	1.54	1.10	1.28	1.23	—	—
k_H/k_D	1.1[d]	1.0[e]	1.0[e]	4.6[f]	5.7[g]	1.1[g]

---

a. Current work; b. reference 1; c. all values ±.05; d. ±.4; e. approximate; f. ±.5; g. See Figure 1.

The preferential abstraction of H_a over H_b ($k_a/k_b > 1$) for 2-aminohexane radical cation correlates this reaction with the other processes shown (Table I). The lack of discrimination against deuterium in all the cation radicals fits the proposal offered above that these intramolecular hydrogen transfers occur with lowered energies of activation and earlier, more reactant resembling, transition states than their neutral counterparts.

The similar isotope effects for 2-hexanone triplet and 2-hexyloxy radical and the parallel decrease with introduction of positive charge support proposals of the parallel nature of these intermediates.[16]

Acknowledgement

We are grateful to the National Institutes of Health, General Medical Sciences, for generous support of this research.

References

1. For alcohol molecular ions and alkoxy radicals see: (a) M.M. Green, J.G. McGrew II, and J.M. Moldowan, J. Amer. Chem. Soc., 93, 6700 (1971); (b) M.M. Green, J.M. Moldowan, and J.G. McGrew II, J. Org. Chem., 39, 2166 (1974); and references therein.

2. For the carbonyl analogy see S. Meyerson and J.D. McCollum, in Advances in Analytical Chemistry and Instrumentation, Vol. 2, Wiley and Sons, N.Y., 1963, p. 184 ff; F.P. Boer, T.W. Shannon, and F.W. McLafferty, J. Amer. Chem. Soc., 90 7239 (1968); D.G.I. Kingston, J.T. Bursey, and M.M. Bursey, Chem. Revs., 74, 215 (1974); G. Eadon, J. Diekman, and C. Djerassi, J. Amer. Chem. Soc., 92, 6205 (1970); J. Diekman, J.K. MacLeod, C. Djerassi, and J.D. Baldeschwieler, ibid., 91, 2069 (1969); C. Fenselau, J.L. Young, S. Meyerson, W.R. Landis, E. Selke, and L.C. Leitch, ibid., 91, 6847 (1969); N.C. Deno, R. Fishbein, and J.C. Wyckoff, ibid., 92, 5274 (1970); F.W. McLafferty, and W.T. Pike, ibid., 89, 5953 (1967); S. Meyerson, Int. J. Mass Spectrom. and Ion Phys., 1, 309 (1968); and references throughout these papers.

3. For the McLafferty rearrangement isotope effect see: (a) Kingston et. al., in reference 2 and references therein; (b) J.K. MacLeod and C. Djerassi, J. Amer. Chem. Soc., 89, 5182 (1967); (c) reference 1.

4. For alcohol molecular ion isotope effects see: (a) W. Benz and K. Biemann, J. Amer. Chem. Soc., 86, 2375 (1964); (b) S. Meyerson and L.C. Leitch, ibid., 86, 2555 (1964); (c) M.M. Green, R.J. Cook, J.M. Schwab, and R.B. Roy, ibid., 92, 3076 (1970); (d) reference 1.

5. For ketones see: (a) D.R. Coulson and N.C. Yang, ibid., 88, 4511 (1966); (b) A. Padwa and W. Bergmark, Tetrahedron Letters, 5795 (1968); (c) F.D. Lewis, J. Amer. Chem. Soc., 92, 5602 (1970).

6. For alkoxy radicals see: (a) reference 1; (b) C. Walling and J.A. McGuiness, J. Amer. Chem. Soc., 91, 2053 (1969); (c) G.F. Larson and R.D. Gillion, ibid., 97, 3444 (1975).

7. R.A. More O'Ferrall, J. Chem. Soc. (B), 785 (1970); W.H. Saunders, Jr., J. Chem. Soc. (Chem Comm.), 850 (1973); K.H. Lee, S.E. Loke, and G.H. Yeoh, J. Chem. Soc. (Perkin II), 10 (1975); J.R. Keefe and N.H. Munderloh, J. Chem. Soc. (Chem. Comm), 17 (1974); M. Simonyi, I. Fitos, J. Kardos, I. Lukovits, and J. Pospisil, ibid., 252 (1975); P.J. Smith and L.M. Noble, Can. J. Chem., 53, 263 (1975); L. Melander, Acta Chem. Scand., 25, 3821 (1971); J. Bigeleisen, Pure and Applied Chemistry, 8, 217 (1964); W.H. Saunders, Jr., A.F. Cockerill, Mechanisms of Elimination Reactions, Wiley-Interscience, N.Y., 1973, p. 71 ff; W.A. Pryor, and K.G. Kneipp, J. Amer. Chem. Soc., 93, 5584 (1971); R.P. Bell, Chem. Soc. Revs., 3 (4), 513 (1974) and numerous references therein; K.B. Wiberg, Chem. Revs., 55, 713 (1955); F.H. Westheimer, ibid., 61, 265 (1961).

8. W.A. Pryor, Free Radicals, McGraw-Hill Publ., 1966, p. 162, 163, 175; E.S. Huyser, Free Radical Chain Reactions, Wiley-Interscience, 1970, p. 106; G.A. Russell in Free Radicals, Vol. I, Ed. by J.K. Kochi, Wiley-Interscience, 1973, p. 311 ff; K.B. Wiberg and E.L. Motell, Tetrahedron, 19, 2009 (1963); K.B. Wiberg and L.H. Slaugh, J. Amer. Chem. Soc., 80, 3033 (1958).

9. The low energies of activation (A.P. - I.P.) for elimination reactions such as loss of water from alcohol cation radicals and the McLafferty rearrangement may be correlated with the low intensity molecular ions observed with rearrangement is possible. These ideas are discussed in: D.H. Williams and I. Howe, Principles of Organic Mass Spectrometry, McGraw-Hill, 1972, Chapter 4; M.M. Green in Topics in Stereochemistry, Vol. 9, Ed. by E.L. Eliel and N.L. Allinger, Wiley-Interscience, 1975; R.G. Cooks, J.H. Beynon, R.M. Caprioli, and G.R. Lester, Metastable Ions, Elseiver Publ., 1973.

10. W. Carruthers, Some Modern Methods of Organic Synthesis, Cambridge University Press, 1971, p. 172 ff; J.W. Wilt in, Free Radicals, Vol. I, Ed. by J.K. Kochi, Wiley-Interscience, 1973, p. 390 ff. and references therein.

11. E. Schmitz and D. Murawski, Chem. Ber., 99, 1493 (1966).

12. E.J. Corey and W.R. Hertler, J. Amer. Chem. Soc., 82, 1657 (1960).

13. O. Mitsunobu, M. Wada, and T. Sano, ibid., 94, 679 (1972).

14. K. Mislow and M. Raban, Top. Stereochem., 1, 1 (1967).

15. D.Y. Curtin and D.B. Kellom, J. Amer. Chem. Soc., 75, 6011 (1953); see reference 1.

16. P.J. Wagner, Accounts Chem. Res., 4, 168 (1971).

HIGH PRESSURE ION-MOLECULE REACTIONS IN FLUOROMETHANES

M. Joanne Pabst, Hiok Seng Tan and J. L. Franklin
Chemistry Department, Rice University
Houston, Texas 77001

ACKNOWLEDGMENT

The authors are pleased to acknowledge support of this work by the Robert A. Welch Foundation.

Conventional high pressure mass spectrometric techniques have been used to study the ion molecule reactions occurring in CH_3F, CH_2F_2, CHF_3, and CF_4 at pressures up to one torr. At low pressures our results are in good agreement with studies reported by other workers,[1-10] but at elevated pressures we were able to observe a number of higher order reactions which have not been reported previously.

The experiments were carried out in a quadrupole mass spectrometer equipped with a conventional high pressure source. Both have been described in detail elsewhere.[11]

In CH_3F the major primary ions are the parent ion CH_3F^+, and the fragments CH_2F^+ and CH_3^+. The parent ion undergoes a proton or hydrogen atom transfer reaction producing CH_3FH^+. The protonated parent ion then undergoes a nucleophilic displacement reaction, condensing with a neutral and eliminating a HF molecule to form $(CH_3)_2F^+$. CH_3^+ undergoes a hydride transfer reaction producing CH_2F^+, and CH_2F^+ reacts through a third order process also forming $(CH_3)_2F^+$. $(CH_3)_2F^+$ undergoes a series of condensation-elimination reactions which involve condensation of the ion with a neutral forming an excited collision complex which upon further collision eliminates H_2 and/or HF molecules to form $C_3H_8F^+$ and three other products. $C_3H_8F^+$ undergoes a similar sequence producing $C_4H_8F^+$ and three other products, and $C_4H_8F^+$ begins a third sequence forming four additional products. Nineteen stable condensation products are also observed in the high pressure spectrum. These are produced by collisional stabilization of excited collision complexes.

In CH_2F_2 the major primary ions are the parent, $CH_2F_2^+$, and the fragments CH_2F^+, CHF_2^+, CHF^+, and CF^+. As in CH_3F, the parent ion reacts to form the protonated parent which then undergoes a nucleophilic displacement reaction producing a dialkylfluoronium ion, in this case $C_2H_4F_3^+$. The fragments undergo fluoride ion transfer reactions producing CH_2F^+. CH_2F^+ condenses with the neutral forming an excited collision complex which upon further collision can be stabilized forming the stable condensation product, $C_2H_4F_3^+$ (major product), or can react producing $C_2H_6F^+$ (minor product). $C_2H_4F_3^+$ and $C_2H_6F^+$ then undergo a series of reactions producing several higher order products. At high pressures 4 additional stable condensation products are also observed.

In CHF_3 only a small amount of the parent ion is observed, the major primary ions being the fragments CF_3^+, CF_2^+, CF^+ and CHF_2^+. The fragments undergo fluoride ion transfer reactions producing CHF_2^+ which comprises 98.5% of the total ion intensity by 75μ. CHF_2^+ reacts only very slowly with the parent neutral producing a small amount of condensation product, $CHF_3 \cdot CH_2F^+$, at high pressures. Several additional ions were observed at high pressures but were believed to be results of a small impurity in the system.

Only fragments- CF_3^+, CF_2^+, CF^+, F^+, C^+, CF_3^{++}, and CF_2^{++} - are observed in the primary spectrum of CF_4. The singly charged fragments undergo fluoride ion transfer reactions producing CF_3^+ which appears to be quite unreactive with the parent neutrals. The only condensation product observed at high pressures is a very small amount of $CF_4 \cdot CF^+$.

Comparing the results obtained for the four systems, it is obvious that reactivity decreases with increasing fluorine substitution in the neutral. This is evidenced not only by the fewer products formed in the more substituted systems, but also by the slower rates of the reactions which do occur.

Both experimental and theoretical rate constants have been calculated whenever possible, and are listed in Table 1. In comparing the reactions of a particular ion with different neutrals, the theoretical rates predict the same ordering of reactivity as was experimentally observed. Since the theoretical rates are actually measures of collision frequencies, this indicates that the major factors contributing to the reactivity may be the parameters which determine collision frequency, i.e., polarizability, dipole moment, and reduced mass.

REFERENCES

1. A. G. Marshall and S. E. Buttrill, Jr., J. Chem. Phys., 52, 2752 (1970)
2. N. A. McAskill, Aust. J. Chem. 23, 2301 (1970)
3. A. A. Herod, A. G. Harrison and N. A. McAskill, Can. J. Chem. 49, 2217 (1971)
4. A. G. Harrison, G. P. Nagy, M. S. Chin and A. A. Herod, Int. J. Mass Spectrom. Ion Phys., 9, 287 (1972)
5. J. M. S. Henis, M. D. Loberg, M. J. Welch, J. Amer. Chem. Soc., 96, 1665 (1974)
6. R. J. Blint, J. B. McMahan, J. L. Beauchamp, J. Amer. Chem. Soc., 96, 1269 (1974)
7. A. G. Harrison and N. A. McAskill, Aust. J. Chem., 24, 1611 (1971)
8. J. B. McMahan, R. J. Blint, D. P. Ridge, and J. L. Beauchamp, J. Amer. Chem. Soc., 94, 8934 (1972)
9. N. A. McAskill, Aust. J. Chem., 23, 893 (1970)
10. J. L. Beauchamp, D. Holtz, S. D. Woodgate and S. L. Patt, J. Amer. Chem. Soc., 94, 2798 (1972)
11. S. M. Schildcourt and J. L. Franklin, J. Chem. Phys., 51, 4055 (1969)
12. S. K. Gupta, E. G. Jones, A. G. Harrison and J. J. Myher, Can. J. Chem. 45, 3107 (1967)

TABLE 1. EXPERIMENTAL AND THEORETICAL RATE CONSTANTS
($k \times 10^{10}$ in cc/molecule sec.)

	k experimental		k theory[a]
CH_3F	15 eV	200 eV	
CH_3F^+	18.6	23	20.1
CH_3^+	7.8	10.9	24.4
CH_4F^+	9.5	13.6	20.0
CH_2F^+	34.5[b]	28.0[b]	-
$C_2H_6F^+$	2.3[b]	1.5[b]	-
CH_2F_2	15 eV	200 eV	
CF^+	-	11.2	18.7
CHF^+	-	13.2	18.6
CHF_2^+	2.6	6.0	16.9
$CH_2F_2^+$	11.3	17.7	16.8
CH_2F^+	11.0[b]	16.1[b]	-
$C_2H_4F_3^+$	0.516[b]	0.516[b]	-
$C_2H_6F^+$	0.588[b]	-	-
CHF_3		200 eV	
CF^+		8.7	16.2
CF_2^+		9.3	14.2
CF_3^+		6.4	13.3
F^+		19.6	19.0
CF_4		200 eV	
CF^+		3.3	8.3
CF_2^+		2.7	7.0
C^+		12.3	12.2
F^+		18.7, 8.2	10.0

a theoretical rate constants calculated from formula:[12]

$$k = 2\Pi e \left(\frac{\alpha}{\mu}\right)^{1/2} + \frac{2\Pi e \mu_D}{\mu} \left(\frac{\mu i}{2\varepsilon_e}\right)^{1/2} \ln\left[1 + 2\left(\frac{\mu \varepsilon_e}{\Pi k \mu i T}\right)^{1/2}\right]$$

b $k \times 10^{27}$ in $cm^6/molecule^2$-sec

MASS SPECTROMETRIC STUDY OF ION-MOLECULE REACTIONS IN C_2H_3F AND $C_2H_2F_2$

H. S. Tan, M. Joanne Pabst and J. L. Franklin
Chemistry Department, Rice University
Houston, Texas 77001

ACKNOWLEDGMENT

The authors are pleased to acknowledge support of this work by the Robert A. Welch Foundation.

Previous studies of ion-molecule reactions in C_2H_3F[1-4] and in CH_2CF_2[7,8] have been made at low to medium pressures but a limited amount of work has been done on C_2H_3F[5,6] at elevated pressures. The present investigation was undertaken to determine the effect of pressure and energy upon product distribution and reaction order and rate.

A quadrupole mass filter furnished with a high pressure source capable of operating at pressures up to about one torr was employed. The operation of the instrument and techniques employed have been described previously.[9] Nominal electron energies of 12.5 and 200 eV and a source field strength of 10.2 v/cm were used. No electron beam collimation magnets were employed in order to eliminate discrimination between primary and secondary ions. Source pressure was measured directly with a MKS Baratron pressure meter Type 77, which was calibrated up to 50μ pressure by a McLeod gauge. The ion source temperature remained at approximately 44°C as measured by a Chromel Alumel thermocouple.

C_2H_3F: At 12.5 eV electron energy initially only $C_2H_3F^+$ was detected.[10] Therefore, the consecutive reactions of the $C_2H_3F^+$ alone could be followed up to a pressure of 385μ. The rate of decay of $C_2H_3F^+$ was found to be third order with a rate constant of 1.61×10^{-25} cc^2 $molecule^{-2}$ sec^{-1}. At low pressures the $C_3H_3F_2^+$, $C_3H_4F^+$, $C_3H_5^+$, $C_4H_5F^+$ and $(C_2H_3F)_2^+$ are produced by the parent ion. The product distribution ratio of $C_3H_3F_2^+$: $C_3H_4F^+$:$C_3H_5^+$ has been determined to be 0.66:0.17:0.17, in good agreement with the third order values obtained by Harrison et al.[1,2] and the second order distribution obtained from the ion cyclotron studies[3,4]. The principal reaction sequences of $C_3H_3F_2^+$, $C_3H_4F^+$ and $C_3H_5^+$ are as follows:

$$C_3H_3F_2^+ \xrightarrow{2M} C_5H_6F_3^+ \xrightarrow{2M} C_7H_9F_4^+ \xrightarrow{2M} C_9H_{12}F_5^+,\ C_9H_{11}F_4^+ \qquad (1)$$

$$C_3H_4F^+ \xrightarrow{2M} \begin{cases} C_5H_7F_2^+ \xrightarrow{2M} C_7H_{10}F_3^+ & (2a) \\ C_5H_6F^+ \xrightarrow{2M} C_7H_9F_2^+ & (2b) \end{cases}$$

$$C_3H_5^+ \xrightarrow{2M} C_5H_7^+,\ C_5H_8F^+ \qquad (3)$$

where M represents the C_2H_3F molecule.

At 200 eV electron energy, the fragment ions $C_2H_2^+$, $C_2H_3^+$, C_2HF^+, $C_2H_2F^+$ and the parent ion $C_2H_3F^+$ comprise about 90% of the total ionization at near zero pressure. The ionic products from the parent ion are identical to those obtained in the 12.5 eV study. Except at pressures higher than 400μ, the $(C_2H_3F)_3^+$ and $(C_2H_3F)_4^+$ produced by the successive reaction of $(C_2H_3F)_2^+$ can also be observed. The $C_2H_2^+$ and C_2HF^+ mainly react by charge transfer to form the $C_2H_3F^+$. The $C_2H_2F^+$ reacts with C_2H_3F to form $C_2H_3^+$, $C_2H_4F^+$, CHF_2^+, $C_2H_3F_2^+$, and $C_4H_4F^+$. The $C_2H_3^+$ reacts to produce both $C_2H_4F^+$ and $C_4H_5^+$. At higher pressures, the secondary $C_2H_3F_2^+$,

reacts further by successive addition of a molecule to form $MC_2H_3F_2^+$, $M_2C_2H_3F_2^+$ and $M_3C_2H_3F_2^+$. The $C_2H_4F^+$ also reacts successively with the C_2H_3F to form $C_4H_6F^+$, $C_6H_8F^+$ and $C_8H_{11}F_2^+$. The $C_4H_5^+$ AND CHF_2^+ may react respectively to form $C_6H_7^+$ and $C_3H_3F_2^+$.

CH_2CF_2: At 12.5 eV electron energy, only $CF_2CH_2^+$ is observed.[11] $CF_2CH_2^+$ reacts only by a third order process to form $(CF_2CH_2)_2^+$. The rate constant[7,8] was measured to be 5.98 x 10^{-26} cc^2 $molecule^{-2}$ sec^{-1}. At higher pressures (above 3.5μ), three main ionic products $C_3H_2F_3^+$, $C_2H_3F_2^+$ and $(CF_2CH_2)_3^+$ and the minor ions $C_3H_3F_2^+$ and $C_4H_3F_3^+$ are formed by the further reaction of $(CF_2CH_2)_2^+$. The further reactions of the three main ionic products may be accounted by the following schemes,

$$C_3H_2F_3^+ \xrightarrow{2M} MC_3H_2F_3^+ \xrightarrow{2M} M_2C_3H_2F_3^+ \qquad (4)$$

$$C_2H_3F_2^+ \xrightarrow{2M} MC_2H_3F_2^+ \xrightarrow{2M} (M_2C_2H_3F_2^+,\ M_2C_2H_2F^+) \qquad (5a)$$

$$\xrightarrow{M} M_2HF_2^+ \qquad (5b)$$

and $$(CF_2CH_2)_3^+ \xrightarrow{2M} M_2C_2HF^+ \xrightarrow{2M} M_3C_2HF^+ \qquad (6)$$

where M represents the CF_2CH_2 molecule.

At 200 eV electron energy, the mass spectrum of 1,1 difluoroethylene is complicated even at a pressure as low as 0.22μ. All together there are 16 primary ions, C^+(3.1%), CH^+(2.8%), CH_2^+(11.3%), F^+(1.3%), C_2^+(2.1%), C_2H^+(2.3%), $C_2H_2^+$(2.8%), CF^+(17.3%), CHF^+(1.1%), CH_2F^+(13%), C_2F^+(0.6%), C_2HF^+(10.3%), $C_2H_2F^+$(16.4%), CF_2^+(0.7%), $C_2HF_2^+$(1.8%) and $CF_2CH_2^+$(11.0%). However, all the primary ions except F^+, CF^+, CHF^+, CH_2F^+ and $C_2H_2F^+$ may undergo charge transfer to form the parent ion $CF_2CH_2^+$, which reaches about 45% of total ionization at 35μ pressure. Although $CF_2CH_2^+$ is mainly produced by charge transfer, the ionic products produced from the $CF_2CH_2^+$ at 200 eV are in general similar to those at the 12.5 eV study described earlier. The F^+ and CHF^+ may react to form $C_2H_2F^+$. The second order characteristic reaction of CF^+ may produce $C_2H_2F^+$ and CHF_2^+, while the $C_2H_2F^+$ reacts to form $C_2H_3F_2^+$, $C_3H_3^+$, $C_3H_4F^+$, $C_4H_3F_2^+$ and $C_3H_3F_2^+$. CH_2F^+ reacts in a third order process, which give a rate constant of 7.8 x 10^{-26} cc^2 $molecule^{-2}$ sec^{-1} to produce CF_3^+ and $C_2H_3^+$. At higher pressures most of the secondary ions undergo reactions which involve addition of a molecule of CH_2CF_2 and elimination of a HF molecule from the products.

The disappearance rate constants of the primary and secondary ions in both C_2H_3F and CF_2CH_2 systems are shown in Table 1 and 2. In the C_2H_3F system the rate constants of $C_2H_3F_2^+$, $C_3H_4F^+$, $C_3H_5^+$ increase in that order. Similarly, in the CF_2CH_2 system the rate constants of $C_3H_2F_3^+$, $C_3H_3F_2^+$, $C_3H_4F^+$ also increase in that order. Evidently, each successive substitution of an H atom by an F atom to the analogous $C_3H_5^+$ decreases the reactivity of the substituted ions as indicated in Table 1 and 2.

REFERENCES

1. J. A. Herman and A. G. Harrison, Can. J. Chem., 47, 957 (1969)
2. N. A. McAskill and A. G. Harrison, Int. J. Mass Spectrom. Ion Phys., 5, 193 (1970)
3. R. M. O'Malley and K. R. Jennings, Int. J. Mass Spectrom. Ion Phys., 2, 441 (1969)
4. V. G. Anicich and M. T. Bowers, Int. J. Mass Spectrom. Ion Phys., 11, 329 (1973)

5. M. T. Praet and J. P. Delwiche, Int. J. Mass Spectrom. Ion Phys., 12, 193 (1973)
6. L. W. Sieck, R. Gorden, Jr., S. G. Lias and P. Ausloos, Int. J. Mass Spectrom. Ion Phys., 15, 181 (1974)
7. V. G. Anicich and M. T. Bowers, J. Amer. Chem. Soc., 96, 1279 (1974)
8. R. M. O'Malley and K. R. Jennings; M. T. Bowers and V. G. Anicich, Int. J. Mass Spectrom. Ion Phys., 11, 89 (1973)
9. S. M. Schildcrout and J. L. Franklin, J. Chem. Phys., 51, 4055 (1969)
10. H. S. Tan, M. J. Pabst and J. L. Franklin, Int. J. Mass Spectrom. Ion Phys. (in press)
11. A paper detailing this study will be submitted to Int. J. Mass Spectrom. Ion Phys.
12. S. K. Gupta, E. G. Jones, A. G. Harrison and J. J. Myher, Can. J. Chem., 45, 3107 (1967)

TABLE 1. TOTAL ION DISAPPEARANCE RATE CONSTANTS IN VINYL FLUORIDE

Ion	This work $\times 10^{-10}$ cc^3 $molecule^{-1}$ sec^{-1}	Harrison[1] cc^3 $molecule^{-1}$ sec^{-1}
$C_2H_2^+$	19.3 (± 1.2)	19.5
C_2HF^+	19.3 (± 1.2)	19.5
$C_2H_2F^+$	10.3 (± 0.6)	7.5
$C_3H_5^+$	4.9 (± 0.9)	
$C_3H_4F^+$	2.2 (± 0.7)	
$C_3H_3F_2^+$	0.5	
$C_2H_4F^+$	4.2 (± 0.7)	
$C_2H_3F_2^+$	1.9 (± 0.4)	
$C_4H_5^+$	0.8 (± 0.08)	

TABLE 2. TOTAL ION DISAPPEARANCE RATE CONSTANTS IN CF_2CH_2

Ion	Experimental K $\times 10^{-9}$ cc $molecule^{-1}$ sec^{-1}	Theoretical $K\varepsilon_e$[12] $\times 10^{-9}$ $molecule^{-1}$ sec^{-1}	$K/K\varepsilon_e$
C^+	3.43	2.93	1.44
CH^+	3.88	2.31	1.68
CH_2^+	2.91	2.25	1.29
F^+	2.88	2.00	1.44
C_2^+	2.60	1.85	1.41
C_2H^+	2.89	1.82	1.59
$C_2H_2^+$	2.29	1.80	1.27
CF^+	0.88	1.71	0.52
CHF^+	1.77	1.69	1.05
C_2F^+	1.91	1.56	1.22
C_2HF^+	1.84	1.55	1.19
CF_2^+	2.15	1.50	1.43
$C_3H_4F^+$	0.349		
$C_3H_3F_2^+$	0.124		
$C_3H_2F_3^+$	0.066		

ION MOLECULE REACTIONS IN Ar GAS*

Wei-Cheng F. Liu and D. C. Conway
Department of Chemistry
Texas A&M University
College Station, Texas 77843

ABSTRACT

The rate constant k_1 for the reaction $Ar^+(^2P_{3/2}) + 2Ar \rightarrow Ar_2^+ + Ar$ has been measured mass spectrometrically in a drift tube ion source at 77-296°K. The experimental procedure and the method of analysis have been described[1] for the 195 and 296°K data except the Ar was purified further by passage over Ti at 900°C. At 296°K the rates of the side reactions were reduced significantly from those of the previous experiments, yet k_1 was found to be $(2.3\pm0.2)\times10^{-31}$ cm^6/sec, in agreement with the previous result.[1] At 195°K k_1 was found to be 3.0×10^{-31} cm^6/sec. At 77°K, where the Ti furnace was not used, the $^2P_{3/2}$ and $^2P_{1/2}$ states of Ar^+ appear to react at the same rate, and the Ar_2^+ formed from the $^2P_{1/2}$ Ar^+ does not appear to dissociate at a significant rate. Using an approximate procedure to correct for impurity reactions, k_1 was found to be 5.2×10^{-31} cm^6/sec. The rate constant for the formation of Ar_3^+ and the equilibrium constant for the reaction $Ar_3^+ + Ar = Ar_4^+$ were also determined at 77°K.

*This research was supported by the Robert A. Welch Foundation and has recently appeared in the literature.[2]

[1]W. F. Liu and D. C. Conway, J. Chem. Phys. 60, 784 (1974).

[2]W. F. Liu and D. C. Conway, J. Chem. Phys. 62, 3070 (1975).

PROTON ABSTRACTION REACTIONS IN THE SYSTEMS H_2O-NH_3, H_2CO-NH_3, CH_3OH-NH_3 AND CH_3OH-H_2O.

Zeev Karpas and Fritz S. Klein

Isotope Department, Weizmann Institute of Science, Rehovot, Israel.

Proton transfer reactions in the gas phase have recently become the subject of intense study [1]. These investigations serve as a test for current theories on ion-molecule interactions and as a source of thermodynamic data, like standard free energy changes, heats of formation and bond energies for ionic species and for chemical ionization data.

The rates of positive ion proton transfer reactions of the type $AH^+ + B \rightarrow BH^+ + A$ seem to follow the predictions of the average dipole orientation (ADO) and the locked-in dipole (LD) models reasonably well [2]. On the other hand, negative ion proton abstraction reactions like $A^- + BH \rightarrow B^- + AH$ show divergent behaviour [3].

The relative rate constants of the following proton abstraction reactions were measured at room temperature by ICR:

1. $NH_2^- + CH_3OH \rightarrow CH_3O^- + NH_3$
2. $NH_2^- + H_2O \rightarrow OH^- + NH_3$
3. $NH_2^- + H_2CO \rightarrow HCO^- + NH_3$
4. $OH^- + CH_3OH \rightarrow CH_3O^- + H_2O$

Calculation of the heats of reaction, based on published thermochemical data and double resonance experiments show all reactions to be exothermic. Relative rate constants have been experimentally determined by the method of Anicich and Bowers [4], from the slopes of the plots of the intensity ratio of secondary to primary ions as a function of the neutral reactant density, as shown in figure 1.

Taking reaction 2 ($NH_2^- + H_2O$) as reference, the experimental relative rate constants are given in column 2 of Table 1. These ratios are compared with the relative rates calculated for the ion-induced dipole (G+S) model (column 3), the locked-in dipole (column 4) and the ADO model (column 5). The calculated exothermicities of the reactions are shown in the last column of Table 1.

None of the models comes close to the experimental value, and even varying the constant "c" in the ADO model has little effect. All these models predict only small variations in the rate constants (±15% GS, ±7% ADO) compared to a factor of 6.2 (reactions 1 and 3) in the experiment. However, it is not difficult not to notice the correlation between the calculated exothermicities of the reactions and the experimental values. It is easy to accomodate all experimental data if one allows for activation energies for these reactions which are inversely proportional to their exothermicities [5]. Temperature effects for these reactions are measured by the method described in the following paper.

References

1.a D.K. Bohme, "Interactions Between Ions and Molecules", Plenum,N.Y.1975
b H.I.Schiff & D.K.Bohme, Int. J. Mass Spectrom.Ion Phys. 16,167 (1975).
c T. Su & M.T. Bowers, JACS 95, 7609 (1973).
d W.T. Huntress, Jr., J.K. Kim and L.P. Theard, this volume R1.
2.a B.H.Solka & A.G. Harrison, 21st Conf. ASMS, San-Francisco, p.30 (1973)
b A.G. Harrison, P.H. Lin and C.W. Tsang, this volume G-2.
3. D. Betowski, J.D. Payzant, G.I. Mackay & D.K. Bohme, Chem. Phys. Lett. 31, 321 (1975).
4. V.G. Anicich & M.T. Bowers, Int. J. Mass Spectrom. Ion Phys. 11, 329 (1973).
5. M.T. Bowers, W.J.Chesnavitch & W.T. Huntress,Jr., ibid, 12,357 (1973).

TABLE 1: Relative rate constants and heat of reaction

#	reaction	exp	G+S	LD	ADO	$-\Delta H$ k cal/mole
1	$NH_2^- + CH_3OH$	1.17	1.32	1.00	1.18	23
2	$NH_2^- + H_2O$	1.00	1.00	1.00	1.00	17
3	$NH_2^- + CH_2O$	0.19	1.04	1.09	1.11	4 ± 4
4	$OH^- + CH_3OH$	0.53	1.30	0.98	1.17	6

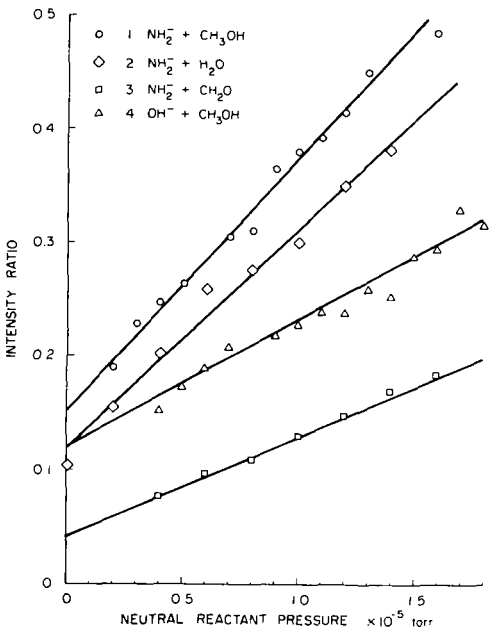

Figure 1: Ion intensity ratio [secondary]/[secondary] + [primary] as a function of the neutral Reactant Pressure.

Negative Ion Molecule Reactions at Low Ion Energies

Itzhak Dotan (Duchovny) and Fritz S. Klein
Isotope Department, Weizmann Institute of Science,
Rehovot, Israel

A considerable number of thermal ion molecule rate constants has been published and even more is known about rates at ion energies of several electron volt [1]. Information on rates in the suprathermal range, which is more difficult to study, is scarce. However, ion reactivity at these energies is of prime interest since it reflects the more intimate characteristics of the interaction potential while high energy rates are generally represented by the peripherals. From the applied aspect, intermediate energy range interactions are rather important in upper atmosphere phenomena [2].

Several years ago we developed [3] an experimental method to measure the energy dependence of rates of positive ion molecule interactions by varying the relative reactant energy either (a) isothermally over a temperature range of 325 to 650°K, or by (b) accelerating the ionic reactant in a pulsed electric field to accurately controlled energies in the range of thermal to about 1 eV kinetic energy. We have now perfected this method to include negative ion molecule interactions.

The experimental method was described by Schnitzer and Klein [3]. A schematic diagram of the instrument is given in figure 1. The negative reactant ions were generated by dissociative electron attachment, which at the chosen energies and neutral reactants produced thermal or near thermal ions.

The following reactions have been studied:

1. O^- $(NO_2,NO)NO_2^-$. (Figure 2). This charge exchange is exothermic by 0.815 eV (∿ 19 kcal/mole) [4]. The rate constant shows a negative energy dependence which is paralleled by a negative temperature effect. Both a 200° temperature increase or an addition of ∿0.05 eV ion kinetic energy cause the reaction rate to fall by 40%. A similar decrease of rate constant was also observed [5] at higher ion energies.

2. $O^-(N_2O,NO)NO^-$ (Figure 3). This atom exchange is exothermic by 0.14 eV (3 kcal/mole) [6]. The experimental energy effect on the rate constant is only slightly negative by both methods of investigation (25% rate decrease for 200° and almost constant at low accelerations). At higher energies (> 5 eV) a steep decrease with energy was observed by

Paulson [8] and Stockdale et al. [5].

3. O^- $(D_2;D)$ OD^- (Figure 4). The atom exchange is exothermic by 0.3 eV (∿ 5 kcal/mole) [8]. The energy effect on the rate is positive (a factor of three per eV; qualitative thermal measurements show a similar trend). These results are in qualitative agreement with the data of McFarland et al. [8].

4. SO^- (SO_2,SO) SO_2^- (Figure 5). The charge exchange is exothermic by 0.13 eV (∿ 3 kcal/mole). The energy and thermal effects are positive. A potential barrier with an experimental activation energy of 300±40 cal/mole may explain these data.

5. $SO^-(SO_2,S)$ SO_3^- (Figure 6). This atom exchange is thermoneutral (within experimental error). The energy effect is positive and can be rationalized by invoking a small activation energy. A similar effect was observed by Platzner et al. [9].

Presently we are qualitatively comparing the energy effect of the thermal Boltzman distribution with the slightly distorted distribution of the accelerated ion relative energy.

References

1. M. Henchman, Ion Molecule Reactions, J.L. Franklin, Ed., 101-259 (1972).
2. E.E.Ferguson, Accounts Chem. Res. 3, 402 (1970).
3. R. Schnitzer & F.S. Klein, Int. J. Mass Spectrom. Ion Phys. 16, 385 (1975).
4. T.O. Tiernan & C. Lifschitz, J. Chem. Phys. 59, 3162 (1973).
5. J.A.D. Stockdale et al., Phys. Rev. 184, 81 (1969).
6. R. Marx et al., J. Chem. Phys. 58, 3267 (1973).
7. J.F. Paulson, J. Chem. Phys. 52, 959 (1970).
8. M. McFarland et al., J. Chem. Phys. 59, 6624 (1973).
9. I. Platzner, G. Levin & F.S. Klein, Adv. Mass Spectrom. 5, 217 (1970).

PULSING CIRCUITRY SCHEMATIC DIAGRAM

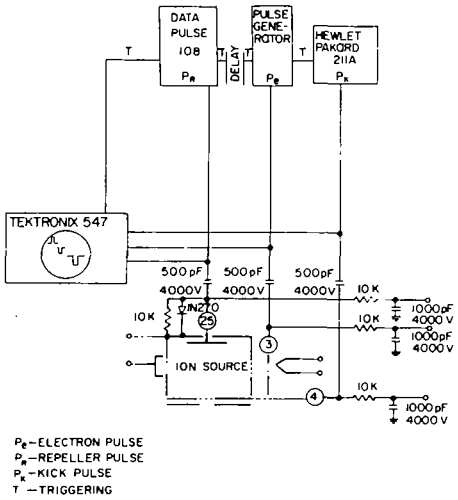

Figure 1

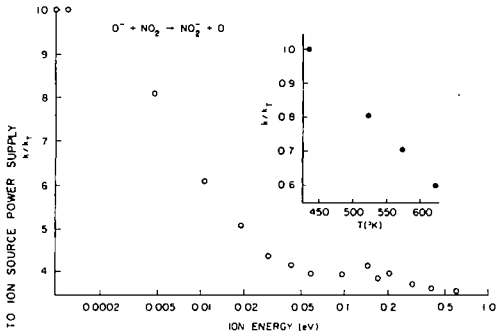

Figure 2

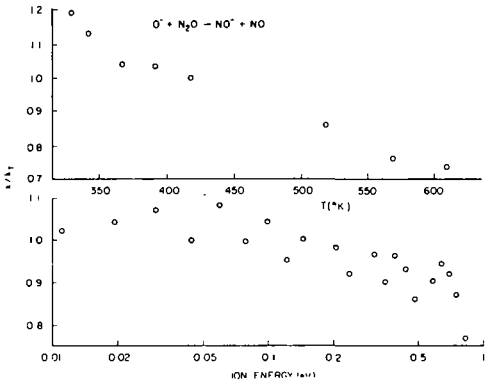

Figure 3

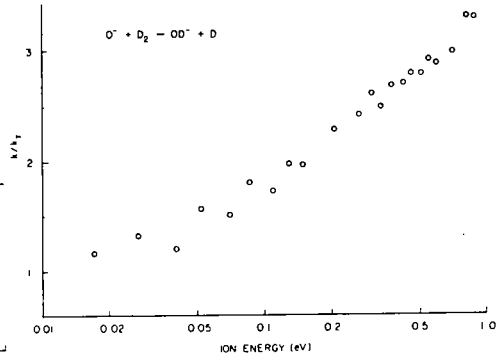

Figure 4

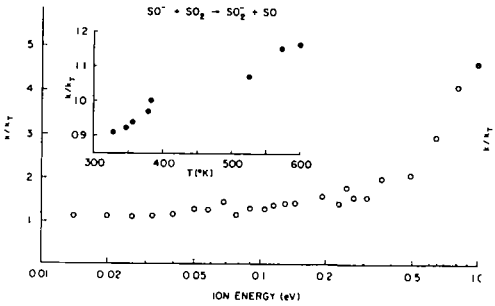

Figure 5

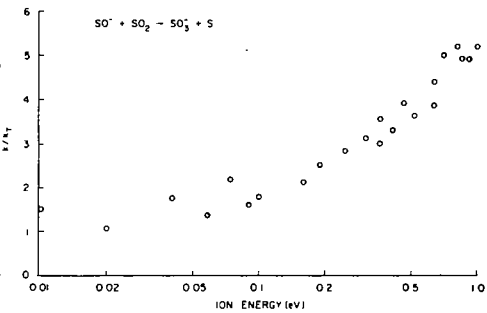

Figure 6

ENDOERGIC ION-MOLECULE-COLLISION OF I^- ON H_2O

Kamel M. A. Refaey* and J. L. Franklin
Chemistry Department, Rice University
Houston, Texas 77001

ACKNOWLEDGMENT

The authors are pleased to acknowledge support of this work by the Robert A. Welch Foundation.

Endoergic reactions of negative ions with neutral molecules proved to be useful in determining the electron affinities of several species. Tandem mass spectrometers separated by a collision chamber are frequently employed[1-3] for this purpose. An ion source with separate ionization and collision chambers employed earlier by Refaey and Chupka[4,5] for positive ions, was adapted for the investigation of negative ions,[6] employing primary halide ions formed by pair production as projectiles.

In the present investigation, the primary ion is formed dissociative resonance capture. This technique has been used successfully to study both charge-exchange and ion-molecule-reactions employing I^- produced by electron resonance capture of HI as the primary ion.[7-9]

Work reported here has been carried out on a Bendix time-of-flight (T.O.F.) mass spectrometer. The ion source with separate ionization and collision chambers was especially constructed for the purpose of these investigations. I^- ions produced in the ionization chamber by the electron resonance capture of HI are pulsed to the desired energy to enter the collision chamber containing H_2O vapor molecules. Both I^- ions and products of collision are further accelerated to a final potential of 3500 volts where they enter the flight tube of the mass spectrometer through a 2.5 mm in diameter hole. Detailed description of the ion source and its operation has been given elsewhere.[8]

Distilled H_2O vapor was introduced into the collision chamber at room temperature after repeated freezing and thawing under vacuum.

Because of the fact that the initial translational energies of the secondary ions vary widely, the mass resolution of the instrument is greatly reduced. Consequently, we were unable to resolve OH^- and OH_2^- or OD^- and OD_2^- ions. In most instances, however, it is possible to determine from energy considerations which secondary ion is observed.

The energy dependences of the cross sections of ions formed by collision of I^- with H_2O are shown in Fig. 1. The curve, marked by circles, starts with a long tail which is partly attributable to background ions but which may also include some H_2O^-. If this is H_2O^-, the electron affinity of water must be approximately 2.6 eV. It is emphasized that this is speculative.

A definite onset occurs at about 3.2 eV and can be only OH^- formed by the reaction

$$I^- + H_2O \rightarrow OH^- + HI.$$

This results in $\Delta H_f(OH^-) = -37$ kcal/mole in good agreement with values determined by others.[10]

A rather broad onset in the region 6.3 - 6.8 eV can be attributed to either or both of the reactions

$$I^- + H_2O \rightarrow OH^- + H + I(^2P_{3/2}) - 6.4 \text{ eV}$$

$$\rightarrow O^- + H_2 + I(^2P_{3/2}) - 6.7 \text{ eV}$$

The corresponding reactions in which $I(^2P_{1/2})$ is formed will occur at about 7.3 and 7.7 eV respectively. A discontinuity at 7.5 eV can be attributed to either process.

A strong discontinuity at 4.6 eV and a weaker one at 8.9 eV cannot be interpreted.

A massive ion (curve marked by triangles) having a definite onset of 3.9 eV is IO^- formed together with H_2. This results in $\Delta H_f(IO^-) = -15$ kcal/mole and EA(IO) = 2.6 eV in very good agreement with values determined previously. A definite deflection in this curve appears at 5.0 eV and is difficult to understand. Conceivably, it might be HIO^- for which we would compute a heat of formation of -42 kcal/mole but it is difficult to accept this without further evidence. Similarly, it might be HI^- for which we compute the heat of formation to be 1 kcal/mole but with reservations. It is possible that the ion is I^- which has suffered a loss of 5 eV upon collision with a water molecule. This very nearly is the exact amount of energy required to break the OH bond in water and such an energy loss mechanism might be expected to occur with a large cross section. The energy lost by I^- could be sufficient to cause the I^- peak to shift to an apparently higher mass and thus appear near IO^-. We are unable to resolve these differences at this time.

Although H^- was detected as a secondary ion, its intensity was too low to permit measurements.

REFERENCES

1. B. M. Hughes, C. Lifshitz and T. O. Tiernan, J. Chem. Phys. 59, 3162 (1973).
2. J. F. Paulson, J. Chem. Phys. 52, 963 (1970).
3. D. Vogt, Int. J. Mass Spectrom. Ion Phys. 3, 81 (1969).
4. K. M. Refaey and W. A. Chupka, J. Chem. Phys. 43, 2544 (1965).
5. K. M. Refaey and W. A. Chupka, 14th Annual Conference on Mass Spectrometry and Allied Topics, p. 197, Dallas, May (1966).
6. W. A. Chupka, J. Berkowitz and D. Gutman, J. Chem. Phys. 55, 2724 (1971).
7. K. M. A. Refaey and J. L. Franklin, J. Chem. Phys. 61, 733 (1974).
8. K. M. A. Refaey and J. L. Franklin, submitted to J. Chem. Phys.
9. K. M. A. Refaey and J. L. Franklin, submitted to Int. J. Mass Spectrom. Ion Phys.
10. J. L. Franklin and P. W. Harland, Annual Review of Physical Chem. 25, 485 (1974).

* Physics Department, Cairo University, Cairo, Egypt.

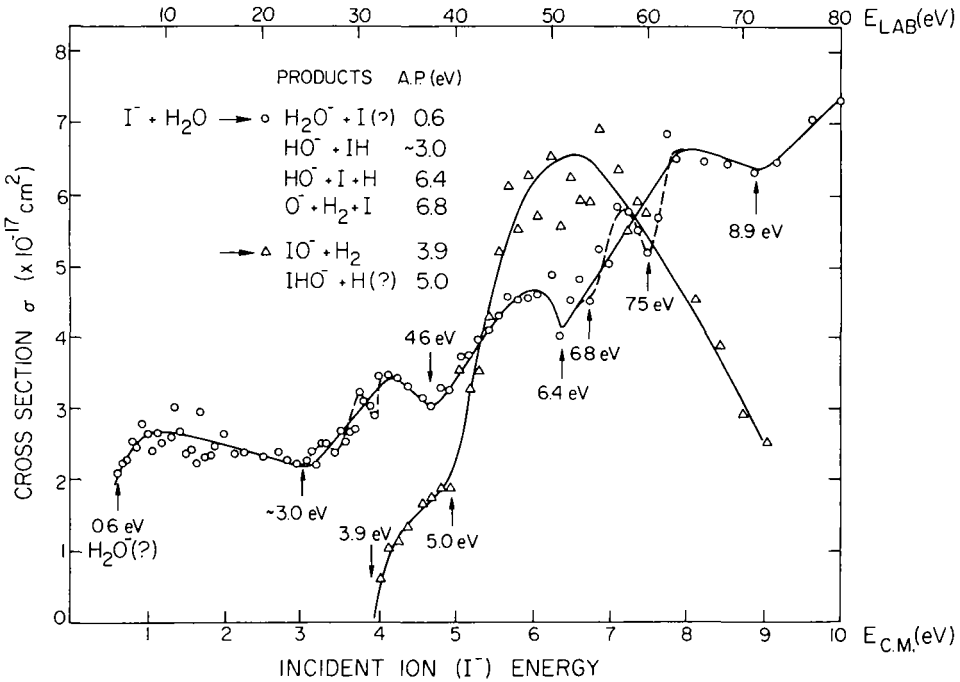

FIGURE CAPTION

Figure 1. Results of Collision of I^- on H_2O

NEGATIVE ION SPECTRA OF SOME SULPHIDES AND SOME OXIDES OF NITROGEN*

Kamel M. A. Refaey**
Physics Department, Cairo University
Cairo, Egypt

Hydrogen sulfide[1] and NO_2[2] have been subjected to collision with I^- at various energies and several endoergic ion-molecule reactions determined. The method employed, as discussed in paper P-6, used a time-of-flight mass spectrometer equipped with a collision chamber adjacent to the ionization chamber. Ions from the ionization chamber are pulsed at variable energies into the collision chamber and product and unreacted primary ions are extracted and analyzed. I^- ions formed by dissociative resonance capture were employed as projectiles.

Figure 1 gives the variation in cross section for the various secondary ions as a function of energy in the center of mass. Because of the poor resolving power of the instrument for secondary ions the mass peaks for HS^- and S^- could not be resolved. However, the energy onsets observed could in most instances be interpreted in terms of one or the other ion.

There are several scattered points below the point a (1.7 eV). These points can be ignored as background intensities. If a corresponds to the formation of HS^- according to

$$I^- + H_2S \rightarrow HS^- + HI \qquad (1)$$

then one obtains $\Delta H_f(HS^-) = -19$ kcal mole^{-1}. This value in combination with $\Delta H_f(HS) = 34.10^3$ kcal mole^{-1} gives EA = 2.3 eV. This value is in good agreement with those reported in the literature.[4,5]

Point b (4.2 eV indicates the appearance of S^- according to

$$I^- + H_2S \rightarrow S^- + I + H_2 \qquad (2)$$

which gives $\Delta H_f(S^-) = 19.1$ kcal mole^{-1}. This value in turn gives EA (S) = 2.1 eV. Two other onsets for S^- give values that are less precise but are nevertheless rather close to the accepted heat of formation.

Table 1 summarizes the results for H_2S.

TABLE 1. RESULTS OF COLLISION OF I^- ON H_2S

Collision Products	A.P. eV	ΔH_f(ion) kcal mole^{-1}	E.A. eV
$HS^- + HI$	1.7	-19	2.3
$S^- + HI + H(?)$	5.8	24	1.9
$S^- + I_{2p3/2} + H_2$	4.2	19.1	2.1
$S^- + I_{2p3/2} + 2H$	8.8	22	2.0
$IS^- + H_2$	2.5	5.5	3.1
$IHS^- + H$ (?)	4.5	- 0.5	1.1
$H^- + IHS$	4.8	25[a]	
$H^- + I + HS$	6.5	39	
$H^- + IS + H$ (?)	9.3	77[b]	
$H^- + I + S + H$	10.5	45	

a - ΔH_f(IHS) b - ΔH_f(IS)

Collision of I^- on NO_2 gives rise to the secondary ions NO_2^-, IN^- and O^-. NO^- ions were also observed but with rather low cross sections. The results shown in Figure 2 indicate that NO_2^- appears at 0.95 eV according to

$$I^- + NO_2 \rightarrow NO_2^- + I \qquad (3)$$

which gives EA (NO_2) = 2.1 eV. This value is in general agreement with several reported values.[4,5]

The rise in the cross section curve at 4.1 eV has been reproduced in other measurements and can be attributed to the formation of NO_2^- in an electronically excited state about 3.05 eV above the ground state. This view is supported by the fact that the isoelectronic molecule NOF has an excited state[6] 3.7 eV above the ground state.

The onset for the formation of IN^- at 2.7 eV results from the reaction

$$I^- + NO_2 \rightarrow IN^- + O_2 \qquad (4)$$

which gives $\Delta H_f(IN^-)$ = 23 kcal $mole^{-1}$ in good agreement with the results of collision of I^- on N_2O. $\Delta H_f(IN)$ has been obtained from collision of I^- on NO as 53 kcal $mole^{-1}$. Thus EA (IN) = 1.3 eV. The cross section curve for IN^- shows a small increase at about 6.0 eV (3.3 eV above onset). This increase has been observed more clearly in other measurements and was also pronounced in IN^- curve from N_2O. This can probably be attributed to the formation of IN^- in electronically excited state. The isoelectronic molecule IO has an excited state about 2.7 eV above the ground state.

The results of collision of I^- on NO_2 are summarized in Table II.

TABLE II. RESULTS OF COLLISION OF I^- ON NO_2

Collision Products	A.P. eV	ΔH_f (ion) kcal $mole^{-1}$	EA (eV) This Work	EA (eV) Best Estimate
$NO_2^- + I$	0.95	-39	2.1	>2.1 ± 0.1
$NO_2^{-*} + I$	4.1			
$IN^- + O_2$	2.7	23	1.3	1.3 ± 0.2
$IN^{-*} + O_2$	6			
$O^- + I + NO$	5.0			

* This work was performed at Rice University under a grant from the Robert A. Welch Foundation to Professor J. L. Franklin.
** Present Address: Chemistry Department, Rice University, Houston,Texas

REFERENCES

1. Kamel M. A. Refaey, J. Chem. Phys. (submitted)
2. Kamel M. A. Refaey, Int. J. Mass Spectrom. Ion Phys. (submitted)
3. Selected values of Chemical Thermodynamic Properties, Technical Note, US Nat. Bur. Stand. 270-3 (1968)
4. J. Berkowitz, W. A. Chupka and D. Gutman, J. Chem. Phys.,55, 2733(1971)
5. E. Herbst, T. A. Patterson and W. C. Lineberger, J. Chem. Phys., 61, 1300 (1974)
6. G. Hurzberg, "Electronic Spectra of Polyatomic Molecules"
7. G. Hurzberg, "Spectra of Diatomic Molecules"

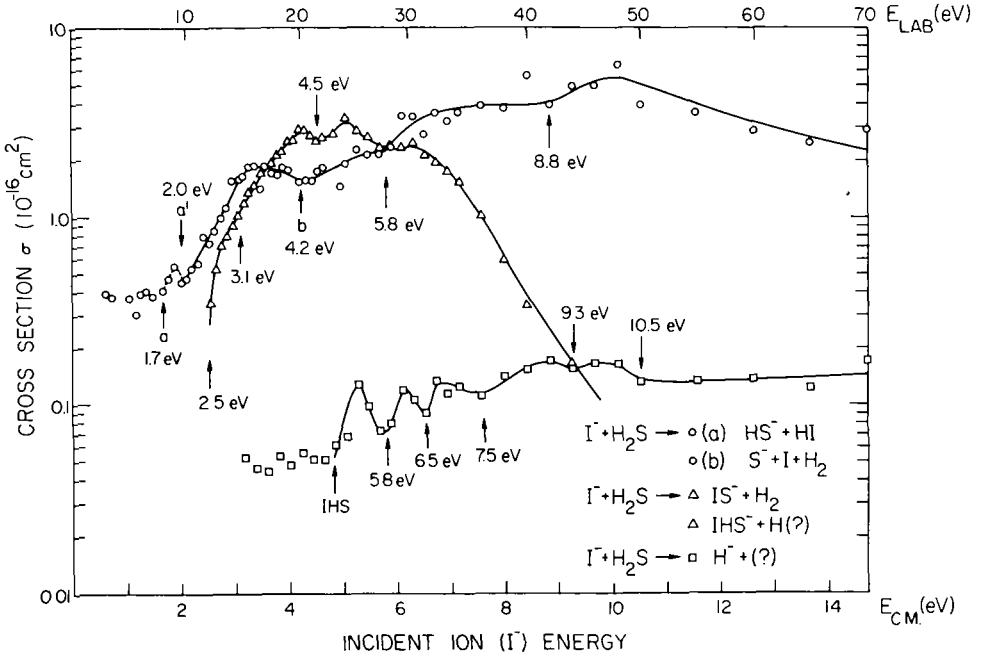

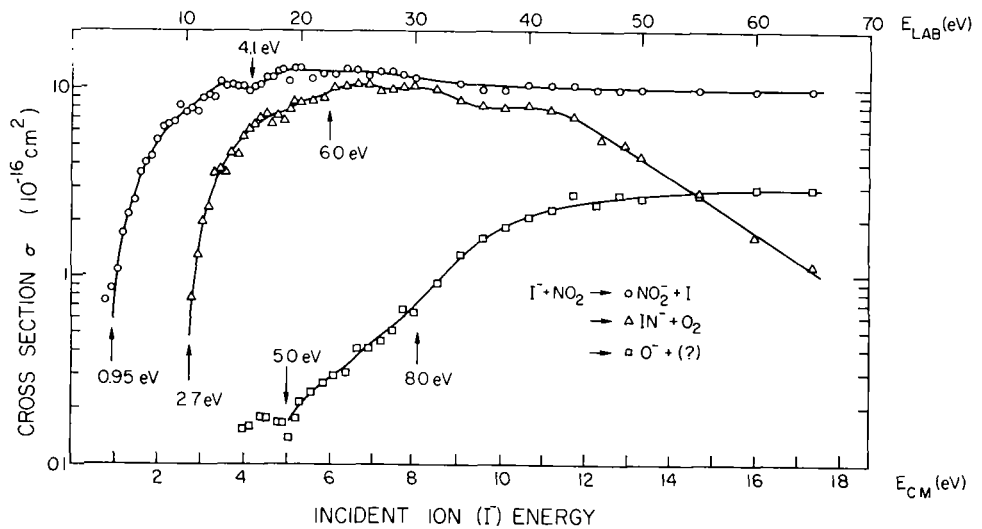

FIGURE CAPTIONS

Figure 1. Results of Collision of I^- on H_2S

Figure 2. Results of Collision of I^- on NO_2

Measurement of Thermal Electron Dissociative Attachment Rates for Halogen Gases.

G. D. Sides* and T. O. Tiernan*

Aerospace Research Laboratories, (LJ), Wright-Patterson AFB, Ohio 45433

Abstract

A flowing afterglow system has been used to measure the rates of dissociative electron attachment in the halogen gases fluorine, chlorine and bromine. A flowing afterglow apparatus previously described was modified to incorporate a filament (thermionic emission) source for these measurements[1]. In addition, the apparatus was interfaced to a minicomputer for data acquisition and control purposes. The operation of the flowing afterglow system was checked by determining the rates of electron attachment to sulfur hexafluoride and oxygen and comparing these with previously reported data. Results for the various halogens will be reported and discussed.

[1]American Society for Mass Spectrometry, 21st Annual Conference on Mass Spectrometry and Allied Topics, San Francisco, May 1973.

*Present Address: Department of Chemistry, Wright State University, Dayton, Ohio 45431

This work will be described fully in a paper to be submitted to Journal of Chemical Physics.

DISSOCIATIVE ATTACHMENT AND ION MOLECULE REACTIONS IN PHOSPHORUS AND ARSENIC CHLORIDES

J. G. Dillard, R. Pauls, and C. E. Compton
Chemistry Department
Virginia Tech
Blacksburg, VA 24061

ABSTRACT

Dissociative electron capture processes and negative ion-molecule reactions in PCl_3, $POCl_3$, $PSCl_3$, and $AsCl_3$ were noted. The principal ion in the dissociative processes is Cl^- with some formation of $AsCl_2^-$ and PCl_2^- in $AsCl_3$ and PCl_3, respectively. Parent molecular negative ions are formed in $POCl_3$ and in $PSCl_3$ at low electron energies. Subsequent fragmentation of the parent ions occurs via loss of Cl.

Negative ion-molecule reactions occur via Cl^- transfer to PCl_3 and $AsCl_3$ from $POCl_n^-$ ions. No transfer was noted in the neat gas since no chrlorine containing ion is sufficiently abundant to undergo a Cl^- transfer. No ion transfer processes were noted in $PSCl_3$ or in $POCl_3$ in the neat gases. Fluoride ion transfer was studied in mixtures of SF_6-PCl_3 and SF_6-$AsCl_3$. No F^- transfer was noted in SF_6 mixtures with $POCl_3$ or $PSCl_3$. In $POCl_3$ and $PSCl_3$, collisional dissociative secondary reactions were noted.

MASS-SPECTROMETRIC SAMPLING OF THE IONIC AND NEUTRAL SPECIES PRESENT IN DIFFERENT REGIONS OF AN RF DISCHARGE IN METHANE

by

M. J. Vasile and G. Smolinsky
Bell Laboratories
Murray Hill, New Jersey 07974

The ionic and neutral products of RF discharges in methane produced by capacitive and inductive coupling have been examined. The configurations studied were (1) axial sampling through an internal RF capacitor electrode, (2) axial sampling through an electrically grounded internal capacitor electrode, (3) radial sampling of a capacitively coupled discharge through an electrically floating electrode, and (4) axial sampling of an inductively coupled discharge through a grounded electrode. Major differences in the ions observed occur between configurations (1) and (3), above. In the former, the dominant ions found are C^+, CH^+, CH_2^+, CH_3^+, $C_2H_2^+$, and $C_2H_3^+$, with very little abundance of ions containing more than three carbon atoms. In the latter, the ions CH_3^+, CH_5^+, $C_2H_3^+$, and $C_2H_5^+$ are dominant, with a significant fraction of the total comprising C_4 to C_6 ions. The dissimilarity observed between these two cases clearly can be attributed to the difference in energy of the electrons which cause the ionization and the difference in kinetic energy of the primary ions which undergo ion-molecule reactions to yield secondary ions. Ions containing two or more carbon atoms have been shown to result from ion-molecule reactions rather than from primary ionization of C_2 neutrals. The neutral gas composition is also a function of position in the discharge and is clearly related to the energy available at any particular sampling point.

RELATIVE PROTON AFFINITIES OF ETHYLENE AND WATER

Yip-Hoi Li and Larry I. Bone
Department of Chemistry, East Texas State University, Commerce, Texas 75428

The difference in proton affinities of C_2H_4 and H_2O has been measured in a quadrupole mass spectrometer using electron impact in a field free, high pressure source. Experiments were carried out at four different temperatures (365°K, 402°K, 409°K, and 421°K) and at various mole fractions of H_2O ranging from 0.35 to 0.65. The mass spectra of each mole fraction was studied as a function of total pressure. The percent of total ionization was then plotted as a function of total pressure as shown in Figure 1.

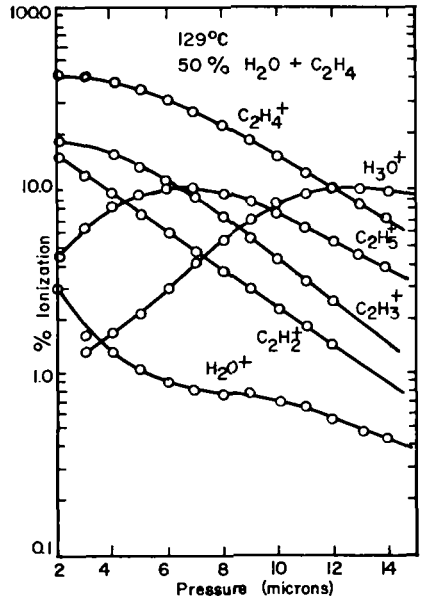

Figure 1. Percent Ionization as a Function of Total Pressure.

At pressures below 3 microns, the actual percent of ionization was calculated by summing all peaks in the spectrum. At higher pressures, where large clusters start to dominate, the peaks of importance were measured on a relative basis and plotted assuming $C_2H_2^+$ is not produced by any reaction and reacts only by first order process. That is, the straight line observed for $C_2H_2^+$ in Figure 1 is simply extrapolated and other ion intensities are plotted relative to it.

Both $C_2H_5^+$ and H_3O^+ are produced by second order proton transfer from initial fragments, exchange a proton by

$$C_2H_5^+ + H_2O \rightleftarrows C_2H_5 + H_3O^+ \qquad 1)$$

and react further by clustering with both neutral reactants. Both ions in reaction 1 exhibit a maximum intensity at intermediate pressure. The rates of production and reaction were equated at each maxima giving two sets of simultaneous equations containing the equilibrium constant for reaction 1. Without any assumptions concerning values for the rate constants involved, the equilibrium constant was calculated by itterative techniques.

The equilibrium constant was measured as a function of temperature and a van't Hoff plot gave an enthalpy difference for reaction 1 of -3.9 kcal/mole and an intercept corresponding to an entropy difference of -5 cal/deg mole. Mass discrimination effects which are inherent in the use of both a quadrupole analyzer and an electron multiplier are at best difficult to quantify. In this study, these effects cause the $H_3O^+/C_2H_5^+$ ratio and thus the equilibrium constant to be too large by some multiplicative factor. The use of a van't Hoff plot allows accurate measurements of $\Delta H°$ with the inherent error contributing only to the $\Delta S°$ term.

We conclude that the proton affinity of H_2O is 3.9 kcal/mole greater than the proton affinity of C_2H_4. We estimate that the observed entropy difference is probably 2-3 e.u. too high as a result of mass discrimination effects. The entropy difference for reaction 1 is probably low, as expected.

This work was supported by the Robert A. Welch Foundation.

LONG RANGE TRIMETHYLSILYL GROUP MIGRATIONS IN STEROID MASS SPECTRA

C.J.W. Brooks, S.J. Gaskell and A.G. Smith,

Department of Chemistry, The University,

Glasgow, G12 8QQ, Scotland.

During a study of 5-cholestene-3β,26-diol (26-hydroxycholesterol) (I) in human brain [1], we used cholesterol oxidase [2] to effect selective oxidation, giving 26-hydroxy-4-cholesten-3-one (II) which was characterised by gas chromatography-mass spectrometry (GC-MS) of derivatives.

Salient features of the 70eV mass spectrum of the trimethylsilyl (TMS) ether of II are recorded in Table 1. The base peak at m/e 196 amounted to 7.6% of the total ionisation (Σ 50) in the 70eV spectrum and 22.7% in the 20eV spectrum. Spectra were recorded by GC-MS with OV-17 liquid phase, thus ensuring separation between the enone TMS ether and the corresponding enol di-TMS ether. The mass spectrum of 3,5-cholestadiene-3,26-diol di-TMS ether showed an abundant molecular ion and few prominent fragment ions. The ion at m/e 196 amounted to 10% of the base peak.

The Figure indicates a possible origin of the ion of m/e 196. Inspection of models suggests that interaction between the side-chain TMSO group and the 3-oxygen is feasible following fragmentation across ring B. Ions of m/e 196 also occur in the spectra of TMS ethers of related side-chain hydroxylated steroid 4-en-3-ones (Table 2). The mechanism shown in the Figure remains speculative since we have no evidence for the terminus of migration of the TMS group, nor that the migration occurs in a single step.

Table 1. Mass spectrometric data (70eV) for 26-trimethylsilyloxy-4-cholesten-3-one*

ions	(m/e > 100)	rel. int.
472	$M^{+\cdot}$	33
457	$[M-15]^+$	22
382	$[M-90]^{+\cdot}$	2
229	$[M\text{-side-chain-}42]^+$	37
196	(see text)	100
124	"ring A" fragment [3]	38

* GC-MS analysis (LKB 9000); similar data were obtained via direct insertion probe (Du Pont 490F).

The origin of the ion at m/e 196 in the spectrum of the TMS ether of II was investigated by high resolution mass measurement and by examination of the spectra of the $^2H_9$-TMS and 3-^{18}O analogs. The mass was determined (AEI MS9) as 196.1287 amu ($C_{11}H_{20}OSi$: calculated, 196.1284). $^2H_9$-labelling resulted in a shift to m/e 205, confirming retention of the TMS moiety. The 3-^{18}O compound (62.5 ^{18}O atom per cent) gave a spectrum containing ions at m/e 191 and 193 of relative intensity consistent with the ^{18}O enrichment. The ion of m/e 196 may therefore be attributed to combination of the side-chain TMS group with a nuclear fragment containing

ring A. The possibility of an inter-molecular mechanism was investigated by simultaneous GC-MS analysis of 26-trimethylsilyloxy-4-cholesten-3-one, its [$^2H_9$]-TMS analog and its [3-^{18}O]-[$^2H_9$]-TMS analog. A spectrum recorded at the top of the emerging chromatographic peak was consistent with an intramolecular process (→ m/e 196, 205 and 207) and indicated that an intermolecular route (→ 196, 198, 205 and 207) could not account for more than 10% of the rearrangement.

Table 2. Occurrence of the ion of m/e 196 in the spectra of the TMS ethers of side-chain hydroxylated 4-en-3-ones.

	Side chain	% of Base peak
C_8 :	26-OTMS	100
	25-OTMS	5
	24-OTMS	6
	22-OTMS (22-epimers) (i)	56
	(ii)	33
	20-OTMS	0.5
C_7 :	25-OTMS	15
C_5 :	24-OTMS	100
C_3 :	22-OTMS	25

Migration of a TMS group under electron impact has been widely studied in steroids and other compounds. Sloan et al. [4] demonstrated interaction between TMSO groups attached to steroid rings A and D. The dominance of the rearrangement we describe for the 4-en-3-ones probably stems from the facile cleavage of ring B, which provides the necessary conformational flexibility.

A full account of this work to be published [5].

This work was supported by the Medical Research Council and the Science Research Council.

References

1. Smith, A.G.; Gilbert, J.D.; Harland, W.A.; Brooks, C.J.W. Biochem. J. (1974) 139, 793.

2. Smith, A.G.; Brooks, C.J.W. J. Chromatog. (1974) 101, 373.

3. Shapiro, R.H.; Djerassi, C. J. Amer. Chem. Soc. (1964) 86, 2825.

4. Sloan, S.; Harvey, D.J.; Vouros, P. Org. Mass Spectrom. (1971) 5, 789.

5. Gaskell, S.J.; Smith, A.G.; Brooks, C.J.W. Biomed. Mass Spectrom., in press.

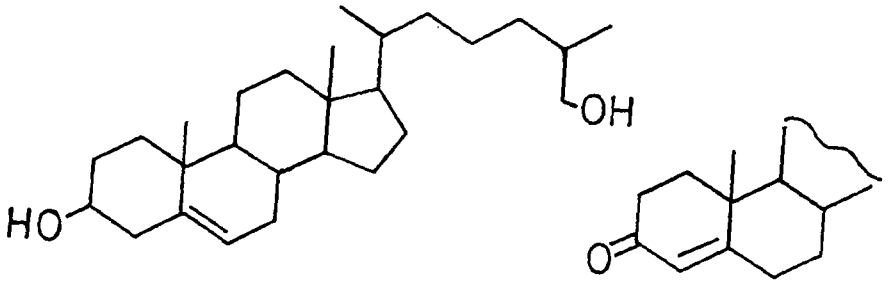

(I) (II)

Figure. Proposed mechanism for the formation of ion m/e 196:

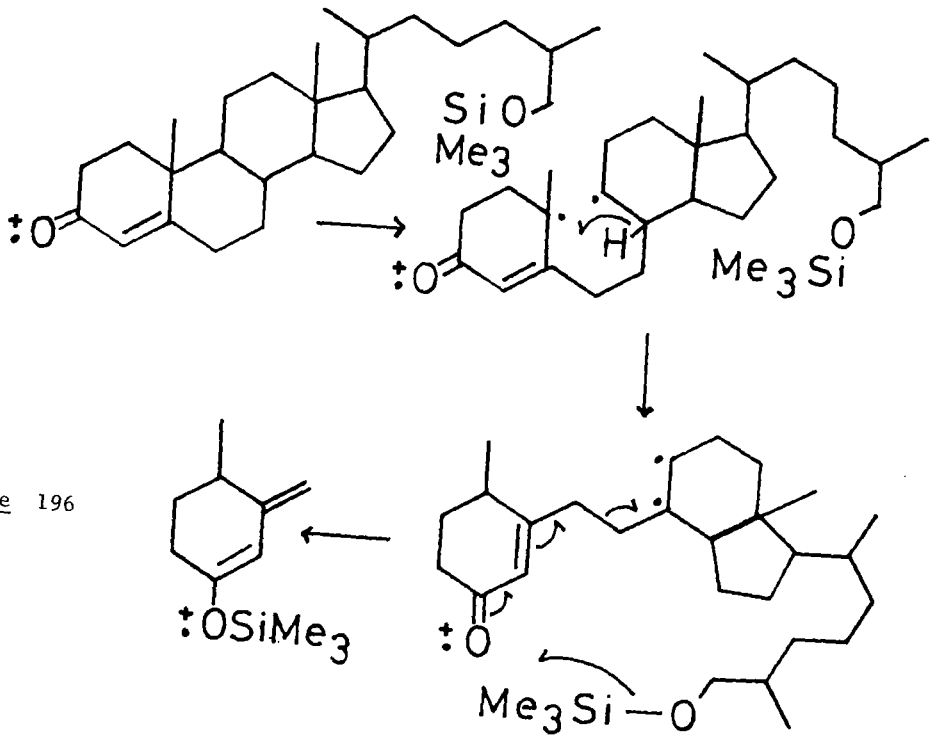

SELECTIVE INTRODUCTION OF TMS GROUPS IN TRYPTAMINE: PREPARATION OF N-TMS DERIVATIVES OF TRYPTAMINES

N. Narasimhachari and K. Leiner

Galesburg State Research Hospital
Galesburg, Illinois 61401

In an earlier paper it was shown that N-methyltryptamine and N-methylserotonin yield mono and di-TMS derivatives respectively. The mass spectra of those compounds showed that the trimethylsilyl group (TMS) was attached to the indolic nitrogen (N_I) and not to the secondary amino nitrogen (N_W).[1] We have now extended this partial trimethylsilylation reaction to other indolethylamines, particularly the primary amines. Bis (trimethylsilyl) trifluoroacetamide plus 1% trimethylchlorosilane (Regisil^R) was used as the silylating agent. The free amines (100μg) were heated with 100μl of this reagent in a sealed tube (Pasteur pipettes sealed at both ends) at 100°C for 15 minutes. Tryptamine, α-methyltryptamine and 5-methoxytryptamine yielded a mono-TMS and 5-hydroxytryptamine a di-TMS derivative as the major (90%) product. The mass spectra of these derivatives showed the presence of free amino group and substitution of TMS group in the indolic nitrogen. Thus for example, the mass spectrum of tryptamine-mono-TMS derivative showed the molecular ion at m/e 232 ($M^{\cdot+}$) the major fragment ion at m/e 202 $(M - 30)^+$ (70%), and the base peak at m/e 73, of the TMS group. Similarly 5-methoxytryptamine-mono-TMS, 5-hydroxytryptamine di-TMS were characterized by the molecular ion at m/e 262 ($M^{\cdot+}$), 320 ($M^{\cdot+}$) and $(M - 30)^+$ at m/e 232 and 290 respectively.

The presence of the free amino group in those derivatives was further confirmed by their conversion to the isothiocyanate derivatives using carbon disulfide, in ethyl acetate solution or on column injection of the TMS derivative and carbon disulfide.[2] The amine-TMS-NCS derivatives were identical with the amine-NCS-TMS derivatives reported earlier[3] in GC and GC-MS characteristics. As an illustrative example the GC data and mass spectra of tryptamine-mono N_I-TMS and its NCS derivative are shown in Figure 1. The advantages of these derivatives over the functional group analysis using the base peak at m/e 174[4] are obvious in the sense that these derivatives yield structural information of the parent amine. Full details of this paper will be published elsewhere.

1. N. Narasimhachari et al., J. Chromatographic Sci. 9:502,(1971)
2. N. Narasimhachari and P. Vouros, Anal. Biochem. 45:154,(1972)
3. N. Narasimhachari and P. Vouros, Biomed. Mass Spectrometry 1: 367, (1974)
4. F. P. Abramson et al., Anal. Biochem. 51:482, (1974).

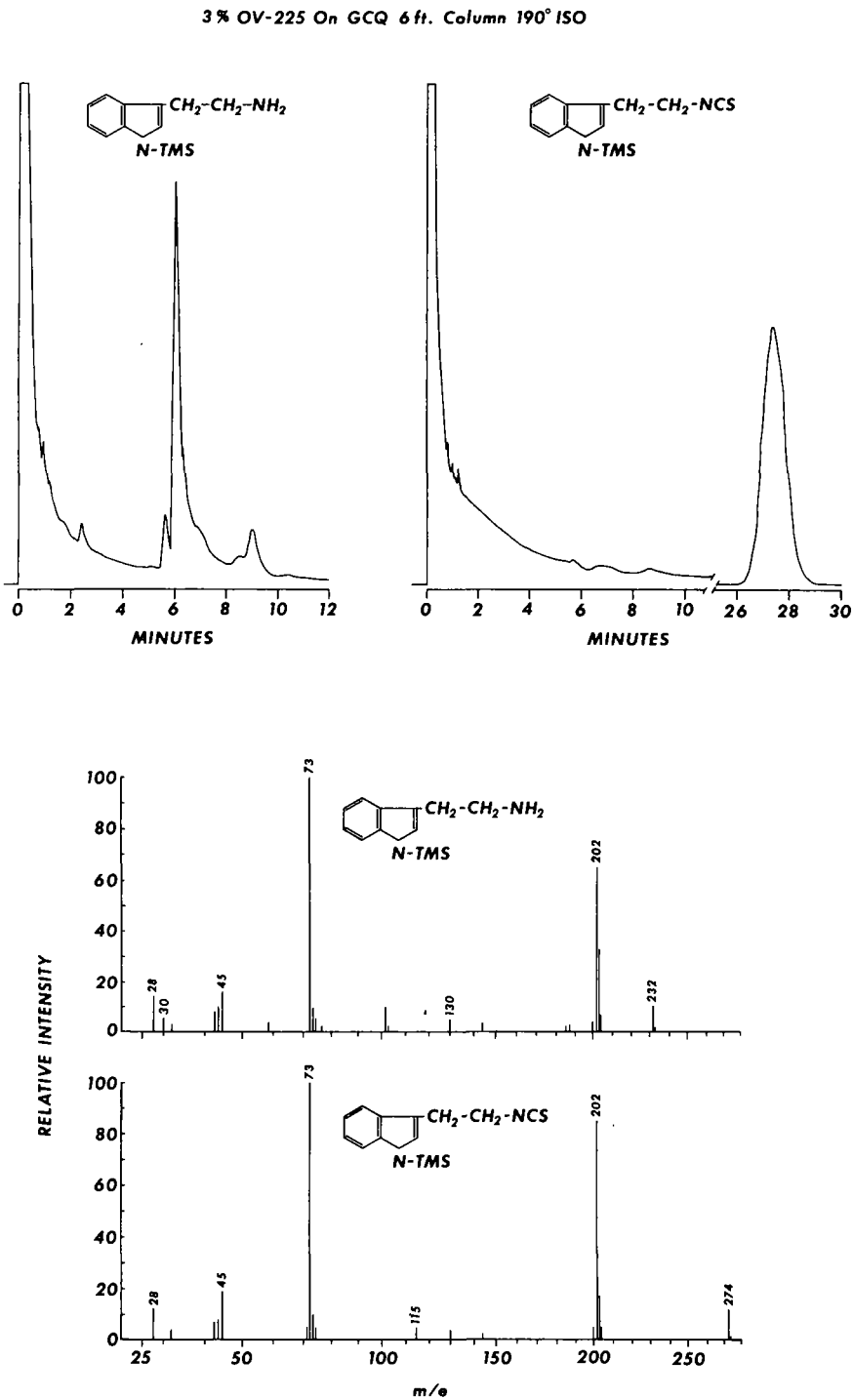
3% OV-225 On GCQ 6 ft. Column 190° ISO
CH2-CH2-NH2
N-TMS
CH2-CH2-NCS
N-TMS
0 2 4 6 8 10 12
MINUTES
0 2 4 6 8 10 26 28 30
MINUTES
RELATIVE INTENSITY
100 80 60 40 20 0
73
202
28
30
45
130
232
274
115
25 50 100 150 200 250
m/e

Fig. 1

I0,II-dihydroxy-protriptyline:Formation Via a Stable Epoxide Intermediate

CLAUDIO PANTAROTTO,GIORGIO BELVEDERE,ROBERTO FANELLI, VINCENZO ROVEI and ALBERTO FRIGERIO.

Ist."Mario Negri", Via Eritrea 62,20I57 Milan, Italy.

Unstable epoxides have been recognized as intermediates in the formation of dihydroxy derivatives of drugs.[I] Recently, stable epoxides of tricyclic drugs have been isolated from human and rat urine.[2] An investigation into the metabolic fate of protriptyline has revealed an oxidative metabolic transformation occurring in the rat species which leads to two urinary metabolites,namely I0-II-epoxy-protriptyline and I0-II-dihydroxy-protriptyline;the latter,previously identified ,also appears as its glucuronide.[3] The identification ofthese metabolites has been made by means of T.L.C., G.L.C.,M.S.and G.L.C.-M.S.analyses and the proposed structures were confirmed by comparison with authentic pure standard obtained by synthesis.

This work is being submitted for publication to the J.of Pharm.Sci.

[I] M.Stafford et al.,Res.Commun.Chem.Pathol.Pharm.8,593-606,I974

[2] A.Frigerio et al.,J.Pharm.Sci. 63,I536-I540,I974.

[3] S.F.Sisenwine et al.,J.Pharm.Exp.Ther.,I75,5I-59,I970.

GC/MS OF THERMALLY STABLE SULFONYLUREA DERIVATIVES

H. C. Ashline and W. E. Braselton, Jr.

Department of Medicine
Medical College of Georgia
Augusta, Georgia 30902

The sulfonylurea drugs tolbutamide, chlorpropamide and tolazamide have been used as oral antidiabetic agents for 15 years, but in spite of their widespread use, the pharmacokinetics and mechanism of action of these compounds are not well understood. Development of an adequate analytical method for measurement of the drugs and their metabolites is a necessary first step for clinical research in this area.

Thus far, gas chromatographic methods of quantitation have been hampered by the thermal decomposition of the sulfonylureas and their N-methyl derivatives during GLC analysis.[1,2] We have now been able to develop a method for formation of thermally stable derivatives of this class of compounds, and in this paper we describe their mass spectral and GLC characteristics. In addition we present a method for quantitation of serum levels of the drugs and some of their metabolites.

N-Methyl (N-Me) derivatives of chlorpropamide, tolazamide, tolbutamide and the tolbutamide metabolites hydroxytolbutamide and carboxytolbutamide were prepared by reaction with diazomethane; N-trideuteromethyl derivatives by reaction with [D_6]-dimethylsulfate. N-Me,N'-trifluoroacetates (TFA) and N-Me,N'-pentafluoropropionates (PFP) were then prepared by reaction with the appropriate anhydride (Fig. 1).

Mass spectra (70 eV, Finnigan quadrupole) of the TFA derivatives of chlorpropamide and tolbutamide were compared with the spectra of the PFP derivatives (Fig. 2). Several prominent ions arising by direct cleavage were seen (m/e 91 and 155 of tolbutamide, and corresponding ions 101 and 175 of chlorpropamide) as well as several rearrangement ions, which contain the perfluoroacyl group (50 a.m.u. between the TFA and PFP derivative). In addition, ion m/e 153 (203 of the PFP) was common to both chlorpropamide and tolbutamide, indicating a central portion of the molecule. The following scheme is proposed to account for the fragment ions observed in these compounds, as well as the corresponding derivatives of the tolbutamide metabolites:

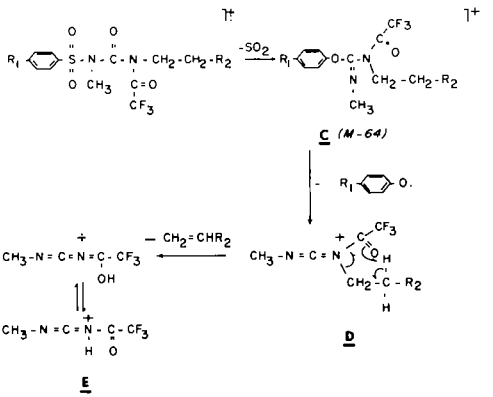

This is based on a similar rearrangement observed in the fragmentation of N-Me-tolbutamide[3], and was confirmed by the spectra of the N-CD_3,N'-TFA derivatives of chlorpropamide and tolbutamide, which resulted in a 3 a.m.u. shift in the fragments containing the N-CH_3 (N-CD_3).

An exception to the above mode of fragmentation was shown by tolazamide (Fig. 3) which did not undergo the loss of SO_2 and subsequent rearrangement.

The N-Me,N'-perfluoroalkyl derivatives were stable to GLC conditions as evidenced by their mass spectra, so the chromatographic mobilities were examined on several types of liquid phases, indicated in Table 1.

Table 1. GC/MS Relative Retention Times of Sulfonylurea N-Me,N'-TFA Derivatives.

Sample	3% OV-1, 210°	3% OV-17, 230°	3% SP 2401, 230°
Chlorpropamide	0.80	0.86	0.81
Tolbutamide	1.00	1.00	1.00
OH-Tolbutamide	1.39	1.26	1.97
COOH-Tolbutamide	1.97	2.06	1.97
Tolazamide	2.88	3.51	2.22

The excellent GLC characteristics and sensitivity to electron-capture detection made possible the quantitation of the compounds in small serum samples using the following procedure:

50 µl of serum were acidified with 50 µl of 1 N HCl and extracted with 5 ml ethyl acetate. One ml of the ethyl acetate fraction was dried with N_2 and reacted with 0.5 ml of diazomethane, 50 µl of MeOH for 5 min to prepare the N-Me-sulfonylurea. This was dried with N_2 and reacted 30 min at 65° with TFAA:pyridine:ethylacetate (15:7:100) to form the N-Me, N'-TFA derivative. This was again dried with N_2, and dissolved in 5 ml of cyclohexane, and 1 µl injected into the GLC with a known amount of reference standard (tolbutamide N-Me,N'-TFA for chlorpropamide measurement, chlorpropamide N-Me,N'-TFA for tolbutamide measurement). Samples were chromatographed on a 1.8 m x 2 mm i.d. glass column of 3% OV-1 on Gas Chrome Q at 180°, gas flow 37 ml/min. Quantitation was by the relative peak height method from a standard curve.

Measurements of serum levels of chlorpropamide were obtained on a normal subject following ingestion of 250 mg of chlorpropamide, and on a patient with chlorpropamide induced hypoglycemia, following withdrawal of treatment with the drug (Fig. 4). The values were compared with those obtained by MID on parallel samples. MID was performed by repetitively scanning ions m/e 153 of tolbutamide (external standard) and chlorpropamide, and m/e 175 and 195 of chlorpropamide for 600 msec each. The GLC conditions were the same as those used for the electron capture measurements.

The quantitative results obtained by GLC with electron capture detection were comparable to those obtained by MID (Fig. 4). In addition, mass spectra of the sulfonylurea compounds extracted from serum of patients treated with the drugs, and examined by GC/MS were identical to the reference compounds. These results indicate that the less expensive and less complicated GLC method can be used for blood level measurement of sulfonylurea drugs, a procedure we are now routinely employing.

References

1 Wickramasinghe, J.A.F. and S.R. Shaw, J. Pharm. Sci. 60, 1669 (1971).

2 Simmons, D.L., R.J. Ranz and P. Picotte, J. Chromatog. 71, 421 (1972).

3 Sabih, K., Biomed. Mass Spectrom. 1, 163 (1974).

4 This work was supported by a grant from the Upjohn Company.

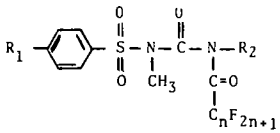

	R_1	R_2
Tolbutamide	CH_3-	-C_4H_9
Hydroxytolbutamide	$C_nF_{2n+1}COO$-	-C_4H_9
Carboxytolbutamide	CH_3OCO-	-C_4H_9
Chlorpropamide	Cl-	-C_3H_7
Tolazamide	CH_3-	-$C_6H_{12}N$

FIGURE 1. Sulfonylurea N-Methyl,N'-Perfluoroacyl Derivatives.

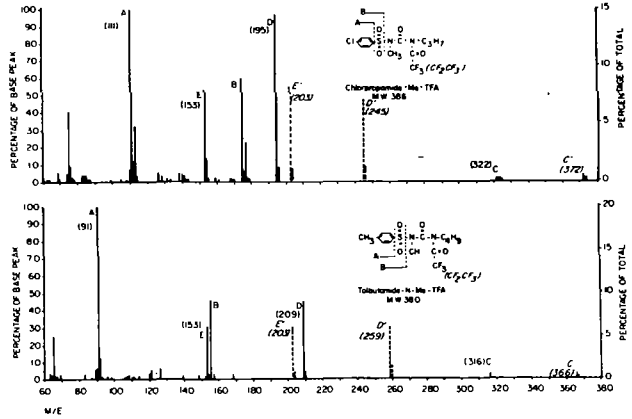

FIGURE 2. Mass spectra (70 eV) of N-Me,N'-TFA derivatives of tolbutamide and chlorpropamide. The 50 a.m.u. increases observed in the spectra of the corresponding PFP derivatives are indicated by dashed lines.

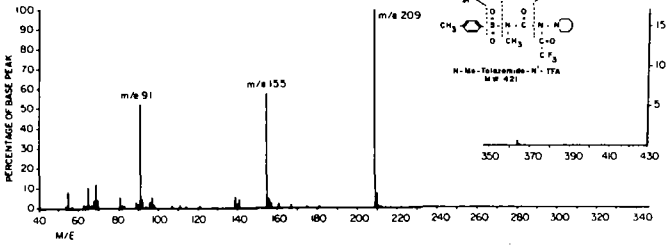

FIGURE 3. Mass spectrum (70 eV) of tolazamide-N-Me, N'-TFA.

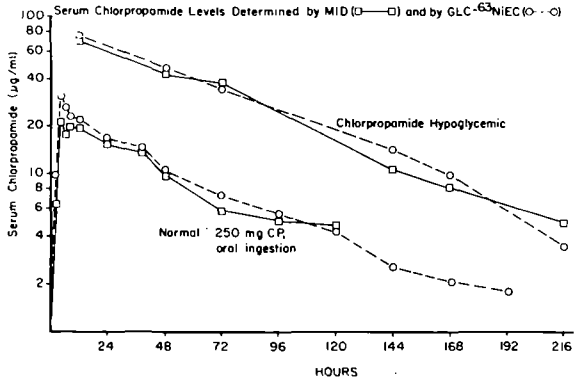

FIGURE 4.

Precision and Accuracy in Measuring Picomole Quantities of Norepinephrine by Quadrupole-Selected Ion Monitoring

R. C. Murphy, J. A. Zirrolli, K. Clay, S. E. Hattox and R. Helbig

Department of Pharmacology
University of Colorado Medical Center
Denver, Colorado 80220

Quadrupole mass spectrometers have been described as being well suited for selective ion monitoring for quantitative measurement of minute quantities of biologically produced molecules. There have been few reports of studies designed to evaluate the precision and accuracy with which these instruments can be expected to operate under such conditions. Errors in measurement could arise from various sources; and considering the gas chromatography-mass spectrometer alone, one might expect potential errors from i) physico-chemical differences between the internal standard and the desired compound to be measured, and ii) parameters of the GC-MS system affecting sensitivity and thus fidelity of the data. Evaluation of these points has been the goal of the present study using a commercial gas chromatography-mass spectrometer-computer system (Finnigan Corp.) in the quantitation of the neurotransmitter, norepinephrine (NE) (I) using α-methylnorepinephrine (MNE (II) and deuterated norepinephrine (DNE) (III) (1).

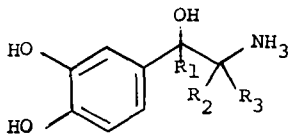

I $R_1 = R_2 = R_3 = H$

II $R_1 = R_2 = H,\ R_3 = CH_3$

III $R_1 = R_2 = R_3 = D$

An equimolar stock solution of these catecholamines was carefully made in 0.1 N HCl. Preparation of the pentafluoropropionyl derivatives were made according to the procedure of Costa et al. (2). The derivatized compounds were separated on the gas chromatograph and the ions at m/e 176 and 190 were monitored as described by Costa (2), and in addition the ion at m/e 178 which is specific for the deuterated norepinephrine was monitored. The area under each ion-envelope was integrated and normalized to 10.00 for the area for norepinephrine (m/e 176). Figure 1 summarizes the resultant data with each point representing the mean of five analyses of one sample and the sample-standard deviation indicated by the error bars. From three to eight samples were prepared at each dilution level indicated in Fig. 1.

The results from the quantitative measurement of DNE demonstrate very good accuracy and precision. The measurement of the MNE from the same sample and by the same technique was unsatisfactory. Figure 1 shows that the m/e 178 abundance (DNE) was always found at the theoretical value of 10.0. In contrast, the abundance of m/e 190 (MNE) varied considerably within each dilution level as well as replicate analyses of the same sample as evidenced by the error bars.

Possible factors producing such a dicotomy in results include i) chemical degradation of the sample before or during the analysis, ii) measurement of fragment ions whose abundance might be sensitive to small changes in ion source parameters, especially temperature, or iii) a change in ionization conditions or ion detection sensitivity during or between

in ionization conditions or ion detection sensitivity during or between analyses. This latter possibility could play a major role since NE elutes many seconds apart from MNE but simultaneously with DNE. Further evidence of this latter possibility is the readily observed phenomenon on the oscilloscope when focusing the ion source using perfluorotributylamine. Changing the various ion source voltages such as lens, extractor, ion energy (acceleration voltage), and resolution can greatly alter the ratio of m/e 69 to m/e 219.

A quantitative measurement of the isotopes of xenon was undertaken to evaluate the contribution of ion source parameters alone. Xenon was chosen since it is an monoatomic gas having several isotopes of known abundance. These facts would eliminate the first two possible sources of error mentioned above. Xenon (760 torr) was introduced into the mass spectrometer at 2×10^{-6} torr by means of a viscous leak (150 cm x .0178 cm capillary). The isotopes at m/e 129, 131, and 136 were measured by selected ion monitoring while opening and closing a valve at the low pressure end of the inlet. Abundance was measured by integration of the appropriate mass unit. Several parameters effected isotope ratios - electron multiplier voltage, lens voltage, and ion energy. Figure 2 shows the ratio of 131/129 and 136/129 measured five times each, after nine intervals. Every attempt was made to minimize the fractionation of xenon and keep the instrument parameters constant except ion energy. The results show that even over a seven amu difference, a loss in precision and accuracy can be observed as compared to the two amu difference. While the magnitude of the errors was substantially less than the norepinephrine case, the trend towards a mass-dependent error is evident.

These experiments with a quadrupole mass spectrometer indicate a paradoxical loss of precision and accuracy in a mass-dependent manner becoming severe even at 14 amu. This error was not related to the absolute amount of sample in the ion source, and may prevent the use of homologous compounds as internal standards if high precision and accuracy are desired. An understanding of this phenomenon must await further experimentation.

REFERENCES

1. R. C. Murphy: J. Labelled Compds., in press.

2. E. Costa, A. R. Green, S. H. Koslow, H. I Leferen, A. V. Revuelta, and C. Wang: Pharm. Rev. 24, 167 (1972).

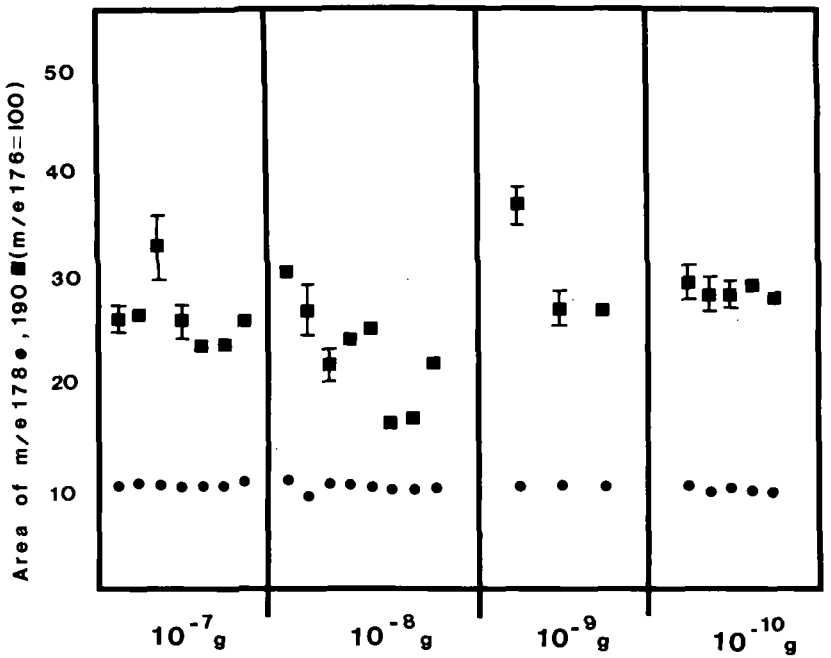

FIGURE 1: Relative area of deuterated norepinephrine (m/e 178 ●) and α-methylnorepinephrine (m/e 190 ■) to norepinephrine in a derivatized aliquot from an equimolar mixture of all three at the indicated dilution level. Each point is the mean of five determinations with the error bars indicating one standard deviation.

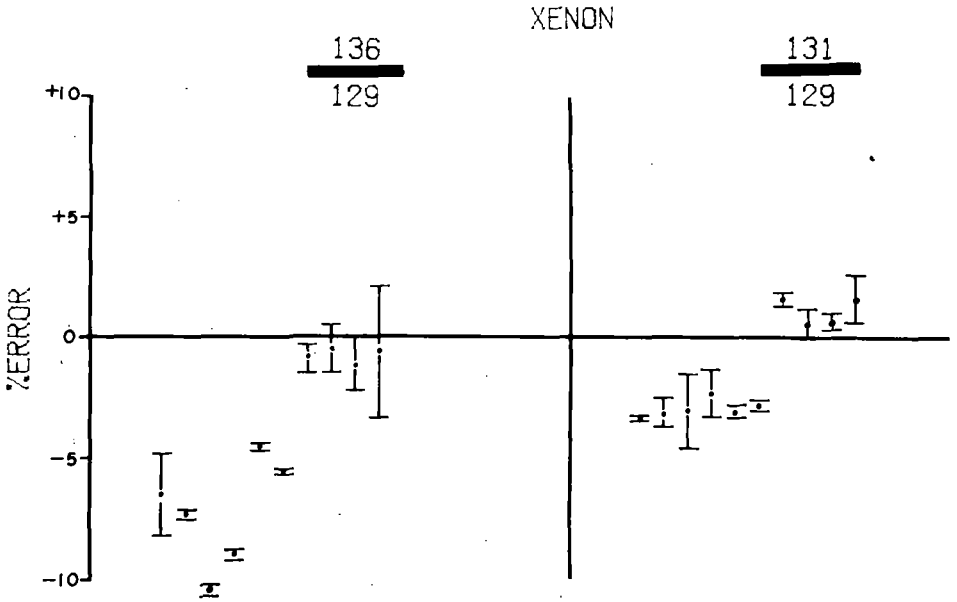

FIGURE 2: Error in the calculated ratios of the indicated isotopes of xenon from published values. Each point is the mean of five measurements after introduction of xenon into the ion source.

Differentiation of Endogenous N-methyl Derivatives in Serum Extracts from Artifacts Caused by N-methylation in the Injector of the Gas Chromatograph.

Lan K. Wong, Catherine E. Costello, and K. Biemann

Department of Chemistry, M.I.T., Cambridge, MA 02139

N,N'-dimethoxymethylphenobarbital (DMMP, I), a potentially useful anticonvulsant, is known to be metabolized to phenobarbital (II) in humans. There have been some indications that phenobarbital is further methylated in vivo to give N-methylphenobarbital (mephobarbital, III). However, detection of N-methylphenobarbital in serum extracts of DMMP patients seems to be very dependent on extraction and gas chromatographic procedures. This has led us to suspect that N-methylphenobarbital might arise from some thermally induced reaction between phenobarbital and an agent in the serum extract during gas chromatography.

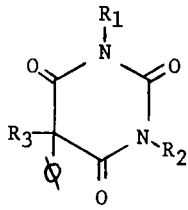

	R_1	R_2	R_3
(I)	CH_2OCH_3	CH_2OCH_3	CH_2CH_3
(II)	H	H	CH_2CH_3
(III)	CH_3	H	CH_2CH_3
(IV)	H	H	CD_2CD_3
(V)	CH_3	H	CD_2CD_3
(VI)	CH_3	CH_3	CH_2CH_3
(VII)	CD_3	CD_3	CH_2CH_3
(VIII)	CD_3	CH_3	CH_2CH_3

When a serum extract obtained from a DMMP patient was coinjected with a sample of phenobarbital-ethyl-d_5 (IV) into a gas chromatograph and the eluents examined by mass spectrometry, both unlabelled N-methylphenobarbital (III) and N-methylphenobarbital-ethyl-d_5 (V) were detected as evidenced by the selected ion records of m/e 218 and m/e 219 (fig. 1), base peaks of the two compounds, respectively. In another experiment, phenobarbital was added to a serum extract which was devoid of any drug components and the mixture was subjected to GC-MS analysis. Again N-methylphenobarbital was detected. These results prove that an agent in serum extract is indeed capable of N-methylating phenobarbital under gas chromatographic conditions. However, they cannot rule out the possibility that some of the N-methylphenobarbital detected could be due to endogenous methylation.

To clarify this ambiguity, we designed an experiment in which all available free amide positions were trideuteromethylated with excess trimethyl-d_9 anilinium hydroxide (TMAH-d_9) at the injection port of the gas chromatograph. This procedure could suppress any N-methylation by the alkylating agent present in serum. In doing so, detection of any further unlabelled N-methyl compounds would be indicative of endogenous methylation. Thus, a serum extract obtained from a DMMP patient was coinjected with the TMAH-d_9 reagent for GC-MS analysis. At the point where N,N'-dimethylphenobarbital (VI) was expected to elute in the gas chromatogram, only the N,N'-dimethyl-d_6 species (VII) was detected. The mass spectrum (fig. 2) did not contain any ion of m/e 235. This ion would have been the

base peak of the N-methyl-d_3,N'-methyl species (VIII) (fig. 3), should N-methylphenobarbital have been present and trideuteromethylated subsequently by TMAH-d_9. Thus, it can be concluded that N-methylphenobarbital is not a metabolite from DMMP or phenobarbital, but merely a GC artifact. Also other compounds such as diphenylhydantoin and fatty acids appear to be methylated by the serum alkylating agent to N-methyldiphenylhydantoin and methyl esters, respectively. In addition to its utility for clarifying the ambiguity presented by this artifact production, the TMAH-d_9 reagent would be useful for quantitation of mephobarbital in the presence of phenobarbital when a mass spectrometer is used in drug analysis.

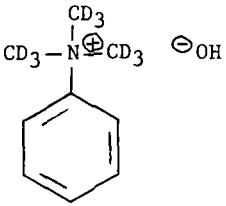

Trimethyl-d_9 anilinium hydroxide

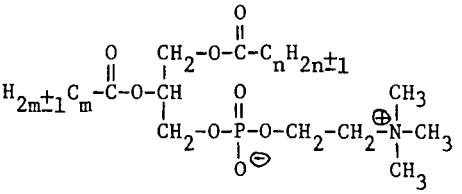

m = 15,17
n = 15,17 Lecithin

The trimethyl quarternary amine structure of TMAH-d_9 suggested to us that a choline derivative might be the methylating agent in serum responsible for the formation of these artifacts. Lecithin (phosphatidyl choline) seemed to be a likely candidate since the fatty acid side chains of this compound cause it to be soluble in the organic solvents employed in most extraction procedures during drug analysis. Indeed, GC-MS analysis of a mixture of phenobarbital and a benzene solution of lecithin revealed the formation of N-methylphenobarbital. The extent of methylation was comparable to that due to the methylating agent present in serum.

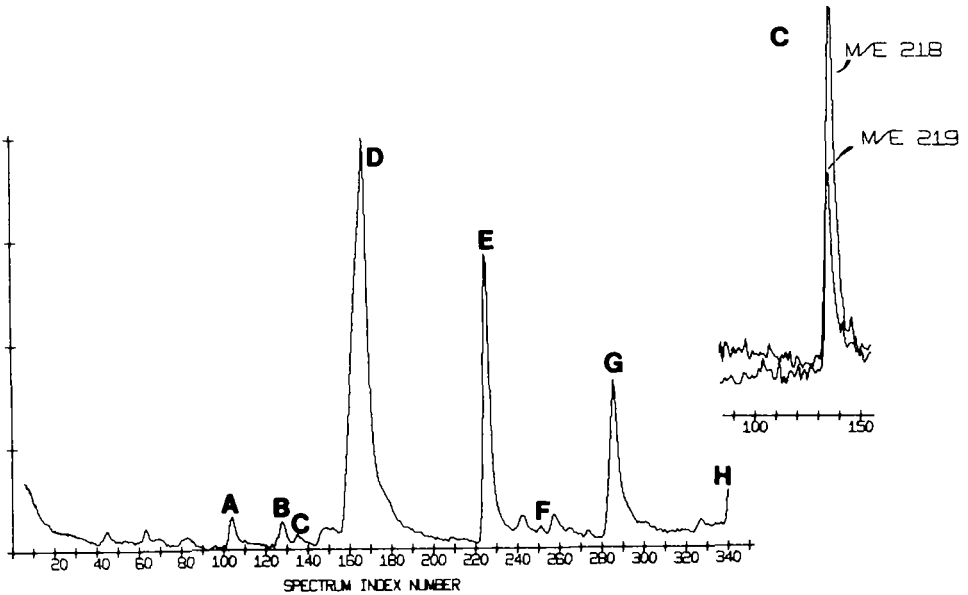

Figure 1

Figure 2

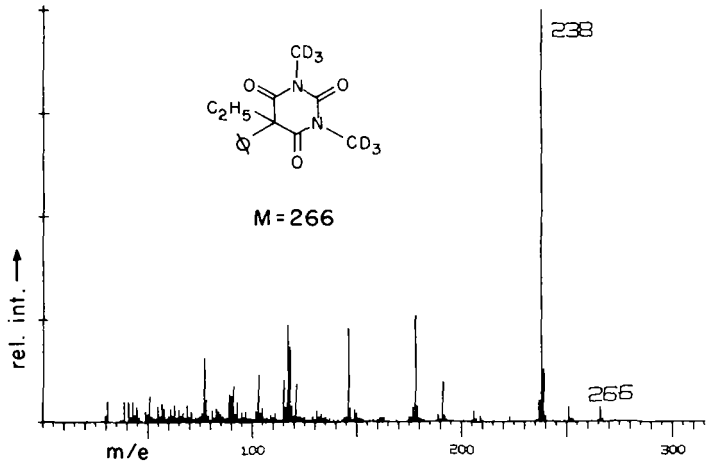

Figure 3

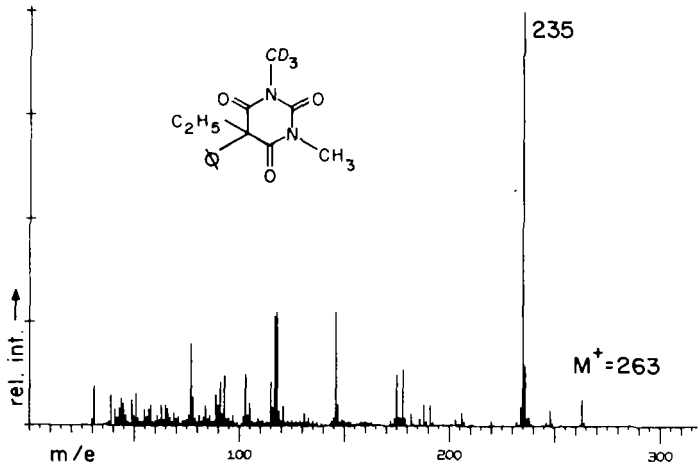

Fig. 1: Total ion plot of serum extract obtained from DMMP patient coinjected with phenobarbital-ethyl-d_5:
A,B = phthalate plasticizers
C = N-methylphenobarbital (d_0 and d_3)
D = phenobarbital
E = tri-2-butoxyethyl phosphate (impurity from B-D Vacutainer)
F = N-methyl phenyl-p-methylphenyl hydantoin
G = phenyl-p-methylphenyl hydantoin; H = cholesterol.
The selected ion records of ions m/e 218, m/e 219 for component C are shown in the top right insert.

Fig. 2: Mass spectrum obtained during GC-MS analysis after TMAH-d_9 derivatization of serum extract from phenobarbital patient. Note that ion m/e 235 is absent.

Fig. 3: Mass spectrum of N-methyl,N'-methyl-d_3 phenobarbital.

Negative Ion Mass Spectral Studies of Some Underivatized Nucleosides

Costello L. Brown and Virginia Hanson

Chemistry Department
California State University
Los Angeles, California
90032

Negative ion studies have been carried out on the following underivatized nucleosides: thymidine, adenosine, uridine, inosine and guanosine. Despite the volatility problems and also the fact that these molecules are not particularly promising candidates to produce good negative ions, we were able to obtain negative ion spectra at 70 eV and also at voltages below 8 eV on all compounds investigated. The spectra for these compounds are not complex and contain relatively few peaks, which were dominated by an ion derived from the base fragments of the molecules. Molecular ions were consistently detected only at voltages less than 2 eV. Sugar-derived fragments were rarely observed.

It is apparent from these initial investigations that negative ion spectra can provide structurally significant information for the analysis of nucleosides. The spectra obtained show significantly enhanced parent ions, no rearrangement ions and fewer peaks.

Ionization efficiency curves were obtained on the more prominent peaks.

Structural Studies on the Modified Nucleoside Q, Isolated From E.coli Transfer RNA.

H. Kasai, Z. Ohashi, F. Harada, S. Nishimura, N. J. Oppenheimer*, P. F. Crain, J. G. Liehr, D. L. von Minden, and J. A. McCloskey

National Cancer Center Research Institute, Tokyo, Japan; University of California, San Diego, California*; and Baylor College of Medicine, Houston, Texas.

The structure of the unknown modified nucleoside Q, present in the first position of the anticodons of E. coli $tRNA^{Tyr}$, $tRNA^{His}$, $tRNA^{Asn}$, and $tRNA^{Asp}$, is proposed to be 7-(4,5-cis-dihydroxy-1-cyclopenten-3-yl-aminomethyl)-7-deazaguanosine (I). The structure of Q was deduced from studies of its chemical reactivity, and spectral data, including UV absorbance, proton NMR, and mass spectrometry. A complete high resolution mass spectrum of the N-acetyl-permethyl derivative established the presence of the 7-deazapurine nucleus and the cyclopentenediol side chain. These unusual structural features were further confirmed by mass spectra of the N-acetyl-pertrimethylsilyl, pertrimethylsilyl, and di-O-isopropylidene-pertrimethylsilyl derivatives.

The structure of Q is unique in that its 7-deazaguanine base represents the first example of purine skeleton modification in a nucleoside from tRNA. A complete account of this work is in press in Biochemistry.

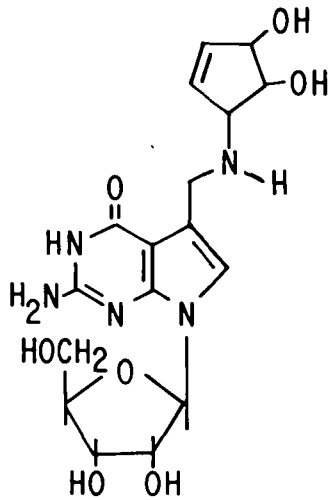

I

Hydrogen Rearrangement Reactions in the Mass Spectra of Nucleosides

S. E. Hattox, Institute for Lipid Research, Baylor College of Medicine, Houston, Texas 77025.

K. H. Schram and J. A. McCloskey, Department of Biopharmaceutical Sciences, University of Utah, Salt Lake City, Utah 84112.

The mass spectra of C-perdeuteriouridine (uridine-d_8)(1)(1), uridine-3'-d(2), 1-(β-D-xylofuranosyl)uracil-3'-d(3) and 1-(β-D-arabinofuranosyl) uracil-2'-d(4) were examined in an effort to determine the identity of specific hydrogens involved in various hydrogen transfer and elimination reactions which occur following electron ionization. The results of these studies will have application in the determination of the biosynthetic pathways of nucleoside antibiotics and minor nucleosides in RNA, and in studies of the distribution and metabolism of nucleosides of medicinal interest.

Analysis of the spectrum of 1 versus uridine made possible the identification of ions and elimination reactions involving skeletal hydrogens. It was found that loss of water from the molecular ion (m/e 252) involves a hydroxyl group and a skeletal hydrogen from the ribose ring. The mass spectra of 2,3 and 4 (2) indicate that initial loss of water does not involve the hydrogens in the 2' or 3' positions of these compounds. Also of interest is that in the b^+2H ion (m/e 113 for uridine) of 2, 3 and 4 the hydrogen transferred is not from the 3' position or the 2' position of 2. The spectrum of 1 shows that a significant amount of skeletal hydrogen is transferred to form the b+2H ion (m/e 116).

The ions at m/e 57 and m/e 73 in the spectrum of uridine are intense peaks derived from the carbohydrate moiety and were shown to have the compositions C_3H_5O and $C_3H_5O_2$ respectively. The data in Table 1 support the presence of the 5', 4' and 3' carbon atoms of the ribose ring as proposed by DeJongh et al., (4). The ion at m/e 73 (Table 2) is thought to contain the 1', 2' and 3' carbon atoms and to have the structure shown. Similar analysis of the trimethylsilyl derivatives (5) of 1, 2, 3 and 4 shows that the ion at m/e 129 in the spectrum of uridine-$(TMS)_4$ has a structure analogous to the ion at m/e 57 in the free nucleoside but contains an OTMS group. Likewise, the ion at m/e 217 is the TMS analog of the m/e 73 species in the free nucleoside (Table 3).

These results lead to the following conclusions:

1) The skeletal hydrogens at the 3' position of 2 and 3 and at the 2' position of 4 do not undergo significant transfer to the base or are lost as water.

2) The ion of m/e 57 in the free nucleosides and m/e 129 in the TMS derivatives contain the 5',4' and 3' carbon atoms.

3) The ion of mass 73 in the free nucleosides and mass 217 in the TMS derivatives contain the 3', 2' and probably the 1' carbon atoms.

Table 1

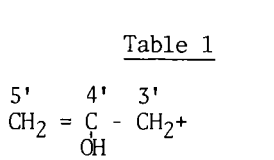

compound	m/e	shift
uridine	57	0
1	61	4
2	58	1
3	58	1
4	57	0

Table 2

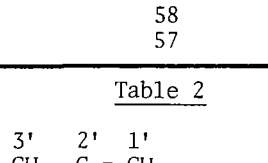

compound	m/e	shift
uridine	73	0
1	76	3
2	74	1
3	74	1
4	74	1

Table 3

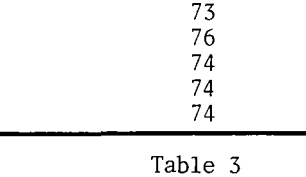

compound	m/e	shift
uridine	217	0
1	220	3
2	218	1
3	218	1
4	218	1

References

1) S. E. Hattox and J. A. McCloskey, Anal. Chem., 46, 1378 (1974).
2) Prepared by reduction of the 2' and 3' keto-ditrityl nucleosides using sodium borodeuteride. A. F. Cook and J. G. Moffatt, J. Amer. Chem. Soc., 89, 2697 (1967).
3) J. A. McCloskey and K. Biemann, J. Amer. Chem. Soc., 84 2005 (1962).
4) D. C. DeJongh, T. Radford, J. D. Hribar, S. Hanessian, M. Bieber, G. Dawson and C. C. Sweeley, J. Amer. Chem. Soc., 91, 1728 (1969).
5) J. A. McCloskey, A. M. Lawson, K. Tsuboyama, P. M. Krueger and R. N. Stillwell, J. Amer. Chem. Soc., 90, 4182 (1968).

STERICALLY CROWDED SILYL GROUPS AS DIRECTORS OF FRAGMENTATION IN THE MASS SPECTRA OF 2'-DEOXY-NUCLEOSIDES

by

John B. Westmore and Michael A. Quilliam
Department of Chemistry, University of Manitoba,
Winnipeg, Canada

and

Kelvin K. Ogilvie
Department of Chemistry, McGill University,
Montreal, Quebec, Canada

The use of alkylsilyl groups for the protection of hydroxyl functions in various molecules, in particular ribonucleosides and 2'-deoxy-nucleosides, has been studied. In addition to having desirable properties for synthetic procedures the alkylsilyl group imparts valuable characteristic properties to the nucleosides for thin-layer chromatography, gas chromatography and mass spectrometry. For our purposes, the groups of greatest synthetic value, arranged in order of increasing steric crowding around the silicon atom, were

$\underline{i}\text{-}C_3H_7(CH_3)_2Si\text{-}$	$\underline{cyclo}\text{-}C_4H_8(\underline{i}\text{-}C_3H_7)Si\text{-}$	$\underline{t}\text{-}C_4H_9(CH_3)_2Si\text{-}$
DMIPS	TMIPS	TBDMS
$(\underline{i}\text{-}C_3H_7)_2CH_3Si\text{-}$	$(\underline{i}\text{-}C_3H_7)_3Si\text{-}$	$\underline{cyclo}\text{-}C_4H_8(\underline{t}\text{-}C_4H_9)Si\text{-}$
DIPMS	TIPS	TMTBS

The steric effects of the substituents influence rates and selectivities of substitution or replacement at various hydroxyl functions.

The isomeric pairs, I and II, can be distinguished by TLC, or by GC on a non-polar column such as OV-1. The mass spectra of the

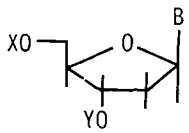

I

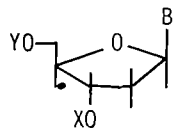

II

B = T, U or A

X or Y = H or silyl group

isomers are characteristically different. Elimination of a bulky alkyl group from the silyl moiety of the molecular ion (which is not itself detectable) occurs very readily to give an ion having the charge localized on the silyl residue. Subsequent fragmentation is quite

different for I and II. Many ions are formed by skeletal rearrangements, their formation being governed by the steric accessibility of electron-rich parts of the molecule to the positively charged siliconium residue.

The mass spectral behaviour of these silyl derivatives is quite different from that of trimethylsilyl derivatives. The rearrangements that involve migration of an intact silyl group are suppressed while those influenced by interaction with the siliconium center are enhanced. This observation should allow a more detailed study of siliconium ion interactions and accentuate certain types of structural information.

References:

M. A. Quilliam, K. K. Ogilvie and J. B. Westmore, Biomed. Mass Spectrom. 1, 78 (1974)

K. K. Ogilvie, E. A. Thompson, M. A. Quilliam and J. B. Westmore, Tetrahedron Lett. 2865 (1974)

K. K. Ogilvie, K. L. Sadana, E. A. Thompson, M. A. Quilliam and J. B. Westmore, Tetrahedron Lett. 2861 (1974)

M. A. Quilliam, K. K. Ogilvie and J. B. Westmore, J. Chromatography 105, 297 (1975)

THE CHARACTERIZATION OF N-PHOSPHONOMETHYLGLYCINE AND ITS METABOLITE AMINOMETHYLPHOSPHONIC ACID BY GC/MS/COM AND ISOTOPIC DILUTION TECHNIQUES[1]

Melvin L. Rueppel* and John T. Marvel
Agricultural Research Department
Monsanto Agricultural Products Company
St. Louis, Mo. 63166

N-Phosphonomethylglycine (PMG), the active ingredient of Roundup(R) herbicide, is characterized by low toxicity, negligible environmental impact, and rapid degradation to CO_2 via aminomethylphosphonic acid (AMP). Aminoalkylphosphonates, in general, may be derivatized at microgram levels with trifluoroacetic anhydride followed by diazo-n-butane esterification. The structure of these derivatives have been confirmed spectrally (^{1}H-NMR and GC/MS/COM) and major mass fragments assigned by HRMS in order to permit isotopic dilution techniques. Purified metabolic samples of PMG and AMP (<1 ppm in soil and plants) have been derivatized and characterized by GC/MS/COM thereby confirming chromatographic characterizations. The applicability of isotopic dilution techniques to the unambiguous characterization of low purity, difficultly derivatized plant metabolic samples have been demonstrated using ^{13}C-enriched PMG appropriately.

[1] Complete discussions of these results will be submitted to J. Agr. Food Chem. and Biomedical Mass Spectrometry.

IDENTIFICATION OF NOVEL DITERPENOID ALKALOIDS IN *DELPHINIUM AJACIS* BY MASS SPECTROMETRY

Presented at the
American Society of Mass Spectrometry
Houston, Texas
May 25-30, 1975

George R. Waller and Robert H. Lawrence, Jr.
Biochemistry Department
Oklahoma State University
Stillwater, Oklahoma

Alkaloids with diterpenoid skeletons have been isolated from several families of Ranunaclacae--mainly *Aconitum* and *Delphinium*. These compounds have long been of interest because of their pharmacological properties and complex structures. Many of these compounds are among the most toxic materials of plant origin known to man. They cause nausea, excessive salivation and frequent swallowing; death is usually thought of being due to paralysis of the respiratory center.

This paper will briefly familiarize you with the diterpenoid alkaloids occurring in *Delphinium ajacis*, our methods of extraction and analysis, their distribution in the plant, and their occurrence in tissue cultures of *Delphinium ajacis*.

The common larkspur, *Delphinium ajacis*, is widely distributed in the western United States where it has been a common cause of cattle poisoning. In fact, more cattle deaths in the U.S. can be attributed to larkspur poisoning than from any other poisonous plant. Sheep and horses are much less susceptible. Research shows that these plants furnish good range forage without risk for sheep. It is also a common plant in home gardens. *Delphinium ajacis* has been shown to produce alkaloids of two main diterpenoid skeletal types which are antipodal to the steroids.

Ajaconine is the only atisine skeletal type conclusively identified in *D. ajacis*. It is derived from a tetracyclic diterpine in which carbons 19 and 20 are linked with the nitrogen of B-amino ethanol; it has a C-17, C-9 ether bridge, and contains one secondary hydroxyl group (Figure 1).

Three lycoctonine-type alkaloids have been positively identified in *D. ajacis* extracts (delcosine, acetyldelcosine, and delsoline). These are derived from a pentacyclic diterpene where carbon atoms C-19 and C-20 are linked with a nitrogen of ethylamine; they all contain at least three methoxyls, one secondary hydroxyl group and two tertiary hydroxyl groups--the difference between the three being their substitution on the five-membered ring which is gydroxyl for delcosine, methosyl for delsoline, and this position is acetylated in acetyldelcosine (Figure 1).

The extraction procedures that have been used in this paper demonstrate that they are highly specific and provide a shortened and quantitative procedure:

1. Drying the tissue and grinding to a powder
2. This is soaked in 10% acetic acid for one hour, after which it is sonicated for three minutes.
3. This acetic acid extract is washed with carbon tetrachloride, then made basic to pH 13 with 5N NaOH being careful to keep below about 10° C. This is then extracted with carbon tetrachloride followed by chloroform. This chloroform extract containing diterpenoid alkaloids can then be analyzed directly.

Analysis of this chloroform extract utilized TLC, GLC, GC-MS, and direct probe-MS. TLC analysis on Silica Gel-G using benzene:ethylacetate: diethylamine served only as a rough quantitative assay.

Analysis by GLC and GC-MS required the development of an all glass solid injection system to prevent partial dehydration and epimerization of the diterpenoid alkaloids and to prevent high liquid phase bleed resulting from solvent stripping of the OV-61 columns used.

Major fragment ions that are characteristic of the compound and which have low cross contribution from the other compounds are selected. The cross contribution is determined as are the response factors from known amounts of pure compounds.

Probe runs are then analyzed by repetitive scans in the high mass range (where most of the important fragment ions occur). The ion intensities of the interpretive fragment ions are plotted--the area under each curve is determined and corrected for cross contributions and response factor to arrive at a total μg estimation for each known compound. Unknowns are monitored by their characteristic fragment ions and estimated relative to the knowns.

Table 1 shows the results using the direct probe-Mass Spectrometry method in the analysis of extracts of seeds from the D. ajacis plants. The total diterpenoid alkaloid content in terms of the known alkaloids was lowest in the roots, lower leaves, and upper leaves and highest in the seeds, mature fruit, immature fruit and the flowers. Thus all plant parts analyzed contained from 0.02% to 0.46% diterpenoid alkaloids. Delcosine was the predominant diterpenoid alkaloid in all tissues studied.

Some transport of diterpenoid alkaloids may be occurring out of the lower leaves and this appears to be fairly non-selective.

The elemental composition of the M^{+}-189 ion d is common to delcosine, acetyldelcosine, delsoline, and the unknowns reported except M. W. 329.

We postulate that these represent compounds where (1) all free hydroxyls are methylated (MW=509), (2) C-14 is acetylated and two of the remaining three hydroxyls are mythylated (M=523) and (3) similar to the 523 with the last free hydroxyl methylated (M=537). These characteristics are predominant in lower leaves but are present in all parts except roots. The plant contains a considerable amount of unknown diterpenoid alkaloids.

An additional unknown has been isolated from the roots with a molecular weight of 329, and the parent ion is the base peak. The root unknown is in about the same concentration as ajaconine. Preliminary information indicates that this may be hetisine, an atisine-type alkaloid not previously identified in D. ajacis.

In summary, I have described the method of extraction, analysis, distribution of alkaloids in the plants and their occurrence in tissue cultures of Delphinium ajacis. Some tentative structures and suggestions were described concerning their possible role in biosynthesis of diterpenoid alkaloids of D. ajacis.

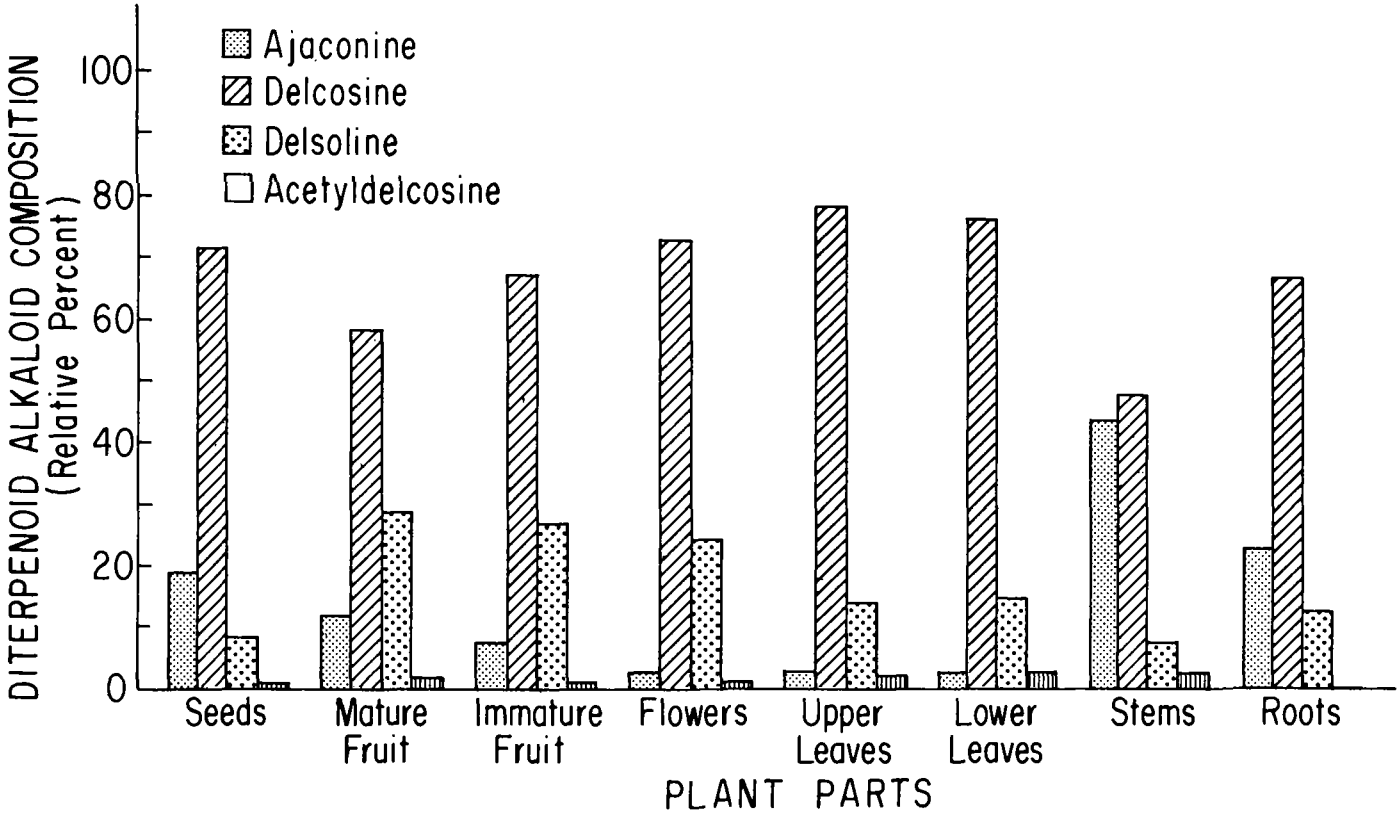
Ajaconine
Delcosine
Delsoline
Acetyldelcosine
DITERPENOID ALKALOID COMPOSITION
(Relative Percent)
100
80
60
40
20
0
Seeds
Mature Fruit
Immature Fruit
Flowers
Upper Leaves
Lower Leaves
Stems
Roots
PLANT PARTS

TABLE 1

FIGURE 1

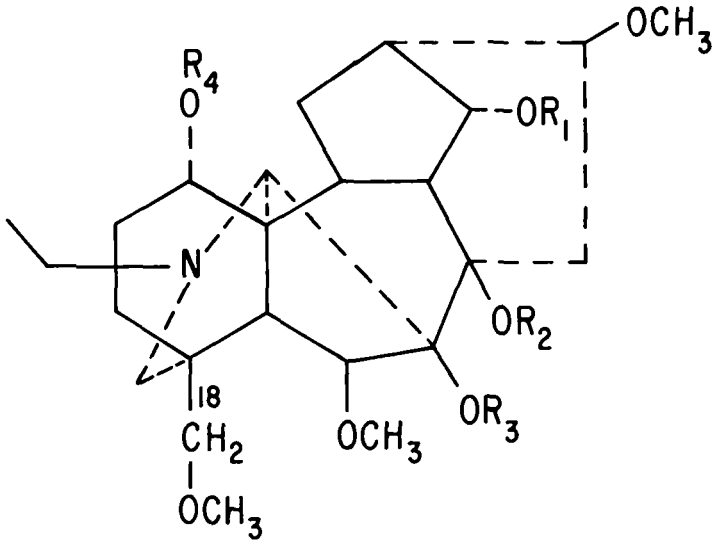

UNKNOWN DITERPENOID ALKALOIDS FROM *D. AJACIS* – PROPOSED STRUCTURES
(Lycoctonine Skeletal Type)

$R_1 = R_2 = R_3 = R_4 = CH_3$	M. W. = 509
$R_1 = COCH_3$; $R_2 = R_3 = CH_3$; $R_4 = H$	M. W. = 523
$R_1 = COCH_3$; $R_2 = R_3 = R_4 = CH_3$ (other combinations of R are possible)	M. W. = 537

KNOWN ALKALOIDS

$R_1 = R_2 = R_3 = R_4 = H$	Delcosine	M. W. = 453	*D. AJACIS*
$R_1 = CH_3$; $R_2 = R_3 = R_4 = H$	Delsoline	M. W. = 467	*D. AJACIS*
$R_1 = COCH_3$; $R_2 = R_3 - R_4 = H$	Acetyldelcosine	M. W. = 495	*D. AJACIS*

EI AND FI MASS SPECTRA OF THE FLUORESCAMINE DERIVATIVES OF SOME BIOLOGICALLY IMPORTANT PRIMARY AMINES INCLUDING AMPHETAMINES AND AMINO ACIDS

N. Narasimhachari
Galesburg State Research Hospital
Galesburg, Illinois 61401

E. Kempster and M. Anbar
Mass Spectrometry Research Center
Stanford Research Institute
Menlo Park, California 94025

In a preliminary report the electron impact mass spectra of the fluorescamine derivatives of some primary amines including amphetamines and the ethyl esters of aminoacids were presented and the fragmentation patterns discussed.[1] We have now extended this study to several other compounds with the primary amino function and all the essential amino acids. In addition, the Field Ionisation mass spectra of the fluorescamine derivatives of a few typical amines (e.g. dopamine, d-amphetamine, tryptamine and 5-hydroxytryptamine) and amino acid mixture are also obtained using the Field Ionisation source described by Anbar and Aberth.[2]

Preparation of Fluorescamine Derivatives: The methods used for the pure standards of amines and aminoacid ethylesters were essentially the same as described earlier.[1] For the preparation of the free amino acid derivatives, the acit was first dissolved in borate buffer (pH 9.0) and then treated with fluorescamine reagent in ethyl alcohol. The mixture was acidified to pH 2 with 0.5N HCl and extracted twice into ethyl acetate. The ethyl acetate layer was washed with water dried over sodium sulfate and evaporated to dryness under vacuum. For biological samples the ethyl acetate extract containing the amines is treated with an alcoholic solution of fluorescamine and after 30 minutes the fluorescamine derivative was extracted into borate buffer (pH 9.0). The aqueous phase was then separated and the organic layer discarded. The buffer extract was then acidified to pH 2 with 0.5N NCl and reextracted into ethyl acetate, the extract dried over sodium sulfate and evaporated under vacuum.

El Spectra: The EI spectra were obtained on a Varian Ch-7 mass spectrometer using a solid sample probe and ionization potential of 70 eV. One or two micrograms of the sample was used and flash heated to 250°C.

The parent ion in the mass spectrum of these derivatives is the $(M - 18)^{+}$ ion. The loss of H_2O from the carboxylic acid may be the easy thermal dehydration giving rise to the lactone as in fluorescamine. The loss of 16 amu from the parent ion is due to loss of oxygen atom from the spiran ring. The fluorescamine derivatives of the amines and amino acids gave the parent M - 18 ion which is 260 amu higher than the amino compound. The spectra also show highly abundant radical ion R+ characteristic of the amine and the fragment ions derived from it, thus giving structural information of the parent amine. Thus for example

the mass spectrum of fluorescamine derivative of 3-hydroxy-4-methoxy phenethylamine is characterized by the fragments shown in Scheme I.

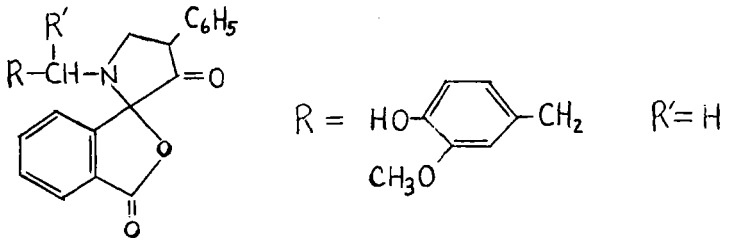

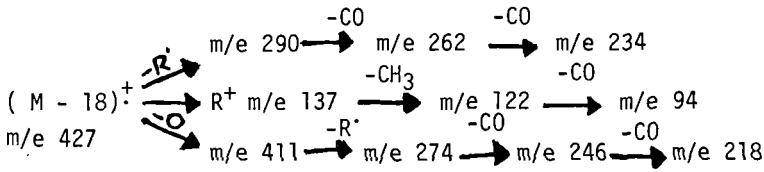

FI Spectra: The Field Ionization mass spectra of the samples were obtained using the SRI multipoint Field Ionization Source and the Extranuclear laboratories Elfs Quadrupole Instrument. The samples were heated from 150 to 300°C. In the cases studied, the compounds gave the M-18 ion as the only parent ion. Thus, tryptamine, 5-hydroxytryptamine, dopamine, 5-methoxytryptamine and d-amphetamine derivatives gave the $(M - 18)^{+\cdot}$ ions at m/e 420, 436, 413, 450 and 395 respectively. Of these, only tryptamine F gave an additional fragment ion at m/e 404 probably by loss of oxygen atom. The FI spectra of the fluorescamine derivative of oxygen atom. The FI spectra of the fluorescamine derivatives of a mixture of 5 amino acid ethylesters are given in Table I.

Compound	m/e $(M - 18)^{+\cdot}$	m/e $(M - 18 - O)^{+\cdot}$
Glycine	363	none
Alanine	377	none
Valine	405	389
Phenylalanine	453	437
Tyrosine	469	453

In a preliminary study of the amine and amino acids in cerebrospinal fluid we used the fluorescamine derivatives and identified tryptamine, phenylalanine alanine and glutamic acid.

1. N. Narasimhachari, Biochem. Biophys. Res. Comm., 55:231, (1973).
2. M. Anbar and W. H. Aberth, Anal. Chem., 46:59A, (1974).

Proton Transfer Reactions from H_3^+ Ions to N_2, O_2, and CO Molecules.

W. T. Huntress, Jr., J. K. Kim, and L. P. Theard,
Jet Propulsion Laboratory, Pasadena, CA 91103.

The rate constants for proton transfer from H_3^+ ions to N_2, O_2, and CO have been measured as function of hydrogen buffer gas partial pressure. The rate constant for proton transfer from H_3^+ to N_2 shows a very large pressure dependence, increasing from 1.0×10^{-9} cm^3/sec at low H_2 partial pressures to 1.7×10^{-9} cm^3/sec at high H_2 partial pressures. The rate constants for proton transfer from H_3^+ to O_2 and CO are constant with partial pressure of H_2; giving values of 6.4×10^{-10} cm^3/sec and 1.7×10^{-9} cm^3/sec, respectively. The role of excess vibrational energy in H_3^+ ions and of equilibrium between forward and back reaction are discussed. Back reaction is observed only for the reaction of H_3^+ ions with O_2, and an equilibrium constant of $K = 2.0 \pm 0.11$ kcal/mole higher than that of H_2.

INTERNAL ENERGY EFFECTS AND ISOTOPE EFFECTS IN HYDRON TRANSFER REACTIONS TO ETHANE

Richard D. Smith* and Jean H. Futrell
Department of Chemistry
University of Utah, Salt Lake City, Utah 84112

Bimolecular processes involving proton transfer and/or hydride ion abstraction comprise some of the simplest, most common, and fundamentally interesting ion-molecule reactions. Recently we have undertaken a detailed study, using a tandem-Ion Cyclotron Resonance mass Spectrometer, of a series of reactions of the form:

$$YD^+ \ (YH^+) + C_2H_6 \ (C_2D_6) \quad \text{products} \qquad (1)$$

where Y is an atom or molecule (eg., Ar, D_2, N_2, CO_2, N_2O, CO, or CD_4). Reactions of YD^+ (YH^+) (where Y = Ar, D_2, N_2, CO_2, or CD_4) are examined as a function of the average number of YD^+ (YH^+) -D_2 (H_2) collisions in the source chamber prior to extraction and injection into the ICR cell.

The present work utilized a tandem-ICR mass spectrometer for the study of both the bimoleculer ion-molecule reactions and the metastable (unimolecular) reactions. The instrument and technique have been described previously.[1,2]

The D_3^+ and CD_5^+ reactant ions were prepared from pure samples of D_2 and CD_4. The remaining reactant ions (ArD^+ N_2H^+, N_2OD^+, CO_2D^+, CO_2H^+, and COD^+) were prepared from a 25 to 1 (35 to 1) mixture of D_2 (H_2) to Y (where Y = Ar, N_2, N_2O, CO_2, and CO). The product distributions and rate constants for reaction of these ions with C_2H_6 (C_2D_6) are determined as a function of the average number of collisions in the Dempster source.[3]

The total rate constants for reaction of ArD^+, D_3^+, CO_2D^+ and CD_5^+ are given in Table 1 for the highest and lowest valves of $\bar{n}$ attained.

Table 1 Absolute Rate Constants[a]

Reaction	Rate Constant[b] Excited (low $\bar{n}$)	Relaxed (high $\bar{n}$)	Collision Rate Constant[c]
$ArD^+ + C_2H_6$	18.5	14.0	11.8
$D_3^+ + C_2H_6$	23.8	20.4	22.1
$CO_2D^+ + C_2H_6$	10.5	9.3	11.6
$CD_5^+ + C_2H_6$	12.8	12.1	13.9

[a]In $10^{-10}cm^3mol^{-1}sec^{-1}$. Uncertainty in absolute rate constants is ± 15 percent; for relative rates approximately ± 5 percent.

[b]"Excited" corresponds to the initial reactant ion distribution, at low $\bar{n}$, and "relaxed" corresponds to the "final" distribution at high $\bar{n}$.

[c]Calculated from the Langevin theory, $= 2\Pi e \left(\frac{\alpha}{\mu}\right)^{\frac{1}{2}}$, using the average polarizability of the neutral.

The product distributions obtained in this work are summarized in the following table:

TABLE 2

Heats of Reaction and Product Disbributions for "Excited" and "Relaxed" Reactant Ions

Reaction	Product Ion	ΔH_R(eV)[a]	Product Distribution initial (excited)	final (relaxed)
$ArD^+ + C_2H_6$	$C_2H_5^+$	-1.55	0.58	0.54
	$C_2H_4D^+$	-1.55	0.22	0.42
	$C_2H_3^+$	+0.62	0.10	0.02
	$C_2H_2D^+$	+0.62	0.10	0.02
$D_3^+ + C_2H_6$	$C_2H_6^+$	-1.7	0.00	0.00
	$C_2H_5^+$	-1.20	0.55	0.40
	$C_2H_4D^+$	-1.20	0.39	0.60
	$C_2H_3^+$	+0.96	0.03	0.00
	$C_2H_2D^+$	+0.96	0.03	0.00
$N_2H^+ + C_2D_6$	$C_2D_6H^+$	-1.15	0.00	0.09
	$C_2D_5^+$	-0.65	0.65	0.40
	$C_2D_4H^+$	-0.65	0.35	0.51
$CO_2D^+ + C_2H_6$	$C_2H_6D^+$	-0.6	0.09	0.51
	$C_2H_5^+$	-0.10	0.27	0.05
	$C_2H_4D^+$	-0.10	0.64	0.44
$CO_2H^+ + C_2D_6$	$C_2D_6H^+$	-0.6	0.09	0.57
	$C_2D_5^+$	-0.10	0.43	0.31
	$C_2D_4H^+$	-0.10	0.48	0.12
$CD_5^+ + C_2H_6$	$C_2H_6D^+$	-0.5	0.26	0.58
	$C_2H_5^+$	-0.03	0.16	0.05
	$C_2H_4D^+$	-0.03	0.58	0.37
$N_2OD^+ + C_2H_6$	$C_2H_6D^+$	-0.2	----	0.89
	$C_2H_5^+$	+0.03	----	0.10
	$C_2H_4D^+$	+0.03	----	0.01
$COD^+ + C_2D_6$	$C_2D_7^+$	-0.03	----	0.84
	$C_2D_5^+$	+0.44	----	0.16

[a]Heat of reaction for ground state reactants and products.

The metastable decompositions of $C_2H_6D^+$ and $C_2D_6H^+$ ions were examined by injecting these ions into the ICR spectrometer and monitoring the $C_2X_5^+$ product ions. Very large iostope effects were observed;[3] the $C_2H_5^+/C_2H_4D^+$ ratio of products observed for the decomposition of $C_2H_6D^+$ was found to decrease from 0.15 to 0.01 as the $C_2H_6D^+$ were increasingly relaxed in the source.

These results (discussed in detail elsewhere[3]) illustrate the relationship between internal energy and the lifetime of the $C_2H_7^+$ reaction complex generated by proton transfer, and the corresponding isotope effects. We presume that this intermediate may also be involved as a transient species in the reaction of CH_3^+ with CH_4 to generate $C_2H_5^+$ as a final product. Stable $C_2X_7^+$ products are produced from the less energetic reactants, N_2H^+, CO_2X^+, (X = H or D) N_2OD^+, COD^+ and CD_5^+ while reaction of D_3^+ produces $C_2X_7^+$ ions too short-lived to be observed without collisional stabilization.

This research has shown that the mechanism of hydride abstraction (or proton transfer followed by H_2 elimination without isotopic exchange) decreases rapidly in favor of proton transfer followed by random X_2 elimination, as the excess energy decreases. An interesting conclusion is that hydride abstraction deposits significantly less energy in $C_2X_5^+$ products than proton transfer reactions. We find that only proton transfer products undergo further decomposition to form $C_2X_3^+$ products.

The N_2H^+ - C_2D_6 results provide evidence that these reactions partition a significant amount of energy as relative translation of the products. A polarization-stripping model can be used to rationalize the conversion to translational energy. Additionally, the $C_2H_5^+$ - D_2 reaction generates scrambled $C_2H_4D^+$ and $C_2H_3D_2^+$ products anticipated for a $C_2H_5D_2^+$ reaction intermediate species. This reverse reaction of the decomposition of $C_2H_7^+$ has a slow rate of ($10^{-12} > k > 10^{-13} cm^3/mol^{-1}sec^{-1}$) and the translational and internal energy dependence is best explained on the basis of a modest activation energy barrier to this reaction.

---

* Present Address: Naval Research Laboratory, Washington, D.C.

References

1. R.D. Smith and J.H. Futrell, Int. J. Mass Spectrom. Ion Phys., 17, 233 (1975).

2. D.L. Smith and J.H. Futrell

3. R.D. Smith and J.H. Futrell, Int. J. Mass Spectrom. Ion Phys., submitted.

ICR Study of the Gas Phase Chemistry of Li^+, Na^+, K^+

JOHN ALLISON and DOUGLAS P. RIDGE
University of Delaware
Department of Chemistry
Newark, Delaware 19711

Reaction of Na^+[1] with tC_4H_9Cl follows the scheme outlined in reactions (1) - (3).

$$Na^+ + tC_4H_9Cl \longrightarrow C_4H_8Na^+ + HCl \quad (1)$$

$$C_4H_8Na^+ + tC_4H_9Cl \longrightarrow (C_4H_9Cl)Na^+ + C_4H_8 \quad (2)$$

$$(C_4H_9Cl)Na^+ + tC_4H_9Cl \longrightarrow (C_4H_9Cl)_2Na^+ \quad (3)$$

The metal induced elimination is quite general, other examples being reactions (4) - (6).

$$Na^+ + tC_5H_{11}Cl \longrightarrow C_5H_{10}Na^+ + HCl \quad (4)$$

$$Li^+ + iC_3H_7Cl \longrightarrow C_3H_6Li^+ + HCl \quad (5)$$

$$Li^+ + CH_3COCl \longrightarrow CH_2COLi^+ + HCl \quad (6)$$

Halide ion transfer, so typical of the solution chemistry of the alkali metal ions, has been observed only in instances where it is the only energetically accessible reaction pathway as in reactions (7) and (8). The elimination shows some specifity with regard to the stereochemistry of the

$$Li^+ + C_6H_5CH_2Cl \longrightarrow C_6H_5CH_2^+ + LiCl \quad (7)$$

$$Li^+ + \text{1-adamantyl chloride} \longrightarrow C_{10}H_{15}^+ + LiCl \quad (8)$$

substrate. Li^+ eliminates HCl from both nC_4H_9Cl and tC_4H_9Cl, but Na^+ eliminates HCl only from tC_4H_9Cl. By analogy with reaction (1) we might expect the alkali metal ions to dehydrate alcohols, and in fact, reaction 9 is observed

$$Li^+ + tC_4H_9OH \longrightarrow \begin{cases} \xrightarrow{90\%} H_2OLi^+ + C_9H_8 \\ \xrightarrow{10\%} C_9H_8Li^+ + H_2O \end{cases} \quad (9)$$

Li^+ does not dehydrate nC_4H_9OH or iC_3H_7OH, and Na^+ does not dehydrate any of the three alcohols.

In looking for reactions of the alkali metal ions with inorganic species, reaction (10) was observed which parallels reaction (11). This suggested that there might be other parallels between the chemistry of Li^+ and Co^+. The chemistry in a mixture of $CoNO(CO)_3$ and iC_3H_7Cl was examined. Co^+ generated by electron impact reacted as indicated in Table I. Although halide transfer becomes a relatively important process, elimination of HCl is dominant. A similar pattern is observed with Fe^+ generated by electron impact on $Fe(CO)_5$. In fact, the transition metal ions dehydrohalogenate all of the substrates observed to be dehydrohalogenated by the alkali metal ions.

$$Li^+ + CoNO(CO)_3 \longrightarrow CoNO(CO)_2Li^+ + CO \quad (10)$$

$$Co^+ + CoNO(CO)_3 \longrightarrow Co_2NO(CO)_2^+ + CO \quad (11)$$

In examining reactions of the metal ions with other alkyl halides the oxidative addition, reaction (12), was identified. The alkali metal

$$M^+ + CH_3I \rightarrow MCH_3^+ + I \qquad M{=}Fe,\ CO \qquad (12)$$
$$M^+ + CH_3I \rightarrow MI^+ + CH_3$$

ions were unreactive toward CH_3I. A limit on the metal carbon bond strengths in MCH_3^+ may be deduced from reaction (12). Limits on a number of bond strengths may be deduced from reactions observed in this study, and some of them are given in Table II.

We have initiated a study of the use of alkali metals as an ionization reagent in a conventional mass spectrometer. A filament coated with a mixture containing Li_2O is mounted inside the source. The emitted Li^+ is observed to react with tC_4H_9Cl from $C_4H_9^+$ and $C_4H_8Li^+$ in a ratio that depends on the filament bias. A more positive bias favors $C_4H_9^+$. It appears to be feasible to obtain very simple spectra using Li^+ as an ionization reagent.

TABLE I

		Co	Fe	Li
$M^+ + iC_3H_7Cl \rightarrow$	$C_3H_6M^+ + HCl$	60%	61%	97%
	$HClM^+ + C_3H_6$	5%	<2%	3%
	$C_3H_7^+ + MCl$	35%	39%	<0.5%

TABLE II

Limits On Bond Strengths
Inferred from Metal Ion Reactions

(M = Li,Fe,Co)	$D(C_3H_6 - M^+)$	$\geq$ 18.9
(M = Li,Na,Fe,Co)	$D(C_4H_8 - M^+)$	$\geq$ 17.0
(M = Li,Fe,Co)	$D(CH_2CO - M^+)$	$\geq$ 20.5
	D(Co - Cl)	$\geq$ 73.8
	D(Fe -Cl)	$\geq$ 72.8
	D(Fe - OH)	$\geq$ 82.4
(M = Fe,Co)	$D(M^+ - I)$	$\geq$ 55.6
(M = Fe,Co)	$D(M^+ - CH_3)$	$\geq$ 55.6

1) Alkali metal ions were generated using the method of J. P. Blewitt and E. J. Jones, Phys. Rev. 50, 464 (1936). Reactions were identified using conventional ion cyclotron reasonance techniques.

Temperature Dependence of Ion-Molecule Reactions Studied by ICR.

S. E. Buttrill, Jr. and G. Ringer, Dept. of Chem., Univ. of Minnesota, Minneapolis, MN 55455

A new ICR cell has been designed and constructed for operation over a wide temperature range. The entire cell is contained within a box of 0.8 mm copper which is suspended from a copper heat sink. In addition to the standard source, analyzer, and ion collection regions, the cell includes a pressure measuring region so that neutral gas densities within the box may be measured directly. The filaments are mounted on posts extending down from the heat sink outside the box in order to minimize local heating. Preliminary results on the reaction of hydrogen ion with hydrogen will be presented together with studies on the temperature dependence of ionic equilibria.

FOURIER TRANSFORM ION CYCLOTRON RESONANCE SPECTROSCOPY

M. Comisarow and A. G. Marshall
Department of Chemistry
University of British Columbia
Vancouver, B. C., Canada V6T 1W5

Conventional ion cyclotron resonance (ICR) spectrometers yield mass spectra by sequentially exciting the cyclotron motion of the sample ions and simultaneously detecting that excited cyclotron motion, one mass at a time. Typically, about 20 minutes are required to obtain a mass spectrum of reasonable signal to noise ratio over the mass range 15-200. Fourier transform ion cyclotron resonance (FT-ICR) spectrometers[1-5] yield the whole mass spectrum in the time which a conventional ICR spectrometer would require to scan through just one line in the mass spectrum by operating in the following manner: The spectrometer excites the cyclotron motion of all ions which are present in the sample at once, and then stores the time domain transient signal which results from that excited cyclotron motion. Since the time domain signal contains contributions from all ions whose motion has been excited, the frequency domain signal which is obtained by numerical Fourier transformation[6] of the time domain signal will contain the whole mass spectrum. Examples of FT-ICR time domain signals and the corresponding mass spectra are contained in references 1 , 2 , and 4.

While conventional ICR spectrometers generally have been considered to be low resolution mass spectrometers, FT-ICR spectrometers can be used obtain high resolution mass spectra[4]. This feature of FT-ICR spectroscopy which first was theoretically predicted[5] and then was experimentally demonstrated[4] can also be used to extend the mass range of ICR spectrometers. Figure 1 shows a FT-ICR mass spectrum which extends to m/e = 1185. An example of an ultra high resolution FT-ICR mass spectrum is given in Figure 2. Figure 3 shows a FT-ICR mass spectrum over a wide mass range.

The published literature[1-4] and Figures 1 to 3 show preliminary results obtained on a prototype instrument which demonstrate the feasibility of the FT-ICR technique and it is reasonable to extrapolate and predict the mass spectral performance expected of a full scale FT-ICR spectrometer. A full scale FT-ICR spectrometer with a suitable minicomputer should have the following features and capabilities and should:

1. Produce mass spectra up to 10,000 times faster than a conventional ICR instrument, or
2. Be up to 100 times as sensitive as conventional ICR spectrometers. This feature is obtained by accumulation of (up to 10,000) time domain signals, prior to Fourier transformation.
3. Yield high resolution mass spectra. A routine resolution of 10,000 at m/e = 1000 does not seem unattainable.
4. Automatically produce mass spectra which are calibrated throughout the mass range. Since the FT-ICR spectrometer simultaneously measures the cyclotron frequencies of all excited ions, the masses of those ions can be determined if the mass of any one ion is known. Such a calibration does not require that the magnetic field be accurately known. Even if empirical correction factors are found

to be required, this feature of FT-ICR spectroscopy will be very useful. N_2+ will probably be the most convenient calibrating mass, even for masses up to 1000.

5. Be easier to operate than conventional ICR instruments since the mini-computer required for numerical Fourier transformation can also be used carry out many of the routine instrumental operations.
6. Retain all of the capability of conventional ICR spectrometers. This is very important since ICR spectrometers have been used in a very wide variety of mass spectrometric experiments.

REFERENCES

1. M. Comisarow and A. G. Marshall, Chem. Phys. Lett. 25, 282, (1974)
2. M. Comisarow and A. G. Marshall, Chem. Phys. Lett. 26, 489, (1974)
3. M. Comisarow and A. G. Marshall, Can. J. Chem. 52, 1997, (1974)
4. M. Comisarow and A. G. Marshall, J. Chem. Phys. 62, 293, (1975)
5. M. Comisarow and A. G. Marshall, Proceedings of 22nd ASMS meeting, Philadelphia, May 19-24 1974, paper W4, page 492 of proceedings.
6. J. W. Cooley and J. W. Tukey, Math. Comp., 19, 297, (1965)

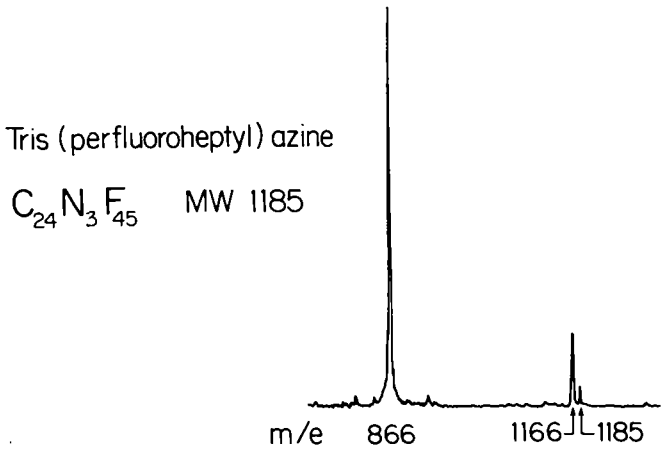

Figure 1. FT-ICR mass spectrum of Tris(perfluoroheptyl) azine from m/e=866 to m/e=1185.

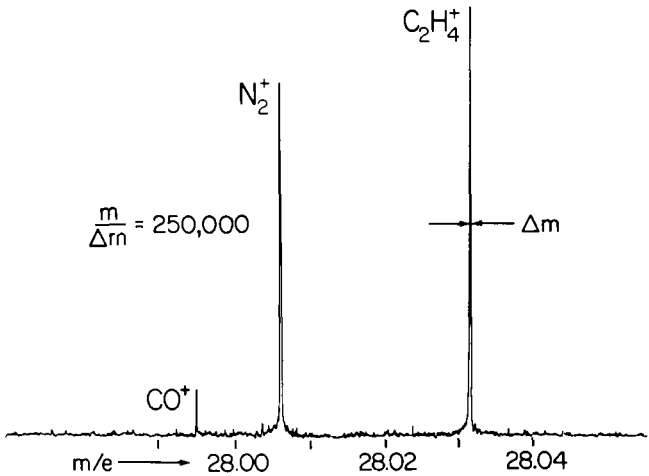

Figure 2. Ultra-high resolution FT-ICR mass spectrum of a ternary mixture of CO, N_2, and ethylene near m/e = 28.

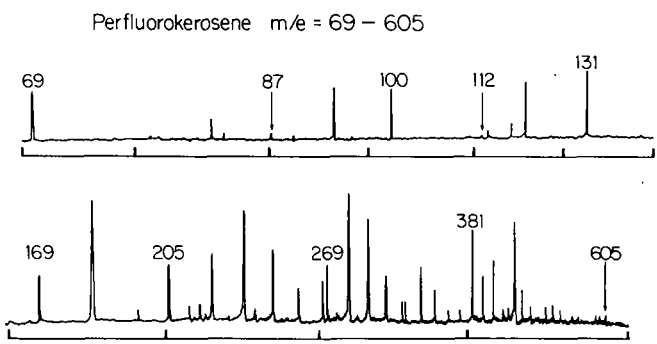

Figure 3. FT-ICR mass spectrum of PFK obtained using the spectral segment extraction technique[5]. The displayed intensities in each of the ten spectral segments were scaled by factors of (low mass to high mass) 0.125, 4, 2, 2, 1, 1, 1, 2, 4, and 4, respectively.

Charge Transfer to Hydrogen Halide and Halogen Molecules from Atomic and Diatomic Ions[1]

by

Sharon G. Lias

National Bureau of Standards

Washington, DC 20234

The charge transfer from Xe^+, Kr^+, and Ar^+ to HI, HBr, HCl, Br_2, and Cl_2 and from O_2^+ and N_2^+ to HI, HBr, and HCl have been investigated, using the NBS pulsed ion cyclotron resonance mass spectrometer. This study was initiated to ascertain to what extent the rate or probability of charge transfer to these molecules is influenced by such factors as the matching of energy levels between reactant ion and product ion, or the Franck-Condon factors linking appropriate energy levels of the product ion and the ground state reactant molecule. In many cases, the atomic and diatomic ions studied here undergo particle transfer reactions with these molecules in addition to transferring charge and this study also attempts to elucidate factors which govern the relative probabilities of charge transfer or particle transfer for a given ion-molecule pair.

The Figure shows in schematic form the photoelectron spectra of HI, HBr, HCl, Br_2, and Cl_2, as well as the recombination energies of the $^2P_{3/2}$ and $P_{1/2}$ states of the Xe^+, Kr^+, and Ar^+ ions. Also shown (by dotted lines) are the threshold energies for the dissociations: ($HX^+ \rightarrow H + X^+$) or ($X_2^+ \rightarrow X + X^+$), where X is the appropriate halogen atom. The rate constants for charge transfer from thermal Xe^+, Kr^+, and Ar^+ ions to HI, HBr, HCl, Br_2, and Cl_2 (in units of cm^3/molecule-second x 10^{11}) are superimposed on the Figure in the appropriate areas. In parentheses

are the ratios of these rate constants to the estimated rate constants for collision of the particular ion-molecule pairs. An examination of these efficiencies shows that all of these charge transfer reactions occur with a low probability. In fact, of the fifteen ion-molecule pairs discussed here, only six undergo charge transfer with a probability greater than about 0.01-0.03. These six are: Ar^+-HBr, Ar^+-Br_2, Ar^+-Cl_2, Kr^+-HI, Xe^+-HBr, and Xe^+-Cl_2, which are, for the most part, the ion-molecule pairs for which near resonant energy states can be seen on the figure. The Ar^+-Br_2 pair, which does not show a resonant energy level in Figure 1 reacts with an efficiency of 0.064, but the reaction results largely or entirely in the formation of Br^+ product ions: $Ar^+ + Br_2 \rightarrow Br^+ + Br + Ar$. Repulsive states do not appear in photoelectron spectra; the position of a repulsive curve crossing with respect to the rare gas ion recombination energy and the internuclear distance of the neutral molecule could influence the probability for charge exchange occurring through dissociation. Experiments were also performed to see if similar correlations can be made for the charge transfer reactions of the diatomic ions O_2^+ and N_2^+ to these molecules. Again, as in the case of the atomic ions, the probability of charge transfer is rather low for all these pairs, and again, there does seem to be a correlation between the existence of resonant energy states and the probability of charge transfer.

The Kr^+, Ar^+, and N_2^+ ions also undergo the alternate reaction: $M^+ + HX \rightarrow MH^+ + X$ with the hydrogen halides, in competition with charge transfer. Except when charge transfer is favorable, the rate of this reaction is proportional to the reaction exothermicity.

[1]Submitted for publication to Int. J. Mass Spectrom. Ion Phys.

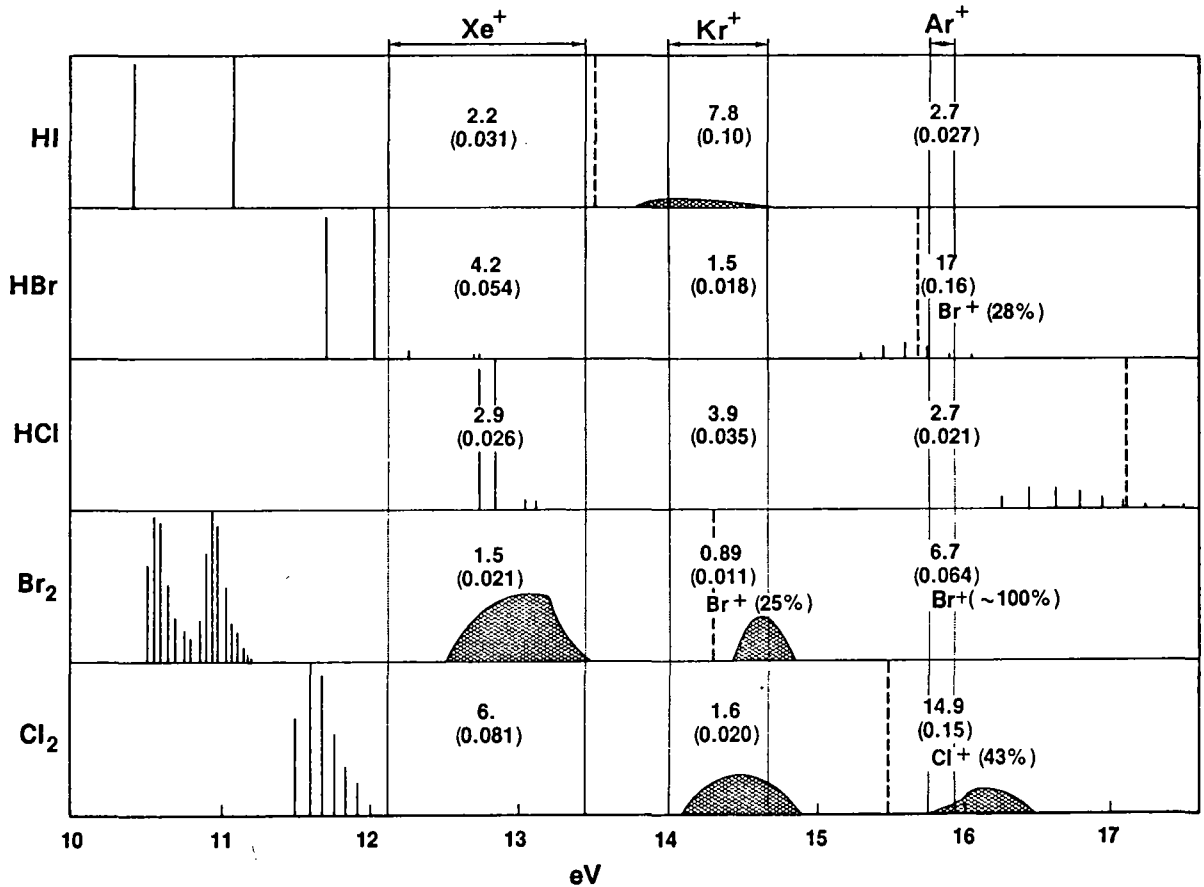
Xe+
Kr+
Ar+
HI
2.2
(0.031)
7.8
(0.10)
2.7
(0.027)
HBr
4.2
(0.054)
1.5
(0.018)
17
(0.16)
Br+ (28%)
HCl
2.9
(0.026)
3.9
(0.035)
2.7
(0.021)
Br2
1.5
(0.021)
0.89
(0.011)
Br+ (25%)
6.7
(0.064)
Br+(~100%)
Cl2
6.
(0.081)
1.6
(0.020)
14.9
(0.15)
Cl+ (43%)
10
11
12
13
14
15
16
17
eV

Comparison of Energy Dependencies of Ion-Molecule Reactions. W. LINDINGER, F. C. FEHSENFELD, D. A. ALBRITTON, A. L. SCHMELTEKOPF, and E. E. FERGUSON, NOAA/ERL Aeronomy Laboratory, Boulder, CO 80302

Several ion molecule reactions have been studied in a temperature dependent flowing afterglow between 300°K and 900°K. These reactions include

$$O^+ + N_2 \rightarrow NO^+ + N \qquad (1)$$

$$CO_2^+ + O_2 \rightarrow O_2^+ + CO_2 \qquad (2)$$

$$NH_3 + H_2 \rightarrow NH_4^+ + H \qquad (3)$$

and

$$N_2OH^+ + CO \rightleftharpoons COH^+ + N_2O \qquad (4)$$

These reactions, which all exhibited strong temperature dependences, were also studied in a flow-drift apparatus as a function of E/N in helium and argon buffers. The drift-tube results are discussed in terms of the kinetic energy imparted to the ions by the electric field. The intercomparisons of the variable temperature flowing afterglow and the flow-drift results allows one to assess the importance of ion kinetic energy in determining the rate constants and to estimate the effects associated with ion kinetic energy distributions and/or partitioning of energy into vibrational or rotational excitation of the drifting ions.

A Quantitative Investigation of the Role of Franck-Condon Factors in Charge-Transfer Reactions

Jane Gale and Michael Henchman, Department of Chemistry, Brandeis University, Waltham, Mass. 02154 and John F. Paulson, AFCRL, Bedford, Mass. 01730.

In a continuing investigation of accidentally resonant charge-transfer reactions between atomic ions and polyatomic molecules,[1] the cross sections of fifteen such reactions (involving the ions D^+, O^+, Ar^+, Kr^+ and Xe^+ with methane, ethane and propane) have been measured on the AFCRL tandem mass spectrometer. In eight cases, separate measurements on the Brandeis pulsed tandem machine gave surprisingly good agreement, even though differing collection efficiencies of less than unity are to be expected in each case. In the relative energy range used (> a few eV), the cross sections show little energy dependence. This behavior and the invariance of the product spectrum with relative energy demonstrate the processes to be resonant. The thermal translational energies of the products show that they result from essentially rectilinear trajectories at comparatively large reactant separations.

Under these conditions it may be appropriate to enquire if the cross sections for such processes, occurring at a distance, may be correlated with measureable properties of the isolated reactants. Such an approach underlies the phenomenological theory of Förster[2] for the transfer of excitation energy at long range, also involving a radiationless transition. Förster identifies the probability for energy transfer P as being proportional to the square of the interaction matrix element

$$P \propto [\langle \psi_A \psi_{B*} | Op | \psi_{A*} \psi_B \rangle]^2$$

where A* and B represent donor and acceptor respectively. If the operator is an electronic one and if the Born Oppenheimer approximation applies, the wave functions ψ may be written as product functions of their electronic and vibrational parts, φ and χ.

$$P \propto [\langle \varphi_A \varphi_{B*} | Op | \varphi_{A*} \varphi_B \rangle]^2 [\langle \chi_A \chi_{A*} \rangle \langle \chi_{B*} \chi_B \rangle]^2$$

where the final term represents Franck-Condon factors. Further analysis of the operator shows that P may be formulated in terms of transition probabilities of isolated species.

$$P \propto [\langle \varphi_A | Op | \varphi_{A*} \rangle \langle \varphi_{B*} | Op | \varphi_B \rangle]^2 [\langle \chi_A \chi_{A*} \rangle \langle \chi_{B*} \chi_B \rangle]^2$$

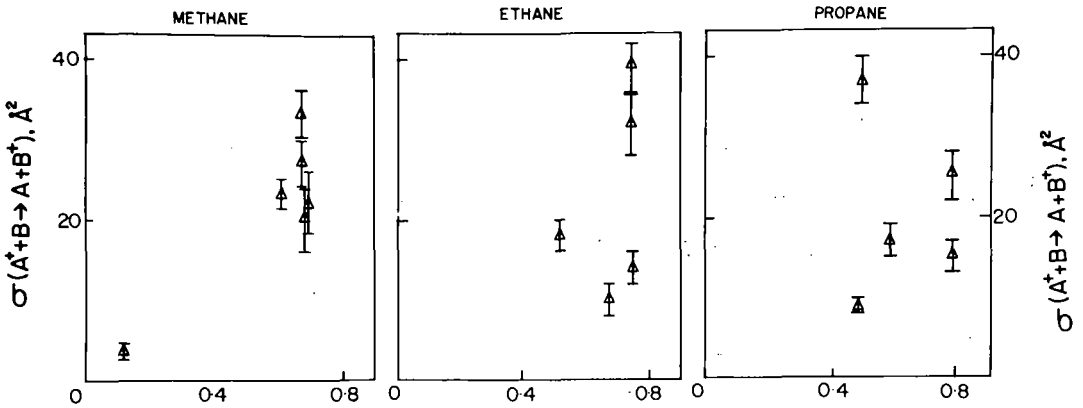

FIGURE 1

RELATIVE FRANCK-CONDON FACTORS

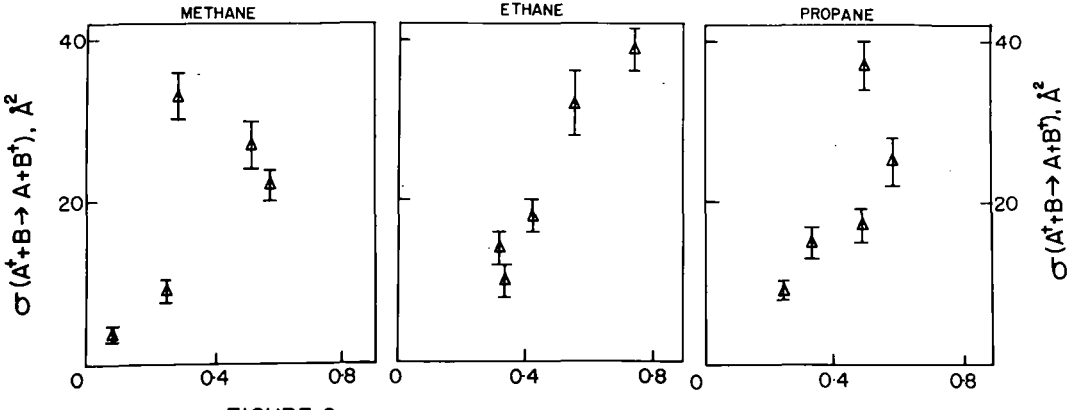

FIGURE 2

RELATIVE F-CF x $\sigma(A^+ + A \rightarrow A + A^+)$

In seeking the relevance of this formalism to charge transfer, we note that recent interest in correlating such cross sections with Franck-Condon factors is effectively conducted at the second stage of the Förster analysis. Our own data, so analysed in Figure 1, using experimental Franck-Condon factors from threshold electron spectroscopy,[3] demonstrate a propensity rule: where these factors differ significantly (e.g. methane), they exercise a controlling influence on the cross section: where they do not (e.g. ethane), other factors are influential.

While we now have reason to believe that the Förster formalism at the third stage should not be applicable to charge transfer, we have nevertheless enquired if the cross sections may be correlated empirically with properties of the ionic reactant for a common target molecule. We have tried the symmetric charge transfer cross section as a measure of the ion's transition probability and this is shown in Figure 2. A correlation is demonstrated (with the exception of two data points, whose reliability may be questioned on other grounds). This correlation is entirely empirical, is of some interest and may be related, plausibly in a qualitative way, to the distances over which electrons may tunnel.

References:

(1) J. Gale, M. J. Henchman, A. J. Masson and J. Paulson, Proceedings of the 22nd ASMS Conference (1974) p. 253.

(2) T. Förster, "Modern Quantum Chemistry," Section III (O. Sinanoglu, ed.) Academic Press, New York (1965), pp. 93-157.

(3) R. Stockbauer and M. G. Inghram, J. Chem. Phys. 54, 2242 (1971).

Excitation Functions from Rate Constants Measured under Non-Maxwellian Conditions

Jide Ige and Michael Henchman, Department of Chemistry, Brandeis University, Waltham, Mass. 02154

We have previously considered the extent to which rate constants, measured by different techniques may be compared.[1] Consider an isothermal measurement $k(T)$ and a non-isothermal measurement $k(T^*)$, characterized by an effective temperature T^*. For $T = T^*$, so long as the relative velocity distributions $P(v_r, T)$ and $P(v_r, T^*)$ are rather similar, the magnitudes of $k(T)$ and $k(T^*)$ should be comparable directly, irrespective of the form of the excitation function $\sigma(v_r)$. To establish a reliable "best value" for a rate constant, it is important to use methods for which $P(v_r, T^*)$ approaches $P(v_r, T)$.

Consider now the different task of using a diversity of rate-constant data to yield by deconvolution the microscopic excitation function $\sigma(v_r)$. Since the direct measurement of $\sigma(v_r)$ is hard at the lowest energies, such rate-constant data are generally the sole information available. To proceed, detailed knowledge of the distribution functions $P(v_r, T^*)$ is needed but unavailable. For the task of extracting $\sigma(v_r)$, the requirements are the exact opposite from those for establishing best values for rate constants. Methods should be sought with the greatest difference in their distribution functions to give rate constants as different from each other as possible in order to force the excitation function to become increasingly unique.

For one method, the drift-tube, an empirical distribution function has been proposed[2] and shown to be reasonable through theoretical analysis by Viehland and Mason. We have explored the application of this to the reaction $O^+(N_2,N)NO^+$ in three respects:

I. Can the deconvolution be avoided by presenting rate constant data $k(T^*)$ as phenomenological cross sections $q(\bar{v}_r)$ where $q(\bar{v}_r) = k(T^*)/\bar{v}_r$ with $\bar{v}_r$ the mean relative velocity estimated from the value of T^*? Is $q(\bar{v}_r)$ an acceptable estimate of $\sigma(\bar{v}_r)$? In Figure 1, q_{exp} is the drift-tube rate constant data of Johnsen and Biondi[3]; q_{theory} is a best fit to this, obtained by convoluting the optimum trial excitation function σ with the Woo and Wong distribution

function; and $f = q_{theory}/\sigma$ is a measure of the acceptability ranging from ~ 3 at 0.04 eV to 1.3 at 0.6 eV.

II. Should k(T) (afterglow) be expected to differ significantly from k(T*) (drift-tube) and how do available data agree? In Figure 2, k_{DT} is the drift-tube data of Johnsen and Biondi[3]. A trial σ has been fitted to this and used to predict the corresponding k(T) plot for isothermal measurements. The identity of k(T) and k(T*) within experimental limits of measurement suggest the suitability of drift-tube measurements for obtaining "best values" for rate constants and extending the accessible temperature range: isothermal measurements add no additional information to aid deconvolution of σ. The data points are isothermal measurements of the NOAA group and k_{DT}(exp) their alternative set of drift-tube data[4].

III. In Figure 3, how does the trial excitation function, σ_{theory}, deconvoluted from rate constant data[3], agree with direct beam measurements of σ (data points[5])? At 1.0 eV, it appears excellent but at 0.7 eV a factor of 2 too low.

References:

(1) J. Ige and M. Henchman, Proceedings of the 22nd ASMS Meeting (1974), p. 148.

(2) S. B. Woo and S. F. Wong, J. Chem. Phys. 55, 3531 (1971).

(3) R. Johnsen and M. A. Biondi, J. Chem. Phys. 59, 3504 (1973).

(4) W. Lindinger, F. C. Fehsenfeld, A. L. Schmeltekopf and E. E. Ferguson, J. Geophys. Res. 79, 4753 (1974).

(5) R. F. Stebbings, B. R. Turner and J. A. Rutherford, J. Geophys. Res. 71, 771 (1966); J. A. Rutherford and D. A. Vroom, J. Chem. Phys. 55, 5622 (1971).

Figure 1

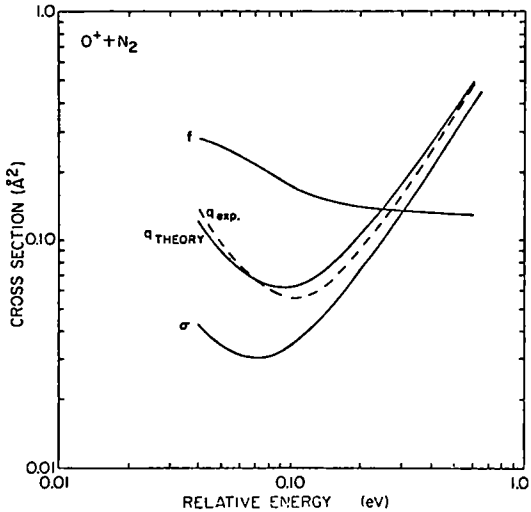

Figure 2

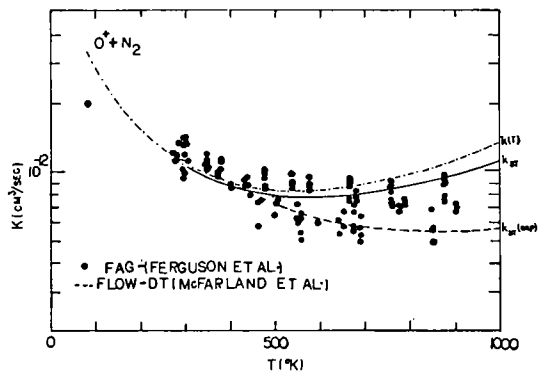

Figure 3

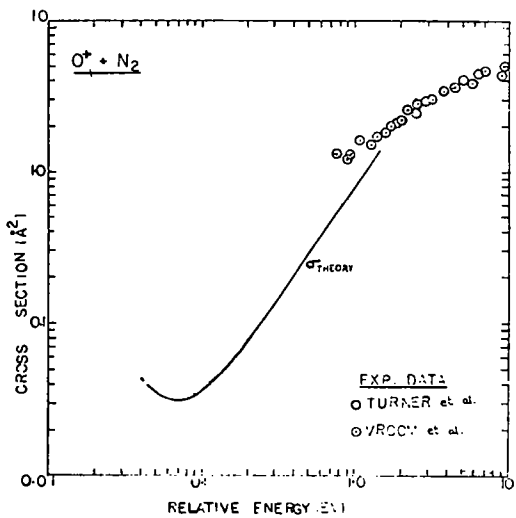

HEATS OF FORMATION OF GASEOUS HYDROCARBON IONS

ALAN GOREN and BURNABY MUNSON
Department of Chemistry
University of Delaware
Newark, Delaware 19711

Differences in heats of formation of tertiary alkyl ions have been reported previously from high pressure mass spectrometric studies. The results of our experiments are in generally good agreement with the earlier work.

A duPont (CEC) 21-110B mass spectrometer was modified earlier for chemical ionization studies[2]. Additional modifications have been made to study equilibrium reactions of alkyl ions. The path length for ions was increased to 1.5 cm, the areas of the electron entrance and ion exit holes were reduced, and the connections were made more vacuum tight. A preheating zone (20 cm x 0.016 cm i d stainless steel tubing) was added and the glass inlet lines (20 cm x 0.4 cm i d) were heated in five sections. All of these and the source were maintained at the same temperatures. A grid was placed between the focus plates and the source block to reduce the potential penetrations into the source and also to reduce the collisionally induced decompositions just outside the source. The majority of the experiments were performed on mixtures of constant composition at pressures of 0.4 to 2.0 torr at temperatures of 70 - 250°C. No repeller voltage was used in these experiments, although a small repeller voltage had no effect on the results. Using the Langevin Treatment to estimate the mobilities of the ions, we obtain values of several hundred microseconds for the residence times of the ions in our source at 1 torr and an assumed field strength of 1 v/cm. The apparent equilibrium constants, $K = (MH)I_N + /(NH)I_M+$, approached a constant value for pressures above 1 torr. From plots of log K vs 1/T one obtains the heats and entropies of the reactions. Table I shows data for butyl, pentyl, and hexyl ions. The internal consistency of these data is very good as well as the agreement with previous work. ΔS for these reactions is not significantly different from zero. The negative heats of reaction, however, indicate a greater stability of the higher alkyl ions.

TABLE I
THERMOCHEMISTRY OF HYDRIDE TRANSFER REACTIONS

Reaction	ΔH°(kcal/mole)	ΔS°(cal/°mole)
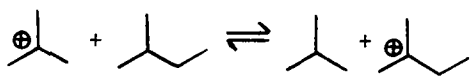	-2.80 ± .20 (-3.6, -3.3)*	-1.81 ± .49 (-2.3, -2.7)
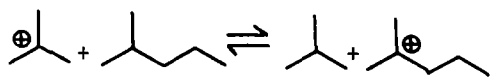	-4.60 ± .22 (-3.8)	-3.81 ± .47 (+1.61)
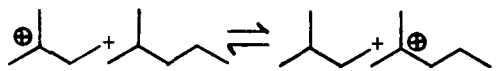	-1.86 ± .25	-0.05 ± .70
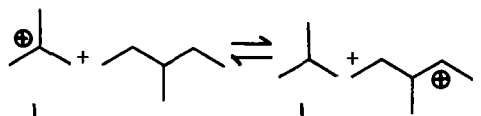	-3.85 ± .45 (-4.8)	-1.74 ± .94 (-0.1)
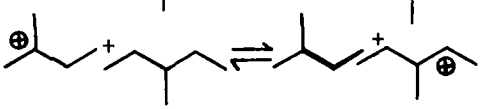	-1.79 ± .21	-1.22 ± .41

The equilibrium constants for mixtures of i-C_4H_{10} and 2,3-dimethylbutane (1) and i-C_4H_{10} and 2-methylcyclopentane (2) did not attain an apparently constant value. ΔH for the other C_6 hydrocarbons was not a sensitive function of pressure, however, nor were the ΔH values for reactions (1), -5.2 $\pm$ 0.5 kcal/mole, or reaction (2), -4.1 $\pm$ 0.8 kcal/mole. The hydride affinities of the C_6 ions are 3.9 to 5.2 kcal/mole lower than the hydride affinities of t-C_4H_9.

Table II shows data for mixtures of i-C_4H_{10} or i-C_5H_{12} with 2-methylhexane and 3-methylhexane. From an extrapolation of the data of Table I or from the concept that the hydride affinities of the tertiary heptyl ions should be about the same as the hydride affinities of the hexyl ions, we expected ΔH for t-$C_4H_9^+$ and the t-heptanes would be -5 to -6 kcal/mole. The value in Table II is much more negative than this. A similar anomaly has been noted by Field and co-workers.[1] We have no explanation for these observations and feel that they may be the result of an unknown instrumental artifact. It is significant to note that our data are self-consistent and agree well with those data of Field and co-workers for the pentyl and hexyl ions. However, our data are not particularly selfconsistent and do not agree quantitatively with the anomalous work of Field and co-workers for the heptyl ions.

TABLE II
THERMOCHEMISTRY OF HYDRIDE TRANSFER REACTIONS

Reaction	$\Delta H°$(kcal/mole)	$\Delta S°$(cal/°mole)
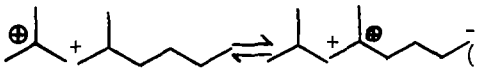	-12.9 $\pm$ 1.0 (-17.9)	-23.5 $\pm$ 0.5 (-28.8)
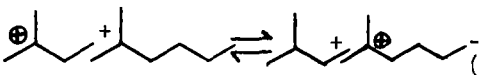	-14.3 $\pm$ 1.2 (	-29.7 $\pm$ 1.3
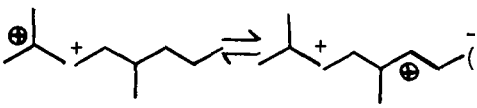	-14.3 $\pm$ .7 (-25.2)	-27.5 $\pm$ 2.1 (-40.0)
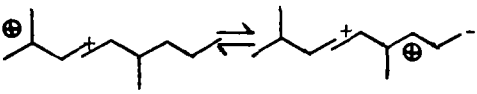	-12.7 $\pm$ 1.1	-27.5 $\pm$ 2.0

Values in parenthesis from ref. 1

1a) J. J. Solomon and F. H. Field, J. Amer. Chem. Soc. 95, 4483 (1973).
b) J. J. Solomon, M. Meottner, and F. H. Field, J. Amer. Chem. Soc. 96, 3727 (1974).
c) J. J. Solomon and F. H. Field, J. Amer. Chem. Soc. 97, 2625 (1975)
d) J. J. Solomon and F. H. Field, unpublished data.

2 J. A. Michnowicz, Ph.D. Thesis, University of Delaware, 1972.

PROTON AFFINITIES OF INORGANIC COMPOUNDS

DANNE SMITH and BURNABY MUNSON
Department of Chemistry
University of Delaware
Newark, Delaware 19711

Although the proton affinities of many compounds are known, the proton affinities of several strong acids and common solvents have not yet been determined. Ion-molecule reactions have been studied which involved several sulfur-containing species in order to put limits on their proton affinities.

Mixtures of CH_4 and SO_2 were studied in a mass spectrometer which had been modified for high pressure operation and mixtures of CH_3F and SO_2 were studied in an ICR mass spectrometer. In the CH_4/SO_2 experiments, CH_5^+ reacted rapidly by proton transfer to form SO_2H^+, but the $C_2H_5^+$ ions gave no indications of any reactions. The limits of the proton affinity of SO_2 are 151 kcal/mole < PA(SO_2) < 159 kcal/mole from

$$CH_4F^+ + SO_2 \longrightarrow SO_2H^+ + CH_3F$$

$$C_2H_5^+ + SO_2 \longrightarrow \text{no reaction}$$

The experiments with SO_3 were much more difficult than the experiments with SO_2 because of the difficulties in handling gaseous SO_3. The pressure of SO_3 could not be controlled accurately and it was very difficult to obtain SO_3 without sulfuric acid. Experiments were made by adding SO_3 from a bulb of fuming sulfuric acid directly into the source of the high pressure mass spectrometer containing gases which gave a series of reactant ions. One observed the changes in the ionic distributions as the pressure of SO_3 decreased. 128 kcal/mole < PA(SO_3) < 142 kcal/mole, from

$$CH_5^+ + SO_3 \longrightarrow SO_3H^+ + CH_4$$

$$CHO^+ + SO_3 \not\longrightarrow SO_3H^+ + CO$$

Estimates of the proton affinity of sulfuric acid were made by obtaining CI spectra of H_2SO_4 with several reactant ions obtained from pure gases or mixtures. The sulfuric acid was introduced into the source by a direct insertion probe and the vapor phase concentration of sulfuric acid could be controlled by changing the temperature of the sample. Preliminary experiments indicated that PA(C_2H_4) = 159 kcal/mole < PA(H_2SO_4) < PA(C_3H_6) = 178 kcal/mole.

Similar experiments with HSO_3F showed PA(CH_4), PA(CO), PA(SO_2) < PA(HSO_3F) < PA(C_2H_4), or 151 kcal/mole < PA(HSO_3F) < 159 kcal/mole.

Preliminary experiments with CF_3SO_3H showed PA(CH_4), PA(CO) < PA(CF_3SO_3H) < PA(C_3H_6) or 142 kcal/mole < PA(CF_3SO_3H) < 178 kcal/mole.

Precision and Accuracy in Isotope Ratio Determinations.*

RAY S. NEWBURY, Lawrence Livermore Laboratory
Livermore, California 94550

The determination of absolute fission cross section ratios using the threshold cross sections technique avoids the weighing of fissile materials (with attendant ~1% uncertainties), but requires isotope ratio determinations with uncertainties of <0.1%. We are measuring these ratios on a 34 cm double focusing 60° sector instrument using surface ionization with pulse counting. A description of our internal standardizing technique whereby precisions (and, presumably, accuracies) of isotope ratios to better than 0.1% are obtained is given. Rhenium (187/185 ratio = 1.672 ± 0.002) is used as an example.

* Work performed under the auspicies of the U.S. Atomic Energy Commission.

The Triple Filament Thermal Ionization Source (TFTIS) and High Precision Isotope Abundance Ratios

Larry J. Moore

National Bureau of Standards
Institute for Materials Research
Analytical Chemistry Division
Washington, D. C. 20234

Although thermal isotopic fractionation effects for the single filament analysis of small quantities of elements have been correlated with the simple atomic Rayleigh distillation model, the TFTIS has received much less theoretical attention. Empirical fractionation corrections for the TFTIS, in combination with synthetic mixtures of high purity separated isotopes, have been used to determine absolute abundance ratios and atomic weights at NBS for Ag, Cu, Mg, Pb, U, Rb and K. Modifications of the isotopic analysis techniques thus derived have been applied to the high accuracy analysis of trace metals in Standard Reference Materials by isotope dilution. The conclusion to be drawn from these measurements is that the simple atomic Rayleigh distillation model is inadequate to explain the mass discrimination effects observed for the TFTIS, even for high purity salts.

For the above absolute abundance measurements these generalizations can be drawn:

(1) Known sources of systematic isotope measurement error are minimized.

(2) High purity materials are used.

(3) Only a small fraction of sample loaded into the instrument is actually consumed during analysis.

The theoretical analysis of Kanno [1] has suggested that molecular vaporization may play an important role in the fractionation effects observed for multiple filament sources. A comparison of actual NBS empirical corrections for absolute abundance measurements with those calculated via the Kanno model reveals a consistent prediction of direction (i.e., absolute/experimental <1 for light nuclide/heavy nuclide) for all the above elements. However, the empirical correction factor is always closer to theoretical than predicted for the atomic model. Thus:

(1) The atomic (square root of atomic masses) Rayleigh model is incorrect for most multiple filament analyses for samples of moderate size.

(2) The molecular evaporation model may be only partially correct since the empirical correction factor implies an evaporating species of higher molecular weight than that which might be expected for the pre-evaporation species <u>presumed</u> present on the filament.

The molecular vaporization interpretation has been applied to the TFTIS analysis of the polynuclidic elements Ca, Sr, Nd and Sm, resulting in typical intra-analysis ratio drifts of ∿0.005-0.02%/amu/hour, and nearly as precise (and therefore accurate) between analyses.

Recently documented intra-analysis ratio drifts opposite the conventional distillation model may be explained by a modification of the Kanno model to incorporate translations between distillation curves of varying molecular mixtures during analysis.

The assumption of molecular vaporization at the sample filament is buttressed by electron diffraction identification of Ca compounds of the type CaxReyOz, and by numerous Knudsen cell experiments in the literature where alkali, alkaline earth and rare earth salts are evaporated as molecules (including dimers and trimers) in the temperature range <∿1100 °K, which is the approximate operating range for the isotopic analysis of the salts described here. Although an *'a priori'* extrapolation of equilibrium Knudsen cell measurements to those of the Langmuir evaporation is not possible, it is likely that some molecular vaporization occurs in the TSTIS.

Applications of this approach include the proven ability to measure abundance ratios of microgram and submicrogram quantities of Ca, Sr, Nd and Sm in a relatively short analysis period with precisions ≤0.01% per amu, making it useful for the hyperfine resolution of radiogenic isotopic components in geological, biological and nuclear studies, and for high accuracy isotope dilution measurements. Also, the use of identified high molecular weight species in combination with a proven Rayleigh distillation and relative abundance measurements would permit the calculation of well characterized atomic weights from mass spectrometric measurements alone.

Until definitive Langmuir evaporation measurements are made, the extent and exact role of any molecular vaporization in the TFTIS remains unresolved. In the interim the Kanno model, including the present modifications, is extremely useful as a working model in the interpretation and prediction of fractionation effects observed in this laboratory for the TFTIS.

A more detailed version of this research is being submitted for publication elsewhere.

[1] Kanno, H., Bull. Chem. Soc. Japan 44, 1808-1812 (1971).

Iron Concentration in Porcine Blood and Standard Reference Material Copper Benchmarks by Isotope Dilution Mass Spectrometry

Ernest L. Garner and Lura P. Dunstan

National Bureau of Standards
Institute for Materials Research
Analytical Chemistry Division
Washington, D. C. 20234

The concentration of iron in a sample of porcine blood and in three copper benchmark Standard Reference Materials (SRM's) was determined by thermal ionization isotope dilution mass spectrometry. An enriched isotope of ^{57}Fe was used as the spike to alter the $^{56}Fe/^{57}Fe$ ratio for the isotope dilution measurement. This approach eliminated any major effects of isobaric interference of Cr and Ni on the concentration measurement.

Iron was separated from the matrix by ion exchange chromatography. All reagents were purified by sub-boiling distillation [1]. Known weights of sample and ^{57}Fe spike were dissolved in a mixture of nitric and hydrofluoric acids (5:1). After dissolution and evaporation of the solution to dryness, the residue was converted to the chloride using hydrochloric acid. The residue was then dissolved in 10N hydrochloric acid and loaded onto a column containing 100-200 mesh strongly basic anion exchange resin. The column was washed with 6N hydrochloric acid to remove interferring elements, and the iron was removed with 0.2N hydrochloric acid. The fraction containing iron was evaporated to dryness and dissolved in nitric acid (1+9) for mass spectrometric analysis.

The ion source used for this work was triple filament rhenium ribbon with approximately 50 μg of iron on each sample filament. Iron, as $FeCl_3$, was dissolved in nitric acid (1+9) and evaporated to dryness on the filaments using electrical currents and heat lamps. The residue, a mixture of iron oxides, was reduced in a hydrogen atmosphere to a mixture of metallic iron, which was predominant, and iron oxides. Stable and slowly changing Fe^+ ion currents of 1×10^{-12}A were routinely obtained. When necessary, either larger sample sizes or more intense ion currents were utilized for the isotopic analysis of natural samples and the ^{57}Fe spike.

The concentration of iron in the porcine blood was found to be 393.1 ± 0.8. The indicated uncertainty (ts) was calculated for four 1 g subsamples taken from the same vial of serum. Analysis of the copper benchmark SRM's was more extensive and included both 1 g and 0.25 g subsamples. These materials were initially cast as bars, converted into chips, and then prepared as lots labelled MARKED, UNMARKED and

COMPOSITE. The composite was a blend of the other two lots. Using 1 g samples for analysis, a distinct trend between marked and unmarked ends of the bar was observed. The initial values determined for the composite subsamples were, exclusive of SRM 396, intermediate with respect to the values for the marked and unmarked lots. The deviation of SRM 396 from this pattern was believed to be sample inhomogeneity, an assumption that was partially supported by a replicate preparation and analysis of subsamples of all three lots of this material. Analyses of 0.25 g subsamples of these SRM's gave an increase in the range of concentration values of all positions which was at least a factor of three more than the uncertainty in the measurement. It was concluded that the amount of material analyzed and inhomogeneity were critical factors in the analysis of the copper benchmarks. The average values for three composite subsamples of SRM's 394, 395 and 396 were 153.2 ± 2.7, 94.54 ± 2.1 and 142.1 ± 1.3, respectively. The indicated uncertainties are the range and are large enough to cover the observed effects of sample inhomogeneity for a 1 g subsample of the composite.

The initial concentration determinations by thermal ionization isotope dilution mass spectrometry have demonstrated competiveness with other analytical techniques. For 1 g of material with an iron concentration of 100 μg, the method is accurate to slightly less than 1%. The error components are ratio determination, calibration of the spike, variability of the analytical blank, and variability of the isotopic fractionation between analyses. The analytical blank varied between 100-200 ng. Efforts to evaluate some of the components of the analytical blank (environment, ion exchange resin, reagent, apparatus, filaments, etc.) were only partially successful but it was possible to identify the filament blank as the most likely obstacle to reducing the analytical blank below 50 ng. A reduction of the analytical blank is necessary before the technique can be effectively applied to submicrogram concentrations.

[1] Kuehner, E. C., Alvarez, R., Paulsen, P. J. and Murphy, T. J., Anal. Chem., 44, 2050-2056 (1972).

Determination of the Absolute Isotopic Abundance and Atomic Weight of Terrestrial Potassium

E. L. Garner, T. J. Murphy, J. W. Gramlich, P. J. Paulsen, L. A. Machlan and I. L. Barnes

National Bureau of Standards
Institute for Materials Research
Analytical Chemistry Division
Washington, D. C. 20234

and

S. S. Goldich
Northern Illinois University
Department of Geology
DeKalb, Illinois 60115

Absolute values have been obtained for the isotopic abundance of potassium in a reference sample of potassium chloride (Standard Reference Material 985) [1], and more than 70 potassium containing minerals representing widely varied geological and geographical locations [2].

Two solid sample thermal ionization mass spectrometers were calibrated with synthetic potassium standards, prepared from chemically pure and nearly isotopically pure ^{39}K and ^{41}K separated isotopes. The potassium separated isotopes were assayed as the perchlorates and then converted to the chlorides for mixing and mass spectrometric analysis using a tantalum triple filament technique. The resulting absolute isotopic abundances of the Standard Reference Material, in atom percents, are:

$$^{39}K = 93.2581 \pm 0.0029$$

$$^{40}K = 0.011672 \pm 0.000041$$

and

$$^{41}K = 6.7302 \pm 0.0029.$$

The atomic weight calculated from this isotopic composition is:

$$39.098304 \pm 0.000058.$$

The indicated uncertainties are the sum of the uncertainties in the isotopic composition of the separated isotopes, the chemical assay and mixing of the separated isotope solutions, and the mass spectrometric ratio measurements. Each error component is at least as large as the 95% confidence limits.

The mineral samples investigated in this study were chosen to encompass a wide range of geologic conditions, and particular attention was given to include samples which might be expected to show isotopic variations, if such variations exist in nature. Although the mineral survey data shows a slight bias of a few part in ten thousand (relative to the standard) toward a greater abundance of ^{41}K, no significant isotopic variations have been observed.

[1] Garner, E. L., Murphy, T. J., Gramlich, J. W., Paulsen, P. J., and Barnes, I. L., Absolute Isotopic Abundance Ratios and the Atomic Weight of a Reference Sample of Potassium, J. Res. NBS, (to be published).

[2] Garner, E. L., Goldich, S. S., Gramlich, J. W., Machlan, L. A., and Murphy, T. J., Absolute Isotopic Composition of Terrestrial Potassium (in preparation).

SIMULTANEOUS DETECTION OF URANIUM ISOTOPES*

R. E. Powell, N. R. Daly and N. J. Freeman

MOD(PE), AWRE, Aldermaston,
Reading RG7 4PR, England.

The accurate measurement of isotopic ratios is an important requirement in a number of scientific areas, e.g. nuclear power development, fissile material accountancy, standardization of reference materials, geochronology and fractionation studies. In the mass spectrometry of solids a thermal ionization technique is normally applied. In this case some of the causes of imprecision are the time variation of ion beam intensity and the small number of ions that are available for measurement.

These problems can be largely overcome by collecting ion beams simultaneously in ion collectors that are almost 100% efficient. A scintillation detector has been developed at AWRE that can simultaneously measure two ion beams. The efficiency of the detector is essentially 100%, hence the system is insensitive to gain changes within its component elements. Using the 235/238 isotope ratio from NBS 350 standard uranium samples, the standard deviation between runs under the same measurement conditions is 0.04%, which is comparable to the statistical limit for counting 10^7 ions on the 235 isotope. This is sufficient to demonstrate a variation of measured isotopic ratio as the filament temperature is varied during a uranium analysis.

---

* This paper will be submitted for publication in Rev. Sci. Instr.

URANIUM ISOTOPE ANALYSIS ON-SITE BY QUADRUPOLE MASS SPECTROMETRY

M. W. Siegel
Extranuclear Laboratories, Inc.
Pittsburgh, Pennsylvania 15238

F. E. Jones
Allied Chemical Corporation
Idaho Falls, Idaho 83401

INTRODUCTION: The nuclear reactor industry requires large numbers of routine isotopic abundance measurements for reactor site monitoring and accounting of uranium and plutonium. These analyses are presently done in laboratory installations employing large magnetic mass spectrometers frequently costing in excess of $100K and comparable in performance capability to the instruments used to establish primary isotope standards. Many routine analyses could well be conducted on site with instruments capable of lesser precision and accuracy. It was recently proposed that a good quadrupole instrument might demonstrate adequate analytical abilities (comparable to smaller magnetic instruments), while at the same time providing significant advantages in cost, weight, stability during transportation, ease of operation and ease of mini-computer interfacing. The results reported herein represent a preliminary test of this idea with uranium. A regular production quadrupole mass spectrometer package (Extranuclear Laboratories 'spectrEL' system) was modified to accept a surface ionization source through the air-lock normally used with its solids probe. It was felt that if this essentially standard system could approach minimal performance requirements and remain cost competitive with gamma-ray spectrometry in the proposed application, then the construction of a fully dedicated prototype instrument would be justified.

INSTRUMENT: The instrument consists of a standard quadrupole, standard ion optics system modified slightly for surface ionization, and the associated single stage vacuum system and electronics package. Detection is by a particle multiplier mounted off-axis, followed by an impedance transforming preamplifier. Mass command is available in three modes (internal sweep, DMP and computer), each of which is ultimately traceable to a 0 to 10 volt signal corresponding linearly to 0 to 350 amu. The DMP (Digital Mass Programmer) mode was used in these experiments. The DMP is a 16 channel device each of whose channels stores a digital START MASS (amu), WIDTH (amu), RATE (amu/sec), and GAIN, the last being the programmed gain of a linear signal scaling amplifier placed after the impedance changing preamplifier. Most of the data discussed herein were collected by using four DMP channels set to monitor ^{234}U, ^{235}U, ^{236}U, and ^{238}U with 0.75 amu sweep width. The samples were NBS standards U-Nat, U-050, U-200, U-500 and U-930. The programmed gains were set so that each isotope's peak signal produced about half scale deflection on a 0 to 1 volt strip chart recorder. This recording method takes full advantage of the available precision, as isotopic abundance ratios are essentially the reciprocal gain ratios, the exact recorder deflection providing a correction factor of order unity. Some data were collected by using a single channel to scan the entire mass range of interest.

ION SOURCE: The samples were deposited on canoe-shaped rhenium filaments prepared in advance by spotwelding approximately 1 cm x 1 mm x 50 μm foil elements to the kovar posts of a standard low cost two pin metal-in-glass button. Heating current for operation as a U^+ surface ionization source is empirically determined, and corresponds to near-white heat. Residual oxides which have a lower vapor pressure than the metal are observed as UO_2^+ and UO^+ for the first few minutes, but thereafter the U^+ dominates. A micro-

gram loading produces a stable ion source for 30-40 minutes, providing adequate time for several repeat measurements. Filament change time, from vacuum to vacuum, is about 5 minutes with our air-lock arrangement. Because real-life samples will be radioactive alpha emitters, sample size in this system is limited to a total of 1 μg of uranium metal. A small drop (1 - 10 μl) of sample solution (usually $UO_2(NO_3)_2$) at the appropriate concentration is dried onto the filament by mild ohmic heating. Sucrose treatment of the prepared filament and mild heating of the filament in 2×10^{-5} torr benzene vapor significantly improve the observed ratio of uranium to uranium oxides. This pretreatment might be eliminated via the use of double filaments, not tested in these measurements.

REQUIREMENTS AND PROCEDURE: The set of suggested minimum requirements on precision and accuracy set down in advance of these tests were: ±1%, ±1% for >5 atom %; ±2%, ±2% for 0.50 to 5.0 atom %; ±8%, ±4% for 0.10 to 0.50 atom %; and ±35%, ±20% for 0.01 to 0.10 atom %. Precision is defined as the 95% confidence limit (Student-t). Accuracy is defined as the fractional deviation of the mean result from the standard value. Since isotopic ratios were actually measured, the limits on each measurement are determined by combining the individual requirements in quadrature. A linear correction factor of approximately 1.7% per amu deviation from mass 235 was determined by a single calibration run with U-500, and this factor was used to correct all subsequent measurements. It was anticipated in advance that in the field similar calibration runs would be made at approximately daily intervals. Additional requirements were imposed on resolution, abundance sensitivity and peak shape. These were tested at the instrument settings used for measurements and determined to be satisfactory. No adjustment of any instrument parameter was made after the initial setup.

RESULTS AND CONCLUSIONS: Typically five to fifteen rapidly repeated measurements are averaged to obtain a "run". Each result is an average of approximately three runs made on each of two different filaments of the same sample material. The percentage results as Precision/Accuracy compared to the requirements (parenthesis) are:

Ratio	U-Nat	U-050	U-200	U-500	U-930
$^{238}U/^{235}U$	1/0.4 (8/4)	1.5/0.7 (2.2/2.2)	2.5/0.5 (1.4/1.4)	2.8/0.1 (1.4/1.4)	6/0.4 (1.4/1.4)
$^{236}U/^{235}U$	--	24/10 (35/20)	8/4.5 (8/4)	18/3 (35/20)	46/24 (35/20)
$^{234}U/^{235}U$	--	23/8 (35/20)	14/32 (8/4)	8/2 (2.2/2.2)	11/5 (2.2/2.2)

The bulk of the data easily satisfy the suggested accuracy requirements (particularly in the important $^{238}U/^{235}U$ ratio), and more marginally satisfy the precision requirements. The two or three anomalously bad results involve ratios of very small numbers. While not every measurement satisfies the pre-stated requirements, the overall picture from this preliminary experiment is sufficiently encouraging to suggest that continued development would be productive.

Carbon Dating Mass Spectrometry--Background Reduction Techniques, Rafael Schnitzer, William H. Aberth, and Michael Anbar, Stanford Research Institute, Mass Spectrometry Research Center, Menlo Park, CA 94025

The mass spectrometry technique to measure the isotope ratio $^{12}C/^{13}C/^{14}C$ uses the formation of the stable negative ions CN^-.[1] These ions are produced efficiently from N_2 and CO_2 in a duoplasmatron negative ion source. When $^{15}N_2$ is used, the isotope ratio will be

$$^{12}C^{15}N/^{13}C^{15}N/^{14}C^{15}N = (27)/(28)/(29) \quad .$$

The ambient isotope ratio $^{14}C/^{12}C = 1/10^{12}$ requires that the background level at mass 29 should be reduced below the 10^{-12} level compared with the mass 26 ion current with $^{14}N_2$ as reactant gas. At the time of our last year's report[1] this background was as high as 10^{-8}. The background reduction techniques explored during 1974-75 include: (a) ion source modification, (b) inlet system gas purification, (c) ion beam photodetachment background reduction.

Ionization Source

Two major modifications have been introduced to improve ion source operation. These are: a hollow cathode[2] with no extra pumping, and an air cooled Z electrode as illustrated in Fig. 1. The advantages of these changes are: (1) prolonged operation for hundreds of hours compared to a filament operated ion source, which could not be operated for more than 10 hours without replacement; (2) input power is reduced by at least an order of magnitude and the source is thus operated at considerably lower temperatures; (3) the extracted ion currents have not changed, although the arc current has been reduced from $\sim$ 2 A to $\sim$ 200 mA; and (4) the Z electrode is kept even cooler by internal air cooling to minimize outgassing which may contribute to the background. The cooler mode of source operation minimized the potential contribution of $^{29}Si^-$ or $^{28}SiH^-$ to mass 29 background.

Inlet System and Gas Purification

Although only high purity gases are being introduced to the ion source we have found that a major contribution to mass 29 originates from hydrocarbons. Two ionic species are involved; first $C_2H_5^-$, which is formed from the fragmentation of long chain hydrocarbons, and second $^{12}C_2HD^-$, formed from ethane,[3] from $CH_2 + C^-$, or possibly by some other processes. The gases are therefore subjected to a purification procedure as illustrated in Fig. 2. The high pressure gases pass over heated copper oxide to oxidize any hydrocarbon impurities to $CO_2 + H_2O$. In addition a microwave discharge is applied to the low pressure region followed by a second copper oxide oven. The discharge breaks up residual hydrocarbons in an oxidizing atmosphere and the CuO oxidizes them further. This procedure reduced the background level to 10^{-10}.

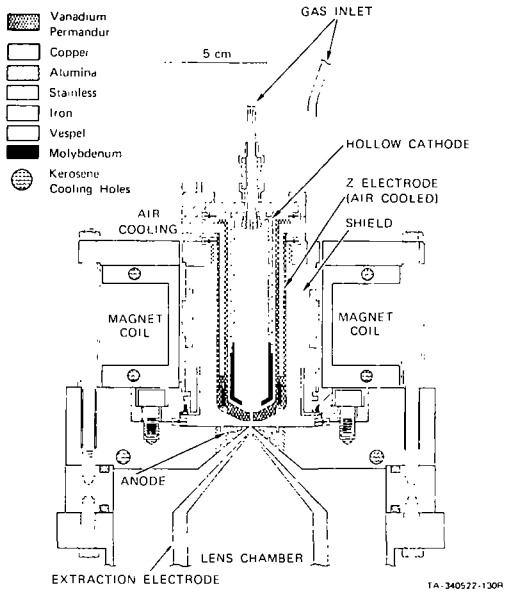

FIGURE 1 CROSS SECTIONAL VIEW OF THE DUOPLASMATRON OPERATED AS AN UNPUMPED HOLLOW CATHODE

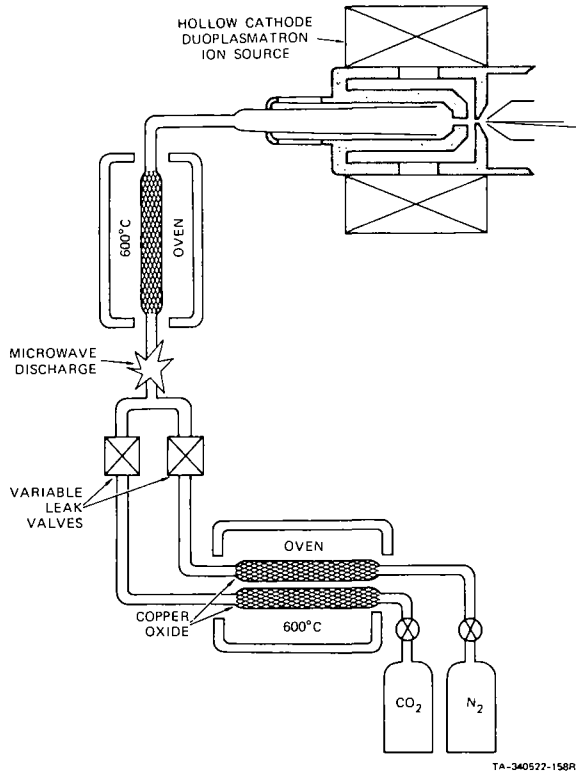

FIGURE 2 INLET SYSTEM GAS PURIFICATION

As $C_2H_2^-$ as well as COH^- can be formed from H and C originating from H_2O and CO_2, our next step is to remove as far as possible the H_2O originating from the oxidation of the tracer hydrocarbons.

Background Reduction by Photodetachment of Undesired Ionic Species

The residual background ions ($^{13}C_2HD^-$, $C_2H_5^-$, COH^-) are expected to be of lower electron affinity compared with that of CN^- (3.5 eV). Some of these ions could be in excited states having even lower electron affinities. Therefore, photons with energies lower than 3.5 eV interacting with the mass 29 ion beam could photodetach or dissociate the undesired background components. We have tested the feasibility of this approach. The experimental set up is illustrated in Fig. 3. A laser with photon energy of 1.8 eV and power output of 1 joule per pulse (3×10^{18} photons) interacted with the ion beam along a 30 cm path. The pulsing rate was 12 pulses per minute and the pulse duration was 0.6 msec. The photon beam diameter was 8 mm as compared to 1 mm of the ion beam. The laser triggered the scaler counter and the ratio of "laser on"/"laser off" measured the photoattachment plus photodissociation effects. Measurements were taken on masses 28, 29, and 30 ions beams. No significant changes were recorded in the beam intensities of mass 28 and 30. An attenuation of 5 to 10% was observed on the mass 29 beam. An average photodetachment cross section $\sigma = 10^{-18}$ cm^2 was calculated. This photodetachment approach is not practical at the moment because of the short duty cycle of pulsed operation. On the other hand, it may prove to be an adequate method for low level beam background reduction when a continuous intense laser beam becomes available.

References

1. R. Schnitzer, W. Aberth, H. L. Brown, and M. Anbar, Proceedings of the 22nd Annual Conference on Mass Spectrometry and Allied Topics, Philadelphia (May 1974) p. 64.
2. H. J. Roden, Proceedings of 2nd Symposium on Ion Sources and Formation of Ion Beams, Berkeley (1974) VII-7.
3. H. J. Dawson, A. J. Ferrer-Correia, Proceedings of 23rd Annual Conference on Mass Spectrometry and Allied Topics, Houston (May 1975), E-10.

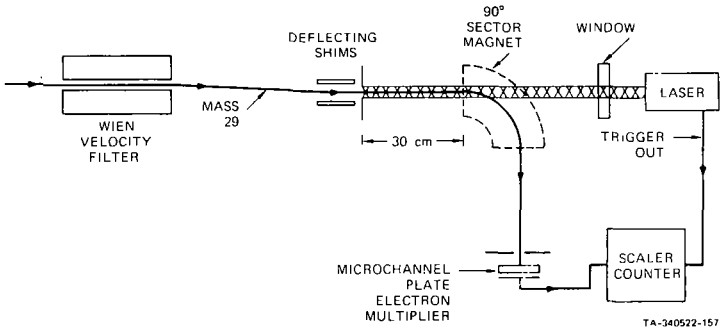

FIGURE 3 ION BEAM PHOTODETACHMENT EXPERIMENT

Isotope Ratios from GCMS

D.E. Matthews and J.M. Hayes

Departments of Chemistry and Geology
Indiana University
Bloomington, Indiana 47401

Recently, many laboratories have developed capabilities for determining isotope ratios using GCMS. As the technique becomes more widely used, it becomes increasingly important to study the fundamental limitations on the precision of the method. Certainly, one fundamental limitation is imposed by ion statistics. It should be obvious that the number of ions collected constitutes the ultimate limiting factor on the precision of a single determination. Another category of fundamental limitations arises from the observation pattern used to determine the isotope ratios.

An example of a limitation due to the observation pattern used is provided by figure 1, where two ion beams are being measured such that beam 1 is observed for the first portion of the GC peak, ion beam 2 is observed for the second portion, and ion beam 1 is again observed for the remainder. Under these conditions it is visually obvious that an error will result in the measured ratio such that the apparent abundance of ion beam 2 will be artificially enhanced. Although it is not expected that anyone would make a measurement under these conditions, if an obvious error occurs in figure 1, then an error probably still exists when the beams are switched more frequently. This "peak cycling error" can formally be defined as $\Delta R = (R - R^*)/R^*$ where R^* is the true ratio, and R is the ratio measured from the observed GC peak. Although the number of measurement cycles completed per GC peak is an important factor influencing the peak cycling error, other factors, such as the degree of completion of the last measurement cycle, the peak shape, the pattern of observation used, time delays, the setting of starting and stopping thresholds, and isotopic fractionation by the GC column also have an effect. With the development of a suitable computer program, the peak cycling error can be calculated as a function of any of these parameters. However, in this report we will consider only the following: (1) the effect of the number of measurement cycles (the last cycle is likely to be incomplete--here we report average errors for randomly variable degrees of completion), (2) the effects of the pattern of observation used, and (3) Gaussian shaped GC peaks.

The pattern of observation usually takes the form of one of two different scanning algorithms. A unidirectional scan could be performed by observing 3 ion beams, A, B, C, in the following order: ABCABC..., or a bidirectional scan could be performed using the order: ABCCBA... . Both the sign and magnitude of the peak cycling error depend on the scanning algorithm chosen. The results of trial calculations are shown in figure 2, in which the peak cycling error, ΔR (%), is plotted as a function of the number of measurement cycles per peak. A measurement cycle is defined as the time required for a single observation of the ions of interest, together with all associated delays, etc. Curves for both unidirectional and bidirectional scans are given. Note that the ΔR curve for the bidirectional scan has two branches, depending on whether the number of measurement cycles per peak is odd or even. For either the unidirectional or the bidirectional scan, the error is systematic, with the sign of the error being opposite for the two types. The dotted line in figure 2 gives the absolute value of the bidirectional scan curve for the even

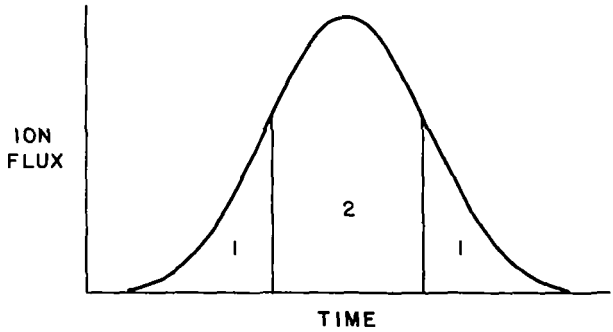

Figure 1. Illustration of the peak cycling error in isotope ratio determinations by GCMS.

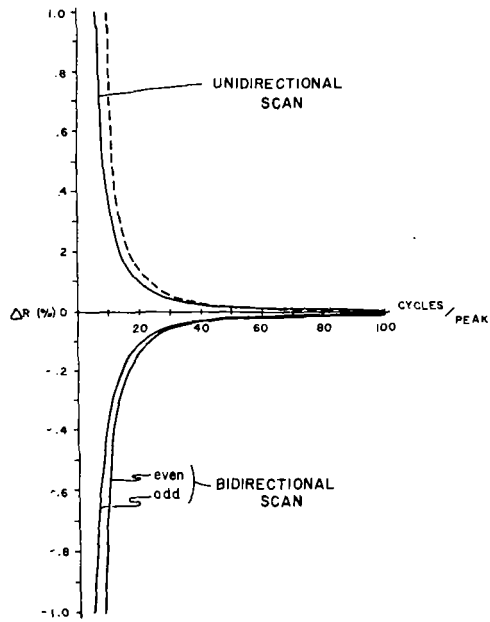

Figure 2. Calculated peak cycling error; ΔR, versus the number of measurement cycles per peak.

cycle case, showing that a larger peak cycling error occurs when the bidirectional scan is used.

To demonstrate the existence of the peak cycling error, a computer-controlled GCMS system was used in the ion counting mode (1,2,3). To provide accurately reproducible GC peaks, an exponential dilution flask with two 8-port valves was used in connection with a blank 28 meter glass capillary column yielding subnanomole amounts of xenon gas within GC peak widths of 16 seconds. The observed xenon isotope ratios were shown to follow the theoretical unidirectional and bidirectional curves of figure 2, with the observed error being, if anything, somewhat worse than predicted.

Modern chromatographic techniques can produce peaks only a few seconds wide, and chances for significant peak-cycling errors are, therefore, relatively great. Taking the calculations shown in figure 2 as a guide, it can be seen that at least 25 measurement cycles are required in a peak if the average error (bidirectional scan) is to be held below 0.1%. Even if the GC peak is only 5 sec wide, this still allows 200 msec/cycle, and it appears that the requirement is not impossibly stringent. Indeed, it is necessary to avoid cycling too rapidly, a circumstance which can occur because at very low cycle times a relatively large fraction of the cycle time will be spent in delays waiting for power supplies and amplifiers to settle. This programmed waste of time can significantly reduce the efficiency of measurement and lead to relatively low precision.

A detailed report of this work is being prepared for publication. We gratefully acknowledge the support of the National Aeronautics and Space Administration (grant no. NGR 15-003-118).

---

1. D.A. Schoeller, J.M. Hayes, C.A. MacPherson, R.F. Blakely, and W.G. Meinshein, Proc. of the 20th Ann. Conf. on Mass Spectrometry and Allied Topics, p. 231 (1972).

2. J.M. Hayes and D.A. Schoeller, Proc. of the 21st Ann. Conf. on Mass Spectrometry and Allied Topics, p. 53 (1973).

3. D.A. Schoeller, J.M. Hayes, Anal. Chem. 47, 408 (1975).

An International Mass Spectral Search System (MSSS)

S. R. Heller, EPA, PM-218, Washington, D.C. 20460, G.W.A. Milne, H.M. Fales, A. Bridy, NIH, Bethesda, Md 20014 and R.S. Heller, University of Maryland, College Park, Md 20742

The status and future of the MSSS will be presented and discussed. At present the MSSS is used by over 100 groups in the U.S., Canada and Europe via the Cyphernetics Corporation PDP-10 computer and network.

The data base consists of about 40,000 semi-certified spectra, and the data base is expected to grow to over 50,000 by early 1976. The data base, in computer tape is being made available through the NTIS, Springfield, Virginia, as NBS Tape #8. A printed form of the data base is expected to be available early in 1976.

At present there are some two dozen options in the MSSS, with new features consistently being added. Future options expected to be available shortly include STIRS, PBM, isotope analysis, substructure search, isotope labeling and search of the MSDC literature bulletin files.

The authors wish to acknowledge the support of EPA, NIH, FDA, NBS and MSDC for the MSSS. In addition acknowledgment is made to the following firms which have or are interfacing their data systems to MSSS: AEI, Dupont, Finnigan, H-P, INCOS, JEOL, Nuclide, System Industries and Varian-MAT.

A GENERAL METHOD FOR MOLECULAR ION PREDICTION

R. Geoff Dromey, Bruce G. Buchanan, Dennis H. Smith, Joshua Lederberg and Carl Djerassi. Departments of Computer Science, Genetics, and Chemistry. Stanford University, Stanford, California 94305.

Assignment or identification of the molecular ion plays a key role in structural elucidation from mass spectral data. In this paper we propose a general method for molecular ion prediction. The method has a heuristic and algorithmic basis. It predicts a ranked set of candidate molecular ions. In most instances the correct molecular ion can be found in the top three to five ranked candidates. If the molecular ion is present in the spectrum it is almost always ranked highest. Only an abbreviated description of the method can be given here. A more complete description can be found elsewhere.[1]

BASIC POSTULATE FOR PROPOSED METHOD:

Crucial to the present method for molecular ion prediction is the following postulate. "There exists at least one SECONDARY LOSS in a spectrum that will match a PRIMARY LOSS from the molecular ion irrespective of whether the molecular ion peak is present in the spectrum." A "PRIMARY LOSS" in this context is a composition or mass of a fragment that is lost from the molecular ion. A SECONDARY LOSS set for a particular spectrum is made up of a combination of losses from all fragment ion peaks other than any possible molecular ion and all compositions or masses in the lower half mass range of the spectrum. Restating the basic postulate we can say that for every mass spectrum there is a high probability that any mass or composition lost from the molecular ion will be also observed as a loss from one fragment ion to another or will itself appear as a fragment ion in the lower regions of the mass spectrum.

PREDICTION OF MOLECULAR ION CANDIDATES:

The secondary loss set explained above can be generated by calculating mass (or composition if high resolution) differences between all pairs of peaks in a spectrum. To complete the set the lower masses in the spectrum can be included. In generating these losses an accumulative intensity index is calculated for each loss by adding the ion intensities of the pair of peaks involved in the loss. Intensities of corresponding peaks in the lower half of the spectrum are also added to the appropriate indices.

With the secondary loss set in hand, candidate molecular ions can be generated. To do this the mass of each member of the secondary loss set is added to the mass of each member of the upper half of the spectrum. The associated intensity indices are also added cumulatively. Candidates generated in this way with masses less than the highest mass in the spectrum are immediately discarded. Those candidates with masses greater than the highest mass peak are further tested to see if they form feasible losses with respect to existing peaks in the spectrum. The ones that do not form consistent losses are rejected as candidates. When the exhaustive generation is complete we are left with a set of candidates, each with an associated ranking index (accumulated during generation). In many cases tests on the spectrum indicate that only even mass candidates need be generated; in other cases both odd and even mass candidates are generated. A sample set of results is given in Tables 1 and 2. The method has been implemented as a computer program that will accept either high or low resolution mass spectral data. In the latter case the program works with compositions instead of masses.

[1] R.G. Dromey, B.G. Buchanan, D.H. Smith, J. Lederberg, C. Djerassi, "Applications of Artificial Intelligence for Chemical Inference. XIV. A General Method for

TABLE 1

Sample Set of Results Showing Molecular Ion Prediction and Ranking

Compound	Mol formula	Highest mass present	Fragment missing[a]	Mol wt	Ranked at no.[b]
Ritalin (2)	$C_{14}H_{19}NO_2$	172 (M - 61)	$C_2H_5O_2$	233	4
Pentobarbital (3)	$C_{11}H_{18}N_2O_4$	197 (M - 29)	C_2H_5	226	2
Mebutamate (4)	$C_{10}H_{20}N_2O_4$	175 (M - 57)	C_4H_9	232	3
Tridecan-7-one	$C_{13}H_{26}O$	155 (M - 43)	C_3H_7	198	4
Succinic acid methyl ester	$C_6H_{10}O_4$	116 (M - 30)	CH_2O	146	2
Caprylic acid methyl ester	$C_9H_{18}O_2$	129 (M - 29)	C_2H_5	158	3
Glutaric acid methyl ester	$C_7H_{12}O_4$	129 (M - 31)	CH_3O	160	1
Maleic acid butyl ester	$C_{12}H_{20}O_4$	173 (M - 55)	C_4H_7	228	2
N-TFA a-alanine[c] butyl ester	$C_9H_{14}NO_3F_3$	186 (M - 55)	C_4H_7	241	2
N-TFA norleucine butyl ester	$C_{12}H_{20}NO_3F_3$	227 (M - 56)	C_4H_8	283	2
N-TFA valine butyl ester	$C_{11}H_{18}NO_3F_3$	227 (M - 42)	C_3H_6	269	2
N-TFA threonine butyl ester	$C_{12}H_{15}NO_5F_6$	323 (M - 44)	C_3H_8	367	1
N-TFA phenylalanine butyl ester	$C_{15}H_{18}NO_3F_3$	216 (M - 101)	$C_5H_9O_2$	317	4
n-Undecyl alcohol	$C_{11}H_{24}$	154 (M - 18)	H_2O	172	1

[a]These fragment composition losses from the molecular ion are only postulated. Their validity could only be confirmed by high-resolution studies. [b]Note "ranked at number 1" is the program's best choice for a molecular candidate. [c]TFA refers to the trifluoroacetyl derivative.

Predicting Molecular Ions in Mass Spectra". Journal of Organic Chemistry, 40 (1975), 770.

TABLE 2
A Summary of Ranking Results Is Given for
Various Classes of Compounds Tested

Class	Mol ion in top 3	Mol ion in top 5	Total no. of compds
Amines	62	67	68
Alcohols[a]	51	54	57
Ketones	42	44	44
Ethers	33	34	34
Acetals	13	14	14
Amino acid derivatives	9	11	13
Thioethers	11	12	12
Drug compounds	6	8	9
Methyl esters	6	8	8
Butyl esters	4	5	6

[a]Program failed to generate the correct candidate for one alcohol, tert-butyl alcohol.

Automatic Identification of Mass Spectra. A Goodness of Fit Measure Derived from Hypothesis Testing

Stanley L. Grotch

Jet Propulsion Laboratory
Pasadena, California

Abstract

The heart of all file searching procedures is the algorithm used to measure goodness of fit. In the comparison of two coded spectra, the weights chosen for each mass have, in previous work, generally been obtained in an *ad hoc* manner.

It is shown, using binary encoded mass spectra (position of the most intense peak/14amu), that these weights may be chosen, a priori, in a way which maximizes the separation between spectra which are the same and those which are independent.

This result follows directly from considerations of hypothesis testing. Consequently, the effects of errors on the choice of weighting is expressed analytically.

Extensive tests using this procedure with binary codes invariably gave results which were superior to all other weighting techniques tested.

* * *

A detailed description of this work is tentatively scheduled for publication in "Analytical Chemistry" in July, 1975.

A Probability Based Matching System Applicable to a Large Diverse File of Reference Mass Spectra. F. W. MCLAFFERTY, GAIL M. PESYNA, H. E. DAYRINGER, and R. VENKATARAGHAVAN, Cornell Univ., Dept. of Chem., Ithaca, NY 14850

The PBM system, which calculates a "confidence index" related to the average number of randomly-selected compounds whose mass spectra would have to be examined to find data which match the particular reference spectrum to the same degree as does the unknown, has now been made applicable to reference mass spectra collected under a wide variety of instrumental conditions. Average results on over 900 randomly-selected "unknowns" indicate that PBM is clearly superior in recall and precision to retrieval methods presently in use, even those which employ a substantially larger proportion of the mass spectral peaks. PBM employs a "reverse search" procedure, making it especially advantageous for mass spectra of unknown mixtures. Search of a file of 35,000 reference spectra on a laboratory PDP-11/45 computer requires ~15 seconds. Both PBM and the "Self-Training Interpretive and Retrieval System" are now available by local phone call through the TYMNET international network to the Cornell IBM 370/168 using a data base that is more comprehensive than any other available.

WHAT IS A "FACTOR" IN THE FACTOR ANALYSIS OF MASS SPECTRA

R. W. Rozett and E. McLaughlin Petersen

Chemistry Department
Fordham University
Bronx, New York 10458

The factor analysis (FA) of mass spectra [1-4] produces the factors of the data set. The usefulness and interpretation of these factors is not immediately obvious. The main concern of the present study is to develop meaningful interpretations of the factors of mass spectral data.

In a general sense a factor is an independent property which lies hidden behind the interdependent, correlated and redundant properties which are measured in a set of mass spectra. It is one of the less numerous, simpler, and independent characteristic petterns which lie behind the set of fragmentation patterns. It is an empirical function which represents one axis of a coordinate system in which the original measurements may be represented simply and efficiently.

The factors of a data set are not unique. Four different kinds of factors have been found useful for mass spectral data: principal, typical, basic, and partial factors.

PRINCIPAL FACTORS

Principal (component) factors are the set of eigenvectors which result from the eigenanalysis of the covariance matrix derived from the original mass spectral measurements. They are useful to determine the dimensionality of the data matrix, i.e. the number of factors needed to reproduce the original data matrix adequately.

TYPICAL FACTORS

After determining how many essentially different kinds of behavior are present in the spectra, one can try to pick out from the measured spectra the best representative of each kind of behavior. These are the typical factors. In our study of the isomers of $C_{10}H_{14}$ three factors were found to be present. Therefore we determined which three of the 22 isomers best represent the three factors. The same procedure can be carried out with typical masses. The three most representative masses are identified.

BASIC FACTORS

A molecular property which can account for the variation observed in a set of mass spectra is called a basic factor. Basic factors are potentially of great significance for mass spectra. Their identification would be equivalent to the derivation of mass spectra . In fact, if one could identify all the basic factors of a mass spectral data set, it would produce an empirical theory of mass spectra which would provide an interface between a fundamental derivation of spectra and mass spectral libraries. Only future work can establish whether such a program can be realized.

PARTIAL FACTORS

One can look on a set of mass spectra as a kind of mixture of various components. FA is able to look for the components of the mixture. Partial factors or component factors are these constitutive parts of the mixture. Linear combinations of the components regenerate the observed mass spectral data set. Partial factors preserve the characteristics of the mass spectral data set, just as the components of a mixture preserve the properties of the mixture. Partial factors need not be found among the observed spectra, unlike typical factors. One does not expect to find pure examples of each basic type of behavior among the observed compounds. A partial factor is a sort of pure and perhaps unobserved typical factor. The set of mass spectra as a whole, and each spectrum individually, is treated as a weighted average of the partial factors.

In specifically mass spectral terms, we resolve the observed spectrum into a set of partial mass spectra. The set of all the fragmentation patterns are analyzed into a smaller set of simpler fragmentation patterns. Each partial or component mass spectrum is associated with a particular ion dissociation pathway, or with the dissociation of a single important ion. All the techniques of mass spectral analysis can then be applied to the partial mass spectra, which now contain the information present in the original spectra in a condensed and simplified way.

REFERENCES

(1) R. W. Rozett and E. McLaughlin, Twenty Second Annual Conference on Mass Spectrometry, Philadelphia, PA, May 19-24, 1974, p441.

(2) R. W. Rozett and E. McLaughlin Petersen, Anal. Chem., 47, 1400 (1975).

(3) J. B. Justice, Jr., Doctoral Dissertation, University of North Carolina at Chapel Hill, 1974.

(4) E. McLaughlin Petersen, Doctoral Dissertation, Fordham University, New York, 1975.

A SIMPLE SEARCH SYSTEM FOR MASS SPECTRA

by J.F. Smith, R.J. Mathews and J.D. Morrison
La Trobe University, Bundoora, Australia

In 1972, because of an improvement in computing facilities at La Trobe University, it became possible for the Department of Physical Chemistry to set up a computer library of mass spectra. The only previous experience in this area was with a GC-MS-PDP/9 system in which a series of limited libraries of compounds pertaining to current problems were stored on tape and used in comparisons with GC-MS analyses. Only the 6 most intense peaks of each library entry were stored and comparisons were made with the 6 largest peaks of unknown spectra. If a mass match occurred in the comparison of the unknown with the library spectrum, the smaller of the peak intensities was divided by the larger and a fractional similarity calculated. These similarities were summed for all 6 peaks. A perfect match yields a result of 6 which can be converted to 100% similarity. This we call the RATIO method.

Since most of the problems were tackled in a standard way, we were able to use retention time as a further search criterion.

There are many factors to be considered when establishing a data file. Perhaps the most important is the success of the search algorithm but the speed of the search, the ease of housekeeping and the computer storage required must also receive consideration. We were anxious to use the best available techniques when setting up our data system and hence decided to examine all of the published comparison algorithms. To do this, a library of 550 mass spectra drawn from the literature was set up. Another 250 spectra of compounds known to be in the library but whose spectra had been obtained from different sources were used as unknowns. The data were divided into subsets, according to molecular class. The criteria used for measuring success have been published elsewhere (1)(2). The results of the tests are difficult to summarise in a short paper. We found that certain algorithms performed better than others for particular library subsets. For example the ratio method was slightly better for terpenoids than the other methods. Perhaps the most useful test in the case of a general library, is the percentage number of times a given algorithm gives the correct answer as its first choice. If this test is performed on a comparison of complete spectra, the method of Reed and his co-workers, denoted by the DIV method (divergence) (3) performed marginally better than that published by Crawford and Morrison (4), called below the AID method (Absolute Intensity Difference), which was again slightly better than the ratio method (78.0:76.0:75.8)%. All other tests performed at levels about 10% lower than this. When only matching 8 peaks the figures became 77.7:76.5:75.9% and it is interesting to note that the success rate is not significantly lower than when matching full spectra. This point will be discussed below. In terms of computer time the ratio method is slightly faster than the AID algorithm which is significantly faster than the DIV method. (.95:1:1.4) Matching complete spectra takes about 3.5 times longer than matching 8 peaks.

On the basis of these findings it was decided, at least for the time being, to continue to use the 6 peak ratio method for the following reasons:

(i) Both the DIV and the AID method require normalisation to total ionization whereas the ratio method requires normalisation to the base peak. Thus the ratio data is stored in a readily comprehens-

ible form which assists human manipulation of data. The base peak can be inferred, saving one word of computer storage.

(ii) 6 peaks, although not as successful as 8 peaks, had the advantage that the data pertaining to one compound could be conveniently stored on one teletype line or one card image. 28 characters are required for the mass intensity pairs, leaving 3 for the molecular weight and 40 for the name of the compound. The correct answer is almost always in the first 4 choices.

(iii) The ratio method performed marginally better on terpenoids which were at the time the subject of a number of research projects at La Trobe University.

For speed of search, the file is ordered according to a common parameter and the search conducted by the commonly used bisection method. Three such files have been established, ordered by molecular weight, base peak and by largest neutral fragments. To enter or change data, the files are merely edited at the appropriate place.

Finally to return to the point made earlier, that searching a limited number of peaks is generally as successful as searching full spectra. This may be further illustrated as in Fig. 1 where the results of two tests are shown. In both cases the % success is plotted against the number of peaks used for the search. In the upper curve the DIV method was tested using only peaks above mass 40 for a set of low molecular weight compounds. One observes a steep increase with the number of peaks, then a plateau region with a slight fall off. In the lower curve AID on terpenes gave the same rapid increase in success rate up to a maximum and then a marked decrease as the number of peaks used was increased further. The upper curve is a typical case, the lower curve is the best example of decreasing success that was observed.

One wonders if there is any basis in theory for these findings. If a general library of mass spectral data is thought of as an information system, one may compute the average information content at each mass, using Shannon's $P_i \Sigma \ln P_i$ definition of information content, where P_i is the probability (i.e. the intensity) of the ith peak. The result of this is the curve shown in figure 2. This is a much smoothed envelope of a violently fluctuating curve but illustrates the fact that most of the information in a library of mass spectra is contained in the low masses. This is merely a reflection of the fact that most spectra have their most intense peaks at the low mass end of the scale. The presence of a fixed level of noise lowers the precision to which a peak height can be measured and thus is effectively a base line shift as shown.

In any comparison of an unknown with a library the first peaks compared are likely to fall in the high information zone and this accounts for the rapid rise in the success characteristic. As more peaks are used there is an increasing tendency for them to be high mass peaks where the increment of information is much smaller, giving rise to a plateau region. Finally, if noise plays any part, increasing the number of peaks may actually decrease the information content and the success rate may fall.

1. Mathews R.J. & Morrison J.D., Aust. J. Chem. 27 (1974) 2167.
2. Mathews R.J. & Morrison J.D., Aust. J. Chem. (submitted)
3. Forbman, S., Reed, R.I., Robertson D.H. and Silva M.E.F., Int. J. Mass Spectrom. Ion Phys., 12 (19B) 123.
4. Crawford L.R. & Morrison J.D., Anal. Chem., 40 (1968) 1464.

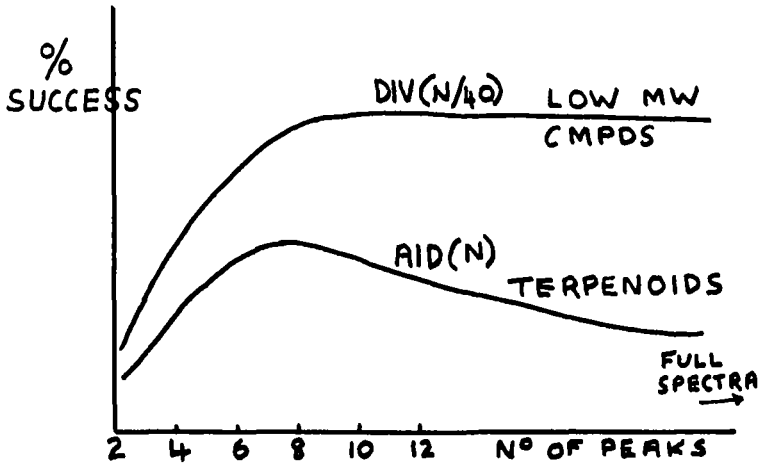

FIGURE 1.

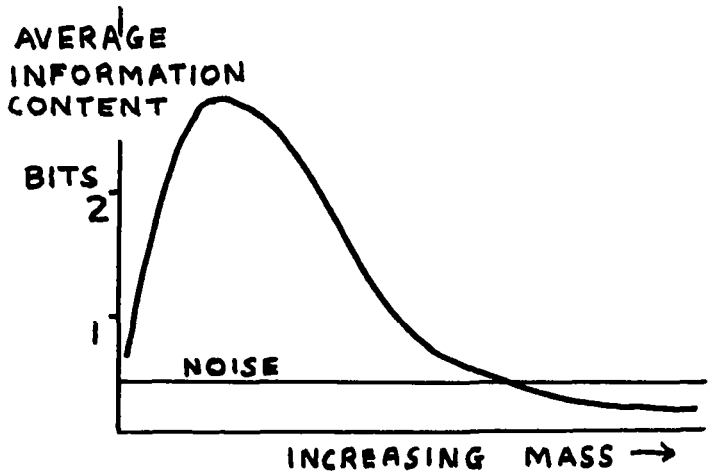

FIGURE 2.

Applications of a GC-MS Data System Using a New Library Search System

J.R. Chapman, K.R. Compson, R.M. Elliott, D. Hazelby, G. Shackleton
AEI Scientific Apparatus Ltd, Manchester M31 2LD, England

Library search is now accepted as a very useful adjunct to a low resolution data system. However in certain cases the library search may not yield an unambiguous result and on these occasions accurate mass measurements are particularly helpful. The DS50 data system in combination with a double beam mass spectrometer such as the MS3074 or the MS1073 allows the data from low resolution scans to be examined both by library search and accurate mass measurement techniques. This paper describes the library search programme used with the AEI DS50 data system and gives some examples of its use in combination with a double beam mass spectrometer.

The library search system has been fully described elsewhere[1] and only a brief description is necessary. The spectrum is reduced to a 120 bit spectrum signature, which is compared with the signatures of the spectra in the library to produce a matching score. This type of spectrum signature is very compact, allowing a large library to be stored on the disc of a mini computer, and the search is also very fast. The speed is further enhanced by a routine which requires each possible match to reach a certain percentage of the maximum score after checking only 16 bits of the signature. If the predetermined percentage has not been attained then that possibility is rejected. This feature greatly increases the overall speed of the search.

The spectrum signature is designed to contain only structurally significant data so that in cases in which a compound is not included in the library the system gives the operator a valuable indication of the compound type. This is illustrated in figures 1 and 2. This spectrum was obtained from a sample of tobacco smoke that was described in paper C-2. Spectra were obtained at 1000 resolving power with a scan speed of 1 second per decade. The result leaves no doubt that the compound was a $C_{10}H_{16}$ terpene, and in fact, all of the first 10 selections were of this type of compound. The GC retention time confirmed that the compound was limonene.

Figure 2 illustrates a situation in which the result is less clear. The library search results strongly indicate that this material had a furan type structure. The lower table gives the mass measurements of two of the major peaks. These show that the compound contained only one oxygen and in conjunction with the library search results point to its identity being ethyl methyl furan. This compound was in fact not in the library and so could not have been correctly identified by the library search routine alone.

Another example of the combination of library search with double beam mass measurement is shown in figures 3 and 4. Figure 3 is a chromatogram of a derivatized extract of the urine of a patient who had been treated with anticonvulant drugs and figure 4 shows how one of these peaks was identified by the combined use of library search and double beam mass measurement. The library search clearly indicates the compound type and the mass measurements confirm that the first choice is correct.

These examples illustrate the way in which the library search programme identifies compounds and particularly the compound type and show how the results can frequently be confirmed or refined by the use of double beam mass measurement.

Naegli and Clerc Anal.Chem. vol. 46, pp 739-744 July 1974

FORMULA	% SCORE	COMPOUND
$C_{10}H_{16}$	96.6	D - LIMONENE
$C_{10}H_{16}$	96.1	LIMONENE
$C_{10}H_{16}$	96.1	CAMPHENE
$C_{10}H_{16}$	94.6	ALPHA FENCHENE

Figure 1

FORMULA	% SCORE	COMPOUND
$C_{12}H_2O$	96.5	2, 5 - DI - TERT - BUTYLFURAN
$C_6H_6O_2$	95.3	2 - FURYL METHYL KETONE
$C_6H_6O_2$	95.3	FURYL METHYL KETONE
$C_7H_8O_2$	94.5	2-FURYL ETHYL KETONE

NOMINAL MASS	COMPOSITION	MASS MEASUREMENT ERROR
110	$C_7H_{10}O$	0.7 mMU
95	C_6H_7O	0.3 mMU

Figure 2

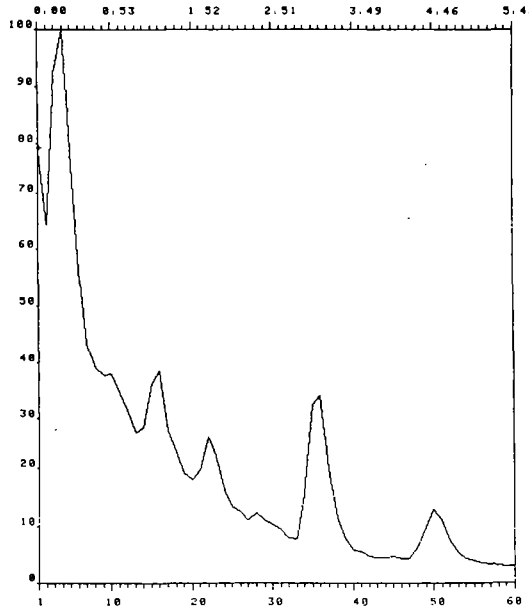

Figure 3

FORMULA	% SCORE	COMPOUND
$C_{18}H_{18}N_2O_2$	88.9	5 - P - METHYL 5(N, N DIMETHYL) PHENYLHYDANTOIN
$C_{19}H_{23}NO_4$	87.9	8, 14 - DIHYDROSALUTARIDINE
$C_{17}H_{16}O_2N_2$	87.4	DIPHENYL HYDANTOIN
$C_{18}H_{18}N_2O_3$	87.3	5 - P - ANISYL 5(N, N DIMETHYL) PHENYL HYDANTOIN

NOMINAL MASS	COMPOSITION	MASS MEASUREMENT ERROR
294	$C_{18}H_{18}N_2O_2$	0.2 mMU
217	$C_{12}H_{13}N_2O_2$	2.6 mMU
132	$C_9H_{10}O$	1.2 mMU

Figure 4

AN EXTENSION TO THE ROLE OF THE DEDICATED DATA SYSTEM IN GC-MS

P Powers, M J Wallington, J A V Hopkinson, VG Data Systems Limited, Altrincham, Cheshire, England and G L Kearns, The Kearns Group, Stamford, Conn 06902, USA.

At the 1974 Meeting we announced[1] a new series of Data Systems for use in Organic Mass Spectrometry. A particular feature of these systems is their high speed, especially in the processes of acquisition, real time mass measurement and in the generation of mass chromatograms. This paper describes some of the improvements made recently to these systems, improvements which take advantage of their speed and which have particular importance in GC-MS.

Perhaps one of the most difficult aspects of the interpretation of a GC run is the correct identification of partially resolved GC components. The use of mass chromatograms to connect one or more masses with each part of such a component is well known but this process relies on the chemist having prior knowledge of which masses to choose. Even with very fast chromatogram generation the identification of a complete unknown can be slow and tedious.

It was shown[2] in 1974 at this meeting that this problem could be eased dramatically if the computer were to calculate all possible mass chromatograms and present the user with a summary of the data. The principle of this approach is shown diagrammatically in Figure 1. At the top is a typical unresolved chromatogram peak which has been characterised by taking a number of mass spectrometer scans across it. The data system now calculates mass chromatograms for all masses up to mass 2000 and examines each one for maxima. All maxima occurring at any one retention taken together then form the true mass spectrum of the chromatogram component eluting at that time. Thus in Figure 1 masses 250, 251, 254, 255 and 258 form part of the true mass spectrum of scan 108 whereas masses 251, 252, 253, 254, 255 and 257 form part of the true mass spectrum of scan 113. Masses which are present but which have not maximised can be discounted since they are formed from background or other interfering ions. The mass reconstructed spectra therefore truly represent the intrinsic components of the GC peak and when a reconstructed gas chromatogram is formed from these data by the addition of all maximising masses, a chromatogram of much increased resolution results. In practice, of course, the resolution increase is limited by the fact that the spectrometer takes a finite time to scan. Nevertheless the result is quite dramatic, as can be seen from Figure 2.

The upper trace shows a conventional reconstructed total ion chromatogram of a perfume sample. The lower trace shows the mass reconstructed chromatogram which results from the mass maximising process. The broad peak between scans 80 and 90 (extreme right of upper box) and the poorly resolved triplet between scans 100 and 125 (extreme left of lower box) are just two that have been definitively resolved.

A further advantage of this process is the fact that background and other interfering ions are automatically rejected. Of course this rejection can in theory be achieved by the use of successive subtraction. In the case of the unresolved triplet in Figure 2 such a process becomes virtually impossible since unique normalising masses cannot be found for each component. Simple components like the broad peak between scans 80 and 90 do however allow the capability of the mass maximising process to be compared with the result of meticulous subtraction. Figure 3 shows this for spectrum 86 of the perfume sample referred to above. The top box shows the mass reconstructed or cleaned up spectrum produced by Mass Max and the lower box shows the result of subtracting spectrum 83 from 86. M/e 164 was used as a normalising mass in this subtraction since this was a prominent mass in spectrum 83.

The subtracted spectrum required considerable operator interaction to obtain. The MassMax spectrum was obtained entirely automatically and in real time.

The fact that these data are obtained in real time means that the cleaned up spectra can be reported in any of the Interscan report formats of the data system. Figure 4 shows a new form of report which gives substantially more information than do other formats. The report gives the masses of the most prominent peaks in each group of ten masses. The heading identifies the group of ten and each number on each line identifies the final digit. Thus the prominent masses of the real component at scan 86 of the same perfume sample are immediately revealed in real time as 29, 32, 43, 58, 69, 71, 81, 95, 109, 110, 126 and 142. The success of the MassMax process in separating such complicated GC components led us to attempt a much more difficult but nontheless typical problem. We prepared a mixture of pesticides some of which have not only similar retention times but almost identical mass spectra too. Such mixtures are impossible to separate by subtraction but the MassMax process proves to be remarkably successful, as can be seen from Figure 5. The outer envelope shows the original TIC trace and the inner curve the separated result. These data were taken from a VG 7070 mass spectrometer coupled to a VG 2040 data system. Of particular note is the increased precision with which retention time may be measured. The success of this work opened the way for us to implement software for the actual subtraction of gas chromatograms. Such difference chromatogram data are useful where the user needs to know the difference between two GC samples rather than the identification of each component.

The software uses library searching techniques coupled with retention time data to ensure that peaks are the same before normalised intensity subtraction is performed. Figure 6 shows an output from the subtraction of two pesticide runs. A mixture of Dieldrin and DDT was taken as a standard with the mixture shown in Figure 5 taken as sample. The second isomer of DDT was used for intensity normalisation. Peaks unique to the sample are listed on the left and their library identifications on the right.

References (1) P Powers et al, Paper W1 presented at 22nd Conference ASMS Philadelphia 1974 (2) J E Biller & K Biemann, Paper U1 presented at 22nd Conference ASMS Philadelphia 1974.

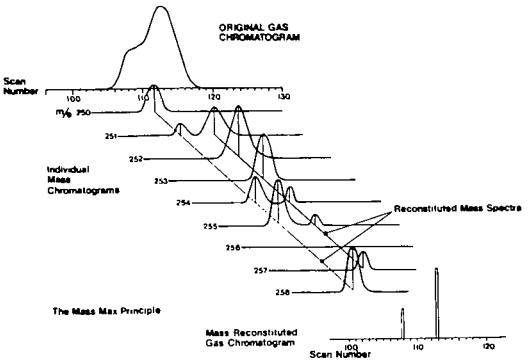

Figure 1

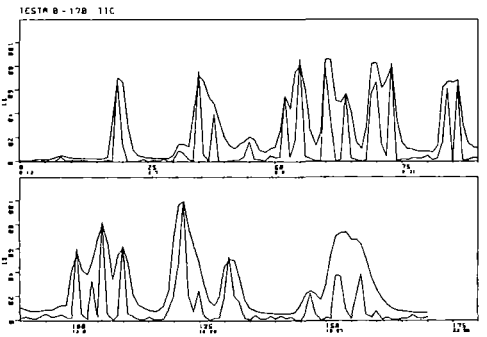

Figure 2

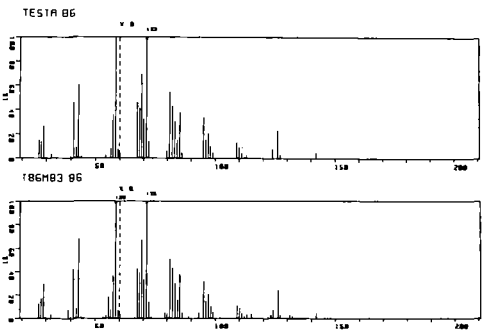

Figure 3

2 'MassMax' Peaks only

[illegible]

[illegible]	[illegible]	[illegible]	[illegible]	[illegible]	[illegible]	[illegible]
[illegible]	[illegible]	[illegible]	28	54	174	10.13*0
[illegible]	[illegible]	[illegible]	32	52	158	10.21*0
[illegible]	[illegible]	[illegible]	28	79	297	10.30*0
[illegible]	[illegible]	[illegible]	55	119	1361	10.38*0
[illegible]	[illegible]	[illegible]	164	121	1467	10.46*0
[illegible]	[illegible]	[illegible]	26	123	1445	10.55*0
[illegible]	[illegible]	[illegible]	58	107	1497	11. 3*0
[illegible]	[illegible]	[illegible]	45	94	687	11.11*0
[illegible]	[illegible]	[illegible]	32	80	346	11.20*0
[illegible]	[illegible]	[illegible]	28	75	256	11.28*0
[illegible]	[illegible]	[illegible]	39	72	220	11.37*0

Figure 4

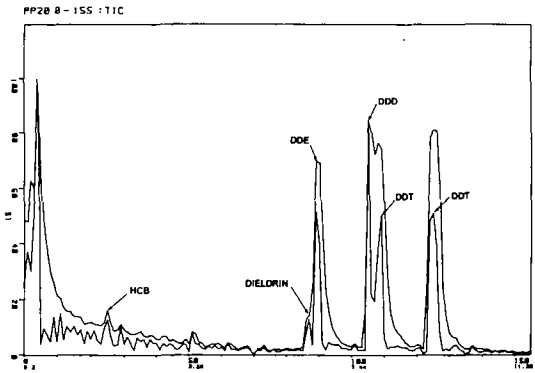

Figure 5

SUBTRACTION REPORT GC30- GC20

TIME RANGE : 6M 00S - 10M 00S
NORM PEAK : 9M 43S / 9M 38S
T/HOLD STD : 5%
T/HOLD SAM : 20%

TIME	SAMPLE(-)	SAM/STD	STANDARD(+)	DEL T	IDEN
6.49		-15.9		-0.05	DIELDRIN
6.58	-100.6				DDE
8.12	-159.2				DDD
8.29		-60.8		-0.04	DDT
9.43		STD		-0.05	DDT

Difference Chromatogram Output

Figure 6

REAL-TIME GAS CHROMATOGRAPHY-HIGH RESOLUTION MASS SPECTROMETRY AND THE ANALYSIS OF COMPLEX ORGANIC MIXTURES

B. J. Kimble, F. C. Walls, R. W. Olsen and A. L. Burlingame
Space Sciences Laboratory,
University of California, Berkeley, California 94720

The combination of low resolution gas chromatography with real-time high resolution mass spectrometry (GC/HRMS), described previously,[1,2] provides accurate mass measurements of all peaks in spectra obtained by continuous cycle operation. The instrumentation currently employed in this laboratory utilizes a faster scan cycle time (9.6 sec between m/e 800-60) and this now permits the use of open tubular capillary columns for the analysis of complex organic mixtures. The operational parameters are summarized in Table 1.

The mass measurement accuracy was determined from data obtained using 15 N-containing fragments from heptacosafluorotributylamine (HFTBA); the HFTBA was introduced from a glass inlet system together with PFK and with He flowing into the ion source to give an indicated pressure of 2.6×10^{-6} torr. The 15 selected N-containing ions covered the mass range m/e 114-614, and 18 high resolution mass spectra were recorded to provide a total of 270 mass measurements. The mass measurement error distribution is shown in Fig. 1 as a histogram; 100% of the measurements were within 17.5 ppm, and 96% were within 10 ppm. The smallest peak considered in these measurements contains about 30 ions and the dynamic intensity range for these masses is 30:1. The potential dynamic range of the system is >130:1 assuming that the smallest peak again contains about 30 ions.

Evaluation of the separator performance was achieved by sweeping repetitively once a second over m/e 74 using the peakmatching oscilloscope of the MS902. This output was also monitored on a storage oscilloscope and provided a "response profile" during elution of methyl stearate from the gas chromatograph. Fig. 2a shows the maximum response for the $C_3H_6O_2$ ion at m/e 74 from methyl stearate (100 ng injected on the GC column) plotted against the indicated source pressure. The pressure was varied by adjustment of the make-up He flowrate into the separator. In Fig. 2b, the source pressure was maintained at an indicated value of 4.8×10^{-6} torr (the maximum point on the curve in Fig. 2a), and the maximum $C_3H_6O_2$ response was determined for various amounts of methyl stearate injected onto the GC column. The reason for the significant nonlinearity of the $C_3H_6O_2$ response with respect to amount of methyl stearate introduced <u>via</u> this separator is unclear at present, particularly since the FID response to methyl stearate was linear over at least the range 5-500 ng injected on this column.

The data for methyl stearate shown in Table 2 were obtained under normal operation as a GC/HRMS system (parameters as in Table 1, source temperature 250°C). Under the GC conditions used, the methyl stearate peak eluted in about 20 sec; thus it seemed necessary to evaluate the effect of a 9.6 sec scan cycle time with respect to the peak elution profile in terms of mass measurement accuracy. Ten separate injections were made of 100 ng of methyl stearate; Table 2 shows the mass measurement errors in ppm and the corresponding intensities for the $C_3H_6O_2$ and molecular ions. Under these conditions, the relative intensity of the molecular ion is only about 4% of the $C_3H_6O_2$ ion, and the maximum intensity for the molecular ion represents about 10 ions, with a signal-to-noise ratio of about 6:1. The data show that even with 2 scans/GC peak, the molecular ion was detected in all cases despite the low intensity.

The fast scan cycle time now available with this GC/HRMS instrumentation permits the recording of complete high resolution mass spectra of components eluting from open tubular capillary columns and the system is currently in use for the analysis of many types of complex organic mixtures.

This work was supported by NIH Grant RR-719-02 and NASA Grant NGL 05-003-003.

---

[1]B. J. Kimble, R. E. Cox, R. V. McPherron, R. W. Olsen, E. Roitman, F. C. Walls and A. L. Burlingame, Presented at the 22nd Annual Conference on Mass Spectrometry and Allied Topics, Philadelphia, Pa., May 19-24, 1974, p. 315.

[2]_____, J. Chromatog. Sci., 12, 647 (1974).

Table 1.

REAL-TIME CAPILLARY GC/HRMS SYSTEM

GC: 175 ft x 0.030 in. i.d. glass SCOT OV-101
Effluent splitter: variable to FID and/or MS
Make-up He inlet to separator: variable flow

SEPARATOR: second stage stainless steel Ryhage jet
inlet jet diameter 0.010 in.
outlet jet diameter 0.012 in.
jet separation 0.020 in.
115 liter/sec diffusion pump

MS: modified MS902

dynamic resolution	10,000
scan rate	6 sec/decade (exponential)
mass range	m/e 800-60
scan time	7.2 sec
rescan time	2.4 sec
cycle time	9.6 sec

DATA ACQUISITION: LOGOS-II
Digitization rate 50 kHz

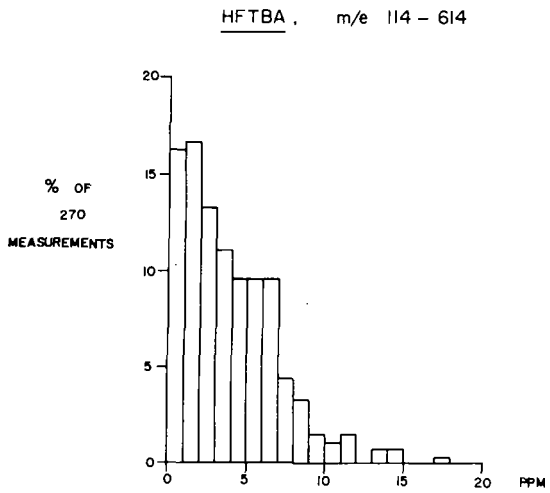

Figure 1.

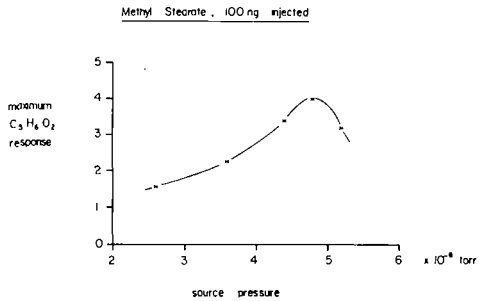

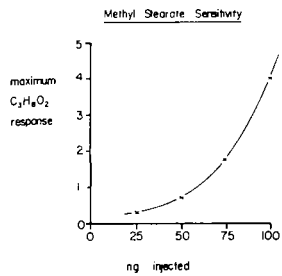

Figure 2.

Methyl Stearate 100 ng

Scan	m/e 74.0368 Error	m/e 74.0368 Intensity	m/e 298.2871 Error	m/e 298.2871 Intensity
22	-3.07	2437	–	–
23	2.40	4888	7.24	111
24	-8.87	1520	24.7	84
81	-5.97	5406	0.28	264
82	3.54	2350	-4.27	92
130	1.31	7077	–	–
131	-0.55	3806	23.2	217
180	3.47	7208	–	–
181	4.77	3169	32.0	104
228	9.23	5859	–	–
229	1.02	4037	2.47	295
280	-0.49	5595	-13.91	97
281	-4.48	2823	–	–
332	2.98	3066	1.45	50
333	-4.24	1599	–	–
379	-3.34	2374	–	–
380	-1.59	3889	5.79	125
428	-0.43	5463	10.52	83
429	-1.75	2261	-21.17	192
480	4.03	7387	1.70	130
481	1.02	2641	-13.01	166

Table 2.

T-10

Instrumentation and Data Reduction for Collisional Activation Spectra. T. WACHS, P. F. BENTE, III, F. W. MCLAFFERTY, and C. C. VAN DE SANDE, Cornell Univ., Dept. of Chem., Ithaca, NY 14850

A "reversed geometry" Hitachi-RMU-7 has been further modified to obtain improved CA spectra for the study of ion structures. A confined collision region has been added to decrease the effect of main ion beam scattering and eliminate interfering first-field decompositions. Resolution of peaks, broadened due to the relatively large energy release in the CA process, has been improved by increasing the accelerating potential from 4 to 8 KV and by placing a potential on the collision chamber itself. The latter also separates CA and unimolecular metastable peaks of the same mass. Data collection, CATTING, ESA control, least squares smoothing, data plotting, and mass and abundance determination are done via a DEC PDP-8 computer. Using this system, measurement of the energy transferred in the CA of simple hydrocarbon ions gives values consistent with breakdown curves.

T-11

A Computer-controller AVA Unit for Routine Biological Assay Processing.

R. B. Spencer and R. W. Walker, Merck & Co., Rahway, NJ 07065

Drug metabolism studies using the isotope dilution technique and a GC/MS system in the AVA mode of operation are often conducted. AVA operation allows detection of specific ions (i.e., specific m/e values) characteristic of the compounds of interest. A Varian MAT Spectro System 100 computer system provides data acquisition and processing capabilities for regular operation of the LKB 9000, but does not have an AVA capability. An LKB model 9066 AVA accessory unit is used, with subsequent manual workup of the data. Computer control of the AVA unit and processing of the data have been provided by making additions and modifications to the data system and AVA unit. Control of the AVA unit is possible through an interface board designed for this purpose. Assembly language subroutines callable from BASIC language programs running in the Varian 620/i computer provide AVA unit control and data acquisitions capabilities. Comparisons of the computer mode of operation with the previously used manual operation show good agreement of results, with a virtually complete elimination of the need for manual handling of the data.

Low-Cost Computer System for Quadrupole Mass Spectrometers.

Philip S. Berger, Peter D. Norbert and William F. Holmes,
Washington University Medical School, St. Louis, Missouri

The development of computer hardware and software especially applicable to GC/MS analyses is described. Data can be acquired by three methods of mass scanning--incrementing at 0.1 mass unit intervals with peak detection, incrementing by successive integer mass values corrected for mass defect, and selected ion monitoring. Where appropriate, fractional mass information can be stored with peak intensities. A display interface with digital bar and character generators has been designed, which can be used with a standard refreshed display oscilloscope. The display allows presentation of spectra during data acquisition and rapid, convenient examination and processing of stored data. Control of data storage during the GC run, plus a very compact data format helps to increase the effective file storage space.

Extension of the Mass Range for Selected Ion Monitoring by Computer Control of the Magnetic Field. NORMAN D. YOUNG, JOHN F. HOLLAND, JAMES N. GERBER and CHARLES C. SWEELEY, Biochemistry Department, Michigan State University, East Lansing, Mich. 48824

Selected Ion Recording (formerly Selected Ion Monitoring) techniques are routinely being used for precise quantitative analysis of multi-component mixtures on GC-MS systems. Nearly all magnetic sector mass spectrometers implement this technique by switching the accelerating voltage to focus the ions of interest (1-4). However, the accelerating voltage may be switched only over a limited mass range without significant loss of sensitivity due to defocusing of the ion source (5). This limited sampling range often makes it impossible to monitor and quantitate more than one compound in a single GC injection. To circumvent this problem, the accelerating voltage and the magnetic field were both put under control of a dedicated minicomputer. With these controls, a series of SIR analyses can be performed at any magnetic field setting. This provides the opportunity to monitor any eluting compound that can be separated in time from preceeding and succeeding compounds by an interval of ten seconds or longer.

The instrument configuration consists of a LKB 9000 mass spectrometer interfaced to a PDP 8/E minicomputer. A 10 bit digital to analogue converter is used to control the accelerating voltage from 3300 to 3700 volts.

To illustrate the magnetic field switching method, an experiment was designed to analyze a complex mixture of three biogenic amines and an internal standard. As seen in Table I, each compound was assigned an ion set. Each set contains ions that are indicative of the compound it represents. Each set also specifies a retention time when the computer is to switch to the next ion set. Figure I shows the variations of the magnetic field during data collection. The magnetic field is ramped to an appropriate setting and a SIR analysis is performed by monitoring the indicated ions with the accelerating voltage. At the specified retention time, the magnetic field is switched to a new value in preparation for the next ion set. The maximum time for a magnetic field switch is 8 seconds.

Figure IIa shows the gas chromatogram of the mixture which includes a series of hydrocarbons. Figure IIb shows the computer output for the experiment. The multiplication factors next to the peaks are used to provide good visual presentation. The computer can integrate each ion peak, subtract baseline and output corrected peak height and area. In general, the precision and sensitivity are identical to the traditional SIR approach.

In conclusion, computer control of the magnetic field and accelerating voltage makes the magnetic sector mass spectrometer a viable tool for performing SIR analysis on multicomponent mixtures. This method will be expanded in greater detail in a future publication being submitted to *Analytical Chemistry*.

This work was supported by a NIH Grant RR-00480.

REFERENCES

1. J. F. Holland, C. C. Sweeley, R. E. Thrush, R. E. Teets and M. A. Bieber, Anal. Chem., 45, 308 (1973).

2. W. F. Holmes, W. H. Holland, B. L. Shore, D. M. Bier and W. R. Sherman, Anal. Chem., 45, 2063 (1973).

3. J. T. Watson, D. R. Pelster, B. J. Sweetman, J. C. Frolich and J. A. Oates, Anal. Chem., 45, 2071 (1973).

4. C. C. Sweeley, W. H. Elliott, I. Fries and R. Ryhage, Anal. Chem., 38, 1549 (1966).

5. C. C. Sweeley, J. F. Holland, N. D. Young and R. B. Blaiser, "Proceedings of the 22nd Annual Conference on Mass Spectrometry and Allied Topics." Philadelphia, PA., May, 1974.

SET I

Compound: Tryptophol (T_{ol})

Ions: 453,454

Retention Time for Switch: 7:00

SET II

Compound: Tryptamine (T_{am})

Ions: 276,289

Retention Time for Switch: 11:00

SET III

Compound: 5-methoxytryptamine (T_{me})

Ions: 482,483

Retention Time for Switch: 12:40

SET IV

Compound: Methyl Stearate (MeS)

Ions: 298,299

Retention Time for Switch: 15:00

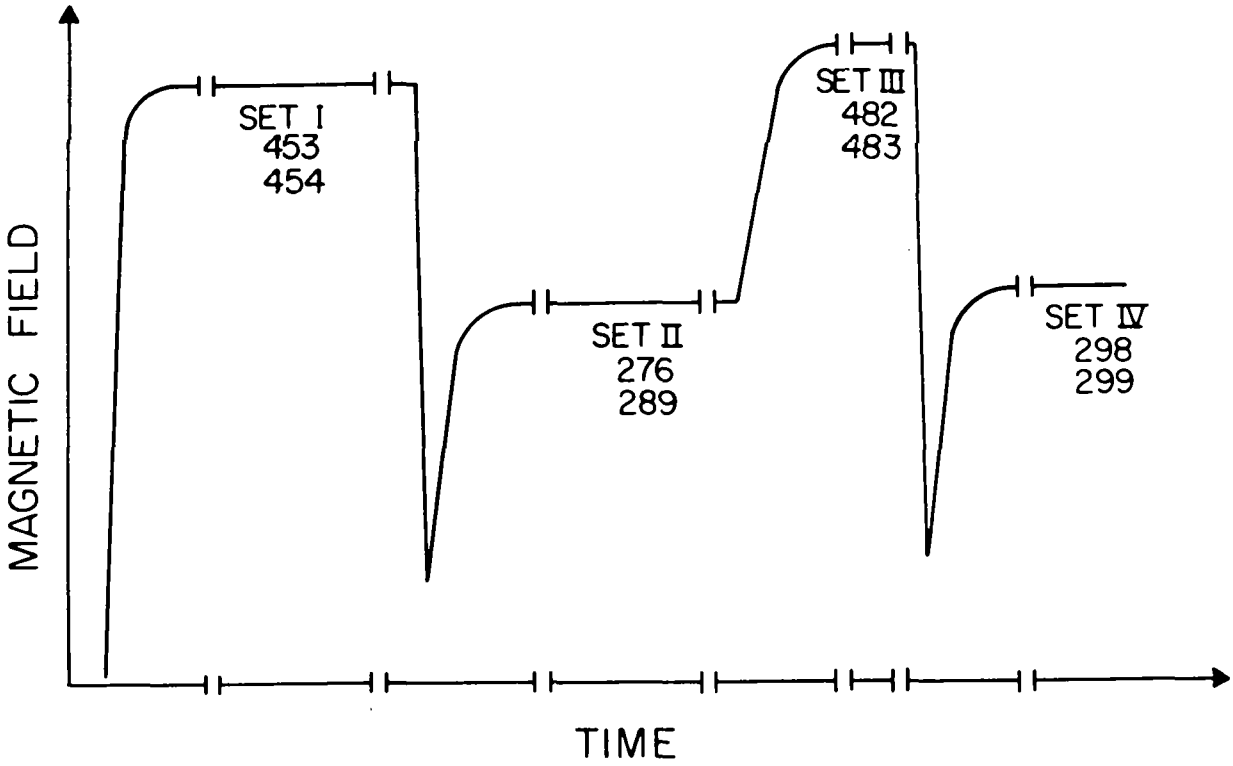
MAGNETIC FIELD
TIME
SET I
453
454
SET II
276
289
SET III
482
483
SET IV
298
299

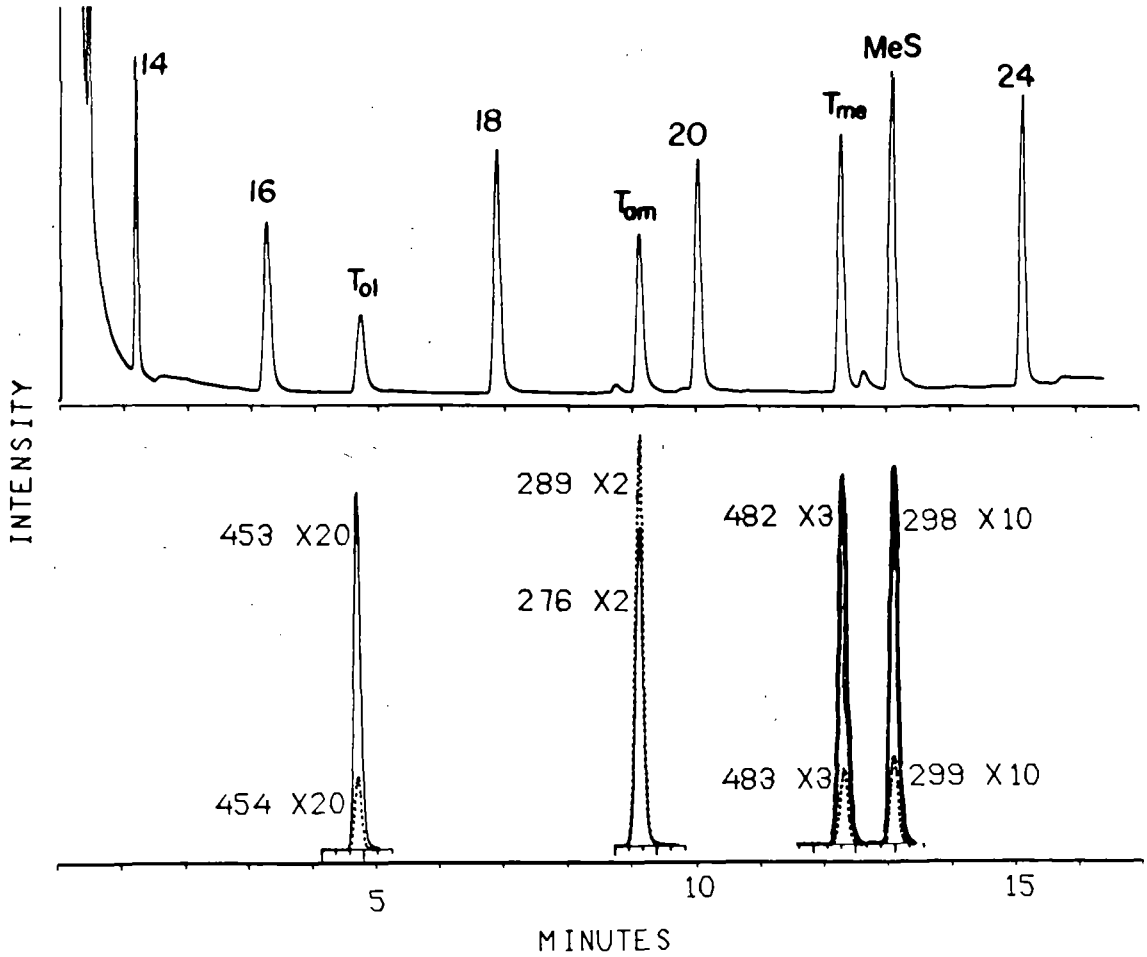
14
16
T_{ol}
18
T_{om}
20
T_{me}
MeS
24
INTENSITY
453 X20
454 X20
289 X2
276 X2
482 X3
298 X10
483 X3
299 X10
5
10
15
MINUTES

T-14

The Use of a Programmable Calculator for Mass Spectrometer Control and Data Processing.

Jeffrey L. Hayden*, Tony C.D. Knight**, and Stephen W. Smith***

A Hewelett-Packard 9830A programmable calculator system has been used during the testing of mass spectrometers to be flown to Mars as part of the Viking Mission. The calculator system was used to control the operation of the spectrometers during the testing and calibration program, to acquire and store the mass spectral data and to process and display the data. The system, its performance, its limitations and merits are discussed.

*Univ. of Minn., School of Physics and Astron., Minneapolis, Minn. 55455.
**Martin Marietta Corp. P. O. Box 179, Denver, Colorado 80201
***Bendix Corporation, 3300 Plymouth Road, Ann Arbor, Michigan 48107.

T-15

Voltage Scanning of a Double Focussing Mass Spectrometer Under Computer Control.

K. B. Denson, S. P. Taylor, and J. M. Hayes, Indiana University, Department of Chemistry, Bloomington, Ind. 47401.

A CEC 21-110B double focussing mass spectrometer has been modified to permit voltage scanning over a wide range under computer control. The ion accelerator and electrostatic analyzer potentials can be controlled individually, permitting either conventional mass scanning or the controlled observation of metastable ions, either under computer control or in a manual mode. For GC-MS applications, the speed with which the voltage can be scanned should permit implementation of a very flexible selective ion monitoring (SIM) scheme, even when glass capillary columns, with their narrow peak widths, are used in the chromatographic system. The effect of decreased accelerating voltage on sensitivity has been examined and will be compared with the sensitivity under magnetic scan conditions.

On-Line Control of High Resolution Mass Spectrometers. I. Peak Matching*

Del W. Bissett, C. Cone and F. C. Maseles,
U.T. Austin, Dept. of Chem., Austin, Tx. 78712

A special purpose interface for on-line control of the accelerating voltage and electric sector voltage of a DuPont (CEC)21-110 high resolution mass spectrometer by a PDP 8-I laboratory computer has been constructed, using Digital Equipment Corporation M-series logic modules. The interface provides the program inputs for a Fluke high precision programmable voltage source (Model 3330B). For peak matching the output voltage of this supply is used directly to provide the voltages of the positive and negative field plates, and also the accelerating voltage reference; thus simply replacing the standard electric sector supply with a programmable one. For metastable scans either electric sector or accelerating voltage can be independently scanned under computer control by a straightforward change in the interconnections of the various supplies.

Ion intensities are read by a scaler in the interface connected to a homemade ion counting amplifier. A parallel analog signal from a diode pump is fed to the standard oscilloscope which is externally triggered by a scan start pulse from the interface. The operator can thus visually monitor peaks being scanned under computer control at the same time that digital peak intensity information is being acquired by the computer. A range of scan rates is program selectable, utilizing a clock in the interface.

For the initial application of peak matching we quickly obtained a precision of measurement comparable to that found by manual measurement using this mass spectrometer. Presently for ratios of two peaks with a mass difference of less than two percent both the accuracy and the precision of measurement are less than 1ppm but for wider ratios less satisfactory results are obtained. A careful study of the sources of error is underway and when completed a full paper will be prepared for publication.

*The financial support of the Robert A. Welch Foundation is gratefully acknowledged.

SEQUENCE DETERMINATION OF OLIGODEOXYRIBONUCLEOTIDES BY MASS SPECTROMETRY AND COMPUTERIZED PATTERN RECOGNITION. J.L. Wiebers and J.A. Shapiro, Dept. of Biological Sciences, and S.P. Perone and D.R. Burgard, Dept. of Chemistry, Purdue Univ., West Lafayette, IN 47907.

A novel strategy for the sequence analysis of oligodeoxyribonucleotides has been devised which is based upon the direct structural analysis of intact, underivatized oligonucleotides by mass spectrometry with subsequent analysis of the spectral data by computerized pattern recognition techniques. The pyrolytic and electron impact conditions of the spectrometer permit the cleavage of oligonucleotides of varying chain length and composition yielding reproducible fragmentations and characteristic m/e values which can be used to reveal purine and/or pyrimidine base sequence information. The selection of optimum features (which can be the relative intensities of certain m/e values, or the ratios of peak heights of specific ions, or, the linear combination of such values) has been done by an interactive feature selection method employing multidimensional K-nearest neighbor analysis. Certain features reveal the location (5' or 3' terminus) of a residue in a dinucleotide and these have been incorporated into a computer program which can be used to determine the sequence of any of the dinucleotides that occur in DNA. Other specific features indicate which nucleotides within an oligonucleotide are adjacent and are included in the program. Knowledge of the nucleotide pairs present, in conjunction with the information as to the 3' or 5' position of a residue in the pair, permits the reconstruction of the sequence of the original oligonucleotide. The 3' and 5' terminals of the intact molecule can be confirmed by trifluoroacetylation of the 3' and 5' hydroxyl groups with subsequent mass spectral identification of the diagnostic ions for these sites. Twenty-two model oligodeoxyribonucleotides of defined sequence and of varying chain length have been analyzed by the mass spectral-pattern recognition method. (Supported by NSF Grant BMS 74-22213.)

UPACS - Computerized Mass Spectrometry System

L. Baczynskyj, J. F. Zieserl, M. D. Kenny,
J. B. Aldrich and D. J. Duchamp

UPACS - the Upjohn Physical and Analytical Chemistry System - is an IBM 1800 based time-sharing computer system for laboratory automation. Since the acquisition of the computer in 1968, the following instruments have been interfaced to it:

1. One X-ray diffractometer (Syntex P 1).
2. One NMR ^{13}C and ^{1}H spectrometer (Varian XL 100).
3. One CD/ORD spectropolarimeter (Cary 60).
4. One liquid scintillation spectrometer (Packard Tri-Carb) plus balance.
5. Two elemental analyzers (Perkin-Elmer 240) plus balance.
6. Five gas-liquid chromatographs with automatic injection.
7. Three mass spectrometers with GLC attachments.

The computer is a 32 K (16 bit) machine. A distinctive feature of UPACS is the fact that all instruments interfaced to the IBM 1800 can operate simultaneously, without interference and the data acquisition and data reduction are performed in real-time. Other such systems using larger computers have been described.[1]

In 1969 our first GC-MS instrument (LKB 9000) was interfaced to the computer.[2] A second mass spectrometer (Atlas MAT CH4) was interfaced in 1971. Since the acquisition of the Varian MAT CH7 and the replacement of the CH4 with the CH5 DF, a second generation interface has been built and the software rewritten. This new system allows simultaneous scanning of the three GC-MS instruments (CH5 DF, CH7 and LKB) in the low resolution and metastable (CH5 only) modes. Other modes, such as high resolution for the CH5 DF, are under development.

The I/O devices used in the mass spectrometry laboratory are three terminals (30 ch./sec., Texas Instrument Silent 700) one at each instrument and a 30" plotter (Calcomp) shared with other users.

To set up a mass spectrometry experiment a series of commands (at present 34) are available. The print, plot, store and background subtraction functions can also be implemented using interface buttons at the mass spectrometers.

The schematic of the interface is shown in Figure 1. The intensities of the ions are digitized at the interface using a 12 bit A/D converter with 4 gain ranges (1, 8, 64, 512). The output of the digital mass marker (binary), the ion intensities and the time (32 bits) are transmitted to the computer at user selected rates 5, 2.5, 1.25, 0.625, 0.312 or 0.156 KHz. A block of 8 words is sent at the chosen sampling rate if any or all three mass spectrometers are on line, scanning, and the intensity signal is above threshold.

The data enters the IBM 1800 computer through a high-speed digital input data channel which puts the data into a 2 K core buffer area in a cyclic fashion. Data are reduced in real time by data acquisition programs written in IBM 1800 assembler language and always present in computer core. Three types of data collection are used:

1. High points are picked in real time (for low resolution).
2. Intensities are averaged (n points where n is set according to experiment type).
3. High resolution peak data are extracted (under development).

Scanning is initiated by pushing a button at the instrument or automatically by computer clock. Actual start and termination of scan is computer-controlled. Scanning is terminated when a preset time expires or when a designated mass is reached. Results of this preliminary data reduction are placed in a raw file on disk.

Three types of files are used in the processing of the data:

1. Three RAW DATA files (one for each instrument).
2. Three TEMPORARY files (one for each instrument) that can accommodate up to 80 spectra of 1,500 ions each.
3. One PERMANENT file that can contain approximately 2,000 mass spectra.

The raw data processing program (MSMRV) processes the data according to experiment type. For low resolution scans it assigns masses and intensities for each ion, normalizes the scans and transfers them to the temporary (scratch) file. It checks for printing, plotting, background subtraction and storing options. It also provides for calibration of the mass markers and transmission tests of various bits (time, mass, gain, intensity).

Further processing of the data in the temporary file is performed by several programs:

1. MSPLO plots mass spectra in various formats with scale expansion, labelling and other available options.
2. MSPRN prints the final report (3 formats) of various scans.
3. MSAVG does the averaging, subtraction and background subtraction function of spectra.
4. MSAUX is used to store, recall, and delete spectra in the permanent file and to print a directory of spectra.

For scans of metastable ions (defocussing modes), MSMRV assigns sequence numbers to the various scans and transfers them to the CH5 temporary file. Scans of metastable ions are then processed by MSMCL, which finds high points, centers of peaks at 3/4 height, averages several scans, and smoothes the data, if requested. The final calculations are performed by MSPPP. It correlates point numbers with voltages and masses, prints reports, and plots the spectrum of the scan.

Most of the processing programs use integer arithmetic and are written in FORTRAN for a multiuser system (up to 60 different operators are using the GC-MS facilities in one year).

REFERENCES

1. See, for example, D. Hennenberg, K. Casper, B. Weimann and E. Ziegler, in "Advances in Mass Spectrometry," Vol. 6, A. R. West, Ed., Appl. Sci. Publ., Ltd., Barking, Essex, 1974, p. 477.
2. D. A. Griffith, in "Biochemical Applications of Mass Spectrometry," G. R. Waller, Ed., Wiley-Interscience, 1972, p. 58.

FIGURE 1

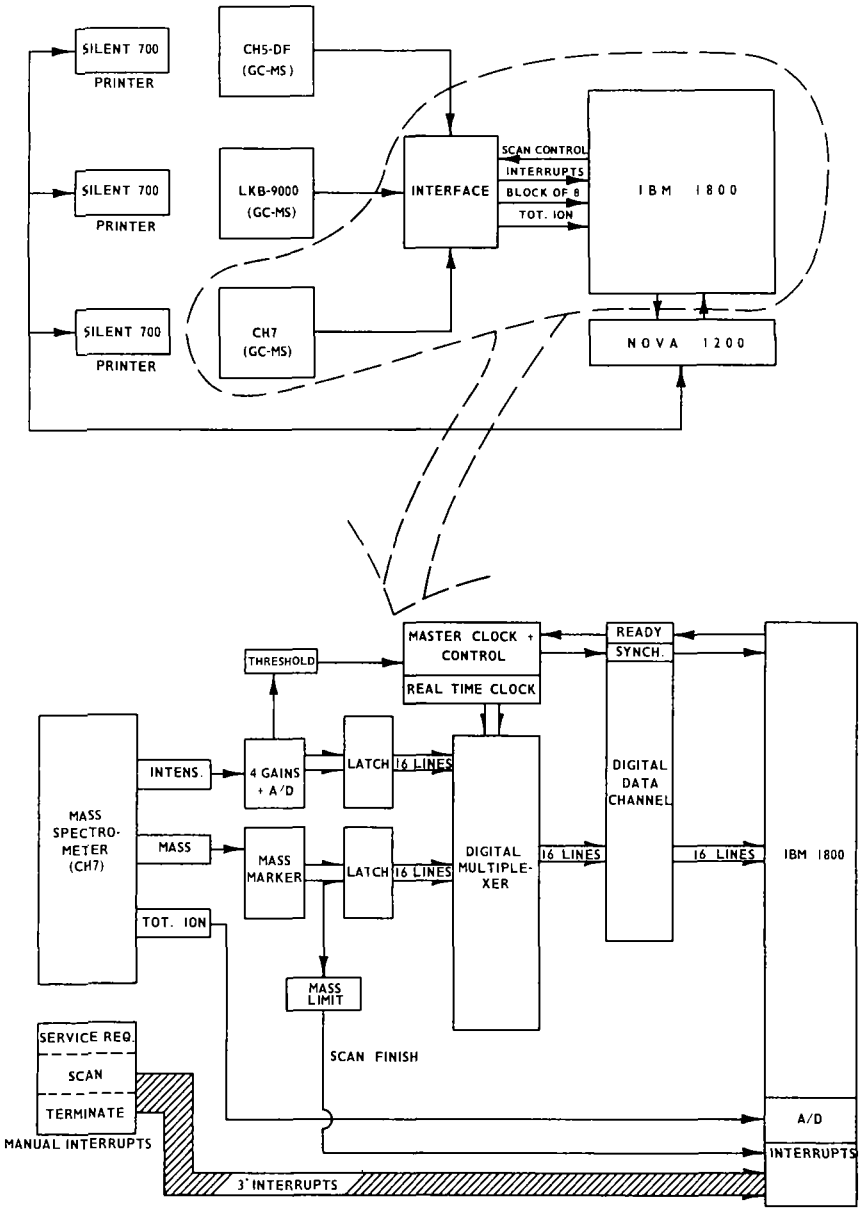
SILENT 700
PRINTER
SILENT 700
PRINTER
SILENT 700
PRINTER
CH5-DF
(GC-MS)
LKB-9000
(GC-MS)
CH7
(GC-MS)
INTERFACE
SCAN CONTROL
INTERRUPTS
BLOCK OF 8
TOT. ION
IBM 1800
NOVA 1200
MASTER CLOCK + CONTROL
REAL TIME CLOCK
READY
SYNCH.
THRESHOLD
MASS SPECTRO-METER (CH7)
INTENS.
MASS
TOT. ION
4 GAINS + A/D
MASS MARKER
LATCH
16 LINES
LATCH
16 LINES
DIGITAL MULTIPLE-XER
16 LINES
DIGITAL DATA CHANNEL
16 LINES
IBM 1800
MASS LIMIT
SCAN FINISH
SERVICE REQ.
SCAN
TERMINATE
MANUAL INTERRUPTS
A/D
INTERRUPTS
3' INTERRUPTS

Plasma Amino Acid Analysis by Isotope Ratio GC/MS/Computer Techniques. MARTIN F. SCHULMAN and FRED P. ABRAMSON, George Washington U., Depts. of Pathology and Pharmacology, Washington, DC 20037.

A complete description of this work appears in Biomedical Mass Spectrometry, 2: 9 (1975).

U-2

DETERMINATION OF ^{3}H, ^{14}C, and ^{18}O BY GC-MS. APPLICATION TO STEROL METABOLISM

Brian S. Middleditch,* Marcell Gut,** and Shlomo Burstein*

*Department of Cell Biology, Baylor College of Medicine
Houston, Texas 77025
and
**The Worcester Foundation for
Experimental Biology
Shrewsbury, Massachusetts 01545

Isotope ratios are derived, in submicrogram amounts, from repetitive mass spectral scans. Incubation of [4-^{14}C]cholesterol with an adrenal preparation yields [4-^{14}C]-(22R)-22-hydroxycholesterol (I) and [4-^{14}C]-(20R,22R)-20,22-dihydroxycholesterol (II). The specific activity of II is derived from m/e 461 and 463 (C-1 to C-21) of the TMS derivative. These ions also give the ^{18}O-content at C-20 of [4-^{14}C;20,22-^{18}O]-II formed with $^{16}O_2$ and $^{18}O_2$. The total ^{18}O-content in the side-chain (hence that at C-22) is determined from m/e 289, 291, and 293 (C-20 to C-27). The binomial distribution of these ions shows that the oxygen atoms in the side-chain of each molecule of II derive from separate oxygen molecules. Equal amounts of ^{18}O, reflecting the composition of the atmosphere, are found at C-20 and C-22. Incubation of I with $^{18}O_2$ yields [20-^{18}O]-II without scrambling of oxygen atoms.

Supported by USPHS grants CA 15423 and AM 3419.

Publication is contemplated.

HIGH PRECISION ISOTOPE RATIO MEASUREMENTS BY CI/MS*

D. L. Hachey, P. A. Szczepanik,
W. F. Bryant, and P. D. Klein

Division of Biological and Medical Research
Argonne National Laboratory
Argonne, Illinois 60439

Biomedical isotope ratio measurements are most commonly made using electron impact mass spectrometry (EI/MS). Electron ionization provides a stable, reproducible ionization process that is essential for high precision isotope ratio measurements. EI/MS, however, is a relatively energetic ionization process that results in extensive fragmentation of complex biological molecules. The mild ionization process involved in chemical ionization (CI/MS) generally produces a simple fragmentation pattern with only two or three ions predominating, and thus greatly improves the ion yield for a particular fragment. In order to assess the suitability of using CI/MS to measure isotope ratios, we examined several different classes of biological compounds enriched with ^{2}H, ^{13}C and ^{15}N.

The CI mass spectrometer used in this study was the Biospect, a quadrupole mass spectrometer equipped with a CI ion source. Isotope ratios were measured using a stable isotope ratiometer-multiple ion detection system which was designed and built at Argonne (1). Isotope enriched compounds used in this work were urea-1-^{15}N, chenodeoxycholic acid-24-^{13}C, and methadone-$^{2}H_5$ hydrochloride.

In order to determine the precision with which isotope ratios could be measured by gas chromatography and CI/MS, a standard mixture of bile acids was prepared that contained lithocholic, deoxycholic, chenodeoxycholic, and cholic acids. The natural ^{13}C abundance was determined for the four bile acids in a single GLC run using the ion that results from complete dehydration of the steroidal hydroxy groups. The results from five consecutive runs are summarized in Table I. With the exception of the cholic acid results, these data indicate that isotope ratios can be determined with a precision of 0.4% and with a relative accuracy that agrees to within 99.3% of the theoretical value.

Table I. Determination of the Natural ^{13}C Abundance of Individual Bile Acids in a Mixture by Gas Chromatography and CI/MS.

Bile acid:	Lithocholic	Deoxycholic	Chenodeoxycholic	Cholic
Mean Ratio (n = 5)	27.52%	27.55%	27.46%	29.11%
SD	0.15	0.08	0.08	0.43
Theory	27.75	27.72	27.72	27.68

Isotope dilution curves were prepared for urea samples that contained 0.03% to 10% excess urea-1-^{15}N, for bile acid samples that contained 0.5% to 100% excess chenodeoxycholic acid-24-^{13}C, and for methadone samples that contained 0.05% to 100% excess methadone-$^{2}H_5$. Dilution curves were constructed by graphing the difference in isotope ratio between the enriched

sample and standard compound against the mole ratio of isotope labeled compound to unlabeled compound. The data were treated as logarithms in these graphs in order to display the accuracy of an isotope ratio measurement over a wide range. The dilution curves were linear over the concentration ranges listed above. Figure 1 shows that the dilution curve obtained for methadone samples is linear over 3½ orders of magnitude and is usable to mole ratios down to 5×10^{-4}. Table II summarizes the linear regression data obtained for several dilution curves. The standard errors associated with the slopes are typically between 1% and 3% and correlation coefficients are better than 0.998, indicating a close fit of the data to the regression line. Thus an experimentally determined isotope ratio can be related to the mole ratio with good accuracy.

Table II. Regression Analyses of Isotope Dilution Curves.

Compound	Slope	Intercept
Chenodeoxycholic acid-24-^{13}C (By CI/MS)	0.6771 ± 0.0184	-0.3551 ± 0.0259
Chenodeoxycholic acid-24-^{13}C (By EI/MS)	0.8451 ± 0.0153	-0.1784 ± 0.0285
Methadone-$^{2}H_5$ (Direct dilution)	0.9895 ± 0.0138	-0.2057 ± 0.0312
Methadone-$^{2}H_5$ (Inverse dilution)	1.0107 ± 0.0153	0.1793 ± 0.0221

(1) P. D. Klein, J. R. Haumann and D. L. Hachey, Clin. Chem. 21 (1975) in press.

*Work supported by the United States Energy Research and Development Administration.

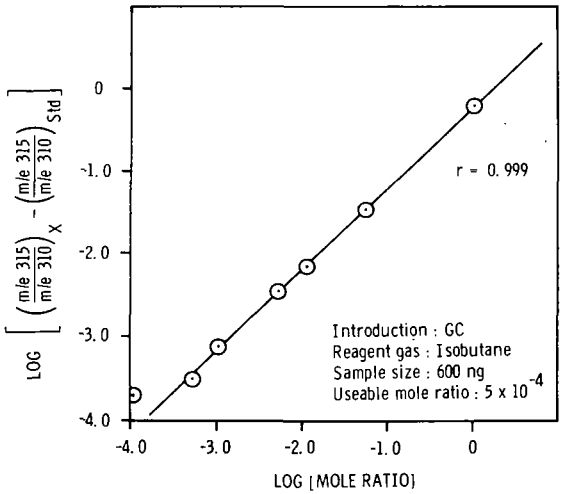

Figure 1. Isotope dilution curve for methadone-$^{2}H_{5}$.

A Procedure to Measure Total Body Water in Infants Using $H_2{}^{18}O$

J. A. Zirrolli and R. C. Murphy

Department of Pharmacology
University of Colorado Medical Center
Denver, Colorado 80220

The measurements of total body water (TBW), extracellular water (ECW), and intracellular water (ICW) are a useful aid in understanding many physiological processes, both normal and abnormal. The principle of measuring water spaces is quite simple and is based upon the dilution into the space to be measured of an exactly known amount of some "tracer" compound. Then by determining the equilibrium concentration of the tracer, the volume or space into which it has diffused can be calculated. The most ideal tracer for TBW should be water itself and this paper describes a procedure for measuring TBW using $H_2{}^{18}O$. Although deuterium oxide is relatively inexpensive compared to ^{18}O labelled water, it does have several disadvantages as a TBW tracer. First, and most important, it is known that D_2O in large doses can lead to toxic reactions, while there is no known toxicity associated with $H_2{}^{18}O$. Second, there is some evidence[1] which shows that $H_2{}^{18}O$ may more accurately measure TBW than D_2O due to the ability of the deuterium label to be diluted also into a readily exchangeable hydrogen pool consisting of hydroxyl, carboxyl, amino, etc. hydrogens.

This procedure was designed for use in low weight newborn infants and to approximate the clinical situation, baby pigtail macaque monkeys weighing from 1.5 to 3.0 kg were used as the animal model. The monkeys were anesthesized with phenobarbital and the femoral artery and vein were cannulated. Approximately 1.0 to 1.5 gm of $H_2{}^{18}O$ in saline was injected through the venous cannula and 0.3 ml samples of blood were obtained through the arterial cannula at various time points after the injection. Aliquots of the blood sample (50-100 µl) were vacuum distilled and the water collected and sealed in ampoules containing 30 mg of guinidine hydrochloride. The water was converted to CO_2 [2] by heating the sealed ampoule at 200°C and the reaction (I) was complete in 16 hours.

$$2\,H_2O + NH_2\text{-}\overset{NH}{C}\text{-}NH_2 \longrightarrow CO_2 + 3\,NH_3 \qquad \text{I}$$

After the amonnia was removed with a sulfuric acid trap, the ratio of $C^{16}O^{18}O$ to $C^{16}O^{16}O$ (M/e 46 to M/e 44) was determined with a CEC 21-620 cycloidal mass spectrometer with a gold foil molecular leak using the cyclic scanning mode. The volume of distribution of $H_2{}^{18}O$ could be calculated from these blood ratios and ratios determined from standard dilutions of $H_2{}^{18}O$ in $H_2{}^{16}O$. A typical distribution curve of $H_2{}^{18}O$ as a funtion of time is shown in the first figure and equilibrium with TBW (found to be 67% of the monkey's total body weight) occurs in approximately 30 minutes.

To verify the accuracy of this method, the TBW of a 3.0 kg monkey was determined simultaneously with $H^{18}O$, tritiated water, and antipyrine (a drug which is easily quantitated by a spectrophotometric method). The results listed in the second figure show that although there may be real differences in the initial (one minute) distribution of these tracers, at equilibrium (ninety minutes) they all approximate the same water space.

We are now preparing to use this $H_2{}^{18}O$ method in newborn infants with idiopathic respiratory distress syndrome (IRDS or hyaline membrane disease) to correlate the degree of this disease state with the infants edematous condition.

REFERENCES

1. Lifson, N., Gordon, G. B., McClintock, R., J. Appl. Physiol., 7, 704, 1955.

2. Boyer, P. D., Graves, D. J., Suelter, C. H., Dempsey, M.E., Anal. Chem., 33, 1906, 1961.

FIGURE 1: Distribution of $H_2{}^{18}O$ in blood

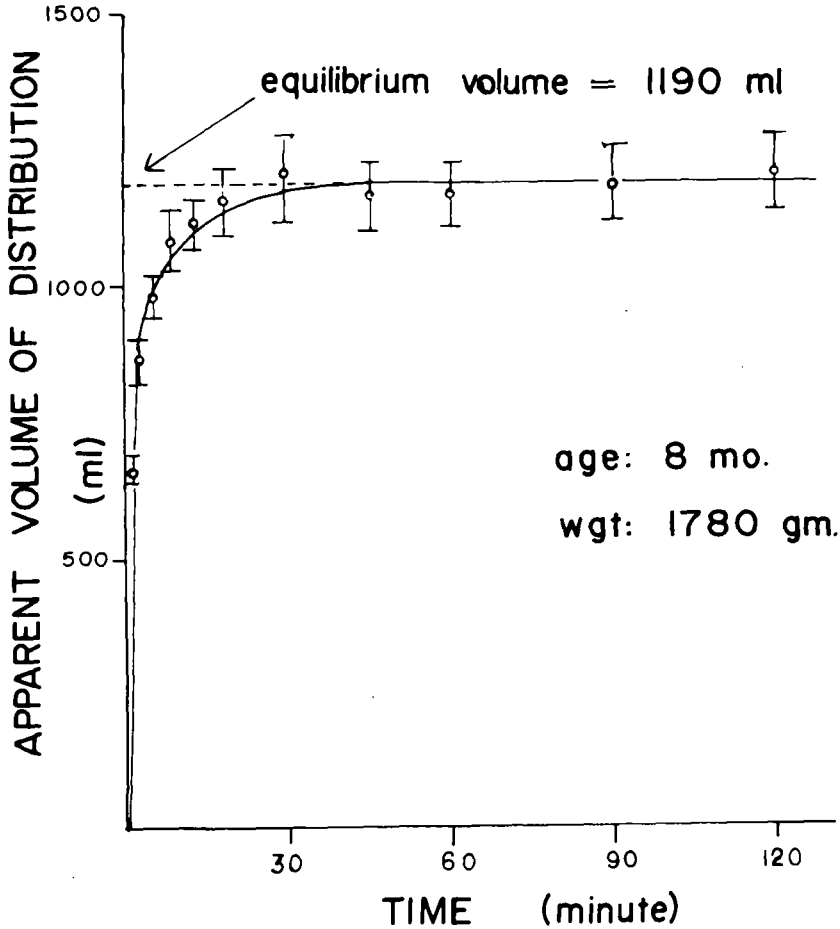

FIGURE 2: COMPARISON OF METHODS

	$H_2{}^{18}O$	^3H_2O	ANTIPYRINE*
1 MINUTE SPACE (ML)	968 + 30	1089 + 30	1384 + 70
90 MINUTE SPACE (ML)	2042 + 70	2085 + 50	2160 + 100
HALF - LIFE (DAY)	3.81 + .08	4.47 + .26	

* 2,3-DIMETHYL-1-PHENYL-3-PYRAZOLIN-5-ONE

A COMPARISON BETWEEN $^{14}CO_2$ AND $^{13}CO_2$ MEASUREMENTS IN THE BREATH OF RATS FED SODIUM ACETATE

Robert S. Ampulski and Robert W. Boggs
The Procter & Gamble Company
Miami Valley Laboratories
Cincinnati, Ohio 45247

ABSTRACT

$^{13}CO_2/^{12}CO_2$ ratios have been determined by monitoring m/e 45 and 44 from the expired breath of animals fed ^{13}C labeled materials. Rats, dosed with $Na^{13}CO_2CH_3$, were placed in a glass cage. A constant air flow through the cage was continuously monitored on a high resolution SM-1 mass spectrometer operating in the peak matching mode. The ion intensity of m/e 44 and 45 were alternately recorded. The appearance and decay of excess $^{13}CO_2$ could be observed and interpreted in terms of the metabolism of sodium acetate. Details of experimental design along with examples and limitations are discussed. The mass spectral method was compared to the classical radiochemical method of measuring $^{14}CO_2$ and found to be in excellent agreement.

INTRODUCTION

Presented here is an alternative method to the use of radioactive ^{14}C in metabolism studies of organic compounds to CO_2. This is a mass spectrometric method which allows for both the integral and total quantitation of $^{12}CO_2$ and $^{13}CO_2$. The mass spectral method was compared to the classical method of $^{14}CO_2$ analysis. Rats were dosed with a solution containing both sodium (1-^{13}C)-acetate and sodium (1-^{14}C)-acetate and placed in a respiration cage. The respired rat breath was then analyzed for $^{12}CO_2$ and $^{13}CO_2$ via mass spectrometry and $^{14}CO_2$ via radiochemistry.

EXPERIMENTAL

The experimental system shown in Fig. 1 consisted of a tank of compressed breathing air (a), flow meters (b), a small gas respiratory chamber with a single inlet and an outlet (c), a gas chromatographic splitter valve inlet system to the mass spectrometer (d), an SM-1B mass spectrometer, an automatic attenuating strip chart recorder (e), fritted glass scrubbing towers containing 6% sodium hydroxide solution (f), metering valves, and interconnecting tubing.

The mass spectrometer was operated in the peak switching mode with a dwell time of 15 sec each on m/e 44 and 45. The cycle time was 30 seconds. The peak intensities were recorded on an automatically attenuated strip chart recorder controlled by the peak switching circuit. Flat topped mass peaks with a resolution of $M/\Delta M = 2000$ were obtained by narrowing the entrance slit and opening the collector slit. The mercury diffusion pump traps were cooled with dry ice methanol to prevent CO_2 condensation inside the trap. The normal source operating pressure was 2×10^{-5} torr. The analyzer was maintained at 1×10^{-6} torr. The air flow rate through the respiration cage was arbitrarily maintained at 200 ml/min. A small fraction of the cage air effluent was admitted to the mass spectrometer through a gas chromatograph splitter valve on a line-of-sight inlet probe. The remaining air was bubbled through 6% sodium hydroxide solution for collection of $^{14}CO_2$.

The excess $^{13}CO_2$ was calculated from the measurement of the respiratory CO_2 before dosing and at time intervals after dosing. Total CO_2 was determined by comparison with a standard 2% CO_2 in air (Matheson primary standard).

During each time interval the $^{14}CO_2$ was determined in the 6% NaOH trapping solutions by diluting the samples to 250 ml with 6% NaOH, taking a 1 ml aliquot to which a scintillation cocktail was added, and counting on a Packard scintillation counter. Results were reported as % recovery.

RESULTS AND DISCUSSION

The integral and total recoveries of $^{13}CO_2$ as a function of time are shown in Fig. 2. A comparison of the 180 min and 300 min recoveries for the radiochemical and mass spectrometric methods are shown in Table 1.

Table 1. CO_2 Recovery

	% Recovered ± S.D.	
Time After Dosing	$^{13}CO_2$	$^{14}CO_2$
180 min (n = 10)	73 ± 9	73 ± 12
300 min (n = 5)	81 ± 3	79 ± 5

As can be seen the total recoveries agree remarkably well. A comparison of the differential $^{13}CO_2$ and $^{14}CO_2$ methods is shown in Fig. 3. The integral $^{13}CO_2$ and $^{14}CO_2$ recoveries are shown in Fig. 4. It can be seen that both methods are comparable. A linear regression analysis of $^{13}CO_2$ on $^{14}CO_2$ is depicted in Fig. 5. The slope of the line is very nearly 1 and the intercept is .008 (zero within experimental error).

The present limitations of the experimental method described are shown in Table 2.

Table 2. Limitations

Ratio precision	± 1%
Time resolution	30 sec
Sample size (rat)	13 mg/kg
Sodium (1-^{13}C)-acetate 90 atom % ^{13}C	1.4×10^{-4} mol/kg

SUMMARY AND CONCLUSIONS

The method presented here is a continuous, real time, concise, and reproducible method for measuring respired CO_2. It is both a differential and an integral method from which total recoveries and kinetics can be obtained. The results of the method are comparable to the traditional radiochemical method of $^{14}CO_2$ analysis. Time resolution could probably be increased by the use of a mass spectrometer with a double collector. The ratio precision and thus the lower limit of amounts fed could probably also be improved by the use of double Faraday cup collectors. Despite these present limitations, meaningful results can be obtained on physiological sized samples

ACKNOWLEDGMENTS

The authors express their appreciation to Fred Schroeder, Frank Duke, Tom Davis, Gail Engerholm and Bob Bruce for their technical assistance.

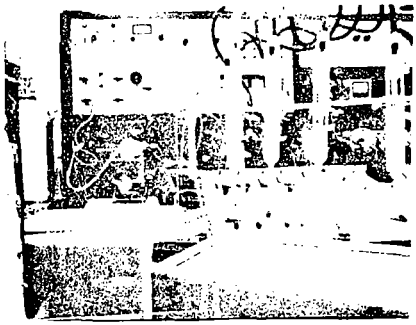

Fig. 1

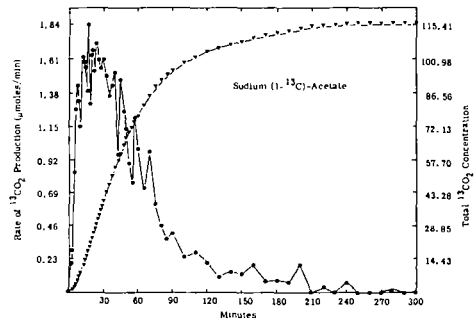

Fig. 2

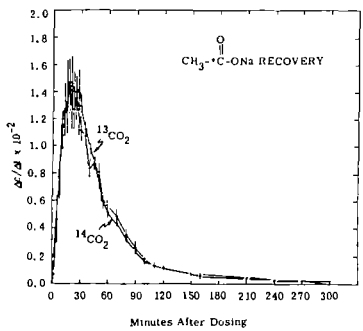

Fig. 3

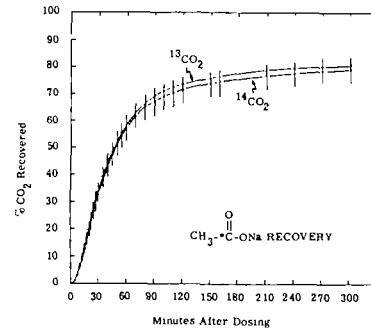

Fig. 4

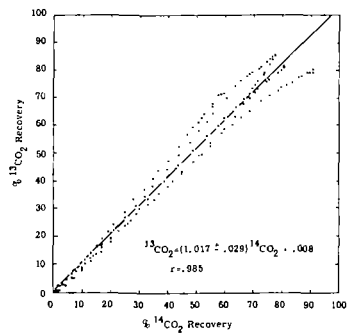

Fig. 5

IN VIVO MEASUREMENT OF GLUCOSE METABOLISM IN CHILDREN WITH STABLE ISOTOPICALLY LABELLED METABOLITES

D. M. Bier, K. J. Arnold, M. Haymond
L. D. Gruenke, and D. M. Kipnis. Depts.
of Pediatrics and Medicine, University of
California, San Francisco and Washington
University School of Medicine, St. Louis;
and Dept. of Pharmaceutical Chemistry,
University of California, San Francisco.

Continuous four hour intravenous infusions of glucose-6,6-d_2 and alanine-2,3,3,3-d_4 (metabolically non-recycling labels) given at a rate approximately 1% of the estimated flux of each has permitted the simultaneous determination of hepatic "new" glucose production and estimation of venous blood alanine (the principal gluconeogenic amino acid) turnover in 21 children with various hypoglycemic conditions.

50 - 500 μl blood samples were drawn at appropriate intervals during the isotope infusion. Proteins were precipitated with 3M perchloric acid. The supernatant was neutralized with 20% KOH, the resultant potassium perchlorate precipitate removed by centrifugation, and the supernatant re-acidified with HCl to pH 2. The acidified sample was subsequently passed over two disposable columns in tandem: Dowex-1-Formate and Dowex-50-H^+, each resin bed approximately 0.5 x 1.0 cm depending on sample size. The glucose containing fraction passes through both columns, is collected, dried under N_2, and converted to the 6-O-acetyl-1,2:3,5-di-O-(n-butane-boronyl)-α-D-glucofuranose by addition of pyridine and butane boronic acid in molar excess, sonication, and subsequent addition of a molar excess of acetic anhydride. The alanine fraction is eluted from the Dowex-50 column with 2M NH_4OH, dried under N_2, and converted to the TMS derivative with molar excess addition of acetonitrile: BSTFA::1:1 followed by sonication and room temperature reaction for 12 - 16 hours.

Isotopic enrichment was subsequently determined by GC-MS with specific ion recording on one of two systems: a computer-controlled LKB-9000 or an AEI MS12 with a voltage sweeping circuit. Virtually identical isotopic enrichments were found in blood samples measured on both systems.

The glucose and alanine flux rates determined in the children studied are shown in the following table. Since the three normal children were larger and older than the hypoglycemic children, direct comparisons in turnover data between these groups is not yet possible. Individual

GLUCOSE AND ALANINE TURNOVER RATES IN CHILDREN DETERMINED WITH STABLE ISOTOPICALLY LABELLED METABOLITES

Condition	Glucose Turnover (mg/kg·min)	Alanine Turnover (μmoles/kg·min)
Normal Children (3)	5.2, 7.6, 3.5	9.2, 16.8, 12.7
Ketotic Hypoglycemia (6)	6.7 ± 0.5	8.9 ± 1.1
Cyanotic Heart Disease (7)	7.1 ± 0.8	8.0 ± 0.8
Galactosemia (1)	6.6	8.8
Leucine Sensitivity (1)	10.6	9.2
Glucose-6-Phosphatase Def. (1)	-	3.6
Unclassified Conditions (2)	10.4, 7.3	14.5, 9.0

values or mean ± SE are presented (where applicable). The numbers in parenthesis represent the number of patients investigated with each condition. These data represent the first in vivo determinations of postabsorptive hepatic "new" glucose production and venous alanine flux in the pediatric age group.

GC/MS Analysis of Polypeptides and Proteins Containing Arginine, Lysine and Proline Using Dipeptidylaminopeptidase Mixtures

William E. Seifert* and Richard M. Caprioli*
Department of Chemistry, Purdue University
West Lafayette, Indiana 47907

In the work described in this paper, a method was devised for the routine analysis of polypeptides and proteins involving the combination of enzymatic and gas chromatographic/mass spectrometric techniques. Two enzymes, dipeptidylaminopeptidases I and IV, were used separately and as a mixture to hydrolyze polypeptides and proteins to dipeptides. The dipeptides were then analyzed by gas chromatography/mass spectrometry.

Dipeptidylaminopeptidases hydrolyze peptides by releasing dipeptides from the N-terminal end of the substrate. Dipeptidylaminopeptidase I (DAP I) has the widest range of specificity, generally hydrolyzing all bonds except those involving a proline residue or in which the N-terminal amino acid is arginine or lysine. Dipeptidylaminopeptidase IV (DAP IV) preferentially releases dipeptides from substrate peptides having a penultimate proline residue. Experiments were performed to demonstrate that DAP I and DAP IV could be used as an enzymatic mixture to circumvent some of the specificity limitations of using DAP I alone to hydrolyze peptides. The enzymes were found to be compatible with each other when used as a mixture. Experiments with S-carboxymethylated soybean trypsin inhibitor (Kunitz) and ribonulease S-peptide demonstrated that the DAP I/DAP IV mixture was able to hydrolyze polypeptides having penultimate proline residues as well as N-terminal arginine or lysine residues. Polypeptides the size of proteins were degraded to dipeptides with the DAP I/IV mixture.

A nearest-neighbor analysis approach was devised to obtain primary structure information from polypeptides without obtaining overlap information. Identification of the sequence of the amino acid residues in a dipeptide identifies one of the nearest-neighbors for each amino acid. Using the information obtained from a nearest-neighbor analysis of the DAP I hydrolysate of BSA**, the action of plasma protease on bovine serum albumin to give the fragment BSA** was elucidated. A nearest-neighbor approach was also used to align the first 44 residues of spinach plastocyanin using homology considerations.

The results obtained in this study indicate that the DAP-GC/MS method of analysis provides the protein chemist with a technique by which a wide range of problems dealing with the primary structure of polypeptides and proteins may be solved. The technique requires only 10-25 nanomoles of sample, considerably less than that required by the automatic sequenator, with the possibility of being used on picomolar amounts of sample. In addition to the determination of amino acid sequences by the dipeptide overlap method, the DAP-GC/MS technique can be used in a nearest-neighbor approach to complement classical methods of sequence determination, as a method for easily verifying published sequences, as well as a method for obtaining primary structure information such as the location of modified residues.

Part of this work has been published in Biochem. Biophys. Res. Comm., 64, 295-303 (1975).

* Present address: Department of Biochemistry, University of Texas Medical School at Houston, Houston, Texas 77025

DETECTION OF ASPARAGINE AND GLUTAMINE IN PEPTIDES SEQUENCED BY DIPEPTIDYLAMINOPEPTIDASE I VIA GAS CHROMATOGRAPHY-MASS SPECTROMETRY.

M. A. Yound and D. M. Desiderio, Institute for Lipid Research and Department of Biochemistry, Baylor College of Medicine, Houston, Texas 77025.

One of the newest methods for obtaining the amino acid sequence of an oligopeptide by means of mass spectrometry is the use of an enzyme which sequentially cleaves dipeptides from the oligopeptide (1,2). The resulting mixture of dipeptides is derivatized and subjected to GC-MS for separation and sequencing. A second portion of the original peptide is subjected to one step of the Edman degradation procedure and the resultant shortened peptide is subjected to the same procedure as above and the two sequences are overlapped. In the ideal case, the sequence of the original peptide is obtained.

One difficulty with this procedure is the derivatization procedures employed up to now have resulted in hydrolysis of asparagine and glutamine side chains of the original peptide with loss of some structural information A simple straightforward method for differentiating asparaginyl/glutaminyl dipeptides from aspartyl/glutamyl dipeptides is presented (3). Very simply, the technique involves two separate methods to form methyl esters. The first method employs 0.1 N HCl/methanol at room temperature for four hours to reveal all dipeptides except those containing the nonvolatile (for a GC column) asparagine and glutamine-containing ones. The second procedure employs 0.1 N HCl/methanol at 45°C for sixteen hours. This procedure solvolyses asparagine and glutamine side chains and new pairs of aspartic or glutamic acid-containing dipeptides occur in the GC-MS where none had occurred previously. Therefore, one obtains a means of unequivocally establishing the position of asparagine and glutamine residues in the original peptide.

This approach was proven feasible with a synthetic pentadecapeptide which contains two Asn residues, four Gln residues and one Asp residue out of a total of fifteen amino acids. No difficulties were experienced during the proposed differential esterification method and both the Asn dipeptide an Gln dipeptide were appropriately found.

During the development of this methodology, a new method to analyze asparagine and glutamine amino acid was found (4). TMS-methylthiazolinone derivatives were prepared, hydrolysis of the amide side chains was avoided, and the products were elucidated by GC-MS.

References

(1) P. X. Callahan, J. E. McDonald and S. Ellis, in Methods of Enzymology, C. H. W. Hirs and S. N. Timasheff, Eds., Vol. 25, Academic Press., New York, 1972, p. 282.

(2) R. M. Caprioli, W. E. Seifert and D. E. Sutherland, Biochem. Biophys. Res. Commun., 55, 67 (1973).

(3) M. A. Young and D. M. Desiderio, Anal. Biochem., in press.

(4) M. A. Young and D. M. Desiderio, Anal. Letters, 8, 1 (1975).

IDENTIFICATION OF OLIGOPEPTIDES IN MIXTURES BY MICRODISTILLATION IN A MASS SPECTROMETER

Ronald D. Grigsby and Eric J. Norman
Department of Biochemistry and Biophysics
and
Paul E. Pulley
Data Processing Center
Texas A&M University
College Station, Texas 77843

A number of programming improvements have been made in the analysis of elimination curve data obtained by the microdistillation of mixtures with a probe inlet.[1] Confidence intervals can now be determined for all parameters, and sufficient information can be resolved from the composite spectra to allow identification of di- and tripeptide derivatives by comparison with standard spectra on tape.

A question that arises in any attempt to analyze composite spectra obtained by probe distillation concerns the capability of the technique for distinguishing between peaks originating from components of very similar volatility present in a mixture. To answer this question three binary mixtures of dipeptide derivatives having reversed sequences were run as well as a mixture of five dipeptide derivatives all containing a common amino acid in the N-terminal position.

The binary mixtures contained the N-acetyl-O-n-butyl derivatives of (1) Tyr-Gly and Gly-Tyr; (2) Tyr-Ala and Ala-Tyr; and (3) Tyr-Leu and Leu-Tyr. When the computer was provided with the resolved relative intensities for the components of the mixtures, it correctly identified each compound. Furthermore, the results showed that the derivatives containing tyrosine in the N-terminal position had slightly higher volatilities than those having tyrosine present in the opposite sequence.

The mixture of five dipeptide derivatives contained Tyr-Gly, Tyr-Ala, Tyr-Leu, Tyr-Glu, and Tyr-Trp. Each component was identified correctly even though the derivatives of Tyr-Gly and Tyr-Ala had almost identical volatilities. In fact, Tyr-Ala had a slightly higher volatility than Tyr-Glu as might be expected by replacing the α-hydrogen of glycine with the methyl group of alanine.

As a test of the method with tripeptides, the N-acetyl-O-n-butyl derivatives of Met-Leu-Gly, Leu-Gly-Phe, and Leu-Trp-Leu were run as a mixture. All three were identified from the standard spectra on tape.

A detailed description of the technique and results including its application to more complex mixtures will be submitted for publication in Biomedical Mass Spectrometry.

---

1. R.D. Grigsby, C.O. Hansen, D.G. Mannering, W.G. Fox, and R.H. Cole, Anal. Chem., 43, 1135 (1971)

MASS SPECTROMETRY OF SOME BORANE-REDUCED DIPEPTIDES AND THE PERMETHYLATION PRODUCTS

Richard M. Thompson, Frederick L. Weitl, and Roger W. Roeske

Department of Pediatrics and Biochemistry
Indiana University School of Medicine
Indianapolis, Indiana 46202

A small group of CBZ- and t-BOC-protected dipeptide esters were reduced with borane in THF between -20° and 0°C. The products of principal interest from these reductions, obtained in 30-70% isolated yields, had the following general structure:

$$R\text{-}O\text{-}CO\text{-}NH\text{-}CH(R')\text{-}CH_2\text{-}\overset{+}{N}H_2\text{-}CH(R'')\text{-}COOR'''\ Cl^-$$

These protected diamino-acids can be inserted into synthetic peptides with the amine function providing a site of attachment for an affinity label.

The mass spectra of these reduced compounds (LKB-9000-S, direct probe analysis of the HCl salts) showed the following general fragmentation when R' and R'' = H or i-C_4H_9 and R'' = H or CH_3:

$$\underset{a}{R\}}\underset{b}{O\}}\overset{c}{\{CO}\text{-}NH\text{-}CH(R')\overset{d}{\}\{CH_2}\text{-}NH\text{-}CH(R'')\underset{e}{\}\{COOR'''}$$

Ion d, which arises by C-C cleavage, is the most interesting ion because of the previous observation by Biemann and co-workers [J. Am. Chem. Soc., 81, 2274 (1959)] that the ion formed by C-C cleavage in the spectra of polyamino alcohols obtained by exhaustive LAH reduction was the amine-fragment. The corresponding amine fragments were not observed in our mass spectra. The C-terminal amino acid can be characterized from the mass of d when R''' is known.

Another significant ion, f, (R.I. = 60 to 100%) may arise from the loss of b+H from e and may be represented as follows:

$$O{=}C{=}N\text{-}CH(R')\text{-}CH_2\text{-}\overset{+}{N}H{=}CH(R'')$$

Together, ions d and f can be used to identify the nature of R' and R'', the amino acid side chains.

Two principal volatile products resulted from the permethylation of these compounds:

$$R\text{-}O\text{-}CO\text{-}\underset{\underset{CH_3}{|}}{N}\text{-}CH(R')\text{-}CH_2\text{-}\underset{\underset{CH_3}{|}}{N}\text{-}CH(R'')\text{-}COOCH_3$$

I

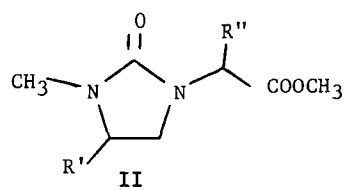

II

I and II were separated and analyzed by GC-MS(SE-30 columns). The spectra of I contain ions due to cleavage along the backbone similar to the parent compounds including the C-terminal fragment due to C-C cleavage. The principal fragmentation of II is loss of the carboxymethyl group (59 amu) forming the following stable ion which was the base peak in all cases:

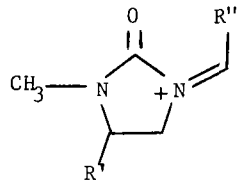

II was characterized as a cyclic urea from the various molecular ions, the mass spectral fragmentations, the methylation patterns (determined with CD_3I), accurate mass measurements, and the observation that the same product formed regardless of the protecting group. In contrast, no hydantoins were formed by the permethylation of unreduced protected dipeptide esters.

Supported in part by the James Whitcomb Riley Memorial Association and the Grace M. Showalter Residuary Trust.

CHEMICAL IONIZATION MASS SPECTRA OF DERIVATIZED PEPTIDES

M. Mudgett, D.V. Bowen and F.H. Field

The Rockefeller University

New York, New York 10021

ABSTRACT

The first CI spectra of derivatized peptides were reported in 1970 (1). The methane spectra of permethylated acetylated peptides were found to give sequence ions of high intensity characterizing both the N-terminal and C-terminal sequences. Other investigators (2,3) have confirmed the intensity of high mass sequence ions in CI spectra and the general utility of CI spectra for the sequencing of peptides.

In view of these results and of the utility of isobutane CI-MS in other sequencing work, we investigated the isobutane chemical ionization spectra of 40 di-, tri-, tetra-, and pentapeptides as their permethylated N-acetyl derivatives. All peptides were purchased from commercial sources and an attempt was made to include at least one example of every amino acid at the N-terminal and C-terminal positions.

The acetylation and permethylation procedures were essentially those developed by Lederer (4). Peptides containing arginine were first treated with hydrazine to convert arginine to ornithine. Peptides containing methionine were acetylated and permethylated without prior treatment of the sulfhydryl group. Most of the spectra reported were obtained from 10-100 nmole aliquots of derivatives prepared from 1-10 μmoles of peptide. Satisfactory results have been obtained with 1-5 nmole aliquots of derivatized peptides prepared from 10 nmoles of peptide.

In a typical isobutane CI-MS spectrum, both N-terminal and C-terminal sequence ions are observed. The average relative intensity of each sequence ion has been determined. An estimate of the probability of each type of sequence ion has also been made. The most intense and most common

N-terminal sequence ion is the N-acylium ion. The C-ammonium ion occurs as frequently but tends to have a somewhat lower relative intensity.

Ten glycine-containing peptides showed varying degrees of C-methylation. This produces sequence ions typical of alanine and is a potentially serious source of artifacts. (5)

The EI, methane-CI and isobutane-CI spectra of several peptides have been compared. All spectra were obtained with a DuPont 21-492 mass spectrometer interfaced to a VG-2040 data system. The results confirmed the advantages of CI-MS over EI-MS for sequencing permethylated acetylated peptides.

REFERENCES

1. Gray, W.R., Wojcik, L.H. and Futrell, J.H., BBRC, 41, 1111-1119 (1970).
2. Kiryushkin, A.A., Fales, H.M., Axenrod, T., Gilbert, E.J. and Milne, G.W.A., Organic Mass Spectrometry, 5, 19-31 (1971).
3. Schier, G.M., Halpern, B. and Milne, G.W.A., Biomedical Mass Spec., 1, 212-218 (1974).
4. Thomas, D.W., F.E.B.S. Letters, 5, 53-56 (1969).
5. Mudgett, M., Bowen, D.V., and Kindt, T.J., Biomedical Mass Spectrometry. In press.

EXPERIMENTAL RESULTS AND AN ATTEMPT AT AN INTERPRETATION FOR SECONDARY ION EMISSION FROM TARGETS BOMBARDED BY A Cs^+ ION BEAM

Pierre VALLERAND and Marcel BARIL

Department of Physics, University of Laval
Quebec, Que., Canada, G1K 7P4

Several authors have observed that the emissivity of different elements shows a proportionality with the logarithm of the difference between the work function (ϕ) and the ionisation potential (I) or the electron affinity (A) depending on whether it concerns positive or negative emission respectively. One[1] author supposes the existence of a plasma in the impact zone of the primary beam. This observation may imply the existence of a thermodynamic equilibrium between the various species of the pulverisation product. The knowledge of the concentrations of the low elements in the matrix permits the adjustment of two parameters, one being the electronic density and the other the plasma temperature. Dissociation formulae[3] have been applied by Andersen to determine the concentrations of all other elements.

According to these authors, the proportionality of the logarithm of the secondary ions current with the ionisation potential or electron affinity may justify the description of the emission of secondary ions by a thermal model. Zurela[2] supposes a localised elevation of temperature in the immediate region where the secondary ion leaves the target. In modifying Dobretsov's equation is the case of the emission of a fast particle (non thermodynamic equilibrium). Zurela obtains temperatures between 2000 and 8000°K for the pulverisation centres. On the opposite, Andersen supposes the existence of a macroscopic temperature: Saha-Eggert's equations describes the thermodynamic equilibrium between the plasma's various components. The temperatures obtained are of the order of 11,000°K. It should be noted that Zurela and Andersen obtain high temperatures for elements having a good affinity for oxygen.

We present in Fig. 2 the emissivity, for negative ions, of a few constituents of an Bronze phosphorus alloy. These measurements have been done with an achromatic mass spectrometer[4] described in Fig. 1. The energy of the Cs^+ ion was 5 KeV at a current density of 100 μsm/cm^2 the vacuum being around 1X 10^{-7} torr. In the case of the emission of negative ions, Saha-Eggert's equation is written:

$$\log (N_{M^-}/N_{M^o}) = 15.38 + \log (g_{\mu^-}/g_{M^o}) - 1.5 \log T + 5040\, E_a/T + \log ne^- \qquad (1)$$

where the terms used are identical to those used in reference (1). The left part of Equ. 1 is estimated through the simple following expression[5]:

$$N_{M^-}/N_{M^o} = \frac{i_s^{M^-}}{i_p \times S^M \times \alpha^M \times C^M} \qquad (2)$$

(where $i_s^{M^-}$ and i_p are the secondary and primary ion current respectively; S^M, the atomic sputtering yield; α^M, the transmission of spectrometer; C^M, the concentration of species) which permits us to write Saha-Eggert equation under the form:

$$\log (i_s^M/C^M) = K + \frac{5040}{T} E_a \qquad (3)$$

K being a constant. According to this equation, the curve of the graph on Fig. 2 suggests the existence of a temperature around 3100°K.

Note that Zurela obtains a similar result for a pure copper target when he supposes a non equilibrium state. The same author, from Hennequin and Slodzian's results, calculates the mean temperature of emission centres, according to his model; the result being that, in spite of a factor 5 difference in the energy of the primary ions (Hennequin Ar^+: 8 KeV), Zurela Ar^+: 40 KeV), there are but few temperature variations with the energy of the primary ions. According to the measurements made by Vallerand and Baril, a variation, however limited, of the energy of the primary Cs ions, between 2 and 6 KeV, does not bring a detectable variation of the temperature. According to their results, the preceding authors are of the opinion that the correction of the secondary ion current observed must take into account the proportion between the different masses involved in the secondary ionic emission phenomena. For example: the momentum transfer between a primary ion and an atom from the target will be different according to the proportion of the masses involved. It therefore becomes necessary to take into account the multiple values possible for the primary ion's mass, for the ejected particle's mass and for the target's apparent mass. A study of these phenomena is presently being conducted.

---

1. Andersen; G.A., Heinthorne; T.R., Analytical Chemestry, Vol. 45, p. 1421 (1973).

2. Zurela; Z., Int. J. Mass Spectr. Ion Phys., Vol. 12, p. 33 (1973).

3. Boumans; P.W.J.M., "Theory of Spectrochemical Excitation", Hilger and Watts Ltd, London.

4. Vallerand; P., Baril; M., Canadian Journal of Physics, Vol. 52, p. 482 (1974).

5. Werner; H.W., Vacuum, Vol. 22, p. 613 (1972).

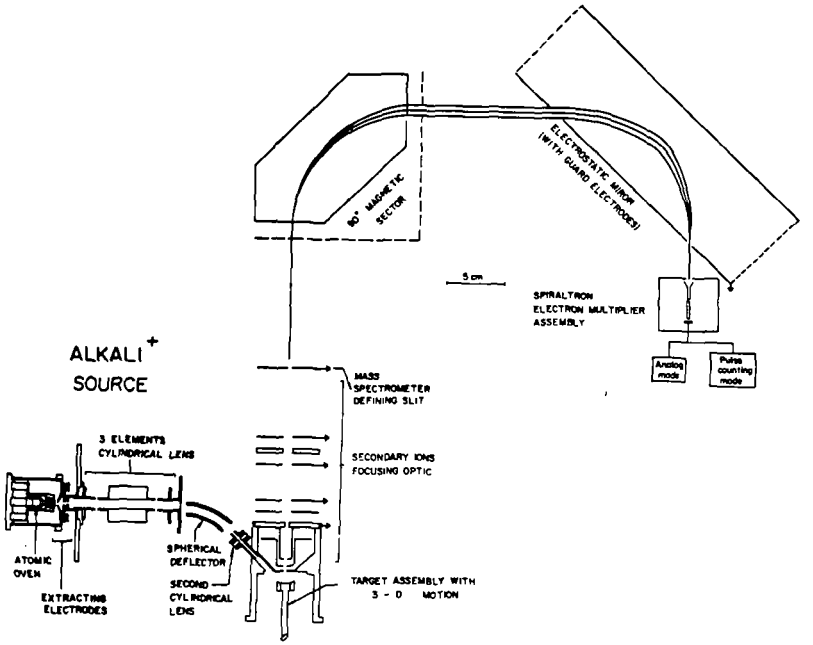
90° MAGNETIC SECTOR
ELECTROSTATIC MIRROR (WITH GUARD ELECTRODES)
5 cm
SPIRALTRON ELECTRON MULTIPLIER ASSEMBLY
Analog mode
Pulse counting mode
ALKALI+ SOURCE
MASS SPECTROMETER DEFINING SLIT
3 ELEMENTS CYLINDRICAL LENS
SECONDARY IONS FOCUSING OPTIC
SPHERICAL DEFLECTOR
ATOMIC OVEN
EXTRACTING ELECTRODES
SECOND CYLINDRICAL LENS
TARGET ASSEMBLY WITH 3 - D MOTION

Fig. 1

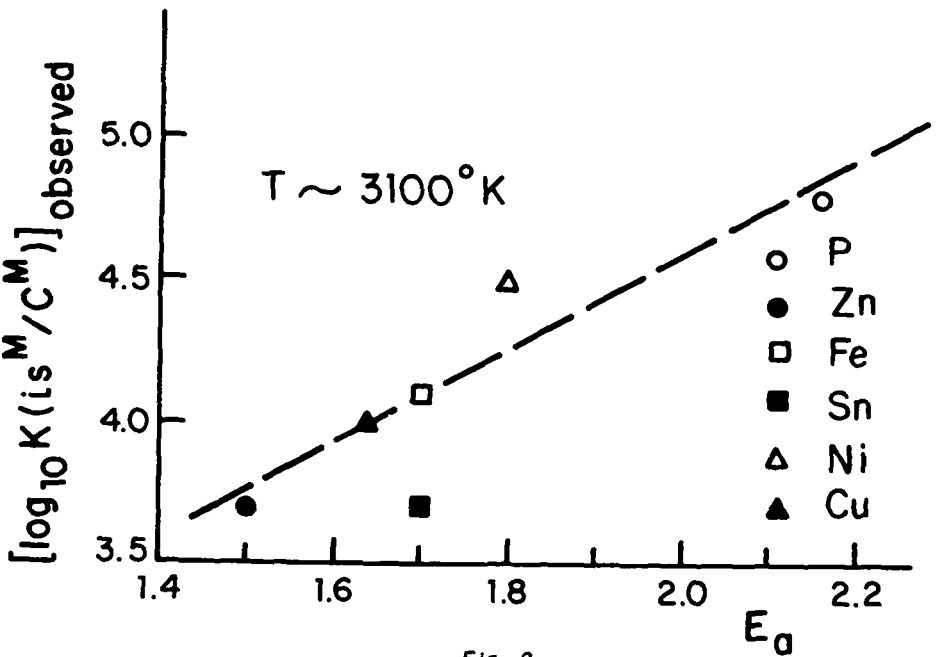
$[\log_{10} K(is^M/C^M)]_{observed}$
5.0
4.5
4.0
3.5
T ~ 3100°K
P
Zn
Fe
Sn
Ni
Cu
1.4
1.6
1.8
2.0
2.2
E_a

Fig. 2

LOW ENERGY ION SCATTERING SPECTROMETRY (ISS) OF THE SiO_2/Si INTERFACE

William L. Harrington, R.E. Honig, R. Williams and A.M. Goodman
RCA Laboratories
Princeton, New Jersey 08540

The Si-SiO_2 system is a vital part of present semiconductor device technology. The thin region making up the SiO_2/Si interface is the dominant factor in many aspects of MOS behavior--surface states, surface charge, radiation damage, dielectric breakdown, etc.--and for this reason has received a great deal of attention by analytical techniques. High energy backscattering, in particular the work of Sigmon, Chu, Lugijjo, and Mayer [1], has reported a rapidly decreasing O/Si ratio as one measures thinner and thinner oxide films. This work is interpreted as showing excess Si near the interface which has been pulled out of the oxide during the initial stages of oxide growth. However, the limit of depth resolution by this technique is on the order of 200 Å, so that only integrated values over such thicknesses can be obtained. From these data, one can only infer the Si-rich interface.

Low energy ISS, on the other hand, has the unique advantage that rare gas ions scattered from a surface as ions in a single, atomic collision can be restricted almost entirely to the outermost atomic layer. Thus, this technique has been used to measure SiO_2 stoichiometry and to examine the SiO_2/Si interface in greater detail than previously reported.

Assuming that excess Si does exist at the interface, it is inconceivable that these substrate atoms could move large distances into an oxide. For this reason, a thermal oxide of about 1000 Å, as shown in Figure 1, was chosen as a standard for SiO_2. In this and all subsequent ISS depth profiles, the scattering response for O was multiplied by 1.72

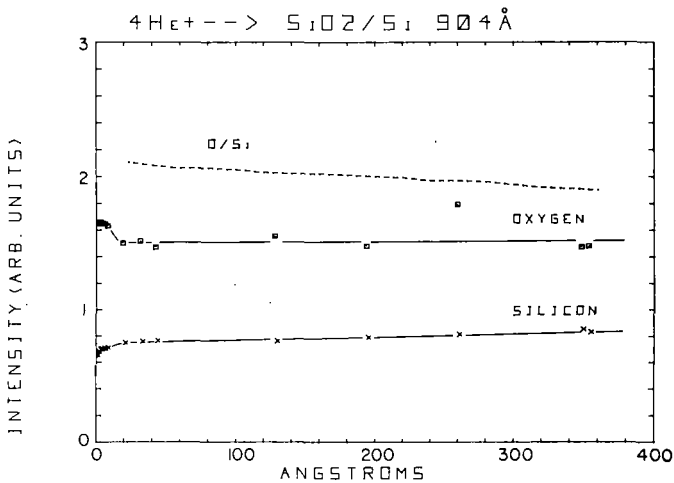

Figure 1. ISS responses from a 904 Å oxide layer on Si used as a standard for SiO_2.

as an empirical, relative scattering cross section correction, which for the 904 Å oxide standard produces an O/Si ratio of 2.0. The oxide thicknesses quoted are those measured by ellipsometry before ISS profiling. Starting with this 904 Å oxide and etching down to thinner layers, it was shown that the O/Si ratio remained 2.0 at the surface of oxides down to a thickness of 44 Å.

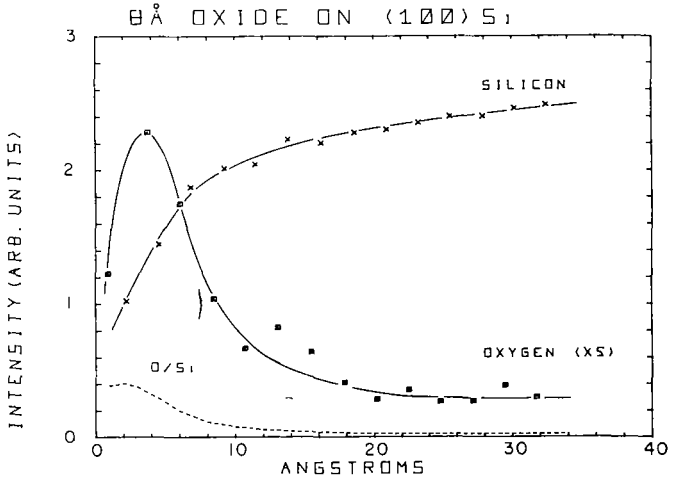

Figure 2. ISS depth profile of residual 8 Å oxide on (100) Si

Because it is difficult to controllably etch films much thinner than this, wafers of both (100) and (111) Si were etched to bare Si, and then 600°C oxides of known thicknesses were grown and profiled. For an 8 Å oxide on both (100) and (111) Si (Figure 2), the O/Si ratio is only 0.4 at the maximum O response. Growth from 8 to only 15-16 Å, as shown for (111) Si in Figure 3, produces an oxide which on the outer surface has an O/Si ratio of 2.0. This observation establishes a region

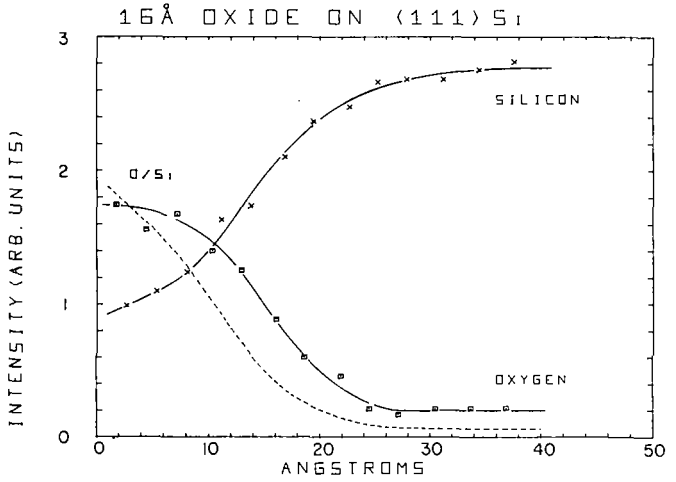

Figure 3. ISS depth profile of 16 Å oxide grown at 600°C on (111) Si

of 10-15 Å of initial oxide growth that could contain excess Si, thus reducing the O/Si ratio. At thicknesses sufficient to establish enough signal statistics, as shown in Figure 4 for a 96 Å oxide, one can clearly detect a step in the Si signal before the O begins to fall.

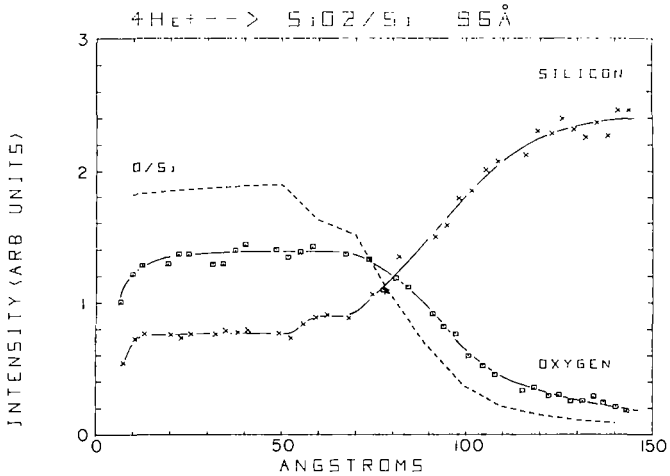

Figure 4. ISS depth profile of SiO_2/Si etched down to 96 Å. The step in the Si response corresponds to 1.5×10^{14} at/cm^2 excess Si per monolayer extending 3-4 molecular layers into the oxide.

This plateau indicates excess Si at the interface, again corresponding to a region of 10-15 Å in thickness. Using the Si atom density of 7.9×10^{14} at/cm^2 in the thermal SiO_2 region as a point of calibration, one can calculate rather directly that the Si-rich plateau corresponds to a Si density of 9.4×10^{14} at/cm^2. Therefore, there is an excess Si density of 1.5×10^{14} at/cm^2 per monolayer (about 20%) which extends out into the oxide 10-15 Å or about 3-4 molecular layers.

(1) T.W. Sigmon, W.K. Chu, E. Lugujjo, and J.W. Mayer, Appl. Phys. Lett., Vol. 24, No. 3, 105-107 (1974).

Boron Implanted Silicon- A Comparison of SIMS Total Concentration Profiles with Electrical Measurements

by

C.W. Magee, W.L. Harrington, R.E. Honig and C.P. Wu
RCA Laboratories, Princeton, N.J. 08540

Secondary Ion Mass Spectrometry (SIMS) is ideally suited for the determination of ion-implanted dopant profiles due to its high (sub parts-per-million) sensitivity and good depth resolution. There is, however, a subtle problem associated with the use of this technique to determine ion implanted dopant distributions in semiconductors, and that is the inability of SIMS to differentiate between substitutional and interstitial dopant atoms. It is most important to be aware of this limitation because only those dopant atoms which are in substitutional positions in the lattice have any effect on the electrical characteristics of the material. Therefore, it is the depth profile of only the substitutional, or "electrically active" dopant atoms which is of use to the solid state device engineer.

Annealing an implant distribution is thought to leave approximately 99% of the dopant atoms in substitutional positions in the lattice and thus electrically active. Our previous studies of ion implanted boron in silicon seemed to indicate that this percentage of active dopant atoms might be considerably lower in the tails of the profiles where most electrical junctions occur. This study was undertaken to gather more information on that question.

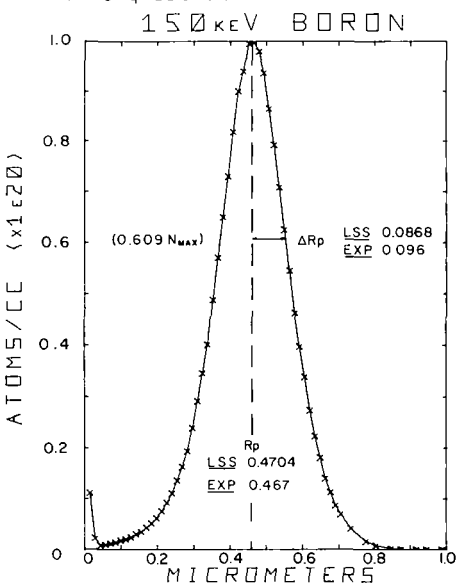

Figure 1

Figure 1 shows the SIMS profile for a 150keV boron implant into silicon which we used as a sensitivity calibration for all subsequent profiles. We used the area under the curve to compare with the Ndose (in atoms/cm^2) as measured on the implant machine for the calibration reference. The Rp (range) and ΔRp (straggle) agree well with the values predicted by LSS theory.

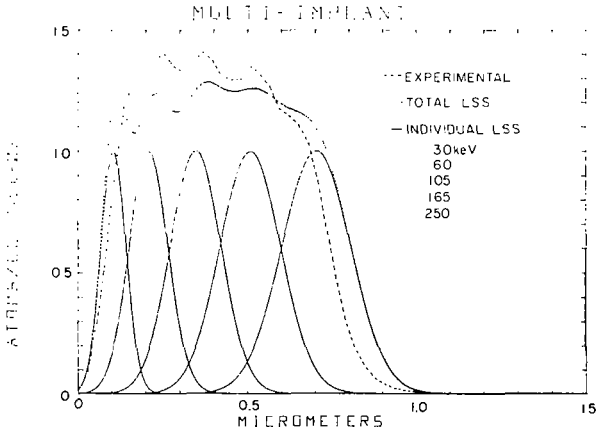

Figure 2

Figure 2 shows the implant distributions in the sample on which the comparisons between SIMS and electrical measurements were made. It is a multi-implant of boron in silicon made at 30, 60, 105, 165, and 250keV. Note how the experimental SIMS profile shows the humps in the distribution as predicted by the LSS composite of the five implants. (We do not see the predicted hump from the 30keV implant because it was put in first and subsequently washed out by the other implants penetrating through it).

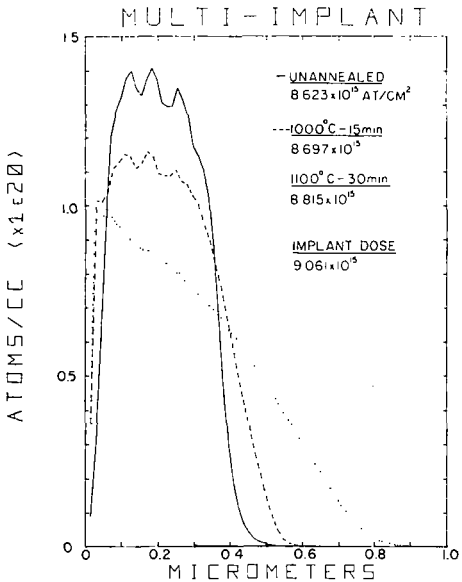

Figure 3

Figure 3 shows the effect of annealing on the distribution. The three profiles were not normalized to each other in concentration, only to the single implant shown in Figure 1. The doses, however, all agree well with the sum of the measured doses for the five implants.

In order to compare our profiles of total boron to profiles of electrically active boron, we had to get some kind of electrical data on the boron distributions. Accurate spreading resistance measurements on

such shallow distributions are practically impossible to obtain so we used angle lapping and staining to determine the electrical junction depth. This is the depth at which the concentration of electrically active P-type boron atoms equals the level of intrensic N-type dopant atoms in the silicon ($1x10^{16}$ atoms/cm^3). Figures 4 and 5 show the results for two annealing conditions.

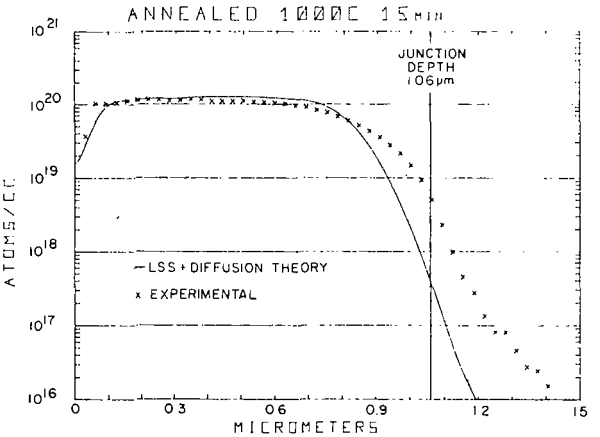

Figure 4

Angle lapping and staining of the sample annealed at 1000°C for 15 minutes revealed a junction at 1.06 micrometers which means that at that depth, the substitutional boron concentration had dropped to $1x10^{16}$ atoms/cm^3 . But at 1.06 micrometers, the SIMS measurements indicated a total boron concentration of $5x10^{18}$ atoms/cm^3 resulting in an electrically active fraction of about 0.2%. Note that this depth of 1.06 micrometers is even shallower than the depth at which the unannealed profile reaches $1x10^{16}$ atoms/cm^3. Similarly, the 1100°C-30 minute sample in Figure 5 showed about 1% of the boron electrically active at the junction.

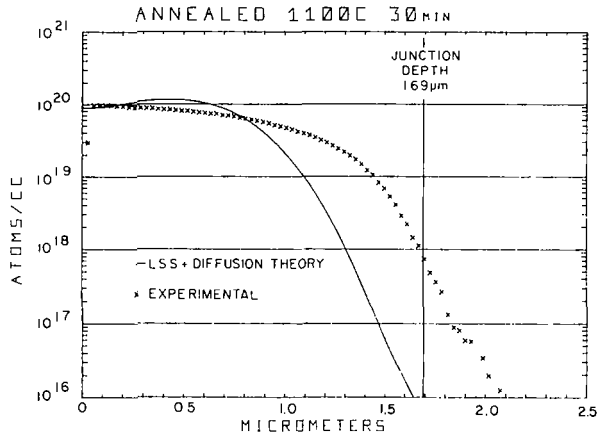

Figure 5

This low degree of electrical activity in the tails of the implants seems reasonable in light of the fact that at those depths, the lattice crystallinity has been undisturbed by implantation. This results in a very low concentration of vacant substitutional sites into which the implanted boron atoms may move during the annealing stage.

TEST OF A QUANTITATIVE CORRECTION PROCEDURE FOR SIMS ANALYSIS

David S. Simons, Judith E. Baker, and Charles A. Evans, Jr.
Materials Research Laboratory
University of Illinois
Urbana, Illinois 61801

Introduction

Several methods have been proposed for the conversion of secondary ion intensities to elemental composition. These include the use of empirical sensitivity factors [1], the quantum mechanical model of adiabatic surface ionization advanced by Schroeer [2], and the local thermal equilibrium (LTE) approach of Andersen and Hinthorne [3,4]. The LTE model has been subjected to the most extensive testing, and it has achieved some success as a semi-quantitative correction procedure, particularly when applied to mineral samples [4]. However, some questions remain about the general applicability of the LTE approach. Since it is available in the form of the CARISMA computer program only to users of one particular ion microprobe, one might wonder whether it would work as well on other types of SIMS devices which have different conditions of ion bombardment, extraction, and energy acceptance. Also, the CARISMA program incorporates thousands of constants into its data base, and the question should be asked whether this amount of complexity is necessary to achieve an acceptable semiquantitative analysis. For these reasons, we have developed a greatly simplified computer program based on the LTE model, which is similar to the approach used by Shimizu and coworkers in Japan [5,6]. The basis of the model is the Saha-Eggert ionization equation, which describes the dissociation equilibrium between neutral atoms and positive ions in a plasma of temperature T and electron density N_e. Once the temperature and electron density are supplied, the ion/neutral ratio of any element can be calculated from the Saha-Eggert equation.

Simplified LTE Model

Compared to the full CARISMA computer program described by Andersen and Hinthorne [4], the simplifications used in the present work are as follows:

1. Corrections for the production of negative ions are not included. Such corrections may prove to be important for the more electro-negative elements such as the halogens.

2. An empirical oxide correction is used for those elements which have oxide ion intensities greater than 20% of the atomic ion intensity. In these cases, the sum of both intensities is used in the subsequent analysis. This procedure replaces the theoretical oxide correction incorporated into the CARISMA program.

3. Partition functions for the positive ions and neutral atoms are represented by fifth order polynomial functions of temperature [7]. Although this form is only stated to be accurate between 1500°K and 7000°K, we assume its validity at all temperatures. The dependence of the partition functions on electron density is ignored.

Results

The simplified LTE correction procedure has been tested using three NBS standard reference metal alloys and two well-characterized insulators.

Data were taken in the ion counting mode on the AEI IM20 ion microprobe. For the metallic samples, a primary beam of positive oxygen ions was used with an impact energy of 15 keV. For the insulators, negative oxygen ions were used with an impact energy of 35 keV. The primary beam diameter was 16-20 micrometers, and the beam was rastered over an area 75 micrometers square or larger, in order to average over sample inhomogeneities. Complete sets of data were taken from three different spots on each sample. Results for each material are summarized below.

SRM 661 LOW ALLOY STEEL: Fe and Ni were used as internal standards. Most of the other elements were corrected such that the calculated concentrations were within a factor of 2 of the bulk values. Mo was a factor of 25 too low. The empirical oxide correction was not used for Mo because of interferences between MoO and Fe and Ni dimers. The full CARISMA computer program consistently underestimates Mo concentrations by more than a factor of 6 [4]. The average error of fit, excluding internal standards, ranged between 68% and 103% for the three spots. The average error of the CARISMA program for a comparable sample, SRM 461, was 76% [4].

SRM 121d STAINLESS STEEL: Fe, Cr, and Ni were used as internal standards. All elements were corrected within a factor of 2 except Mo, which was a factor of 40 too low. Again, no oxide correction was used. The average fitting error was 41%-48%. The error for a comparable sample, SRM 101e, analyzed using CARISMA, was 53% [4].

SRM 162a MONEL: Ni and Cu were used as internal standards. The fit in this case was not considered satisfactory. The simple LTE program assigned the Cu internal standard a value 30%-45% too low, and the resulting average error for the trace elements was between 118% and 154% for the three spots. The CARISMA analysis of a similar monel yielded an average error of 57% [4]. We are continuing to investigate the reason for the failure of the simple LTE model in this case.

LAKE COUNTY LABRADORITE: In this feldspar mineral, Si and Al were taken as internal standards. Ion counts from 5 other elements were measured, and all were corrected within a factor of 2. The average fitting error ranged between 16% and 43%. The CARISMA fitting error for a similar labradorite mineral was 48% [4].

K252 NBS GLASS: This glass contains 6 cations at concentrations between 1 and 22 atomic percent. Si and Ba were used as internal standards. The other elements were all corrected within a factor of 2, with average fitting errors falling between 23% and 45%.

Conclusion

We have found our simple LTE correction program for SIMS data to provide a satisfactory semiquantitative analysis in 4 of the 5 reference materials tested. We also note indirect evidence which suggests that, for most of these materials, there is no advantage in accuracy to be gained by using the full complexity of the CARISMA computer program.

Acknowledgement

This work was supported by the National Science Foundation under Grants DMR-72-03026 and MPS 74-05745.

References

1. J. A. McHugh, "Secondary Ion Mass Spectrometry," in Methods and Phenomena, Methods of Surface Analysis, edited by S. P. Wolsky and A. W. Czanderna, Elsevier, Amsterdam, (to be published).

2. J. M. Schroeer, T. N. Rhodin, and R. C. Bradley, Surface Science 34, 571 (1973).

3. C. A. Andersen and J. R. Hinthorne, Science 175, 853 (1972).

4. C. A. Andersen and J. R. Hinthorne, Anal. Chem. 45, 1421 (1973).

5. R. Shimizu, T. Ishitani, and Y. Ueshima, Jap. J. Appl. Phys. 13, 249 (1974).

6. R. Shimizu, T. Ishitani, T. Kondo, and H. Tamura, Anal. Chem. 47, 1020 (1975).

7. L. de Galan, R. Smith, and J. D. Winefordner, Spectrochim. Acta 23B, 521 (1968).

A more complete account of this work will be submitted for publication in Analytical Chemistry.

Ion Microprobe Analysis for Niobium Hydride in Hydrogen-Embrittled Niobium

Peter Williams and Charles A. Evans, Jr.
Materials Research Laboratory
and
Martin L. Grossbeck and Howard K. Birnbaum
Department of Metallurgy and Mining Engineering
University of Illinois, Urbana, Illinois 61801

Hydrogen-embrittled niobium samples have been examined in an ion microprobe to verify the mechanism of embrittlement by stress-induced precipitation of niobium hydride. A fractured Nb-2 at.% H sample was examined in detail. Mass-analysed images of the fracture region of the sample were obtained using Nb^+, NbH^+, H^+, and NbO^+ ions. The images clearly demonstrate the presence of a hydrogen-rich phase at the fracture site. NbH^+/Nb^+ secondary ion current ratios from the fracture sample were compared with current ratios from macroscopic NbH precipitates in a Nb-5.5 at.% H sample. The ratios obtained at the fracture surface and away from it appear characteristic of niobium hydride and Nb-H solid solution respectively. Scanning electron microscope and electron diffraction studies together with the ion microprobe analysis provide strong evidence in support of the theory of hydrogen embrittlement by stress-induced precipitation of niobium hydride.[1,2]

A more complete account of this work will be submitted to Analytical Chemistry.

This work was supported in part by the National Science Foundation under Grants DMR-72-03026 and MPS-74-05745, the Office of Naval Research under Contract N00014-67-A-0305-0020, and the U.S. Energy Research and Development Administration under Contract AT(11-1)-1198.

1. D. C. Westlake, Trans.-AIME 245, 1969 (1969).
2. T. W. Wood and R. D. Daniels, Trans.-AIME 233, 898 (1965).

POSITIVE AND NEGATIVE ION MASS SPECTRA OF METAL COMPLEXES OF NICKEL (II) WITH HYDRAZINE-S-METHYL-DITHIOCARBOXYLATE LIGANDS

J. G. Dillard and C. F. Battrell
Chemistry Department
Virginia Tech
Blacksburg, VA 24061

ABSTRACT

The positive ion mass spectra of nickel (II) complexes with the bidintate ligand L^- ($R_2C{=}N{-}N{-}\overset{S}{\underset{C}{}}{-}SCH_3^-$) $R{=}CH_3$, H and C_6H_5, are characterized by the formation of the base peak, the parent molecular ion. Fragmentation of the parent ion is found to proceed via clevage of Ni-N and Ni-S bonds. Loss of HL and L are dominant processes. Methyl rearrangement processes occurs and subsequent loss of SCN is noted. In instances where the ligand is tridentate, Ni(L)Cl, loss of Cl, HCl, and ligand fragment are observed. An intense (100%) molecular ion, $Ni(L)Cl^+$, is also detected.

Negative ion mass spectra reveal the formation of parent molecular ions for $R{=}CH_3$. Resonance capture processes at electron energies near zero were noted for $Ni(L)_2$ where $R{=}CH_3$.

NEGATIVE ION CHEMISTRY OF THE MOLYBDENUM FLUORIDES*

D. L. Hildenbrand
STANFORD RESEARCH INSTITUTE
Menlo Park, California 94025

Some negative ion processes involving the molybdenum fluorides were studied by electron impact mass spectrometry, and threshold energies for dissociative capture processes yielding MoF_5^-, MoF_4^- and $MoOF_3^-$ were evaluated. A 12-inch radius, 60° sector magnetic mass spectrometer was used. Gaseous MoF_6 containing a $MoOF_4$ impurity was admitted to the ion source through a molybdenum Knudsen cell, but even at room temperature there was sufficient reduction to yield significant amounts of MoF_5 and Mo_2F_{10} in the entering neutral beam, as evidenced by positive ion spectra. The assigned processes and their threshold energies are listed in Table I. Since the enthalpies of most of the corresponding neutral processes are available from our high temperature equilibrium measurements, the threshold energies can be used to estimate the electron affinities of neutrals associated with the negative ions, as shown in the table. The estimated EAs are lower bounds, since it is assumed that products separate with only thermal energy. Similar measurements on the tungsten fluorides yielded $EA(WF_5) \geq 0.4$ eV, $EA(WF_4) \geq 0.9$ eV, and $EA(WOF_3) \geq 0.3$ eV, all comparable to those reported here for the molybdenum fluorides.

Table I

Process	ΔH_o°, eV	Result
$MoF_6 + e \rightarrow MoF_5^- + F$	3.6 ± 0.1	$EA(MoF_5) \geq 4.1 - 3.6 \geq 0.5$ eV
$Mo_2F_{10} + e \rightarrow MoF_5^- + MoF_5$	0.3	$EA(MoF_5) \geq 1.2 - 0.3 \geq 0.9$ eV
$MoF_5 + e \rightarrow MoF_4^- + F$	3.0	$EA(MoF_4) \geq 3.8 - 3.0 \geq 0.8$ eV
$MoOF_4 + e \rightarrow MoF_4^- + O$	5.0	$EA(MoF_4) \geq 5.8 - 5.0 \geq 0.8$ eV
$MoOF_4 + e \rightarrow MoOF_3^- + F$	3.8	$EA(oOF_3) \geq 4.1 - 3.8 \geq 0.3$ eV

*Research sponsored by the Air Force Office of Scientific Research.

Application of Field Desorption Mass Spectrometry to Inorganic Chemistry, Michael Anbar and Gilbert A. St. John, Stanford Research Institute, Mass Spectrometry Research Center, Menlo Park, CA 94025

A new type of field desorption source has been constructed (Fig. 1) comprising the basic structure of the SRI multipoint source, substituting the multipoint emitter with a metal rod (1 mm O.D.) with a rough surface (~ 0.5 mm in diameter), acting as the field ionizing or field desorbing surface. Three types of surfaces have been tested--broken tungsten and titanium rods, polished iron etched with HCl, and etched iron rods coated with colloidal gold by dipping in chloroauric acid. The different surfaces showed very similar ionization efficiencies when placed within 50 μm from a grid or a slit counter electrode. Voltages in the range 1 to 5 kV have been applied to induce field desorption, typically using 1 to 3 kV. The total source structure can be heated up to 400°C. Typically temperatures in the range of 100°C to 200°C have been used for most of the materials tested. Our technique differs from conventional field desorption, using carbon or metal dendrites deposited on a wire, by the extreme simplicity of preparation of the active surfaces and by the much lower temperatures applied to the ionizing surface.

The ions formed were accelerated to 7 kV and mass analyzed by a 45° sector magnet. The sample loading was done by immersion of the rod tip in a solution of the tested material or by deposition of a microliter droplet from a micro-syringe onto the active surface. Occasionally a 10% polyvinyl alcohol solution (PVA) was used as matrix for inorganic substrates. The polymer was found to facilitate better control of the rate of field desorption.

This field desorption technique has been applied to a large number of inorganic species and to certain nonvolatile thermolabile organic materials. In this paper we shall present just a few examples of these spectra. Fig. 2 shows the field desorption characteristics of different chlorides. Whereas LiCl field desorbs in the form of Li^+ plus Cl^+, NaCl produces substantial yields of Na_2Cl^+ and $Na_3Cl_2^+$ ions. In the case of NH_4Cl we observe field desorbed predominant clusters as complex as $(NH_4)_5Cl_4^+$ It seems that the relative polarizability of the cation and the anion contribute to the probability of cluster formation. This suggestion is borne out in the case of the iodides which shows the existence of $Li_3I_2^+$ with no evidence for the analogous sodium, potassium or cesium species. Interestingly enough in both NaCl and NaI we find the formation of Na_2^+ with no evidence for the analogous dimers in the case of the other alkaline metals. Other factors may exist affecting the stabilities of the polyatomic ions. These are, however, preliminary results obtained by manual scanning and a more extensive study is called for. Such an investigation should examine concentration, temperature, and field intensity effects. The mass spectra should be measured by multi-scanning

rather than by single manual scanning to produce a more quantitative and reproducible mass spectrum.

Other examples of field desorption spectra of inorganic species are those of potassium orthophosphate and ammonium nitrate (Fig. 3). In the case of ammonium nitrate we observe clusters of the hydrated compounds carrying an excess of H^+. This behavior should be compared with that of field ionized ammonium nitrate (same figure) where only traces of the parent ion are detected and most of the ions formed are of fragments resulting from thermal decomposition of the substrate.

The same broken tungsten ionization tip has been used to field desorb organic molecules. In the latter case we found that using a 1% sucrose solution containing 10^{-6} M NaCl enhances the desorption of organic materials. Fig. 4 shows three spectra produced by this technique--folic acid, glutathione, and maytansine, three highly thermolabile nonvolatile materials. The relatively low temperatures allow field desorption without thermal breakdown. The sucrose containing medium may provide a molten matrix in which the organic solute may migrate to the regions of high field strengths; the sodium ions dispersed in the matrix may allow ionization by charge transfer. This action of sodium ions is different from the "cationization" reported by Shulten, as the folic acid and glutathione molecular ions are produced and not their sodium salts. Experiments are in progress to establish ionization efficiencies and optimal conditions for this new mode of field desorption of organic compounds.

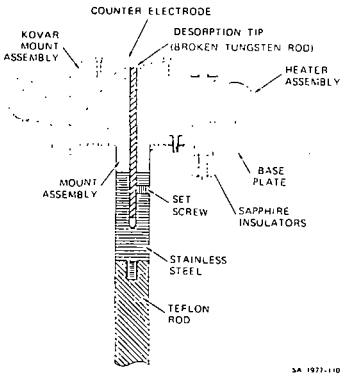

FIGURE 1 FIELD DESORPTION IONIZER WITH SAPPHIRE INSULATORS

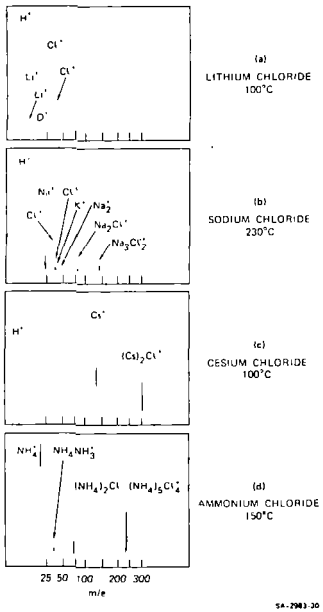

FIGURE 2 FIELD DESORPTION SPECTRA OF MONOVALENT CHLORIDES

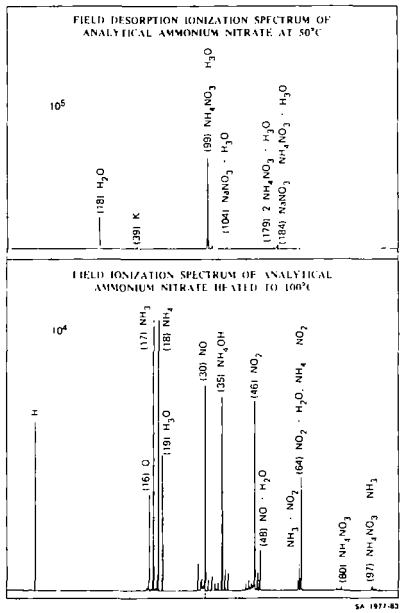

FIGURE 3

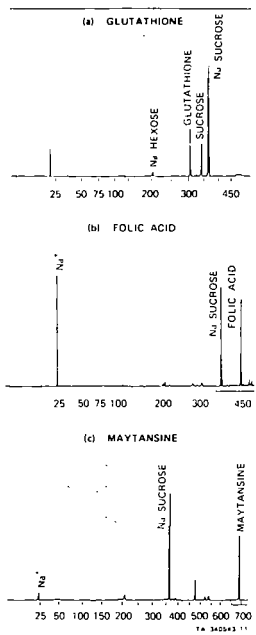

FIGURE 4 FIELD DESORPTION SPECTRA

MASS SPECTRA OF SILVER SALTS

Gerald D. Roberts and Edward White, V

Smith Kline & French Laboratories
Philadelphia, Pennsylvania 19101

Reports on the electron impact mass spectra of copper (I) carboxylates[1] and recently on silver (I) carboxylates[2] have appeared. We have examined the spectra of some aliphatic, alicyclic, and aromatic silver carboxylates and some salts other than carboxylates. Field desorption spectra have been obtained on some of these salts.

The compounds examined under electron impact are listed in Table I. Those listed as successful gave spectra showing ions containing silver atoms and did not appear to undergo extensive thermal decomposition. Those listed as unsuccessful gave no ions containing silver.

TABLE I

Compounds for which Electron Impact Mass Spectra were Attempted

Successful (Silver Containing Ions Observed)	Unsuccessful (Silver Containing Ions Absent)
$AgO_2C(CH_2)_nCH_3$ n=0,1,2,4,6,8,10	$AgO_2C(CH_2)_nCH_3$ n=12,16
$AgO_2CC(CH_3)_3$	$AgO_2CCH{=}CH_2$
$AgO_2C(CF_2)_nCF_3$ n=0,2	$AgO_2CCH{=}C(CH_3)_2$
$AgO_2C{-}C_3H_5$ (cyclopropyl)	$AgO_2CCH_2CH{=}CH_2$
$AgO_2C{-}C_{10}H_{15}$ (adamantyl)	AgO_2CCH_2CN
$AgO_2C{-}C_6H_5$	$AgO_2C{-}C_6H_4{-}R$
$AgO_2C{-}C_6F_5$	R=p-dimethylamino
$AgO_2C(CH_2){-}C_6H_5$	R=p-chloro R=o-methoxy
$AgSCF_3$	$AgSCH_2CH_3$
	$AgSCOCH_3$
	$AgO_3S{-}R$
	$R{=}CH_3$: p-tolyl
	$AgOPO(OC_6H_5)_2$

$Ag^{II}(C_8H_4N_2)_4$ (phthalocyanine)	Ag^{II} (picolinate)$_2$
	Ag-benzotriazole
	Ag-adenine

The spectra of the silver carboxylates are consistent with the previous proposals that in the vapor phase copper (I) and silver (I) carboxylates exist mainly as the dimeric species (I). The ion corresponding to (I) is generally weak or absent with the most abundant

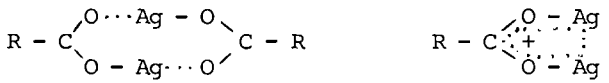

(I) (II)

ion being (II) in most cases. The ions $Ag_3[O_2C(CH_2)_n\text{-}CH_3]_2^+$ are observed at low abundance for the compounds with n=1,2, and 4.

The fragmentation of silver acetate was examined by the use of deuterium labelling and both accelerating voltage and DADI metastable ion techniques. The proposed fragmentation with the observed metastable ions indicated by m* is:

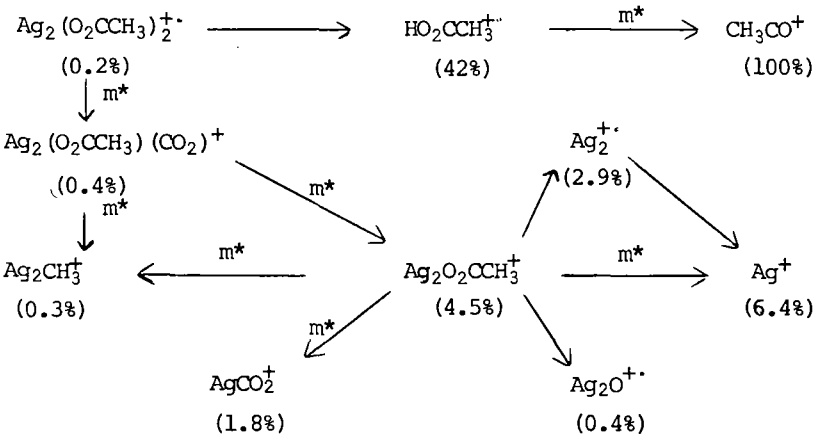

An ion was observed in several of the carboxylates corresponding to $AgNa(O_2C\text{-}R)^+$ which prompted us to examine lithium and sodium acetates both of which appear to volatilize as tetramers and at temperatures much higher than the 200°C required for silver carboxylates.

For $AgSCF_3$ the spectrum is complex with the highest mass ion observed being $Ag_4(SCF_3)_3^+$ suggesting that the volatile species is the tetramer.

The field desorption spectra of the three compounds examined all show the ions Ag_nX_{n-1} for X=acetate (n=1 to 6), X=p-chloro-benzoate

(n=1 to 4), and X=methanesulfonate (n=1 to 7).

References

1. D.A. Edwards and R. Richards, J. Chem. Soc. Dalton, 2463 (1973).

2. S.K. Adams, D.A. Edwards, and R. Richards, Inorg. Chim. Acta, 12, 163 (1975).

THERMAL STABILITY OF THIN FILMS BY MODULATED BEAM MASS SPECTROMETRY

Margaret A. Frisch and Wilhad Reuter
IBM Research, Box 218, Yorktown Heights, N.Y. 10598

We have developed a technique in which the thermal stability of thin films can be examined, leading to, in certain cases, the determination of reaction order and activation energy. The volatilization of impurities, even at low nanogram levels, can also be studied, enabling one to distinguish between surface vaporization and bulk diffusion. The method involves the controlled heating of the sample at a precise linear rate, usually in the range of 1 to 100 degrees/min. The molecular beam, after modulation at 20 c/s, is analyzed by repetitve scans in an automated quadrupole mass spectrometer. Kinetic data on non-equilibrium processes can be derived from the shape of the temperature-intensity curve, employing the analytical methods derived by P. A. Redhead(1).

As an example, we have applied this concept to the characterization of amorphous Gd-Co films, prepared by bias sputtering in a krypton atmosphere. In the sputtering process, the rare gas is entrapped in the film up to as much as 30 atomic %, which amount is dependent on the bias voltage. One of the concerns is the stability of these films in respect to their crystallization behavior and whether the presence of krypton aids or hinders the stabilization of the amorphous phase. Secondly, since the binary Gd-Co system undergoes significant oxidation in air, the stability of the krypton in the oxide phase was also of interest.

Two 12000Å samples were examined by this technique: one which was exposed to air for several weeks; the other, because it had been exposed to air for a short time, was sputter-cleaned to remove the oxide layer. The samples were placed in a molybdenum Knudsen cell with a 1 mm diameter by 5 mm long orifice. Around the circumference of the cell was wound a heater which afforded the precise control of the sample temperature from room temperature up to as high as 1100° K. Several heating rates were employed during these analyses. From preliminary experiments, the principal desorption phases were ascertained and during these instances the sample was heated at 4 degrees/minute. When the sample was observed to crystallize, the temperature was held constant, usually around 770° K, in order to observe other phenomena under isothermal conditions; e.g. diffusion of interstitially trapped krypton and slower nucleation processes.

In Figure 1, the krypton ion signal at m/e=84 is plotted as a function of time for the sputter-cleaned Gd-Co film. At 770° K, the film was observed to crystallize by the sudden increase in the krypton signal. The ion current decayed to zero during the next ten minutes but reached a

second maximum about forty minutes later. We have correleated these events to those observed by electron microscopy on similar films(2). Two types of homogenous nucleation processes have been observed in the case of α-Ge thin films, surface and volume nucleation, which depended on the gas contamination on the surface and in the bulk. The surface nucleation is kinetically one to two orders of magnitude faster than the bulk nucleation which is hindered by gaseous contamination. The krypton release during the latter phase is believed to be the kinetically slower volume nucleation while the initial burst is associated with surface nucleation. A small amount of krypton was also observed at about 450° K, which is the release of krypton trapped in the residual oxide layer. However, from the relative integrated signals, the extent of this surface oxidation is considerably less than 100 Å.

The second sample, which was exposed to air for several weeks, showed a substantially different response to the thermal treatment (Figure 2). Essentially the bulk of the krypton is incorporated in the oxide phase and is easily removed at the very low temperature of 371° K. In the region of the crystallization temperature, the signal was observed over a wide range, beginning around 740° K. The low temperature peak results from the crystallization of the amorphous oxide phase and the sharpness of the response indicates a high nucleation rate.

These experiments are being extended to ascertain the effect of film thickness on the ratio between surface and volume nucleation. In addition, the activation energy of the nucleation processes are under study by varying the temperature of the isothermal phase.

The complete description of this work is under preparation for submission to Surface Science.

(1) P. A. Redhead, Vacuum, 12, 203(1962).

(2) A. Barna, P. B. Barna and J. F. Pocza, J. of Non-Crystalline Solids, 8-10, 36(1972).

High Resolution CIMS: A General Method.

Donald F. Hunt and William F. Reid, Department of Chemistry, University of Virginia, Charlottesville, VA. 22901.

In an earlier report[1] we described the use of argon-water CIMS for obtaining HR CI mass spectra containing all the EI type fragment ions plus an M+1 ion characteristic of MW. PRK is used as an internal standard in this procedure. HR CI(CH_4) spectra can also be obtained since the PRK fragment ions occur at the same m/e values as found in EI spectra. In this paper we outline a general method for obtaining HR CI spectra with reagent gases such as nitric oxide, isobutane, and ammonia which fail to promote fragmentation of either PRK or PFTBA. These latter reagent gases are particularly useful for obtaining elemental composition data on poly-functional, acid-labile, organic samples.

[1]D. F. Hunt and J. F. Ryan III, Anal. Chem., 44, 1306 (1972).

MECHANISMS IN METHANE CHEMICAL IONIZATION SPECTRA

BARBARA L. JELUS and BURNABY MUNSON
Department of Chemistry
University of Delaware
Newark, Delaware 19711

Deuterium labelling of compounds has been very common and useful in elucidating ionic decomposition pathways in electron ionization mass spectra. Labelling studies have been reported previously for chemical ionization mass spectra. CI mass spectra involve an initial attack by the reactant ions and one may therefore label the reactant ions as well as the molecules being studied in efforts to understand the mechanisms of reaction. Studies with labelled reagent gases have been reported previously. There is the additional complication in CI studies that the product ions may undergo ion-molecule reactions with the labelled reagent gas or with impurities.

A series of experiments were done using CD_4 (Merck, Sharpe, and Dohme) as the reagent gas. These experiments were complicated by the presence of impurities in the three samples of CD_4 that were tried. The high pressure mass spectrum of CD_4 in these experiments, therefore, was not directly comparable to the CH_4 spectrum. The CD_4 spectrum at high pressures has significant amounts of hydrogen-containing ions and also has larger abundances of high molecular weight ions. The samples may contain some unsaturated hydrocarbons as impurities.

Table Ia shows the data for a series of hydrocarbons. The relative amount of deuterium incorporation into the ions is small and to a rough approximation, independent of the hydrocarbon structure. This absence of significant incorporation of deuterium in the ions indicates that any $(M+D)^{+*}$ intermediates formed by deuteron transfer from CD_5^+ to the alkanes do not live long enough for the incoming deuteron to become equivalent to the hydrogens on the carbon atom in the sample molecule. One could best consider these $(M+D)^{+*}$ intermediates as involving protonation of a C-H bond to form a 3-center CHD bond which decomposes by the elimination of HD. A possible alternative mechanism is that of H^- transfer to CD_5^+ without the intermediacy of any complex. We have no good explanation for the differences among the spectra of the hydrocarbons. A small amount of D_2O in the CD_4 could be responsible for some of the deuterium incorporation.

The alkyl halides are relatively well behaved and similar to the hydrocarbons in their behavior, Table Ib. Any $(M+D)^{+*}$ intermediates decompose almost exclusively by DX elimination to give the undeuterated alkyl ions. This observation supports the hypothesis that the attack and subsequent decomposition are localized in the molecules. No significant contribution can be present from a process which involves proton transfer to one of the carbon atoms followed by migration of a proton down the carbon chain toward the halogen atom with eventual elimination of HX. The differences among the primary, secondary, and tertiary halides are somewhat too small for us to be certain that they are real.

The spectra of the alcohols, however, are more difficult to interpret, Table Ic. There is significant incorporation of deuterium into the ions for these cyclic alcohols and there are striking differences between the isomeric compounds. Explanations of these differences are not obvious. The larger amounts of ionic incorporation of deuterium in the alcohols than for the hydrocarbons or alkyl halides may be related to the differences in lifetimes of the $(M+D)^{+*}$ complexes. The differences, however, may also result from multiple collision processes which have not yet been considered.

TABLE I
Ionic Incorporation of Deuterium
(a) CD_4 Spectra of Alkanes

Compound	$M-H^+$ % Ionization	$\frac{M+D-H_2^+}{M+D-HD^+}$
2,2-dimethylbutane	36	.010 ± .005
3-methylhexane	49	.034 ± .006
n-octadecane	30	.038 ± .021
cyclohexane	81	.087 ± .037
decalin	82	.027 ± .007
5-α-androstane	64	.031 ± .006
protoadamantane	66	.058 ± .015

(b) CD_4 Spectra of Alkyl Halides

	$(M-X)^+$ % Ionization	$\frac{(M+D-HX)^+}{(M+D-DX)^+}$
1-chlorobutane	93	.019 ± .004
1-chloro-3-methylbutane	92	.013
1-chlorohexane	92	.010
1-bromododecane	40	.010
1-chlorooctadecane	16	.016 ± .006
2-chlorobutane	91	.034 ± .005
bromocyclohexane	89	.025 ± .006
2-chloro-2-methylpropane	95	.045 ± .011

(c) CD_4 Spectra of Alcohols

	$(M-OH)^+$ % Ionization	$\frac{(M+D-HX)^+}{(M+D-DX)^+}$
5-α-androstan-17β-ol	.43	.10 ± .02
5-β-androstan-3α-ol	.43	.21 ± .01
2-<u>exo</u>-protoadamantanol	.69	.33 ± .11
2-<u>endo</u>-protoadamantanol	.65	.07 ± .01

Atmospheric Pressure Ionization (API) Mass Spectrometry. Relation of Sensitivity of Detection to the Ion Source Pressure.

I. Dzidic, D. I. Carroll and E. C. Horning, Baylor College of Medicine, Houston, TX 77025.

Several different API sources recently developed in this laboratory offer a number of advantages apart from the ease of sample introduction. The most important of these are the high sensitivity and selectivity of sample detection. Parameters which permit the operation of high pressure sources to achieve these objectives will be discussed.

A NEW HYPERSENSITIVE SYSTEM FOR TRACE GAS ANALYSIS

N. M. Reid and J. B. French
Institute for Aerospace Studies
University of Toronto

and

J. A. Buckley
Sciex Ltd.
Toronto

A new instrument has been developed for the hypersensitive detection, based on mass spectrometry, (< 1 in 10^{10}) of trace gases in the atmosphere or other applications where large sample volumes but very low concentrations are involved. The aim has been, from the outset, to develop a multipurpose instrument which was not only hypersensitive to many compounds but also met the requirements of (a) a very fast response to allow it to work in real-time without the necessity for sample pre-separation, or concentration, which means it had to be free of memory effects from sample hangup on walls; and (b) portability, ruggedness, ease of operation, and requiring only electrical power for operation. Typical applications include the real time analysis of human breath for clinical, diagnostic or screening applications, airborne geochemical exploration by the detection of trace gas anomalies above ore bodies, nerve gas detection, etc.

SYSTEM DESCRIPTION

This trace atmospheric gas analyser (TAGA) is believed to be unique in that it offers the following combination of advantages:

Real Time
1. Continuous sampling to 100 L/min.
2. Operation at ambient temperature and humidity.
3. Fast dynamic response, clearout in seconds.
4. No wall interactions.

Hypersensitive
5. Currently detects less than 1 in 10^{10}
6. Estimated detectability limit of first commercial model 1 in 10^{13}.

Wide Range
7. Positive identification by mass spectrometry.
8. Sensitive to a wide range of compounds (e.g. containing O, S, P, N and halogens).

Adaptability
9. Field portable, requiring only electrical power.
10. Can also be used as an inlet system for an existing GC/MS or MS system.
11. Can be modified to handle discrete samples (e.g., peak from GC).
12. Multi-mode spectral response which is ideally suited to computerized data handling and analysis.

Currently there are no practical instruments available which combine extreme sensitivity with the capability of detecting a variety of trace gases of interest in air. Many sensitive laboratory systems involve sample preparation and/or integration and hence do not possess real-time capability, and most are designed for the case of micro-sample analysis

(such as gas chromatographic effluents) rather than the case of extremely dilute traces in relatively large sample flows, such as the air sampling application.

A prototype TAGA is now in operation at the Institute for Aerospace Studies, University of Toronto, and has been described in detail in the Ph.D. thesis of J. A. Buckley, "A Hypersensitive Real Time Trace Atmospheric Gas Analyser"[1]. The basic approach is to use mass spectrometry to identify and quantify trace gases in air. To make this practical for parts ratios in the range of interest between 1 in 10^6 to 1 in 10^{14}, it is necessary to produce a massive degree of pre-separation as pre-selection of the trace gas molecules from air molecules before their introduction into the mass spectrometer. This is done by an extremely rapid preferential ionization at atmospheric pressure of the trace gas molecules using ions produced in a primary ionization process from air and water contained in the air (reactant ions). This is thus an application of atmospheric pressure chemical ionization. It is also equally necessary to maximize all the sequence of transfer coefficients that exist between the original "signal" trace molecules in air and their final arrival as mass-analyzed ions per second at the detector. The concepts used to do this have been verified in the laboratories and patent applications have been filed.

A continuous stream of 5 to 100 liters per minute of air is drawn through the mixing and settling region of the instrument into an atmospheric ion molecule reactor. In this region primary ion production from the air occurs using for example a β-emitting tritium foil, rapidly followed by secondary ion molecule reactions with the trace gas molecules present. The end results of this are the formation of stable product ions of the trace gases with an unusual high efficiency. These ions, produced at atmospheric pressure, are then concentrated and introduced with high efficiency into the vacuum chamber. These three features, that is, high efficiency atmospheric pressure ionization, concentration and high efficiency ion transfer contribute to the unusually high sensitivity obtained with this technique. Another feature is that the sample of air which is analyzed at no time has come in contact with the walls of the instrument, removing wall-memory effects which have plagued all ultrasensitive gas analysis techniques and allowing real time monitoring of rapidly changing conditions.

The trace gas ion mixture is allowed to expand into the vacuum system where the neutral gas is cryopumped using an ultra-high capacity cryopump and the ions are focussed using a series of ion lenses, and mass analyzed using a quadrupole mass-spectrometer with unit resolution up to m/e = 1000. Ion detection is carried out using a high gain channel electron multiplier followed by a fast and very sensitive solid state electrometer or by a discriminator and ion counter. Both positive and negative ions can be analyzed and detected. The output signal from the electrometer and counter can be handled in various ways - either by display on an oscilloscope, on an X-Y or chart recorder or most efficiently by a dedicated mini-computer with a suitable interface.

REFERENCE

1. "A Hypersensitive Real Time Trace Atmospheric Gas Analyser, J.A.C. Buckley, Ph.D. Thesis, University of Toronto, 1974.

Argon-Ozone-Water CIMS: A New Method for Determining the Location of Double Bonds

D. F. Hunt, F. W. Crow and T. M. Harvey
Department of Chemistry
University of Virginia
Charlottesville, Virginia 22901

In the analysis of biological samples such as drug metabolites and insect pheromones, the complexity of the mixtures and the size of the sample preclude isolation and wet chemical structure elucidation. Combined Gas Chromatography/Mass Spectrometry has proven to be an excellent method of analysis. Many of these biological samples contain a double bond whose position is crucial to the activity of the compound and therefore knowledge of the olefin position is also crucial. The extensive scrambling and olefin isomerization which takes place under EI conditions in a mass spectrometer preclude its use in determining double bond position.

If a larger sample were isolated, the method of choice would be ozonolysis of the sample and subsequent cleavage of the molozonide to form the ketones or aldehydes which would indicate the double bond position. This same chemistry can be done in the gas phase in the source of a chemical ionization mass spectrometer.

Ozone was made in a Welsbach ozonizer and trapped at dry ice/acetone temperatures on silica gel.[1] On warming, the ozone was admitted as a reagent gas into the mass spectrometer. Undried argon was used to produce Ar/H_2O spectra of the sample and molozonide cleavage products. By this method one should have observed the $M+1^+$ ions of the aldehydes or ketones resulting from cleavage of the molozonide to the appro priate carbonyl compounds. (Fig. 1).

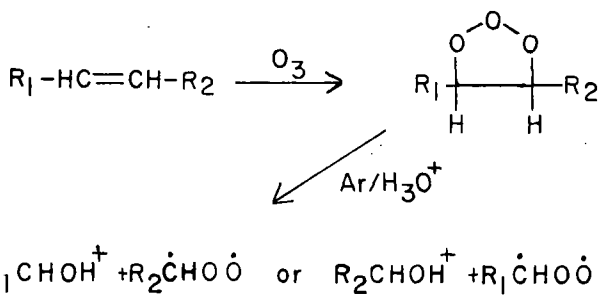

Fig. 1

A mixture of ozone and argon, in a ratio of 1:7, was admitted into the mass spectrometer at a total pressure of 1 torr. In an oxidizing atmosphere the lifetime of a filament is shortened; therefore, the Townsend discharge electron

source was used in this experiment.[2]

Styrene derivatives having the general form* were examined.[3] A peak at m/e 107 was always seen, corresponding to the $M+1^+$ ion from benzaldehyde, an expected ozonolysis product. Abundances of other ions varied. In most cases $M+1^+$ ions from the parent olefin were observed and occasionally the carbonyl compound corresponding to the other ozonolysis product.

Long chain fatty olefinic alcohols were also examined.[4] Molecular ions for the olefin were not observed and only the $M+1^+$ ion from the aldehyde resulting from the nonfunctional side of the molecule was seen. The alcohol containing fragment was not observed.

Experiments with long chain fatty olefinic acids showed both aldehydes expected from ozonolysis.[5] These were seen in the form of their $M+1^+$ ions.

The methyl esters of the above acids were also examined.[6] Their $Ar/O_3/H_2O$ spectra showed $M+1^+$ ions for the parent olefin and both $M+1^+$ ions corresponding to the aldehydes formed from ozonolysis.

These studies reveal that more work is necessary to understand why the ions and reactions observed vary between different series of compounds. However, the utility of the technique can be shown even with a compound whose response is less than ideal. (Fig. 2).

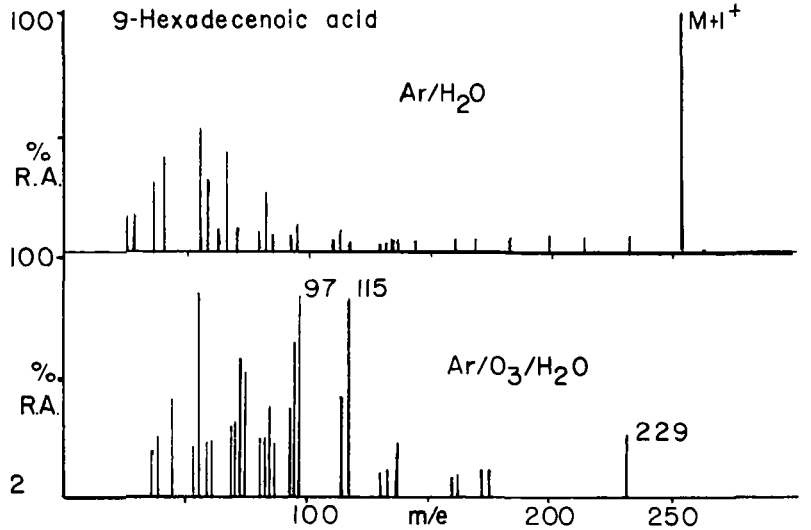

Fig. 2

The Ar/H_2O spectrum of 9-hexadecenoic acid shows a prominent $M+1^+$ ion giving the molecular weight. The fragmentation indicates little or no branching. No information is gained as to the position of the double bond. In the $Ar/O_3/H_2O$ spectrum this acid does not behave like the other acids. It shows only one fragment from the ozonolysis reaction, m/e 115 corresponding to protonated heptaldehyde. The acidic end of the

compound is not observed. Other prominent peaks are m/e 229, protonated heptaldehyde dimer and m/e 97, which is m/e 115-H_2O. This spectrum is adequate to position the double bond.

Investigations to this point have shown a great deal of promise. One can gain important information from small amounts of material avoiding lengthy wet chemical procedures. Future work will be sensitivity studies and investigation into the utility of $Ar/O_3/H_2O$ CIMS in analyzing cyclic olefins.

1. G. A. Cook, A. D. Kiffer, C. V. Klumpp, A. H. Malik and L. A. Spence, "Ozone Chemistry and Technology, Advances in Chemistry Series," 21 (1959).
2. D. F. Hunt, G. C. Stafford, J. W. Russell, 23rd Annual Conference on Mass Spectrometry and Allied Topics, Houston, Texas (1975).
3. Trans cinnamyl alcohol, trans-cinnimaldehyde, α-methyl-cinnimaldehyde, trans-4-phenyl-3-butene-2-one, trans-cinnamic acid, benzilidene acetophenone, trans-β-methyl-styrene.
4. Palmitoleyl alcohol, elaidyl alcohol, eicosenyl alcohol, erucyl alcohol, nervonyl alcohol.
5. Myristoleic acid, palmitoleic acid, elaidic acid, cis-5-eicosenoic acid, erucic acid, nervonic acid.
6. Methyl myristoleate, methyl palmitoleate, methyl elaidate, methyl cis-5-eicosenoate, methyl erucate, methyl nervonate.

*

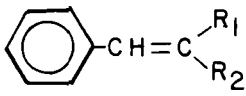

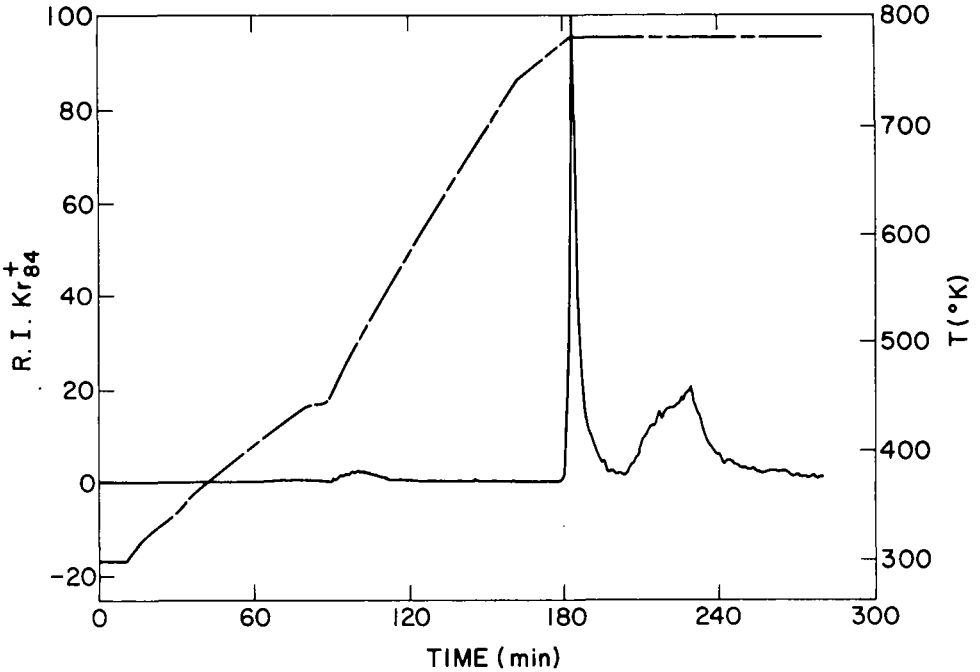

Fig.1 Thermal Release of krypton from amorphous Gd-Co film. Surface cleaned by ion sputtering.

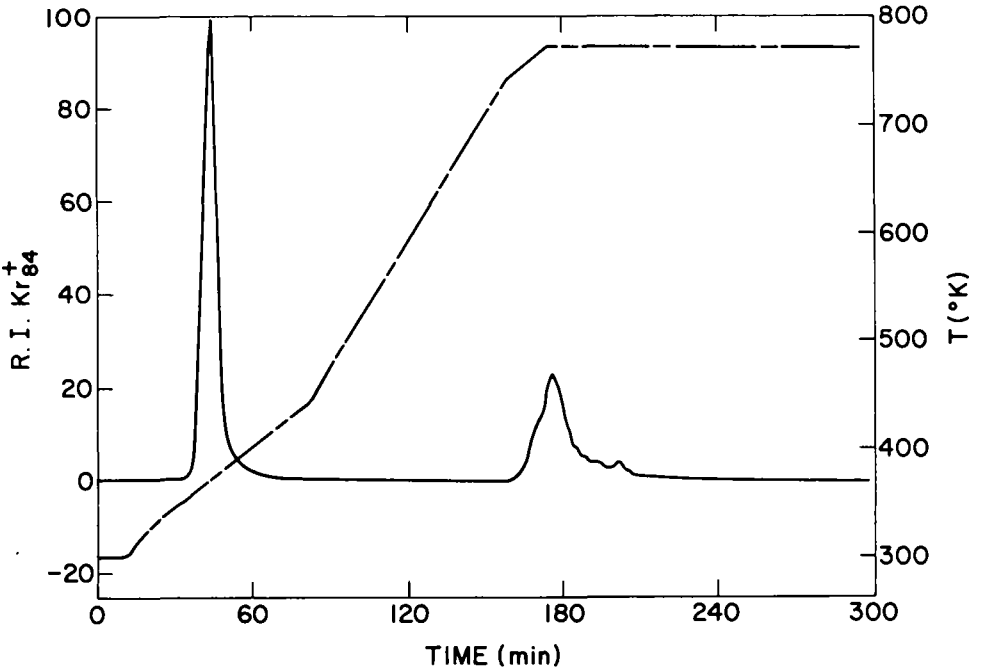

Fig. 2 Thermal release of krypton from air oxidized amorphous Gd-Co film.

Negative Chemical Ionization Mass Spectrometry: A Potential New Method For Analyzing Mixtures of High Molecular Weight Aromatic Hydrocarbons

Donald F. Hunt, George C. Stafford, and John W. Russell
Chemistry Department
University of Virginia
Charlottesville, Virginia 22901

Research to explore the utility of negative ion chemical ionization (NCI) mass spectrometry for the analysis of complex mixtures of high molecular weight, aromatic hydrocarbons found in high boiling petroleum fractions, synfuels, and coal liquefaction processes has been facilitated by our newly developed Townsend electric (TD) discharge source.[1] This new technique appears to be at least two orders of magnitude more sensitive than the widely used low voltage high resolution technique[2] and should prove applicable to the analysis of trace quantities of sulfur, oxygen, and nitrogen containing aromatics in complex mixtures under low resolution conditions.

Introduction of H_2 into the TD source at 3 torr affords H^-, OH^-, and a population of low energy electrons. The addition of a polynuclear aromatic sample affords a NCI spectrum which is devoid of small fragment ions and exhibits peaks only in the molecular weight region ($M-1^-$, $M^{\cdot-}$, and $M+1^-$). Experiments with phenanthrene using deuterium as a reagent gas suggest that these ions are formed in part by the following reactions:

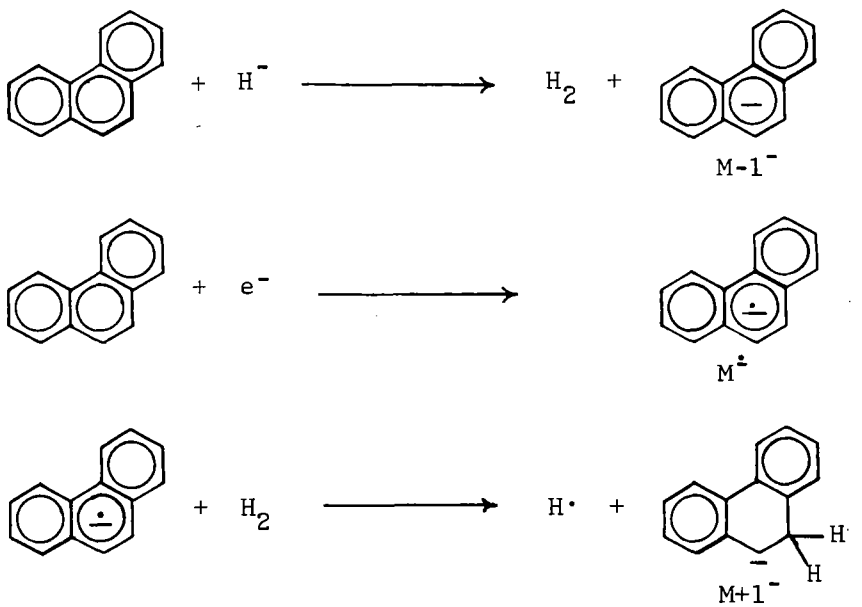

Ideally, for hydrocarbon mixture analysis one would prefer to see single ion spectra from each constituent. Having concluded that the M^- and M+1 ions both required initial capture of a thermal electron, we reasoned that these ions could be eliminated from the above spectrum if a suitable scavenger could be found that would preferentially react with the thermal electron population but be unreactive toward H^-. Nitrogen dioxide seemed to fit the necessary criteria and indeed works well under our experimental conditions. When NO_2 is added to the hydrogen flowing into the CI source ($H_2/NO_2 = {}^{10}/_1$), NO_2^- is produced in high abundance and only the $M\text{-}1^-$ ion remains in the phenanthrene spectrum.

In addition to our studies using hydrogen as a reagent gas, we have extended our research to explore the use of O_2 as a reagent gas. When oxygen is introduced into the TD source at 1 torr, a NCI spectrum consisting of O^-, O_2^-, and NO_2^- (derived from air impurity) is obtained. Addition of acenaphthylene to this ionic plasma affords a NCI spectrum which contains two intense ions, M^- and ($M+O_2\text{-}OH\cdot$). Similar spectra were obtained from aromatic quinones.

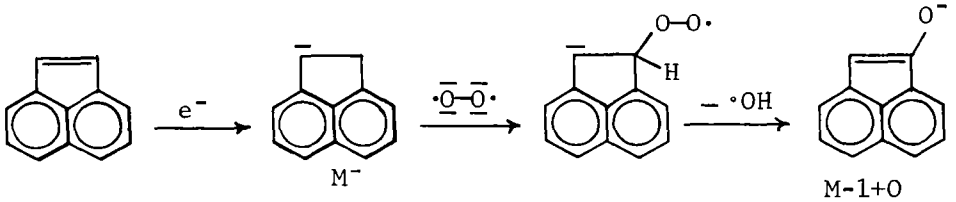

Polynuclear aromatic compounds were found to give NCI spectra which contain only M+15 and M+30 ions. Dibenzo- and benzothiophene were found to undergo gas phase oxidations, and the ion arising from the sulfone (M+32) accounts for the most abundant ion in the spectrum.

From an analytical viewpoint, this gas phase oxidation could be used to facilitate the analysis of the $C_3\text{-}SH_4$ doublet in a complex hydrocarbon mixture without resorting to high resolution techniques. In theory, this could be accomplished by running the hydrogen NCI spectrum to obtain the total integrated intensity of the M-1 peak for the two components being studied. On running a second experiment using oxygen as a reagent gas, the sulfur containing component should be moved 32 mass units higher, and both compounds could be easily quantitated.

Sensitivity studies (Single Ion Monitoring) indicate that oxygen NCI is an extremely sensitive technique for detecting compounds at the picogram level. A 2 picogram sample of the pesticide TCDD could easily be detected with a 50:1 S/N ratio, and a 200 femtogram sample of dibenzothiophene was detected with a S/N ratio of 100:1.

1. D. F. Hunt, C. N. McEwen, and T. M. Harvey, Anal. Chem., in press.

2. (a) T. Aczel, D. E. Allan, J. H. Harding, and E. A. Knipp, Anal. Chem., 42, 341 (1970); (b) B. H. Johnson and T. Aczel, ibid., 39, 682 (1967); (c) T. Aczel, J. Q. Forster, and J. H. Karchmer, 157th Meeting of the American Chemical Society, Minneapolis, Minn., Apr. 13-18, 1969, Preprints of the Division of Fuel Chemistry, Vol 13, No. 1, p. 8; (d) J. L. Shultz, T. Kessler, R. A. Friedel and A. G. Sharkey, Jr., Fuel, 51, 242 (1972).

WATER CHEMICAL IONIZATION OF LIPID MATERIALS

S. E. Buttrill, Jr.
Department of Chemistry
University of Minnesota
Minneapolis, Minnesota 55455

In many respects water is the ideal reagent gas for compounds such as those important in lipid analysis. Both normal water and D_2O are readily available in very high purity at very low cost. With a proton affinity of approximately 165 kcal/mole, water will protonate almost all oxygen-containing compounds. The spectrum of pure water is extremely simple, consisting of H_3O^+ at m/e 19 and clusters of this ion with additional water molecules at m/e 37, 55, 73, and 91. Finally, when both source temperature and water pressure are carefully kept constant, the relative intensities of cluster ions of the form $MN^+(H_2O)_n$ with n = 0, 3 are sensitive to both the structure and stereochemistry of the sample molecule M.

The water CI spectra of the various types of compounds studied can only be briefly summarized here.

Methyl esters. At a typical source temperature of 110°C and about 0.2 torr water pressure, the base peak is always $M+H^+$, the acylium ion ($M+H^+$ - MeOH) has a relative intensity of 0.05. The clustered ion M+19 is about 0.15 ± 0.05 for saturated esters and somewhat lower for unsaturated compounds.

Triglycerides. Smaller triglycerides such as trioctanoin show large peak $M+H^+$ peaks and peaks corresponding to the loss of a molecule of carboxylic acid from the protonated molecule ($M+H^+$ - RCOOH). A smaller RCO^+ peak is also present at about 0.05 relative intensity (RI). No water clusters are present at 130°C. For larger triglycerides such as tristearin, no molecular ion is observed at 270°C using water, methanol, diethyl ether as reagent gas. An ion at ($M+NH_4^+$) present using ammonia as reagent gas, but no $M+H^+$. The other peaks are similar to those of the lower triglycerides with base peak at ($M+H^+$ - RCOOH) and small peaks for RCO^+, R^+, and $RCOOH_2^+$.

Free acids. Underivatized carboxylic acids yield strong water CI spectra at about 140°C. Base peak is $M+H^+$ with $M+H^+$ - H_2O being about 0.20 RI. Water cluster ions at M+19 and M+37 are always present at this temperature.

Diglycerides. At 170°C, the base peak for compounds such as dipalmitin is $M+H^+$ - H_2O with $M+H^+$ being about 0.3 RI. The ion ($M+H^+$ - RCOOH) with RI of 0.8 and small peaks for RCO^+ and $RCOOH_2^+$ make it a simple matter to identify diglycerides from their water CI spectra.

The structural information available from the water cluster ions frequently observed is illustrated by the spectra of diethyl maleate and fumarate obtained at 130°C and shown in Fig. 1. The protonated maleate diester, which is the cis isomer, can form an intramolecular hydrogen bond, thus saturating all of the hydrogen bonding sites on the ion. This cyclic structure is unaccessible to the protonated trans isomer, so it readily hydrogen bonds to a molecule of water.

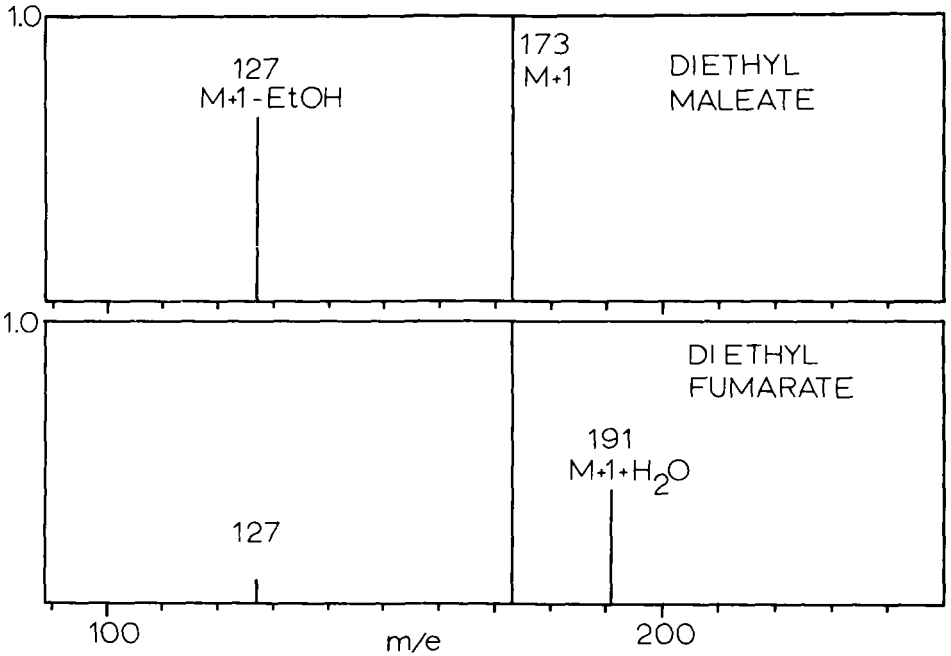

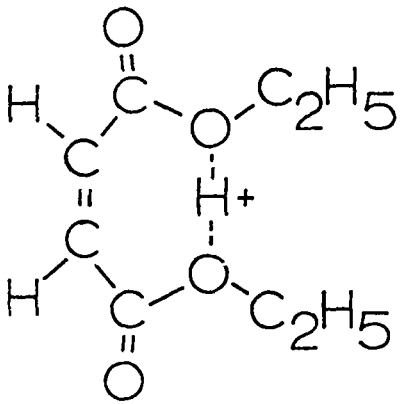

Maleate

Fumarate

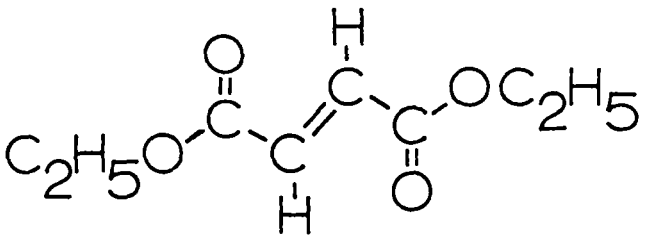

Reagent Gas Cluster Ion Additions to Neutral Molecules

H. S. Swofford, Jr., Philip Price, D. P. Martinsen and S. E. Buttrill, Jr.

Dept. of Chemistry, Univ. of Minnesota
Minneapolis, Minnesota 55455

The principle reagent gas ions formed in water Chemical Ionization Mass Spectrometry (CIMS) are $H^+(H_2O)_n$ where n = 0-6 (1,2). Water CIMS spectra often demonstrate a similar type of clustering. In addition to the formation of MH^+, peaks corresponding to $MH^+(H_2O)_n$ are often observed where n = 1-3.

We observed that difunctional compounds tend to accentuate the formation of $MH^+(H_2O)_n$ clusters. Previously (3) it was noted that variations in cluster ion peak intensities might yield structural and conformational information. An important property of difunctional compounds is the distance between functional groups. A series of difunctional straight chain aliphatic nitriles was used as a simple model to study, $NC(CH_2)_nCN$ where n = 1-6.

All experiments were performed at a source and inlet temperature of 110° ± 5°C. Figure 1 shows the variations in water reagent gas cluster ion intensities with source pressure, as observed with our instrument. It can be seen that the source pressure must be above approximately 0.2 torr before clusters containing three or four water molecules form an appreciable fraction of the total ion current (TIC). The maximum sample TIC occurs below 0.1 torr, however, most of the signal at this pressure is due to MH^+ ions and not clusters. Since the sensitivity falls off with increasing pressure, it was advantageous to work at the lowest source pressures still conducive to clustering, 0.22 to 0.23 torr. Clustering between sample and water reagent gas was also studied as a function of sample concentration. Until the sample concentrations reach one to three thousand parts per million, little variation in clustering is observed. All spectra determined by injection were, therefore run on 100 to 200 ppm aqueous solutions.

With the present apparatus, CIMS spectra may be taken by directly injecting solutions into DuPont's inlet system (3). Samples may also be placed on the solids probe with reagent gas supplied at sufficient pressure by injecting 10 to 30 µl of water into the batch inlet.

The spectra of the six model dinitriles are plotted in figure 2 as percent of total sample ion current, and the points for each type of cluster are connected by solid lines. Thus, each solid curve represents the relative intensity of a particular type of sample-water cluster as the sample is varied from dicyano methane to 1,6-dicyano hexane.

The curves reveal that, based solely on relative clustering intensities, one can differentiate between various configurations of dinitriles. As the distance (number of methylene groups) between nitriles is increased, (A) the molecular ion (MH^+) falls rapidly to a steady value, (B) the $MH^+(H_2O)$ ion increases, (C) the $MH^+(H_2O)_2$ ion passes through a maximum at a separation of 4 methylenes, and (D) the $MH^+(H_2O)_3$ ion passes through a maximum at a separation of 2 methylenes and then decreases to zero at 5 methylenes.

As a test of the validity of this method for determining the distance between nitrile groups, the spectra of four compounds different from the six model compounds were determined. The observed relative cluster intensities for these four compounds are shown in Figure 3. Also shown are the predicted values as read from the appropriate positions along the curves in Figure 2. Since two of the test compounds contain a double bond between the nitriles, a shift to the left was made when reading from the curves.

It is well known that the fragmentation observed in Cl spectra can reveal valuable structural information. This study demonstrates that reagent gas clustering provides a second source of structural information from CI spectra. Interactions between other functional groups and various reagent gasses will be the subject of further studies. This work has been submitted to Analytical Chemistry.

This work was supported by NSF Grant No. GP-38764X.

References

1. D. Beggs and F. H. Field, J. Am. Chem. Soc., 93, 1567 (1971).
2. D. F. Hunt, C. N. McEwen, and R. A. Upham, Anal. Chem., 44, 1292 (1972).
3. P. Price, D. P. Martinsen, R. A. Upham, H. S. Swofford, Jr., and S. E. Buttrill, Jr., Anal. Chem., 47, 190 (1975).

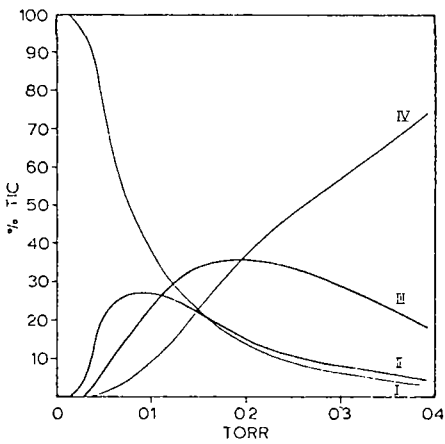

Figure 1. Ions in H_2O reagent gas versus source pressure, I = $H^+(H_2O)$, II = $H^+(H_2O)_2$, III = $H^+(H_2O)_3$, IV = $H^+(H_2O)_4$.

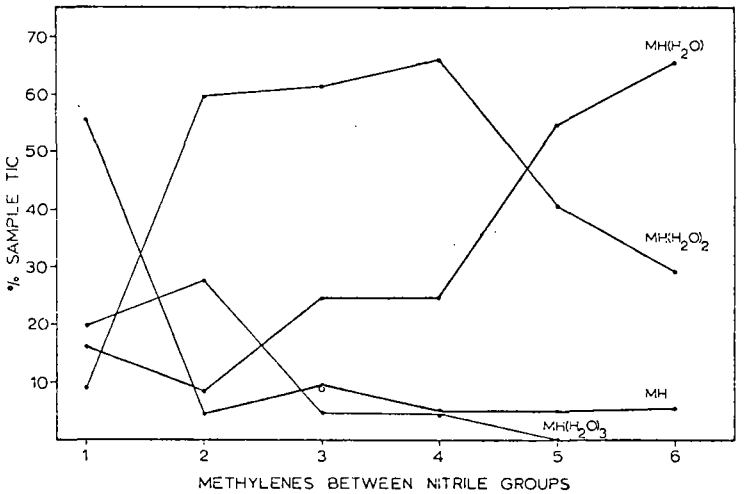

Figure 2. Cluster ion intensities versus separation between nitrile groups for six aliphatic dinitriles.

COMPOUND		MH	MH(W)	MH(W)$_2$	MH(W)$_3$
	PRED.	12	9	52	26
	OBS.	15	23	39	23
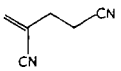	PRED	10	25	61	5
	OBS	9	29	60	2
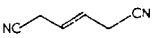	PRED	6	25	65	4
	OBS	6	21	66	7
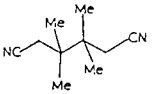	PRED	5	25	66	4
	OBS	5	15	72	7

Figure 3. Predicted versus observed ion intensities for four test compounds.

PROTON LOCALIZATION IN CHEMICAL IONIZATION FRAGMENTATION. Ian Jardine and Catherine Fenselau, Department of Pharmacology and Experimental Therapeutics, The Johns Hopkins University School of Medicine, Baltimore, Md. 21205.

Several workers studying chemical ionization spectra of deuterium-labeled samples have observed that the isotope labels are partially scrambled with hydrogen atoms before the M + H ions decompose (1,2). Consequently it has been suggested that the proton transferred in ionization is not specifically localized in the molecule (2). We have now studied the effects of temperature and proton affinity on the randomization of the ionizing proton.

In order to distinguish hydrogen atoms originating in the sample from protons transferred from methane reagent gas, a series of D_{11}-cyclohexyl compounds was used. D_{11}-Cyclohexylamine and D_{11}-cyclohexylsulfide were synthesized from commercial samples of D_{11}-cyclohexanol and D_{11}-cyclohexylbromide. This series provides a range of proton affinities and all four compounds form $C_6D_{11}^+$ fragment ions by elimination of small neutral molecules.

$$c\text{-}C_6H_{11}X \xrightarrow{(H^+)} C_6H_{11}^+ + HX$$

m/e 83

$$c\text{-}C_6D_{11}X \xrightarrow{(H^+)} C_6D_{11}^+ + HX$$

m/e 94

$X = NH_2$, SH, OH, Br

We have found in the cases of D_{11}-cyclohexylamine, D_{11}-cyclohexylsulfide and D_{11}-cyclohexanol that the elimination of HX leads to $C_6D_{10}H^+$ ions as well as $C_6D_{11}^+$ ions, in amounts which increase, for a given compound, as the source and gas temperature is decreased from 200° to 100°. No $C_6D_{10}H^+$ ions are formed from D_{11}-cyclohexylbromide at any of the temperatures studied, but only $C_6D_{11}^+$ ions. The bromide has the lowest proton affinity of the four compounds. Cyclohexylamine, with the highest proton affinity, showed the most scrambling, with as many as one $C_6D_{10}H^+$ ion formed for every two $C_6D_{11}^+$ ions at 100°. Delocalization of hydrogen atoms in the alcohol and sulfide was intermediate between that in the bromide and amine.

One consistent interpretation of all these observations is that less scrambling is observed in those systems which fragment faster. At higher temperatures fragmentation proceeds more quickly and, indeed, less exchange is observed between deuterium atoms in the ring and hydrogen atoms on the functional group.

Proton affinity also may be correlated with ion lifetimes. Field has predicted (3) that the extent of fragmentation in which a small neutral molecule is eliminated in chemical ionization will be inversely proportional to the proton affinity of the small molecule eliminated. We have confirmed this correlation by determining the ratios of $\frac{M + H}{C_6H_{11}}$ in thirteen cyclohexyl derivatives. The higher the proton affinity, the larger the ratio and the smaller the extent or rate of fragmentation. Within this series cyclohexylamine fragments less rapidly than cyclohexylsulfide or cyclohexanol and cyclohexylbromide fragments extremely rapidly. This

order is inversely proportional to the extent of scrambling observed in the four deuterium-labeled analogs.

Our results, which will be published elsewhere, show that protons transferred from methane reagent gas may be delocalized in longer-lived parent ions.

1. F. H. Field and M. S. B. Munson. J. Amer. Chem. Soc. 89, 4272 (1967).
2. C. Fenselau, J. H. Duncan and H. M. Fales. Proceedings of the Nineteenth Annual Conference on Mass Spectrometry and Allied Topics, Atlanta, Georgia, May 2-7, 1971.
3. F. H. Field. Chemical Ionization Mass Spectrometry, in MTP International Review of Science, Vol.5, A. Maccoll (Ed.), Butterworth's, London, 1972.

REACTIONS OF AMMONIA AND WATER IN THE CHEMICAL IONIZATION MASS SPECTROMETRY OF BIFUNCTIONAL ACIDS AND ESTERS.

Robert J. Weinkam and Joseph Gal

Contribution from the Department of Pharmaceutical Chemistry, School of Pharmacy, University of California San Francisco, California, 94143.

The chemical ionization induced fragmentation of monofunctional n-alkyl carboxylic acids and methyl esters proceeds through the protonated molecular ion by two major pathways,[1] hydride abstraction leading to $(M-H)^+$, and unimolecular elimination of water or methanol, respectively, to give the acylonium ions $R{\cdot}C{\equiv}O^+$. The spectra of mono and bifunctional carboxyl compounds are compared in Table 1, which presents the methane cims of dodecanoic (1) and dodecan-1,10-dioic (2) acids, and the esters methyl dodecanoate (3) and methyl dodecan-1,10-dioate (4). The second functional group has the effect of reducing hydride abstration and increasing elimination of water and methanol. The increased fragmentation of the bifunctional acid (2) and methyl ester (4) suggests the presence of a bifunctional interaction leading to a stabilized product ion $(MH-HOR)^+$, R=H, CH_3.

The relative fragmentation of the mono and diacetoxy decanes,(5) and (6), Table 1, support this scheme. The dominant loss of acetic acid in the monoacetate was greatly reduced by the presence of the second function. This can be explained by assuming that the isomeric acetates and methyl esters eliminate alcohol by the same mechanism.

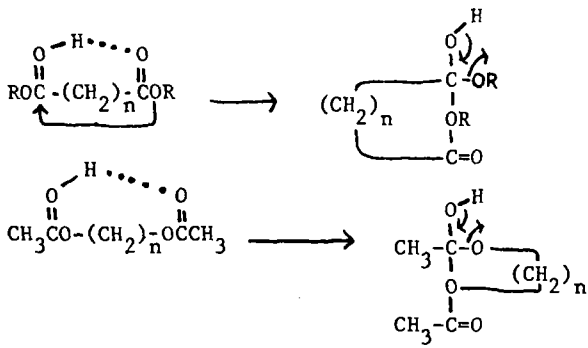

The extent to which the second functional group can facilitate the elimination of water in a dicarboxylic acid is a function of the interfunctional chain length. Figure 1 presents the isobutane cims of a series of dicarboxylic acids in which the percent total sample related ionization (%Σ) of $(MH)^+$ declines and %Σ $(MH-HOH)^+$ increases as the interfunctional polymethylene chain is lenghthened.

The proton complex suggested as an intermediate in this fragmentation scheme would increase the proton affinity of the bifunctional molecule by the free energy released on formation of the intramolecular hydrogen bond. As the proton affinity of ammonia (207 ± 3) is close to that of long chain methyl ester (205 ± 3) the increased proton affinity of the bifunctional molecule would shift the equilibrium, $M + NH_4^+ \rightleftarrows (M + NH_4)^+ \rightleftarrows (MH)^+ + NH_3$,

towards the protonated molecular ion $(MH)^+$. Figure 2 shows the percent associated ion $(M + NH_4)^+$ and protonated molecular ion $(MH)^+$ relative to the number of methylene groups in the series of methyl dicarboxylates.

It seems feasible to suggest that the increase in the $(M+NH_4)^+/(MH)^+$ ratio results from an increase in the ammonium ion affinity in the larger ring systems, n=4 to 10, by way of ammonium ion complex formation. The alternate explanation, a decrease in proton complex stability, is not consistent with studies on the gas phase stability of analogous complexes.

The ci induced fragmentation reactions of monofunctional carboxylic acids appears to be directly related to the difference in proton affinity of the reagent ion and that of the carboxylic acid group (190 $\pm$ 3 kcal/mole). The dependence on relative proton affinities does not hold for dicarboxylic acids, however. Figure 3 shows the percent total sample related ion current (%Σ) carried by the protonated molecular ion for a series of dicarboxylic acids, $HO_2C(CH_2)_nCO_2H$, on ionization by the reagent gases methane, water and isobutane.

The processes involved in the reaction of dicarboxyl compounds with hydrogen bond donor reagent gases such as water is indicated by the reaction series. Figure 4, of dimethyl esters. This presents the dependence of the percent total sample related ion current of the protonated molecular ion MH^+ and fragment ion $(MH-HOCH_3)^+$, on interfunctional separation, n, for the series $CH_3O_2C(CH_2)_nCO_2CH_3$. In this series an additional major ion $(MH-14)^+$, was present in the spectra of those compounds having more than three methylene units. This ion corresponds to the exchange of reagent gas water for methanol of the ester function, in effect, gas phase hydrolysis.

The exchange reactions observed between bifunctional carboxylic acids and esters and protic reagent gases occur through bimolecular reaction pathways which have defined structural and chemical requirements. Although it is not possible to state conclusively the details of the reaction pathway the diverse data presented can be understood through a reaction model involving initial coordination of the reagent gas with the bifunctional sample molecule involving complimentary hydrogen bonding. This species may then decompose through the exchange reaction pathway, $RO_2C(CH_2)_nCO_2R + H_3O \rightarrow [RO_2C(CH_2)_nCO_2R \cdot H_3O]^+ \rightarrow RO_2C(CH_2)_nCO_2H_2^+ + HOR$.

Acknowledgement. Supported in part by the NIH Research Career Development Award 1-K4-GM-00007.

REFERENCES

To be submitted to Organic Mass Spectrometry.
(1) M. S. B. Munson and F. H. Field, J. Amer. Chem. Soc., 88, 4337 (1972).
(2) M. S. B. Munson, Anal. Chem., 43, No. 13, 28A (1971).

1

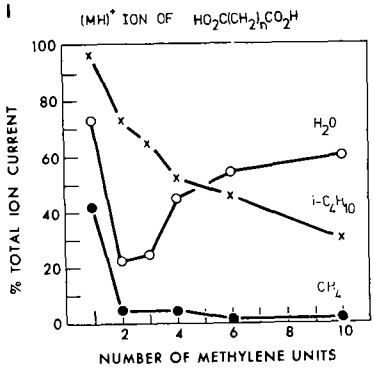

2

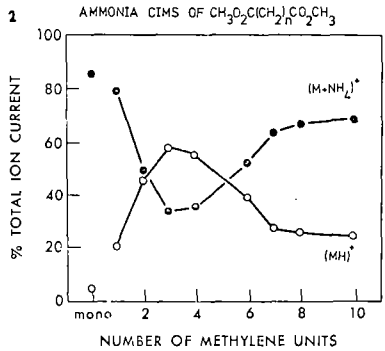

3

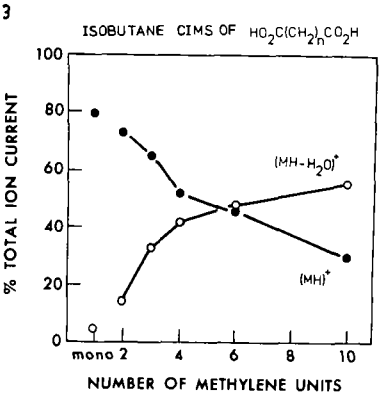

4

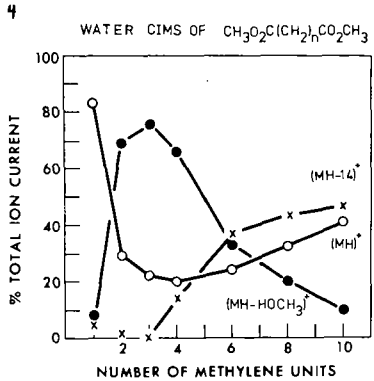

Table 1 Methane (280°C) Chemical Ionization Mass Spectra of Mono and Di(methyl) Alkyl Acids, Esters and Ketones

No	Compound	R = C_2F_5	MH[a]	M -R	MH -H_2 -HOR	MH -H_2 -HOR	MH -H_2 -2HOR	MH -H_2 -2HOR
1	$HO_2C(CH_2)_{10}CH_3$	79	100	73	43	26		
2	$HO_2C(CH_2)_{10}CO_2H$	1	3	1	100	4	1	4
3	$CH_3O_2C(CH_2)_{10}CH_3$	33	100	33	13	3		
4	$CH_3O_2C(CH_2)_{10}CO_2CH_3$	14	59	3	100	8	1	1
5	$CH_3CO_2(CH_2)_{10}H^b$	1	48	1	100	14		
6	$CH_3CO_2(CH_2)_{10}O_2CCH_3^c$	1	180	2	9	3	70	5

[a] Includes ^{13}C isotopes [b] R = H for acids 1 and 2. R = CH_3 for methyl esters 3 and 4. R = CH_3CO for ketones 5 and 6. [c] $CH_3(CH_2)_8^+$ 139 rel intensity [d] $CH_3CO_2H_2$ 202 rel intensity

Hydrogen Rearrangements in Esters Following Chemical Ionization

F.M. Benoit and A.G. Harrison,
Univ. of Toronto,
Dept. of Chemistry,
Toronto, Ont.

In the CI mass spectra (H_2 and CH_4) of n-propyl esters the major fragmentation pathway is the loss of C_3H_6 from the MH^+ and $MC_2H_5^+$ ions following migration of a propyl hydrogen atom to the carboxyl function. The first report on the CI mass spectra of esters involving the loss of olefin from the alcoholic portion of the molecule suggested that such a reaction could reasonably be attributed to a McLafferty rearrangement with the migrating hydrogen originating from the gamma position: however no labelling experiment was conducted. Our examination of deuterium labelled derivatives of n-propyl acetate and n-propyl benzoate reveals that the gamma position is not the unique source of the migrating hydrogen but that all three propyl sites contribute to the reaction with about 50% of the hydrogen atoms coming from C-3 (Table 1).

Table 1. The source of the migrating hydrogen in n-propyl acetate and n-propyl benzoate.

	propyl acetate			propyl benzoate		
	C-1	C-2	C-3	C-1	C-2	C-3
$MH^+(H_2)$	26	24	50	26	25	49
$MH^+(CH_4)$	24	24	52	30	22	48
$MC_2H_5^+(CH_4)$	29	21	50	27	22	51

Consequently, elimination of olefin in these esters cannot be attributed to a McLafferty rearrangement which requires[2] the specific abstraction of a hydrogen atom from C-2. Our analysis of 2,2,3,3,3-d_5-n-propyl benzoate reveals an abundant daughter ion (9-11%) retaining two deuterium atoms (originally located in the propyl group). We estimate that the reagent and propyl hydrogen atoms have become indistinguishable in about 25% of the daughter ions of the reaction of interest; in these ions the transfer reaction appears to be stepwise.

We consider that protonation in molecular ions dissociating via the reaction of interest is likely to occur at either of the oxygen atoms although in reacting ions of higher internal energy attack of the proton can be shown to occur exclusively at the propoxy oxygen atom[3]. Thus, two forms of the protonated molecular ion, (a) and (b), which are not interconvertible according to a recent review[4], are generated. The main

(a) (b)

driving force for H atom migrations has been shown[5] to be the presence of an electron deficient (or charged) site. Consequently, we suggest that migration of a propyl hydrogen atom can occur to either oxygen atom. Should migration occur

to the protonated oxygen atom subsequent loss of olefin is rapid, no interchange of reagent and propyl hydrogen atoms is likely, and the overall reaction is concerted. However, should H atom migration occur to the unprotonated oxygen atom, the intermediate ion is sufficiently stable to allow, via a series of equilibrium processes, the propyl and reagent hydrogen atoms to randomize (either partially or completely) prior to the loss of olefin.

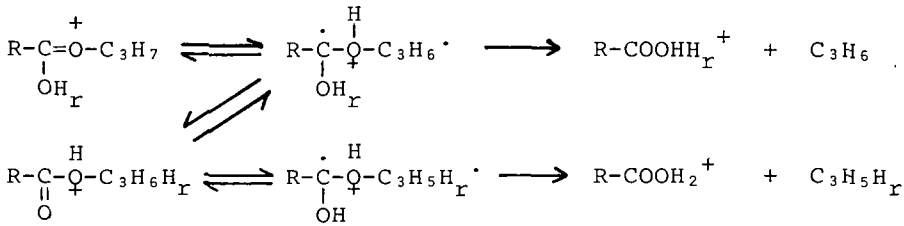

We suggest that the participation of all three propyl sites in the reaction of interest is largely due to propoxy oxygen acting as a recipient site for the transferred hydrogen atom.

References.

1. M.S.B. Munson, and F.H. Field, J. Amer. Chem. Soc., 88, 4337 (1966).
2. D.G.I. Kingston, J.T. Bursey, and M.M. Bursey, Chem. Rev., 74, 215 (1974).
3. C.V. Pesheck and S.E. Buttrill, J. Amer. Chem. Soc., 96, 6027 (1974).
4. M.A. Winnik, Org. Mass Spectrom., 9, 920 (1974).
5. F.P. Boer, T.W. Shannon, and F.W. McLafferty, J. Amer. Chem. Soc., 90, 7239 (1968).

Chemical Ionization Mass Spectrometry of Compounds of Biological Interest

M.E. Rennekamp, J. Shabanowitz and D.V. Bowen

The Rockefeller University

New York, New York 10021

ABSTRACT

Several synthetic peptide analogues of antibiotics have been examined by isobutane CI-MS. These peptides are cyclic polymers of proline and valine with 8, 10 or 12 residues in the ring. These cyclic peptides show almost no fragmentation under isobutane CI-MS conditions at source temperatures around 250°C - 300°C. The few fragment ions which are formed appear to be characteristic of the peptide structure and indicate that the fragmentation occurs by the loss of an even number of residues. These experiments have shown the utility of chemical ionization with peptides of molecular weight as high as 1600. Peak matching with perfluoro-s-triazines has been used to obtain accurate mass measurements of the $(M+1)^+$ ions of these peptides under CI conditions.

Studies of some organo-metallic compounds have emphasized the utility of source insertion chemical ionization[1]. In this technique the sample is applied to the tip of a glass rod which is then inserted into the source so that the sample is within 1 or 2 mm of the electron beam. We believe that this brings the sample into the region of the CI reactant gas plasma. Bis-thioglyceryl mercury gave useful spectra by source insertion chemical ionization. The major ion observed was $(M+1)^+$ and a strong ion was observed corresponding to loss of water. When bis-thioglyceryl mercury was examined from a standard probe-cup, only mercury ions were seen and no spectra characteristic of the organo-metallic compound were obtained. Gold thioglucose did not give usable spectra by this technique or by standard probe-cup insertion.

Source insertion chemical ionization has also been used to obtain the

spectra of three classes of quaternary ammonium compounds[2]. As previous EI studies lead one to expect, these compounds volatilize with thermal loss of alkyl halide. The CI spectra of the resulting thermolysis products are useful for characterizing the parent compound. This technique has been particularly useful in the development of an assay for choline in the presence of acetylcholine. Commercial samples of acetylcholine are often contaminated with significant amounts of choline, which is readily formed by hydrolysis of the acetylcholine. In order to establish the quality of acetylcholine samples before their use in biological experiments, we developed a simple source insertion chemical ionization assay. A sample of acetylcholine is placed on the tip of a glass rod and inserted into the mass spectrometer. Acetylcholine in the sample volatilizes at about 150°C. The Source Insertion Probe distillation thus gives two peaks whose areas are proportional to the amount of acetylcholine and of choline in the sample. This assay can detect 1 mole percent of choline in acetylcholine.

(1) Baldwin, M.A.; McLafferty, F.W. Org. Mass Spectrom. 1973, 7, 1353-1356.

(2) Shabanowitz, J.; Brynes, P.; Maelicke, A.; Bowen, D.V.; Field, F.H. Biomed. Mass Spectrom. 1975, in press.

MECHANISTIC STUDIES OF THE DECOMPOSITION OF URETHANE FOAMS USING CHEMICAL IONIZATION MASS SPECTROMETRY

F.D. Hileman, K.J. Voorhees, L.H. Wojcik, J.H. Futrell, and I.N. Einhorn
Flammability Research Center & Departments of Chemistry & Material Science
University of Utah, Salt Lake City, Utah 84112

A rigid urethane foam was prepared by reacting 4, 4'-diphenylmethane-diisocyanate and propoxylated trimethyolpropane. This foam was then pyrolyzed and the lower molecular weight degradation products were readily identified using conventional GC-ETMS techniques. The higher molecular weight products have been much more difficult to analyze since they consist principally of the pyrolysis products of the polyol used in the preparation of the foam. A sample chromatogram of these heavy molecular weight products is shown in Figure 1. The mass spectra in Figure 2A shows the extensive fragmentation that a sample polyol, dipropoxytrimethylolpropane undergoes during electron impact conditions. Since all the various polyolpyrolysis products gave similar mass spectra under electron impact conditions, this technique proved of little use in the identification of these pyrolysis products.

Contrast the EI spectra in Figure 2A with the methane CI spectra of the same compound shown in Figure 2B. The fragmentation was nearly eliminated with a strong M+1 ion at m/e 251. Thus, using GC-CIMS, it was possible to obtain strong M+1 ions for each of the eluted peaks thus greatly simplifying product identification. Helium was typically used as carrier gas with isobutane as reagent gas using the "reagent switching" technique to generate the chemical ionization mass spectrum. Isobutane was selected as reagent gas to minimize the fragmentation of the polyol, especially the loss of water. The reason for this was that the polyol can lose water in the pyrolysis process and thus confusion could result in peak identification as to whether the water loss occurs in pyrolysis or in the ion source. Using this technique the product identifications given in Table 1 were possible. The high number of alkenes present in the pyrolysis products strongly suggests that one of the decomposition mechanisms was a concerted reaction (1) as shown in Figure 3. This mechanism was supported by the chemical ionization identification of the 4,4'-diphenylmethanediamine in the pyrolysis residue resulting from the degradation of the isocyanate.

References

1. J.H. Saunders and J.K. Backus, "Thermal Degradation and Flammability of Urethane Polymers," Rubber Chem. and Tech., 39, (1966), p. 461.

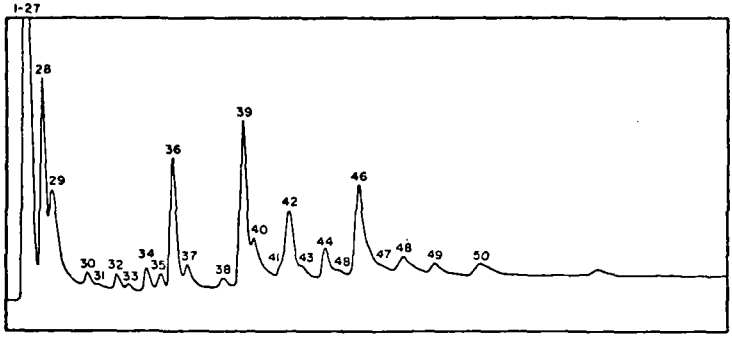

Figure 1. Rigid urethane foam pyrolyzed at 1000°C separated on a UC-98 column. Flame ionization detector response.

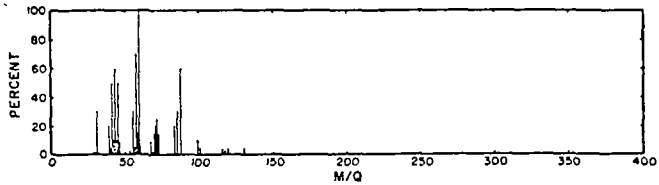

Figure 2a EI spectrum.

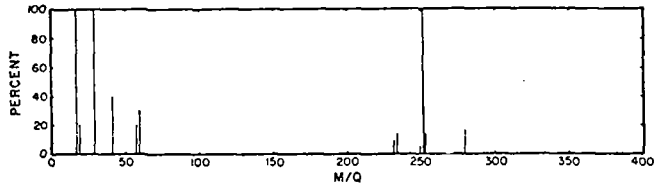

Figure 2b. CI spectrum

Figure 2. A comparison of EI and CI spectra of Dipropoxy TMP.

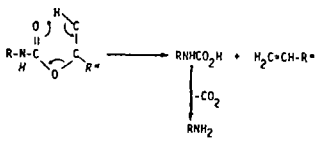

Figure 3. Proposed mechanism for thermal decomposition of rigid urethane.

TABLE I

THERMAL DECOMPOSITION PRODUCTS RESULTING FROM A RIGID-URETHANE FOAM ON 12' 10% UC-98

Peak Number	Compound	
28	Benzonitrile	GCMS+GCCIMS
29	Aniline	GCMS
30	N.I.*	
31	N.I.	
32	dipropoxydiene-TMP	GCCIMS
33	N.I.	
34	monopropoxy-TMP	GCCIMS
35	dipropoxy-one-TMP	GCCIMS
36	dipropoxyene-TMP	GCCIMS
37	dipropoxyene-TMP	GCCIMS
38	tripropoxydiene-TMP	GCCIMS
39	dipropoxy-TMP	GCCIMS
40	dipropoxy-TMP	GCCIMS
41	tripropoxy-one-TMP	GCCIMS
42	tripropoxyene-TMP	GCCIMS
43	tetrapropoxydiene-TMP	GCCIMS
44	tripropoxy-TMP	GCCIMS
45	tetrapropoxydiene-TMP	GCCIMS
46	tripropoxy-TMP	GCCIMS
47	tetrapropoxyene-TMP	GCCIMS
48	tetrapropoxyene-TMP	GCCIMS
49	tetrapropoxy-TMP	GCCIMS
50	tetrapropoxy-TMP	GCCIMS
51	N.I.	

*No identification.

On-Line Hydrogen/Deuterium Exchange in Capillary Gas Chromatography/ Chemical Ionization Mass Spectrometry (GC-CIMS) as a Means of Structure Analysis of Complex Mixtures.

W. J. Richter, W. Blum and J. G. Liehr,
Zentrale Funktion Forschung, CIBA-GEIGY AG, Basle, Switzerland

It was shown by HUNT et al. [1] that deuterium exchange of acidic hydrogen atoms can be effected in an on-line fashion by means of chemical ionization using D_2O as reactant under customary CI conditions. Direct sample insertion of selected single compounds, containing OH and NH-groups gave excellent exchange efficiency even in instances in which up to five acidic protons were present in the molecule [1]. Since the number of exchangeable hydrogen atoms represents a distinct structural parameter, its determination appears particularly useful in the analysis of constituents of mixtures, rather than single compounds, by GC-MS techniques. The diagram shows a dual gas glass capillary GC-MS system operating in the CI mode, which is capable of performing such an exchange on mixtures of high complexity.

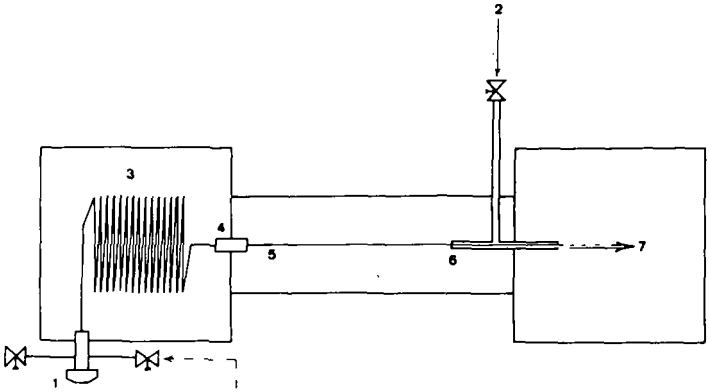

Independent choices of optimal carrier and reactant gases (1 and 2) are possible by admixing the latter behind the glass capillary column (3). Owing to the small carrier gas flow in capillary columns, compared to large ones of reactant gas, no special enrichment device is required. Direct coupling of the thin-film capillary is afforded via a platinum capillary (5) [2]. It is part of a coaxial interface (6) [3] that serves the common admission of both gases, without prior mixing, to the CI source of a Finnigan 1015 quadrupole mass spectrometer (7). Polar reagent gases such as water or methanol and their deuterated analogs can thus be admitted without interacting unfavorably with the inside wall coating of the interface capillary. These coatings are built up, during initial use, by stationary phase bleeding from the column and are necessary for due operation of the system.

In order to illustrate the potential use and the performance of this system with respect to GC resolution and exchange quality attained, a mixture of o-, m- and p-phenylenediamine was subjected to non-exhaustive N-methylation. The objective was to generate a variety of products with different numbers of acidic hydrogen atoms to be determined. The three starting materials would allow the presence of not less than 18 partly

isomeric and partly homologous compounds in such a model mixture.

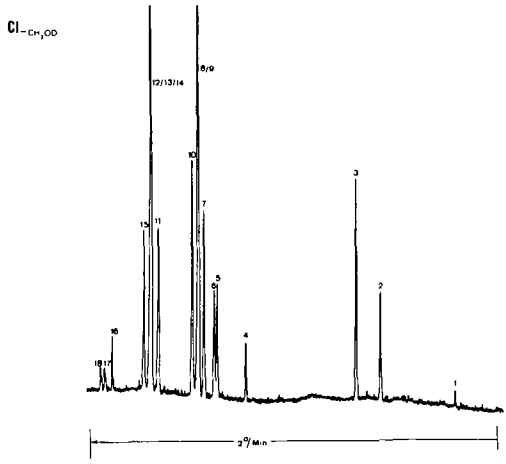

The above figure shows the gas chromatogram of the resulting mixture, obtained by analog recording of integrated total ion current as a function of time. Comparison of this trace with an FID gas chromatogram obtained in a parallel GC analysis without MS coupling revealed that practically no loss of the high separation efficiency of the glass capillary column had occurred. The mass shifts observed between successive GC-CIMS runs, in which methanol and methanol-O-D were used as reactants, furnished the number of exchangeable H-atoms for every single component. This number had to be consistent with the degree of methylation that was known from the m/e values of the MH^+ ions. Classification of the components into homologues is thus readily accomplished. Identification of the substitution type (ortho-, meta-, or para-) required, however, supplementary methylation experiments using the pure isomers instead of a mixture thereof. The detailed analysis of the CI spectra continuously taken and processed by a FINNIGAN 6000 computer system during the runs disclosed that, indeed, all 18 possible compounds were present in the mixture. Incomplete separation was observed only in two instances, i.e. for the components 8/9 and 12/13/14.

The quality of exchange is best exemplified by the CI(CH_3OH) and CI(CH_3OD) spectra of the unreacted phenylenediamines (MW108) which each contains four acidic H-atoms. Exchange of all four hydrogen atoms affords quasimolecular ions MD^+ at m/e 114. Calculations reveal total H/D exchanges in excess of 96 %. Correspondingly, the CI(CH_3OH) spectrum exhibits MH^+ quasimolecular ions at m/e 109. $M^{+\cdot}$ ions at m/e 108 as possible products of charge exchange are largely absent when using methanol as the reactant. Concomitant charge exchange, to which donor-substituted aromatic compounds are rather susceptible, would definitely interfere with evaluating the results, particularly when trace amounts or incompletely separated components are to be analyzed.

References:

1. D. F. Hunt, C. N. McEwen and R. A. Upham, Anal. Chem., 44, 1292 (1972)
2. N. Neuner-Jehle, F. Etzweiler and G. Zarske, Chromatographia 6, 211 (1973)
3. W. Blum and W. J. Richter, Finnigan Spectra 5/1 (1975)

The Analysis of Polymer Degradation Products by Chemical Ionization Mass Spectrometry.

D. A. Chatfield, F. Hileman, K. J. Voorhees, J. H. Futrell, and I. N. Einhorn, The Flammability Research Center and the Departments of Material Science and Chemistry, The University of Utah, Salt Lake City, Utah 84112

Methodology has been developed for the quantitative analysis of the thermal degradation products from polymeric materials. Combinations of gas (GC) and liquid (LC) chromatography and simultaneous electron impact (EI) and chemical ionization (CI) mass spectrometry are key factors in the separation and identification of the volatile products and aerosol residues that are formed in the presence of oxidative or inert atmospheres. A computerized and extensively modified AEI MS-30 provides simultaneous EI and CI mass spectra on line from a GC. Less volatile products are LC-separated for analysis by CI/MS. Methane is often the CI reagent gas of choice for the identification of unknown compounds but ammonia and isobutane are valuable when complex mixtures are involved. The application of the above techniques to a study of the thermochemistry of several improved polymeric materials will be discussed.

Surface Chemical Ionization of Arginine and Two Isobaric Tripeptides.*

R. D. MacFarlane, R. Skowronski, A. Hassell, and D. F. Torgerson, Texas A & M University, Department of Chemistry and Cyclotron Institute, College Station, Texas 77843

The amino acid, arginine, and two isobaric tripeptides, gly-leu-ala and ala-leu-gly, have been studied by the method of surface chemical ionization. The reactive ions were nascent H^+, H^- and Na^+ produced directly in the sample by intensely ionizing high energy heavy ions. In each case, the quasi-molecular ions $(M+1)^+$, $(M-1)^-$, and $(M+Na)^+$ were observed in good yield. The positive and negative quasi-molecular ions were produced with comparable intensity. Considerable fragmentation of the arginine quasi-molecular positive ion was observed, mainly the result of the release of small stable molecules and homolytic cleavage. New observations for the tripeptides include the attachment of up to 3 Na^+ ions and the preference for fragment ions associated with the N-terminal part of the tripeptide.

*Work supported in part by the U.S. AEC and The Robert A. Welch Foundation.

Quantitative Analysis of Fatty Acids in Biological Systems by Chemical Ionization Reconstructed Mass Chromatography

JOSEPH D. WANDER, SEYMOUR M. SABESIN, LOIS B. KUIKEN, NORMAN W. FLYNN, JAMES B. RAGLAND, and FREDERICK PETTY

Stout Laboratory for Neuroscience and Department of Medicine University of Tennessee Center for the Health Sciences Memphis 38163

The chemical ionization (c.i.) mass spectrum (m.s.) of the Me ester (FAME) of a fatty acid in an isobutane-plasma is dominated by a single ion $(M+1)^+$ formed by capture of H^+; c.i. (methane) also affords this ion, plus a second major ion formed by loss of H^- $(M-1)^+$. As mixtures of FAMEs are separable by gas chromatography (g.c.), we investigated the use of reconstructed mass chromatography of the intense $(M+1)^+$ ions as a potentially sensitive and specific method for one-step quantitative determination of fatty acid profiles.

Use of unpurified isobutane as a g.c. carrier/c.i. reagent gas gave good g.c. separations and funnelled nearly all of the ionization of each component FAME into the $(M+1)^+$ species; however, it soon became clear that the performance of the ion source suffers rapid degradation from such usage, and the performance of the g.c. column also seemed to be degraded.

These difficulties were averted by the use of methane as the carrier/reagent gas, but the fact that two ions, differing by 2 mass numbers, are produced from each FAME requires a complete g.c. separation of those pairs of FAMEs (*e.g.*, Me stearate, M.W. 298, and Me oleate, M.W. 296) that form an ion in common. A 1m x 2mm (i.d.) tubular glass column packed with 3% EGSS-X on Gas Chrom Q, programmed from 130-210° at 6°/min, gave the separation in Figure 1, detected as a net current of ions at $230 \leq m/e \leq 330$. Figure 2 was constructed from the same run by recalling (*i.e.*, retrospectively monitoring) ion currents observed at *m/e* ratios characteristic of the individual $(M+1)^+$ ions of five FAMEs; thus, (a) the overlapped responses to Me linoleate (18:2) and Me nonadecanoate (19:0) are deconvoluted, and (b) the base line perturbation is removed from the response of

Me arachidonate (20:4), facilitating area calculations. Areas so measured, were found to fit (r>0.999) the concentration--response expression:

$$ln(moles/mole_{17:0}) = m\,ln(area/area_{17:0}) + b$$

in which mole and area ratios are expressed relative to the internal standard Me heptadecanoate (17:0).

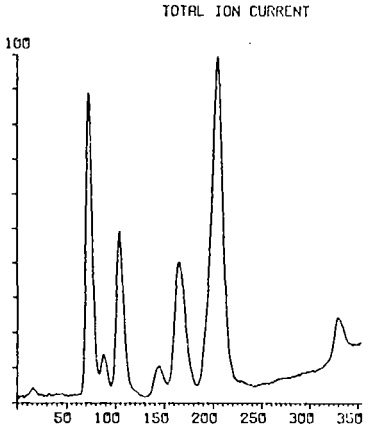

Figure 1

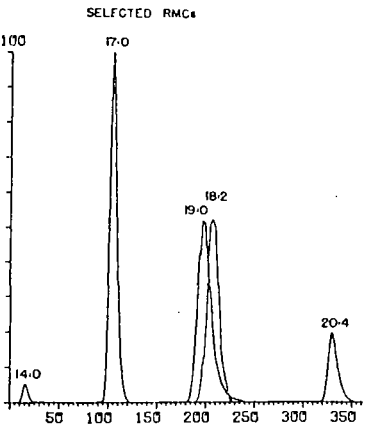

Figure 2

TABLE

Calibration Parameters for and Measured Amounts of FAMEs

FAME	*m*	*b*	*rel. conc. range*	*conc. (nmole/ml)*	*±(%)*
14:0	0.871	0.262	0.01-10	27	7.0
16:0	0.826	0.426	0.01-50	540	5.5
16:1	0.835	1.308	0.01-10	300	5.2
18:0	0.853	0.497	0.01-10	108	11.1
18:1	0.832	0.903	0.01-50	865	4.0
18:2	0.863	1.747	0.1-10	2380	3.8
18:3	0.836	0.946	0.01-10	32	10.1
20:4	0.868	1.259	0.1-10	430	4.6

Analytical data in the TABLE were obtained as follows: cholesteryl nonadecanoate (901 nmole) was added to pooled, normal, human plasma (1 ml). Cholesteryl esters were isolated, transesterified, and mixed with 17:0 (352 nmole). Average (triplicates of triplicates) amounts of constituent fatty acids (measured as FAMEs) in this fraction were calculated by inserting area ratios into the expression above.

A detailed version will be submitted for publication in *Lipids*.

PROTON TRANSFER MASS SPECTROMETRY OF RAPIDLY HEATED α-AMINO ACIDS*

Robert C. Pierce and Lewis Friedman
Department of Chemistry
Brookhaven National Laboratory
Upton, New York 11973

The proton transfer mass spectra of 19 α-amino acids have been obtained by evaporation of 5-8 nmol samples from a rapidly heated Teflon surface[1] followed by NH_4^+ single collision ionization (samples of much less than one nanomole are chemisorbed strongly and thus give rate data which are not representative of the bulk evaporation, see Figure 1). The protonated amino acid parents are observed in all samples and serve as the base peak in all spectra but two. Time (temperature) evolutions of fragment ions are coincident with those of the protonated parent in nearly all cases, indicating that deamination, dehydration, and loss of formic acid occur predominantly in the gas phase (see Figure 1). The NH_3 chemical ionization mass spectra of rapidly heated amino acids reveal a lesser degree of fragmentation than the corresponding NH_4^+ proton transfer spectra due to the gas phase stabilization of PH^+ species by neutral NH_3 collisions in the CI source. This observation supports a gas phase mechanism for fragment ion formation. Each amino acid displays a characteristic onset temperature for evaporation (see Table I) which is independent of sample size in the range 2-10 nmol. The analysis of the rates of sample evaporation yield respective rate constants with activation energies (E_a's) for evaporation of the form

$$k_2 = e\,\frac{kT}{h}\,e^{\Delta S^{\ddagger}/R}\,e^{-Ea/RT}. \qquad (1)$$

Large variations in the entropies of activation ($\Delta S^{\ddagger}$'s) are obtained from the preexponential terms in the evaporative rate constant k_2. If the rate limiting step in the evaporation were the transition from activated solid or melt substantially positive $\Delta S^{\ddagger}$ values would be expected. The measurements indicate a large number of the $\Delta S^{\ddagger}$ values are either negative or close to zero. This range of $\Delta S^{\ddagger}$ values would be consistent with an evaporative rate limiting step in which an energized molecule must orient itself in a highly constrained configuration relative to the bulk lattice to achieve an activated state. The subsequent evolution of that molecule into the gas phase would proceed relatively more rapidly. The following mechanism

$$N_s \underset{k_{-1}}{\overset{k_1}{\rightleftharpoons}} N_s^* \qquad \text{(reversible energization, fast)} \qquad (2)$$

$$N_s^* \xrightarrow{k_2} N_s^{\ddagger} \qquad \text{(activation, rate limiting)} \qquad (3)$$

*Research performed under the auspices of the U. S. Energy Research and Development Administration.

and $N_s^{\ddagger} \xrightarrow{k_3} N_g$ (evolution, fast), (4)

where N_s^* is an energized molecule, $N_s^{\ddagger}$ is an activated molecule and N_g is a gaseous neutral, is consistent with these observations.

Extrapolation of the relative evaporation rate data to mass spectrometric studies employing slow sample heating of amino acids and peptides indicates that species containing arginine, histidine, and tyrosine would be considerably more difficult to non-destructively evaporate than those containing exclusively the other amino acid residues. This appears to be in line with the general observations in systems involving both slow heating and rapid heating of these compounds.[1,2]

A detailed account of this work will be submitted to the Journal of the American Chemical Society.

References

1. R.J. Beuhler, E. Flanigan, L.J. Greene, and L. Friedman, J. Amer. Chem. Soc., 96, 3990 (1974).

2. R.J. Beuhler, E. Flanigan, L.J. Greene, and L. Friedman, Biochemistry, 13, 5060 (1974).

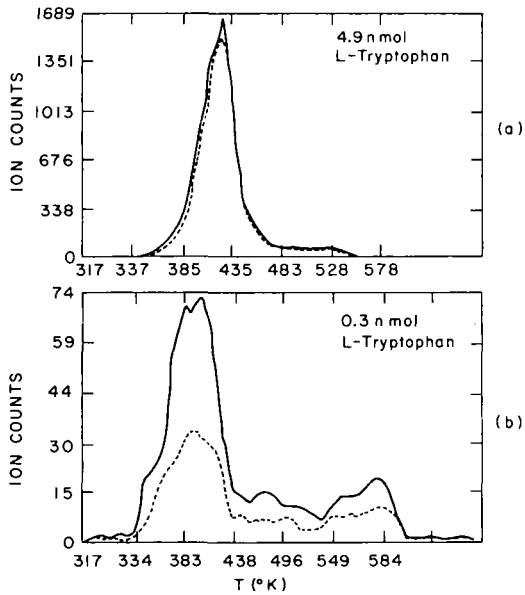

Figure 1. Time (temperature) dependent evolution of ionic species originating from rapid heating of L-Tryptophan samples (~10°/sec). The solid line corresponds to the ion PH^+ (m/e = 205) and the dashed line to the ion PH^+-NH_3 (m/e = 188).

Table I.

Amino Acid Kinetic Evaporation Parameters

Amino acid	Ea (kcal/mol)	$\Delta S^{\ddagger}$(eu)	Temperature of PH^+ evolution (°K)	ln $k_{60°}$	$A_{60°}$
Gly	23±1	−0.5±2.7	325±3	−7.5	1.4 (13)
β-Ala	25±1	7.8±2.8	318±5	−5.3	8.7 (14)
D-Ala	25±2	4.7±5.5	342±8	−6.8	1.8 (14)
DL-Val	19±2	−15.5±5.8	320±5	−8.1	7.6 (9)
L-Leu	20±1	−9.6±2.6	323±4	−6.8	1.4 (11)
L-Phe	21.5±1.5	−3.5±3.9	342±4	−6.2	3.1 (12)
L-Tyr	24±2	−14.4±4.4	412±3	−15.6	1.3 (10)
L-Trp	21±2	−9.2±5.0	340±6	−8.2	1.8 (11)
DL-Ser	20±1	−16.8±2.5	354±6	−10.3	3.9 (9)
DL-Thr	23±2	−1.9±5.2	341±6	−7.8	6.5 (12)
L-Asp	23±1	−13.5±2.5	370±3	−13.6	2.2 (10)
L-Glu	29±1	9.1±2.4	353±8	−12.1	1.6 (15)
L-Lys	21±2	−19.0±4.6	397±2	−13.1	1.3 (9)
L(+)-Arg	32±2	0.5±4.1	441±3	−21.2	2.2 (13)
L-His	34±2	13.5±4.4	392±3	−17.9	1.5 (16)
DL-Met	32±2	17.7±5.9	363±7	−12.6	1.2 (17)
L-Cys	23±1	−6.6±2.9	337±3	−10.1	6.4 (11)
L-Pro	12±2	−32.9±5.5	323±3	−5.5	1.3 (6)
L-Asn	21±2	−12.9±5.1	358±3	−10.0	2.8 (10)

Positive and Negative CIMS of N-Trifluoroacetyl-n-butyl Esters of Amino Acids

Donald F. Hunt, George C. Stafford and Cathy Devine
Department of Chemistry
University of Virginia
Charlottesville, Virginia 22901

The N-trifluoroacetyl-n-butyl ester of amino acids are well suited for separation and detection by gas chromatography using an electron capture detector.[1] In some cases several amino acids from a protein hydrolysate may elute together thus making identification and quantitation difficult. One may elect to use combined gas chromatography-mass spectrometry as an aid in the analysis. However, the electron impact mass spectrum of the N-trifluoroacetyl-n-butyl ester amino acids have been investigated and are characterized by a weak or absent molecular ion, and abundant fragmentation.[1]

We undertook a study of the mass spectra of these amino acid derivatives to see what advantages both positive and negative chemical ionization might offer over electron impact. In the positive mode, methane CI affords an abundant $M+1^+$ ion and much less fragmentation than electron impact. The fragmentation that does occur takes place at the ester functional group and involves loss of butanol or butyl formate.

Sample fragmentation can be eliminated completely by introducing a small amount of ammonia into the source containing CH_4 at one torr. Under these conditions the methane reagent ions are consumed and NH_4^+ is produced as the major reagent ion. The proton affinity of NH_3 is higher than the proton affinity of the amino acid derivatives, thus no protonated (M+1) ion is observed. Ammonia CI spectra, however, does show an $M+18^+$ ion corresponding to attachment of NH_4^+ to the sample molecule.

Due to the high electronegativity of the trifluoroacetyl group, it was expected that the derivatized amino acid would yield abundant negative ions. To test this possibility hydrogen was employed as the reagent gas in our recently developed Townsend discharge CI source.[2] In the negative ion mode H^- and OH^- are the principal reagent ions observed. The OH^- is produced from trace quantities of H_2O present in the source. With hydrogen as a reagent gas the amino acid derivatives give an $M-1^-$ ion as the base peak. Fragment ions usually produced by cleavage at the ester function group were also observed. In an effort to reduce fragmentation a less basic reagent plasma was generated by introducing methanol, acetone and nitromethane to remove H^- and OH^- from the plasma. Even with the least basic reagent plasma of hydrogen/nitromethane extensive fragmentation was observed. However, with NO_2 as a reagent gas at about one torr in the negative mode, the amino acid derivatives afford spectra with abundant $M-1^-$ ions

and reduced fragmentation as compared with hydrogen. Typical fragment ions correspond to loss of 57 ($M-C_4H_5$) and 113 (CH_3CONH_2)

In conclusion, we find that under CI conditions it is possible to select a reagent gas that will provide abundant ions characteristic of the structure and molecular weight of the N-trifluoroacetyl-n-butyl esters of amino acids.

1. E. Gelpi, W. A. Koenis, J. Gibert and J. Oro, J. Chromat. Sci., 7, 604 (1969).

2. C. N. McEwen, T. M. Harvey and D. F. Hunt, Abstracts 22nd Annual Conference on Mass Spectrometry and Allied Topics, Philadelphia, PA, May 1974, No. X-5.

Bacterial Fingerprinting With Isobutane Chemical Ionization Mass Spectrometry.

Frederick Petty, Robert C. Rendtorff, Robert W. Chandler, Norman Flynn, and Joseph D. Wander, Univeristy Tenn. Center for Health Sci., Memphis , TN 38163.

In an attempt to develop a rapid and simple method for bacterial identification we have investigated *E. coli*, *S. aureus*, *S. pyogenes*, *S. fecalis*, *H. influenzae*, *K. pneumoniae*, *N. gonorrheae*, *N. meningitidis*, and *P. aeruginosa*. A small bacterial colony is placed directly into a 1 x 10 mm capillary tube, heat killed, and subsequently rapidly heated to 350°C in the source of a Finnigan 1015D mass spectrometer operated in the chemical ionization mode with isobutane as a reagent gas. Under these conditions the spectra produced are relatively "simple" and may be compared with unknown spectra either manually or with a computerized library search. Preliminary results for the above bacterial species will be presented and the potential applications of this technique in medicine will be discussed.

CHEMICAL IONIZATION MASS SPECTROMETRY OF PENICILLIN

T.L. Chang and C.F. Kuhlman, Wyeth Labs. Inc., P.O. Box 8299, Philadelphia, Pa. 19101

Penicillin is a well known broadspectrum antibiotic. However, in spite of its wide application in many medicinal fields, relatively few mass spectrometric investigations have been made on this compound. The main reason is that it is rather difficult to obtain a good mass spectrum for interpretation. Most penicillins are not very volatile and they are thermally unstable at high temperature. They also produce a very small molecular ion or no molecular ion under conventional EI condition. Since the CI is known to produce an intense MH^+ ion, we felt that the CI technique may produce better mass spectrometric information than the EI.

Four types of medicinally important penicillins were studied. They were ampicillin, hexacillin, pencillin V and dichloxacillin. They were first investigated in their free acid form and then investigated after methylation and silylation. For practical purposes, it would be most convenient that all penicillins could be examined in their free acid form. However, the preliminary examination of free acid penicillins produced a mixed result. Ampicillin and hexacillin produced a very satisfactory CI spectra. They showed an intense protonated molecular ion along with several key fragment ions. Pencillin V showed a protonated molecular ion with a disappointingly weak intensity of less than 1%. Nevertheless, this is an improvement over the EI spectrum which shows no molecular ion at all. The CI spectrum of dichloxacillin showed only the key fragment ions but no protonated molecular ion. The most important fragmentation of all penicillins is the cleavage of the β-lactum ring as shown in the following scheme. Another important fragment ion is the R^+ ion. These key fragment ions and the protonated molecular ion offer vital structural information for all penicillins investigated. High resolution mass measurement was obtained for all CI ions. The major drawback of the CI investigation of free acid penicillins continued to be the thermal instability of these compounds. In all cases, the free acid penicillins were carefully examined at the lowest possible temperature to produce desired CI spectra. If the probe temperature was raised to approximately 200°C, mass peaks of the thermally decomposed products begin to appear in the spectrum.

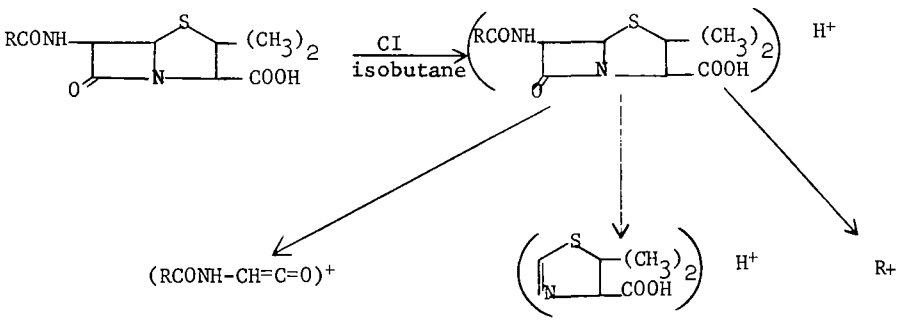

Methylation and silylation are two commonly used techniques to increase the volatility of non-volatile or thermally unstable compounds. Both derivatization techniques produced surprisingly successful results for penicillins. All derivatized penicillins produced an intense protonated molecular ion along with key fragment ions described previously. All spectra was recorded easily at a probe temperature of approximately 100°C. The derivatization procedure undertaken was also extremely simple. About 10-20 μg of sample was placed in a sample capillary tube and 2-5 μl of the derizatization agent was added. The capillary tube was placed on the probe tip and inserted into the instrument for rough pumping. This rough pumping removed the excess derivatization agent. Five minutes later the instrument was turned on and the spectra obtained.

The detailed manuscript of this paper will be published elsewhere.

Quantitative Determination of Glycine (and Other Amino Acids) in Subnanomole Quantities Using Chemical Ionization Mass Fragmentography

NORMAN W. FLYNN, HUGH N. TUCKER, SAMUEL V. MOLINARY, JOSEPH D. WANDER, and FREDERICK PETTY

Stout Laboratory for Neuroscience and Department of Biochemistry University of Tennessee Center for the Health Sciences, Memphis 38163

Quantitative determination of glycine (and other amino acids) is necessary not only to facilitate the diagnosis of diseases associated with faulty metabolism of amino acids, but also to examine the distribution in neural tissue of these compounds, of which several have tentatively been identified as neurotransmitters. Gas chromatography (g.c.) using a 45cm x 2mm (i.d.) glass column packed with 0.3% EGA on Chromosorb G, coupled with a chemical ionization (c.i.) mass spectrometer operated in selective ion monitoring mode (mass fragmentography), provides a specific assay for picomole quantities of these compounds in biological specimens.

In general, minimal fragmentation of *N*-trifluoroacetamido *n*-butyl ester (TAB) derivatives of amino acids occurs subsequent to chemical ionization (c.i.) in the presence of either methane or isobutane. C.i. of TAB-glycine ($CF_3CONHCH_2CO_2C_4H_9$,TAB-Gly) affords two main ions, *m/e* 228 (M+1) and *m/e* 172 (M+1-C_4H_8). [C.i. of TAB-γ-aminobutyric acid (TAB-GABA) likewise produces two principal ions, *m/e* 256 (M+1) and *m/e* 182 (M+1-BuOH)] The capture ion preponderates from c.i.(isobutane), whereas the fragment is favored by c.i.(methane); with either gas, the base peak contributes >50% of the total ionization >*m/e* 100.

TAB-Gly-d_2 was used as an internal standard; essentially no isotopic discrimination occurs on the short g.c. column. The expression:

$$[\text{TAB-Gly}]/[\text{TAB-Gly-}d_2]=m(\text{area}_{\text{Gly}}/\text{area}_{d_2})+b$$

(m=2.17, b=0.020, methane; m=2.09, b=0.0545, isobutane) is used to convert relative area measurements into relative concentration values over a concentration range from approximately 1 nmole/μl to 1 pmole/μl of TAB-Gly. (r >0.9998).

The analytical procedure consists of spiking 1ml of plasma or urine with 625 nmole of gly-d_5, sedimenting macromolecules, lyophilizing the supernatant, and esterifying and acylating the residue; after removal of reagents and dilution to a volume of 100 μl, the products (1 μl) are injected on column for analysis. The TABLE contains values measured for specimens from 3 pediatric patients.

TABLE

Quantities of glycine ([μg/ml] ±S.E.) detected in biological specimens by c.i. mass fragmentography

Specimen	*c.i. (methane)*	*c.i. (isobutane)*	*g.c.*
plasma (*a*)	0.290±.002	0.290±.001	0.22
urine (*b*)	0.344±.022	0.351±.001	0.37
urine (*c*)	2.30 ±.02	2.20 ±.02	2.27

(*a*) Normal; (*b*) Controlled maple syrup urine disease; (*c*) Hyperglycinemia of unknown origin.

The practicability of extending this general procedure to the measurement of neurotransmitters is illustrated for rat ventral spinal tissue (prepared by Dr. John G. Wood, Anatomy). In Figure 1, *m/e* 174 (TAB-Gly-d_2) and *m/e* 184 (TAB-GABA-d_2) are signals from internal standards, relative to which those of the natural compounds are measured. Figure 2 shows that aspartic and glutamic acids are also resolved on the short g.c. column, so it will be possible to measure at least four potential neurotransmitters in a single analysis.

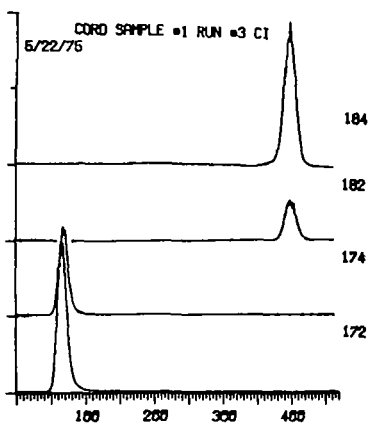

Figure 1

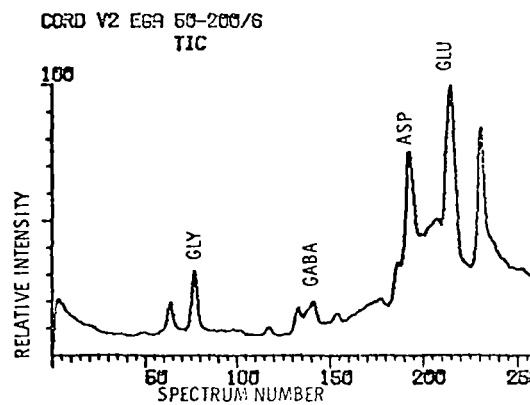

Figure 2

DETERMINATION OF ACTIVE HYDROGEN IN ORGANIC COMPOUNDS USING GC/EIMS OR CIMS

C. N. McEwen and F. G. Kitson
Central Research and Development Department
E. I. du Pont de Nemours and Company
Wilmington, Delaware 19898

Assignment of the structure of an unknown is considerably aided by a knowledge of the acidic hydrogen content (i.e., OH, NH, SH) of the molecule. Methods have been reported for exchanging hydrogen for deuterium by equilibrating the sample in D_2O or CH_3OD before injection into an EI ion source.[1] Exchange in a CI source was shown to occur when D_2O ($\geq$0.4 torr) is used as a reagent gas.[2] Exchange of compounds injected onto a GC column is reported to occur if the column is first equilibrated with D_2O (a base such as $Ba(OH)_2$ is usually added to also exchange active CH hydrogens)[3]. This latter method requires that the column be dedicated to H/D exchange experiments.

We find a simple and expedient means of exchanging hydrogen for deuterium on compounds eluting from a GC into either an EI or CI ion source is to leak a small amount of D_2O into the GC-MS inlet line on the mass spectrometer side of the separator. The D_2O pressure in the EI source is sufficiently low so as not to produce $M+D^+$ ions, and in the CI source sufficiently high so that $(D_2O)_nD^+$ are the major reagent ions with a variety of "filler" reagent gases including methane but not H_2O or NH_3.

Exchange under both EI and CI conditions was shown to involve D_2O adsorbed on glass or stainless steel heated GC-MS inlet walls. Neither D_2O^+ in EI or D_3O^+ in CI was necessary for exchange to occur. Exchange of CH hydrogens was insignificant in the compounds examined except for compounds such as β-diketones which have a high enol content.

Fragment ions from exchanged compounds are very helpful in assigning structure and elucidating the mechanisms of fragmentation. Electron impact is superior for this application, whereas chemical ionization is often better for determining the total acidic hydrogen content, since CIMS usually produces an enhanced MH^+ ion (MD^+ when D_2O is used).

Experimental

The EI exchange experiments were done on a Du Pont 21-490 (all metal GC-MS inlet) mass spectrometer, and the CI experiments were done on either a Du Pont 21-491 or 21-492 (all glass GC-MS inlet) mass spectrometer. All of the 21-490 series instruments were equipped with gas reservoirs.

Injection of 10μl of D_2O into the reservoir - followed by a two minute wait and pump-out - equilibrated the reservoir with D_2O. Two 5μl injections of H_2O at the end of the experiment removes D_2O from the system.

At the beginning of a GC run 3 to 10μl of D_2O is added to the reservoir and leaked into the GC-MS inlet line through a gold leak during the GC run. The inlet system is kept at 250° and the source block at 200°.

---

1. (a) K. Biemann, "Mass Spectrometry," McGraw-Hill, New York, N.Y., 1962, Chap. 5; (b) H. Budzikiewicz, C. Djerassi, and D. H. Williams, "Structure Elucidation of Natural Products by Mass Spectrometry," Vol. 1, Holden-Day, Inc., San Francisco, Calif., 1964, Chap. 2.

2. (a) D. F. Hunt, C. N. McEwen and R. A. Upham, Anal. Chem., 44, 1292 (1972); (b) D. F. Hunt, C. N. McEwen, and R. A. Upham, Tetrahedron Lett., 4535 (1971).

3. G. M. Anthony and C. J. W. Brooks, Chem. Commun., 200 (1970).

ABSOLUTE UNIMOLECULAR DECAY RATES OF ENERGY SELECTED METASTABLE IONS

T. Baer, A. S. Werner and B. P. Tsai
Department of Chemistry
University of North Carolina
Chapel Hill, N.C. 27514

We have investigated a variety of energy selected metastable ions and have measured their absolute rates of fragmentation by Photoion-Photoelectron Coincidence (PIPECO). The technique, which has been previously described,[1] is based on analyzing the asymmetric time of flight (TOF) distribution of fragment ions produced from metastable precursor ions which have reacted in the 6 cm long acceleration region. The ion internal energy is fixed by using an energy analyzed (zero kinetic energy) photoelectron as the "start" for the ion TOF determination.

We have now measured fragmentation rates for various isomers of butadiene,[1] of ethyl chloride,[2,3] 1,2 dichloroethane,[2,3] propargyl chloride,[2,3] and bromobenzene. The results for bromobenzene are shown in Figs. 1 and 2. Two interesting features were revealed in this study.

HCl loss from the chloroethanes and Cl loss from propargyl chloride proceed via a two component exponential decay to form the same product ion. This is similar to Andlauer and Ottinger's data on benzene,[4] in which the two components proceeded to different final products. Two component decay rates can arise in two ways. A) If the initial excitation populates two different electronic states which are isolated from each other then decomposition will occur independently from the two states. B) A second mechanism involves the excitation to a single initial state, but a subsequent isomerization reaction which is competitive with direct dissociation. An analysis of this mechanism leads to a two component decay rate. If one is willing to accept isolated states in the framework of the statistical theory, then neither mechanism violates any assumptions of the statistical theory (QET or RRKM).

The second feature which is emerging from these results concerns the absolute rates. In our previous study[1] of the $C_4H_6^+$ dissociation, we noted that the statistical theory predicts a rate which is nearly 3 orders of magnitude too slow at threshold. However, the theory and experiment appeared to converge at higher energies (.5 eV above threshold). A similar trend is apparent in Ottinger's[5] benzonitrile data. At the time of this meeting we did not know where the true onset for Br loss from $C_6H_5Br^+$ was, so that we could not compare our data with the theory. We did, however, use the theory to calculate an onset (i.e. a kinetic shift). Earlier in this meeting, Gordon[6] presented data on H loss from benzene which was in reasonable agreement with an earlier study by Lifshitz[7] from which one can derive a heat of formation of $C_6H_5^+$ of 258 kcal/mol. Our calculated kinetic shift is in good agreement with this $C_6H_5^+$ heat of formation. This means that for Br loss from bromobenzene, the QET and experiment agree. Perhaps it is too early to begin to generalize about the correspondence between theory and experiment, but the following pattern appears to be establishing itself. The energy flow among the internal modes of an isolated molecule can not be described statistically near threshold. However, as the energy is increased the energy flow becomes progressively more statistical. We are continuing our investigations on other metastable ions in order to test these ideas.

1. A. S. Werner and T. Baer, J. Chem. Phys. 62, 2900 (1975).
2. T. Baer, A. S. Werner and B. P. Tsai, J. Chem. Phys. 62, 2497 (1975).
3. B. P. Tsai, A. S. Werner and T. Baer, submitted to J. Chem. Phys.

4. B. Andlauer and Ch. Ottinger, Z. Naturforsch. 27a, 293 (1972).
5. C. E. Klots, Z. Naturforsch. 27a, 553 (1972).
6. S. M. Gordon and N. W. Reid, Paper D-12, this conference.
7. C. Lifshitz, A. M. Peers, M. Weiss, M. J. Weiss, Adv. Mass Spectrom. 6, 871 (1973).

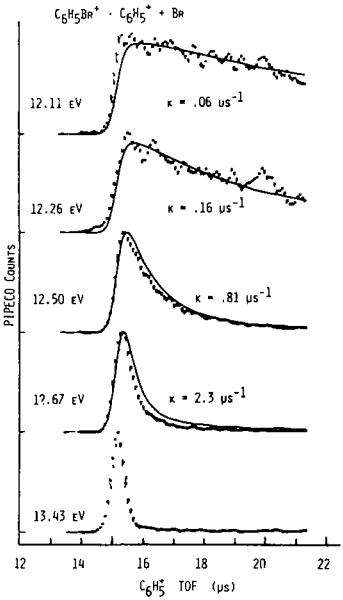

Fig. 1

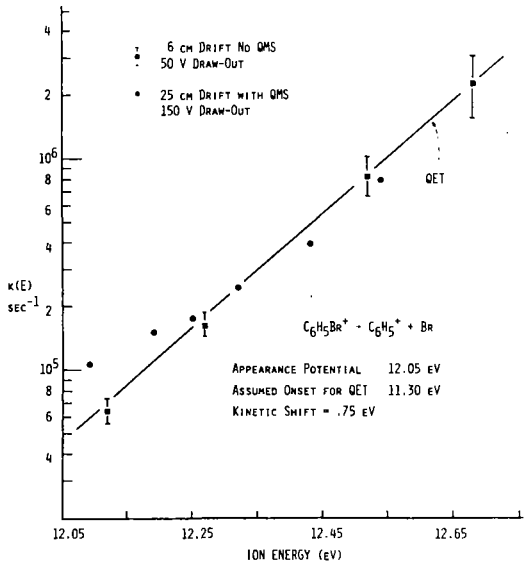

Fig. 2

Field Ionization Kinetics (FIK). Decomposition and Isomerization of $C_4H_8^{+\cdot}$ Radical Ions.

Roger P. Morgan and Peter J. Derrick, Dept. Chem., University College, London WC1H OAJ UK.

Field ionization kinetics (FIK) allows the kinetics of ion decompositions to be determined over a time range extending through picoseconds to microseconds.[1] We report FIK results for the decompositions induced by ionization of the six netural C_4H_8 isomers and of specifically ^{13}C labelled 2-methylpropenes and but-2-enes. These results, together with earlier FIK results for deuterium labelled alkenes,[2] suggest that the $C_4H_8^{+\cdot}$ ions from all six isomers isomerize to a common mixture of interconverting structures within nanoseconds. Major decomposition pathways of the mixture of structures are delineated, and the rates of skeletal rearrangements determined.

1(a) P.J. Derrick and A.J.B. Robertson, Proc. Roy. Soc. Ser. A., 324, 491 (1971).
(b) H.D. Beckey, H. Hey, K. Levsen, and G. Tenschert, Int. J. Mass Spectrom. Ion Phys. 2, 101 (1969).

2 P.J. Derrick and A. L. Burlingame, Accounts Chem. Res. 7, 328 (1974)

A New Method for Structure Determination of Ion-Molecule Reaction Products. PAUL P. DYMERSKI and F. W. MCLAFFERTY. Cornell Univ., Dept. of Chem., Ithaca, NY 14850

Recent modifications of the collisional activation (CA) mass spectrometer (reversed RMU-7) to permit high source pressures while maintaining high resolution have made possible a new method for examining structures of ion-molecule reaction products. This technique has been applied in two areas: (1) To produce ions for structural analysis as products of high-pressure reactions. Protonation of ethylene oxide and examination of the $C_2H_5O^+$ product is discussed in abstract Y-11. (2) To "derivatize" butyl ions by reaction with acetyl chloride to enhance structural differences of the isomeric $C_4H_9^+$ ions.

Under low pressure CA conditions all four isomeric $C_4H_9^+$ cations have similar CA spectra. Condensation of $C_4H_9^+$ with acetyl chloride occurs exclusively by the reaction:[1]

$$C_4H_9^+ + CH_3COCl \longrightarrow C_6H_{11}O^+ + HCl$$

with HCl formation involving hydrogen abstraction exclusively from the butyl ion. CA spectra of the $C_6H_{11}O^+$ ion product shows characteristic differences when formed from different butyl ion isomers. These spectra indicate that n- and sec-$C_4H_9^+$ ions are isomerized to a common structure, presumably sec-$C_4H_9^+$. Tert-$C_4H_9^+$ is a unique and stable structure, while the iso-$C_4H_9^+$ ion apparently isomerizes to a mixture of 72% sec- and 28% tert-$C_4H_9^+$ under the experimental conditions employed.

[1] J. R. Hass and K. R. Jennings, Adv. Mass Spectrom., 6, 711 (1974).

Field Ionization Kinetics Studies of Cleavage and Rearrangement Reactions in Ketones and Alcohols.

Donald G. Patterson, Richard B. Scott and Peter Brown,
Arizona State University, Dept. of Chem, Tempe, Az. 85281

The standard field ionization source (wire type anode) of a Varian-Atlas SM1B double focussing mass spectrometer has been modified to a blade type emitter, for field ionization kinetics measurements. Potential profiles have been calculated for this ion source geometry, and ion lifetimes and rate constants for unimolecular gas phase decompositions assigned. This approach has provided important mechanistic information for reactions of ionized d-labelled phenyl alkyl ketones, and for H_2O elimination from acenaphthenols.

UNIMOLECULAR DECOMPOSITION OF METASTABLE IONS OVER AN EXTENDED TIME SCALE OF 10^{-6} 10^{-3}sec

Richard D. Smith* and Jean H. Futrell
Department of Chemistry
University of Utah, Salt Lake City, Utah 84112

The observation of the decomposition of metastable ions--e.g., in double-focusing mass spectrometers--is typically limited by the experimental configuration to a particular time interval of several microseconds to tens of microseconds with an initial observation time of 10^{-6}sec to 10^{-5} sec. The combination of modest rates and short sampling times often results in insufficient sensitivity to observe specific processes which are postulated to occur.

Here we report on a new technique which utilizes a tandem Dempster-ICR mass spectrometer to observe directly all metastable decomposition processes, for mass selected ions, occurring between approximately 3 x 10^{-6}sec and 4 x 10^{-3}sec. The technique is especially sensitive to slow metastables and extends the range of rate constants which can be observed to processes as slow as 10^{2}sec^{-1}. The system initially selected for examination was the propane molecular ion, $C_3H_8^+$, since extensive experimental[1,2,3] and theoretical[2,4] work is available for comparison.

The instrument used in this study is a tandem Dempster-ICR mass spectrometer previously described.[5] In the present experiments ions are formed by 60 eV electron impact in the Dempster source under essentially zero collision conditions; an average repeller field of 20 volt/cm was used for ion extraction. The accelerating potential was varied from 800-3800 volts to change the time before injection into the ICR cell; at 3800 volts the time interval is 2.7 ± 0.3 μsec between ion formation and injection into the ICR cell for an ion of m/z 44. Ions are mass-selected and decelerated to near thermal energy before introduction into the ICR section. The ICR section employed drift potentials of +0.0 volt and -0.5 volt and trapping potentials of 1.5 volt in this study; the corresponding residence time is 4 msec. Ion detection utilized a variable frequency marginal oscillator calibrated for each ion frequency.

We have studied the metastable unimolecular decay reactions of $C_3H_8^+$ to form $C_3H_7^+$, C_3H_6 and $C_2H_4^+$. In Table 1 the data confirm overall excellent agreement with the QET predictions of Vestal and Futrell,[2,4] provided the time scale is shifted by a factor of about 10. Since the calculation of absolute rates presents a most severe challenge to the theory, disagreement of this magnitude is not unexpected. Adjustment of the parameters in the original calculations[4] would effect excellent agreement between theory and experiment; indeed an increase in the activation energy of about 0.05 eV for reaction (1) would give essential agreement. Further adjustments in vibrational frequencies lead to precise agreement as previously noted.[3] Since these shifts in calculational parameters would generate negligible changes in the relative produce (metastable) intensities, we may conclude that the results in Table 1 lend support to the QET as a suitable framework for discussing these processes.

TABLE 1. Product Distribution for $C_3H_8^+$ from QET[4] for t = 0.25 μ seconds to t = ∞ and Present Results for t = 2.7 μ seconds to t = 4 msec.

	QET	Experimental
$C_3H_8^+$	.887	.864 ± .02
$C_3H_7^+$	.102	.118 ± .006
$C_3H_6^+$	.000	.010 ± .001
$C_2H_4^+$	.011	.008 ± .001

The unimolecular decomposition of the methane molecular ion, and its deutero analogs, have also been studied with the Tandem-ICR. The results for the present study and those from the previous work of Ottinger[6] and Hills, Vestal, and Futrell[7] are presented in Table 2. The work of Hills et al.[7] utilized a modified double focusing instrument while Ottinger used a metastable defocusing technique. The previous work of Dibeler and Rosenstock[8] (not compared in Table 2) was performed on a conventional mass spectrometer and detected only the CD_4^+ $CD_3^+ + D$ metastable transition.

TABLE 2. Intensities of Metastable Transitions in Methane and Deuteromethanes[a]

REACTION		PRESENT RESULTS[b]	PREVIOUS RESULTS[b]	
			Hills et al.[7]	Ottinger[6]
CH_4^+	$CH_3^+ + H$	0.061 ± 0.008	0.009	0.019
CH_3D^+	$CH_3D^+ + H$	0.099 ± 0.015	0.016	0.031
$CH_2D_2^+$	$CHD_3^+ + H$	0.133 ± 0.020	0.028	0.033
CHD_3^+	$CD_3^+ + H$	0.184 ± 0.028	0.040	0.050
CD_4^+	$CD_3^+ + D$	0.080 ± 0.010	0.015	0.032

a. Time to injection into ICR cell is $1.8 \pm 0.3\ 10^{-6}$ sec. for all studies attained by variation of experimental parameters.
b. Metastable intensities in percent of total ionization.

As with the propane molecular ion, QET is qualitatively correct in predicting the relative rate for these processes but gives less than satisfactory values for the absolute rate constants. The QET calculations of Hills et al.[7] predict metastable intensities too small to be observable even for their shorter minimum observation time (a minimum rate constant of 7.2×10^8 sec^{-8} for CH_4^+). This descrepancy may be due to the partial failure of QET for molecules as small as methane. Possible sources of error in the calculations include failure of the classical approximation for the reaction coordinate and errors in frequency assignments for the parent ion. It is also possible to rationalize the present results in terms of a tunneling process, as suggested by Rosenstock[9] and Klots.[10]

* Present address: Naval Research Laboratory, Washington, D. C.

References

1. Ch. Ottinger, J. Chem. Phys., 47, 1452, (1967).
2. M. Vestal and J.H. Futrell, J. Chem. Phys., 52, 978, (1970).
3. P.W. Ryan, J.H. Futrell, and M.L. Vestal, Chem. Phys. Lett., 18, 329, (1973).
4. a. M. Vestal, J. Chem. Phys., 43, 1356, (1965).
   b. M. Vestal and A.G. Lener, ARL Report 67-0114, Jan. 1967.
5. D.L. Smith and J.H. Futrell, Int. J. Mass Spectrom. and Ion Phys., 14, 171, (1974).
6. Ch. Ottinger, Z. Naturforsch., 20a, 1232, (1965).
7. L.P. Hills, M.L. Vestal, and J.H. Futrell, J. Chem. Phys., 54, 3834 (1971).
8. V.H. Dibeler and H.M. Rosenstock, J. Chem. Phys., 39, 1326, (1963).
9. H.M. Rosenstock, Advan, Mass Spectrom., 4, 523, (1968).
10. C.E. Klots, Chem. Phys. Lett., 10, 422, (1971).

SIMULTANEOUS OBSERVATION OF FIRST AND SECOND FIELD FREE REGION METASTABLE PROCESSES IN AN INSTRUMENT OF REVERSED NIER-JOHNSON GEOMETRY

Woodfin V. Ligon, Jr. and Jimmy L. Webb

General Electric Corporate Research & Development

Schenectady, New York 12301

ABSTRACT

Metastable defocusing on an instrument with "normal" geometry (ESA before magnet) completely deflects the main beam in the ESA such that none of the main beam ions reach the 2^d field free region (FFR). This is, however, not the case in an instrument with reversed geometry. Scanning up the accelerating voltage with constant magnetic field effectively scans down through the main beam ions such that they sequentially come to focus at the β slit. None of these ions will pass the ESA because their energy is too high. Metastable daughters of these ions formed in the 2^d FFR will, however, pass the ESA and be observed if fortuitously $(m_2/m_1)x(V_2/V_o) \simeq 1.00$ where m_2 is the mass of the metastable daughter, m_1 the parent mass, V_2 is the new accelerating voltage and V_o is the normal accelerating voltage. These ions can be observed superimposed on metastable daughters from the 1st FFR. This phenomena is especially likely in cases of consecutive losses of the same mass.

The Observation of Metastable Transitions in a Double Focussing Mass Spectrometer Using a Linked Scan of Accelerating Voltage and Electric Sector Voltage

A. F. Weston and K. R. Jennings
University of Warwick, Coventry, England, CV4 7AL
R. M. Elliott & S. Evans, AEI Scientific Apparatus Ltd., Manchester, England

Metastable transitions which occur in the first field-free region of a double focussing mass spectrometer of Nier-Johnson geometry have been investigated by scanning simultaneously at fixed magnetic field the accelerating voltage V and the energy V^o transmitted by the electric sector such that $V^{\frac{1}{2}}/V^o$ is constant throughout the scan. At one point during the scan, $V = V^o$ so that ions formed in the source are transmitted by the electric sector and the magnet is set such that the parent ions of interest, m_1^+, are collected. A scan is then initiated at V = O and a mass spectrum is obtained of m_1^+ and all daughter ions m_2^+ formed from it. The minimum value of m_2/m_1 is set by the instrumental maximum of V and the value chosen for $V = V^o$. In the MS50 instrument (A.E.I. Scientific Apparatus Ltd.), $V_{max} = 8$ kV so that for $V = V^o = 2$ kV, $m_2/m_1 = 0.5$ but by using $V = V^o = 1$ kV, it is possible to reduce m_2/m_1 to 0.35.

Because of the double focussing properties of the combined electric and magnetic sectors, all daughter ions m_2^+ transmitted by the β-slit are focussed at the same point at the collector slit so that narrow peaks approximately symmetrical in shape are obtained. The resolution is largely unaffected by the amount of internal energy released or by the spread of energies transmitted by the β-slit. Hence no information on the release of internal energy can be obtained from this type of scan, but the narrow peaks given by the daughter ions greatly facilitates the determination of their masses.

Although reduction in β-slitwidth reduces peak intensities, it is desirable to work with a narrow β-slit in order to minimise the observation of spurious peaks which may arise from contributions due to ions formed from parent ions differing in mass by a single mass unit from the ion under study, especially if appreciable internal energy is released. For example, when tuned to the m/q = 99 peak in the mass spectrum of CF_3CH_2OH, a linked scan gave peaks at m/q = 100, 99, 98, 82, 81 and 80 when the β-slitwidth was 0.30 inches, but when this was reduced to 0.05 inches, peaks were observed only at m/q = 99 and 81, indicating the loss of a molecule of water by the CF_3CHOH^+ ion. When used in this manner, the linked scan gave rapid and useful results in a wide variety of systems.

A number of the finer details of linked scan spectra were investigated further. In most scans, no peaks are observed until $V = V^o$ when a peak corresponding to m_1^+ is seen. If a peak is seen when $V < V^o$, this is due to the formation of a singly charged daughter ion from a doubly charged parent ion, e.g., in the mass spectrum of toluene, $90^{++} \rightarrow 63^+ + 27^+$ and when tuned to m/q = 45, a peak due to the 63^+ ion is observed before that due to the 90^{++} ions.

In other scans, weak signals were observed corresponding to apparent metastable transitions which were chemically impossible and these were ascribed to the collection of daughter ions m_2^+ formed by decomposition of m_1^+ ions during the time taken to traverse the accelerating region. Such decompositions give rise to signals which are apparently due to a given daughter ion being formed from a continuous range of precursor masses and any linked scan set up to investigate daughter ions from a parent ion of mass between m_1^+ and m_2^+ will give a signal indicating the formation of m_2^+ ions. The origin of a signal of this type can be confirmed by carrying out a scan of V at fixed electric sector voltage with the magnet set to collect m_2^+ ions under normal conditions. For example, in the mass spectrum of toluene, $m/q = 65^+$ ions formed from $m/q = 91^+$ ions in the accelerating region produce signals for any linked scan for parent ions of $m/q = 91^+$ down to 65^+.

Another unexpected feature in certain linked scan spectra was the observation of a broad peak. This type of peak arises from a consecutive decomposition of the type

$$m_1^+ \rightarrow m_2^+ \rightarrow m_3^+$$

in which m_2^+ ions formed in the first field free region are transmitted by the electric sector before further decomposition to give m_3^+ occurs. The release of internal energy broadens the range of voltages over which m_3^+ ions are collected. In the trifluoroethanol spectrum, a broad peak was observed arising from the decompositions

$$81^+ \rightarrow 61^+ \rightarrow 60^+$$

and reduction of the β-slitwidth does not alter the peak shape but merely reduces the intensity.

In general, the linked scan provides a convenient method of identifying daughter ions of a given parent ion and the sharpness of the peaks minimises difficulties encountered in the observation of daughter ions of adjacent masses. When used in collaboration with the accelerating voltage scan, detailed information on energy release can also be obtained for each metastable transition.

Energy Partitioning and Ring Size in Cyclic Transition States.

R. G. Cooks, R. W. Kondrat and J. H. Beynon, Dept. of Chem., Purdue Univ. W. Lafayette, Indiana 47907, A. Maquestiau and R. Flammang, Univ. de L'etat A. Mons, Faculte Des Sci., Mons, Belgique.

The evidence in favor of a 4-centered vs. 6-centered intermediates in the elimination reactions of the molecular ions of phenetoles, acetanilides, phenyl acetates and alkyl benzenes will be reviewed. Energy partitioning measurements on metastable ions in these systems are interpreted in terms of a stepwise 1, 3-hydrogen transfer mechanism or a 1,5-hydrogen transfer mechanism. By the study of partially deuterated phenetoles it is shown that two distinct processes occur in the energy spectra of metastable ions. One is associated with a relatively large and the other with a smaller kinetic energy release. Higher energy metastable ions, selected on the basis of their isotope scrambling behavior, give more of the larger kinetic energy release. All results are therefore consistent with the interpretation that ions of the lowest energy react predominantly by a stepwise 1,3-hydrogen transfer or a 6-centered process while for higher energy ions a concerted 4-centered mechanism is dominant.

METASTABLE TRANSITION ANALYSIS

by E. J. Gallegos
Chevron Research Company, Richmond, California

Introduction

This paper describes the use of mass analyzed ion kinetic energy (MIKE) spectra in the analysis for specific organic components in a mixture. In many cases, this technique gives much of the same information obtained by single ion detection GC-MS, the advantage being that MIKE spectra are obtained in only a small fraction of the time required for GC-MS.

Metastable transition analysis is based on the ability of a double-focusing mass spectrometer to detect specific ionic decomposition processes and identify products and related progenitors without interference from other reaction processes and related ion participants.

The technique is described, and three samples of its application are given. These are terpane, sterane, and alkylphthalate analysis in complex organic mixtures.

Theory

Metastable transitions in mass spectrometry were first reported by Hipple and Condon[1] in 1945. The theories of metastable transitions are summarized in a recent book by R. G. Cookes et al.[2] Even so, a short review of the theories pertinent to this work will be given here. Figure 1 gives a graphic description of metastable transitions and where they are formed.

Results

Metastable transition analysis is possible only if a decomposition process can be found that is uniquely characteristic of a compound or compound type.

There are many systems which obey the requirements for metastable analysis. Three examples of this are given.

Terpanes and Steranes

Terpanes and steranes are characterized by base peaks at m/e 191 and 217, respectively, in their mass spectra. Figures 2 and 3 show the metastable spectra of authentic cholestane and gammacerane, respectively.

Figures 4 and 5 show the metastable scan of 191 and 217, respectively, of the saturate fraction of Green River shale.[3] Table I compares the metastable transition results with GC-MS results.

Table I

		GC-MS	Metastable Analysis
Terpanes	C_{31}	1.0	1.1
	C_{30}	13.6	13.6
	C_{29}	2.3	2.3
Steranes	C_{29}	10.3	10.3
	C_{28}	7.6	6.4
	C_{27}	1.9	1.8

Alkylphthalates

Alkylphthalates can be characterized by a large m/e 149 fragment. Figure 6 shows the metastable spectra of a pure alkylphthalate, top, and phthalate in an organic concentrate from water, bottom.

Even in the presence of other components which form an m/e 149 ion on electron impact, the progenitors are sufficiently different in mass that the phthalate metastable peaks are clearly resolved.

Summary

Metastable transition analysis has many of the benefits of GC-MS without requiring actual physical separation of molecules.

References

1. J. A. Hipple and E. U. Condon, Phys. Rev. 68, 54 (1945).

2. R. G. Cooks, J. H. Beynon, R. M. Copriol, and G. R. Lester, "Metastable Ions," Elsevier Scientific Publishing Company 1973.

3. E. J. Gallegos, Anal. Chem. 43, 1151 (1971).

FIGURE 1

METASTABLE TRANSITION SCHEMATIC

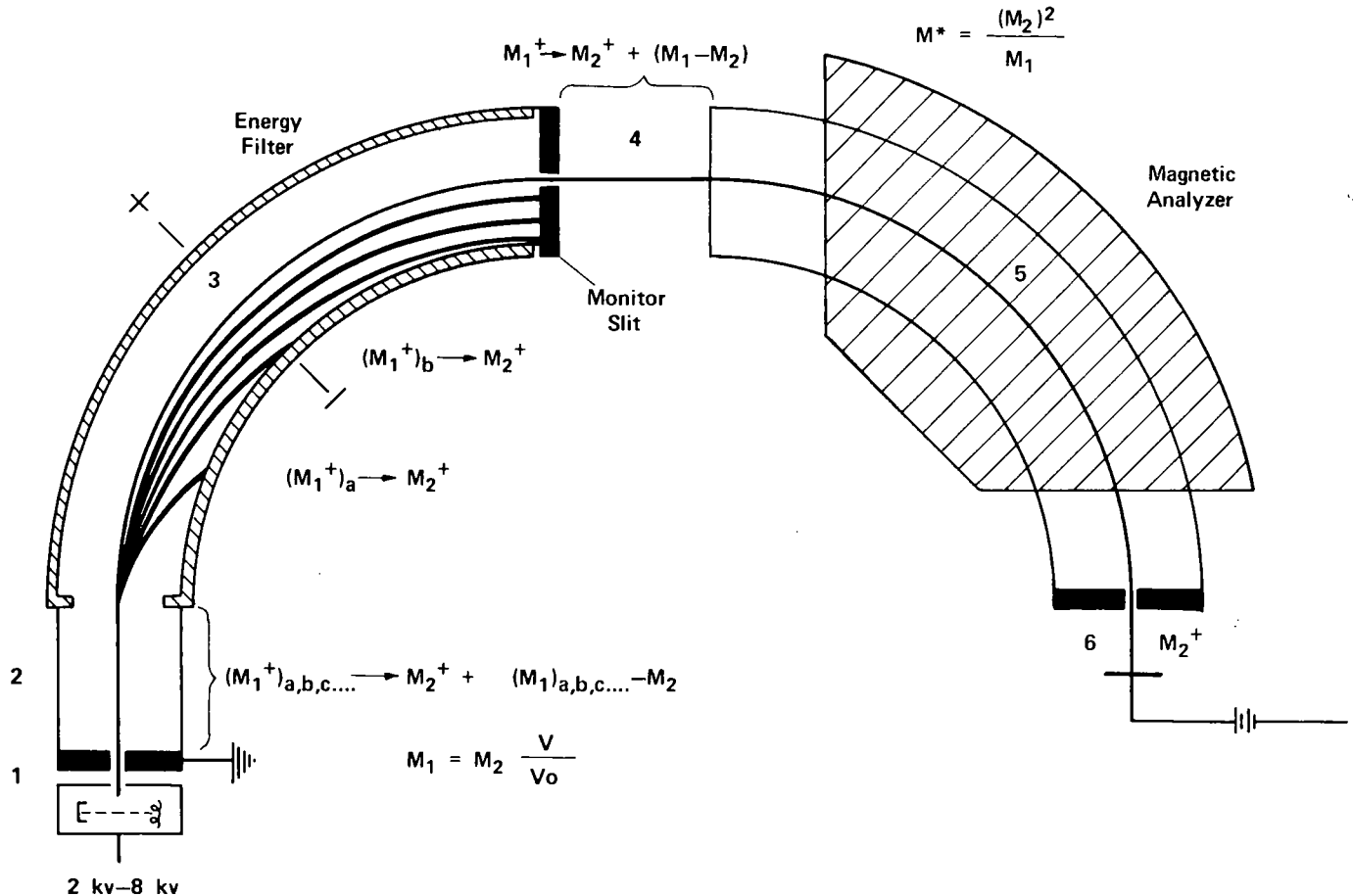

FIGURE 2

METASTABLE SPECTRUM OF m/e 217 OF CHOLESTANE

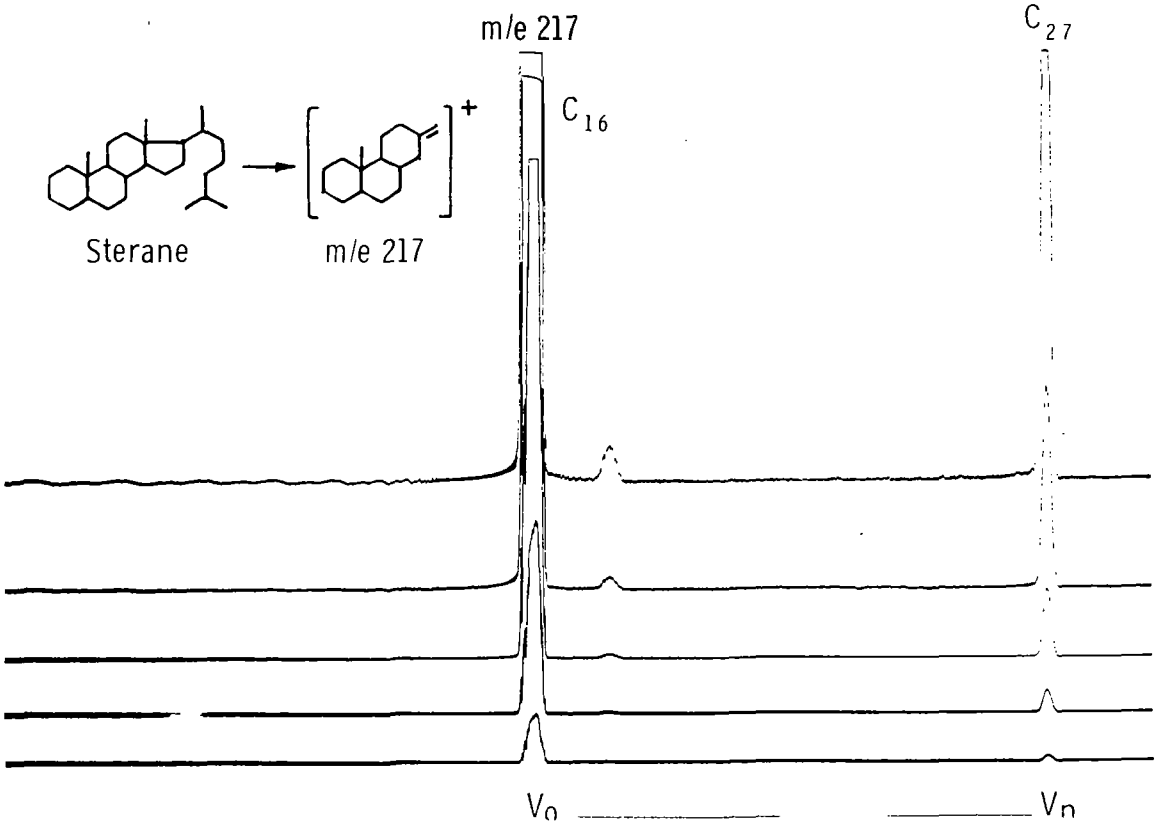

FIGURE 3

METASTABLE SPECTRUM OF m/e 191 OF GAMMACERANE

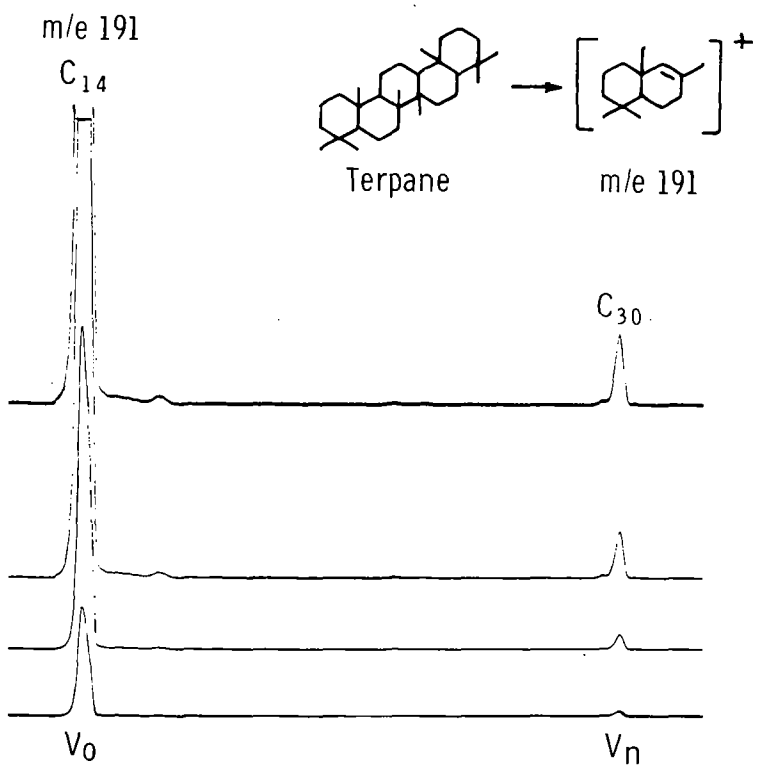

FIGURE 4

m/e 191 METASTABLE SPECTRUM

(TERPANES)

SATURATES, GREEN RIVER, COLORADO, EOCENE, OUTCROP

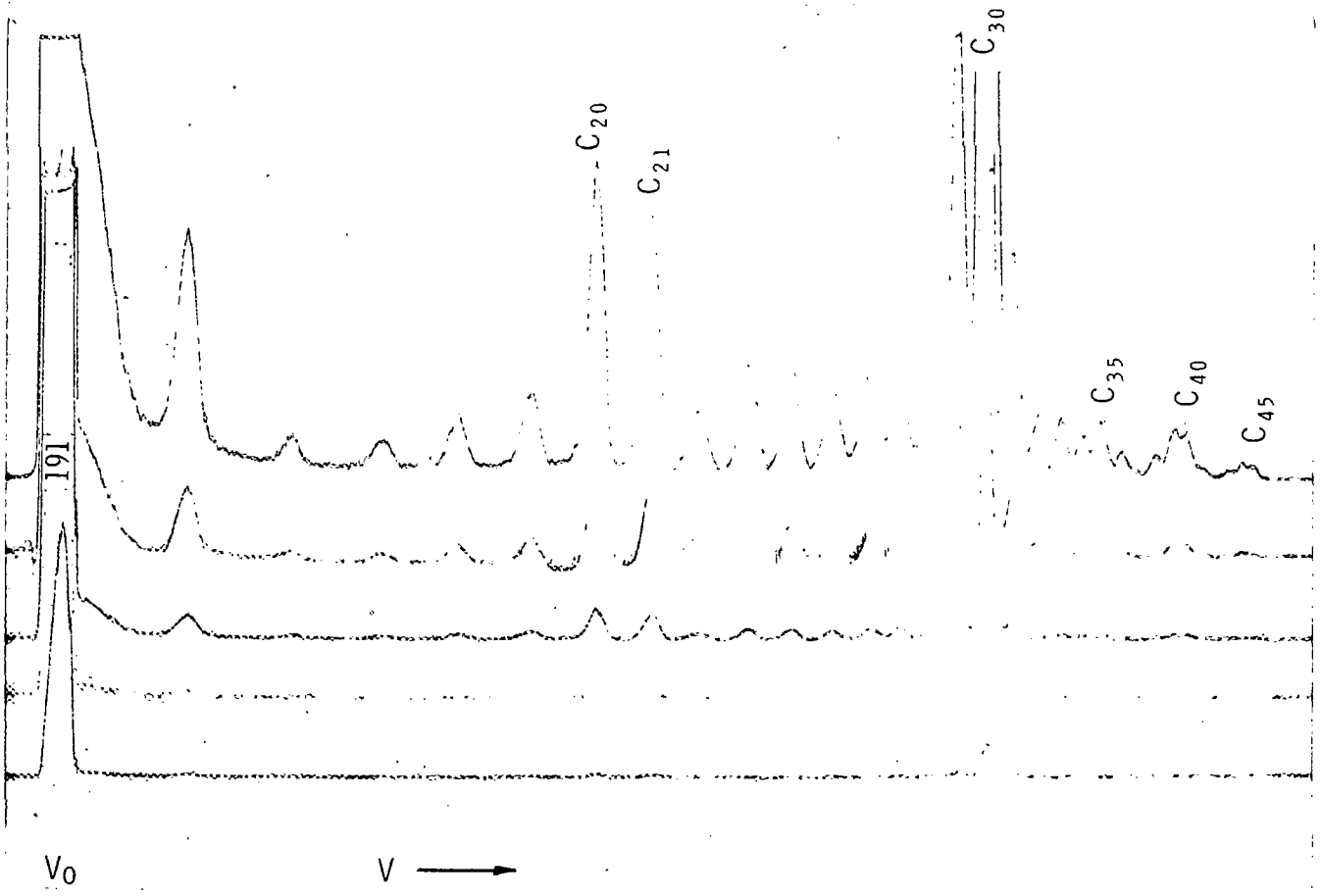

FIGURE 5

m/e 217 METASTABLE SPECTRUM
SATURATE FRACTION OF GREEN RIVER SHALE

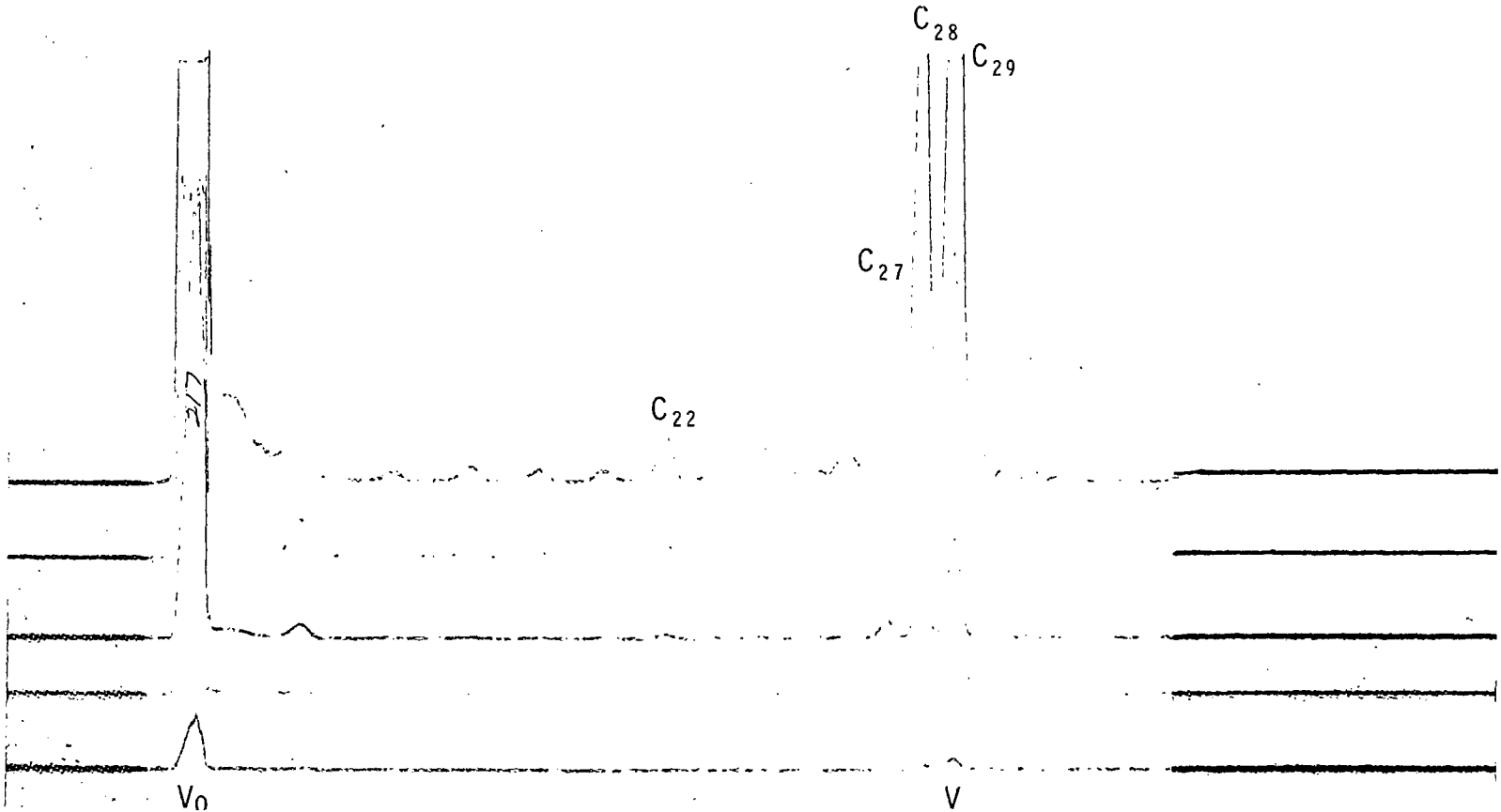

FIGURE 6

METASTABLE SCAN OF m/e 149 OF PURE n-DIBUTYL PHTHALATE AND PHTHALATES IN ORGANICS FROM A WATER SAMPLE

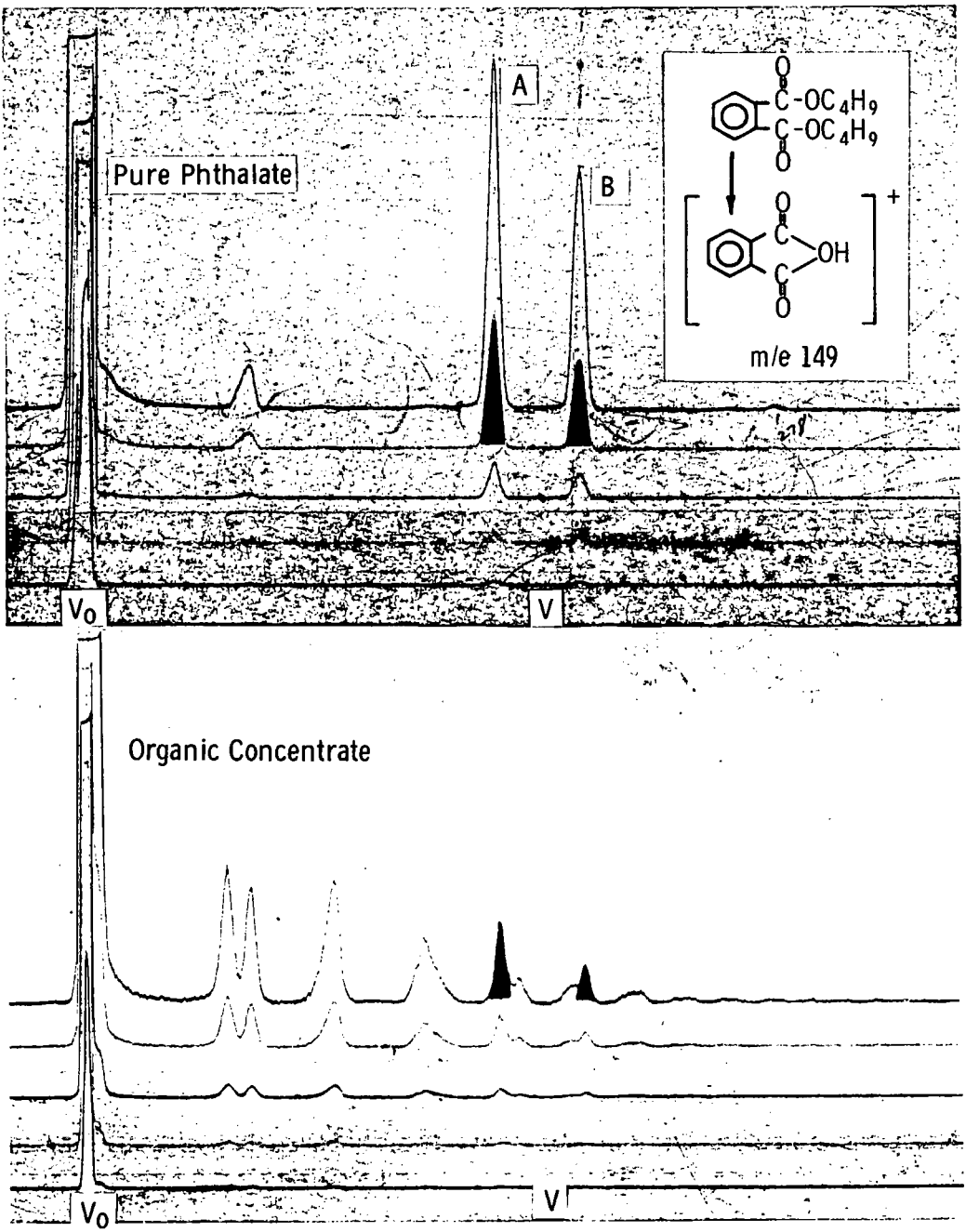

THE STRUCTURES OF FRAGMENTING $C_2H_4O^{+\cdot}$ IONS.[1]

JOHAN K. TERLOUW and JOHN L. HOLMES
Department of Chemistry
University of Ottawa, Ottawa K1N 6N5
Ontario, Canada.

Metastable ion peaks for the fragmentation $C_2H_4O^{+\cdot} \rightarrow C_2H_3O^+ + H^\cdot$ have been studied in the first field-free region of a double focussing mass spectrometer under conditions of good energy resolution. Four isomeric $C_2H_4O^{+\cdot}$ ions were generated $\overset{CH_2-CH_2}{\diagdown O \diagup}{}^{+\cdot}$ (a), $CH_3CHO^{+\cdot}$ (b), $CH_2{=}CHOH^{+\cdot}$ (c) and ${}^+CH_2\text{-}O\text{-}\dot{C}H_2$ (d) from ethylene oxide, acetaldehyde, ethylvinylether (loss of C_2H_4) and dimethylether (loss of H_2) respectively. Each fragmented producing a different ${}^1m^*$ peak having a characteristic shape and kinetic energy release. (b) and (c) show non-composite m^* peaks with $T_{0.5}$ values of 43 and 580 meV respectively while the shape of the m^* for (a) and (d) ($T_{0.5}$ = 430 and 320 meV respectively) suggests that they are both composite peaks in which different proportions of two isomeric daughter ions are generated. The above ions a/d, b and c do not therefore interconvert prior to fragmentation and their characteristic ${}^1m^*$ peaks permit their unequivocal identification, thus providing a powerful method for ion structure determination.

In agreement with some recent collisional activation data[2] it was found that the unbranched aldehydes, cyclic alcohols and 2-haloethanols investigated generated (c) type $C_2H_4O^{+\cdot}$ ions. These are also produced by glycidol and α-furfuryl alcohol. Some compounds generated composite ${}^1m^*$ peaks, e.g. 1,3-dioxolane produced (a) and (c) ions, while compounds which produce prominent $C_2H_5O^+$ ions having the protonated acetaldehyde structure[3], generate m/e 44 ions of structures (b) and (c). In isopropanol these components were separated by a deuterium labelling experiment. The other stable $C_2H_5O^+$ isomer ($CH_3\text{-}\overset{+}{O}{=}CH_2$) is found in the spectrum of ethylene glycol dimethylether and in this case $H^\cdot$ loss appears to generate m/e 44 ions of structure (d). Contrary to earlier proposals[4], pyruvic acid does not generate (b) type ions but produces predominantly ions of structure (c).

The isoelectronic sulphur and nitrogen containing ions have also been investigated. In the case of the sulphur compounds, isomerisation to one common ion structure appears to occur, but the nitrogen containing ions can exist in different isomeric forms, related to the stable C_2H_4O ions.

1 J.L. Holmes and J.K. Terlouw, Can. J. Chem., (in press, 1975).

2 C.C. Van de Sande and F.W. McLafferty, J. Amer. Chem. Soc., (in press, 1975).

3 F.W. McLafferty, R. Kornfeld, W.F. Haddon, K. Levson, P.F. Bente III, S.C. Tsai and H.D.R. Schuddemage, J. Amer. Chem. Soc., 95, 3886 (1973).

4 N.J. Turro, D.S. Weiss, W.F. Haddon and F.W. McLafferty, J. Amer. Chem. Soc., 89, 3370 (1967).

THE ENERGETICS AND METASTABLE CHARACTERISTICS OF FRAGMENTING $C_3H_6^{+\cdot}$ IONS

JOHN L. HOLMES, GWYNETH M. WEESE and JOHAN K. TERLOUW
Department of Chemistry
University of Ottawa, Ottawa K1N 6N5
Ontario, Canada.

Metastable ion peak shapes, dimensions and relative abundances have been measured for the three fragmentations $C_3H_6^{+\cdot} \rightarrow C_3H_4^{+\cdot} + H_2$; $C_3H_6^{+\cdot} \rightarrow C_3H_5^{+} + H^{\cdot}$ and $C_3H_6^{+\cdot} \rightarrow C_3H_3^{+} + H^{\cdot} + H_2$ $C_3H_6^{+\cdot}$ ions were derived from propene, cyclopropane, tetrahydrofuran, cyclohexanone, 2-methyl but-1-ene and cis-pent-2-ene. Activation energies for these fragmentations have been evaluated from A.P. measurements. Three daughter ion dissociations ($C_3H_5^{+} \rightarrow C_3H_3^{+} + H_2$; $C_3H_5^{+} \rightarrow C_3H_4^{+\cdot} + H^{\cdot}$ and $C_3H_4^{+\cdot} + C_3H_3^{+} + H^{\cdot}$) have been similarly examined.

Ion structures have been determined and the metastable energy releases have been correlated with the thermochemical data. It was concluded that the molecular ions of propene and cyclopropane become structurally indistinguishable prior to fragmentation, in agreement with other workers[1,2], but that differences in their metastable ion characteristics can be ascribed wholly to internal energy differences. It was also concluded that fragmenting $C_3H_6^{+\cdot}$ ions generated from the various precursor molecules are structurally indistinguishable and cannot be classified with either molecular ion of the isomeric C_3H_6 hydrocarbons[3]. The relative abundances of the metastable peaks can be correlated with the photoelectron spectra of the isomers. The pathway for the consecutive fragmentation which generated the metastable ion peak (m/e 42 → m/e 39) was shown to be

$$C_3H_6^{+\cdot} \rightarrow CH_2 = C = CH_2^{+\cdot} + H_2 \rightarrow$$ $$+ H^{\cdot}$$

The activation energy of the fragmentation $C_3H_5^{+} \rightarrow C_3H_3^{+} + H_2$ has been measured by determining the A.P. of $C_3H_3^{+}$ from thermally generated allyl radicals. This and related thermochemical measurements confirm earlier suggestions[4] that the cyclopropenium ion is generated at threshold. The metastable peak for this fragmentation is composite (flat top upon flat-

top) and the components arise from the cogeneration of the isomeric cyclopropenium and propargyl cations[5].

1. M.L. Gross and P.H. Lin, Org. Mass Spectrom. 7, 795 (1973).

2. A.Y.-K. Lau, B.H. Solka and A.G. Harrison, Org. Mass Spectrom. 9, 555 (1974).

3. J.L. Holmes and J.K. Terlouw, Org. Mass Spectrom. (in press 1975).

4. P. Goldberg, J.A. Hopkinson, A. Mathias and A.E. Williams, Org. Mass Spectrom. 3, 1009 (1970).

5. J.L. Holmes, A.D. Osborne and G.M. Weese, Org. Mass Spectrom. (in press 1975).

The effect of Ortho-and 2,6-Substitution Patterns on the loss of NO· from Substituted Nitrobenzenes by M. K. Hoffman and M. D. Friesen, Dept. of Chemistry, K.S.U., Manhattan, KS 66506.

This work will be published in Organic Mass Spectrometry.

SEMIEMPIRICAL MOLECULAR ORBITAL CALCULATIONS USED TO STUDY SUBSTITUENT EFFECTS

G.H. Loew and R.F. Kirchner
Dept. of Genetics
Stanford Univ. Med. Center
Stanford, CA 94305

J.G. Lawless
Planetary Biology Div.
NASA-Ames Res. Center
Moffett Field, CA 94035

An attempt has been made to establish molecular criteria suitable for describing the substituent effect on the intensity of the $COCH_3^+$ fragment in the mass spectra of a series of substituted acetophenones. Good correlation to observed intensity ratios is obtained using the ratio of calculated values of the ionization potential of the molecule to the bond density of the cleaving bond. This correlation is comparable to those obtained from the use of Hammett constants by previous investigators. It has the advantage, though, of being related to fundamental properties of the molecules which vary with substituent and can be directly calculated in their "gas phase" state. Calculated ionization potentials as a function of substituent exactly parallel measured values in cases where these two results can be compared. Though bond density variations are very small, the validity of their approximate correlation to experimental values of (AP_{F^+} - IP_M) was established in a test case. It appears that these criteria, which can be calculated and used in a predicitive fashion, will be useful in understanding substituent effects.

Some Aspects of the Ionic Chemistry of C_6H_6

M. L. Gross, S. B. Bronczyk, R. Aerni,
D. H. Russell, G. A. Gallup and D. Steinheider

Department of Chemistry
University of Nebraska
Lincoln, Nebraska 68508

The purpose of this study is to gain structural information on various C_6H_6 radical cation by investigating their ion-molecule reactions using ICR spectrometry.

Under drift-cell conditions, we found no evidence for the bimolecular reaction, $C_6H_6^+ + C_6H_6 = C_{12}H_{12}^+$. Instead, a rather facile reaction of ionized benzene with 2-propyliodide was discovered. The relative rate constants for disappearance of $C_6H_6^+$ k_D and for appearance

$$C_6H_6^+ + C_3H_7I \rightarrow \underset{\underline{m/e}\ 121}{C_6H_6\text{-}C_3H_7^+} + I$$

of m/e 121 k_A for a series of compounds which produce abundant $C_6H_6^+$ ions are reported on Table I. All the compounds produce $C_6H_6^+$ ions which in turn form m/e 121, except tropone. The disappearance of

Table I

Source of $C_6H_6^+$	k_D	k_A
benzene	1.00	1.00
anisole	0.99	0.97
styrene	1.00	1.00
cyclooctatetraene	1.00	0.82
benzaldehyde	1.53	1.16
chroman	1.52	1.17
tropone	0.80	--

$C_6H_6^+$ from tropone is due to a charge exchange reaction to form $C_3H_7I^+$.

The C_6H_6 radical cations produced from various acyclic isomers of benzene (1,3-hexadiene-5-yne, 1-5-hexadiyne, 2,4-hexadiyne, and 1-4-hexadiyne exhibit totally different bimolecular chemistry. No m/e 121 is observed for these compounds. Instead a series of internal reactions occur. For example, ionized 1,3-hexadiene-5-yne reacts with its neutral precursor to form $C_7H_7^+$, $C_8H_6^+$, $C_9H_7^+$, $C_9H_8^+$, $C_{10}H_7^+$, $C_{10}H_8^+$, $C_{11}H_9^+$. Interestingly, ionized benzene is inert with neutral 1,3-hexadiene-5-yne.

In addition, all of the acyclic C_6H_6 isomers produce $C_6H_6^+$ ions which react with 1,3-butadiene to give $C_8H_7^+$, $C_9H_9^+$, and $C_{10}H_{10}^+$. Once again, ionized benzene shows none of this chemistry.

We conclude that at least two different structures exist for $C_6H_6^+$ ions. Considering the disparity in the bimolecular chemistry of ionized benzene (and other compounds in Table I) and the similarities among the acyclics, we suggest that ionized benzene retains it's ring-closed form.

The detailed results will be published in "J. Amer. Chem. Soc."

A second aspect of this work is an ab initio SCF calculation on the mechanism of hydrogen scrambling in ionized benzene. We have found that the energy of the isomerized structure shown in Figure 1 is 1.8 eV above an undistorted benzene ion. Because approximately 3.2eV are required to open the ring and 4.9 eV are needed for fragmentation, the structure in Figure 1 is a reasonable intermediate in the hydrogen scrambling process.

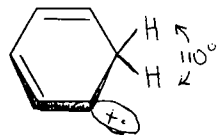

Figure I.

CHLORINE AND BROMINE KINETIC ISOTOPE EFFECTS FROM ISOTOPE-RATIO MASS SPECTROMETRY

James W. Taylor, Donald G. Graczyk, John F. Willey and Robert L. Julian

Department of Chemistry
University of Wisconsin
Madison, Wisconsin 53706

The measurement of heavy atom kinetic isotope effects presents a difficult experimental problem because of the magnitude of these effects. Experimental precision required for chlorine measurements is in the range of one part in 10^4 whereas for bromine the desired precision is one part in 10^5.

To approach these precision limits we have modified our Nuclide RMS-6-60 instrument to accept capacitive integration of the two ion currents from m/e 50 and 52 for chlorine work using CH_3Cl as the sampling gas and m/e 94 and 96 for bromine with CH_3Br as the sampling gas. The instrumental approach is similar to that reported in the literature[1,2] and the conversion of the Cl^- into CH_3Cl has been previously described.[3-5] For our instrumental modification, however, we employed Burr-Brown 3523L operational amplifiers and used a Julie DM-1010 6½ digit digital voltmeter to produce the ratios directly.

Chemical reactions producing chloride and bromide from mechanistically different reactions have been investigated in these laboratories and the chlorine heavy-atom KIE (kinetic isotope effects) used as a probe to mechanism and transition state structure.[6-7] Preliminary data with bromine values for the S_N1 reaction of t-butyl bromide solvolysis in methanol at 20°C gave a bromine KIE of $1.0027_2 \pm 0.0001_5$ compared to the chlorine KIE value of $1.0105_8 \pm 0.0001_5$. For a S_N2 reaction, n-butyl bromide plus thiophenoxide in methanol, the bromine and chlorine KIE values were $1.0014_3 \pm 0.0001_5$ and $1.0089_5 \pm 0.0001_5$, respectively. The capacitive integration modification appeared to improve the instrumental precision by a factor of five, but the measured isotope effects still yielded the same uncertainty. These latter results suggest that the major uncertainty resides in one of the chemical conversion steps - a conclusion we are investigating at the present time.

---

1. M. C. Jackson and W. A. P. Young; *Rev. Sci. Inst.*, *44*, 32 (1973).
2. R. D. Beckinsdale, N. J. Freeman, M. C. Jackson, R. E. Powell and W. A. P. Young; *Int. J. Mass Spec. Ion Phys.*, *12*, 299 (1973).
3. J. W. Taylor and E. P. Grimsrud; *Anal. Chem.*, *41*, 805 (1969).
4. C. R. Turnquist, J. W. Taylor, E. P. Grimsrud and R. C. Williams; *J. Amer. Chem. Soc.*, *95*, 4133 (1973).
5. D. G. Graczyk and J. W. Taylor; *J. Amer. Chem. Soc.*, *96*, 3255 (1974).
6. R. C. Williams and J. W. Taylor; *J. Amer. Chem. Soc.*, *95*, 1710 (1973).
7. R. C. Williams and J. W. Taylor; *J. Amer. Chem. Soc.*, *96*, 3721 (1974).

MASS FRAGMENTOGRAPHIC STUDIES OF SULFUR COMPOUNDS: Some 1-(5-Ethyl-2-thienyl)-1-thiaalkanes

by

Pisal Chandrasurin, Norman G. Foster and Robert W. Higgins*
Texas Woman's University, Department of Chemistry
P. O. Box 23973, Denton, Tx. 76204

Fragmentation studies of the mass spectra of 15 high purity compounds of the 1-(5-ethyl-2-thienyl)-1-thiaalkane series are presented. The molecular ion intensities are moderately strong and easy to verify due to the presence of two sulfur atoms in the molecule. Prominent ions occur in all spectra at m/e 144 and 129. Often the ion of largest intensity is found among alkyl or alkenyl ions. A total of seven different ion species are base peaks for the compounds reported.

The m/e ion at 144 represents a rearrangement ion formed by a hydrogen atom transfer concurrent with cleavage at the sulfur-carbon bond between the thio sulfur atom and the alkyl chain. Additional prominent ions come from ring fragmentations known to occur for the alkylthiophenes. Alkyl ions appear at potentials about equal to the rearrangement ions, about 2 ev higher than the molecular ion. A small but diagnostically useful ion at mass 112 apparently formed by cleavage between the thiophene ring and the thio sulfur atom, and carrying the 5 positioned ethyl group is reported.

The methyl and ethyl compounds are exceptions to the correlations developed in this work. The methyl compound shows an intense ion at mass 143 due to the loss of a methyl group. The 144 ion has an intensity corresponding to the expected isotopic contribution from the 143 ion. A second methyl group is lost from this compound to produce a rather unexpected rearrangement ion of only modest intensity at mass 128. The ethyl compound exhibits its base peak at m/e 157 due to the loss of a methyl group. This molecule does not lose a second methyl group. Metastable peaks from reactions to establish these processes for rearrangements were all observed. Low ionization data are presented in support of suggested mechanisms of fragmentation.

No identification interference with known thienylthiaalkane or thiophenic types of compounds is encountered. The plethora of alkyl type ions might prove to be misleading to the mass spectroscopist unwarned of the behavior of this variety of sulfur compound. Persons using only three or four peaks as in mass fragmentography should anticipate experiencing difficulties with positive identifications.

*deceased

PARTIAL MASS SPECTRA - 1-(5-Ethyl-2-thienyl)-1-Thiaalkanes

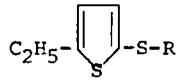

A. Straight Chain Compounds, %Σi

R=	nC_3	nC_4	nC_5	nC_7	nC_8	nC_9
MW	186	200	214	242	256	270
M^+	4.42	4.04	3.61	2.25	1.97	1.74
144	4.17	7.99	9.40	9.44	7.51	6.95
129	10.30	11.86	10.56	6.71	5.05	3.64
Σ Alkyls	14.93	18.05	18.06	37.88	44.32	51.26
Σ Ring Fragments	19.96	21.73	17.19	15.23	14.08	8.73

B. Branched Chain Compounds, %Σi

R=				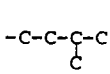	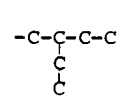	
MW	186	200	200	214	228	226
M^+	2.28	3.61	3.41	2.84	2.16	12.47
144	4.57	9.75	11.57	8.13	11.77	16.34
129	9.28	10.50	13.43	7.11	6.45	8.98
Σ Alkyls	30.82	25.53	22.23	35.21	39.68	30.32
Σ Ring Fragments	18.32	20.57	26.35	16.61	13.84	15.52

Σ Alkyls = 41, 43, 55, 57, 69, 71, etc.

Σ Ring Fragments = 39, 45, 51, 53, 59, 65.

TGA-MS-COMPUTER ANALYSIS OF POLYPHOSPHAZENE COMPOSITES

M.L. Bazinet, W.G. Yeomans and C. Merritt, Jr.

US Army Natick Laboratories, Natick, Massachusetts 01760

One of the more insidious health hazards in the use of plastic materials is the toxicity due to the volatile products evolved during a fire.

This study is concerned with the compounds produced by degradation of polyphosphazene polymers. The instrumentation used for analysis of slow thermal decomposition of phosphazene polymers consists of a duPont Thermal Gravimetric Analyzer, a Perkin-Elmer Gas Chromatograph directly coupled to a duPont 21-491 Mass Spectrometer. An ion counter at the multiplier output provides a digital signal for a Hewlett Packard Model 2116 computer which is used for acquiring the mass spectral data generated during the GC elution of the decomposition products. A disc is used for interim storage of the spectral data prior to transfer to a DEC PDP-15/76 Computer System for subsequent processing.

The analysis procedure consists of weighing and decomposing a sample of the polymer in the TGA chamber at a heating rate of 10°/minute. The heated area is constantly flushed with an atmosphere of helium or oxygen which sweeps the volatile gases onto a GC column, cooled to $-100^{o}C$ for condensation of the volatiles. An oxygen atmosphere flowing at the rate of (60) cc/min was used and the frozen GC column was flushed with helium for five minutes to remove the residual oxygen. When the decomposition has progressed to the desired limit the flow of gases from the TGA is interrupted. Then the program to operate the GC oven at between -100 and $+300^{o}C$ is started. Adjustment of the capillary valve interface at the exit end of the GC column allows the chromatographic elution of volatile components to emerge into the ion source which is kept at about 6×10^{-6}Torr, as measured by the ionization gauge. A chromatogram is provided by an auxillary FID and mass spectra are recorded repetitively during elution.

Figure 1 shows a typical thermogram of the degradation of [poly bis (meta chlorophenoxy) phosphazene] showing a decomposition range of about one hour when the rate is set at 10 deg/minute. The major weight loss, 80% of the sample, occurs between 350 and $450^{o}C$. Figure 2 shows a chromatogram of the volatiles produced from the thermal degradation of chlorophenoxyphosphazene polymer. The low molecular weight compounds obtained such as benzene, phenol, chlorophenol, dichlorophenol, dibenzofuran and other diphenyl compounds can be seen to be structurally related to the polymer. The mass spectra of later eluates show high mass fragments that correspond to the cyclotriphosphazene ring with various fragments of the chlorophenoxy groups attached.

A pyrolysis-GC-MS system, employing a time of flight mass spectrometer (Bendix Model MA 2) was used to study fast decomposition. In this case a 2 milligram sample of chlorophenoxy-

phosphazene was placed in a small platinum boat and pyrolyzed at 600°C for one minute with a 40 ml/minute flow of an oxygen atmosphere. The GC column was a 1/8 inch x 6 foot SP-2300 column. The subambient temperature programmer cooled the oven to -100°C. After a five minute flush with helium at a flow rate of 15 ml/minute the needle valve to the mass spectrometer was opened, thus allowing the sample volatiles to enter the TOF source. The GC oven program was then started. A Columbia Scientific Industries Model 260 spectrum digitizer was used to record the mass spectra. The chromatogram was recorded from the total ion current monitor.

Figure 3 shows the chromatogram of the pyrolysis products from the TOF analysis. In comparison with the TGA analysis the low molecular weight compounds obtained by rapid heating are essentially the same as those observed for slow heating. In rapid pyrolysis the decomposition is more extensive and only small amounts of high molecular weight compounds are observed.

The products observed during thermal decomposition can differ due to different heating rates. Therefore the problem in these experiments is to simulate the natural fire conditions where plastic materials can be exposed to the entire heat spectrum from low heat to instant combustion, since the center of intense heat can be the polymer material itself, while similar polymer material is slowly heated by virtue of being a distance from the heat source.

As preliminary survey tests we used the TGA slow heating rate of 10°/minute thus taking over an hour to reach the same temperature as the pyrolysis method of rapid heating rate of one minute to heat to 600°C. These methods have provided the information needed to evaluate the materials formed from the thermal decomposition of polyphosphazene polymers.

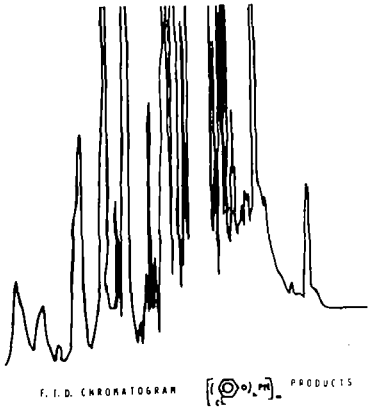

Figure 1

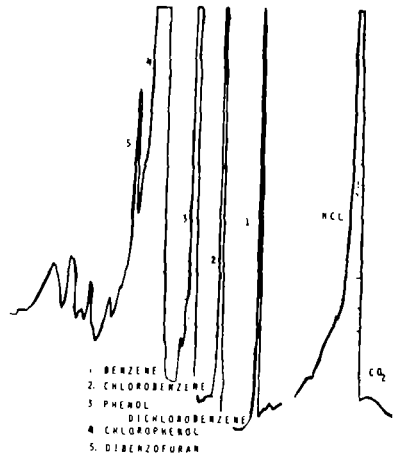

Figure 2

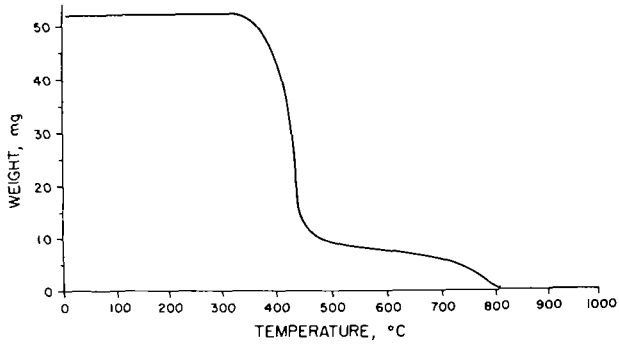

Figure 3

The Mass Spectra of an Amide and some Thioamide

by R.I. Reed and Rahmat Borhani,
Chemistry Department, University of Glasgow,
Glasgow, G12 8QQ, Scotland.

Previous studies of the mass spectra of organosulphur compounds have been concerned mainly with dithiocarboxylic acid esters,[1] dialkyl sulphites,[2] dimethylthio carbamates[3] and substituted thioureas.[4] In two cases[1,2] the occurrence of a McLafferty rearrangement has been reported as a major fragmentation and an intermediate process.

The present investigation reports the mass spectra of an amide and some thioamide which have been synthesised

It appears that the main route of the breakdown is:

Molecule → Molecular ion → Alkyl or Morpholine ion

no comfirmatory metastable peaks could be detected. In every case the occurrence of C-N< bond cleavages, accompanied by a hydrogen migration to the amine part, was observed. A four membered ring transition state[5] can be assumed as a probable mechanism, or it can indicate the formation of a five membered ring although it should be admitted that a sulphur atom often simulates the system -CH=CH- (Diagram 1). In each instance, there are prominent ions at m/e = 57 and m/e = 87 except for diethylamino-1-butyrothioamide, where they appear at m/e = 58 and m/e = 73. The ion at m/e = 57 is ($C_3\overset{+}{H}_7N$) as determined by exact mass measurement. Equally m/e = 87 represent the separation of the morpholino fragment. There is a well defined metastable ion[6] at m/e = 37.34 corresponding to the transition state of $\overset{+}{87} \rightarrow \overset{+}{57}$. Accurate mass measurement gives evidence to prove the pathway.

Decomposition of the base peak ($C_3\overset{+}{H}_7N$) in the first three spectra is probable, to form significant ions at m/e = 28 and m/e = 29. This is supported by the appearance of two intense metastable ions at m/e = 13.76 and m/e 14.75, respectively. However, the results of mass measurement show little evidence of the mechanism (Diagram 2). Finally a similar decomposition as well as further high resolution spectra were observed for diethylamino-1-butyrothioamide (Diagram 3 and 4).

Experimental:

The four compounds were all obtained by a small modification of the customary synthesis. The morpholino-1-butyroamide was first prepared from the appropriate ketone and morpholine by the usual method.[7] The thioamide is prepared by a slight modification of the method of R.Mayer

and K. Gewald[8] obtained by cooling the product with methanol in a mixture of dry ice and acetone. Methanol was removed under vacuum. The purity of all compounds was checked by gas-liquid chromatography.

The mass spectra were obtained upon a GEC-AEI-MS 902S mass spectrometer at 70 eV and a trap current of 500 μA using a direct inlet system at 120°.

References:

1. N.H. Leon, Org. Mass Spec. 6 (1972) 407.
2. A.A. Gamble, J.R. Gilbert and J.G. Tillett, J.Chem.Soc. B. (1965) 655.
3. James C. Tou and R.M. Rodia, Org. Mass Spec. 6 (1972) 493.
4. M.A. Baldwin, Alicza M. Kirkien, A.G. Loudon and Allan MacColl, Org. Mass Spec. 4 (1970) 81.
5. F.W. McLafferty, Anal. Chem. 31 (1959) 82.
6. J.H. Beynon, "Mass Spectrometry and its application to organic chemistry", Elsevier Publishing Company, Amsterdam, 1960, p.251 et seq.
7. Practical Hand Book of Organic Chemistry, English translation by B.J. Hazzard p.432.
8. R. Mayer and K. Gewald, Angew. chem. internat. edit. 6 (1967) 294.

1.

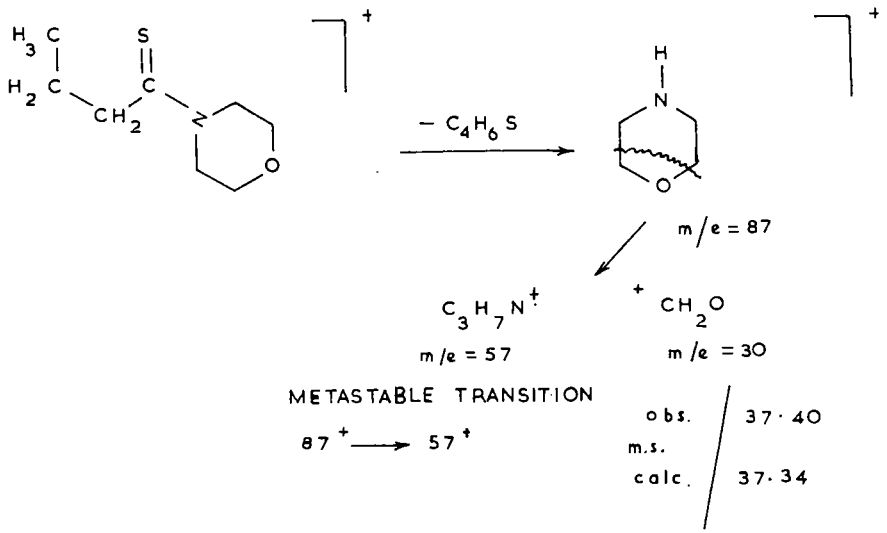

2.

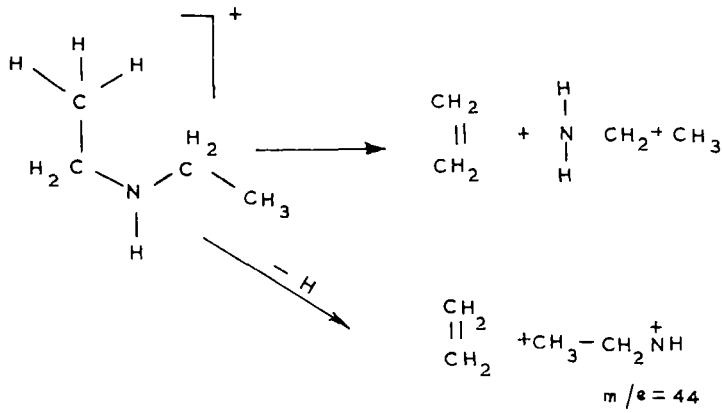

3.

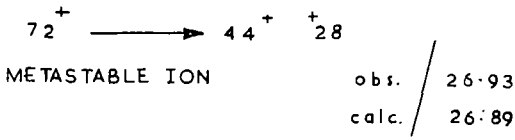

Results of Mass Measurement at m/e = 44

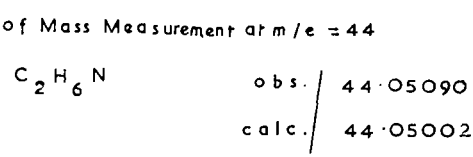

4. Results of Mass Measurement

m/e	Formula		Observed	Calculated
28	CH_2N	large peak	28.018740	28.018723
	C_2H_4	small peak	28.031310	28.031298
29	CH_3N	large peak	29.026499	29.026547
	C_2H_5	small peak	29.039173	29.039123
30	CH_4N		30.034323	30.034371
57	C_3H_7N		57.057108	57.057846
58	C_3H_8N		58.065483	58.065671
73	$C_4H_{11}N$		73.089050	73.089145
87	C_4H_9ON		87.068069	87.068410

Topological studies by bifunctional interactions in mass spectrometry.

S. Najm, G. Wolff, G. Teller, and R. E. Wolff, Univ. Louis Pasteur, Inst. de Chimie, Strasbourg, France.

Interactions between functional groups carried by chains attached to aromatic rings only take place with sufficiently long chains.[1] This can be used advantageously for studying the relative positions of phenolic functions of mono- and polycyclic aromatic systems; the phenolic groups are transformed into an ester of a ω-carboxyalkyl phenol-ether or ester; the occurence of the bifunctional interactions have been related to the relative positions of the phenolic substituents and the length of the alkyl chains; the mechanisms of these interactions has also been studied. The extension of this procedure to aromatic amines, aminophenols and non-aromatic systems will be discussed.

[1] R.E. Wolff, M. Greff, G. Teller, and G. Wolff, Organic Mass Spectrom. 1975, 10, in press.

Field Desorption Studies on Peptides and Peptide Antibiotics on an MS902 Spectrometer

Howard R. Morris*, Karen E. Batley and Edwin C. Barton
(Medical Research Council Group, University Chemical Laboratory, Lensfield Rd., Cambridge, England)

Instrument Modification

A basic A.E.I. EI/FI source has been modified for FD studies as described by Schulten and Beckey for a CEC mass spectrometer (1). We have examined three basic geometries for ion focussing (a) the original A.E.I. geometry (b) a simple single lens system designed by Dr P. Derrick (c) a double lens system based on a Beckey design. Experiments in the FI and FD modes have shown little difference (within an order of magnitude) between these geometries as measured by ion current at the collector slit at 1400 resolving power.

Mass Marking

A mass counting system is described which uses a PDP8/DS10 system for data acquisition, using fluorocarbon standards as references in both the FD(FI) and EI modes.

Peptides and Peptide Antibiotics

We have been primarily interested in FD in connection with our studies on protein and glycoprotein structures (2,3). From our studies to date presented on a number of peptides of varying lengths, encompassing most of the common amino acids, and including acetyl and acetyl permethyl derivatives, the following conclusions have been reached.

1) No complete sequence information was generated from <u>any</u> of the samples studied, despite attempts to fragment by thermal degradation on the wire. Examples of Met.Phe.Gly, Tyr.Leu.Pro.Glu.Phe and Ser.Val.Thr.Pro.Leu.Gly.Ala.Phe are given to demonstrate this.

2) Serious 'salt effects' are observed for peptides containing traces of inorganic salts, as is inevitable in many column separative procedures. Ion current is spread between a number of signals including $(M-H+Na)^+$, $(M+Na)^+$, $(M-H+2Na)^+$ etc. leading to complex spectra, and difficulty in molecular ion recognition.

3) Many less polar samples desorb from the wire too quickly to obtain accurate repeatable results in one sample loading.

We have solved two of the above problems as follows:

a) desalting of the sample prior to FD removes problem 2. We find that electrophoresis is the only reliable method and this is demonstrated on Tyr.Leu.Pro.Glu.Phe.

b) rapid desorption from the wire can be alleviated as follows. The compound under study is first dissolved in a suitable solvent. When in solution a more polar co-solvent is added in restricted volume so as not to throw the compound out of solution. This has the effect of delaying desorption from the emitter and 'spreading' desorption over more milliamp (temperature) values. In the latter respect the addition of a co-solvent appears to have a similar effect to an indirect heating device for the wire (4). The corollary of the above process i.e. dissolution followed by discrete addition of a less polar solvent is helpful in reducing desorption temperatures for very polar samples e.g. folic acid analogues and some

antibiotics.

We have as yet found no simple solution to the lack of sequence data in FD spectra, and we conclude that in its present state FD is of dubious value in sequence studies even as a complementary approach.

A more promising application of FD mass spectrometry is in the study of complex molecules whose structures are largely known as a result of other chemical and spectroscopic work. Two examples of this under study in our laboratory are the antibiotics echinomycin and triostin. From the proposed structures (5,6) the molecular weights are 1084 for echinomycin and 1086 for triostin respectively. Our FD studies of these compounds show that a) echinomycin has an actual molecular weight of 1100.4 as measured against the 1066 signal in the FI spectrum of perfluoroheptyl triazine. Further chemical and spectroscopic studies have enabled us to propose a revised structure for echinomycin, having a thioacetal rather than a dithian cross link (7), and a model of the revised structure can now explain its biological activity.

b) triostin C does possess the disulphide bridge structure assigned (5) by observation of an $M^{+\cdot}$ at 1086. The spectrum also shows the presence of 1088 and associated signals, indicating some dithiol triostin in the sample. This fact is presently being investigated by the comparison with the ^{1}HNMR spectrum of triostin C which shows that despite its crystallinity triostin C is not a pure compound(8).

The solvent effects discussed for peptides earlier are well demonstrated in these less polar antibiotic samples.

Acknowledgements

The authors thank Dr D.H. Williams for his interest in the initial modification of our source, and Professor H.D. Beckey for allowing experts in his laboratory to be consulted. We are grateful to the British Medical Research Council for financial support.

References

1) Schulten H.L. and Beckey H.D. (1973) Org.Mass Spectrom., 7, 861.
2) Morris H.R., Williams D.H., Midwinter G.G. and Hartley B.S. (1974) Biochem.J., 141, 701.
3) Morris H.R., Batley K.E., Harding N.G.L., Bjur R.A., Dann J.G. and King R.W. (1974) Biochem.J., 137, 409.
4) Winkler H.U. and Beckey H.D. (1973) Org.Mass Spectrom., 7, 1007.
5) Otsuka H. and Shoji J. (1967) Tetrahedron, 23,1535.
6) Keller-Schierlein W., Mihailovic M. Lj. and Prelog V. (1959) Helv. Chim. Acta, 42, 305.
7) Dell A., Williams D.H., Morris H.R., Smith G.A., Feeney J. and Roberts G.C.K. (1975) J.Amer.Chem.Soc., 97, 2497.
8) Personal Communication, Dr D.H. Williams.

* Present address : Dept. of Biochemistry, Imperial College, London SW7 2AZ.

Organic Ion Structures From Collisional Activation Spectra.

BASTIAAN VAN DE GRAAF, P. P. DYMERSKI, C. C. VAN DE SANDE, TAKAO NISHISHITA, N. M. M. NIBBERING, and F. W. MCLAFFERTY. Cornell Univ., Dept. of Chem., Ithaca, NY 14850

Collisional activation (CA) spectra have proven to be uniquely useful for structural characterization of isomeric organic ions because such spectra are essentially independent of ion internal energy. Isomers in addition to those previously postulated are shown to be stable for $C_8H_9^+$ and $C_9H_{11}^+$ ions. The behavior of the odd-electron $C_2H_4O^{+\cdot}$ and $C_3H_6O^{+\cdot}$ isomeric ions is in general similar to that expected from the mass spectra of the corresponding molecules. Seven $C_3H_5O^+$ ions are distinguishable, and in particular cases are formed by unexpected pathways. Stable cyclic $C_2H_5O^+$ and $C_2H_5S^+$ ions have been identified. $C_2H_5S^+$ and $C_3H_7S^+$ ions are similar to their oxygen and nitrogen containing analogs in relative stability and formation pathways, but interesting differences can be noted. The proposed cyclic structure of the tetra-methylenechloronium ion has been confirmed by the study of 1-chlorohexane-1,1-d_2 and -4,4-d_2.

INTERPRETATION OF THE MASS SPECTRUM OF AN ORNITHINE-CONTAINING LIPID

M. L. Gross and D. R. Hilker
Department of Chemistry

and

H. W. Knoche and J. M. Shively
School of Life Sciences
University of Nebraska
Lincoln, Nebraska 68508

The electron-impact mass spectrum of an ornithine-containing lipid from Thiobacillus thiooxidans has been interpreted from high resolution spectra, low voltage scans, and complete metastable studies using high voltage scans. The interpretation is consistent with the structure worked out by Knoche and Shively (1) using more classical procedures.

Evaporation from a direct inlet leads to dehydration of the zwitterionic substance to form a 2-piperidone-containing lipid--see scheme 1.

The most noteworthy features of the fragmentation of the $[M-H_2O]^+$ are shown in scheme 2. There are three initial decompositions. A^2 McLafferty rearrangement involving the carbonyl function of 19-carbon fatty acid with the charge going with either fragment accounts for two ions at m/e 350 (rel.A = 17%) and m/e 312 (rel A = 1.4%). The third fragmentation produces m/e 368 (0.5% rel A). Interestingly, these fragmentations serve to degrade the lipid into component parts, a phenomenon of considerable interpretive value.

The remainder of the spectrum consists of expected fragmentation of the initially formed fatty acid and fatty amide ions. Carbonyl-directed cleavages, McLafferty rearrangements, and remote hydrogen transfers account for most of the nitrogen and oxygen-containing ions. In addition, approximately 45% of the total ion current consists of hydrocarbon ions.

The detailed results will be published soon.

Reference:

(1) H. W. Knoche and J. M. Shively, J. Biol. Chem., 247, 170(1972).

Scheme 1

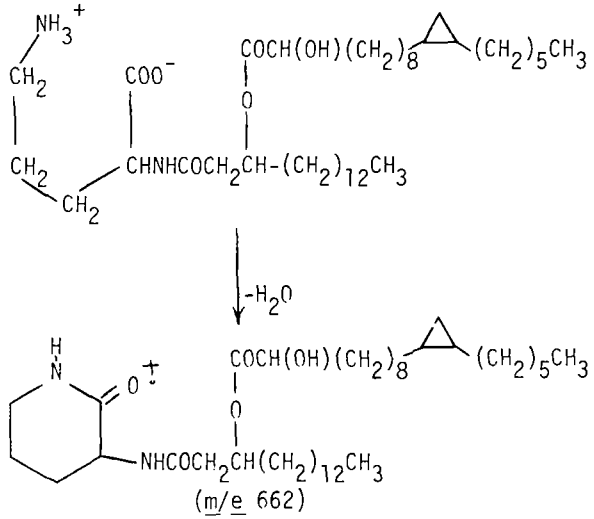

Scheme 2

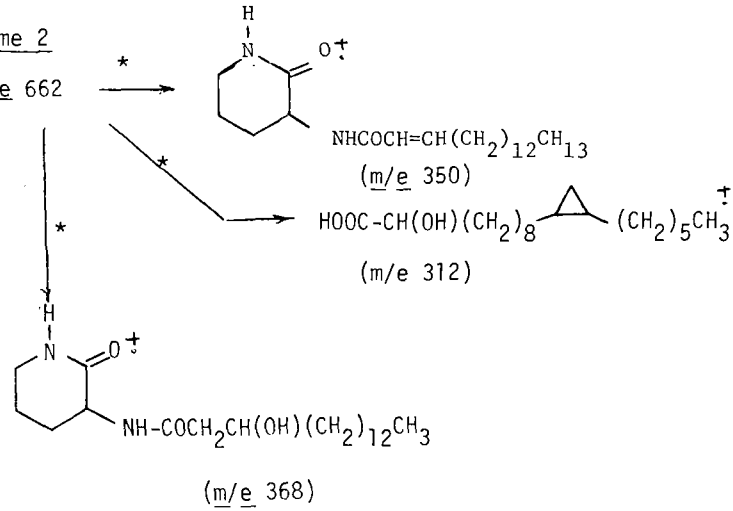

Mass Spectrometry of Cyclopropyl alkyl Benzenes.

Thomas H. Kinstle and Sally Andrewson, Bowling Green State University, Dept. of Chem., Bowling Green, Ohio 43403.

The fragmentation mechanisms of a series of cyclopropylalkyl substituted benzenes, 1, were investigated using extensive deuterium labeling, metastables, and low energy impact

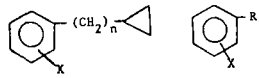

1; n=0,1,2,3
x=o or p-NO_2
o or p-NH_2

2; R=CH_3, Et, i-Pr, tBu
x=o or p NO_2

techniques. The charasteristic cleavage of the cyclopropane rings have been elucidated and the dependence of these processes as a function of n and the nature and location of the aromatic substiutent have been evaluated. Comparisons of the behavior of 1 with the non-cyclopropyl containing analogs 2 have demonstrated the unique influence of the cyclopropane ring in several "ortho-effect" fragmentations.

NEW REFERENCE COMPOUNDS FOR M/E ABOVE 1000

Roy W. King
Department of Chemistry, University of Florida
Gainesville, Florida 32611

Keith B. Baucom
PCR, Inc., P.O. Box 1466, Gainesville, Florida 32602

Perfluorokerosene, the traditional reference substance for high- and low-resolution mass spectrometry, suffers from very low ion intensities above m/e 700 and is usually considered unusable above mass 1000. An ideal high-mass reference should have the inertness, volatility and regular fragmentation pattern of PFK without its rapid fall-off of intensity with mass, should have no overwhelming peaks (cf. m/e 69 in PFK) and, for single-beam accurate mass measurement, should have all ions mass-deficient with respect to C, H, N, O compounds. A series of oligomers based on the $-CF_2CF_2O-$ unit with aromatic end groups has been developed which shows some of these characteristics.

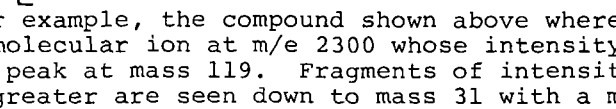

For example, the compound shown above where m+n = 6 shows a molecular ion at m/e 2300 whose intensity is 3% of the base peak at mass 119. Fragments of intensity 0.1% of base or greater are seen down to mass 31 with a maximum separation of 26 mass units. The hydrogen content of the molecule gives rise to clusters of ions separated by one unit which are especially useful for double-beam unit mass marking. Studies are under way to eliminate the hydrogen, making the fragments mass-deficient throughout the spectrum instead of only above mass 300 at present. A repeated spacing of 116 units, corresponding to the $-CF_2CF_2O-$ unit, is prominent in the spectrum and the doubly-charged molecular ion at m/e 1150 with its half mass aids in identifying peaks and counting the spectrum up to mass 2300. The compound is a liquid which can be vaporized by direct insertion at temperatures just above 100°; the spectra described were obtained at 70 ev and an accelerating voltage of 1000 on an AEI MS-30 instrument. Its behavior under ionization conditions other than electron impact has not yet been determined.

The corresponding diamine gives a generally similar spectrum. Shorter-chain related compounds of m.w. 1454 and 1570 have been prepared and show the same intense molecular ions and regular fragments. It is interesting that oligomers based on the branched perfluoropropene oxide unit give intense molecular ions but no appreciable fragments above the M^{++} peak; it appears that the desirable features of the compound described arise from the combination of the tetrafluoroethene oxide chain and the aromatic ends groups. Further work is in progress on this and related compounds.

IONIZATION AND FRAGMENTATION OF SOME SULFOXIDES AND SULFONES INDUCED BY ELECTRON IMPACT

Robert W. Kiser
Department of Chemistry
University of Kentucky
Lexington, KY 40506

Mass spectra of many alkyl and aryl sulfoxides, sulfones, and alkylsulfonates have been reported (1). However, with the exception of some recent photoelectron studies, there is a paucity of information concerning the ionization potentials of these molecules. Further, there are almost no appearance potentials and derived thermochemical data for the various fragment ions formed from these molecules. The goals of this work were to obtain these thermochemical data and to study the mass spectra of additional sulfones by electron impact techiques in an effort to better understand the ionic fragmentation processes in these molecules.

A double-focusing Hitachi RMU-7 mass spectrometer was used in these investigations. Modifications to the basic instrument permitted more detailed ESVV (2) studies of metastable transitions. Rapid voltage scanning of the electric sector (see figure) with simultaneous magnetic field scanning permitted clean separation of multiple metastable peaks and a more complete and accurate conception of the fragmentation processes. Precise mass measurements were made at resolution > 5000 using both the peak-matching method and a computerized data acquisition and reduction technique. Kr, Xe, and H_2O were used as calibrants for the energy scale in the appearance potential measurements; analyses of the ionization efficiency curves were performed using the semi-log plot method and/or the energy compensation technique. Thermochemical data for the molecules were obtained both from the literature (3) and by use of Franklin's method. (4) The molecules studied were SO_2, $(CH_3)_2SO$, $(CD_3)_2SO$, CH_2CH_2SO, $(CH_3)_2SO_2$, $(C_2H_5)_2SO_2$, $CH_3SCH_2S(O)CH_3$, $CH_2(CH_2)_3SO$, $CH_2(CH_2)_3SO_2$, $CH_3OSO_2CH_3$, $C_2H_5OSO_2CH_3$, $CH_2CH{=}CHCH_2SO_2$, $CH_3CHCH_2CH(CH_3)CH_2SO_2$, $(C_6H_5)_2SO_2$, $CH_2SO_2CH_2SO_2CH_2$, $CH_2CH_2SO_2CH(CH_3)SO_2$, and $CH_2CH_2SO_2C(CH_3)_2SO_2$. In the course of this study it was determined that thermal stability of the molecules is a matter of serious concern, e.g., the appearance potentials of the ions formed from butadiene sulfone established that very significant thermal degradation occurs to form butadiene and SO_2. Also, direct probe studies at minimal sample temperatures frequently enhanced the relative abundances of the parent molecule ions and decreased the extent of fragmentation.

The ionization potentials measured for the various sulfoxides were approximately 1.5 ev less than the ionization potentials determined for the corresponding sulfones, e.g., $(CH_3)_2SO$, 9.05 and $(CH_3)_2SO_2$, 10.53 ev; $CH_2(CH_2)_2CH_2SO$, 8.53 and $CH_2(CH_2)_2CH_2SO_2$, 9.90 ev. The alkylsulfonates and sulfones were found to have ionization potentials of about 9.5 to 10.5 ev, obviously dependent upon structure. (The diphenyl sulfone, with I = 8.59 ev, was significantly lower than all other sulfones.) Extended Huckel molecular orbital calculations (5), parameterized with the Hartree-Fock-Slater values for atomic orbital energies given by Herman and Skillman (6) for the Coulomb integrals, and which employed the arithmetic mean formula (7) for overlap integral calculations (K = 1.88), gave minimum ionization potentials (assuming Koopmans theorem to be valid and using experimental geometries) that agreed

rather well with the experimental results. More importantly, these calculations indicate that in the cyclic sulfones and disulfones ionization involves removal of an electron from a molecular orbital that is not localized, but which rather is spread over the entire ring system. Although appearing to involve increased localization on the sulfur atom, approximately the same results are found for the sulfoxides with the EHMO calculations.

Approximate values of heats of formation determined for a subset of the ions examined are (making the usual assumptions about kinetic and excess energies): SO^+, 245; HSO^+, 256; H_2SO^+, 205; CH_2SO^+, 224; CH_3SO^+, 187; $C_2H_4SO^+$, 199; $C_2H_5SO^+$, 175; $C_2H_6SO^+$, 172; $C_3H_5SO^+$, 159; SO_2^+, 209; $C_3H_6SO^+$, 171; $C_4H_8SO^+$, 165; $C_4H_{10}SO^+$, 153; HSO_2^+, 149; $H_2SO_2^+$, 125; $CH_2SO_2^+$, 169; $CH_3SO_2^+$, 144; $C_2H_4SO_2^+$, 152; $C_2H_5SO_2^+$, 125; $C_2H_6SO_2^+$, 121; $C_3H_6SO_2^+$, 176; $C_4H_8SO_2^+$, 142; $C_4H_{10}SO_2^+$, 125; $C_3H_6S_2O_4^+$, 95; $C_4H_8S_2O_4^+$, 75; $C_5H_{10}S_2O_4^+$, 69; $S_2O_3^+$, 116; $C_2H_4S_2O_3^+$, 99; $C_3H_6S_2O^+$, 170; $C_3H_8S_2O^+$, 154; $CH_3SO_3^+$, 128; $CH_5SO_3^+$, 42; $C_2H_5SO_3^+$, 79; $C_2H_6SO_3^+$, 111; $C_3H_7SO_3^+$, 76; $C_3H_8SO_3^+$, 98; and $C_4H_{10}SO_3^+$, 99 kcal/mole. It is noted that heats of formation are lowered by approximately 45 kcal/mole for each additional oxygen atom in an homologous series. Derived proton affinities are: SO_2, 146; CH_3SO_2, 158; and CH_3SO_3H, 184 kcal/mole. Derived ionization potentials are: CH_3SO_2, 8.9 and CH_3SO_3H, 10.2 ev.

A complete report of this study and findings will be submitted for publication soon.

Appreciation is extended to P. A. Purdue and G. Nutter for their valuable assistance in this work.

---

1. S. Meyerson and J. D. McCollum, "Reactions of Isopropyl and Cyclopropyl Phenyl Sulfones under Electron Impact," Div. Phys. Chem., 136th meeting, A.C.S., Atlantic City, 13-18 Sept. 1959; H. Drews, S. Meyerson and E. K. Fields, J. Amer. Chem. Soc., 83, 3871 (1961); D. S. Weinberg, C. Stafford and M. W. Scoggins, Tetrahedron, 24, 5409 (1968); W. E. Truce, R. W. Campbell and G. D. Madding, J. Org. Chem., 32, 308 (1967); R. Smakman and T. J. de Boer, Org. Mass Spectrom., 3, 1561 (1970); and many others.

2. R. W. Kiser, R. E. Sullivan and M. S. Lupin, Anal. Chem., 41, 1958 (1969); and C. Reichert, R. E. Fraas and R. W. Kiser, Int. J. Mass Spectrom. Ion. Phys., 5, 547 (1970).

3. H. Mackle and P. A. G. O'Hare, Tetrahedron, 19, 961 (1963); and H. Mackle, ibid, 19, 1159 (1963).

4. J. L. Franklin, Ind. Eng. Chem., 41, 1070 (1949).

5. R. Hoffmann, J. Chem. Phys., 39, 1397 (1963); ibid, 40, 2474, 2480, and 2745 (1964).

6. F. Herman and S. Skillman, "Atomic Structure Calculations," Prentice-Hall, Inc., Englewood Cliffs, N.J., 1963. 424 pp.

7. M. Wolfsberg and L. Helmholtz, J. Chem. Phys., 20, 837 (1952).

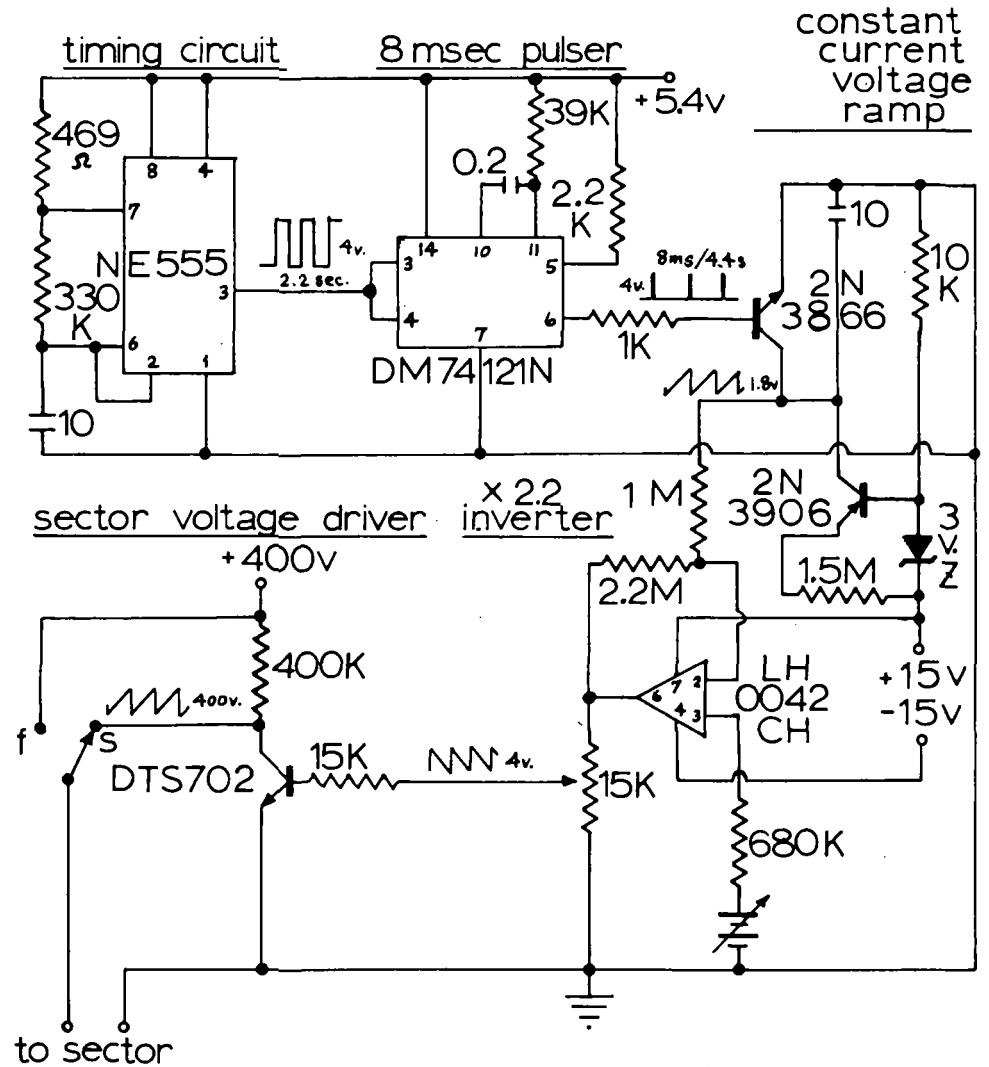

ELECTRIC SECTOR SWEEP CIRCUIT

Studies on the Proteins Ribitol Dehydrogenase, Chloramphenicol Transacetylase, Dihydrofolate Reductase, Azurin and Prothrombin by Mixture Analysis Mass Spectrometry

Howard R Morris*, Anne Dell and Karen E. Batley
(Medical Research Council Group, University Chemical Laboratory Lensfield Rd, Cambridge, England)

The analysis of proteins of unknown structure depends on an ability to sequence minute quantities of peptide(s) of unknown amino acid composition and this has been demonstrated(1). Since then we have been engaged in studies on a number of proteins of unknown structure, the results of which are summarised in this talk. These studies fall into four categories: a) work carried out independently of, but alongside, conventional approaches
b) work on a homologously related sequence
c) independent work on a protein of unknown structure
d) determination of a novel structural feature

a) Ribitol Dehydrogenase and Chloramphenicol Transacetylase

Results have been given for Ribitol Dehydrogenase (2) and are given here (Figure 1) for Chloramphenicol Transacetylase which show an independent determination of over 70% of each of these sequences by mass spectrometry. Many residues have as yet only been determined by mass spectrometry and interesting points arising from the sequence determinations are discussed. These include examples of the power of mixture analysis (2), facile assignments of amides and newly observed fragmentations (3), together with overall success of the strategies employed.

b) Azurin

Clearly the sequence assignment from the mass spectrum can be made more rapidly and with greater confidence if a similar 'template sequence' is available. We are therefore developing an approach for 'screening' homologously related proteins, yielding sequence data of value to evolutionary and other studies. A preliminary attack of this problem gave some 20% of the structure (4) but with refined methods we have now obtained 70% of the sequence of an unknown azurin protein (PfG 149) shown in Figure 2.

c) Dihydrofolate Reductase

The most difficult problem is of course the completely independent structure determination of an unknown protein. We are involved in a study of the sequence of the enzyme dihydrofolate reductase (5), a target enzyme for the chemotherapeutic drug methotrexate. Apart from the numerous protein chemical problems involved we are at the same time developing and testing different approaches to an overall attack on the sequence, and these are discussed.

d) γ-Carboxyglutamic Acid

Mass spectrometry is often most useful when novel structural features are encountered. Some details of our study on the N-terminal sequence of the bovine plasma protein prothrombin are given (6,7). In this work a new amino acid, γ-carboxyglutamic

acid, was assigned by mass spectrometry to ten different positions in the amino acid sequence when classical methods had failed. Evidence for the sequences determined in this study is given.

Acknowledgements

The authors thank the British Medical Research Council for financial assistance, and Miss Valery Barker for excellent work on the amino acid analyser.

References

1) Morris H.R., Williams D.H. and Ambler R.P. (1971) Biochem.J, 125, 189.

2) Morris H.R., Williams D.H.,Midwinter G.G. and Hartley B.S. (1974) Biochem.J., 141, 701.

3) Dell A. and Morris H.R. (1974) Biochem.Biophys.Res.Commun., 61, 1125.

4) Dell A. , Morris H.R., Williams D.H. and Ambler R.P. (1974) Biomed.Mass Spectrom., 1, 269.

5) Morris H.R., Batley K.E., Harding N.G.L., Bjur R.A., Dann J.G. and King R.W. (1974) Biochem.J., 137, 409.

6) Magnusson S., Sottrup-Jensen L., Petersen T.E., Morris H.R. and Dell A. (1974) FEBS Letters, 44, 189.

7) Morris H.R., Thompson M.R. and Dell A. (1975) Biochem. Biophys. Res. Commun., 62, 856.

Legends to Figures

Figure 1 : The partial sequence of Chloramphenicol Transacetylase. Sequences determined by mass spectrometry in upper case lettering. Those determined solely to date by mass spectrometry are underlined.

Figure 2 : Comparison of the type and mutant sequences of a Pseudomonas Azurin. P6009/1 (lower case lettering) shows the classically determined type sequence. PfG 149 (upper case lettering) shows the sequence determined by this mass spectrometric study. The mutations found are underlined.

* Present address : Dept. of Biochemistry, Imperial College, London SW7 2AZ.

CHLORAMPHENICOL TRANSACETYLASE

MET-GLU-LYS-LYS-ILE-THR-GLY-TYR-THR-THR-VAL-ASP-ILE-SER-GLN-
TRP-His-ARG-MET-ALA-Met-Lys-Asp-Gly-GLN-LEU-VAL-LEU-TRP-PHE-
GLN-SER-VAL-ALA-GLN-CYS-THR-TYR-(.....)-SER-SER-LEU-TRP-SER-
GLU-TYR-His-Asp-Asp-Phe-ARG-GLN-PHE-LEU-HIS-LEU-TYR-TYR-SER-
GLN-ASP-VAL-ALA-CYS-TYR-GLY-GLU-ASN-LEU-ALA-TYR-PHE-PRO-LYS-
GLY-PHE-ILE-GLU-ASN-MET-PHE-PHE-VAL-SER-ALA-ASN-PRO-GLN-ALA-
(-TRP-VAL, PHE-THR-SER-PHE-ASP-LEU-ASN-VAL-ALA-Met)(HIS-ILE-
LEU-ALA-ARG-LEU-MET-Asp-Ala-His-Pro-Glu-Phe-ARG-MET-ALA,
TYR-ASN-GLN-THR-VAL-GLN-LEU-ASP-LEU-THR-ALA-Phe, ALA-PHE-LEU-
LYS-THR-VAL-LYS-LYS-Asn-Lys-His-Lys, GLU-ALA-ASP-PHE, HIS-GLU-
GLN-THR-Glu-Thr-Phe, THR-VAL-PHE-HIS,.....)-ASN-MET-ASP-ASN-
PHE-PHE-ALA-PRO-VAL-PHE-THR-MET-GLY-LYS-TYR-TYR-THR-GLN-GLY-
ASP-LYS-VAL-LEU-MET-PRO-LEU-ALA-ILE-GLN-VAL-HIS-HIS-ALA-VAL-
CYS-ASP-GLY-PHE-HIS-VAL-GLY-Arg-Met-LEU-ASN-GLU-LEU-GLN-GLN-
TYR-Cys-Asp-Glu-Trp-Gly-Ala-Gly-Gln.

Figure 1

AZURIN

Ala-Glu-Cys-Ser-Val-Asp-Ile-Gln-Gly-Asn-Asp-Gln-Met-Gln-Phe-
ALA-GLU-CYS-LYS- MET-SER-PHE-

Asn-Thr-Asn-Ala-Ile-Thr-Val-Asp-Lys-Ser-Cys-Lys-Gln-Phe-Thr-
ASN-THR-LYS-ALA-ILE-THR-VAL-ASP-SER-THR-CYS-LYS-THR-PHE-THR-

Val-Asn-Leu-Ser-His-Pro-Gly-Asn-Leu-Pro-Lys-Asn-Val-Met-Gly-
VAL-GLU-LEU-THR-HIS-SER-GLY-ASN-LEU-PRO-LYS-ASN-VAL-MET-GLY-

His-Asn-Trp-Val-Leu-Ser-Thr-Ala-Ala-Asp-Met-Gln-Gly-Val-Val-
HIS-ASN-TRP-VAL-LEU-THR-SER-ALA-ALA-ASN-MET-GLN-PRO-VAL-ALA-

Thr-Asp-Gly-Met-Ala-Ser-Gly-Leu-Asp-Lys-Asp-Tyr-Leu-Lys-Pro-
THR-ASP-GLY-MET-ALA-ALA-GLY-ILE-ASP-LYS-ASP-TYR-LEU-LYS-PRO-

-Asp-Asp-Ser-Arg-Val-Ile-Ala-His-Thr-Lys-Leu-Ile-Gly-Ser-
GLY-ASP-ASP-ILE-ARG- LYS-LEU-LEU-GLY-GLU-

Gly-Glu-Lys-Asp-Ser-Val-Thr-Phe-Asp-Val-Ser-Lys-Leu-Lys-Glu-
ASP-SER-VAL-THR-PHE-ASP-VAL-SER-

Gly-Glu-Gln-Tyr-Met-Phe-Phe-Cys-Thr-Phe-Pro-Gly-His-Ser-Ala-
PHE-PHE-
Leu-Met-Lys-Gly-Thr-Leu-Thr-Leu-Lys
LYS-GLY-THR-VAL-THR-VAL-LYS

Figure 2

Analytical Applications of Photodissociation Spectroscopy

Robert C. Dunbar[‡]

Department of Chemistry, Case Western Reserve University
Cleveland, Ohio 44106

ABSTRACT

Photodissociation spectroscopy is a new ion spectroscopic technique based on observing the wavelength-dependent photolysis of a gas-phase ion under optical irradiation. Methods for obtaining photodissociation using Ion Cyclotron Resonance instrumentation are well developed, and the technique is straight-forward even with a relatively simple spectrometer.

Photodissociation spectra are characteristic of the structure of the ion being irradiated, and provide a way of obtaining optical spectroscopic information about ions. The technique is promising as a way of distinguishing between ions of the same mass but differing structure, and often provides a clear distinction between isomeric ions whose mass spectral fragmentation patterns are indistinguishable.

The potential utility of this technique as an analytical tool supplementing conventional mass spectral analysis is illustrated by the easily differentiated spectra characteristic of various types of hydrocarbon cations. Saturated hydrocarbons, olefins, conjugated dienes and aromatic systems all show characteristic spectra. Saturated hydrocarbons show moderately strong broad absorption bands covering much of the visible and near UV; olefins show relatively weak absorption near 280 nm; conjugated dienes show a strong peak near 350 nm and a weaker peak near 500 nm; while aromatic systems show weak peaks near 260 nm and 450 nm. In this context, a strong peak means a cross section of the order of 3×10^{-17} cm^2 (corresponding to $\log \varepsilon \approx 4$), while a weak peak has a cross section of the order of 3×10^{-18} cm^2 (corresponding to $\log \varepsilon \approx 3$).

[‡]Alfred P. Sloan Fellow

PARTICULATE IMPACT MASS SPECTROMETRY

Frank T. Greene

Midwest Research Institute
Kansas City, Missouri 64110

A new technique for the introduction of "nonvolatile" (very low vapor pressure, thermally unstable) substances into a mass spectrometer is being investigated. In this technique, the substance is dissolved in a suitable solvent and atomized. The resulting aerosol is introduced into a vacuum and the droplets of solution accelerated to nearly molecular velocities by a free-jet expansion. The particulates are collimated into the ion source of a mass spectrometer, where they strike a plate directly above the electron beam. During their flight through the vacuum, the droplets of solution are substantially cooled by evaporation of the solvent, resulting in a low vibrational temperature for the dissolved substance. Upon striking the plate, the droplets presumably evaporate rapidly into the high vacuum of the ion source because of the heat supplied by their inelastic collision with the plate and by heat transfer from the plate. In this very rapid evaporation the solvent appears to carry with it the nonvolatile solute, which passes through the electron beam before striking the ion source walls. Other methods of ionization could also be used.

Preliminary data have been obtained for a number of compounds using electron bombardment ionization and aqueous solutions. These compounds included dicarboxylic and higher acids, sugars and aminoacids. Ascorbic acid was studied intensively. At low electron energies, its spectrum consisted of two peaks, with the molecular ion peak comprising about 10% of the base peak. Arginine was also found to yield a strong molecular ion peak.

This technique appears promising. It should be noted that, at least in principal, it is not limited to mass spectrometry and could be applied to other kinds of spectroscopy.

Preparative Mass Spectrometry. R. G. Cooks and B. H. Solka, Department of Chemistry, Purdue University, West Lafayette, Indiana 47907.

By interacting polyatomic ions of low translational energy with solids or frozen vapors it is possible to effect chemical synthesis. Experiments were done using a plasmatron ion source in conjunction with a Wien mass filter. Reactant ion beams were decelerated to 10 eV or less before interacting with the target surface. The latter was typically a frozen (77°K) organic matrix which was continuously renewed by vapor deposition. Reaction products were transferred from the reactor cryogenically and analyzed by gc/ms. Performance characteristics of the instruments, typical experimental conditions and results will be presented. It is suggested that this general procedure may have value in preparing surfaces with desired chemical characteristics as required in studies of catalysis.

The Kinetics of Radiolytic Gas Phase Reactions by Modulated Molecular Beam Mass Spectrometry.

VALERIE R. KRUGER and DONALD R. OLANDER
Univ. of California, Dept. of Nuclear Engr., Berkeley, CA 94720

An experimental system shown in Fig. 1 was developed to enable on-line mass spectrometric analysis of gas phase radiolysis flow systems, and was applied to observation of the oxygen radiolysis system in particular. In this experimental system, energy from a beam of 1-MeV protons is deposited in the oxygen as it flows through a fast-flow reaction tube. A molecular beam source samples the flow gas, and the resulting molecular beam is then modulated and analyzed with a quadrupole mass spectrometer.

Experimentally determined quantities are the concentrations of atomic oxygen, molecular oxygen, and ozone as functions of reaction time, system pressure, and total absorbed dose. Operating parameters were in the following ranges:

System pressure:	[1.5 - 4.0] Torr
Irradiation time:	[0.2 - 0.3] sec
Total energy deposited:	[0.5 - 15] 10^{12}heV/cm^3
Dose Rate:	[0.2 - 20] 10^{20}heV/gm•sec

Observed concentrations of the radiolysis products atomic oxygen and ozone were of the order:

Atomic oxygen	[5 - 40] 10^{12} atoms/cm^3
Ozone:	[3 - 30] 10^{13} molecules/cm^3

The ozone levels observed are substantially higher than those predicted by pre-existing chemical models, and the discrepancies cannot be explained in terms of increased g-values or of systematic errors in the measurement.

A modification to the chemical model is proposed, in which an excited vibrational state O_2^* is postulated as a precursor to ozone via the reaction:

$$O_2^* + O_2 \rightarrow O_3 + O$$

Calculations including this modification indicate that agreement with the data is improved, although neither the agreement nor the explanation can be considered complete. It is concluded that further investigation of the low-pressure behavior in the oxygen radiolysis system is indicated, particularly with regard to the role of excited species in the chemical mechanism.

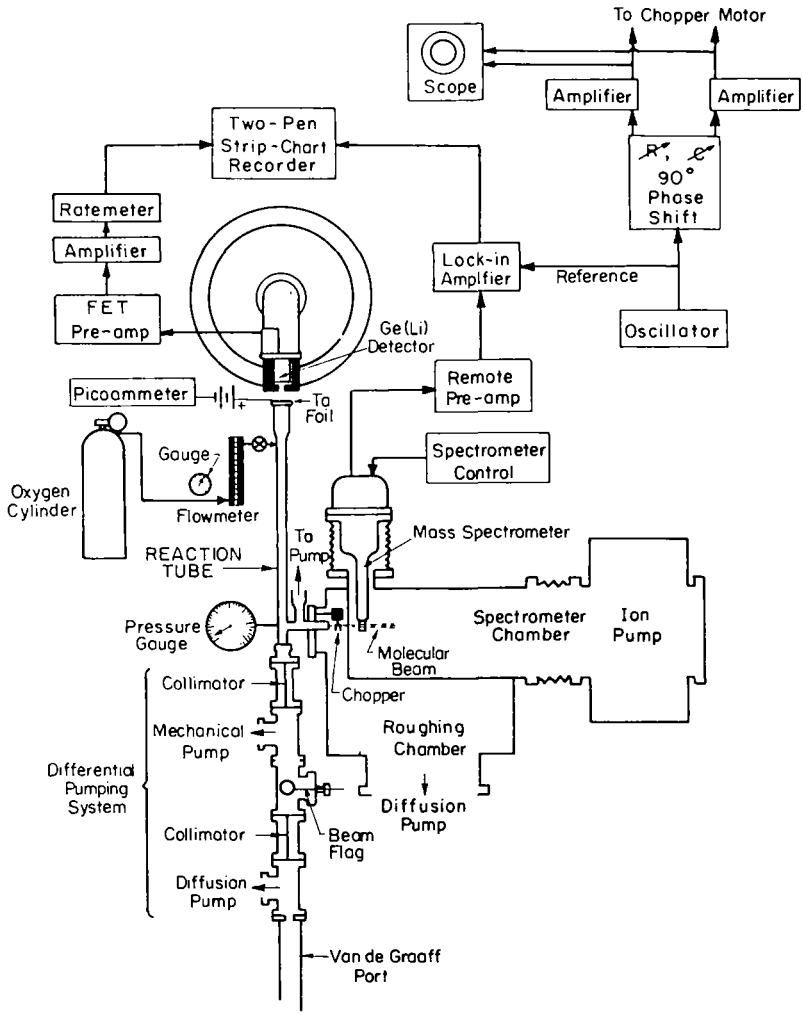

Figure 1. Radiolysis Apparatus

Analysis of μg/kg (ppb) Level Hydrocarbons in Intertidal Zone Sediments and Water by Gas Chromatography-Mass Spectrometry

H.S. Hertz, W.E. May, S.N. Chesler and B.H. Gump

Bioorganic Standards Section
National Bureau of Standards
Washington, D.C. 20234

The purpose of this investigation was to develop analytical techniques adequate to determine the low levels of hydrocarbons anticipated in pollution baseline studies in pristine environments. These techniques must be sensitive at the sub-microgram per kilogram (ppb) level and suitable to handle the paramount problems of realistic analytical blanks and component recoveries. Furthermore, it was desired that these analytical methods ultimately permit the identification and quantitation of individual components among the hydrocarbons present in the samples.

The scheme developed for the analysis of hydrocarbons in marine samples (Figure 1) involves dynamic headspace sampling using a stream of purified nitrogen as a sweep gas for trapping the volatile components on a TENAX-GC packed pre-column for subsequent gas chromatography (GC) or gas chromatography-mass spectrometry (GC-MS). The non-volatile components are then analyzed by coupled-column liquid chromatography (LC). Details of the analytical methodology are presented elsewhere (1). These techniques have been used in this laboratory for the analyses of intertidal zone sediments and water taken from the Prince William Sound and the Northeastern Gulf of Alaska. GC-MS results obtained from sediments taken from two sites of particular interest are discussed below.

Sites I and II are both located in the Northeastern Gulf of Alaska. The gas chromatograms obtained from both of these sediments indicated the presence of a "petroleum hump." The total ion chromatogram for sediment I is presented in Figure 2a. Figure 2b contains the m/e 43 single ion record for this sample. This single ion record helps identify the homologous series which one could not have visually identified in the complex gas chromatogram obtained from this site. The GC-MS analyses of the sediments from Sites I and II confirm that the major constituents are all hydrocarbons. Due to the large number of aromatic hydrocarbons, the presence of petroleum is indicated. This is an expected result for Site I, a known site of seepage, but is a somewhat unexpected result for Site II. The m/e 43 single ion record for Site II reveals some even/odd preference. Thus, some of the hydrocarbons may be of recent biogenic origin. Numerical evaluation of chromatograms from Sites I and II indicated the presence of less than 600 and 150 μg/kg respectively of total hydrocarbons.

One final note of interest concerns the complexity of the petroleum hump, which contains a large number of unresolved hydrocarbons. By the use of single ion records some compounds can be easily resolved. An example is shown in Figure 2c which contains the single ion record for m/e 184, the molecular ion for C_4-substituted naphthalenes.

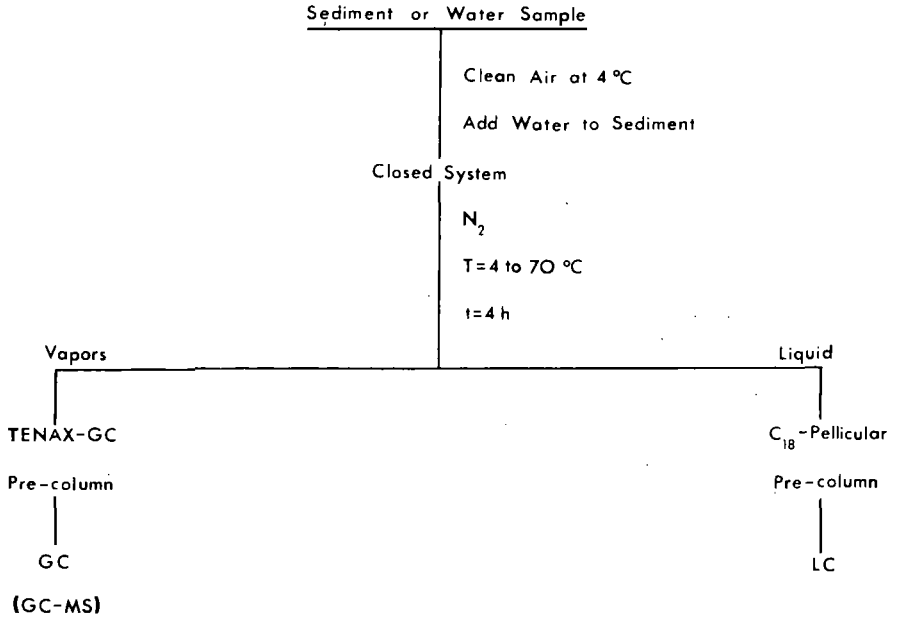

Figure 1. Scheme for analysis of hydrocarbons in marine sediments and water.

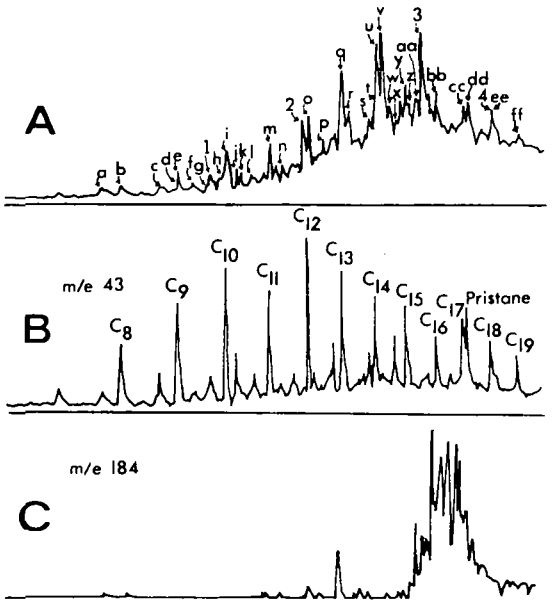

Figure 2. See end of text for caption.

Figure 2. GC-MS analysis of Site I sediment: (A) total ion chromatogram, (B) m/e 43 single ion record, (C) m/e 184 single ion record. C_x = normal saturated alkane containing x carbon atoms. Ø-C_x = benzene substituted with x carbon atoms (e.g. Ø-C_3 could be trimethyl, propyl-, isopropylbenzene, etc.) Peaks labeled 1,2,3,4 are internal standards: mesitylene, naphthalene, trimethylnaphthalene, and phenanthrene, respectively. Identifications followed by "?" are not definite due to incompletely resolved spectra.

a = Ø-C_1
b = C_8
c,d = Ø-C_2
e = C_9
f = Cyclohexane-C_3
g,h = Ø-C_3
i = C_{10}
j,l = Ø-C_4
k = Cyclohexane-C_4
m = C_{11}
n = Cyclohexane-C_5
o = C_{12}
p = Cyclohexane-C_6
q = C_{13}
r = Ø-C_6
s,x = Naphthalene-Et ?
t = C_{14} ?
u,v,w = Naphthalene-$(CH_3)_2$
y = C_{15}
z,aa = Naphthalene-C_3
bb = C_{16}
cc = C_{17}
dd = Pristane
ee = C_{18}
ff = C_{19}

(1) W.E. May, S. N. Chesler, S.P. Cram, B.H. Gump, H.S. Hertz, D.P. Enagonio and S.M. Dyszel, J. Chromatog. Sci., in press.

This study was carried out with partial financial support from the National Oceanic and Atmospheric Administration.

Identification of any commercial product does not imply recommendation or endorsement by the National Bureau of Standards, nor does it imply that the material identified is necessarily the best for the purpose.

Measurement of Reactive Species in Low Temperature Combustion

J. R. Wyatt, J. J. DeCorpo and F. E. Saalfeld
Physical Chemistry Branch
Naval Research Laboratory
Washington, D. C. 20375

Our methods[1,2] for analyzing low temperature combustion processes has been greatly improved with an instrument built at NRL this year. The new analyzer is divided into two chambers: one chamber contains the combustion reactor tube and the second chamber houses an Extranuclear quadrupole mass filter used to analyze the material diffusing from the first chamber. The first chamber is evacuated by a 2400 l/sec diffusion pump and the second by a 1200 l/sec diffusion pump. As in our instruments, previously described[1,2], combustion occurs in a reactor tube which has a small laser-drilled orifice in its wall. Gas effuses from this orifice through a skimmer into the second chamber where the resulting molecular beam is immediately chopped. The chopped beam is then analyzed with the quadrupole filter. This arrangement not only allows the phase angle experiments of Fite to be used, but, by using a lock-in-amplifier, and observing only in currents arising from the chopped beam, all background signals are eliminated. Thus the present instrument is several orders of magnitude more sensitive than our previous analyzer. This affords us the opportunity to detect species whose flame concentrations are appropriately lower. In addition we have used photoionization lamps developed by L. W. Sieck at NBS to reduce the fragmentation of the effusing molecules and to give us better knowledge of the ionizing energy.

The first flame system we studied with our analyzer was the cool flame of acetaldehyde. We observed the same composition of the cool flame profiles reported previously.[3] The most interesting observation in this profile was the presence of methylhydroperoxide, CH_3OOH. This very unstable speices was positively identified in this study, supporting the observation reported earlier. In addition, a careful check was made for the presence of peracetic acid taking advantage of the increased sensitivity of the new instrument. Since peracetic was not detected, we conclude again that methylhydroperoxide is an important chemical intermediate in the cool flame. In the luminous region of the cool flame the concentration of methylhydroperoxide is approximately 0.4% of the acetaldehyde concentration. Carbon monoxide, at 1% is the other major combustion product of the acetaldehyde cool flame. In the second study with the new instrument we added the fire retardant, CF_3Br, to the acetaldehyde cool flame. This agent decomposed into the following products in the flame: CH_3Br, Br_2 and HOBr in the concentration ratio: 10:0.3:0.06. In view of the toxicity and reactibility of these products the concept of quenching a flame with CF_3Br must be seriously reconsidered.

This study will be expanded and published elsewhere in the near future.

1. J. R. Wyatt et al Rev. Sci. Inst. 45, 916 (1975)

2. J. R. Wyatt et al Int. J. Mass Spectrom and Ion Physics 16, 33 (1975)

3. J. R. Wyatt et al Chem. Comm. 14, 533 (1974)

Author Index

Name	Paper No.
Aberth, W.H.	S-7
Abramson, F.P.	U-1
Aczel, T.	H-14
Aerni, R.	Y-5
Alberti, R.	C-6
Albritton, D.A.	R-7
Aldrich, J.B.	T-18
Allen, W.N.	E-9
Allison, J.	R-3
Ampulski, R.S.	I-3,U-5
Anbar, M.	H-6,H-15,J-2, M-3,O-1,Q-13, S-7,V-8
Andrewson, S.	Y-13
Appell, J.	D-5
Argelander, E.J.	C-12
Arison, B.H.	M-4
Armstrong, M.	O-11
Arnold, K.J.	U-6
Artus, J.	O-11
Ashline, H.C.	Q-4
Aspinal, M.L.	C-2
Atkinson, G.H.	K-11
Baczynskyj, L.	T-18
Baer, T.	D-7,X-1
Baker, J.E.	V-4
Baril, M.	V-1
Barnes, I.L.	S-4
Barofsky, D.F.	B-6
Barofsky, E.	B-6
Barton, E.C.	Y-10S
Batley, K.E.	Y-10S,Y-16
Batten, C.F.	D-11
Battrell, C.F.	V-6
Baucom, K.B.	Y-14
Bazinet, M.L.	Y-8
Beckey, H.D.	B-1
Beckey, H.D.	C-10
Beimer, R.G.	C-13
Belvedere, G.	Q-3
Benoit, F.M.	W-11
Bente, III, P.F.	T-10
Berger, P.S.	T-12
Berkowitz, J.	D-1, D-2
Beynon, J.H.	G-6,X-7
Biemann, K.	Q-6
Bier, D.M.	C-5,U-6
Birkinshaw, K.	K-9
Birnbaum, H.K.	V-5
Bissett, D.W.	T-16
Blakley, C.R.	K-6,K-7
Blattner, R.J.	C-11
Blue, G.D.	D-21
Blum, W.	W-14
Boggs, R.W.	U-5
Bone, L.I.	P-11
Booher, N.	J-4
Borhani, R.	Y-9
Botz, F.	E-3
Bowen, D.V.	O-2,U-11,W-12
Bowers, M.T.	E-2
Braselton, Jr., W.E.	Q-4
Brezler, G.L.	I-6
Bridy, A.	T-1
Bronczyk, S.B.	Y-5
Brooks, C.J.W.	Q-1
Brown, C.L.	D-20,Q-7
Brown, H.L.	C-9
Brown, P.	X-3
Bryant, W.F.	U-3
Buchanan, B.G.	T-2
Buckley, J.A.	W-3
Budde, W.L.	A-5,A-8
Burgard, D.R.	T-17
Burlingame, A.L.	T-9
Burstein, S.	U-2
Butler, C.	O-9
Buttrill, Jr., S.E.	L-3,R-4,W-7, W-8
Caprioli, R.M.	U-7
Carel, A.B.	H-16
Carroll, D.I.	H-4,L-1,W-2
Carlson, G.L.	H-5
Carter, D.E.	D-8
Carter, M.H.	A-7
Carter, J.A.	N-2
Chait, E.M.	C-7,C-13
Chandler, R.W.	W-20
Chandrasurin, P.	Y-7
Chang, C.	L-11
Chang, T.L.	W-21
Chapman, J.R.	T-7
Chatfield, D.A.	E-11,H-3,W-15
Chen, A.F.T.	D-20
Chesler, S.N.	Z-5
Chesnavich, W.J.	E-2
Chivalak, C.	K-3
Clay, K.	Q-5
Colby, B.N.	C-12
Cole, C.	K-4
Comisarow, M.	R-5
Compson, K.R.	C-2,T-7
Compton, C.E.	P-9
Cone, C.	T-16
Conway, D.C.	E-8,P-3
Cook, Jr., J.C.	B-2,B-9
Cooks, R.G.	G-6,X-7,Z-3
Costello, C.E.	Q-6

Author Index

Name	Paper No.
Craig, J.C.	C-5
Crain, P.F.	Q-8
Cross, R.M.	C-9
Crow, F.W.	W-4
Crynes, B.L.	H-13
Czuha, M.	C-7
Daly, N.R.	S-5
Dawson, J. H. J.	E-10
Dayringer, H.E.	T-4
DeCorpo, J.J.	Z-6
Dell, A.	Y-16
Denison, A.B.	D-16
Denson, K. B.	T-15
Derrick, P.J.	X-2
Desiderio, D.M.	O-4,U-8
Devine, C.	W-19
Dibeler, V.H.	D-3
Dillard, J.G.	P-9,V-6
Djerassi, C.	T-2
Dobberstein, P.	C-6
Dole, M.	C-8
Dong, P.	D-5
Donike, M.	O-7
Donoho, A.L.	J-11
Donohue, D.L.	N-2
Dotan, (Duchovny), I.	P-5
Dougherty, R.C.	L-7
Dowman, A.A.	C-2
Dromey, R.G.	T-2
Duchamp, D.J.	T-18
Dudenbostel, Jr., B.F.	A-6
Dunbar, R.C.	K-10,Z-1
Dunstan, L.P.	S-3
Dupzyk, R.J.	C-4
Durup, J.	D-5
Durup, M.	D-5
Dyer, R.L.	M-3
Dymerski, P.P.	X-2S,Y-11
Dzidic, I.	H-4,L-1,W-2
Eichelberger, J.W.	A-5,A-8
Einhorn, I.N.	H-3,W-13,W-15
Eldjorn, L.	F-3
Elliott, R.M.	C-2,H-17,T-7, X-6
Elwood, T. A.	E-11
Eshuis, W.	H-10
Eskew, T.J.	I-7,I-8
Evans, Jr., C.A.	C-11,V-4,V-5
Evans, S.	H-17,X-6
Eyler, J.R.	I-2,K-11,K-12
Fales, H.M.	T-1
Fanelli, R.	Q-3
Fehsenfeld, F.C.	R-7
Fennessey, P.V.	M-2
Fenselau, C.	W-9
Ferguson, E.E.	G-3,R-7
Ferrer-Correia, A.J.	E-10
Field, F.H.	E-6,E-7,U-11
Fite, W.L.	C-18,D-13
Flory, D.A.	M-5
Flynn, N.W.	W-17,W-20,W-22
Foltz, R.L.	J-8
Forney, Jr., R.D.	J-8
Foster, N.G.	Y-7
Franklin, J.C.	N-2
Franklin, J.L.	D-8,D-15,D-18, D-19,P-1,P-2, P-6
Freeman, N.J.	S-5
French, J.B.	W-3
French, M.	E-5
Friedman, L.	W-18
Friesen, M.D.	Y-3
Frigerio, A.	Q-3
Frisch, M. A.	H-7,V-10
Frolich, J.C.	M-1
Futrell, J.H.	D-10,E-11,H-3, K-6,K-7,R-2, W-13,W-15,X-4
Gal, J.	W-10
Gale, J.	R-8
Gallegos, E.J.	X-8
Gallo, G.G.	B-10
Gallup, G.A.	Y-5
Games, D.E.	B-7
Garner, E.L.	S-3,S-4
Garrison, A.W.	A-7
Gaskell, S.J.	Q-1
Gerber, J.N.	B-5,T-13
Gershinowitz, H.	E-1
Gieniec, J.	C-8
Gierlich, H.H.	C-10
Glass, G.E.	L-5
Goldich, S.S.	S-4
Goodman, A.M.	V-2
Gordon, S.M.	D-12
Goren, A.	R-10
Graczyk, D.G.	Y-6
Gramlich, J.W.	S-4
Green, M.M.	O-10, O-11
Greene, F.T.	N-4,Z-2
Greenwood, G.J.	H-13
Gregory, P.	J-4
Grigsby, R.D.	U-9
Grimsrud, E.P.	L-4
Gross, M.L.	Y-5,Y-12

Author Index

Name	Paper No.
Grossbeck, M.L.	V-5
Grotch, S.L.	T-3
Gruber, V.F.	M-4
Gruenke, L.D.	C-5,U-6
Guffey, F.D.	H-12
Gump, B.H.	Z-5
Gut, M.	U-2
Hachey, D.L.	U-3
Hadley, F.J.	D-18
Haegele, D.K.	O-3
Hagge, D.E.	H-8,H-20
Hamming, M.C.	H-16
Haney, M.A.	N-2
Hanson, V.	Q-7
Harada, F.	Q-8
Harless, R.L.	A-11
Harrington, W.L.	V-2,V-3
Harrison, A.G.	G-2,W-11
Harrison, W.W.	N-10,N-11
Harvey, Jr., J.	L-6
Harvey, T.M.	A-1,W-4
Hashimoto, S.	J-3
Hassell, A.	W-16
Hatch, F.	C-14
Hattox, S.E.	J-10,Q-5,Q-9
Hawks, R.L.	H-2
Hayden, J.L.	T-14
Hayes, J.M.	S-8,T-15
Haymond, M.	U-6
Hazelby, D.	C-2,H-17,T-7
Heck, H.d'A.	J-2,O-1
Heinen, H.J.	C-10
Helbig, R.	Q-5
Heller, R.S.	T-1
Heller, S.R.	T-1
Henchman, M.	R-8,R-9
Hendricks, L.J.	D-17
Herman, Z.	K-1,K-5,K-9
Hertz, H.S.	Z-5
Herzog, L.F.	I-7
Hierl, P.M.	K-3,K-4
Higgins, R.W.	Y-7
Hildenbrand, D.L.	V-7
Hileman, F.D.	W-13,W-15
Hilker, D.R.	Y-12
Hill, R.M.	J-1
Hiraoka, K.	E-4,E-5
Hites, R.A.	L-9
Hoffman, M.K.	Y-3
Hogan, J.W.	A-4
Hogg, A.M.	I-5
Holland, J.F.	B-5,T-13
Holmes, J.L.	Y-1,Y-2
Holmes, W.F.	T-12
Honig, R.E.	V-2,V-3
Hopkinson, J.A.V.	T-8
Hopper, D.G.	K-8
Horning, E.C.	H-4,J-6,O-5, O-6,W-2
Horning, M.G.	J-1,J-5,O-8, O-9
Hughes, B.M.	K-8,L-10,L-11
Hughes, D.B.	H-10S
Hull, C.W.	C-12,C-13
Hung, A.	O-8
Hunt, D.F.	A-1,A-12,W-4, W-5,W-6,W-19
Huntress, Jr., W.T.	R-1
Ige, J.	R-9
Inghram, M.G.	D-9
Jackson, A.H.	B-7
Jackson, K.M.	I-4
Jacob, L.	B-6
Jamieson, W.D.	H-11
Jardine, I.	W-9
Jellum, E.	F-3
Jelus, B.L.	W-1
Jennings, K.R.	E-10,X-6
Johnson, L.P.	D-4
Johnson, R.L.	H-18,L-8
Jones, E.G.	K-2,K-8
Jones, F.E.	S-6
Julian, R.L.	Y-6
Kanomata, I.	C-1
Kappus, G.	C-6
Karpas, Z.	P-4
Kasai, H.	Q-8
Kearns, G.L.	T-8
Kebarle, P.	E-4,E-5,G-4
Keith, L.H.	A-7
Kellermann, G.	J-1
Kempster, E.J.	H-15,Q-13
Kendall, B.R.	C-21
Kenny, M.D.	T-18
Kim, H.B.	N-1
Kim, J.K.	R-1
Kimble, B.J.	T-9
King, R.	Y-14
Kinstle, T.H.	Y-13
Kipnis, D.M.	U-6
Kirchner, R.F.	Y-4
Kiser, R.W.	Y-15
Kishi, T.	C-3
Kistemaker, P.G.	H-10
Kitson, F.G.	W-23
Klein, F.S.	P-4,P-5

Author Index

Name	Paper No.
Klein, P.D.	U-3
Klots, C.E.	D-6
Knight, T.C.D.	T-14
Knighton, J.R.	C-17
Knights, R.L.	H-8
Knoche, H.W.	Y-12
Konishi, F.	N-9
Kondrat, R.W.	X-7
Kramer, G.M.	G-7
Kronebusch, P.L.	D-1,D-2
Kruger, V.R.	Z-4
Kuehl, D.W.	L-5
Kuhlman, C.F.	W-21
Kuiken, L.P.	W-17
Kusao, K.	N-9
Lampe, F.W.	E-9
Landi, M.	B-10
Lao, R.C.	L-2
Lau, S.S.	O-5,O-8
Lawless, J.G.	Y-4
Lawrence, Jr., R.H.	Q-12
Lee, Y.T.	PL-2
Lederberg, J.	T-2
Leiner, K.	Q-2
Lett, R.G.	H-19
Leung, K.L.	O-4
Lewis, J.W.	A-2
Lewis, R.G.	A-11
Li, Y-H.	P-11
Lias, S.G.	R-6
Liehr, J.G.	Q-8,W-14
Ligon, Jr., W.V.	H-18,L-8,X-5
Lin, D.C.K.	J-8
Lin, P.H.	G-2,L-9
Lin, S.N.	O-6
Lincoln, K.A.	I-1
Lindinger, W.	R-7
Littlejohn, D.P.	C-16
Liu, W-C.F.	P-3
Lo, H.H.	D-13
Locht, R.	D-14
Loew, G.H.	Y-4
Lossing, F.P.	G-1
Lovett, A.M.	M-5
Lumpkin, H.E.	H-14,H-17
MacFarlane, R.D.	C-20,W-16
Machlan, L.A.	S-4
Magee, C.W.	V-3
Mak, N.	B-4
Malm, D.L.	H-9
Margrave, J.L.	D-15,D-19, D-21
Markey, S.P.	H-2,M-2
Marshall, A.G.	R-5
Martin, J.L.	O-10
Martinsen, D.P.	L-3,W-8
Marvel, J.T.	Q-11
Maseles, F.C.	T-16
Mason, F.G.	H-11
Mathews, R.J.	T-6
Matsuda, H.	C-1
Matthews, D.E.	S-8
Mattson, W.A.	N-10,N-11
Mauclaire, G.	D-10
Maurer, K.H.	O-7
May, W.E.	Z-5
McCloskey, J.A.	Q-8,Q-9
McCulloh, K.E.	D-3
McEwen, C.N.	B-3,W-23
McFadden, W.H.	L-1
McGuire, J.M.	A-7
McKinney, C.R.	C-7
McLafferty, F.W.	T-4,T-10,X-2S Y-11
McLeod, P.D.	I-4
McReynolds, J.H.	H-6,J-2,O-1
Meador, R.G.	D-15
Meisels, G.G.	D-11,E-3
Meot-Ner, M.	E-7
Merritt, Jr., C.	A-9,Y-8
Meuzelaar, H.L.C.	H-10
Michelson, H.	C-6
Mickelson, R.W.	H-3
Middleditch, B.S.	U-2
Milne, G.W.A.	H-2,T-1
Moldowan, J.M.	O-11
Molinary, S.V.	W-22
Momigny, J.	D-14
Monkman, J.L.	L-2
Moore, L.J.	S-2
Morgan, R.P.	X-2
Morris, H.R.	Y-10S,Y-16
Morrison, J.D.	D-4,T-6
Mrochek, J.E.	F-2
Mudgett, M.	U-11
Munson, B.	C-14,R-10, R-11,W-1
Murphy, R.C.	J-10,Q-5,U-4
Murphy, T.J.	S-4
Najm, S.	Y-10
Nakagawa, Y.	J-3
Nakamura, N.	N-9
Narasimhachari, N.	Q-2,Q-13
Newbury, R.S.	S-1
Nibbering, N.M.M.	Y-11
Nishimura, S.	Q-8

Author Index

Name	Paper No.	Name	Paper No.
Nishishita, T.	Y-11	Reid, N.M.	W-3
Norbert, P.D.	T-12	Reid, N.W.	D-12
Norman, E.J.	U-9	Reid, W.F.	W-5
Nowlin, J.	J-1	Reiser, R.W.	L-6
Oates, J.A.	M-1	Reiter, R.F.	C-21
Obenhauf, R.H.	B-8	Rendtorff, R.C.	W-20
Oblinger, C.J.	N-5	Rennekamp, M.E.	O-2,W-12
Occolowitz, J.L.	J-11	Reuter, W.	H-7,V-10
Oertli, C.	H-4	Reynolds, W.E.	F-1
Ogilvie, K.K.	Q-10	Richter, W.J.	W-14
Ohashi, Z.	Q-8	Ridge, D.P.	R-3
Ohnuma, T.	J-9	Riggin, M.	K-10
Olander, D.R.	N-7,Z-4	Rinehart, Jr., K.L.	B-2,B-9
Olsen, R.W.	T-9	Ringer, G.	R-4
Oppenheimer, N.J.	Q-8	Roberts, G.D.	V-9
Oro, J.	M-5	Robinson, A.B.	F-1
Orth, R.	K-10	Robinson, L.R.	F-1
Pabst, M.J.	P-1,P-2	Roboz, J.	J-9
Pabst, R.E.	D-15,D-19	Roeske, R.W.	U-10
Pacak, V.	K-5,K-9	Rolinski, E.J.	N-5
Pandey, R.C.	B-9	Rossiter, M.	B-7
Patterson, D.G.	X-3	Roveri, V.	Q-3
Pauls, R.	P-9	Rozett, R.W.	T-5
Paulsen, P.J.	S-4	Rueppel, M.L.	Q-11
Paulson, J.F.	R-8	Russell, D.H.	Y-5
Pebler, A.	H-5	Russell, J.W.	A-1,W-6
Perloff, M.	J-9	Ryan, J.F.	A-11
Perone, S.P.	T-17	Ryan, P.W.	H-3,K-7
Perry, D.L.	D-19	Saalfeld, F.E.	A-10,Z-6
Pesyna, G.M.	T-4	Sabesin, S.M.	W-17
Petersen, E.M.	T-5	St. John, G.A.	H-6,V-8
Petty, F.	W-17,W-20,W-22	Satkiewicz, F.G.	N-8
Phillips, J.M.	D-16	Saunders, R.A.	A-10
Pierce, R.C.	W-18	Schackleton, G.	T-7
Piotrowska, K.	L-7	Scheppele, S.E.	H-13
Ponnamperuma, C.	PL-1	Schmeltekopf, A.L.	R-7
Pope. J.D.	A-7	Schnitzer, R.	H-15,S-7
Pople, J.A.	G-5	Schram, K.H.	Q-9
Porter, C.C.	M-4	Schuetzle, D.	H-8,H-20
Powell, R.E.	S-5	Schulman, M.F.	U-1
Powers, P.	T-8	Schulten, H.R.	B-1
Prater, T.J.	H-8,H-20	Scolnick, M.E.	M-3
Price, P.	W-8	Scott, C.D.	F-2
Pulley, P.E.	U-9	Scott, R.B.	X-3
Puntarotto, C.	Q-3	Seifert, W.F.	U-7
Quilliam, M.A.	Q-10	Seyberth, H.W.	M-1
Radd, R.J.	H-16	Shabanowitz, J.	W-12
Radolovich, G.	N-4	Shapiro, J.A.	T-17
Ragland, J.B.	W-17	Shapiro, R.H.	D-17
Rapp, U.	O-7	Sharkey, Jr., A.G.	H-19
Rasmusson, R.A.	L-4	Sherwood, E.	M-5
Reed, R.I.	Y-9	Shieh, J.J.	O-4
Reeher, J.R.	L-1	Shively, J.M.	Y-12
Refaey, K.M.A.	P-6,P-7	Showronski, R.	W-16

Author Index

Name	Paper No.
Shultz, J.L.	H-19
Siegel, M.W.	D-13,S-6
Sides, G.D.	P-8
Silberberg, M.S.	O-2
Simons, D.S.	C-11,V-4
Smith, A.G.	Q-1
Smith, D.	R-11
Smith, D.H.	T-2
Smith, J.F.	T-6
Smith, R.D.	R-2,X-4
Smith, S.W.	T-14
Smolinsky, G.	P-10
Solka, B.H.	Z-3
Solomon, J.J.	E-6
Soltman, B.	B-5
Sommer, K.R.	J-5
Speis, D.N.	A-6
Spencer, R.B.	H-1,T-11
Sperry, R.R.	M-3
Stafford, G.C.	W-6,W-19
Stalling, D.L.	A-4
Stein, R.P.	C-19
Steinheider, D.	Y-5
Stelzner, R.W.	N-2
Stillwell, R.N.	H-4,J-4
Stillwell, W.G.	J-4,O-8,O-9
Stockbauer, R.	D-9
Stokke, O.	F-3
Stout, S.J.	A-12
Sunshine, I.	J-8
Suzuki, R.	J-9
Sweeley, C.G.	B-5,T-13
Sweeney, G.G.	N-1
Sweetman, B.J.	M-1
Swofford, Jr., H.S.	L-3,W-8
Szczepanik, P.A.	U-3
Takagi, T.	C-3
Takahashi, S.	J-3
Tan, H.S.	P-1,P-2
Tang, S.Y.	K-2
Taylor, C.E.	A-3
Taylor, J.A.	D-11
Taylor, J.W.	Y-6
Taylor, M.L.	L-10,L-11
Taylor, S.P.	T-15
Tayo, S.	C-1
Teller, G.	Y-10
Terlouw, J.K.	Y-1,Y-2
Terwilliger, D.T.	L-10
Testerman, M.K.	I-4
Theard, L.P.	R-1
Thenot, J.P.	J-5,J-6
Thomas, C.R.	N-5
Thomas, R.S.	L-2
Thompson, J.A.	M-2
Thompson, K.R.	N-6
Thompson, R.M.	U-10
Tiernan, T.O.	E-12,K-2,K-8, L-10,L-11,P-8
Titus, D.C.	M-4
Tomassian, A.D.	C-15
Torgerson, D.F.	D-20,W-16
Traeger, J.C.	G-1
Tsai, B.P.	D-7,X-1
Tsang, C.W.	G-2
Tsuyama, H.	C-1
Tucker, H.N.	W-22
Turner, D.L.	E-8
Upchurch, B.T.	H-10S
Vallerand, P.	V-1
Van De Graaf, B.	Y-11
Vanden Heuvel, W.J.A.	M-4
Van De Sande, C.C.	T-10,Y-11
Vasile, M.J.	H-9,P-10
Veith, G.D.	L-5
Venkataraghavan, R.	T-4
Vestal, M.L.	D-10,K-6,K-7
Von Minden, D.L.	Q-8
Voorhees, K.J.	H-3,W-13,W-15
Wachs, T.	T-10
Walker, R.W.	T-11
Waller, G.R.	Q-12
Wallington, M.J.	T-8
Walls, F.C.	T-9
Wander, J.D.	W-17,W-20,W-22
Wang, I.C.	L-3
Wankenne, H.	D-14
Watani, K.I.	J-3
Webb, J.L.	X-5
Weber, J.H.	D-16, H-12
Weese, G.M.	Y-2
Weinkam, R.J.	W-10
Weitl, F.L.	U-1-
Weiss, M.	F-1
Werner, A.S.	D-7,X-1
Westmore, J.B.	Q-10
Weston, A.F.	X-6
White, V, E.	V-9
Whitehead, T.W.	C-12
Wiebers, J.L.	T-17
Willey, J.F.	Y-6
Williams, P.	V-5
Williams, R.	V-2
Wishousky, T.	J-7
Wojcik, L.H.	W-13
Wolff, G.	Y-10

Author Index

Name	Paper No.
Wolff, R.E.	Y-10
Wolstenholme, W.A.	H-17
Wong, L.K.	Q-6
Wood, G.M.	H-10S
Wood, G.W.	B-4
Wu, C.P.	V-3
Wu, R.L.C.	E-12,K-2,L-10
Wyatt, J.R.	Z-6
Yamada, I.	C-3
Yencha, A.J.	K-5
Yeomans, W.G.	Y-8
Yoshioka, Y.	N-9
Young, N.D.	T-13
Young, Y.A.	U-8
Zacchei, A.G.	J-7
Zaletel, J.	C-17
Zerilli, L.F.	B-10
Zierserl, J.F.	T-18
Zirrolli, J.A.	Q-5,U-4
Zune, A.	O-7

ASMS COMMITTEES AND ASTM E-14 SUBCOMMITTEES

II (ASMS) Fundamental Aspects. F. E. Saalfeld, Naval Research Laboratory, Code 6110, Washington D. C. 20375.

III (ASMS) Computers and Data Processing. M. A. Grayson, McDonnell Douglas Research Laboratories, St. Louis, Misouri 63166.

IV (ASTM) Data and Information Problems. C. Merritt, Jr., Pioneering Research Laboratory, U. S. Army Natick Laboratories, Natick, Mass. 01769.

V (ASMS) New Instruments and Techniques. F. W. Karasek, Department of Chemistry, University of Waterloo, Waterloo, Ontario, Canada.

VI (ASMS) Biological Applications. C. C. Fenselau, Department of Pharmacology and Experimental Therapeutics, The Johns Hopkins University School of Medicine, Baltimore, Md. 21205

VII (ASMS) Study of Solids. W. Harrington, RCA Laboratories, Princeton, New Jersey 08540.

VIII (ASMS) High Resolution Studies. H. M. Fales, Laboratory of Chemistry, National Heart and Lung Institute, Bethesda, Maryland 20014.

IX (ASMS) Aids to Education. No Chairman.

XI (ASMS) Environment and Pollution Studies. J. M. McGuire, Southeast Environmental Research Laboratory, Environmental Protection Agency, Athens, Georgia 30601.

Committee II. Fundamental Aspects

Committee II on Fundamental Aspects met at 5:15 PM Monday, May 26, 1975 in the Embassy room of the Shamrock Hilton Hotel, Houston, Texas.

Approximately 25 persons attended the meeting. A list of previous ASMS and ASTM-E-14 symposia was distributed. This list is available from the undersigned upon request. Committee II Chairman reported he had tried to establish joint program between Committee II and other ASMS committees without success. He asked the Committee their opinion on this endeavor. Generally, there seemed to be little or no enthusiasm for the undertaking.

The next discussion was the suggestion of symposium topics for the 1976 ASMS meeting in San Diego. The Committee agreed on the subject of "Thermochemistry of Gaseous Ion" and suggested Henry Rosenstock of NBS arrange the symposium. A motion by G. G. Meisels of Nebraska University to this effect passed without opposition.

Respectively submitted,

F. E. Saalfeld,
Chairman Committee II

ASMS COMMITTEE ON COMPUTERS AND DATA PROCESSING

Under the chairmanship of Steve Heller, the committee concentrated its efforts on two specific tasks; a) the collection and dissemination of mass spectra and b) the collection and dissemination of computer programs for mass spectrometry. The committee chairman and the board of ASMS came to a disagreement over the implementation of this effort. The chairman felt that the committee should solicit financial support to defray the expenses of such an undertaking whereas the board felt that the committee should operate by using the voluntary services of ASMS members. This basic difference of opinion led to the resignation of Steve Heller as committee chairman. Presently, Mike Grayson is chairing the committee on computers and data processing.

SURVEY RESULTS

In July of 1974, a survey of ASMS members was taken to determine; a) the extent and variety of computer applications in mass spectrometry, b) the attitudes toward contribution of mass spectra, c) the attitudes toward software exchange, d) interest in workshop discussion topics for the Houston meeting, and e) the interest in presently available software. In addition, interested members were invited to volunteer their services to assist the committee.

a) Computer Applications

There were 138 replies, 30 from government labs and the remainder split nearly equally between university and industrial labs. Those presently using computers numbered 96; of the non-users, 33 planned to use computers in the near future. Of the computer users, 65 had dedicated systems, 25 worked with batch, off-line systems and 10 were time-sharing with a lab computer. Ten others had some combination of the above facilities in use.

b) Attitudes Toward Spectra Collections

Those who had contributed spectra numbered 49, the majority being able to prepare spectra for contribution in less than an hour. The attitudes of those responding are tabulated below:

No spectra	29	Spectra are proprietary	14
Too few	26	Others derive profit from my contribution	16
Too many	5	No interest	2
Do not know form	7	Other	40
Low quality spectra	16		

An effort was made to contact those 5 respondents who indicated they had too many spectra to contribute in hopes of arranging assistance to encourage their contributions. Respondents (63) indicated that they presently have spectra they could contribute.

c) Attitudes Toward Software Exchange

Of those replying, 35 had given programs to other workers; only 3 of them reported being pestered by the program recipient. Fifty-two reported receiving programs from others of which: 35 felt the exchange had been helpful, 13 were unsure as to the helpfulness of the exchange, and 4 felt they had not been helped at all. Of the respondents, 31 indicated that they had software that they could contribute.

d) Workshop Survey

The interests of the respondents toward current topics in the use of computers in mass spectrometry is summarized in the table below:

	Interested	No Opinion	Not Interested
Data Acquisition	80	32	25
Data Reduction	83	27	26
Data Analysis	108	14	15
Data Search	87	30	20
Heuristics	85	31	21

e) Requests for Materials

A variety of information, listings, etc., were offered to respondents for the asking. Seventy-nine program listings were sent out; 62 copies of Ed Emery's survey were distributed; and 15 copies of Crittenden's dedicated computer software documentation were distributed. The names and addresses of 58 members interested in more information on Dendral were sent to Dennis Smith. Eighteen card decks were requested of which only a few were distributed due to the time and expense involved.

Thirty-five members offered their services to assist the committee in its efforts.

BUSINESS MEETING - May 1975

1) The results of the committee survey were presented to those attending.

2) The status of software exchange efforts was reviewed.

   a) High level language software: The exchange of high level language software is presently being conducted through the services of the Quantum Chemistry Program Exchange (QCPE). At present, two programs are available through QCPE, six programs are in the process of being put up on QCPE, and an effort is underway to solicit more software for exchange. The arrangements with QCPE are experimental at this time and can be summarized briefly as follows: Any programs dealing with all phases of mass spectrometry which are provided to QCPE by this committee can be obtained by any member of ASMS directly from QCPE at the normal handling charges. The ASMS member does not have to be a member of QCPE to request those mass spec related programs. This committee is responsible for advertising the availability of such programs to all ASMS members. QCPE can offer any programs provided through this committee to its own members. Any ASMS member desiring programs available from QCPE which are not contributed through this committee must become a member of QCPE.

   b) Machine level language software: No such service presently exists for exchanging machine language software in computer readable form. The committee has chosen the following approach:

      1) A set of ground rules for exchange of machine language software will be drawn up.

      2) Members interested in contributing such software will complete a form which will be sent to the committee.

      3) The availability of these programs will be announced to the general membership by this committee.

4) Members wishing to obtain such software will send their requests and some computer readable exchange medium to the contributor.

5) The contributor will copy the software onto the computer readable exchange medium and return it to the requestor along with as much documentation as he has available.

In the case of machine level language software, the committee can only act as a central focal point for announcing to the total membership that software which is available for the asking. This is a start in promoting the exchange of such software. Fred Falkner has agreed to coordinate this effort for the committee.

WORKSHOP - May 1975

The following panel members participated in the workshop which was attended by ∿ 125 persons:

J. Carter Cook	University of Illinois
Milt Levenberg	Abbott Labs
Steve Shrader	Shrader Analytical
Hank Fales	NIH
Steve Heller	EPA
Mike Grayson	McDonnell Douglas Research Laboratories

Each panel member discussed briefly his background and application and the topics of reduction and analysis of mass spectral data were opened for discussion. The discussion covered a broad range of topics and many opinions were expressed by those attending.

The consensus of the group was that the use of computers in mass spectrometry, although quite advanced, is far from ideal. Many data systems overlook multiply charged and metastable ions. In some systems, isotope satellite peaks are neglected. Further, computer systems at present do not make use of the full dynamic range of peak intensity available at the analog output of the mass spectrometer collector.

Dedicated systems, while satisfactory for the problems for which they are designed, are difficult to modify for other problem areas. On the other hand, custom systems tend to consume the mass spectrometrist in computer programming.

A brief discussion of file search systems was held and after ∿ 1-1/2 hours the workshop was closed.

COMMITTEE MEMBERSHIP

The following are members of ASMS Committee on Computers and Data Processing:

Ronald Grigsby	K. R. Thompson
Bruce Raby	Brian S. Middleditch
David Bowen	Fred Falkner
Gwendolyn Ball	Derry Fishel
C. Herndon Williams, Jr.	Roy King
W. T. Rainey	Bob Mauldin
Donald Schoengold	Tim Becker
J. P. Lehman	

The time and talents of these members are being applied as effectively as possible to enhance the exchange of software for computers in mass spectrometry.

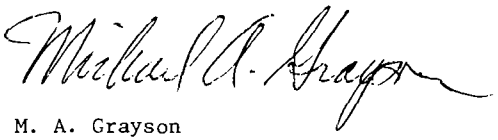

M. A. Grayson
Chairman, Committee on
Computers and Data Processing (III)

ASMS COMMITTEE VI. BIOLOGICAL APPLICATIONS

Chairman: C. Fenselau, The Johns Hopkins University School of Medicine, Baltimore, Maryland 21205

Secretary: W. J. A. VandenHeuvel, Merck, Sharp & Dohme Research Laboratories, Rahway, New Jersey 07065

Activities for 1974-75

1. A workshop on quantitation by gas chromatography mass spectrometry was held at the 1975 ASMS meeting, which addressed the factors limiting the precision of measurements and also the most appropriate ways to report that precision.

2. A symposium on Profiling of Physiologic Fluids was arranged for the 1975 ASMS meeting. Arthur B. Robinson, John E. Mrochek and Oddvar Stokke spoke in the three hour program, which was chaired by C. C. Sweeley.

Minutes from Business Meeting, May 27, 1975

The business meeting of Committee VI was called to order with 51 persons in attendance. Chairperson C. Fenselau introduced the first and major topic - an attempt to concur on the terminology used in describing and reporting the technique employed and record obtained in following the intensities of selected ions vs. time. J. Beynon indicated that the IUPAC Committee on Nomenclature does not insist upon use of a single set of terms, but only desires data reported in concise, understandable language. Suggestions will be "on the table" for 2 years before any decisions are made. Comments can be sent to K. Biemann, a member of the Committee on Nomenclature, or to Dr. Beynon. Several persons spoke in favor of various terms - e.g., mass fragmentography, mass chromatography, selected ion (current) monitoring (recording), ion profile analysis. A vote was taken with the three most widely supported terms on the ballot in an attempt to obtain agreement among the membership of Committee VI on the most appropriate term. It was thought that such a move would help to eliminate the proliferation of terms noted during the past several years. The results: 0 votes for ion profile analysis, 9 votes for mass fragmentography and 33 votes for selected ion recording. Committee VI thus went on record as favoring Selected Ion Recording as the term to be used for the technique now known by a multitude of names, and Selected Ion Record as the term for the resulting record.

J. A. McCloskey, Secretary of ASMS, spoke briefly on a number of topics including - a) the choice of the 1980 meeting site (New York City), b) the scheduling of ASMS meetings to coincide with Memorial Day (this can result in reduced hotel charges), c) the advisability of bringing ideas and comments to the ASMS business meeting, d) the forwarding of suggestions on workshops, symposia and plenary lecturers (submit to C. Fenselau), and e) the possibility of having poster sessions at the 1976 meeting. It was agreed upon during discussion that something must be done to reduce the number of parallel sessions at ASMS meetings. The pros and cons of poster sessions and use of a referee system for screening submitted papers were discussed. A trial run of poster sessions on a voluntary basis is likely for next year. Twenty-six persons participating in an informal poll indicated their willingness to participate in poster sessions, whereas 6 indicated a strong preference for slide talks.

Other topics of interest covered at the meeting included a) the availability of the "Markey Collection" of mass spectrometric data

(contact S. Markey, NIMH, NIH), b) the announcement that a computer program is available (from Dr. Markey) for the calculation of ^{2}H and ^{13}C mole percent in labeled compounds (it is hoped that the program will become available on a time-sharing system similar to the NIH spectral file), c) persons interested in sharing and using computer programs in various areas of mass spectrometry should contact C. Hammer (Department of Chemistry, Georgetown University) of Committee III, d) the workshop on quantitation by GC-MS sponsored by Committee VI, drew 175 attendees, e) the symposium on profiling physiologic fluids, sponsored by Committee VI, drew 140 attendees.

W. J. A. VandenHeuvel, Secretary

Committee VII: Studies of Solids

Business Meeting, May 27, 1975 - Houston, Texas

1. A final report concerning the SSMS round robin studies on steels was distributed and is to be published in the Conference proceedings. No similar study on powder samples is planned at this time.

2. The Committee VII mailing list, which was seriously out of date, has been revised by means of an address card included with the last mailing. Approximately 125 cards have been returned so far.

3. A SSMS Users Directory is to be assembled, using standardized reporting forms, which will summarize the personnel, instrumentation, and applications found in various laboratories. The aim is to provide for more communication between SSMS users. A similar compilation for other solids mass spectrometry techniques was suggested.

4. A quarterly "Solids Mass Spectrometry" newsletter was proposed, to consist of informal descriptions of recent developments which would be out of place in a formal journal. No action was taken, pending further study.

5. Plans were made to sponsor future ASMS symposia and/or Plenary speakers. For the San Diego meeting, the lecture topic of Ion Sputtering was suggested as a general subject of broad application.

6. Possible cooperation with other societies, notably the "Association Francophone de Spectrometrie de Masse des Solids" in sponsoring joint meetings was suggested. As a first effort, contacts at a European mass spectrometry conference or at an east coast ASMS meeting were proposed.

7. A letter was read from Ilford, Ltd. indicating that in their new facilities, the Q-2 plate will still be produced, although certain optical spectroscopy plates are being discontinued.

8. A Solids Workshop was announced for Thursday, May 29, covering the topics (a) Multielement Isotopic Dilution, and (b) Quantitation in SIMS. Summaries of the Workshop will be published in Analytical Chemistry.

W. W. Harrison, Chairman
T. J. Eskew
C. A. Evans, Jr.
F. D. Leipziger
W. L. Harrington
J. A. McHugh

REPORT ON ROUND ROBIN TEST ON NBS STEEL

SRM 661 and 663
Spark Source Mass Spectrometry
ASMS Committee VII 1973 - 74

Twenty-one laboratories participated using instruments made by five manufacturers. The laboratories are located in eight countries.

Each participant was requested to run SRM 663 as a known and from these data calculate RSF values to use to correct the analyses of SRM 661. Both samples were to be run in triplicate.

Each laboratory was also requested to determine in triplicate the ratios of selected isotope pairs of Mo, W, Fe and Cu in SRM 661.

These instructions were followed except that a few laboratories used calculation methods that did not make use of RSF values, and so they did not report RSF values. Three laboratories used electrical detection, while the others used photographic plates.

The results from a statistical evaluation of the reported data are given in the attached table. In the table a laboratory average is the average of the three concentrations of an element reported by that laboratory. A grand average is the average of all the laboratory averages for that element. A study of the complete data and the statistical evaluation leads to the following observations.

1. The Student's "t" test indicates that there are eleven laboratory averages that are significantly different from the others. When these eleven results are omitted, the overall accuracy improves from an average standard deviation of 116 per cent to 44 per cent (lines 12 and 14 in the table).

2. Careful re-examination of the data by the individual laboratories and by the compiler reveals no explanation of, or means to reduce, the scatter.

3. As one might expect, the within laboratory precision is better than the interlaboratory precision (line 6 vs 7).

4. The precision obtained on measuring isotope ratios is better than that obtained on measuring element ratios (line 39 vs 6, 40 vs 7, and 41 vs 8). However, for isotope ratios much different from 2, the precision worsens (compare precision for Fe with the others).

5. The best within laboratory precision is reported by a laboratory using the photographic plate and not electrical detection. However, the average precision for the three laboratories using electrical detection is significantly better than that for all laboratories (line 34 vs 6 and 35 vs 7) and slightly better than that for those laboratories

within the "t" test limits (line 35 vs 9). These comparisons must be viewed with caution because of the small number of laboratories using electrical detection in this collection of data.

6. Because of the discussions over the years concerning RSF values, their magnitude and their interchangeability, the values reported in this round robin are examined from several viewpoints.

7.1 The within laboratory precision of the RSF values is quite good (line 17). The interlaboratory comparison could include only those RSF values relative to the same element. The interlaboratory precision for the fourteen laboratories reporting RSF values relative to Fe is somewhat worse than the within laboratory precision (line 18 vs 17).

7.2 Seventeen laboratories used RSF values. The grand average obtained with each laboratory using its own RSF values are given in line 20. The interlaboratory precision and the accuracy of these results are given in lines 21 and 22 and lines 23 and 24 respectively.

7.3 The data from these seventeen laboratories were recalculated removing the RSF corrections. The grand averages of these uncorrected concentrations, their interlaboratory precision, and their average deviations from the true concentrations are shown in lines 25, 26, and 27. It is obvious that the uncorrected results are less precise and less accurate.

7.4 To determine the effect of all laboratories using the same RSF values, the average of the RSF values relative to Fe were calculated for each element and used to correct the uncorrected data generated in 7.3 above. The grand averages of these "corrected" results and their deviations from the true concentrations are shown in lines 30, 31 and 32. Comparing lines 28 with 31 and 29 with 32 shows the value of each laboratory using its own RSF values.

EVALUATION OF DATA

ASMS COMMITTEE VII ROUND ROBIN 1973-74

Sample NBS SRM 661, Standard NBS SRM 663

Line No.			B	Co	Cu	Zn	As	Mo	Sb	W	Pb	avg
						TRUE CONCENTRATIONS						
1			26	285	370	.85	127	1106	19	46	.067	
						DETERMINED CONCENTRATIONS						
2	Grand Avg		25	290	426	1.83	153	1142	19	57	.18	
3	Range	Lo	3	127	262	.57	46	651	8.3	11	.035	
		Hi	58	391	718	4.8	382	1569	37	162	1.37	
			same. omitting values outside "t" test limits									
4	Grand Avg		24	298	412	1.68	142	1146	17	52	.069	
5	Range	Lo	3	235	262	.57	46	864	8.3	11	0.35	
		Hi	37	391	629	2.8	226	1523	31	97	.19	
						PRECISION, WITHIN LABORATORY Deviation of single values from laboratory avg						
6	avg d,%		21	13	12	23	15	16	22	22	34	20
						PRECISION, INTERLABORATORY Deviation of laboratory avgs from grand avg						
7	avg d,%		33	14	18	35	30	15	31	31	113	36
8	Sd,%		48	20	25	50	45	21	42	51	212	57

same, omitting values outside "t" test limits

9	avg d,%	31	11	15	30	24	12	24	23	41	23
10	Sd,%	42	14	21	38	32	17	32	34	64	33

ACCURACY

Deviation of laboratory avgs from true concentration

11	avg d,%	33	14	21	118	36	15	31	38	200	56
12	Sd,%	47	20	33	160	58	21	42	69	590	116

same, omitting values outside "t" test limits

13	avg d,%	29	12	17	102	28	12	24	27	41	32
14	Sd,%	38	16	26	125	38	17	31	41	65	44

RSF VALUES

14 labs using RSF relative to Fe

15	Grand Avg	1.3	1.2	2.1	8.3	4.1	1.1	6.5	1.0	14
16	Range of) Lo	.12	.44	.68	1.5	.40	.15	1.23	.13	1.2
	Lab Avgs) Hi	3.7	3.5	4.4	20	13	2.4	19	3.6	59

PRECISION, WITHIN LABORATORY

Deviation of single values from laboratory avg for the 11 laboratories reporting RSF for each determination

17	avg d,%	19	16	15	17	22	16	23	15	24	19

PRECISION, INTERLABORATORY

Deviation of laboratory avgs from grand avg 14 labs using RSF relative to Fe

18	avg d,%	60	40	33	70	67	43	73	56	98	60
19	Sd,%	81	64	46	82	95	55	88	87	139	82

EFFECT OF RSF
using data of 17 laboratories
Using Individual RSF Values
Determined Concentration

20	Grand Avg	26	294	438	1.85	155	1127	19	60	.068	
					Precision. Interlaboratory Deviation of laboratory avgs from grand avg						
21	avg d,%	37	14	19	36	36	16	33	33	29	28
22	Sd,%	52	21	27	52	50	23	44	54	34	40
					Accuracy Deviation of laboratory avgs from true concentration						
23	avg d,%	37	15	24	123	40	17	36	46	25	40
24	Sd,%	52	22	37	167	51	23	46	77	29	56
					Taking Out RSF Corrections Determined Concentration						
25	Grand Avg	34	304	808	13.2	413	1313	84	49	.824	
					Precision, Interlaboratory Deviation of laboratory avgs from grand avg						
26	avg d,%	75	20	32	65	43	44	53	49	79	51
27	Sd,%	102	26	42	88	73	56	72	70	109	71
					Accuracy Deviation of laboratory avgs from true concentration						
28	avg d,%	96	21	120	1459	236	52	339	50	1129	389
29	Sd,%	138	29	150	2038	322	70	472	75	1820	568

					Using Grand Avg RSF Values Determined Concentration						
30	Grand Avg	26	238	385	1.60	101	1194	13	49	.059	
					Accuracy Deviation of laboratory avgs from true concentration						
31	avg d,%	80	22	32	124	41	45	51	50	73	58
32	Sd,%	107	26	42	189	62	56	59	75	96	79
					ELECTRIC DETECTION ONLY (3 Laboratories) Determined Concentration						
33	Grand Avg	21	289	376	1.6	140	1124	15	48	.078	
					Precision, Within Laboratory Deviation of single values from laboratory avg						
34	avg d,%	21	9.7	9.3	18	16	22	7.1	13	37	17
					Precision, Interlaboratory Deviation of laboratory avgs from grand avg						
35	avg d,%	20	12	8.1	52	11	16	18	12	78	25
					Accuracy Deviation of laboratory avgs from true concentration						
36	avg d,%	20	13	8.7	88	15	17	21	11	86	31

ISOTOPE RATIOS

		Mo 100/98	W 183/184	Fe 57/56	Cu 65/63	avg
			True Ratios			
37		.405	.470	.0239	.447	
			Determined Ratios			
38	Grand Avg	.409	.473	.0243	.434	
			Precision, Within Laboratory Deviation of Single values from laboratory avg			
39	avg d,%	12	4.3	14	5.9	9.0
			Overall Precision Deviation of single values from grand avg			
40	avg d,%	11	7.0	23	8.5	12
41	Sd,%	16	9.4	36	11	18

Committee VIII on High-Resolution mass spectrometry met with approximately 21 in attendance. There was some agreement that there currently seems to be a strong emphasis on unit resolution instrumentation and data handling rather than accurate mass measurement or other aspects of high-resolution analysis. This was felt to be due to the great demand for analytical systems capable of handling large numbers of relatively routine environmental and biological problems. But in some cases high-resolution analysis was affirmed as an essential step in solving certain special problems. In general, the group expected to see a growth in the need for such systems in the future.

There was general agreement that, after some editing, the specifications for testing high-resolution mass spectrometers developed by Milt Levenberg and David Rosenthal should be sent as letters-to-the-editors of the various mass spectrometry journals.

Several questions were put to the attendees and the results are given below:

1. Everyone present used spectrometers of greater than 6" radius. Thus, users of smaller double-focussing spectrometers apparently do not see themselves in the "high-resolution" camp.

2. 66% nearly always operate at between 6-10,000 resolution; 33% only occasionally that high.

3. 60% operate via on-line computers; 40% use photoplates.

4. 40% do peak-matching less than half-the time; 13% greater than half-time; 47% never.

5. 15% use high-resolution for quantitative analysis as well as accurate mass measurement.

6. 15% feel there is a strong need for resolution greater than 10,000 in their research.

7. 40% felt there was a strong need for spectrometers with higher sensitivity at higher mass (greater than 1,000).

Everyone discussed the need for good internal standards to be used at high mass and nearly everyone said they would be willing to pay at least $100 for suitable samples in the 1-4000 mass range.

Respectfully submitted,
Henry M. Fales

ASMS Committee IX

"Aids to Education"

OBJECTIVES

To disseminate information and aid in providing a better understanding of mass spectrometry and to develop an interest in and enthusiasm for the application of mass spectrometry in all areas of science.

May 27, 1975

Individuals met informally to discuss current activities of the committee. Discussion centered on the need to explore the educational background and technical training desirable for individuals employed or seeking employment as technicians in mass spectrometry laboratories. Details of the recommendations will be available to the membership in the future.

Report of Committee XI
on Environment and Pollution

On Monday, May 26, 1975, a one-day symposium on "Trace Analysis of Environmental Samples" was held. This symposium consisted of 12 invited papers from 10 of the laboratories most active in this area. Attendance at the symposium ranged from a low of 50 to a high of 85.

The most recent membership list for Committee XI shows 89 members. Of these, 8 came to the annual business meeting, which was held after the symposium. Because of the low attendance, no business was conducted. All present members will be contacted by mail during the summer to determine their interest in continued membership as well as their views of the objectives of the Committee.

Respectfully submitted

John M. McGuire
Chairman

Report of ASTM Committee D-2, Research and Development Division 4, Section M on Mass Spectrometry Methods (D02.04.0M)

Thomas Aczel, Chairman, Exxon Research and Engineering Co.
Baytown Research and Development Division Baytown, Texas

ASTM Committee D-2, Division 4, Section M and its Task Groups held two meetings in connection with the 23rd Annual Conference on Mass Spectrometry and the joint meeting of ASTM Committee E-14. These meetings dealt with the development of standardized mass spectral procedures for the analysis of complex mixtures derived from petroleum, coal liquefaction products and shale oils.

Section M has two active Task Groups at the present, one on the analysis of shale oil-gas oil, and one on the analysis of Hydrocarbons from Coal Liquids. The former is chaired by J. Weber, ERDA, Laramie Research Center, the latter by Janet L. Shultz, ERDA, Pittsburgh. The reports of the Task Group Chairpersons are summarized below.

Task Group on Shale Oil (Jim Weber)

The Laramie Research Center is preparing samples which will be used for the cooperative characterization of the olefinic fractions from shale-oil gas oils. These samples will be sent to participants in the cooperative program as soon as possible.

Unfortunately, no clear separation was obtained between aromatics and olefins. The olefins will therefore be hydrogenated using a mild procedure which should not affect the aromatics present in the fraction. Participants in the program will receive, if they so desire, samples of both the hydrogenated and unhydrogenated aromatics.

As far as is known, olefins in shale oil are mainly the C_nH_{2n-2} and C_nH_{2n-4} types with cyclic and dicyclic structures.

Another activity of this Task Group is the comparison of relative low voltage sensitivities. Thomas Aczel of Exxon Research and Engineering Company, Baytown, prepared and distributed 12 samples of aromatic fractions, 430-1050°F, obtained from a number of crudes to be used in this program. Participants will determine the relative low voltage sensitivities of 50 major components of these samples on their own instruments, following a procedure to be mailed to them within July, 1975.

Task Group on Hydrocarbons from Coal Liquids (J. L. Shultz)

Members of this Group have analyzed a saturate fraction, Cut 1, FB39-58 from the Bureau of Mines Synthoil Process. Most laboratories found aromatic components in the sample, with concentration levels ranging from 20 to 92 percent, according to the various analytical methods employed by the participants. Details of these analyses are available from Janet Shultz.

As the first priority of the Group is to develop a satisfactory method for the analysis of saturate samples, it was decided to repeat the separation step. Exxon Research and Engineering Company, Baytown volunteered to prepare saturate fractions according to a

slightly modified version of the ASTM D-2007 procedure which was successful in their Laboratories on coal liquefaction products similar to Synthoil products. The saturate fractions thus obtained will be distributed to participants in the program. Aromatics and polar fractions, as well as the cyclohexane insolubles will also be made available to participants who expressed a desire to analyze these additional samples.

Due to the amount of interest in coal liquefaction and other synthetic fuel technology, the Group decided to sponsor a Symposium on the MS analysis of novel synthetic fuels from coal, shale and tar sands at the 1976 meeting of the American Society for Mass Spectrometry. The proposal was accepted in principle by the Program Chairman. The Symposium will be cochaired by A. G. Sharley of the Bureau of Mines and Thomas Aczel from Exxon Research and Engineering Company.

Report of Section M

Reports of the two Task Groups were transmitted orally to Officers of ASTM E 14 by Thomas Aczel. He proposed that Section M report in the future formally both to ASTM E-14 and ASTM D-2 committees. A formal dependence from E-14 is warranted in his opinion by the close relationship of the activities of the Section to those of Committee E-14.

THE AMERICAN SOCIETY FOR MASS SPECTROMETRY

CONSTITUTION AND BYLAWS

ARTICLE I. NAME

The name of this society shall be "The American Society for Mass Spectrometry".

ARTICLE II. PURPOSE

It is the purpose of this Society to promote and disseminate knowledge of mass spectrometry and allied subjects.

ARTICLE III. MEMBERSHIP

Membership in the American Society for Mass Spectrometry shall be open to any individual, or with approval of the Board of Directors, to any corporate entity with a bona-fide interest in mass spectrometry.

ARTICLE IV. MANAGEMENT

The management of the society shall be vested in the Board of Directors which shall consist of the following members: the officers of the society hereafter listed, two elected members-at-large, the immediate past President, the Chairman of ASTM Committee E-14 on Mass Spectrometry.

The Officers of the Society shall be:

President
Vice-President for Programs, who shall be President-Elect of the Society
Vice-President for Arrangements
Secretary
Treasurer

ARTICLE V. DUTIES OF OFFICERS

Section 1. The President shall be the chief executive officer of this Society; he shall preside at all meetings of the members and directors; he shall have general and active management of the business of this society; he shall see that all orders and resolutions of the

Board of Directors are carried out; he shall execute all bonds, mortgages, and all contracts of this Society and cause or direct the affixing of the corporate seal thereto; he shall have general superintendence and direction of all other officers of this Society and see that their duties are properly performed; he shall submit a report of the operations of the society for the fiscal year to the Board of Directors and members at their annual meeting, and from time to time shall report to the Board of Directors all matters within his knowledge that may affect this Society; he shall be ex-officio a member of all committees except the Nominating and Audit Committees and shall have the power and duties and management usually vested in the Office of President in a corporation; he shall appoint all committees, except as may be otherwise provided; and he shall send, or cause to be sent by the Secretary, notices of any meetings of the Board of Directors.

Section 2. The Vice-President for Programs shall be vested with all the powers and shall perform all the duties of the President during the absence of the latter and shall have such other duties as may, from time to time, be determined by the Board of Directors. The same shall be true of the Vice-President for Arrangements who shall be next in the line of succession. In the event that the President shall be absent at any meeting, the Vice-President for Programs shall preside, and if neither is present at a meeting, then the Vice-President for Arrangements shall preside.

Section 3. The Secretary or a deputy appointed by the President shall attend all meetings of the Board of Directors and all general meetings of the society and act as a clerk thereof; he shall record all votes and minutes of all proceedings; he shall perform such other duties as may be prescribed by the Board of Directors or the President; and he shall be the custodian of the corporate seal and all of the books and records of the society except as may be otherwise provided.

Section 4. The Treasurer shall have charge of the funds of the society and shall deposit them in the name of the society in depositories designated by the Board of Directors; he shall arrange for the payment of all valid society bills and debts from society funds, and shall make a complete and accurate report of the finances of the society at each annual meeting of the members, or at any other time upon request, to the Board of Directors.

ARTICLE VI. DUTIES AND POWERS OF THE BOARD OF DIRECTORS

Section 1. The property and business of the society shall be managed by the Board of Directors.

Section 2. In addition to the general powers of the Board of Directors by virtue of their office, the powers and authority expressly given by law, by terms of the charter of this Society, and elsewhere in these bylaws, the following specific powers are expressly conferred on the Board of Directors.

To purchase or otherwise acquire for the society any property, right or privilege which it is authorized to acquire at such price or consideration, and upon such terms as they deem expedient; to appoint, to remove or suspend subordinate agents or servants, to determine their duties and affix their salaries; to remove or suspend any subordinate officer or servants; to determine who shall be authorized, on behalf of the society, to sign bills, notices, receipts, acceptances, endorsements, checks, releases, contracts and any other instruments; to delegate any of the powers of the Board to any standing committee, special committee, or to any officer or agent of the society, with such powers as the Board may deem fit and proper to grant; generally to do all such lawful acts and things as are not by law, or by charter, or by these bylaws directed or required to be done by members of the Board of Directors.

Section 3. Any action which may be taken at a meeting of the Board of Directors, may be taken without a meeting by a letter ballot sent by and filed with the Secretary of the society and provided all the members of the Board of Directors file ballots.

Section 4. In the event that the office of any elected officer or member of the Board of Directors shall become vacant, the Board of Directors shall immediately fill the vacancy for the remainder of the unexpired term; however, no member who thus fills a vacancy in the office of Vice-President for Programs shall automatically succeed to the presidency, but the society shall in such event elect its next President. A President who vacates office before the conclusion of his term shall not retain membership on the Board of Directors as past-President as described in Article IV.

Section 5. The ballot of the election to membership on the Board of Directors of the society shall be by closed, written ballot.

Section 6. Any member shall be eligible to hold office in the society.

ARTICLE VII. FIDELITY BONDS

The Board of Directors may require such officers or agents to be bonded as it shall deem necessary; for any amount or amounts as it may deem requisite, at the expense of the society.

ARTICLE VIII. LOCATION.

The principal office of this society shall be located in the City of Pittsburgh, Commonwealth of Pennsylvania.

ARTICLE IX. DISSOLUTION.

In the event of either voluntary or involuntary dissolution of the society, the funds or assets of the society, remaining after discharging all just debts of the society or its officers in the name of the society, shall be distributed without encumbrances to a non-profit group, organization or institution of learning engaged in the field of mass

spectrometry within the contemplation of Section 170 (c) (2) of the Internal Revenue Code (1954). The selection of the recipient or recipients shall be made by the majority vote of the Board of Directors in office at the time of dissolution but in no event shall the assets be distributed to any member or members of the society.

ARTICLE X. SOCIETY SEAL

The society shall have a seal, upon which shall be inscribed the name of the society, the year of its creation, and the word "Pennsylvania", the state of the society's incorporation.

ARTICLE XI. AMENDMENTS

Section 1. A proposed amendment to the Constitution and the Bylaws of the society, signed by at least three members of the Board of Directors or by 50 members of the society must be submitted to the Secretary at least fifteen weeks before the regular business meeting of the society at which meeting the proposed amendment may be discussed and amended. The Secretary shall send or cause to be sent the proposed amendment to each member within a reasonable time and at least before or with the notice of the next regular meeting. After the amendment has been discussed at a regular business meeting of the society the Secretary will send a letter ballot on the proposed amendment (as amended at the meeting) to all society members; if two-thirds of the votes obtained by letter ballot are in favor of the proposed amendment it shall be adopted.

Section 2. The Board of Directors shall also have the power to amend the Bylaws by a two-thirds vote of its membership.

Section 3. The Board of Directors is authorized to renumber articles and sections of the Constitution and Bylaws to correspond with any changes that may be made.

BYLAWS

1. Membership

1.1 Application for membership shall be made in writing, on a form to be specified by the Board of Directors. The membership year shall commence October 1 and end September 30.

1.2 Applicants shall be admitted by the action of the Board of Directors and membership thereafter becomes effective upon receipt of dues by the Treasurer.

1.3 Failure to pay dues by April 1 shall automatically terminate membership. Payment of arrears and current dues shall suffice for reinstatement.

1.4 Membership may be terminated without prejudice by written notice to the Secretary, with the requirement that dues up to and including the year of written notice be paid.

1.5 Every member shall have the right to vote and to hold office.

1.6 The books, accounts and records of the society shall be open for inspection to any member of the Board of Directors at any time. Members of the society may upon written request to the Board of Directors, inspect such books, accounts and records of the society at such reasonable times as the Board of Directors may designate.

1.7 The Secretary will prepare or cause to be prepared at least one annual membership report to the Board of Directors.

2. Collections and Disbursements

2.1 Membership classes and dues within such classes shall be determined by the Board of Directors.

2.2 The Board of Directors is authorized to determine separately a registration fee for each general meeting to cover the expenses of holding the meeting. Payment of this fee is a requirement for attendance.

2.3 Disbursements shall be made by approval of a majority of the Board of Directors. Disbursement in excess of $250.00 shall be made by check signed by two members of the Board.

2.4 The fiscal year of the society shall be from October 1 to September 30.

2.5 The Treasurer will prepare or cause to be prepared an annual financial report to the Board of Directors.

3. Terms of Office and Election

3.1 The elected officers and directors-at-large shall hold office for a term of two (2) years, except as otherwise provided in Article VI of the Constitution, with their term year commencing on July 1 and ending on June 30.

3.2 The President shall appoint a nominating committee of not less than three members on or before July 1 of his second year in office. He shall not be a member of this committee. The committee shall nominate a slate of candidates and report in writing to the Board of Directors no later than the first day of the following September. The nominating committee's report will recommend at least one candidate per office and obtain each candidate's consent to serve if elected and a resume for each candidate. This slate of candidates and the resumes will be distributed to the members by the Secretary before November 1.

3.3 Any society member can nominate another member for any office, except President, by submitting to the Secretary before February 15 of the election year:

a. signatures of at least 50 society members endorsing the nomination;

b. signature of the nominee agreeing to hold office if elected;

c. resume of the candidate.

3.4 The Secretary shall prepare or cause to be prepared a letter ballot to be mailed to the membership at the time of the final

meeting notice and requesting return no later than two weeks preceding the annual meeting.

3.5 The election results shall be made known at the next annual business meeting and the new officers shall assume office as specified in paragraph 3.1 of the Bylaws.

4. Committees

4.1 The President shall appoint such committees as are necessary to accomplish the purposes of the society. The terms of these appointments shall not exceed the term of office of the President. He may terminate a committee at any time. Members and chairmen may be reappointed by the incoming President.

5. Meetings

5.1 The society shall meet at least once a year in order to present scientific papers and conduct business. Fifty members shall constitute a quorum for the transaction of business.

5.2 The time and place of the general meeting shall be determined by the Board of Directors.

5.3 Meetings of the Board of Directors may be called by the President or, in his absence, by the Vice-President for Programs. Alternatively, two-thirds of the Board of Directors may call a meeting by written request to the President. Five directors shall constitute a quorum of the Board of Directors.

5.4 A simple majority of those present shall be required to pass any motion at any meeting of the members or Board of Directors, unless otherwise provided.

5.5 Each Director shall be entitled to two weeks notice of any meeting of the Board of Directors.

5.6 Notice of the annual general meeting shall be sent to each member at least thirty days before the meeting.

5.7 The President shall, in response to petition bearing the

signatures of not fewer than twenty members and requesting that the Board of Directors consider a specified question, place this item on the agenda of the first meeting of the Board of Directors which is scheduled to convene on a date not preceding the thirtieth day following receipt of the petition. The member whose signature appears first on the petition shall be entitled to two weeks notice of such meeting, and the same member or a member designated by him shall be entitled to attend such meeting and discuss the specified question with the Board of Directors.

5.8 Whenever any notice is required to be given by the provisions of the Bylaws, a waiver thereof in writing, signed by the person or persons entitled to such notices, whether before, or after the time stated therein, shall be equivalent to the required notice.

6. Compensation

6.1 No member of the Board of Directors of the society shall receive salaries or fees for his services.

6.2 Members of the Board of Directors of the society shall be reimbursed for all reasonable expenses incurred in connection with their official duties.

7. Miscellaneous

7.1 The incoming President shall cause the financial records of the society to be audited within the first six (6) months of his term of office.

7.2 The business of the society shall be conducted in accordance with the latest edition of Roberts' Rules of Order unless otherwise specified herein.

A.S.T.M. Publications on Mass Spectrometry

A. Recommended Practices and Methods of Test*

	Title and Citations in 1975 Books of ASTM Standards
D1137-53 (70)	Analysis of Natural Gases and Related Types of Gaseous Mixtures by the Mass Spectrometer, Part 26.
D1658-63 (74)	Carbon Number Distribution of Aromatic Compounds in Naphthas by Mass Spectrometry, Part 23.
D2424-67 (72)	Hydrocarbon Types in Propylene Polymer by Mass Spectrometry, Part 24.
D2498-68 (73)	Isomer Distribution of Straight-Chain Detergent Alkylate by Mass Spectrometry, Part 24.
D2567-68 (73)	Molecular Distribution Analysis of Monoalkylbenzenes by Mass Spectrometry, Part 24.
D2601-68 (73)	Low Voltage Mass Spectrometric Analysis of Propylene Tetramer, Part 24.
D2786-71	High Ionizing Voltage Mass Spectrometric Analysis of Gas-Oil Saturate Fractions, Part 24.
D2789-71	Hydrocarbon Types in Low Olefinic Gasoline by Mass Spectrometry, Part 24.
E137-68	Evaluation of Mass Spectrometers for Use in Chemical Analysis, Part 42.
E244-69	Atom Percent Fission in Uranium Fuel, Mass Spectrometric Method, Part 45.
E304-68	Use and Evaluation of Mass Spectrometers for Mass Spectrochemical Analysis of Solids, Part 42.

B. Other ASTM Mass Spectrometric Information

AMD11	Index of Mass Spectral Data, 1969, Formerly STP 356).
AMD10a	Mass Spectral Data Structure (Punched Card Index - 3200 cards).
AMD10b	Mass Spectral Data - Name (Punched Card Index - 3500 cards).
AMD10c	Mass Spectral Data - Name (Punched Card Index - 3500 cards).

STP No. 149 Chemical Analysis of Inorganic Solids by Means of Mass Spectrometer, 1951 (out of print, available on microfilm).

STP No. 332a Manual on Hydrocarbon Analysis, 1968 (Revised manual in preparation).

---

*Committee jurisdiction for the mass spectrometric practices and methods is as follows:

Committee D3 - D1137
Committee E10 - E244
Committee E14 - E137 and E304
Committee D2 - all others listed

MASS SPECTROMETRY ORGANIZATIONS

Name	Name and Address for Additional Information
The American Society for Mass Spectrometry	Dr. J. A. McCloskey College of Pharmacy University of Utah Salt Lake City, Utah 84112
The Australian and New Zealand Society for Mass Spectrometry	Dr. J. K. MacLeod The Australian Soc. for Mass Spectrometry Research School of Chemistry The Australian National University Box 4, P.O. Canberra, A.C.T. 2600 Australia
Mass Spectroscopy Society of Japan (MSSJ)	Professor Teruo Hayakawa The Mass Spectroscopy Society of Japan Department of Chemistry Faculty of Liberal Arts and Sciences Univ. of Osaka Prefecture Sakai-shi, Osaka, Japan
Mass Spectroscopy Group	Dr. A. Carrick Instem Ltd. Stafford Street Stone, Staffs England
Arbeitegemeinschaft Massenspektroskopie	Dr. H. F. Grutzmacher, Frachbereich Chemie, Univ. Hamburg, 2 Hamburg, Germany
Groupement pour l'Avancement des Methodes Physiques d'Analyses (G.A.M.S.)	Madame Frere - GAMS 8, 10 rue de Delta 75 Paris 9 eme, France